



Hashemite Kingdom of Jordan



Jordan Journal of



Biological Sciences

An International Peer-Reviewed Scientific Journal

Financed by the Scientific Research and Innovation Support Fund



<http://jjbs.hu.edu.jo/>

المجلة الأردنية للعلوم الحياتية
Jordan Journal of Biological Sciences (JJBS)

<http://jjbs.hu.edu.jo>

Jordan Journal of Biological Sciences (JJBS) (ISSN: 1995–6673 (Print); 2307-7166 (Online)): An International Peer- Reviewed Open Access Research Journal financed by the Scientific Research and Innovation Support Fund, Ministry of Higher Education and Scientific Research, Jordan and published quarterly by the Deanship of Scientific Research , The Hashemite University, Jordan.

Editor-in-Chief

Professor Atoum, Manar F.
Molecular Biology and Genetics,
The Hashemite University

Editorial Board (Arranged alphabetically)

Professor Amr, Zuhair S.
Animal Ecology and Biodiversity
Jordan University of Science and Technology

Professor Hunaiti, Abdulrahim A.
Biochemistry
The University of Jordan

Professor Khleifat, Khaled M.
Microbiology and Biotechnology
Mutah University

Professor Lahham, Jamil N.
Plant Taxonomy
Yarmouk University

Professor Malkawi, Hanan I.
Microbiology and Molecular Biology
Yarmouk University

Associate Editorial Board

Professor Al-Hindi, Adnan I.
Parasitology
The Islamic University of Gaza, Faculty of Health
Sciences, Palestine

Dr Gammoh, Noor
Tumor Virology
Cancer Research UK Edinburgh Centre, University of
Edinburgh, U.K.

Professor Kasperek, Max
Natural Sciences
Editor-in-Chief, Journal Zoology in the Middle East,
Germany

Professor Krystufek, Boris
Conservation Biology
Slovenian Museum of Natural History,
Slovenia

Dr Rabei, Sami H.
Plant Ecology and Taxonomy
Botany and Microbiology Department,
Faculty of Science, Damietta University, Egypt

Professor Simerly, Calvin R.
Reproductive Biology
Department of Obstetrics/Gynecology and
Reproductive Sciences, University of
Pittsburgh, USA

Editorial Board Support Team

Language Editor
Dr. Shadi Neimneh

Publishing Layout
Eng. Mohannad Oqdeh

Submission Address

Professor Atoum, Manar F
The Hashemite University
P.O. Box 330127, Zarqa, 13115, Jordan
Phone: +962-5-3903333 ext.4147
E-Mail: jjbs@hu.edu.jo

International Advisory Board (Arranged alphabetically)

Professor Ahmad M. Khalil

Department of Biological Sciences, Faculty of Science,
Yarmouk University, Jordan

Professor Anilava Kaviraj

Department of Zoology, University of Kalyani, India

Professor Bipul Kumar Das

Faculty of Fishery Sciences W. B. University of Animal &
Fishery Sciences, India

Professor Elias Baydoun

Department of Biology, American University of Beirut
Lebanon

Professor Hala Gali-Muhtasib

Department of Biology, American University of Beirut
Lebanon

Professor Ibrahim M. AlRawashdeh

Department of Biological Sciences, Faculty of Science, Al-
Hussein Bin Talal University, Jordan

Professor João Ramalho-Santos

Department of Life Sciences, University of Coimbra, Portugal

Professor Khaled M. Al-Qaoud

Department of Biological sciences, Faculty of Science,
Yarmouk University, Jordan

Professor Mahmoud A. Ghannoum

Center for Medical Mycology and Mycology Reference
Laboratory, Department of Dermatology, Case Western
Reserve University and University Hospitals Case Medical
Center, USA

Professor Mawieh Hamad

Department of Medical Lab Sciences, College of Health
Sciences , University of Sharjah, UAE

Professor Michael D Garrick

Department of Biochemistry, State University of New York at
Buffalo, USA

Professor Nabil. A. Bashir

Department of Physiology and Biochemistry, Faculty of
Medicine, Jordan University of Science and Technology,
Jordan

Professor Nizar M. Abuharfeil

Department of Biotechnology and Genetic Engineering, Jordan
University of Science and Technology, Jordan

Professor Samih M. Tamimi

Department of Biological Sciences, Faculty of Science, The
University of Jordan, Jordan

Professor Ulrich Joger

State Museum of Natural History Braunschweig, Germany

Professor Aida I. El Makawy

Division of Genetic Engineering and Biotechnology, National
Research Center. Giza, Egypt

Professor Bechan Sharma

Department of Biochemistry, Faculty of Science University of
Allahabad, India

Professor Boguslaw Buszewski

Chair of Environmental Chemistry and Bioanalytics, Faculty of
Chemistry, Nicolaus Copernicus University Poland

Professor Gerald Schatten

Pittsburgh Development Center, Division of Developmental
and Regenerative Medicine, University of Pittsburgh, School
of Medicine, USA

Professor Hala Khyami-Horani

Department of Biological Sciences, Faculty of Science, The
University of Jordan, Jordan

Professor James R. Bamburg

Department of Biochemistry and Molecular Biology, Colorado
State University, USA

Professor Jumah M. Shakhaneh

Department of Biological Sciences, Faculty of Science, Mutah
University, Jordan

Dr. Lukmanul Hakkim Faruck

Department of Mathematics and Sciences College of Arts and
Applied Sciences, Dhofar, Oman

Professor Md. Yeamin Hossain

Department of Fisheries, Faculty of Fisheries , University of
Rajshahi, Bangladesh

Professor Mazin B. Qumsiyeh

Palestine Museum of Natural History and Palestine Institute for
Biodiversity and Sustainability, Bethlehem University,
Palestine

Professor Mohamad S. Hamada

Genetics Department, Faculty of Agriculture, Damietta
University, Egypt

Professor Nawroz Abdul-razzak Tahir

Plant Molecular Biology and Phytochemistry, University of
Sulaimani, College of Agricultural Sciences, Iraq

Professor Ratib M. AL- Ouran

Department of Biological Sciences, Faculty of Science, Mutah
University, Jordan

Professor Shtaywy S. Abdalla Abbadi

Department of Biological Sciences, Faculty of Science, The
University of Jordan, Jordan

Professor Zihad Bouslama

Department of Biology, Faculty of Science Badji Mokhtar
University, Algeria

Instructions to Authors

Scopes

Study areas include cell biology, genomics, microbiology, immunology, molecular biology, biochemistry, embryology, immunogenetics, cell and tissue culture, molecular ecology, genetic engineering and biological engineering, bioremediation and biodegradation, bioinformatics, biotechnology regulations, gene therapy, organismal biology, microbial and environmental biotechnology, marine sciences. The JJBS welcomes the submission of manuscript that meets the general criteria of significance and academic excellence. All articles published in JJBS are peer-reviewed. Papers will be published approximately one to two months after acceptance.

Type of Papers

The journal publishes high-quality original scientific papers, short communications, correspondence and case studies. Review articles are usually by invitation only. However, Review articles of current interest and high standard will be considered.

Submission of Manuscript

Manuscript, or the essence of their content, must be previously unpublished and should not be under simultaneous consideration by another journal. The authors should also declare if any similar work has been submitted to or published by another journal. They should also declare that it has not been submitted/ published elsewhere in the same form, in English or in any other language, without the written consent of the Publisher. The authors should also declare that the paper is the original work of the author(s) and not copied (in whole or in part) from any other work. All papers will be automatically checked for duplicate publication and plagiarism. If detected, appropriate action will be taken in accordance with International Ethical Guideline. By virtue of the submitted manuscript, the corresponding author acknowledges that all the co-authors have seen and approved the final version of the manuscript. The corresponding author should provide all co-authors with information regarding the manuscript, and obtain their approval before submitting any revisions. Electronic submission of manuscripts is strongly recommended, provided that the text, tables and figures are included in a single Microsoft Word file. Submit manuscript as e-mail attachment to the Editorial Office at: JJBS@hu.edu.jo. After submission, a manuscript number will be communicated to the corresponding author within 48 hours.

Peer-review Process

It is requested to submit, with the manuscript, the names, addresses and e-mail addresses of at least 4 potential reviewers. It is the sole right of the editor to decide whether or not the suggested reviewers to be used. The reviewers' comments will be sent to authors within 6-8 weeks after submission. Manuscripts and figures for review will not be returned to authors whether the editorial decision is to accept, revise, or reject. All Case Reports and Short Communication must include at least one table and/ or one figure.

Preparation of Manuscript

The manuscript should be written in English with simple lay out. The text should be prepared in single column format. Bold face, italics, subscripts, superscripts etc. can be used. Pages should be numbered consecutively, beginning with the title page and continuing through the last page of typewritten material.

The text can be divided into numbered sections with brief headings. Starting from introduction with section 1. Subsections should be numbered (for example 2.1 (then 2.1.1, 2.1.2, 2.2, etc.), up to three levels. Manuscripts in general should be organized in the following manner:

Title Page

The title page should contain a brief title, correct first name, middle initial and family name of each author and name and address of the department(s) and institution(s) from where the research was carried out for each author. The title should be without any abbreviations and it should enlighten the contents of the paper. All affiliations should be provided with a lower-case superscript number just after the author's name and in front of the appropriate address.

The name of the corresponding author should be indicated along with telephone and fax numbers (with country and area code) along with full postal address and e-mail address.

Abstract

The abstract should be concise and informative. It should not exceed **350 words** in length for full manuscript and Review article and **150 words** in case of Case Report and/ or Short Communication. It should briefly describe the purpose of the work, techniques and methods used, major findings with important data and conclusions. No references should be cited in this part. Generally non-standard abbreviations should not be used, if necessary they should be clearly defined in the abstract, at first use.

Keywords

Immediately after the abstract, **about 4-8 keywords** should be given. Use of abbreviations should be avoided, only standard abbreviations, well known in the established area may be used, if appropriate. These keywords will be used for indexing.

Abbreviations

Non-standard abbreviations should be listed and full form of each abbreviation should be given in parentheses at first use in the text.

Introduction

Provide a factual background, clearly defined problem, proposed solution, a brief literature survey and the scope and justification of the work done.

Materials and Methods

Give adequate information to allow the experiment to be reproduced. Already published methods should be mentioned with references. Significant modifications of published methods and new methods should be described in detail. Capitalize trade names and include the manufacturer's name and address. Subheading should be used.

Results

Results should be clearly described in a concise manner. Results for different parameters should be described under subheadings or in separate paragraph. Results should be explained, but largely without referring to the literature. Table or figure numbers should be mentioned in parentheses for better understanding.

Discussion

The discussion should not repeat the results, but provide detailed interpretation of data. This should interpret the significance of the findings of the work. Citations should be given in support of the findings. The results and discussion part can also be described as separate, if appropriate. The Results and Discussion sections can include subheadings, and when appropriate, both sections can be combined

Conclusions

This should briefly state the major findings of the study.

Acknowledgment

A brief acknowledgment section may be given after the conclusion section just before the references. The acknowledgment of people who provided assistance in manuscript preparation, funding for research, etc. should be listed in this section.

Tables and Figures

Tables and figures should be presented as per their appearance in the text. It is suggested that the discussion about the tables and figures should appear in the text before the appearance of the respective tables and figures. No tables or figures should be given without discussion or reference inside the text.

Tables should be explanatory enough to be understandable without any text reference. Double spacing should be maintained throughout the table, including table headings and footnotes. Table headings should be placed above the table. Footnotes should be placed below the table with superscript lowercase letters. Each table should be on a separate page, numbered consecutively in Arabic numerals.

Each figure should have a caption. The caption should be concise and typed separately, not on the figure area. Figures should be self-explanatory. Information presented in the figure should not be repeated in the table. All symbols and abbreviations used in the illustrations should be defined clearly. Figure legends should be given below the figures.

References

References should be listed alphabetically at the end of the manuscript. Every reference referred in the text must be also present in the reference list and vice versa. In the text, a reference identified by means of an author's name should be followed by the year of publication in parentheses (e.g.(Brown,2009)). For two authors, both authors' names followed by the year of publication (e.g.(Nelson and Brown, 2007)). When there are more than two authors, only the first author's name followed by "*et al.*" and the year of publication (e.g. (Abu-Elteen *et al.*, 2010)). When two or more works of an author has been published during the same year, the reference should be identified by the letters "a", "b", "c", etc., placed after the year of publication. This should be followed both in the text and reference list. e.g., Hilly, (2002a, 2002b); Hilly, and Nelson, (2004). Articles in preparation or submitted for publication, unpublished observations, personal communications, etc. should not be included in the reference list but should only be mentioned in the article text (e.g., Shtyawy,A., University of Jordan, personal communication). Journal titles should be abbreviated according to the system adopted in Biological Abstract and Index Medicus, if not included in Biological Abstract or Index Medicus journal title should be given in full. The author is responsible for the scuracy and completeness of the references and for their correct textual citation. Failure to do so may result in the paper being withdraw from the evaluation process. Example of correct reference form is given as follows:-

Reference to a journal publication:

Bloch BK. 2002. Econazole nitrate in the treatment of *Candida vaginitis*. *S Afr Med J.* , **58**:314-323.

Ogunseitan OA and Ndoeye IL. 2006. Protein method for investigating mercuric reductase gene expression in aquatic environments. *Appl Environ Microbiol.*, **64**: 695-702.

Hilly MO, Adams MN and Nelson SC. 2009. Potential fly-ash utilization in agriculture. *Progress in Natural Sci.*, **19**: 1173-1186.

Reference to a book:

Brown WY and White SR.1985. **The Elements of Style**, third ed. MacMillan, New York.

Reference to a chapter in an edited book:

Mettam GR and Adams LB. 2010. How to prepare an electronic version of your article. In: Jones BS and Smith RZ (Eds.), **Introduction to the Electronic Age**. Kluwer Academic Publishers, Netherlands, pp. 281–304.

Conferences and Meetings:

Embabi NS. 1990. Environmental aspects of distribution of mangrove in the United Arab Emirates. Proceedings of the First ASWAS Conference. University of the United Arab Emirates. Al-Ain, United Arab Emirates.

Theses and Dissertations:

El-Labadi SN. 2002. Intestinal digenetic trematodes of some marine fishes from the Gulf of Aqaba. MSc dissertation, The Hashemite University, Zarqa, Jordan.

Nomenclature and Units

Internationally accepted rules and the international system of units (SI) should be used. If other units are mentioned, please give their equivalent in SI.

For biological nomenclature, the conventions of the *International Code of Botanical Nomenclature*, the *International Code of Nomenclature of Bacteria*, and the *International Code of Zoological Nomenclature* should be followed.

Scientific names of all biological creatures (crops, plants, insects, birds, mammals, etc.) should be mentioned in parentheses at first use of their English term.

Chemical nomenclature, as laid down in the *International Union of Pure and Applied Chemistry* and the official recommendations of the *IUPAC-IUB Combined Commission on Biochemical Nomenclature* should be followed. All biocides and other organic compounds must be identified by their Geneva names when first used in the text. Active ingredients of all formulations should be likewise identified.

Math formulae

All equations referred to in the text should be numbered serially at the right-hand side in parentheses. Meaning of all symbols should be given immediately after the equation at first use. Instead of root signs fractional powers should be used. Subscripts and superscripts should be presented clearly. Variables should be presented in italics. Greek letters and non-Roman symbols should be described in the margin at their first use.

To avoid any misunderstanding zero (0) and the letter O, and one (1) and the letter l should be clearly differentiated. For simple fractions use of the solidus (/) instead of a horizontal line is recommended. Levels of statistical significance such as: * $P < 0.05$, ** $P < 0.01$ and *** $P < 0.001$ do not require any further explanation.

Copyright

Submission of a manuscript clearly indicates that: the study has not been published before or is not under consideration for publication elsewhere (except as an abstract or as part of a published lecture or academic thesis); its publication is permitted by all authors and after accepted for publication it will not be submitted for publication anywhere else, in English or in any other language, without the written approval of the copyright-holder. The journal may consider manuscripts that are translations of articles originally published in another language. In this case, the consent of the journal in which the article was originally published must be obtained and the fact that the article has already been published must be made clear on submission and stated in the abstract. It is compulsory for the authors to ensure that no material submitted as part of a manuscript infringes existing copyrights, or the rights of a third party.

Ethical Consent

All manuscripts reporting the results of experimental investigation involving human subjects should include a statement confirming that each subject or subject's guardian obtains an informed consent, after the approval of the experimental protocol by a local human ethics committee or IRB. When reporting experiments on animals, authors should indicate whether the institutional and national guide for the care and use of laboratory animals was followed.

Plagiarism

The JJBS hold no responsibility for plagiarism. If a published paper is found later to be extensively plagiarized and is found to be a duplicate or redundant publication, a note of retraction will be published, and copies of the correspondence will be sent to the authors' head of institute.

Galley Proofs

The Editorial Office will send proofs of the manuscript to the corresponding author as an e-mail attachment for final proof reading and it will be the responsibility of the corresponding author to return the galley proof materials appropriately corrected within the stipulated time. Authors will be asked to check any typographical or minor clerical errors in the manuscript at this stage. No other major alteration in the manuscript is allowed. After publication authors can freely access the full text of the article as well as can download and print the PDF file.

Publication Charges

There are no page charges for publication in Jordan Journal of Biological Sciences, except for color illustrations,

Reprints

Ten (10) reprints are provided to corresponding author free of charge within two weeks after the printed journal date. For orders of more reprints, a reprint order form and prices will be sent with article proofs, which should be returned directly to the Editor for processing.

Disclaimer

Articles, communication, or editorials published by JJBS represent the sole opinions of the authors. The publisher shoulders no responsibility or liability what so ever for the use or misuse of the information published by JJBS.

Indexing

JJBS is indexed and abstracted by:

DOAJ (Directory of Open Access Journals)

Google Scholar

Journal Seek

HINARI

Index Copernicus

NDL Japanese Periodicals Index

SCIRUS

OAJSE

ISC (Islamic World Science Citation Center)

Directory of Research Journal Indexing
(DRJI)

Ulrich's

CABI

EBSCO

CAS (Chemical Abstract Service)

ETH- Citations

Open J-Gat

SCImago

Clarivate Analytics (Zoological Abstract)

Scopus

AGORA (United Nation's FAO database)

SHERPA/RoMEO (UK)

المجلة الأردنية للعلوم الحياتية
Jordan Journal of Biological Sciences (JJBS)
ISSN 1995- 6673 (Print), 2307- 7166 (Online)

<http://jjbs.hu.edu.jo>

The Hashemite University
Deanship of Scientific Research
TRANSFER OF COPYRIGHT AGREEMENT

Journal publishers and authors share a common interest in the protection of copyright: authors principally because they want their creative works to be protected from plagiarism and other unlawful uses, publishers because they need to protect their work and investment in the production, marketing and distribution of the published version of the article. In order to do so effectively, publishers request a formal written transfer of copyright from the author(s) for each article published. Publishers and authors are also concerned that the integrity of the official record of publication of an article (once refereed and published) be maintained, and in order to protect that reference value and validation process, we ask that authors recognize that distribution (including through the Internet/WWW or other on-line means) of the authoritative version of the article as published is best administered by the Publisher.

To avoid any delay in the publication of your article, please read the terms of this agreement, sign in the space provided and return the complete form to us at the address below as quickly as possible.

Article entitled:-----

Corresponding author: -----

To be published in the journal: Jordan Journal of Biological Sciences (JJBS)

I hereby assign to the Hashemite University the copyright in the manuscript identified above and any supplemental tables, illustrations or other information submitted therewith (the "article") in all forms and media (whether now known or hereafter developed), throughout the world, in all languages, for the full term of copyright and all extensions and renewals thereof, effective when and if the article is accepted for publication. This transfer includes the right to adapt the presentation of the article for use in conjunction with computer systems and programs, including reproduction or publication in machine-readable form and incorporation in electronic retrieval systems.

Authors retain or are hereby granted (without the need to obtain further permission) rights to use the article for traditional scholarship communications, for teaching, and for distribution within their institution.

- I am the sole author of the manuscript
- I am signing on behalf of all co-authors of the manuscript
- The article is a 'work made for hire' and I am signing as an authorized representative of the employing company/institution

Please mark one or more of the above boxes (as appropriate) and then sign and date the document in black ink.

Signed: _____ Name printed: _____

Title and Company (if employer representative) : _____

Date: _____

Data Protection: By submitting this form you are consenting that the personal information provided herein may be used by the Hashemite University and its affiliated institutions worldwide to contact you concerning the publishing of your article.

Please return the completed and signed original of this form by mail or fax, or a scanned copy of the signed original by e-mail, retaining a copy for your files, to:

Hashemite University
Jordan Journal of Biological Sciences
Zarqa 13115 Jordan
Fax: +962 5 3903338
Email: jjbs@hu.edu.jo

EDITORIAL PREFACE

Jordan Journal of Biological Sciences (JJBS) is a refereed, quarterly international journal financed by the Scientific Research and Innovation Support Fund, Ministry of Higher Education and Scientific Research in cooperation with the Hashemite University, Jordan. JJBS celebrated its 12th commencement this past January, 2020. JJBS was founded in 2008 to create a peer-reviewed journal that publishes high-quality research articles, reviews and short communications on novel and innovative aspects of a wide variety of biological sciences such as cell biology, developmental biology, structural biology, microbiology, entomology, molecular biology, biochemistry, medical biotechnology, biodiversity, ecology, marine biology, plant and animal biology, plant and animal physiology, genomics and bioinformatics.

We have watched the growth and success of JJBS over the years. JJBS has published 11 volumes, 45 issues and 479 articles. JJBS has been indexed by SCOPUS, CABI's Full-Text Repository, EBSCO, Clarivate Analytics- Zoological Record and recently has been included in the UGC India approved journals. JJBS Cite Score has improved from 0.18 in 2015 to 0.58 in 2019 (Last updated on 16 March, 2020) and with Scimago Institution Ranking (SJR) 0.21 (Q3) in 2018.

A group of highly valuable scholars have agreed to serve on the editorial board and this places JJBS in a position of most authoritative on biological sciences. I am honored to have six eminent associate editors from various countries. I am also delighted with our group of international advisory board members coming from 15 countries worldwide for their continuous support of JJBS. With our editorial board's cumulative experience in various fields of biological sciences, this journal brings a substantial representation of biological sciences in different disciplines. Without the service and dedication of our editorial; associate editorial and international advisory board members, JJBS would have never existed.

In the coming year, we hope that JJBS will be indexed in Clarivate Analytics and MEDLINE (the U.S. National Library of Medicine database) and others. As you read throughout this volume of JJBS, I would like to remind you that the success of our journal depends on the number of quality articles submitted for review. Accordingly, I would like to request your participation and colleagues by submitting quality manuscripts for review. One of the great benefits we can provide to our prospective authors, regardless of acceptance of their manuscripts or not, is the feedback of our review process. JJBS provides authors with high quality, helpful reviews to improve their manuscripts.

Finally, JJBS would not have succeeded without the collaboration of authors and referees. Their work is greatly appreciated. Furthermore, my thanks are also extended to The Hashemite University and the Scientific Research and Innovation Support Fund, Ministry of Higher Education and Scientific Research for their continuous financial and administrative support to JJBS.

March, 2020

CONTENTS

Original Articles

- 257 - 265 Regulation of chemoresponsiveness in triple-negative breast cancer: androgen receptor, ABCG2, and microRNA (Review)
Bayan Z. Al-Momany, Hana M. Hammad and Mamoun Ahram
- 267 - 273 Association of Angiotensin Converting Enzyme (ACE) Gene insertion/deletion (I/D) Polymorphism with Obesity and Obesity Related Phenotypes in Malay Subjects
Emilia Apidi, Aliya Irshad Sani, Mohd Khairi Zahri Johari, Rohayu Izanwati Mohd Rawi, Ramlah Farouk, Omar Mahmoud Al-shajrawi, Atif Amin Baig and Nordin Bin Simbak
- 275 - 279 Hepato-Protective Effect of *Curcuma longa* against Paracetamol-Induced Chronic Hepatotoxicity in Swiss Mice
Salima Douichene, Wahiba Rached and Noureddine Djebli
- 281 - 287 Interaction of Atorvastatin and CX3CR1/Fractalkine in Androgen-Dependent Prostate Cancer Cells: Effect on PI3K Pathway
Belal A. Al-Husein, Nizar M. Mhaidat and Razan M. Sweidan
- 289 - 294 Biochemical Composition, Antioxidant Power and Anti-inflammatory of Dehulled *Sesamum indicum* Seeds and Its Coat Fraction
Laila Elhanafi, Zineb Benkhadda Benkhadda, Chainae Rais, Mariame Houhou, Siham Lebtar, Adil Chamo and Hassane Greche
- 295 - 303 Anti-inflammatory and Anti-proliferative Activity of Coconut Oil against Adverse Effects of UVB on Skin of Albino Mice
Snur Mohammed Amin Hassan
- 305 - 311 Influence of water quality parameters on larval stages of *Pseudoleptonema quinquefasciatum* Martynov 1935 (Trichoptera: Hydropsychidae) in streams of western Thailand
Penkhae Thamsenanupap and Taeng On Prommi
- 313 - 320 Antiviral, Antifungal, and Antibacterial Potential Activities of *Ephedra Sinica* in Vitro
Mohamed M. Deabes, Abdou K. Allayeh, Mohamed M Seif, Abdel-Hamied M. Rasmeiy and Khayria M. Naguib
- 321 - 325 Protective effect of Ginger against Sodium Metabisulfite induced Oxidative Stress in Rat
Shahnaz Shekarforoush, Akbar Afkhami Fathabad and Abbas Taheri
- 327 - 337 Molecular Surveillance of Enteroviruses in Al-Zarqa River, Jordan
Ismail Saadoun, Qotaiba Ababneh, Ziad Jaradat and Mamdoh M. Meqdam
- 339 - 344 Phytochemical Analysis, In Vitro Antioxidant Activity and Germination Capability of Selected Grains and Seeds
Radka Vrancheva, Aneta Popova, Dasha Mihaylova and Albert Krastanov
- 345 - 349 Cellulose Content in Selected Plant species along the Dead Sea Coast and the Southern Desert of Jordan
Amal M. Harb and Jamil N. Lahham
- 351 - 357 Inhibitory Effect of Clay/Chitosan Nanocomposite against *Penicillium digitatum* on Citrus and Its Possible Mode of Action
Khamis Youssef and Ayat F. Hashim
- 359 - 364 The Role of Turmeric (*Curcuma longa*) Powder in Improving Liver Function to Increase Vitellogenin Synthesis and Deposition in the Oocytes of Catfish (*Pangasianodon hypophthalmus*)
Cut D. Dewi, Wasmen Manalu, Damiana R. Ekastuti, and Agus O. Sudrajat
- 365 - 372 Effect of Different Applications of Bio-agent *Achromobacter xylosoxidans* against *Meloidogyne incognita* and Gene Expression in Infected Eggplant
Walaa A. Ramadan and Gazeia M. Soliman

- 373 - 376 A Preliminary Assessment on the Habitat Use of Carnivores in Al Mujib Biosphere Reserve Using Camera Trapping
Nashat Hamidan, Zuhair S. Amr and Mohammad A. Abu Baker
- 377 - 384 Evaluation of Nutritional Composition and *In vitro* Antioxidant and Antibacterial Activities of *Codium intricatum* Okamura from Ilocos Norte (Philippines)
Eldrin DLR. Arguelles
- 385 - 391 Associations of GCKR, TCF7L2, SLC30A8 and IGFB Polymorphisms with Type 2 Diabetes Mellitus in Egyptian Populations
Eman A. Awadallah, Nehal S. Hasan, Mona A.M. Awad, Solaf A. Kamel, Rasha N. Yousef, Nevine I. Musa and Eman M. Hassan
- 393 - 403 Toxicities of *Parkia biglobosa* Extract and Dimethoate + Cypermethrin Insecticide on Kidney and Liver of Wistar Rats Fed Treated Okra Fruits
Olajumoke O. Fayinminnu, Olufunso O. Adeniyi and Rotimi Olatunde
- 405 - 414 Pomegranate Peel Extract Activities as Antioxidant and Antibiofilm against Bacteria Isolated from Caries and Supragingival Plaque
Sabria Benslimane, Ouafa Rebai, Rachid Djibaoui, and Abed Arabi

Regulation of chemoresponsiveness in triple-negative breast cancer: androgen receptor, ABCG2, and microRNA (Review)

Bayan Z. Al-Momany¹, Hana M. Hammad¹ and Mamoun Ahram^{2,*}

¹Department of Biological Sciences, School of Science, ²Department of Physiology and Biochemistry, School of Medicine, The University of Jordan, Amman 11942, Jordan

Received: October 8, 2019; Revised: November 27, 2019; Accepted: January 4, 2020

Abstract

Breast cancer is a highly complex, diverse disease that is classified into several subtypes according to the expression of estrogen receptor (ER), progesterone receptor (PR), and human epidermal growth factor receptor 2 (HER2). Such classification is critical as it determines the best therapeutic strategy for the disease. One subtype of breast cancer that lacks the expression of the three receptors is termed triple-negative breast cancer (TNBC). Consequently, TNBC patients do not benefit from therapies that target ER or HER2 and often require systemic therapy. TNBC represents about 15-20% of all newly diagnosed breast cancers and is responsible for about 5% of all cancer deaths annually. A subgroup of TNBCs expresses androgen receptor (AR), which is thought to be a potential therapeutic target. Published reports have indicated that the AR signaling pathway contributes to the growth and progression of this breast cancer subtype. In addition, AR-positive TNBCs have been reported to have a significantly lower rate of pathological complete response to neoadjuvant chemotherapy and are more chemotherapy-resistant. Targets of AR include the multi-drug resistance transporters such as breast cancer resistant protein (BCRP/ABCG2), a primary cause of resistance to chemotherapy. Interestingly, the *ABCG2* gene has also been shown to be targeted by specific microRNA molecules (miRNAs), which are also under the transcriptional regulation of AR. Herein, the roles of AR, ABCG2, and miRNAs in regulating chemoresponsiveness of breast cancer are presented with a proposal to utilize this knowledge in devising a novel therapeutic strategy of TNBC.

Keywords: Breast cancer, Triple negative breast cancer, Androgen receptor, MicroRNA, ABCG2

1. Introduction

Breast cancer is the most common type of cancer that afflicts women worldwide accounting for approximately 11.6% of all diagnosed cancer cases globally and is the leading cause of cancer death among women (Bray *et al.*, 2018). In the USA, the 5-, 10-, and 15-year relative survival rates for breast cancer are 89%, 83%, and 78%, respectively (Miller *et al.*, 2016). While breast cancer rates are higher among women in more developed regions, the disease is expected to cause the death of approximately 627,000 women worldwide, which is almost 15% of all cancer deaths among women (WHO, 2019). Data from the 2016 Annual Statistical Report of the Jordanian Ministry of Health indicated that cancer-associated deaths constitute about 16.2% of total mortality reported in 2012, making it the second leading cause of death in Jordan after cardiovascular diseases (representing 36.4%) (Annual Statistical Report of the Ministry of Health, 2016). Importantly, cancer cases are expected to increase reaching levels that will challenge public and private healthcare systems, potentially jeopardizing access of patients to life-saving treatment (Abdel-Razeq *et al.*, 2015). In particular, breast cancer has been the most common cancer diagnosed in the Jordanian population overall throughout the years with 1067 cases recorded in 2013 and accounting for

19.7% of all cancer cases reported that year (Annual Statistical Report of the Ministry of Health, 2016).

Classification of Breast Cancer and TNBC

Breast cancer is a highly complex, heterogeneous disease in its histology, cellular origin, metastatic potential, mutations, disease progression, therapeutic response and clinical outcome (Ossovskaya *et al.*, 2011). Accordingly, it can be classified into different distinguishable subtypes according to histological features in conjunction with the expression of biomarkers (Lv *et al.*, 2011). The most prominent, classifying biomarkers are hormone receptors including estrogen receptor (ER), progesterone receptor (PR), and human epidermal growth factor-like receptor 2 (HER2). The four clinically important breast cancer classes are: (1) 'luminal A', which is ER- and PR-positive, but HER2-negative, (2) 'luminal B', which is ER-positive and/or PR-positive, and HER2- and Ki-67-positive, (3) HER2-enriched, a disease that is characterized by overexpression of HER2 and is ER- and PR-negative, and (4) 'triple-negative breast cancer' or TNBC where all three receptors are not expressed (ER-, PR-, and HER2-negative) (Rakha *et al.*, 2007; Boyle, 2012; Brouckaert *et al.*, 2013; Lam *et al.*, 2014; Parise and Caggiano, 2014). The majority of TNBCs possess basal-like characteristics.

In the USA, TNBC represents about 15-20% of all newly diagnosed breast cancers, and is responsible for

* Corresponding author e-mail: m.ahram@ju.edu.jo; Dr.Ahram@gmail.com.

about 5% of all cancer deaths annually (Dent *et al.*, 2007). In addition to its lack of expression of ER, PR and HER-2, this class of breast cancer is characterized by expression of genes usually found to be active in basal or myoepithelial cells of the normal breast (Rakha *et al.*, 2007; Rakha *et al.*, 2009). Initially, TNBC was further classified into six subtypes: basal-like 1 (BL1), basal-like 2 (BL2), mesenchymal (M), immunomodulatory (IM), mesenchymal stem-like (MSL) and luminal androgen receptor (LAR) (Lehmann *et al.*, 2011, Masuda *et al.*, 2013). However, in a follow-up study, IM and MSL subtypes were found not to be true TNBC and were removed from this category (Lehmann *et al.*, 2016). Furthermore, both Burstein *et al.* (2015) and Ding *et al.* (2019) classified TNBC into basal-like, immune-activated (BLIA), basal-like immunosuppressed (BLIS), LAR, and MES subtypes. Recently, Jiang *et al.* (2019) classified TNBC into four transcriptome-based subtypes: LAR, IM, BLIS, and mesenchymal-like (MES).

Transcriptional signatures of each breast cancer subtype can be used to support therapeutic decisions, predict outcomes and assist in the management of individual breast cancer patients (Harris *et al.*, 2016; Rakha 2017). In addition, ER, PR and HER-2 expressions not only play an important role in the biology of the tumors, but are also determinants of therapeutic strategy. For example, whereas ER-expressing tumors are treated by targeting the receptor with antagonists such as tamoxifen or with inhibitors of the estrogen-producing enzyme, aromatase, HER2-enriched tumors are treated with HER2 inhibitors such as Trastuzumab or Herceptin® (Lewis Phillips *et al.*, 2008). There is no effective targeted therapy for TNBC due to the lack of expression of these receptors and TNBC patients, therefore, often require systemic anti-cancer therapy to manage the disease (Brady-West and McGrowder, 2011). TNBC is the most sensitive to chemotherapy amongst breast cancer subtypes (Anders and Carey, 2008; Khokher *et al.*, 2013; Cetin and Topcul, 2014). However, TNBC is associated with a higher risk of disease recurrence at earlier times, worse prognosis after recurrence, and higher rates of central nervous system and visceral metastases (Carey *et al.*, 2010). This has been referred to as the triple negative paradox (Carey *et al.*, 2007). Interestingly, since TNBCs differ in their clinicopathologic characteristics, it has been reported that TNBC subtypes also differ in their response to standardized therapeutic efforts (Choi *et al.*, 2012; Masuda *et al.*, 2013).

Structure and Function of Androgen Receptor in Breast Cancer

Testosterone is produced by and released from Leydig cells of the male testes and theca cells of the female ovaries, while dehydroepiandrosterone is produced in the adrenal gland of both genders (Smith *et al.*, 2013). Testosterone acts as both a hormone and a pro-hormone (Smith *et al.*, 2013). It is converted to its more efficacious derivative dihydrotestosterone (DHT) by 5- α -reductase in peripheral tissues, skin, hair follicle, bone, prostate and liver, or by aromatase to the potent estrogen, 17 β -estradiol in ovaries, bone, brain, adipose tissue and prostate (Ellem and Risbridger, 2010; Smith *et al.*, 2013). The levels of circulating androgens decline with age in both men and women, which can affect bone and muscle integrity and

sexual drive in addition to general wellbeing (Davison *et al.*, 2005; Gooren 2010).

At the molecular level, the function of androgens is mediated by activation of androgen receptor (AR). DHT has two fold higher affinity for AR and a five-fold lower rate of dissociation when compared with testosterone (Grino *et al.*, 1990; Tan *et al.*, 2015). AR is a member of the steroid-hormone receptor family, which also includes receptors for estrogen, progesterone, glucocorticoids, and mineralocorticoids (Lubahn *et al.*, 1989). The human AR gene is located on chromosome Xq11-12 and contains a highly polymorphic CAG repeat sequence within exon 1 (Lubahn *et al.*, 1989; Chamberlain *et al.*, 1994). The receptor is ubiquitously expressed in human tissues, with the highest levels reported in reproductive tissues (testes, prostate, uterus and ovaries) as well as liver, breast, adipose and muscle tissues (Bookout *et al.*, 2006). AR-regulated signals are responsible for male sexual differentiation and reproductive development (Bruchovsky *et al.*, 1976). In the absence of ligand, AR exists primarily in the cytoplasm, bound to chaperone proteins that stabilize the receptor in a conformational state that promotes ligand binding (Claessens *et al.*, 2008). In the presence of androgens, in particular testosterone and DHT, AR undergoes a series of conformational changes, dissociates from chaperones, then forms a homodimer that translocates into the nucleus (Claessens *et al.*, 2008). Inside the nucleus, the hormone-AR complex binds to androgen response elements and recruits co-regulatory activators resulting in the regulation of target gene transcription (Claessens *et al.*, 2008). AR expression also has a role in a range of other conditions including acne, male pattern baldness and polycystic ovarian syndrome (Smith *et al.*, 2013). Importantly, AR has been shown to play an important role in the development and progression of a number of cancers such as prostate, endometrial, bladder, kidney and breast (Hunter *et al.*, 2018).

The AR signaling pathway has a role in breast cancer proliferation. Interestingly, both growth stimulatory and growth inhibitory impacts of androgens have been described in breast cancer cells lines (reviewed in Rahim and O'Regan, 2017). Mechanisms underlying these seemingly paradoxical effects are complex. However, the function of AR in breast cancer pathogenesis may depend on the molecular phenotype of the tumor, the relative coexpression of other hormone receptors, and the hormonal environment (Rahim and O'Regan, 2017). AR expression has been identified in 70-90% of breast tumors, similar to ER expression, and it is commonly found in breast tumors that express ER (Obeidat *et al.*, 2018). The prevalence of AR expression in TNBCs is less frequently reported, ranging from 13.7% to 64.3% (Rakha *et al.*, 2007; Luo *et al.*, 2010; McNamara *et al.*, 2013; Asano *et al.*, 2017; Obeidat *et al.*, 2018). This variability may be due to technical differences among the different studies or to the criteria used to define AR positivity (Rakha *et al.*, 2007; Luo *et al.*, 2010; McNamara *et al.*, 2013; Obeidat *et al.*, 2018).

Formerly, androgens, such as fluoxymesterone, testosterone, and calusterone were used for the treatment of advanced breast cancer, resulting in about 18-39% clinical responses (Gucalp and Traina, 2016). However, the undesirable masculinizing side effects of these agents have limited their routine use in the treatment of breast

cancer especially in the advent of newer, less toxic endocrine agents. Currently, there is renewed interest in targeting the AR signaling pathway, particularly in TNBC. In fact, AR-positive TNBC showed preserved androgenic signaling that can be used as a possible therapeutic target similar to ER-positive breast cancers (Lehmann *et al.*, 2011; Gucalp *et al.*, 2013). Several clinical trials currently underway have illustrated the efficiency of anti-androgen therapy for the treatment of AR-positive TNBC (Gucalp *et al.*, 2013; Bonnefoi *et al.*, 2016).

AR-positive TNBCs have different clinicopathologic characteristics than compared to AR-negative TNBCs. One such difference is reported in disease-free survival whereby AR-positive TNBC patients survive longer after recurrence than those with AR-negative TNBCs (Asano *et al.*, 2017). In addition, patients with AR-positive TNBC have a better prognosis and delayed disease recurrence (Luo *et al.*, 2010; Asano *et al.*, 2017). Most AR-positive TNBCs could be categorized as the LAR subtype (Asano *et al.*, 2017), associated with lower Ki-67 index (McNamara *et al.*, 2013), postmenopausal status, positive nodal status (Luo *et al.*, 2010), higher tumor grade, and development of distant metastasis (Rakha *et al.*, 2007). It is also important to note that some studies have suggested positive correlations between AR positivity and progressive disease or poor prognosis (Hu *et al.*, 2011). Thus, debate still exists concerning the clinical significance of AR expression in TNBC (Fioretti *et al.*, 2014).

Reason(s) for the increased survival of patients with AR-positive TNBC have not been identified and might be due to differences in sensitivity to conventional treatments or to the innate nature of this tumor phenotype (Asano *et al.*, 2017). AR-positive TNBCs have been reported to have a significantly lower rate of pathological complete response (pCR), of about 10%, to neoadjuvant chemotherapy (NAC) and are more chemotherapy-resistant (Asano *et al.*, 2016; Lehmann *et al.*, 2016). Therefore, it is hoped, as will be detailed in the next section, that the status of AR expression in TNBC may aid in determining the best strategy of breast cancer treatment and the use of AR-targeted therapy (Gucalp and Traina, 2016).

Role of ABCG2 in Breast Cancer

Development of chemoresistance is a significant obstacle in the effective treatment of breast cancer. Overexpression of multi drug resistance (MDR) transporters is one of the most important causes of chemoresistance (Szakács *et al.*, 2006) and members of the ABC transporter family members are the most widely studied MDR transporters (Gottesman and Ling, 2006). ABC transporters use ATP hydrolysis to control the absorption, distribution, and clearance of numerous substances, including hormones (e.g. folates and dihydrotestosterone), pharmaceutical agents, dietary carcinogens and conjugated metabolites (Huss *et al.*, 2005; Vore and Leggas, 2008). In addition, they have similar trans-membrane domains that can pump chemotherapeutic drugs out of cancer cells against a concentration gradient in an ATP-dependent manner, thus reducing intracellular accumulation of such agents and sparing cancer cells from toxicity (Huss *et al.*, 2005; Vore and Leggas, 2008).

To date, 48 ABC transporters have been identified in the human genome (Vasiliou *et al.*, 2009), among which the most extensively characterized are P-glycoprotein (P-gp/ABCB1), multidrug resistance associated protein-1 (MRP1/ABCC1), and breast cancer resistant protein (BCRP/ABCG2) (Huang *et al.*, 2014; An *et al.*, 2017). ABCG2 is a 72 kDa protein that has many substrates, which include tyrosine kinase inhibitors (TKIs) (e.g. imatinib and gefitinib), anthracyclines (e.g. doxorubicin), camptothecin-derived topoisomerase I inhibitors, disease-modifying anti-rheumatic drugs (e.g. methotrexate), and cyclin-dependent kinase inhibitors (e.g. flavopiridols) (An *et al.*, 2017). Recent studies have demonstrated that transcriptional factors and nuclear receptors and epigenetic factors play important roles in the regulation of ABCG2 expression in different model systems (To *et al.*, 2008a).

An ABCG2-expressing side population (SP) is present in normal and cancerous tissues (Mathew *et al.*, 2009). ABCG2 expression and function are well studied in prostate cancer where expression is found in ~1% of cells in the basal compartment (Huss *et al.*, 2005). ABCG2-expressing prostate tumor cells have been detected in tissue biopsies following androgen deprivation therapy (Huss *et al.*, 2005) and ABCG2 expression is upregulated upon androgen blockade *in vitro* (Huss *et al.*, 2005; Pfeiffer *et al.*, 2011). Moreover, ABCG2-expressing SP cells in the prostate demonstrate multipotency and self-renewal properties, suggesting an enrichment of stem cells in this population (Huss *et al.*, 2005; Foster *et al.*, 2013). An earlier study has shown the ability of ABCG2 to efflux the AR antagonist bicalutamide in prostate cancer tissues (Colabufo *et al.*, 2008). Another study has shown a link between AR signaling and ABCG2 at various levels where inhibition of ABCG2-mediated androgen efflux led to increased nuclear AR expression concomitant with induced expression of AR target genes, delayed cell growth response and cell differentiation mediated by AR, delayed tumor progression and increased overall survival *in vivo* (Sabnis *et al.*, 2017).

In breast cancer, higher levels of ABCG2 were correlated with a reduced efficacy of chemotherapy and poorer outcome in breast cancer patients (Kim *et al.*, 2013). ABCG2 has been described as a stemness marker for various histological breast cancer subtypes (Collina *et al.*, 2015). Furthermore, it was suggested that ABCG2 alone can be considered a suitable marker for breast cancer, in particular for the TNBC phenotype, but this observation was limited to cellular models (Britton *et al.*, 2012). Interestingly, ABCG2 has been shown to be down-regulated in androgen-treated breast cancer cells affecting chemoresistance to mitoxantrone, a topoisomerase II inhibitor (Chua *et al.*, 2016). The last report suggests that AR activation may influence the chemoresponsiveness of breast cancers.

MicroRNA and Their Significance in Breast Cancer

The variable expression of specific genes in tumor cells, including cell surface receptor proteins, mutated genes, and microRNAs (miRNAs or miRs) has been shown to predict the likelihood of cancer progression. miRNAs have significant potential in clinical research since they have important regulatory biological roles, are detected in different tissue types including serum and are relatively stable in formalin-fixed paraffin-embedded

tissue samples, suggesting that they can be used as biomarkers (Sethi *et al.*, 2014; An *et al.*, 2017). MiRNAs are short, single-stranded, non-coding RNAs of 20–25 nucleotides in length, and are widely conserved among species (Christodoulatos and Dalamaga, 2014). Since their discovery in 1993, around 2600 unique mature human miRNAs have been identified and more are expected to be detected (miRBase version 20) (Kozomara and Griffiths-Jones, 2013). Most miRNAs are located in non-coding intronic regions, but some are located in exonic regions (Rutnam *et al.*, 2013). The main function of miRNAs is post-transcriptional gene silencing via directly and specifically base-pairing of their conserved 5'-heptametrical seed sequence with the 3' untranslated region (3'-UTR) of multiple target messenger RNAs (mRNAs). Consequently, they induce either mRNA degradation if base-pairing is perfect or decrease the rate of protein translation if the match is imperfect (Rutnam *et al.*, 2013; Subtil *et al.*, 2014). It is worth noting that miRNAs are not always associated with inhibitory or down regulatory effects. In rare circumstances, dependent on cell cycle phase and co-factor expression, miRNAs can activate mRNA translation, thus up regulating protein levels (Vasudevan *et al.*, 2007).

More than 50% of all translated human genes are regulated by miRNAs and this type of gene regulation controls many facets of cell signaling pathways in both normal and tumor tissues (Rutnam *et al.*, 2013; Subtil *et al.*, 2014). Moreover, each miRNA can regulate numerous target genes, and the same target gene can be regulated by multiple miRNAs, creating a complex network of molecular interactions (Esteller 2011; Mendell and Olson, 2012; Spizzo *et al.*, 2012). The inherent complexity of this regulatory system allows miRNAs to control the global activity of the cell including cell differentiation, proliferation, stress response, metabolism, cell cycle, apoptosis, and angiogenesis (Gebert and MacRae, 2019). Comparison of human plasma or tissue samples from cancer patients vs. cancer-free individuals by miRNA microarray has revealed evidence of deregulation of several miRNAs in many cancers including breast cancer (Sethi *et al.*, 2014; An *et al.*, 2017). Different miRNA expression profiles between cancerous cells and paired normal tissues from the same organ have been documented in a number of studies (Lu *et al.*, 2005; Zhu *et al.*, 2014). As such, it is proposed that miRNAs influence cancer development, metastasis, angiogenesis and drug resistance (Liang and He, 2011; An *et al.*, 2017).

MiRNAs are reported to be aberrantly expressed in human breast cancers compared with normal breast tissue, with affected miRNAs having tumor suppressing or oncogenic effects. Furthermore, several studies have demonstrated that diverse cancer types at different developmental stages display unique miRNA expression profiles (Puppin *et al.*, 2014). Down-regulated miRNAs include miR-10b, miR-125b and miR-145 (Iorio *et al.*, 2005), and the re-introduction of under-expressed miRNAs has been shown to reduce the viability of cancer cells, suggesting tumor-suppressor functions and antiproliferative and /or pro-apoptotic roles (Lu *et al.*, 2005; Zhu *et al.*, 2014). In contrast, oncogenic miRNAs (oncomiRs) display antiapoptotic activities and are over-expressed in cancer cells (Nugent 2014). An example is miR-21, which was found to be overexpressed in breast

tumors compared to matched normal breast tissues (Si *et al.*, 2007). Inhibition of miR-21 resulted in cell growth inhibition in association with increased apoptosis and decreased cell proliferation (Si *et al.*, 2007). Expression of miR-21 was also found to be associated with specific features of breast cancer such as expression of ER and PR, tumor stage, vascular invasion, and proliferation (Yan *et al.*, 2008).

Changes in the expression of miRNAs and/or their functional roles in TNBC, particularly, have also been investigated. Differential expression of some miRNAs have been proposed as prognostic biomarkers such as miR-9, miR-15, miR-588 (Jang *et al.* 2017; Nama *et al.*, 2019). Several circulating miRNAs were identified in the sera of early-stage TNBC patients (miR-126-5p and miR-34a) (Kahraman *et al.*, 2018). In addition, numerous published studies have elucidated the association of miRNAs with TNBC progression or suppression (Piasecka *et al.*, 2018). One example is miR-20a-5p that promotes the growth of triple-negative breast cancer cells through targeting RUNX3 (Bai *et al.*, 2018). MiR-9 was also shown to exhibit a suppressor-like activity in metastatic TNBC cells by direct targeting of NOTCH1 (Mohammadi-Yeganeh *et al.*, 2015). Migration and invasion of TNBC have been proven to be affected by several miRNAs. Examples include miR-124, which regulates epithelial-to-mesenchymal transition (EMT) via targeting ZEB2, thereby inhibiting invasion and metastasis in TNBC (Ji *et al.*, 2019). It was reported that Let-7 miRNA controls metastasis and stemness of TNBC cells by regulating the JAK-STAT3 and cMyc pathways (Lyu *et al.*, 2014). Furthermore, the role of miR-10a in suppressing breast cancer progression via the PI3K/Akt/mTOR pathway was illustrated (Ke and Lou, 2017).

Significant changes in miRNA expression profiles have been observed in drug-resistant cancer cells in comparison with parental drug-sensitive cancer cells (Fojo 2007). Evidence pointing to the role of miRNAs in determining drug sensitivity and MDR is emerging (Wang *et al.*, 2015). One example is miRNA-451 whose expression correlates with an increased sensitivity of MCF-7 cells towards doxorubicin (Kovalchuk *et al.*, 2008). The dysregulation of miRNA expression profiles in cancer cells can lead to resistance towards anti-cancer drugs by abnormally modulating the expression of genes involved in MDR action such as genes encoding ABC transporters, apoptosis and autophagy regulators, regulators of drug metabolism, and genes associated with redox systems (Wang *et al.*, 2015). Therefore, miRNAs may drive tumorigenesis or may be used as diagnostic and prognostic biomarkers, and can potentially be targeted in order to improve treatment responses.

Dysregulation of numerous miRNAs has been linked to the chemoresponsiveness of TNBC (Rizzo *et al.*, 2017; Ouyang *et al.*, 2014). For example, upregulating miR-33a-5p significantly increased cell sensitivity toward doxorubicin in TNBC, but not other breast cancer types (Guan *et al.*, 2019). Downregulation of miR-27b-3p also desensitized cells to tamoxifen in TNBC by increasing NR5A2 and CREB1 expression (Zhu *et al.*, 2016). Interestingly, tamoxifen has also been shown to reverse EMT in TNBC as well as their metastatic capability by down-regulating miR-200 (Wang *et al.*, 2017). One mechanism by which miRNA can affect

chemoresponsiveness of cells is via manipulating DNA repair efficiency as shown for miR-302b (Cataldo *et al.* 2016). Another mechanism has also been illustrated for miR-5195-3p, which enhances the sensitivity of paclitaxel-resistant TNBC cells by down-regulating EIF4A2, a helicase upregulated in proliferating cells (Liu *et al.*, 2019). These findings, and others, strongly implicate the possibility of alternative therapeutic strategies for the disease.

Androgen Regulation of MiRNA in Breast Cancer

Published studies have predominantly focused on the association of AR with miRNA expression in prostate cancer. A few studies, however, have analyzed the regulation of miRNA expression by androgens in breast cancer. For example, Nakano *et al.* (2013) showed that five miRNAs were dysregulated in MCF-7 cells using PCR microarray. Lyu *et al.* (2014) showed that expression of four miRNAs, let-7a, b, c and d was up-regulated in androgen-treated MDA-MB-453 cells while other 7 miRNAs were downregulated. The regulation of miRNA

expression by androgens in MDA-MB-453 cells has also been studied using PCR arrays by Ahram *et al.* (2017) reporting the differential expression of 20 miRNAs. Interestingly, only three microRNAs, let-7a, b, and d were found to be commonly altered in the former two studies but with a different trend where Lyu *et al.* (2014) reported their up-regulation, whereas they were down-regulated by the study of Ahram *et al.* (2017). Ahram *et al.* (2017) also analyzed the regulation of miRNA expression by androgens in MCF-7 and T47D cells. However, none of the reported changes were common with those reported by Nakano *et al.* (2013). These discrepancies in the results could be due to the type and concentration of agonist used, the duration of experiments, and/or passage number of cells. Further work by our group has identified a number of miRNAs, including miR-328-3p, whose expression was up-regulated upon androgen treatment of the TNBC MDA-MB-231 cells (Al-Othman *et al.*, 2018). The general experimental conditions and results of these studies are summarized in Figure. 1.

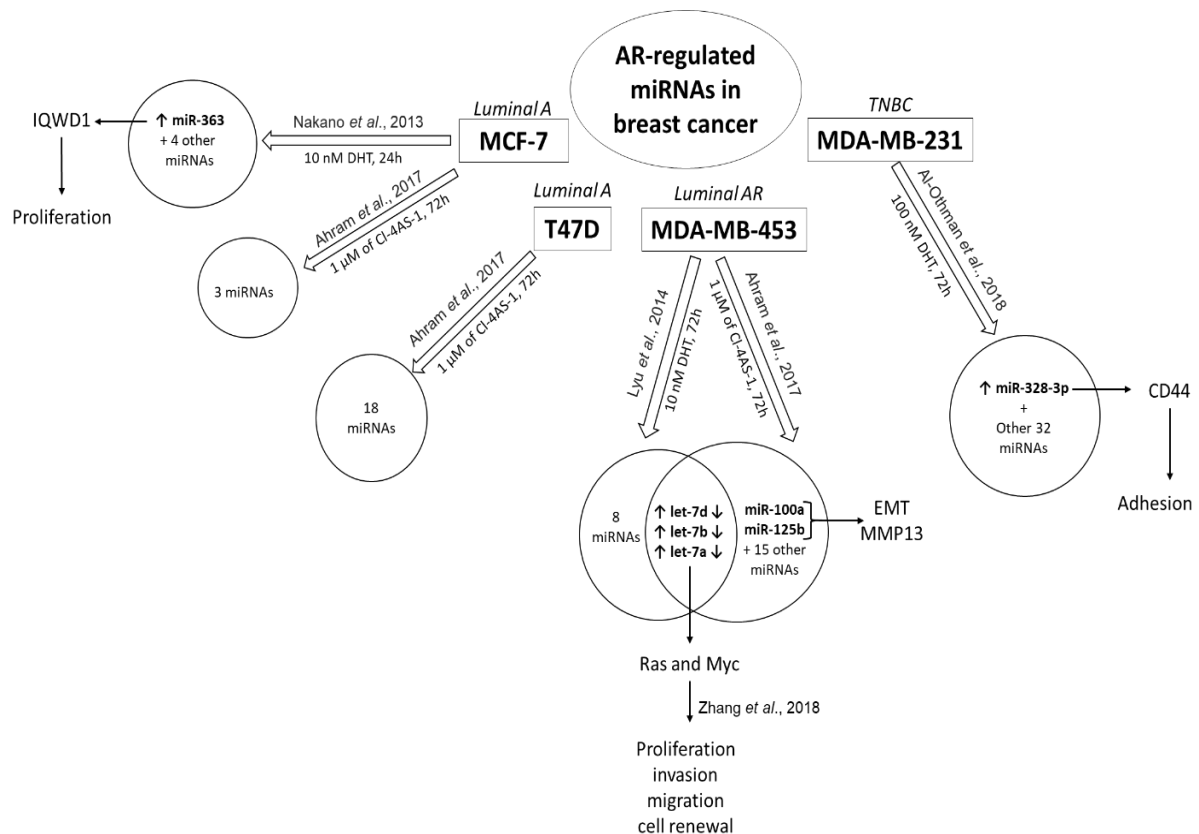


Figure 1. Androgen regulation of miRNAs in breast cancer and their cellular effects

MiRNAs Regulate ABCG2 Levels

A number of miRNAs have been shown to regulate the expression of proteins involved in the chemoresponsiveness of cancer (Pan *et al.*, 2009; Bockhorn *et al.*, 2013; Wang *et al.*, 2019). ABCG2/BCRP was the first MDR transporter found to be regulated by miRNA (To *et al.*, 2008b). To date, several miRNAs have been shown to regulate ABCG2 expression, including miR-328, which has been shown to increase mitoxantrone sensitivity by negatively regulating ABCG2 protein expression via binding to target sites in the *ABCG2* gene 3'-UTR (Pan *et al.*, 2009; Li *et al.*, 2010; Li *et al.*, 2011). Restoration of miR-328

expression as a therapy could therefore improve treatment outcomes, particularly responsiveness to doxorubicin and mitoxantrone, both of which are two substrates for ABCG2 (Pan *et al.*, 2009; Li *et al.*, 2010). Other miRNAs have similar negative regulatory effects on ABCG2 expression including miR-519, miR-520h, miR-212, miR-181a, and miR-487a (Li *et al.*, 2011; Turrini *et al.*, 2012; Jiao *et al.*, 2013; Ma *et al.*, 2013).

2. Conclusion

AR is an important regulator of breast cancer growth and has been proposed to be a potential therapeutic target.

The observations that AR can control cancer chemoresponsiveness can be highly significant in the clinical setting. However, the molecular mechanisms by which it can do so are incompletely characterized. One interesting mechanism is via miRNA molecules that regulate the expression of transporters involved in drug efflux such as ABCG2. Findings that AR can regulate both ABCG2 and its targeting miRNAs constitute an intriguing mechanism of regulation. Understanding of these molecular mechanisms may lead to novel and more effective therapeutic strategies of TNBC based on AR targeting of both ABCG2 and ABCG2-regulating miRNA.

3. References

- Abdel-Razeq H, Attiga F and Mansour A. 2015. Cancer care in Jordan. *Hematol Oncol Stem Cell Ther*, **8(2)**: 64-70.
- Ahram M, Mustafa E, Zaza R, Abu Hammad S, Alhudhud M, Bawadi R and Zihlif M. 2017. Differential expression and androgen regulation of microRNAs and metalloprotease 13 in breast cancer cells. *Cell Biol Int*, **41(12)**: 1345-1355.
- Al-Othman N, Hammad H and Ahram M. 2018. Dihydrotestosterone regulates expression of CD44 via miR-328-3p in triple-negative breast cancer cells. *Gene*, **675**: 128-135.
- An X, Sarmiento C, Tan T and Zhu H. 2017. Regulation of multidrug resistance by microRNAs in anti-cancer therapy. *Acta Pharm Sin B*, **7(1)**: 38-51.
- Anders C and Carey LA. 2008. Understanding and treating triple-negative breast cancer. *Oncology (Williston Park)*, **22(11)**: 1233.
- Annual Statistical Report of the Ministry of Health. 2016. Jordan Cancer Registry, Cancer Incidence in Jordan for 2013. Amman: Ministry of Health; <http://www.moh.gov.jo/>.
- Asano Y, Kashiwagi S, Goto W, Tanaka S, Morisaki T, Takashima T, Noda S, Onoda N, Ohsawa M, Hirakawa K and Ohira M. 2017. Expression and clinical significance of androgen receptor in triple-negative breast cancer. *Cancers*, **9(1)**: 4.
- Asano Y, Kashiwagi S, Onoda N, Kurata K, Morisaki T, Noda S, Takashima T, Ohsawa M, Kitagawa S and Hirakawa K. 2016. Clinical verification of sensitivity to preoperative chemotherapy in cases of androgen receptor-expressing positive breast cancer. *Br J Cancer*, **114(1)**: 14.
- Bai X, Han G, Liu Y, Jiang H and He Q. 2018. MiRNA-20a-5p promotes the growth of triple-negative breast cancer cells through targeting RUNX3. *Biomed Pharmacother*, **103**: 1482-1489.
- Bockhorn J, Dalton R, Nwachukwu C, Huang S, Prat A, Yee K, Chang YF, Huo D, Wen Y, Swanson KE, Qiu T, Lu J, Park SY, Dolan ME, Perou CM, Olopade OI, Clarke MF, Greene GL and Liu H. 2013. MicroRNA-30c inhibits human breast tumour chemotherapy resistance by regulating TWF1 and IL-11. *Nat Commun*, **4**: 1393.
- Bonnefoi H, Grellety T, Tredan O, Saghatchian M, Dalenc F, Mailliez A, L'haridon T, Cottu P, Abadie-Lacourtoisie S, You B and Mousseau M. 2016. A phase II trial of abiraterone acetate plus prednisone in patients with triple-negative androgen receptor positive locally advanced or metastatic breast cancer (UCBG 12-1). *Ann Oncol*, **27(5)**: 812-818.
- Bookout AL, Jeong Y, Downes M, Ruth TY, Evans RM and Mangelsdorf DJ. 2006. Anatomical profiling of nuclear receptor expression reveals a hierarchical transcriptional network. *Cell*, **126(4)**: 789-799.
- Boyle P. 2012. Triple-negative breast cancer: epidemiological considerations and recommendations. *Ann Oncol*, **23**: 7-12.
- Brady-West DC and McGrowder DA. 2011. Triple negative breast cancer: therapeutic and prognostic implications. *Asian Pac J Cancer Prev*, **12(8)**: 2139-2143.
- Bray F, Ferlay J, Soerjomataram I, Siegel RL, Torre LA and Jemal A. 2018. Global cancer statistics 2018: GLOBOCAN estimates of incidence and mortality worldwide for 36 cancers in 185 countries. *CA Cancer J Clin*, **68(6)**: 394-424.
- Britton KM, Eyre R, Harvey JJ, Stemke-Hale K, Browell D, Lennard TWJ and Meeson AP. 2012. Breast cancer, side population cells and ABCG2 expression. *Cancer Lett*, **323(1)**: 97-105.
- Brouckaert O, Schoneveld A, Truyers C, Kellen E, Van Ongeval C, Vergote I, Moerman P, Floris G, Wildiers H, Christiaens MR, Van Limbergen E, Neven P; MBC Leuven, Belgium. 2013. Breast cancer phenotype, nodal status and palpability may be useful in the detection of overdiagnosed screening-detected breast cancers. *Ann Oncol*, **24(7)**: 1847-1852.
- Bruchovsky N, Lesser B, Van Doorn E and Craven S. 1976. Hormonal effects on cell proliferation in rat prostate. *Vitam Horm*, **33**: 61-102.
- Burstein MD, Tsimelzon A, Poage GM, Covington KR, Contreras A, Fuqua SA, Savage MI, Osborne CK, Hilsenbeck SG, Chang JC, Mills GB, Lau CC and Brown PH. 2015. Comprehensive genomic analysis identifies novel subtypes and targets of triple-negative breast cancer. *Clin Cancer Res*, **21**: 1688-98.
- Carey L, Winer E, Viale G, Cameron D and Gianni L. 2010. Triple-negative breast cancer: disease entity or title of convenience?. *Nat Rev Clin Oncol*, **7**: 683-692.
- Carey LA, Dees EC, Sawyer L, Gatti L, Moore DT, Collichio F, Ollila DW, Sartor CI, Graham ML and Perou CM. 2007. The triple negative paradox: primary tumor chemosensitivity of breast cancer subtypes. *Clin Cancer Res*, **13(8)**: 2329-2334.
- Cataldo A, Cheung DG, Balsari A, Tagliabue E, Coppola V, Iorio MV, Palmieri D, Croce CM. 2016. miR-302b enhances breast cancer cell sensitivity to cisplatin by regulating E2F1 and the cellular DNA damage response. *Oncotarget*, **7**: 786-97.
- Cetin I and Topcul M. 2014. Triple negative breast cancer. *Asian Pac J Cancer Prev*, **15(6)**: 2427-2431.
- Chamberlain NL, Driver ED and Miesfeld RL. 1994. The length and location of CAG trinucleotide repeats in the androgen receptor N-terminal domain affect transactivation function. *Nucleic Acids Res*, **22**: 3181-3186.
- Choi J, Jung WH and Koo JS. 2012. Clinicopathologic features of molecular subtypes of triple negative breast cancer based on immunohistochemical markers. *Histol Histopathol*, **27(10)**: 1481.
- Christodoulatos GS and Dalamaga M. 2014. Micro-RNAs as clinical biomarkers and therapeutic targets in breast cancer: Quo vadis? *World J Clin Oncol*, **5(2)**: 71.
- Chua VY, Larma I, Harvey J, Thomas MA, Bentel JM. 2016. Activity of ABCG2 Is Regulated by Its Expression and Localization in DHT and Cyclophosphamide-Treated Breast Cancer Cells. *J Cell Biochem*, **117(10)**: 2249-59.
- Claessens F, Denayer S, Van Tilborgh N, Kerkhofs S, Helsen C and Haelens A. 2008. Diverse roles of androgen receptor (AR) domains in AR-mediated signaling. *Nucl Recept Signal*, **6**.
- Cochrane DR, Bernales S, Jacobsen BM, Cittelly DM, Howe EN, D'Amato NC, Spoelstra NS, Edgerton SM, Jean A, Guerrero J and Gómez F. 2014. Role of the androgen receptor in breast cancer and preclinical analysis of enzalutamide. *Breast Cancer Res*, **16(1)**: R7.
- Colabufo NA, Pagliarulo V, Berardi F, Contino M, Inglese C, Niso M, Ancona P, Albo G, Pagliarulo A and Perrone R. 2008. Bicalutamide failure in prostate cancer treatment: involvement of Multi Drug Resistance proteins. *Eur J Pharmacol*, **601(1)**: 38-42.

- Collina F, Di Bonito M, Li Bergolis V, De Laurentis M, Vitagliano C, Cerrone M, Nuzzo F, Cantile M and Botti G. 2015. Prognostic value of cancer stem cells markers in triple-negative breast cancer. *Biomed Res Int*, **2015**.
- Davison SL, Bell R, Donath S, Montalto JG and Davis SR. 2005. Androgen levels in adult females: changes with age, menopause, and oophorectomy. *J Clin Endocrinol Metab*, **90(7)**: 3847-3853.
- Dent R, Trudeau M, Pritchard KI, Hanna WM, Kahn HK, Sawka CA, Lickley LA, Rawlinson E, Sun P and Narod SA. 2007. Triple-negative breast cancer: clinical features and patterns of recurrence. *Clin Cancer Res*, **13(15)**: 4429-4434.
- Ding YC, Steele L, Warden C, Wilczynski S, Mortimer J, Yuan Y and Neuhausen SL. 2019. Molecular subtypes of triple-negative breast cancer in women of different race and ethnicity. *Oncotarget*, **10(2)**: 198.
- Ellem, SJ and Risbridger G.P. 2010. Aromatase and regulating the estrogen: androgen ratio in the prostate gland. *J Steroid Biochem Mol Biol*, **118(4)**: 246-251.
- Esteller M. 2011. Non-coding RNAs in human disease. *Nat Rev Genet*, **12(12)**: 861.
- Fioretti FM, Sita-Lumsden A, Bevan CL and Brooke GN. 2014. Revising the role of the androgen receptor in breast cancer. *J Mol Endocrinol*, **52(3)**: R257-R265.
- Fojo T. 2007. Multiple paths to a drug resistance phenotype: mutations, translocations, deletions and amplification of coding genes or promoter regions, epigenetic changes and microRNAs. *Drug Resist Updat*, **10(1)**: 59-67.
- Foster BA, Gangavarapu KJ, Mathew G, Azabdafitari G, Morrison CD, Miller A and Huss WJ. 2013. Human prostate side population cells demonstrate stem cell properties in recombination with urogenital sinus mesenchyme. *PLoS One*, **8(1)**: e55062.
- Gebert LF and MacRae IJ. 2019. Regulation of microRNA function in animals. *Nat Rev Mol Cell Biol*, **20(1)**: 21-37.
- Gooren LJ. 2010. Androgens and male aging: current evidence of safety and efficacy. *Asian J Androl*, **12(2)**: 136.
- Gottesman MM and Ling V. 2006. The molecular basis of multidrug resistance in cancer: The early years of P-glycoprotein research. *FEBS Lett*, **580(4)**: 998-1009.
- Grino PB, Griffin JE and Wilson JD. 1990. Testosterone at high concentrations interacts with the human androgen receptor similarly to dihydrotestosterone. *Endocrinology*, **126(2)**: 1165-1172.
- Guan X, Gu S, Yuan M, Zheng X and Wu J. 2019. MicroRNA-33a-5p overexpression sensitizes triple-negative breast cancer to doxorubicin by inhibiting eIF5A2 and epithelial-mesenchymal transition. *Oncol Lett*, **18(6)**: 5986-5994.
- Gucalp A and Traina TA. 2016. Targeting the androgen receptor in triple-negative breast cancer. *Curr Probl Cancer*, **40(2)**: 141-150.
- Gucalp A, Tolane S, Isakoff SJ, Ingle JN, Liu MC, Carey LA, Blackwell K, Rugo H, Nabell L, Forero A and Stearns V. 2013. Phase II trial of bicalutamide in patients with androgen receptor-positive, estrogen receptor-negative metastatic breast cancer. *Clin Cancer Res*, **19(19)**: 5505-5512.
- Harris LN, Ismaila N, McShane LM, Andre F, Collyar DE, Gonzalez-Angulo AM, Hammond EH, Kuderer NM, Liu MC, Mennel RG and Van Poznak C. 2016. Use of biomarkers to guide decisions on adjuvant systemic therapy for women with early-stage invasive breast cancer: American Society of Clinical Oncology clinical practice guideline. *J Clin Oncol*, **34(10)**: 1134-1150.
- Hu R, Dawood S, Holmes MD, Collins LC, Schnitt SJ, Cole K, Marotti JD, Hankinson SE, Colditz GA and Tamimi RM. 2011. Androgen receptor expression and breast cancer survival in postmenopausal women. *Clin Cancer Res*, **17(7)**: 1867-1874.
- Huang S, Ye J, Yu J, Chen L, Zhou L, Wang H, Li Z and Wang C. 2014. The accumulation and efflux of lead partly depend on ATP-dependent efflux pump-multidrug resistance protein 1 and glutathione in testis Sertoli cells. *Toxicol Lett*, **226(3)**: 277-284.
- Hunter I, Hay CW, Esswein B, Watt K and McEwan IJ. 2018. Tissue control of androgen action: The ups and downs of androgen receptor expression. *Mol Cell Endocrinol*, **465**: 27-35.
- Huss WJ, Gray DR, Greenberg NM, Mohler JL and Smith GJ. 2005. Breast cancer resistance protein-mediated efflux of androgen in putative benign and malignant prostate stem cells. *Cancer Res*, **65(15)**: 6640-6650.
- Iorio MV, Ferracin M, Liu CG, Veronese A, Spizzo R, Sabbioni S, Magri E, Pedriali M, Fabbri M, Campiglio M, Ménard S, Palazzo JP, Rosenberg A, Musiani P, Volinia S, Nenci I, Calin GA, Querzoli P, Negrini M and Croce CM. 2005. MicroRNA gene expression deregulation in human breast cancer. *Cancer Res*, **65(16)**: 7065-7070.
- Jang MH, Kim HJ, Gwak JM, Chung YR and Park SY. 2017. Prognostic value of microRNA-9 and microRNA-155 expression in triple-negative breast cancer. *Hum Pathol*, **68**: 69-78.
- Ji H, Sang M, Liu F, Ai N and Geng C. 2019. miR-124 regulates EMT based on ZEB2 target to inhibit invasion and metastasis in triple-negative breast cancer. *Pathol Res Pract*, **215**: 697-704.
- Jiang YZ, Ma D, Suo C, Shi J, Xue M, Hu X, Xiao Y, Yu KD, Liu YR, Yu Y, Zheng Y, Li X, Zhang C, Hu P, Zhang J, Hua Q, Zhang J, Hou W, Ren L, Bao D, Li B, Yang J, Yao L, Zuo WJ, Zhao S, Gong Y, Ren YX, Zhao YX, Yang YS, Niu Z, Cao ZG, Stover DG, Verschraegen C, Kaklamani V, Daemen A, Benson JR, Takabe K, Bai F, Li DQ, Wang P, Shi L, Huang W and Shao ZM. 2019. Genomic and Transcriptomic Landscape of Triple-Negative Breast Cancers: Subtypes and Treatment Strategies. *Cancer Cell*, **35(3)**: 428-440.
- Jiao X, Zhao L, Ma M, Bai X, He M, Yan Y, Wang Y, Chen Q, Zhao X, Zhou M and Cui Z. 2013. MiR-181a enhances drug sensitivity in mitoxantone-resistant breast cancer cells by targeting breast cancer resistance protein (BCRP/ABCG2). *Breast Cancer Res Treat*, **139(3)**: 717-730.
- Kahraman M, Röske A, Laufer T, Fehlmann T, Backes C, Kern F, Kohlhaas J, Schrörs H, Saiz A, Zabler C, Ludwig N, Fasching PA, Strick R, Rübner M, Beckmann MW, Meese E, Keller A and Schrauder MG. 2018. MicroRNA in diagnosis and therapy monitoring of early-stage triple-negative breast cancer. *Sci Rep*, **8(1)**: 11584.
- Ke K and Lou T. 2017. MicroRNA-10a suppresses breast cancer progression via PI3K/Akt/mTOR pathway. *Oncol Lett*, **14(5)**: 5994-6000.
- Khokher S, Qureshi MU, Mahmood S and Nagi AH. 2013. Association of immunohistochemically defined molecular subtypes with clinical response to presurgical chemotherapy in patients with advanced breast cancer. *Asian Pac J Cancer Prev*, **14(5)**: 3223-3228.
- Kim B, Fatayer H, Hanby AM, Horgan K, Perry SL, Valleley EM, Verghese ET, Williams BJ, Thorne JL and Hughes TA. 2013. Neoadjuvant chemotherapy induces expression levels of breast cancer resistance protein that predict disease-free survival in breast cancer. *PLoS One*, **8**: e62766.
- Kovalchuk O, Filkowski J, Meservy J, Ilnytskyi Y, Tryndyak VP, Vasylyf C and Pogribny IP. 2008. Involvement of microRNA-451 in resistance of the MCF-7 breast cancer cells to chemotherapeutic drug doxorubicin. *Mol Cancer Ther*, **7(7)**: 2152-2159.
- Kozomara A and Griffiths-Jones S. 2013. miRBase: annotating high confidence microRNAs using deep sequencing data. *Nucleic acids Res*, **42(D1)**: D68-D73.

- Lam SW, Jimenez CR and Boven E. 2014. Breast cancer classification by proteomic technologies: current state of knowledge. *Cancer Treat Rev*, **40**: 129-138.
- Lehmann BD, Bauer JA, Chen X, Sanders ME, Chakravarthy AB, Shyr Y and Pietenpol JA. 2011. Identification of human triple-negative breast cancer subtypes and preclinical models for selection of targeted therapies. *J Clin Invest*, **121**(7): 2750-67.
- Lehmann BD, Jovanović B, Chen X, Estrada MV, Johnson KN, Shyr Y, Moses HL, Sanders ME and Pietenpol JA. 2016. Refinement of triple-negative breast cancer molecular subtypes: implications for neoadjuvant chemotherapy selection. *PLoS one*, **11**(6): e0157368.
- Lewis Phillips GD, Li G, Dugger DL, Crocker LM, Parsons KL, Mai E, Blättler WA, Lambert JM, Chari RV, Lutz RJ, Wong WL, Jacobson FS, Koeppe H, Schwall RH, Kenkare-Mitra SR, Spencer SD and Sliwkowski MX. 2008. Targeting HER2-positive breast cancer with trastuzumab-DM1, an antibody-cytotoxic drug conjugate. *Cancer Res*, **68**(22): 9280-9290.
- Li WQ, Li YM, Tao BB, Lu YC, Hu GH, Liu HM, He J, Xu Y and Yu HY. 2010. Downregulation of ABCG2 expression in glioblastoma cancer stem cells with miRNA-328 may decrease their chemoresistance. *Med Sci Monit*, **16**(10): 30.
- Li X, Pan YZ, Seigel GM, Hu ZH, Huang M and Yu AM. 2011. Breast cancer resistance protein BCRP/ABCG2 regulatory microRNAs (hsa-miR-328,-519c and-520h) and their differential expression in stem-like ABCG2+ cancer cells. *Biochem Pharmacol*, **81**(6): 783-792.
- Liang LH and He XH. 2011. Macro-management of microRNAs in cell cycle progression of tumor cells and its implications in anti-cancer therapy. *Acta Pharmacol Sin*, **32**(11): 1311.
- Liu M, Gong C, Xu R, Chen Y and Wang X. 2019. MicroRNA-5195-3p enhances the chemosensitivity of triple-negative breast cancer to paclitaxel by downregulating EIF4A2. *Cell Mol Biol Lett*, **24**(1): 47.
- Lu J, Getz G, Miska EA and Alvarez-Saavedra E. 2005. MicroRNA expression profiles classify human cancers. *Nature*, **435**(7043): 834.
- Lubahn DB, Brown TR, Simental JA, Higgs HN, Migeon CJ, Wilson EM and French FS. 1989. Sequence of the intron/exon junctions of the coding region of the human androgen receptor gene and identification of a point mutation in a family with complete androgen insensitivity. *Proc Natl Acad Sci U S A*, **86**(23): 9534-9538.
- Luo X, Shi Y, Li Z and Jiang W. 2010. Expression and clinical significance of androgen receptor in triple negative breast cancer. *Chin J Cancer*, **29**(6): 585-590.
- Lv M, Li B, Li Y, Mao X, Yao F and Jin F. 2011. Predictive role of molecular subtypes in response to neoadjuvant chemotherapy in breast cancer patients in Northeast China. *Asian Pac J Cancer Prev*, **12**(9): 2411-2417.
- Lyu S, Yu Q, Ying G, Wang S, Wang Y, Zhang J and Niu Y. 2014. Androgen receptor decreases CMYC and KRAS expression by upregulating let-7a expression in ER-, PR-, AR+ breast cancer. *Int J Oncol*, **44**(1): 229-237.
- Ma MT, He M, Wang Y, Jiao XY, Zhao L, Bai XF, Yu ZJ, Wu HZ, Sun ML, Song ZG and Wei MJ. 2013. MiR-487a resensitizes mitoxantrone (MX)-resistant breast cancer cells (MCF-7/MX) to MX by targeting breast cancer resistance protein (BCRP/ABCG2). *Cancer Lett*, **339**(1): 107-115.
- Masuda H, Baggerly KA, Wang Y, Zhang Y, Gonzalez-Angulo AM, Meric-Bernstam F, Valero V, Lehmann BD, Pietenpol JA, Hortobagyi GN and Symmans WF. 2013. Differential response to neoadjuvant chemotherapy among 7 triple-negative breast cancer molecular subtypes. *Clin Cancer Res*, **19**(19): 5533-5540.
- Mathew G, Timm Jr EA, Sotomayor P, Godoy A, Montecinos VP, Smith GJ and Huss WJ. 2009. ABCG2-mediated DyeCycle Violet efflux defined side population in benign and malignant prostate. *Cell Cycle*, **8**(7): 1053-1061.
- McNamara KM, Yoda T, Miki Y, Chanplakorn N, Wongwaisayawan S, Incharoen P, Kongdan Y, Wang L, Takagi K, Mayu T and Nakamura Y. 2013. Androgenic pathway in triple negative invasive ductal tumors: its correlation with tumor cell proliferation. *Cancer Sci*, **104**(5): 639-646.
- Mendell JT and Olson EN. 2012. MicroRNAs in stress signaling and human disease. *Cell*, **148**(6): 1172-1187.
- Miller KD, Siegel RL, Lin CC, Mariotto AB, Kramer JL, Rowland JH, Stein KD, Alteri R and Jemal A. 2016. Cancer treatment and survivorship statistics, 2016. *CA Cancer J Clin*, **66**(4): 271-289.
- Mohammadi-Yeganeh S, Mansouri A and Paryan M. 2015. Targeting of miR9/NOTCH1 interaction reduces metastatic behavior in triple-negative breast cancer. *Chem Biol Drug Des*, **86**(5): 1185-1191.
- Nakano K, Miki Y, Hata S, Ebata A, Takagi K, McNamara KM, Sakurai M, Masuda M, Hirakawa H, Ishida T, Suzuki T, Ohuchi N and Sasano H. 2013. Identification of androgen-responsive microRNAs and androgen-related genes in breast cancer. *Anticancer Res*, **33**(11): 4811-4819.
- Nama S, Muhuri M, Di Pascale F, Quah S, Aswad L, Fullwood M and Sampath P. 2019. MicroRNA-138 is a Prognostic Biomarker for Triple-Negative Breast Cancer and Promotes Tumorigenesis via TUSC2 repression. *Sci Rep*, **9**(1): 1-12.
- Nugent M. 2014. MicroRNA function and dysregulation in bone tumors: the evidence to date. *Cancer Manag Res*, **6**: 15.
- Obeidat FN, Ahram M, Al-Khader A, Al Mbaideen S, Hassan H, Altarawneh B and Battah K. 2018. Expression of androgen receptor in invasive ductal breast carcinomas: a clinicopathological study from Jordan. *Ann Saudi Med*, **38**(5): 326-335.
- Ossovskaya V, Wang Y, Budoff A, Xu Q, Lituev A, Potapova O, Vansant G, Monforte J and Daraselia N. 2011. Exploring molecular pathways of triple-negative breast cancer. *Genes Cancer*, **2**(9): 870-879.
- Ouyang M, Li Y, Ye S, Ma J, Lu L, Lv W, Chang G, Li X, Li Q, Wang S and Wang W. 2014. MicroRNA profiling implies new markers of chemoresistance of triple-negative breast cancer. *PLoS One*, **9**: e96228.
- Pan YZ, Morris ME and Yu AM. 2009. MicroRNA-328 negatively regulates the expression of breast cancer resistance protein (BCRP/ABCG2) in human cancer cells. *Mol Pharmacol*, **75**(6): 1374-1379.
- Parise CA and Caggiano V. 2014. Breast Cancer Survival Defined by the ER/PR/HER2 Subtypes and a Surrogate Classification according to Tumor Grade and Immunohistochemical Biomarkers. *J Cancer Epidemiol*, **2014**: 469251.
- Pfeiffer MJ, Smit FP, Sedelaar JP and Schalken JA. 2011. Steroidogenic enzymes and stem cell markers are upregulated during androgen deprivation in prostate cancer. *Mol Med*, **17**(7-8): 657.
- Piasecka D, Braun M, Kordek R, Sadej R and Romanska H. 2018. MicroRNAs in regulation of triple-negative breast cancer progression. *J Cancer Res Clin Oncol*, **144**(8): 1401-1411.
- Puppini C, Durante C, Sponziello M, Verrienti A, Pecce V, Lavarone E, Baldan F, Campese AF, Boichard A, Lacroix L and Russo D. 2014. Overexpression of genes involved in miRNA biogenesis in medullary thyroid carcinomas with RET mutation. *Endocrine*, **47**(2): 528-536.

- Rahim B and O'Regan R. 2017. AR Signaling in Breast Cancer. *Cancers*, **9(3)**: 21.
- Rakha EA and Green AR. 2017. Molecular classification of breast cancer: what the pathologist needs to know. *Pathology*, **49(2)**: 111-119.
- Rakha EA, El-Sayed ME, Green AR, Lee AH, Robertson JF and Ellis IO. 2007. Prognostic markers in triple-negative breast cancer. *Cancer*, **109(1)**: 25-32.
- Rakha EA, Elsheikh SE, Aleskandarany MA, Habashi HO, Green AR, Powe DG, El-Sayed ME, Benhasouna A, Brunet JS, Akslen LA and Evans AJ. 2009. Triple-negative breast cancer: distinguishing between basal and nonbasal subtypes. *Clin Cancer Res*, **15(7)**: 2302-2310.
- Rizzo S, Cangemi A, Galvano A, Fanale D, Buscemi S, Ciaccio M, Russo A, Castorina S and Bazan V. 2017. Analysis of miRNA expression profile induced by short term starvation in breast cancer cells treated with doxorubicin. *Oncotarget*, **8**: 71924-71932.
- Rutnam ZJ, Wight TN and Yang BB. 2013. miRNAs regulate expression and function of extracellular matrix molecules. *Matrix Biol*, **32(2)**: 74-85.
- Sabnis NG, Miller A, Titus MA and Huss WJ. 2017. The Efflux Transporter ABCG2 Maintains Prostate Stem Cells. *Mol Cancer Res*, **15(2)**: 128-140.
- Sethi S, Ali S and Sarkar FH. 2014. Introduction: Role of miRNAs and Their Target Genes in Breast Cancer Metastasis. In *miRNAs and Target Genes in Breast Cancer Metastasis* (pp. 1-6). Springer International Publishing.
- Si ML, Zhu S, Wu H, Lu Z, Wu F and Mo YY. 2007. miR-21-mediated tumor growth. *Oncogene*, **26(19)**: 2799.
- Smith LB, Mitchell RT and McEwan IJ. 2013. *Testosterone: From basic research to clinical applications*. Berlin: Springer.
- Spizzo R, Almeida MI, Colombatti A and Calin GA. 2012. Long non-coding RNAs and cancer: a new frontier of translational research?. *Oncogene*, **31(43)**: 4577.
- Subtil FS, Wilhelm J, Bill V, Westholt N, Rudolph S, Fischer J, Scheel S, Seay U, Fournier C, Taucher-Scholz G and Scholz M. 2014. Carbon ion radiotherapy of human lung cancer attenuates HIF-1 signaling and acts with considerably enhanced therapeutic efficiency. *FASEB J*, **28(3)**: 1412-1421.
- Szakács G, Paterson JK, Ludwig JA, Booth-Genthe C and Gottesman MM. 2006. Targeting multidrug resistance in cancer. *Nat Rev Drug discovery*, **5(3)**: 219.
- Tan ME, Li J, Xu HE, Melcher K and Yong EL. 2015. Androgen receptor: structure, role in prostate cancer and drug discovery. *Acta Pharmacol Sin*, **36(1)**: 3-23.
- To KK, Polgar O, Huff LM, Morisaki K and Bates SE. 2008a. Histone modifications at the ABCG2 promoter following treatment with histone deacetylase inhibitor mirror those in multidrug-resistant cells. *Mol Cancer Res*, **6(1)**: 151-164.
- To KK, Zhan Z, Litman T and Bates SE. 2008b. Regulation of ABCG2 expression at the 3' untranslated region of its mRNA through modulation of transcript stability and protein translation by a putative microRNA in the S1 colon cancer cell line. *Mol Cell Biol*, **28(17)**: 5147-5161.
- Turrini E, Haenisch S, Laechelt S, Diewock T, Bruhn O and Cascorbi I. 2012. MicroRNA profiling in K-562 cells under imatinib treatment: influence of miR-212 and miR-328 on ABCG2 expression. *Pharmacogenet Genomics*, **22(3)**: 198-205.
- Vasiliou V, Vasiliou K and Nebert DW. 2009. Human ATP-binding cassette (ABC) transporter family. *Hum Genomics*, **3(3)**: 281.
- Vasudevan, S., Tong, Y. and Steitz, J.A., 2007. Switching from repression to activation: microRNAs can up-regulate translation. *Science*, **318(5858)**: 1931-1934.
- Vore M and Leggas M. 2008. Progesterone acts via progesterone receptors A and B to regulate breast cancer resistance protein expression. *Mol Pharmacol*, **73(3)**: 613-615.
- Wang J, Yang M, Li Y and Han B. 2015. The role of microRNAs in the chemoresistance of breast cancer. *Drug Dev Res*, **76(7)**: 368-374.
- Wang Q, Cheng Y, Wang Y, Fan Y, Li C, Zhang Y, Wang Y, Dong Q, Ma Y, Teng YE, Qu X, Liu Y. 2017. Tamoxifen reverses epithelial-mesenchymal transition by demethylating miR-200c in triple-negative breast cancer cells. *BMC Cancer*, **17(1)**: 492.
- Wang T, Chen G, Ma X, Yang Y, Chen Y, Peng Y, Bai Z, Zhang Z, Pei H and Guo W. 2019. MiR-30a regulates cancer cell response to chemotherapy through SNAI1/IRS1/AKT pathway. *Cell Death & Disease*, **10(3)**: 153.
- World Health Organization. 2019. Breast cancer. <https://www.who.int/cancer/prevention/diagnosis-screening/breast-cancer/en/>
- Yan LX, Huang XF, Shao Q, Huang MY, Deng L, Wu QL, Zeng YX and Shao JY. 2008. MicroRNA miR-21 overexpression in human breast cancer is associated with advanced clinical stage, lymph node metastasis and patient poor prognosis. *RNA*, **14(11)**: 2348-2360.
- Zhu J, Zheng Z, Wang J, Sun J, Wang P, Cheng X, Fu L, Zhang L, Wang Z and Li Z. 2014. Different miRNA expression profiles between human breast cancer tumors and serum. *Front Genet*, **5**.
- Zhu J, Zou Z, Nie P, Kou X, Wu B, Wang S, Song Z, He J. 2016. Downregulation of microRNA-27b-3p enhances tamoxifen resistance in breast cancer by increasing NR5A2 and CREB1 expression. *Cell Death Dis*, **7(11)**, e2454.

Association of Angiotensin Converting Enzyme (ACE) Gene insertion/deletion (I/D) Polymorphism with Obesity and Obesity Related Phenotypes in Malay Subjects

Emilia Apidi^{1,2}, Aliya Irshad Sani^{1,4}, Mohd Khairi Zahri Johari², Rohayu Izanwati Mohd Rawi², Ramlah Farouk^{1,3}, Omar Mahmoud Al-shajrawi^{1,5}, Atif Amin Baig^{*1,2} and Nordin Bin Simbak¹.

¹Faculty of Medicine, Medical Campus, Universiti of Sultan Zainal Abidin (UniSZA), Kota Campus, Jalan Sultan Mahmud, 20400 Kuala Terengganu, ²Faculty of Health Sciences, Universiti of Sultan Zainal Abidin (UniSZA), Gong Badak Campus, 21300 Kuala Terengganu, Terengganu, Malaysia, ³Yusuf Maitama Sule University, Kano-Nigeria, ⁴Department of Biochemistry, Ziauddin University, Pakistan, ⁵Institute of Marine Biotechnology, Universiti Malaysia Terengganu, 21030 Kuala Nerus, Terengganu, Malaysia

Received July 3, 2019; Revised August 19, 2019; Accepted August 28, 2019

Abstract

Angiotensin converting enzyme (ACE) gene insertion/deletion (I/D) polymorphism has been identified as a potential candidate gene for obesity. The aim of this study was to identify the genotypic and allelic frequencies of ACE gene I/D polymorphism and its association with anthropometric parameters, lipid profiles and the susceptibility for obesity in Malay subjects. This cross-sectional, comparative study involved 219 subjects; 94 obese and 123 non-obese as controls. Anthropometric and lipid profiles were measured according to the standard method, alongside with genotyping analysis by polymerase chain reaction (PCR). Anthropometric and lipid profiles were compared between groups, and the association of this polymorphism with obesity was evaluated. Genotypic frequencies of II (47.9%), DD (42.7%) and DD genotypes (9.6%) in normal group were compared with genotypic frequencies of II (54.5%), DD (36.6%) and DD genotypes (8.9%) in obese group ($P=0.620$). The D allele distribution was 31.0% in normal comparing with 27.0% in obese group ($P=0.410$). Anthropometric parameters and lipid profiles did not differ significantly between the genotypes. However, D allele carriers exhibit consistently higher triglycerides, total cholesterol and LDL-cholesterol levels than the non-carriers without statistical significance. The ACE gene I/D polymorphism is not associated with obesity and obesity related phenotypes in Malay subjects; a weak interaction effect between the D allele with lipid profiles is seen.

Keywords: ACE gene I/D polymorphism, obesity, Malay, anthropometric parameters, lipid profile

1. Introduction

Obesity develops from a sustained positive energy balance that involves the interaction between genetic, environmental and behavioural factors (Yang et al., 2007; Galgani and Ravussin, 2008). The renin-angiotensin system (RAS) is an important regulator of blood pressure, body fluid homeostasis and other metabolic pathways associated with it (Grobe et al., 2013). Angiotensin II is the main effector of this system, produced from angiotensin I (Ang I) and angiotensinogen (AGT) via the effect of renin and angiotensin converting enzyme (ACE)(Frigolet et al., 2013).

In addition to some vital organs and tissues, adipose tissue also hosts a local renin-angiotensin system (Schling et al., 1999; Engeli et al., 2000). Adipose tissue RAS has been implicated in the regulation of visceral adipose tissue accumulation (Acharid et al., 2007) and lipid metabolism (Jones et al., 1997), and thus may contribute towards the

development of obesity and obesity-related metabolic disorders (Yang et al., 2013).

ACE contributes toward effective functioning of the RAS (Lemes et al., 2013). The gene encoding ACE maps to chromosome 17q23, spans 21 kilo bases (kb) long and comprises 26 exons and 25 introns (Sayed-Tabatabaei et al., 2006). A common insertion (I) /deletion (D) polymorphism in intron 16 of the ACE gene has been associated with differences in circulating ACE levels, with DD genotype contributing to the highest, followed by the ID and II genotypes for the intermediate and lowest levels, respectively (Rigat et al., 1990).

The ACE gene I/D polymorphism has been extensively studied for the distribution of ACE genotypes and alleles in different ethnic populations (Jayapalan et al., 2008) and its association with numerous disease conditions including hypertension (Heidari et al., 2014), coronary artery disease (Seckin et al., 2006), insulin resistance (Celik et al., 2010) and obesity (Strazzullo et al., 2003; Yang et al., 2013). However, the mechanism through which this

* Corresponding author e-mail: atifamin@unisza.edu.my.

* **Abbreviations:** Hypoxia-inducible factor-2, ACE; Angiotensin I-converting enzyme, BDNF: Brain-derived neurotropic factor, BLAST: Basic Local Alignment Search Tool, BMI: Body mass index

polymorphism affects obesity and its related phenotypes remains unclear. Therefore, we determine the genotypic and allelic frequencies of ACE gene I/D polymorphism and its association with anthropometric measurements, lipid profile and the risk for obesity in Malay subjects.

2. Materials and Methods

2.1. Subjects

This was a cross-sectional, comparative study. A total of 217 Malay adult subjects, aged between 18-60 years were recruited by a convenience volunteer sampling from educational establishments around Kuala Terengganu, Terengganu, Malaysia. They were 94 obese and 123 non-obese as control, selected after primary obesity screening using body mass index (BMI) which classifies them as obese ($BMI \geq 30\text{kg/m}^2$) and non-obese ($BMI 18.50 - 24.99\text{kg/m}^2$) according to the World Health Organization criteria (WHO, 2000). Those who were eligible but with cardiovascular and respiratory disease, diabetic patients, underweight ($BMI < 18.5\text{kg/m}^2$) and overweight ($25.0\text{kg/m}^2 \leq BMI \leq 29.99\text{kg/m}^2$) were excluded from the study. Study approval was obtained from the Institutional Review Board of the Universiti Sultan Zainal Abidin (UniSZA), the Unit of Planning and Education Policy Research, Ministry of Education, Malaysia and Terengganu State Education Department before conducting the study. All subjects agree to participate and have signed their informed consent.

2.2. Anthropometric measurements

Weight (in kg) and height (in m) were measured to calculate the BMI by dividing the weight by the square of the body height. Waist circumference (WC) was measured between the final rib and the iliac crest at the end of the normal expiration, hip circumference was measured around pelvis at midpoint of maximum protrusion over buttocks by Ergonomic circumference measuring tape (Seca 201). Waist and hip circumferences were obtained to calculate waist-hip ratio (WHR). Waist-height ratio (WHtR) was calculated by dividing the measurement of waist circumference to that of the height. The assessment of body fat percentage (BF%) was done using a Slim Manager N40 (AIIA communications Inc, South Korea). Body adiposity index was determined using the formula: $BAI = [\text{hip (cm)} / \text{height (m)}]^{1.5} - 18$ (Bergman et al., 2011). Abdominal volume index was calculated using waist and waist-hip ratio ($AVI = [2\text{cm (waist)}^2 + 0.7\text{cm (waist-hip)}^2] / 1000$) (Guerrero-Romero and Rodriguez-Moran, 2003). Conicity index was determined based on the previously established formula (Valdez, 1991).

2.3. Blood collection and biochemical assays

Blood samples were drawn after an overnight fast into plain and EDTA-coated tubes (Beckton Dickinson, Franklin Lakes, NJ). After serum separation, total cholesterol, triglycerides and HDL-cholesterol were analysed using an Olympus-AU400 chemistry analyser (Olympus, Tokyo, Japan) by enzymatic calorimetric method. Low-density lipoprotein (LDL) cholesterol was calculated by the Friedewald's formula.

2.4. Blood extraction and Genotyping

The blood extraction procedure was based on manufacturer's protocol (Vivantis, CA, USA).

Genotyping was carried out by polymerase chain reaction (PCR) using the primers described from the previous studies (Rigat et al., 1992; Nikzamir et al., 2008). PCR was carried out

in a total volume of 20 μL containing 1X PCR buffer, 1.7mM MgCl_2 , 0.34mM dNTPs, 0.8 μM of each primer and 1U *Taq* polymerase (Promega, Madison, WI). The amplified products at 190bp, 490bp and both 190bp and 490bp for II, ID and DD genotypes, respectively, and 335bp for confirmatory analysis of ID genotype were resolved on 2% agarose gel and visualized by ethidium bromide staining as shown in Figure 2.

2.5. Statistical analysis

All calculations were carried out using SPSS version 20.0 (IBM Corporation, Armonk, NY). Data was expressed as mean \pm standard deviation (SD) or median (interquartile range). Genotypic and allelic frequencies were determined by manual counting and compared using the chi-square test. Significant differences between groups were evaluated using a one-way ANOVA, Kruskal-Wallis, independent sample *t*-test or Mann-Whitney U test where necessary. A binary logistic regression was used to identify the significant risk factors for obesity, considering their odds ratio (OR), 95% confidence intervals (CI) and the corresponding P-values. A P-value of less than 0.05 was considered as significant.

3. Results

3.1. Characteristics of the study subjects

The anthropometric data and lipid profiles of the study subjects by ACE I/D genotypes are presented in Table 1. All parameters for anthropometric characterization and lipid profiles did not differ significantly between the genotypes, however, total cholesterol and LDL-cholesterol levels were consistently higher in ID and DD subjects than the II subjects without significant differences.

Table 1. Anthropometric measurements and lipid profiles in all subjects according to ACE I/D genotypes.

	ACE genotypes (n=217)			P-value
	II (n=112)	ID (n=85)	DD (n=20)	
Age (year) [†]	36.31 ± 11.27	36.64 ± 9.76	31.70 ± 10.08	0.160
Weight (kg) [†]	66.77 ± 16.93	69.76 ± 18.69	67.29 ± 15.79	0.488
Height (m) [†]	1.59 ± 0.08	1.59 ± 0.08	1.60 ± 0.06	0.786
BMI(kg/m ²) [†]	26.37 ± 5.75	27.40 ± 6.15	26.27 ± 6.16	0.450
WC (cm) [†]	80.60 ± 14.46	83.80 ± 15.12	82.55 ± 16.30	0.326
HC (cm) [†]	98.86 ± 12.93	99.98 ± 10.40	99.98 ± 10.61	0.782
WHR [†]	0.82 ± 0.09	0.83 ± 0.10	0.82 ± 0.10	0.407
WHtR [†]	0.51 ± 0.08	0.53 ± 0.09	0.52 ± 0.10	0.322
CI [†]	1.14 ± 0.10	1.17 ± 0.10	1.17 ± 0.12	0.263
AVI [†]	13.70 ± 4.87	14.74 ± 5.15	14.42 ± 5.68	0.358
BAI [†]	31.53 ± 6.68	31.97 ± 5.30	31.51 ± 6.26	0.872
BF (%) [†]	28.25 ± 8.35	28.76 ± 7.52	26.60 ± 10.80	0.575
TG (mmol/L) [†]	1.00 (0.30-14.30)	1.00 (0.40-7.90)	0.85 (0.50-4.90)	0.677
TC (mmol/L) [†]	5.44 ± 1.39	5.68 ± 1.39	5.55 ± 1.38	0.499
HDL-C (mmol/L) [†]	1.27 ± 0.32	1.36 ± 0.32	1.30 ± 0.38	0.159
LDL-C (mmol/L) [†]	3.85 ± 1.18	3.99 ± 1.25	3.98 ± 1.06	0.720

[†]One-way ANOVA test; [‡]Kruskal-Wallis non-parametric test. Data expressed as mean ± SD, or as median (minimum – maximum) for the skewed data.

Abbreviations: n, number of subjects; BMI, body mass index; WC, waist circumference; HC, hip circumference; WHR, waist-hip ratio; WHtR, waist height ratio; CI, conicity index; AVI, abdominal volume index; BAI, body adiposity index; BF (%), body fat percentage; TG, triglycerides; TC, total cholesterol; HDL-C, high density lipoprotein cholesterol; LDL-C, low density lipoprotein cholesterol

3.2. Genotypic and allelic frequencies of ACE gene I/D polymorphism

The ACE gene II, ID and DD genotype distributions were 47.9%, 42.7% and 9.6% in obese subjects and 54.5%, 36.6% and 8.9% in non-obese subjects, respectively, Figure 1 shows the vasiulization of the ACE alleles and genotypes on the gell picture. There was no significant difference observed between groups (P=0.620). The I allele frequency in obese and non-obese subjects was 69.0% and 73.0%, and the D allele frequency was 31.0% and 27.0%, respectively. The difference in allelic distribution between obese and non-obese was also not significant (P=0.410) (Figure 2).

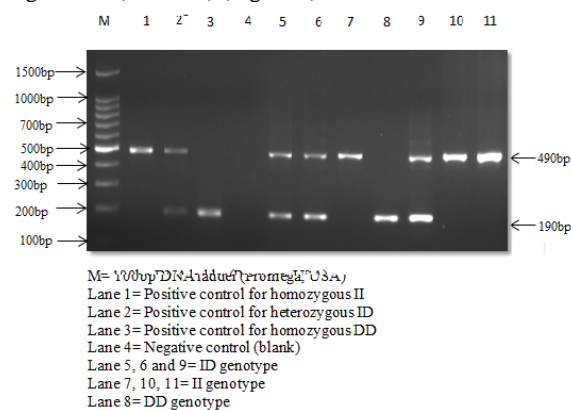


Figure 1. Determination of ACE gene I/D alleles by PCR (separated on a 2% ethidium bromide stained agarose gel)

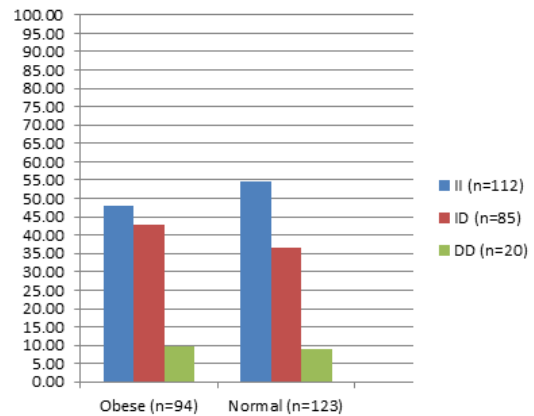


Figure 2. Genotypic and allelic frequencies of ACE I/D gene polymorphism with obesity

3.3. Anthropometric measurements and lipid profiles by ACE I/D genotypes in obese and non-obese subjects

The comparison of anthropometric measurements and lipid profiles in obese and non-obese subjects with their respective ACE I/D genotypes are shown in Table 3 and Table 4. Anthropometric parameters and lipid profiles in obese group did not differ among the genotypes, however, triglycerides, total cholesterol and LDL-cholesterol levels were consistently higher in ID and DD subjects as compared to the II subjects without significant differences (Table 2). In non-obese group, LDL-cholesterol was slightly higher in II subjects than the DD and ID subjects without statistical significance (Table 3).

Table 2. Comparison of anthropometric parameters and lipid profiles in obese subjects grouped by ACE genotypes

	ACE genotypes			P-value ^a	P-value ^b
	II (n=45)	ID (n=40)	DD (n=9)		
Age (year) [†]	40.13 ± 11.11	39.18 ± 8.51	34.44 ± 9.66	0.298	0.378
Weight (kg) [†]	83.74 ± 12.23	85.70 ± 13.89	82.70 ± 7.92	0.706	0.591
Height (m) [†]	1.60 ± 0.08	1.60 ± 0.09	1.59 ± 0.06	0.937	0.879
BMI(kg/m ²) [†]	32.64 ± 3.37	33.20 ± 3.51	32.52 ± 2.42	0.706	0.528
WC (cm) [†]	94.05 ± 10.86	96.10 ± 11.04	97.17 ± 12.82	0.601	0.328
HC (cm) [†]	109.98 ± 12.45	107.80 ± 9.06	109.72 ± 6.55	0.632	0.408
WHR [†]	0.87 ± 0.08	0.89 ± 0.08	0.89 ± 0.12	0.366	0.156
WHtR [†]	0.59 ± 0.06	0.59 ± 0.06	0.61 ± 0.08	0.511	0.293
CI [†]	1.19 ± 0.09	1.21 ± 0.09	1.24 ± 0.14	0.456	0.327
AVI [†]	18.21 ± 4.15	18.86 ± 4.26	19.39 ± 4.89	0.663	0.399
BAI [†]	36.51 ± 6.74	35.19 ± 4.61	36.63 ± 4.50	0.534	0.372
BF (%) [†]	33.87 ± 6.23	33.41 ± 6.01	34.22 ± 8.80	0.918	0.817
TG (mmol/L) [†]	1.20 (0.50 – 14.30)	1.35 (0.60 – 3.60)	2.10 (0.90 – 4.90)	0.403	0.233
TC (mmol/L) [†]	5.48 ± 1.45	5.96 ± 1.43	5.92 ± 1.59	0.294	0.117
HDL-C (mmol/L) [†]	1.16 ± 0.32	1.27 ± 0.25	1.18 ± 0.38	0.247	0.146
LDL-C (mmol/L) [†]	3.89 ± 1.16	4.35 ± 1.28	4.28 ± 1.19	0.216	0.081

[†]One-way ANOVA test; [†] Kruskal-Wallis non-parametric test. Data expressed as mean ± SD, or as median (minimum – maximum) for the skewed data

^a Comparison by one-way ANOVA test (II genotype vs. ID genotype vs. DD genotype) for all variables except for TG by Kruskal-Wallis non-parametric test

^b Comparison by *t*-test (II genotype vs. ID + DD genotypes) for all variables except for TG by Mann-Whitney U test

n, number of subjects; BMI, body mass index; WC, waist circumference; HC, hip circumference; WHR, waist-hip ratio; WHtR, waist height ratio; CI, conicity index; AVI, abdominal volume index; BAI, body adiposity index; BF (%), body fat percentage; TG, triglycerides; TC, total cholesterol; HDL-C, high density lipoprotein cholesterol; LDL-C, low density lipoprotein cholesterol

Table 3. Comparison of anthropometric parameters and lipid profiles in non-obese subjects grouped by ACE genotypes

	ACE genotypes			P-value ^a	P-value ^b
	II (n=67)	ID (n=45)	DD (n=11)		
Age (year) [†]	33.75 ± 10.71	34.38 ± 10.33	29.45 ± 10.29	0.378	0.861
Weight (kg) [†]	55.38 ± 7.36	55.60 ± 7.72	54.68 ± 5.93	0.934	0.974
Height (m) [†]	1.58 ± 0.08	1.58 ± 0.08	1.61 ± 0.06	0.531	0.790
BMI(kg/m ²) [†]	22.17 ± 1.82	22.25 ± 1.89	21.25 ± 1.85	0.198	0.697
WC (cm) [†]	71.56 ± 8.16	72.86 ± 8.27	70.59 ± 4.86	0.590	0.556
HC (cm) [†]	91.39 ± 6.07	93.03 ± 5.36	92.00 ± 4.92	0.333	0.166
WHR [†]	0.78 ± 0.07	0.78 ± 0.08	0.77 ± 0.05	0.791	0.809
WHtR [†]	0.45 ± 0.05	0.46 ± 0.05	0.44 ± 0.04	0.361	0.626
CI [†]	1.11 ± 0.09	1.13 ± 0.10	1.11 ± 0.07	0.570	0.353
AVI [†]	10.68 ± 2.30	11.08 ± 2.31	10.34 ± 1.32	0.517	0.533
BAI [†]	28.18 ± 4.04	29.11 ± 4.13	27.33 ± 3.94	0.316	0.433
BF (%) [†]	24.48 ± 7.43	24.62 ± 6.23	20.35 ± 8.04	0.361	0.593
TG (mmol/L) [†]	0.90 (0.30-4.90)	0.80 (0.40-7.90)	0.70 (0.50-1.20)	0.181	0.416
TC (mmol/L) [†]	5.42 ± 1.35	5.43 ± 1.32	5.25 ± 1.17	0.914	0.917
HDL-C (mmol/L) [†]	1.33 ± 0.30	1.43 ± 0.36	1.39 ± 0.38	0.309	0.136
LDL-C (mmol/L) [†]	3.82 ± 1.21	3.66 ± 1.15	3.73 ± 0.92	0.775	0.485

[†]One-way ANOVA test; [†] Kruskal-Wallis non-parametric test. Data expressed as mean ± SD, or as median (minimum – maximum) for the skewed data

^a Comparison by one-way ANOVA test (II genotype vs. ID genotype vs. DD genotype) for all variables except for TG by Kruskal-Wallis non-parametric test

^b Comparison by *t*-test (II genotype vs. ID + DD genotypes) for all variables except for TG by Mann-Whitney U test

n, number of subjects; BMI, body mass index; WC, waist circumference; HC, hip circumference; WHR, waist-hip ratio; WHtR, waist height ratio; CI, conicity index; AVI, abdominal volume index; BAI, body adiposity index; BF (%), body fat percentage; TG, triglycerides; TC, total cholesterol; HDL-C, high density lipoprotein cholesterol; LDL-C, low density lipoprotein cholesterol.

3.4. sociation of ACE gene I/D polymorphism and other predictor variables with obesity

In a logistic regression analysis, the ACE I/D genotypes were analyzed as categorical variables while age, triglycerides, total cholesterol, HDL-cholesterol and LDL-cholesterol were included as continuous variables (Table 4). There was no evidence that the ACE I/D genotypes can be regarded as an independent risk factor for obesity.

Table 4. Logistic regression analysis for the association of ACE genotypes and other predictor variables with obesity

	OR	95% CI	P-value
Age	1.05	1.03 – 1.08	<0.001
ACE genotypes			
II	1.00 (ref.)		
ID	1.32	0.75 – 2.34	0.335
DD	1.22	0.47 – 3.18	0.687
II + DD	1.30	0.76 – 2.23	0.335
TG (mmol/L)	1.81	1.24 – 2.65	0.002
TC (mmol/L)	1.18	0.97 – 1.44	0.096
HDL-C (mmol/L)	0.19	0.08 – 0.47	<0.001
LDL-C (mmol/L)	1.31	1.03 – 1.65	0.026

Age, TG, TC, HDL-C and LDL-C are included as continuous variables; ACE genotype (II, ID and DD genotypes; II and ID + DD genotypes) are included as continuous variables

TG, triglycerides; TC, total cholesterol; HDL-C, high density lipoprotein cholesterol; LDL-C, low density lipoprotein cholesterol; OR, odds ratio; CI, confidence intervals.

4. Discussion

In this cross-sectional, comparative study, the ACE gene I/D polymorphism was determined for its association with lipid profile, anthropometric measurements and the risk for obesity in Malay adult subjects. The D allele frequency in our study obese group (31.0%) was similar to that range established in other Asian populations between 30.6% - 42.4% for the Indonesian (Sinorita et al., 2010), Korean (Um et al., 2003; Kim, 2009; Yang et al., 2013) and Japanese (Uemura et al., 2000), except for the higher frequency among the Turkish (Bitigen et al., 2007; Akin et al., 2010), Asian Indian (Poornima et al., 2014), Pakistan (Javaid et al., 2011) and Arabs (El-Hazmi and Warsy, 2003). Asia is known for its ethnically diverse populations and therefore could have a diverse patterns of D allele. Comparative studies for obese Africans (Cooper et al., 1997; Mehri et al., 2012) and Caucasians (Alvarez-Aguilar et al., 2007; Bell et al., 2007; Wacker et al., 2008; Fiatal et al., 2011) from different countries confirm their phylogenetic similarities despite being from different geographical areas.

This study found that the ACE gene I/D polymorphism was not a predisposing factor for obesity in Malay, demonstrated by similar D allele distribution in both obese and non-obese groups. Furthermore, logistic regression analysis showed that this polymorphism is unlikely to increase the risk for obesity in this ethnicity. Also, no significant differences between the ACE genotypes in all parameters for anthropometric characterization indicates that this polymorphism was not involved in the regulation of body mass and adipose tissue. Previous studies among the Pakistani (Javaid et al., 2011), Mediterranean

population in Southern Europe (Riera-Fortuny et al., 2005), Turkish (Bitigen et al., 2007), Greeks (Moran et al., 2005) Italian (Strazzullo et al., 2003) and Korean (Yang et al., 2013) populations provide considerable support for the association of this polymorphism with obesity and its associated phenotypes. However, other studies failed to demonstrate any association at all (Nagi et al., 1998; Um et al., 2003; Wacker et al., 2008). Differences in study design (Um et al., 2003; Riera-Fortuny et al., 2005; Javaid et al., 2011), effects of gender and age (Strazzullo et al., 2003; Wacker et al., 2008), racial differences in D allele distributions, different criteria used to define obesity (Uemura et al., 2000; Um et al., 2003; Riera-Fortuny et al., 2005; Kim, 2009) and nutrition profile (Yang et al., 2013) could be the reason for inconsistencies between these studies.

This study also found no significant interaction effect between the ACE gene I/D polymorphism with lipid profiles in the entire subjects, obese and non-obese groups. However, carriers for D allele exhibit consistently higher triglycerides, total cholesterol and LDL-cholesterol without significant differences. The association between this polymorphism and lipid profiles was still at the matter of controversy. Carriers for D allele have been associated with altered lipid values in Japanese (Suzuki et al., 1996), Israeli (Oren et al., 1999), Korean (Kim, 2009) and Mexican (Alvarez-Aguilar et al., 2007) populations. However, results from some other reports were contradictory (Nagi et al., 1998; Uemura et al., 2000; Um et al., 2003). The mechanism by which ACE gene variants may influence lipid levels could be attributable to the specific localization of the renin-angiotensin system in adipose tissue (Schling et al., 1999), which suggests that it may also be involved in lipid metabolism. Differences in ethnic background (Mao and Huang, 2013) and dietary patterns (Yang et al., 2013) may also become significant contributors.

Literature regarding the association of this genetic polymorphism with obesity among Malay subjects is scarce. Although the ACE gene I/D polymorphism was not associated with obesity and its related phenotypes in Malay, the risk imparted by this polymorphism still merits attention. With regard to obese individuals potentially developing favorable metabolic profile (Seo and Rhee, 2014), adipose RAS overexpression is also likely to occur in certain obese individuals (Kalupahana and Moustaid-Moussa, 2012), which could indirectly suggest that further studies are needed to undermine the impact of this genetic polymorphism in obesity among this ethnicity.

5. Conclusion

In conclusion, we have successfully identified the genotypic and allelic frequencies of ACE gene I/D polymorphism in Malay subjects. Although this polymorphism is not associated with obesity in this ethnicity, triglycerides, total cholesterol and LDL-cholesterol levels showed a consistently higher trend in D allele carriers as compared to the non-carriers.

Acknowledgment

This study was supported and funded by the Centre for Research and Innovation Management (CRIM), Universiti Sultan Zainal Abidin (UniSZA), Terengganu, Malaysia

(DPU Grant: UniSZA/13/GU(017)). We also thank the Department of Education Planning and Policy Research, Ministry of Education, Malaysia and Terengganu Education Department for the approval of this study. Participation of all subjects is gratefully acknowledged. We thank all staff and researchers in Faculty of Medicine, Universiti Sultan Zainal Abidin for their support and commitment.

References

- Achard, V., Boullu-Ciocca, S., Desbriere, R., Nguyen, G. and Grino, M., 2007. Renin receptor expression in human adipose tissue. *Am J Physiol Regul Integr Comp Physiol* **292**, R274-82.
- Akin, F., Turgut, S., Bastemir, M., Turgut, G., Kursunluoglu, R., Karasu, U. and Guclu, A., 2010. Angiotensin-converting enzyme gene polymorphism in overweight and obese Turkish patients with insulin resistance. *DNA Cell Biol* **29**, 207-12.
- Alvarez-Aguilar, C., Enriquez-Ramirez, M.L., Figueroa-Nunez, B., Gomez-Garcia, A., Rodriguez-Ayala, E., Moran-Moguel, C., Farias-Rodriguez, V.M., Mino-Leon, D. and Lopez-Meza, J.E., 2007. Association between angiotensin-1 converting enzyme gene polymorphism and the metabolic syndrome in a Mexican population. *Exp Mol Med* **39**, 327-334.
- Bell, C.G., Meyre, D., Petretto, E., Levy-Marchal, C., Hercberg, S., Charles, M.A., Boyle, C., Weill, J., Tauber, M., Mein, C.A., Aitman, T.J., Froguel, P. and Walley, A.J., 2007. No contribution of angiotensin-converting enzyme (ACE) gene variants to severe obesity: a model for comprehensive case/control and quantitative cladistic analysis of ACE in human diseases. *Eur J Hum Genet* **15**, 320-7.
- Bergman, R.N., Stefanovski, D., Buchanan, T.A., Sumner, A.E., Reynolds, J.C., Sebring, N.G., Xiang, A.H. and Watanabe, R.M., 2011. A better index of body adiposity. *Obesity (Silver Spring)* **19**, 1083-9.
- Bitigen, A., Cevik, C., Demir, D., Tanalp, A.C., Dundar, C., Tigen, K., Mutlu, B. and Basaran, Y., 2007. The frequency of angiotensin-converting enzyme genotype and left ventricular functions in the obese population. *Congestive Heart Failure* **13**, 323-7.
- Celik, O., Yesilada, E., Hascalik, S., Celik, N., Sahin, I., Keskin, L. and Ozerol, E., 2010. Angiotensin-converting enzyme gene polymorphism and risk of insulin resistance in PCOS. *Reprod Biomed Online* **20**, 492-8.
- Cooper, R., McFarlane-Anderson, N., Bennett, F.I., Wilks, R., Puras, A., Tewksbury, D., Ward, R. and Forrester, T., 1997. ACE, angiotensinogen and obesity: a potential pathway leading to hypertension. *J Hum Hypertens* **11**, 107-11.
- El-Hazmi, M.A. and Warsy, A.S., 2003. Increased frequency of angiotensin-converting enzyme DD genotype in Saudi overweight and obese patients. *Ann Saudi Med* **23**, 24-7.
- Engeli, S., Negrel, R. and Sharma, A.M., 2000. Physiology and pathophysiology of the adipose tissue renin-angiotensin system. *Hypertension* **35**, 1270-7.
- Fiatal, S., Szigethy, E., Szeles, G., Toth, R. and Adany, R., 2011. Insertion/deletion polymorphism of angiotensin-1 converting enzyme is associated with metabolic syndrome in Hungarian adults. *J Renin Angiotensin Aldosterone Syst* **12**, 531-8.
- Frigolet, M.E., Torres, N. and Tovar, A.R., 2013. The renin-angiotensin system in adipose tissue and its metabolic consequences during obesity. *J Nutr Biochem* **24**, 2003-15.
- Galgani, J. and Ravussin, E., 2008. Energy metabolism, fuel selection and body weight regulation. *Int J Obes (Lond)* **32** Suppl 7, S109-19.
- Grobe, J.L., Rahmouni, K., Liu, X. and Sigmund, C.D., 2013. Metabolic rate regulation by the renin-angiotensin system: brain vs. body. *Pflugers Arch* **465**, 167-75.
- Guerrero-Romero, F. and Rodriguez-Moran, M., 2003. Abdominal volume index. An anthropometry-based index for estimation of obesity is strongly related to impaired glucose tolerance and type 2 diabetes mellitus. *Arch Med Res* **34**, 428-32.
- Heidari, F., Vasudevan, R., Mohd Ali, S.Z., Ismail, P., Etemad, A., Pishva, S.R., Othman, F. and Bakar, S.A., 2014. Association of insertion/deletion polymorphism of angiotensin-converting enzyme gene among Malay male hypertensive subjects in response to ACE inhibitors. *J Renin Angiotensin Aldosterone Syst*.
- Javaid, A., Mansoor, Q., Bilal, N., Bilal, A., Shaukat, U. and Ismail, M., 2011. ACE gene DD genotype association with obesity in Pakistani population. *Int J Bioautom* **15**, 49-56.
- Jayapalan, J.J., Muniandy, S. and Chan, S.P., 2008. Angiotensin-1 converting enzyme I/D gene polymorphism: scenario in Malaysia. *Southeast Asian J Trop Med Public Health* **39**, 917-21.
- Jones, B.H., Standridge, M.K., Taylor, J.W. and Moustaid, N., 1997. Angiotensinogen gene expression in adipose tissue: analysis of obese models and hormonal and nutritional control. *Am J Physiol* **273**, R236-42.
- Kalupahana, N.S. and Moustaid-Moussa, N., 2012. The renin-angiotensin system: a link between obesity, inflammation and insulin resistance. *Obes Rev* **13**, 136-49.
- Kim, K., 2009. Association of angiotensin-converting enzyme insertion/deletion polymorphism with obesity, cardiovascular risk factors and exercise-mediated changes in Korean women. *Eur J Appl Physiol* **105**, 879-87.
- Lemes, V.A., Neves, A.L., Guazzelli, I.C., Frazzatto, E., Nicolau, C., Correa-Giannella, M.L., Velho, G. and Villares, S.M., 2013. Angiotensin converting enzyme insertion/deletion polymorphism is associated with increased adiposity and blood pressure in obese children and adolescents. *Gene* **532**, 197-202.
- Mao, S. and Huang, S., 2013. A meta-analysis of the association between angiotensin-converting enzyme insertion/ deletion gene polymorphism and the risk of overweight/obesity. *J Renin Angiotensin Aldosterone Syst*.
- Mehri, S., Mahjoub, S., Hammami, S., Zaroui, A., Frih, A., Betbout, F., Mechmeche, R. and Hammami, M., 2012. Renin-angiotensin system polymorphisms in relation to hypertension status and obesity in a Tunisian population. *Mol Biol Rep* **39**, 4059-65.
- Moran, C.N., Vassilopoulos, C., Tsiokanos, A., Jamurtas, A.Z., Bailey, M.E., Wilson, R.H. and Pitsiladis, Y.P., 2005. Effects of interaction between angiotensin I-converting enzyme polymorphisms and lifestyle on adiposity in adolescent Greeks. *Obes Res* **13**, 1499-504.
- Nagi, D.K., Foy, C.A., Mohamed-Ali, V., Yudkin, J.S., Grant, P.J. and Knowler, W.C., 1998. Angiotensin-1-converting enzyme (ACE) gene polymorphism, plasma ACE levels, and their association with the metabolic syndrome and electrocardiographic coronary artery disease in Pima Indians. *Metabolism* **47**, 622-6.
- Nikzami, A., Nakhjavani, M., Golmohammadi, T., Dibai, L. and Saffary, R., 2008. Polymorphism in the Angiotensin Converting Enzyme (ACE gene) and ACE activity in Type 2 diabetic patients. *Acta Medica Iranica* **46**, 277-282.
- Oren, I., Brook, J.G., Gershoni-Baruch, R., Kepten, I., Tamir, A., Linn, S. and Wolfowitz, E., 1999. The D allele of the angiotensin-converting enzyme gene contributes towards blood LDL-cholesterol levels and the presence of hypertension. *Atherosclerosis* **145**, 267-71.
- Poornima, S., Subramanyam, K., Khan, I.A. and Hasan, Q., 2014. The insertion and deletion (I28005D) polymorphism of the angiotensin I converting enzyme gene is a risk factor for osteoarthritis in an Asian Indian population. *Journal of Renin-Angiotensin-Aldosterone System*.
- Riera-Fortuny, C., Real, J.T., Chaves, F.J., Morales-Suarez-Varela, M., Martinez-Triguero, M.L., Morillas-Arino, C. and

- Hernandez-Mijares, A., 2005. The relation between obesity, abdominal fat deposit and the angiotensin-converting enzyme gene I/D polymorphism and its association with coronary heart disease. *Int J Obes (Lond)* **29**, 78-84.
- Rigat, B., Hubert, C., Alhenc-Gelas, F., Cambien, F., Corvol, P. and Soubrier, F., 1990. An insertion/deletion polymorphism in the angiotensin I-converting enzyme gene accounting for half the variance of serum enzyme levels. *Journal of Clinical Investigation* **86**, 1343-1346.
- Rigat, B., Hubert, C., Corvol, P. and Soubrier, F., 1992. PCR detection of the insertion/deletion polymorphism of the human angiotensin converting enzyme gene (DCP1) (dipeptidyl carboxypeptidase 1). *Nucleic Acids Research* **20**, 1433-1433.
- Sayed-Tabatabaei, F.A., Oostra, B.A., Isaacs, A., van Duijn, C.M. and Witteman, J.C., 2006. ACE polymorphisms. *Circ Res* **98**, 1123-33.
- Schling, P., Mallow, H., Trindl, A. and Loffler, G., 1999. Evidence for a local renin angiotensin system in primary cultured human preadipocytes. *Int J Obes Relat Metab Disord* **23**, 336-41.
- Seckin, D., Ilhan, N., Ilhan, N. and Ozbay, Y., 2006. The relationship between ACE insertion/deletion polymorphism and coronary artery disease with or without myocardial infarction. *Clin Biochem* **39**, 50-4.
- Seo, M.H. and Rhee, E.J., 2014. Metabolic and cardiovascular implications of a metabolically healthy obesity phenotype. *Endocrinol Metab (Seoul)* **29**, 427-34.
- Sinorita, H., Madiyan, M., Pramono, R.B., Purnama, L.B., Ikhsan, M.R. and Asdie, A.H., 2010. ACE gene insertion/deletion polymorphism among patients with type 2 diabetes, and its relationship with metabolic syndrome at Sardjito Hospital Yogyakarta, Indonesia. *Acta Med Indones* **42**, 12-6.
- Strazzullo, P., Iacone, R., Iacoviello, L., Russo, O., Barba, G., Russo, P., D'Orazio, A., Barbato, A., Cappuccio, F.P., Farinaro, E. and Siani, A., 2003. Genetic variation in the renin-angiotensin system and abdominal adiposity in men: the Olivetti Prospective Heart Study. *Ann Intern Med* **138**, 17-23.
- Suzuki, T., Yokota, H., Yamazaki, T., Kitamura, K., Yamaoki, K., Nagai, R. and Yazaki, Y., 1996. Angiotensin converting enzyme polymorphism is associated with severity of coronary heart disease and serum lipids (total cholesterol and triglycerides levels) in Japanese patients. *Coron Artery Dis* **7**, 371-5.
- Uemura, K., Nakura, J., Kohara, K. and Miki, T., 2000. Association of ACE I/D polymorphism with cardiovascular risk factors. *Hum Genet* **107**, 239-42.
- Um, J.Y., Mun, K.S., An, N.H., Kim, P.G., Kim, S.D., Song, Y.S., Lee, K.N., Lee, K.M., Wi, D.H., You, Y.O. and Kim, H.M., 2003. Polymorphism of angiotensin-converting enzyme gene and BMI in obese Korean women. *Clin Chim Acta* **328**, 173-8.
- Valdez, R., 1991. A simple model-based index of abdominal adiposity. *J Clin Epidemiol* **44**, 955-6.
- Wacker, M.J., Godard, M.P., McCabe, E.H., Donnelly, J.E. and Kelly, J.K., 2008. Sex difference in the association of the angiotensin converting enzyme I/D polymorphism and body mass index. *Med Sci Monit* **14**, Cr353-7.
- WHO, 2000. Obesity: Preventing and Managing the Global Epidemic. Report of a WHO Consultation. WHO Technical Report Series. World Health Organ Tech Rep Ser 894, i-xii, 1-253.
- Yang, S.J., Kim, S., Park, H., Kim, S.M., Choi, K.M., Lim, Y. and Lee, M., 2013. Sex-dependent association between angiotensin-converting enzyme insertion/deletion polymorphism and obesity in relation to sodium intake in children. *Nutrition* **29**, 525-30.
- Yang, W., Kelly, T. and He, J., 2007. Genetic epidemiology of obesity. *Epidemiol Rev* **29**, 49-61.

Hepato-Protective Effect of *Curcuma longa* against Paracetamol-Induced Chronic Hepatotoxicity in Swiss Mice

Salima Douichene, Wahiba Rached* and Nouredine Djebli

Laboratory of Pharmacognosy ApiPhytotherapy, Faculty of Life and Natural Sciences, University of Mostaganem, 27000, Algeria.

Received July 14, 2019; Revised August 25, 2019; Accepted August 31, 2019

Abstract

Curcuma longa L. (*Zingiberaceae*), a natural spice, has been usually used in Algeria to treat gastrointestinal and liver disorders. This study aims to evaluate protective and anti-inflammatory properties of aqueous extract of *C. Longa* rhizome against hepatic damages induced by Paracetamol. The mice were divided into four groups ($n=11$), the hepatotoxicity was induced in mice by oral administration of acetaminophen at the last seven weeks. The aqueous extract was also administered daily for 14 weeks with subjected of Paracetamol, the negative control group, and treated group with turmeric extract. Histopathological study of the liver and several serum markers as serum albumin, gamma GT, blood glucose and transaminases (ALT and AST) were analyzed. The results of biochemical parameters revealed increasing levels in ALT (108.54U/L), AST (256.07U/L), and serum albumin (31.2g/L) in treated intoxicated group compared to Paracetamol intoxicated group. Thus, the results demonstrated decreasing in levels of glycemia (0.3 g/L) and gamma GT (134.20 U/L). Moreover, the liver sections revealed macroscopically significant lesions, (hepatic necrosis) bloating and hydropic lesions, vacuolization and steatosis in intoxicated mice. On the other hand, these lesions are less important in the treated group with only turmeric. Animals were observed for any symptoms of toxicity after administration of extract to ensure its safety. This results show that the extract of *C. longa* has hepatoprotective potential that could be partly attributed to developed as drugs for the treatment of liver diseases.

Keywords: *Curcuma longa*; Paracetamol; mice; hepatotoxicity; hepato-protective effect.

1. Introduction

Paracetamol, known as acetaminophen or APAP, is one of the most commonly used oral analgesics and antipyretics described in the 1960 in the USA (Yoon *et al.*, 2016). It has an excellent safety profile when administered in proper therapeutic doses, but excessive use causes Paracetamol poisoning and generates liver damages (Woolley and Woolley, 2017). In the United States and the United Kingdom, Paracetamol is the most common cause of acute liver failure (Ryder and Beckingham, 2001; Ferri, 2016). The toxic dose of paracetamol is highly variable; in general the recommended maximum daily dose for healthy adults is 4 grams (Freifeld *et al.*, 2014; Twycross *et al.*, 2017). In the first 24 hours following overdose, usually 7g per day (Ferri, 2016; Woolley and Woolley, 2017) people have few or nonspecific symptoms, like abdominal pain or nausea, yellowish skin, blood clotting problems, and confusion occurs (Podolsky *et al.*, 2016; Yoon *et al.*, 2016). Additional complication may include pancreatitis, low blood sugar and lactic acidosis paracetamol toxicity can cause death without treatment after two weeks of exposure (Freifeld *et al.*, 2014; Yoon *et al.*, 2016). There are risk factors which can increase this toxicity, like alcoholism, malnutrition and certain other medications (Ferri, 2016). Paracetamol poisoning is the most common cause of acute liver failure that results not

from paracetamol itself, but from one of its metabolites, N acetyl-*p*-benzoquinone imine (NAPQI) (Webb *et al.*, 2016) which decreases the liver's glutathione and directly damages hepatocytes (Proutet *et al.*, 2014).

Curcuma longa (*Zingiberaceae*) is a rhizomatous perennial herb; the common name of this species is turmeric (Kurkum in Algeria), original from to South Asia especially India and Malaysia (Akramet *et al.*, 2010; Amel, 2015). It is commonly known as a spice and pigment for preparing culinary dishes (Delaveau, 1987; Ghosh *et al.*, 2011). This plant species is well-known in India for its therapeutic properties; its rhizome juice is used orally for the treatment of many diseases such as liver problems, gastrointestinal disorders, asthma, bronchitis, gonorrhea and urinary disorders, or as antihelminthic (Perry *et al.*, 2010). In addition; its essential oils including tumerone, atlantone, and zingiberone are used in the treatment of carminative, stomachic and tonic (Yadav *et al.*, 2017). The anticancer, antidiabetic, antioxidant, anti-inflammatory, and antimicrobial activities of aqueous extracts obtained from the rhizome of *C. longa* were previously reported (Amel, 2015). The turmeric is used in combination with other plants or spices in the food and medical fields. Hence, a mixture of the juice of this plant with dried root of *Pandanus odoratissimus* Linn. f. and water, taken early in the morning orally for 1-week can be used to remedy urinary disorders (Mishra *et al.*, 2015).

* Corresponding author e-mail: itadz@yahoo.fr; djebli_n@yahoo.fr.

The bright yellow color of turmeric originates mainly from polyphenolic pigments known as curcumin(diferuloylmethane) (Lim *et al.*, 2001). Curcumin, the principal curcuminoid found in the rhizome of turmeric, is generally considered its most active compound. Several published studies showed that curcumin has various therapeutic properties, like anticancer effect involving in inhibiting the growth of several different types of cancer, antioxidant, anti-inflammatory, antimicrobial, antidiabetic, hepatoprotective and neuroprotective activities (Lim *et al.*, 2001). The curcumin also exhibited the ability to block NF- κ B and the mutagenic response in *Helicobacter pylori*-infected epithelial cells (Sarkar *et al.*, 2016).

The present study was undertaken to assess the hepatoprotective effect of aqueous extract of *C. longa* rhizomes administrated with paracetamol overdoses induced liver damage in mice, represented by blood transaminases (TGO and TGP), albumin, total protein and sugar levels, confirmed by the histological study of mice's liver. Treatment of mice with only the aqueous extract of *C. Longa* at concentration of 2 mg/kg per day is examined for the first time.

2. Materials and Methods

2.1. Chemicals

All chemicals and reagents were used of analytical grade. Assay kit for serum aspartate aminotransferase and alanine aminotransferase were taken from Dialab, Austria, and Paracetamol (PCM) from Sigma-Aldrich USA.

2.2. Plant Material and Plant Extract Preparation

Turmeric dried rhizomes was purchased from a local market, Algeria. Species identification was performed by botanical Professors of the University of Mostaganem (Algeria). The rhizomes were cleaned, dried, and homogenized in distilled water at a ratio of 1:10 of plant to water and left macerated for 6 hours at 25°C with occasional shaking and stirring. The mixture was then filtered and concentrated, and the resulting liquid was orally administrated to animals with final concentration as 2mg/kg per day.

2.3. Animals

Forty four healthy adult mice, aged of 30 ± 2 days and weighing from 35–40 g, were obtained from Pasteur Institute of Algeria. They were maintained at room temperature (25.5°C) with a 12 h light/dark cycle, and have been given a commercial pellet diet 18 g/day/mouse (obtained from Algerian National Food Office of Cattle) and fresh drinking mineral water.

2.4. Hepatoprotective Assay

The *in vivo* hepatoprotective activity of aqueous extract of turmeric rhizome was determined using the Paracetamol-induced hepatotoxicity test in mice, as previously described by Jarsiah *et al.* (2018) with minor modifications.

The mice were randomly divided into four experimental groups, containing eleven mice in each group. The first group received mineral water and served as negative control group (C). Group II serving as Paracetamol intoxicated group(P) received 100mg/kg at the first seven weeks increased to 200mg/kg at the last seven

weeks. Group III serving as Paracetamol-treated group received paracetamol poisoning doses same as Paracetamol intoxicated group and treated by turmeric extract (P+T) at a dose of 2 mg/kg which showed no signs of toxicity in mice. Finally, Group IV serving as treated turmeric group(T) received 2mg/kg. These doses were administrated orally by force-feeding.

The period of experimentation was 14 weeks under standards laboratory conditions. The animals received the corresponding dose of the respective test solution daily for 14 consecutive weeks. 72 h after the end of experimentation, mice were scarified by decapitation (chloral 3%).

The blood was collected in sterilized centrifuged tubes which were then centrifuged to get serum for biochemical studies. The animals were then sacrificed by cervical dislocation and the liver was removed and dissected out for histopathological studies.

2.5. Determination of Liver Function and Biochemical Parameters

The collected serum was tested according to the standard liver enzymes determination assays comprising glucose, albumin, gamma GT, alanine aminotransferase (ALT), and aspartate aminotransferase (AST) levels were measured using automat COBAS 6000 analyzer.

2.6. Histopathology

The liver tissue was dissected out and fixed in the 10% neutral buffered formaldehyde for 24 hours, dehydrated in gradual ethanol (50–100%), cleared in xylene, and surrounded by paraffin wax. The sections, which were 4–5 μ m thick, were then prepared using rotary a Leica microtome thickness (Leica RM 2125 RTS, Singapore) and stained with hematoxylin and eosin dye 1% for 40 seconds for microscopic observation of histopathological changes in the liver. Next, the liver sections were scored and evaluated according to the severity of the hepatic injury including fatty changes, cell necrosis, lymphocytes, hyaline and ballooning degeneration as described by Jarsiah *et al.* (2018) with slight modifications.

2.7. Statistical Analysis

Statistical analysis data obtained are presented as mean \pm standard error of mean (SEM). The data were performed using one-way analysis of variance (ANOVA) followed by LSD test with $\alpha = 0.05$. This treatment was carried out using the SPSS v. 23.0 program (IBM Corp., Armonk, New York, USA).

3. Results and Discussion

3.1. Determination of liver function and biochemical parameters

Oral administration of paracetamol (100 and 200 mg/kg) for 2 weeks indicated an elevation in serum liver enzymes such as alanine transaminase [Fig. 1-a], aspartate transaminase [Fig. 1-b], gamma GT [Fig. 1-c], blood glucose level [Fig. 1.d], and albumin [Fig. 1.e] compared with the control group. All of these results were ameliorated by coadministration of turmeric aqueous extract. Therefore, These findings may be in concord with many other studies, thus the obtained results were similar with that acquired by of Jarsiah *et al.* (2017) after intraperitoneal injection of 70.150 and 300 mg/kg of APAP to albino Wistar rats, the

overuse of acetoaminophen in mice and rats can caused severe and extensive necrosis cells (liver damages), and increased serum ALT/AST levels in rats. The ameliorative effect of curcumin and its derivates against liver injury induced by several drugs, such as paracetamol (Girish *et al.*, 2009) has been reported. The results attained by Somchit *et al.*(2005), suggested that ethanolic extract of *C.*

longa (100 mg kg^{-1}) has a potent hepatoprotective effect against paracetamol-induced liver damages in rats at 600 mg kg^{-1} expressed by lowered serum liver enzyme activities. Also, Salama *et al.*(2013) reported the hepatoprotective effect of ethanolic extract of this species at 2 and 5 g/kg on thioacetamide induced livercirrhosis in rats with low levels of liver biochemistry.

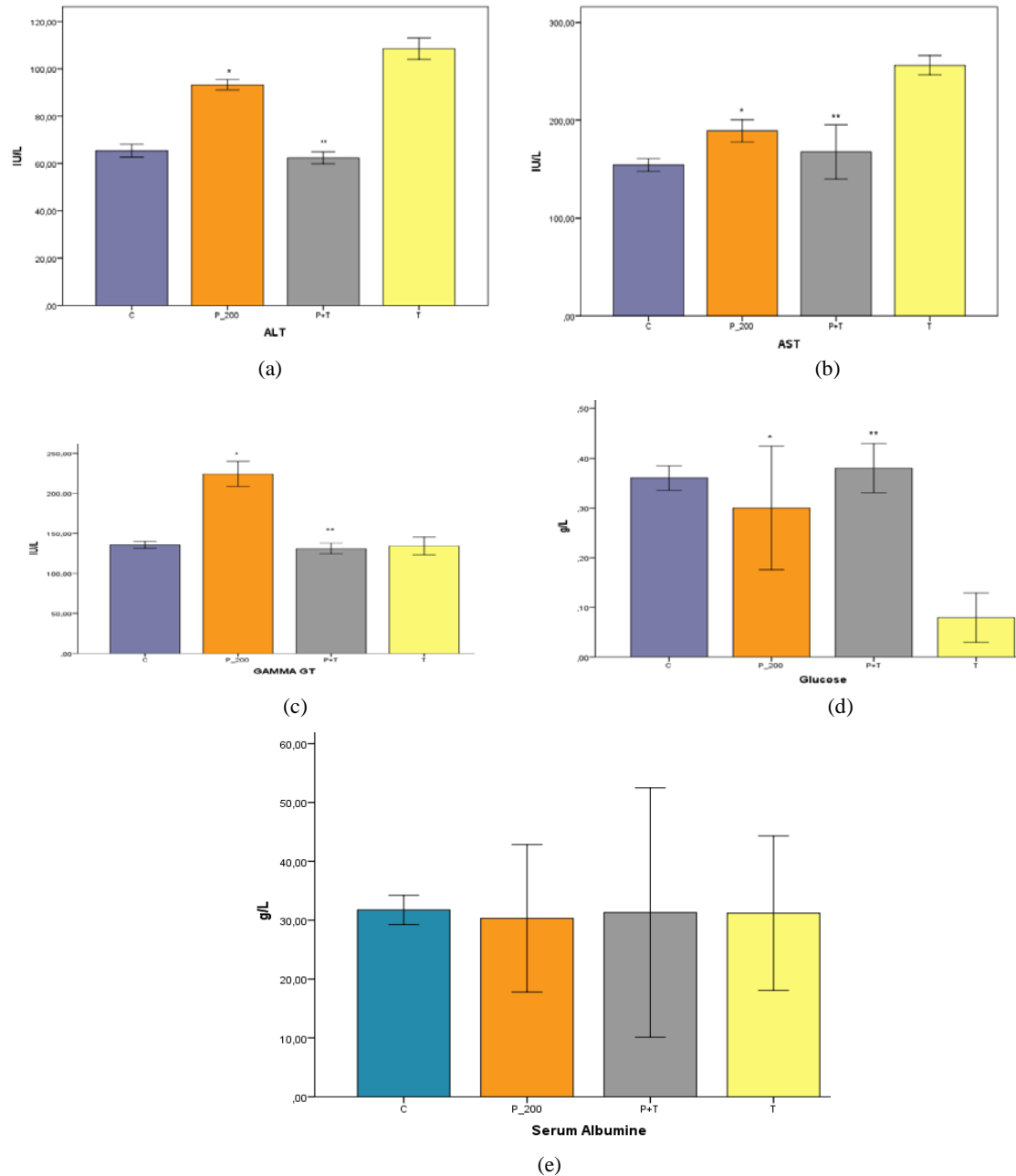


Figure 1. biochemical parameters levels; (a) ALT, (b) AST, (c) Gamma GT, (d) Glucose, and (e) albumin in serum mice of different experimental groups tested for 14 weeks.

The most frequently used preclinical species for drugs hepatotoxicity are rats and mice. The severity of the overall liver injury is very similar between mice and humans (McGill *et al.*, 2012). However the injury process progresses much faster in mice than in humans, with peak transaminases (ALT and AST) values, as indicator of liver cell death, between 12 - 24 h in the mouse (McGill *et al.*, 2013) and 36-48 h in humans after overdose (Lee, 2013). The mouse model of APAP hepatotoxicity is superior to other animal's model and most closely resembles the

human pathophysiology in terms of liver injury and recovery. In the present study, the results showed an increased serum ALT/AST and GT levels in mice, which are proved by Ray *et al.* (1996). An elevation of glucose level in serum of intoxicated group was observed compared to control mouse that may be caused by oxidative stress and NAPQ effect. The administration of phytosome curcumin effectively suppressed paracetamol-induced liver injury evidenced by a reduction of lipid peroxidation level, and elevated of enzymatic antioxidant

activities of superoxide dismutase, catalase, glutathione peroxidase in mice liver tissue (Tung *et al.*, 2017).

The Results showed that curcumin exerts remarkable protective, anti-inflammatory and therapeutic effects of oxidative associated liver diseases against hepatotoxicity induced by paracetamol (Watkins and Seeff, 2006). The ameliorative effect of curcumin and its derivatives against liver injury induced by several drugs, such as paracetamol has been reported (Nabaviet *et al.*, 2014)

In the present study, the results were confirmed by other research, which conclude that the antioxidant ability of curcumin and its derivatives is shown to be the main protective mechanism against drug induced liver damages (Negi *et al.*, 2008). Oetariet *al.* (1996) demonstrated that curcumin is a strong inhibitor of cytochrome P450; it can also normalize antioxidant enzymes and ameliorated acetoaminophen induced liver damage.

3.2. Histopathology

The histological observations of control mice did not show any histological alterations in the hepatocytes. The liver sections showed normal structure with no damage in the central vein and no change in sinusoids and hepatocytes architecture [Fig.2,3,and 4]. In toxic control group, the liver sections showed hepatocytes necrosis with strict damage associated with central vein due to paracetamol .

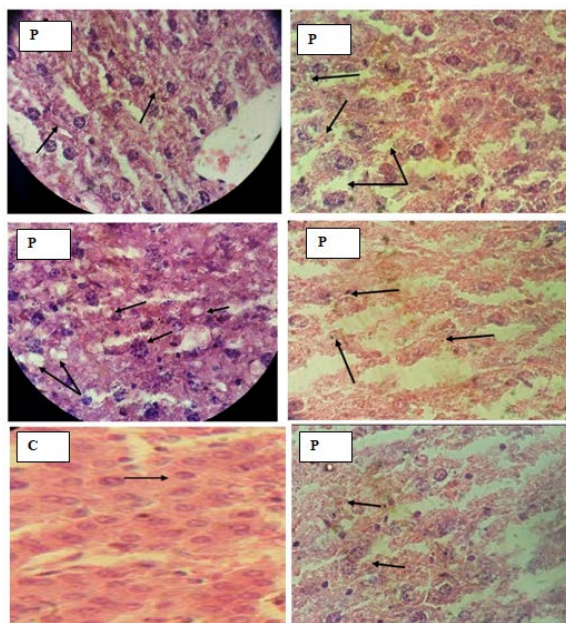


Figure 2. Microscopic study of liver tissue performed by staining (H&E) in mice, (P) intoxicated group with two doses of paracetamol (100 mg/kg, 200 mg/kg) compared with control group (C) (G×100). The black arrows indicate hepatocytes necrosis and strict and severe damage in intoxicated mice tissue, normal structure with no damage in control mice tissue.

In group treated with turmeric aqueous extract, the liver sections showed minor to moderate diffuse granular degeneration and necrosis in liver cells, reduced damage and regeneration of hepatocytes, bile duct, branch of hepatic portal vein and minimal necrosis caused by paracetamol intoxication .

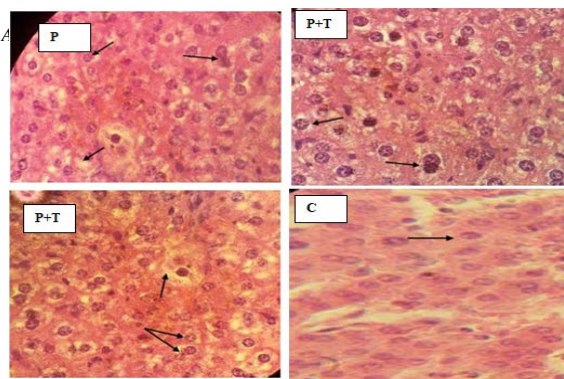


Figure 3. Microscopic study of liver tissue performed by staining (H&E) in mice, (P) intoxicated group with two doses of paracetamol (100 mg/kg, 200 mg/kg) and treated by curcumin (2 g/kg) compared with control group (P+T) (G×100). No specific alterations or damage in liver tissue. The black arrows indicate a best regeneration of liver tissue (cell's mitosis)

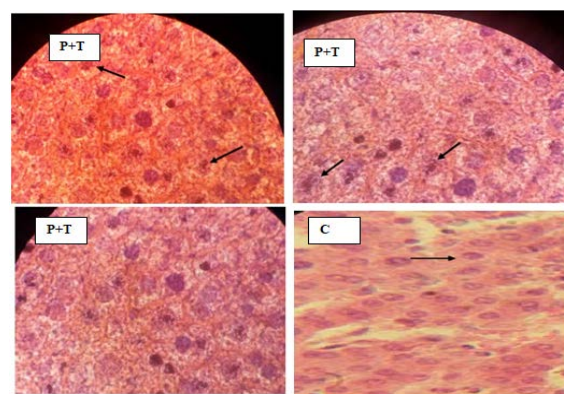


Figure 4. Microscopic study of liver tissue performed by staining (H&E) in mice, (P+T) treated control group with curcumin (2 g/kg) compared with control group (C) (G×100). The black arrows indicate normal structure of liver tissue compared with control.

Histopathology of the liver in control group and treated mice by *C.longa* at a dose of 2g/kg, mice showed no specific pathological changes. Effects of acetoaminophen began to appear from doses of 100mg/kg and 200mg/kg: presence of steatose and different lesions appear mild hyperemia oedema of the portal area and mild infiltration of inflammatory cells and apoptosis were observed, similar results with others studies (Jarsiah *et al.*, 2017), less important in treated group by curcumin. Our histopathological study of APAP toxicity shows obvious difference between the treated poisoned group and the poisoned one. Histopathology and liver biochemistry were significantly lower in the *C. longa* treated groups with a dose of 2mg/kg compared with controls. Similar results were obtained with ethanolic extract of *C.longa* rhizome by Salama *et al.* (2013). Many reports indicated that curcumin induced apoptosis and inhibited hepatocytes proliferation (Wang *et al.*, 2012). The progression of liver damages caused by acetaminophen or paracetamol could be inhibited by the antioxidant activities of curcumin and the normal status of the liver could be preserved (Salama *et al.*, 2013). The model of cell death during paracetamol hepatotoxicity is controversial. Animal studies have concluded that the injury is caused by necrosis, an increasing number of reports suggests that apoptotic cell death plays a significant role.

4. Conclusion

Overall, these outcomes suggest the protective role of aqueous extract of *C. longa* with a weak concentration in the prevention of paracetamol-induced hepatic toxicity in mice cause hepatotoxicity by forming reactive metabolites, which were accompanied with a decrease of chemical parameters in hepatic tissues. Changes in serum liver levels might contribute the molecular mechanisms of the tested plant associated with oxidative modifications in liver tissue. Consequently, the protective effect of *C. longa* against liver damage induced by Paracetamol could be explained by its antioxidant properties. However, clinical studies are necessitated to examine such an effect in humans.

Acknowledgements

The authors are grateful to the MESRS of Algeria for financial support.

References

- Akram M, Shahab-Uddin AA, Usmanhani K, Hannan A, Mohiuddin E and Asif M. 2010. *Curcuma longa* and curcumin: a review article. *Rom J Biol Plant Biol.*, **55** (2): 65-70.
- Amel B. 2015. Microscopic control of Rhizoma *Curcumaelongae* using multivariate analysis. *Planta Med.*, **81** (16): 186.
- Delaveau P. 1987. Les épices: histoire, description et usage des différents épices, aromates et condiments. Albin Michel, Paris, pp. 130-136.
- Ferri FF. (2016). Ferri's Clinical Advisor 2017 5 Books in 1. First ed., Elsevier Health Sciences. Rhode Island, (10): 125-129.
- Freifeld CC, Brownstein JS, Menone CM, Bao W, Filice R, Kass-Hout T, and Dasgupta N. 2014. Digital drug safety surveillance: monitoring pharmaceutical products in twitter. *Drug saf.*, **37** (5): 343-350.
- Ghosh N, Ghosh R, Mandal V, Mandal SC. 2011. Recent advances in herbal medicine for treatment of liver diseases. *Pharm Biol.*, **49** (9): 970-988.
- Girish C, Koner BC, Jayanthi S, Ramachandra Rao K, Rajesh B and Pradhan SC. (2009). Hepatoprotective activity of picroliv, curcumin and ellagic acid compared to silymarin on paracetamol induced liver toxicity in mice. *Fundam Clin Pharmacol.*, **23** (6): 735-745.
- Jarsiah P, Karami M, Nosrati A, Alizadeh A and Hashemi-Soteh MB. 2018. Circulating miR-122 and miR-192 as specific and sensitive biomarkers for drug-induced liver injury with acetaminophen in Rats. *Jundishapur J Nat Pharm Prod.*
- Jarsiah P, Nosrati A, Alizadeh A and Hashemi-Soteh SMB. 2017. Hepatotoxicity and ALT/AST enzymes activities change in therapeutic and toxic doses consumption of acetaminophen in rats. *Int Biol Biomed J.*, **3** (3): 119-124.
- Lee WM. 2013. Drug-induced acute liver failure. *Clin Liver Dis.*, **17** (4): 575-586.
- Lim GP, Chu T, Yang F, Beech W, Frautschy SA and Cole GM. 2001. The curry spice curcumin reduces oxidative damage and amyloid pathology in an Alzheimer transgenic mouse. *J Neurosci.*, **21**: 8370-8377.
- McGill MR, Lebofsky M, Norris HRK, Slawson MH, Bajt ML, Xie Y, Williams CD, Wilkins DG, Rollins DE and Jaeschke H. 2013. Plasma and liver acetaminophen-protein adduct levels in mice after acetaminophen treatment: dose-response, mechanisms, and clinical implications. *Toxicol Appl Pharmacol.*, **269** (3): 240-249.
- McGill MR, Sharpe MR, Williams CD, Taha M, Curry SC and Jaeschke H. 2012. The mechanism underlying acetaminophen-induced hepatotoxicity in humans and mice involves mitochondrial damage and nuclear DNA fragmentation. *J Clin Invest.*, **122** (4): 1574-1583.
- Mishra G, Khosa RL, Singh P and Jha KK. 2015. Hepatoprotective potential of ethanolic extract of *Pandanus odoratissimus* root against paracetamol-induced hepatotoxicity in rats. *J Pharm Bioallied Sci.*, **7**, (1): 45.
- Nabavi SF, Daglia M, Moghaddam AH, Habtemariam S and Nabavi SM. 2014. Curcumin and liver disease: from chemistry to medicine. *Comprehensive Compr Rev Food Sci Food Saf.*, **13** (1): 62-77.
- Negi AS, Kumar JK, Luqman S, Shanker K, Gupta MM and Khanuja SPS. 2008. Recent advances in plant hepatoprotectives: a chemical and biological profile of some important leads. *Med Res Rev.*, **28** (5): 746-772.
- Oetari S, Sudibyo M, Commandeur JN, Samhoedi R. and Vermeulen NP. 1996. Effects of curcumin on cytochrome P450 and glutathione S-transferase activities in rat liver. *Biochem Pharmacol.*, **51**, (1): 39-45.
- Perry MC, Demeule M, Regina A, Moundjian R and Beliveau R. 2010. Curcumin inhibits tumor growth and angiogenesis in glioblastoma xenografts. *Mol Nutr Food Res.*, **54** (8): 1192-1201.
- Podolsky DK, Camilleri M, FitzJG, Kalloo AN, Shanahan F and Wang TC. 2016. Yamada's Textbook of Gastroenterology. 6th ed. John Wiley and Sons, Texas, pp. 1537-3070.
- Prout J, Jones T and Martin D. (2014). Advanced Training in Anaesthesia. OUP Oxford. pp. 166.
- Ray SD, Mumaw VR, Raje RR and Fariss MW. 1996. Protection of acetaminophen-induced hepatocellular apoptosis and necrosis by cholesteryl hemisuccinate pretreatment. *J Pharmacol Exp Ther.*, **279**, (3): 1470-1483.
- Ryder SD and Beckingham JJ. 2001. Other causes of parenchymal liver disease. *Bmj*, **322** (7281): 290-292.
- Salama SM, Abdulla MA, AlRashdi AS, Ismail S, Alkiyumi SS and Golbabapour S. 2013. Hepatoprotective effect of ethanolic extract of *Curcuma longa* on thioacetamide induced liver cirrhosis in rats. *BMC Complement Altern Med.*, **13** (1): 56.
- Sarkar A, De R and Mukhopadhyay AK. 2016. Curcumin as a potential therapeutic candidate for *Helicobacter pylori* associated diseases. *World J Gastroenterol.*, **22** (9): 2736.
- Somchit MN, Zuraini A, Ahmad Bustamam A, Somchit N., Sulaiman MR and Noratunlina R., 2005. Protective Activity of Turmeric (*Curcuma longa*) in Paracetamol-induced Hepatotoxicity in Rats. *Int J Pharmacol.*, **1**: 252-256.
- Tung BT, Hai NT and Son PK. 2017. Hepatoprotective effect of phytosome curcumin against paracetamol-induced liver toxicity in mice. *Braz J Pharm Sci.*, **53** (1).
- Twycross AM, Parker R, McKeever S and Wiseman T. 2017. An integrative review of interventions to support parents when managing their child's pain at home. *Pain Manag Nurs.*, **19** (2): 139-156.
- Wang ME, Chen YC, Chen IS, Hsieh SC, Chen SS and Chiu CH. 2012. Curcumin protects against thioacetamide-induced hepatic fibrosis by attenuating the inflammatory response and inducing apoptosis of damaged hepatocytes. *J Nutr Biochem.*
- Watkins PB and Seeff LB. 2006. Drug-induced liver injury: summary of a single topic clinical research conference. *Hepatology*, **43** (3): 618-631.
- Woolley D and Woolley A. 2017. Practical toxicology: evaluation, prediction and risk, third ed., CRC press, pp. 330.
- Yadav MK, Yadav KS and Patil S. 2017. Characterization of anti-diabetic herbs & potential therapeutic agents in Indian species: A Review. *IOSR J Appl Dent Med Sci.*, **16** (2): 70-78.
- Yoon E, Babar A, Choudhary M, Kutner M, Pysopoulos N. 2016. Acetaminophen induced hepatotoxicity: a comprehensive update. *J Clin Gastroenterol Hepatol.*, **4** (2): 131-142.

Interaction of Atorvastatin and CX3CR1/Fractalkine in Androgen-Dependent Prostate Cancer Cells: Effect on PI3K Pathway

Belal A. Al-Husein^{*}, Nizar M. Mhaidat and Razan M. Sweidan

Department of Clinical Pharmacy, Faculty of Pharmacy, Jordan University of Science and Technology, P.O. Box 3030, Irbid 22110, Jordan

Received April 29, 2019; Revised July 29, 2019; Accepted August 31, 2019

Abstract

Prostate cancer (PC) management lacks any molecular targeted therapies. Statins have shown anticancer effects against PC in both in vitro and in vivo studies. CX3CR1 is a receptor expressed by many cancer cell types, including PC. In this research, we studied the effect of interaction of atorvastatin and CX3CR1/fractalkine on androgen-dependent PC cell line 22Rv1 compared to non-tumorigenic prostatic cells, RWPE-1. Experimental settings were based on investigating the effect of atorvastatin on viability of 22Rv1 and RWPE-1 in the presence and absence of fractalkine. Neutralizing antibody specific for fractalkine was used to neutralize the activity of the receptor in these experiments. MTT viability assay, adhesion assay, and Western blot analysis for expression levels of CX3CR1, phosphorylated Akt and GSK-3 were applied. Results showed that fractalkine partially reversed the 50% inhibition of proliferation mediated by atorvastatin on proliferation and adhesion of 22Rv1 cancer cells. Similar effects were not noticed with normal RWPE-1 cells. Western blotting showed a dose-dependent reduction in the expression of CX3CR1, levels of p-Akt and p-GSK-3 in the presence of fractalkine. This effect was further enhanced when the effect of fractalkine was neutralized using specific antibody. Findings from this study revealed that deprivation of fractalkine is a potential mechanism to enhance anti-proliferative effects of atorvastatin on androgen-dependent prostate cancer cells with no effect on normal cells.

Keywords: Prostate Cancer, Fractalkine, Fractalkine receptor, Atorvastatin, Akt, glycogen synthase kinase-3.

1. Introduction

Prostate cancer (PC) is a major public health problem worldwide and is the second leading cause of cancer deaths among males in the United States (Siegel et al., 2019). PC is characterized by an uncontrolled growth of cancerous prostate cells in male reproductive system. Treatment of PC is highly dependent on stage of the disease. Options available for treatment include watchful waiting, surgery, radiation therapy, androgen deprivation therapy and chemotherapy. Furthermore, immunotherapies have been developed, such as the tumor vaccine sipuleucel-T, and pembrolizumab and were recently incorporated into cancer treatment guidelines (NCCN, 2017). To date, no molecular targeted therapies have been developed for PC.

Chemokines are cytokines that have a wide range of physiological activities such as the ability to stimulate the migration of cells (chemotaxis) and angiogenesis (Luster, 1998). Chemokines and their receptors are extensively expressed in tumors, with different cancer types having different chemokine/receptor expression profiles (Balkwill, 2003). Many studies have illustrated the effect of chemokine-receptor signaling on tumorigenesis process

by promoting tumor growth and progression, angiogenesis, metastasis and modifying the tumor microenvironment to serve the tumor cells' growth (Chow and Luster, 2014). CX3C chemokine receptor 1 (CX3CR1) is a seven-transmembrane G protein-coupled receptor and is considered the only human receptor that binds fractalkine (FKN) or CX3CL1 (Bachelierie et al., 2013). CX3CR1 is expressed in several immune cells, such as natural killer cells (Imai et al., 1997), monocytes/macrophages (Segerer et al., 2002), B and T lymphocytes (Wu, 2014), and microglial cells (Nishiyori et al., 1998). In addition, expression of CX3CR1 has been shown in neurons (Meucci et al., 2000) and many tumors including gliomas, breast, ovarian, and prostate cancers (Ferretti et al., 2014). CX3CR1 has a unique and sole ligand, that is FKN (Macor, 2012). FKN is found in two forms: anchored FKN that functions as an adhesion molecule (Bazan et al., 1997) and soluble FKN which functions as a chemoattractant molecule (Garton et al., 2001). FKN was shown to be overexpressed in PC spinal-metastatic sites compared to primary tumor sites, thus promoting spinal metastasis (Liu et al., 2018). The main source of FKN in spinal tissues is differentiated osteoblasts (Shulby et al., 2004) which drive chemotaxis and homing of PC cells to bone tissue. Normal epithelial prostatic cells and cancerous ones express

^{*} Corresponding author e-mail: belalhusein@just.edu.jo.

^{*} **Abbreviations:** PC: Prostate cancer; FKN: fractalkine; GSK-3: glycogen synthase kinase-3; ATCC: American Type Culture Collection; DMSO: Dimethyl sulfoxide; ANOVA: analysis of variance; FNAb: fractalkine neutralizing antibody, EDTA: Ethylenediaminetetraacetic acid. PBS: Phosphate buffer saline, HMG-CoA: 3-hydroxy-3-methylglutaryl coenzyme A.

CX3CR1 on their surfaces. The expression, however, reduces as cells become androgen-independent (Xiao et al., 2012), indicating a greater role for CX3CR1 in androgen-dependent PC. Stimulation of CX3CR1 in PC cells by FKN will activate downstream signaling pathways, including MAPK, PI3K, and PLC pathways. No known chemicals have the ability to downregulate CX3CR1 expression, and one group used small molecule inhibitors to study the effects of CX3CR1 inhibition (Stout et al., 2018).

Statins are lipid-lowering agents which act by inhibiting HMG-CoA reductase enzyme. Statins are used in practice for management of hypercholesterolemia. Anticancer effects of statins are mediated directly by lowering cholesterol levels and affecting growth factor receptor signaling (Gbelcova et al., 2017), or by indirect "pleiotropic" effects (Ciofu, 2012). Statins affect PC cells by lowering cholesterol levels in lipid rafts and impairing signal transduction pathways involved in cell survival (Zhuang et al., 2005). Pleiotropic effects of statins include anti-proliferative, anti-angiogenic, and pro-apoptotic effects (Kavalipati et al., 2015). Statins affect multiple signaling pathways, including PI3K/Akt and GSK pathways. Atorvastatin is considered one of the most effective statins with a preferable safety profile. A meta-analysis by Bansal et al. showed that statins use was associated with a reduction in the risk of developing PC (Bansal et al., 2012). In addition, statins showed promising results as therapeutic agents for PC management, such as radio sensitization and direct killing effect on PC cells (He et al., 2012). Statin users were shown to have favorable clinical presentation after brachytherapy in localized PC patients (Moyad et al., 2005), reduced levels of prostate-specific antigen (PSA) (Khosropanah et al., 2011), reducing risk of PC recurrence after radical prostatectomy (Hamilton et al., 2010), and reduced mortality (Yu et al., 2013). Atorvastatin decreased FKN/CX3CR1 expression in peripheral blood mononuclear cells in coronary artery disease patients (Damás et al., 2005). It also reduced CX3CR1 levels in peripheral monocytes in patients with Crohn's disease (Grip et al., 2008). It is unknown whether atorvastatin affects the expression of CX3CR1 in PC cells and the impact of such effect is still largely unknown.

In this study, we investigated the effect of atorvastatin on androgen-dependent PC cells, focusing on FKN/CX3CR1 axis. The effect was evaluated via studying cell proliferation, cell adhesion and detecting the expression of CX3CR1 and downstream targets of PI3K pathway, namely Akt and GSK-3 α/β to demonstrate the molecular mechanism of such an effect.

2. Materials and Methods

2.1. Cell Culture

Cell lines were purchased from the American Type Culture Collection (ATCC). Two cell lines were used: androgen-dependent PC cells, 22Rv1 (ATCC® CRL-2505™), and normal prostatic epithelial cells, RWPE-1 (ATCC® CRL-11609™). The 22Rv1 cells were cultured in RPMI high glucose media (Euroclone, Cat# ECB9006L) which contained 1% penicillin/streptomycin (Euroclone, Cat# ECB3001D) and 10% fetal bovine serum (Biowest, Cat# S1600). RWPE-1 cells were cultured in

Keratinocyte Serum-Free Medium (K-SFM, Gibco, Cat# 10724-011) after the addition of K-SFM supplements kit (Cat# 37000-015, providing 0.05 mg/mL bovine pituitary extract and 5 ng/mL recombinant epidermal growth factor). Cells were incubated at 37°C and 5% CO₂. Media replacement was performed every two days.

2.2. Drug Preparation

Atorvastatin calcium salt trihydrate (Sigma-Aldrich, PZ0001) was dissolved in Dimethyl sulfoxide (DMSO, Santa Cruz Biotechnology, SC-358801) to prepare stock solutions of 10 mM. The drug was aliquoted and stored at -20°C.

2.3. Study Design

Both cell lines were cultured with and without Recombinant Human Full Length CX3CL1/Fractalkine (R&D Systems, Cat# 365-FR-025/CF) with different concentrations of atorvastatin (1, 2, 5, 10 and 20 μ M) vs. vehicle-control and incubated for 48 hrs. Then, effects of therapies were studied using the following assays:

2.4. MTT Cell Proliferation Assay

A total of 1×10^5 cells/200 μ l of each cell line was seeded into a 96-well plate for 24 hrs. The media was withdrawn after that and 200 μ l of variable concentrations of atorvastatin (1, 2, 5, 10 and 20 μ M) vs. vehicle-control were added in triplicates. Then, plates were incubated for 48 hrs and 5 μ g/mL FKN neutralizing antibody (FNAb) (R&D System, Cat# MAB3652) was added for 30 minutes, according to previously published work (Shulby et al., 2004). Afterwards, 10 μ l of a freshly prepared MTT solution (prepared by dissolving 0.5 mg of MTT powder in 1 mL of used culture media) was added to each well. After 4 hrs of incubation at 37°C, media was removed and 200 μ l of DMSO was added to each well to dissolve formed formazan crystals. The plate was kept at room temperature in the dark and absorbance was read at 570 nm using microplate reader (EZ Read 400 microplate reader, Biochrom, UK). The same procedure was done in quadruplicates for each concentration while adding FKN 50 ng/mL for 24 hrs, according to previously published work (Guo et al., 2012) for both cell lines.

2.5. Adhesion Assay

A 24-well plate was coated with a monolayer of 50 nM of FKN according to previously published data (Fujita et al., 2012). Coating was performed by diluting FKN with phosphate-buffered saline (PBS, Euroclone, Cat# ECB4053L) and then adding it to the plate and allowing it to dry overnight under UV-light for sterilization. Both cell lines were plated on a different 24-well plates and cultured until 70% confluent, then treated with atorvastatin (1, 2, 5, 10 and 20 μ M) vs. vehicle-control for 48 hrs, each concentration in quadruplicates. Afterwards, cells were treated with 5 μ g/mL of FNAb for 30 min. Next, cells were washed with PBS and were then harvested by adding trypsin-EDTA (Euroclone, Cat# ECB3052D) to each well for 5 minutes. Cells were then collected, rewashed with PBS and then were seeded on the coated plates and incubated at 37°C, 5% CO₂. After 1 hour, cells that didn't attached were washed off, remaining cells were fixed with 2% paraformaldehyde for 5-10 min. Crystal violet stain (prepared by dissolving 2 g crystal violet in 20 mL of 95% ethyl alcohol then adding them to 0.8 g ammonium oxalate

monohydrate that was dissolved in 80 mL deionized water) was applied. The stain was added to each well and incubated at RT for 30 min, subsequently distilled H₂O was used to wash off excess stain. Cells were counted under inverted light microscope. The same procedure was repeated for both cell lines without adding FNAb.

2.6. Western Blotting

A total of 1×10^4 cells of each cell line were seeded in a 6-well plate until 70% confluence. Atorvastatin (1, 2, 5, 10 and 20 μ M) vs vehicle-control was added in duplicates for each concentration for 48 hrs. FKN 50 nM was added to each cell line for 15 minutes. Media was then removed, and cells were washed with ice-cold PBS. A total of 500 μ L of ice-cold lysis buffer (RIPA buffer 10x (Abcam, Cat# ab156034) diluted to 1x with PBS, with the addition of Pierce Protease and Phosphatase Inhibitor Mini Tablets (ThermoFisher Scientific, Cat# A32959), 1 tablet per 10 ml of lysis buffer) was added to each well for 5 minutes. Cells were then scraped and collected in an eppendorf tube. After 30 minutes of incubation on ice, lysates were cleared by centrifugation, and protein concentration was determined by DCTM protein assay (Bio-Rad, Cat# 500-0116). Samples were mixed with 5x laemmli buffer. Equal amounts of protein were loaded into 4–20% Mini-PROTEAN[®] TGXTM polyacrylamide gel (Bio-Rad, Cat# 4561094DC). Afterwards, proteins were electroblotted on UltraCruz[®] Nitrocellulose Pure Transfer Membranes (Santa Cruz Biotechnology, Cat# sc-3724) for 1 hour at 250 mAmp constant current. Protein bands were first detected on the membrane using Ponceau S solution (1g of Ponceau S (Cat# ab146313) + 50 mL acetic acid, completed to 1 L with distilled H₂O). Blots were incubated for 1 hour with 1.25% bovine serum albumin (Sigma Aldrich, Cat# A9418) in PBS then washed three times with PBS containing 1% Tween (PBST) and incubated overnight at 4°C with a 1:1000 Phospho-Akt (pSer473) antibody (Cell Signaling, Cat# 9271). This was followed by washing membrane and probing with 1:5000 secondary HRP conjugated anti-rabbit IgG antibody (Cell Signaling, Cat#7074s). Blots were re-probed with 1:1000 β -actin primary antibody (Abcam, Cat# 8227) followed by 1:5000 secondary HRP conjugated anti-rabbit IgG antibody (Cell Signaling, Cat#7074s). Same procedure was repeated using 1:1000 CX3CR1 (Abcam, Cat# ab8021), 1:1000 Phospho-GSK-3 α/β (Ser21/9) antibody (cell signaling, Cat# 9331), and they were re-probed using 1:1000 GAPDH (Abcam, Cat# ab9485). For the second group, the same procedure was repeated after treating cells with (5 μ g/mL) of FNAb for 30 minutes (R&D System, Cat# MAB3652). Membranes were developed using Amersham ECL Select Western Blotting Detection Reagent (GE Healthcare, Europe GmbH, Cat# RPN2235) and were imaged using C-Digit[®] Blot Scanner (LI-COR, Lincoln, NE). Bands were quantified using the provided Image StudioTM Software version 5.0 for the C-DiGit Blot Scanner.

2.7. Statistical Analysis

All data was presented as mean \pm SEM. To determine significant differences between treatment and control groups, we used the one-way analysis of variance (ANOVA) and conducted post-hoc multiple comparison

analysis. The significance was set at a P value of less than 0.05.

3. Results

In this study, we evaluated the effect of atorvastatin treatment on androgen-dependent prostate cancer cell lines in the presence or absence of FKN. The latter effect was achieved by the addition of FNAb. We used normal prostate epithelial cell lines as control for comparison.

3.1. Effects of Atorvastatin/FKN Interaction on Proliferation

Figure 1 shows the effect of atorvastatin treatment on proliferation of 22Rv1 and RWPE-1 cells. In the presence of FKN, atorvastatin treatment had no effect on viability of RWPE-1 cells; however, it significantly suppressed viability of 22Rv1 cells at a concentration of 20 μ M. When FKN was blocked by FNAb, atorvastatin-induced growth inhibition was enhanced in both cell lines. Cell proliferation was significantly reduced at 20 μ M and 10 μ M of atorvastatin treatment in RWPE-1 and 22Rv1 cells, respectively (Figure 1).

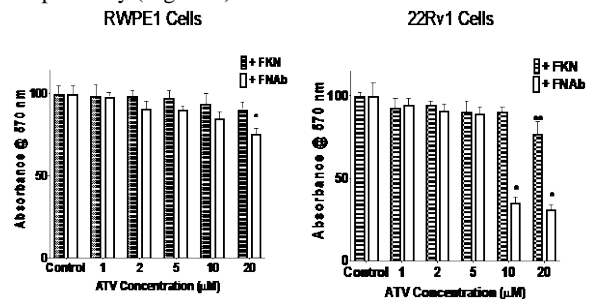


Figure 1. The effect of interaction of atorvastatin and FKN on proliferation of 22Rv1 PC cells compared to RWPE-1 non-tumorigenic cells. FKN: fractalkine; FNAb: fractalkine neutralizing antibody. (*, $P < 0.05$; **, $P < 0.005$)

3.2. Effects of Atorvastatin /FKN Interaction on Adhesion

Adhesion of cells to FKN-coated surfaces is shown in Figure 2. Atorvastatin treatment did not affect adhesion of RWPE-1 cells irrespective of the availability of FKN. On the other hand, atorvastatin induced a dose-dependent inhibition of 22Rv1 cell adhesion in the presence of FKN but not to a significant level compared to control treatment. However, neutralizing the effect of FKN by FNAb enhanced atorvastatin inhibition of 22Rv1 cell adhesion which was significant at 10 μ M concentration of atorvastatin (Figure 2).

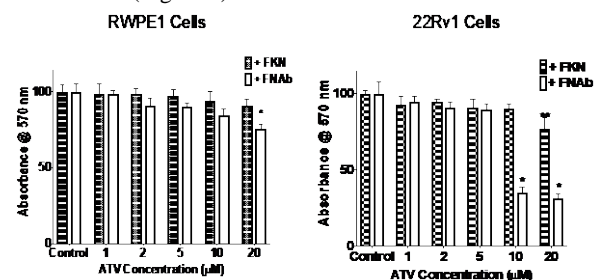


Figure 2. The effect of interaction of atorvastatin and FKN on adhesion of 22Rv1 PC cells compared to RWPE-1 non-tumorigenic cells to FKN coating material. FKN: fractalkine; FNAb: fractalkine neutralizing antibody. (**, $P < 0.005$; ***, $P < 0.0005$;))

3.3. Effects of Atorvastatin/FKN Interaction on CX3CR1 expression and downstream signaling pathways

To further understand the ATV-FKN-CX3CR1 interaction, we investigated the molecular effects of atorvastatin treatment on both cell lines in the presence of FKN as shown in Figure 3. Atorvastatin reduced expression of CX3CR1 in both 22Rv1 and RWPE-1 cells in a dose-dependent manner. In the absence of atorvastatin treatment, the presence of FKN with or without its neutralizing antibody did not alter expression of CX3CR1 compared to vehicle-treated control groups in both cell lines (Figure 3, left panel). In concordance to findings

from viability studies, atorvastatin treatment significantly reduced expression of CX3CR1 at concentrations of 10 and 20 μM in 22Rv1 PC cells, in which neutralizing FKN enhanced the effects of atorvastatin (Figure 3, left panel). Atorvastatin reduced levels of phosphorylated (active) Akt and GSK-3 in both cell lines with greater suppression of expression in 22Rv1 cells (Figure 3, middle and right panels). Similarly, atorvastatin's effect on active Akt and GSK-3 levels was further enhanced when FKN was blocked using FNAb, starting at 10 μM concentration of atorvastatin in 22Rv1 cells.

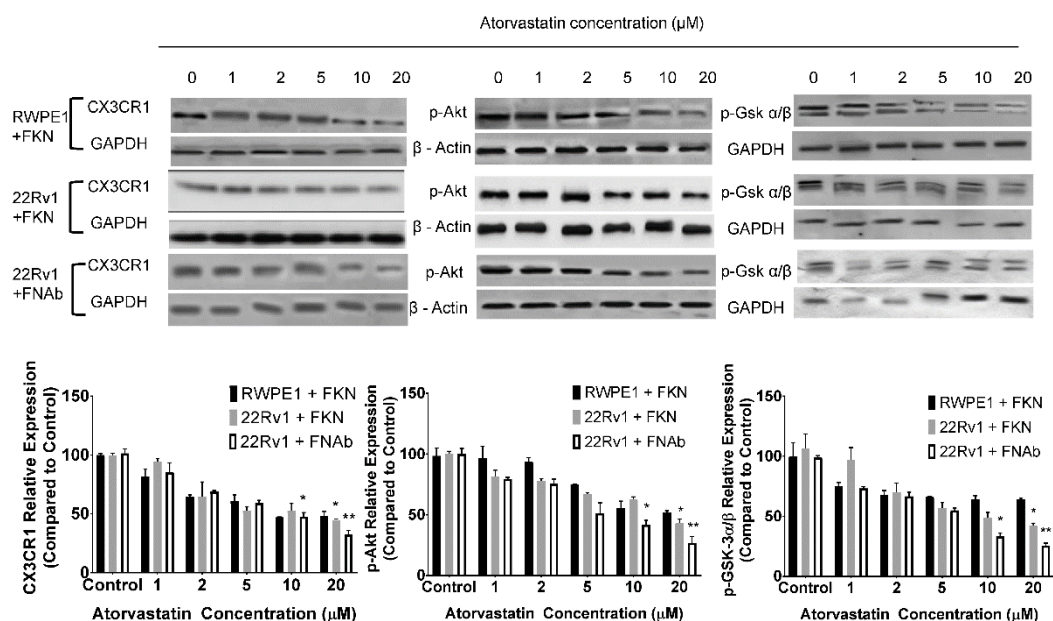


Figure 3. The effect of interaction of atorvastatin and FKN on expression of CX3CR1, p-Akt and p-GSK-3 α/β in 22Rv1 PC cells and RWPE-1 non-tumorigenic cells. Top panel represent Western blot bands for the indicated proteins and the bottom panel indicates densitometric analysis for the expression of each protein compared to the respective vehicle-treated control group. FKN: fractalkine; FNAb: fractalkine neutralizing antibody. (*, $P < 0.05$; **, $P < 0.005$)

4. Discussion

In this study, we have shown the ability of atorvastatin to reduce proliferation and adhesion of 22Rv1 cells in the presence of FKN. These effects of atorvastatin were further enhanced with the use of FNAb to neutralize FKN. On the other hand, we can view those results as that atorvastatin induced reduction of proliferation and adhesion of 22Rv1 cells in the presence of FNAb, and that effect was partially reversed in the presence of FKN. This could suggest the future use of FNAb in combination with other anticancer agents to enhance their effects. Growth and adhesion inhibition induced by atorvastatin was more substantial in 22Rv1 cells compared to RWPE-1 cells. This finding supports a greater selectivity for atorvastatin effects on cancer cells compared to non-cancerous ones further reflecting the potential margin of safety for using atorvastatin. In previous work, we have studied the effect of simvastatin on proliferation of LNCaP cells and it was much higher than what we found using atorvastatin (a more potent statin) (Kochuparambil et al., 2011). Some recent work shows a higher expression profile of multiple lipids in LNCaP cells compared to 22Rv1 cells (Sorvina et

al., 2018). This might explain the reduced sensitivity of 22Rv1 cells to statins, compared to LNCaP cells.

Cell adhesion is essential for growth and survival of cancer cells, as well as cell-to-cell communication (Lodish et al., 2000). Furthermore, cancer cell adhesion is an important step that mediates metastasis to distant sites (Chen, 2012). Progression to metastasis in PC reduces 5-year survival down to 30% (American Cancer Society, 2018). Homing molecules are very important in metastasis of cancer cells in general. Those molecules include integrins, chemokines, as well as selectins. We have previously studied and found an association between integrin $\alpha\beta3$ located on PC-3 cells and its adhesion potential to ICAM-1 in the presence of simvastatin (Al-Husein et al., 2013). Our current study showed reduced adhesion of 22Rv1 cells in response to atorvastatin treatment. This effect was shown in the presence of FNAb while there was no significant effect in the presence of FKN or in normal epithelial prostatic cell, RWPE-1. FKN and its receptor have been shown to enhance the migration of PC cells toward osteoblasts and to promote their adhesion (Shulby et al., 2004). Thus, impairing the interaction between FKN and its receptor could be a promising strategy to prevent progression and metastasis of PC cells to bone, a common site for disease metastasis.

To the best of our knowledge, this is first study to show the ability of atorvastatin to reduce the expression of CX3CR1 in 22Rv1 cells in a dose-dependent fashion. This effect was enhanced by blocking the effect of FKN by FNAbs. This could mean a reduction of both CX3CR1-mediated adhesion as well as CX3CR1-mediated signaling. The latter effect could have multiple implications as it means blockade of both adhesion-mediated signaling facilitated by anchored FKN, or FKN-mediated signaling as a soluble mediator. In addition, downregulation of CX3CR1 prevents the migration of PC cells towards osteoblast cells which bind to FKN on their surfaces (Mantovani, 1999). Collectively, this could be of great importance in management of not only PC, but also lung and kidney cancers, especially in the prevention of spinal metastasis (Liu et al., 2017). Multiple studies have also demonstrated the effect of atorvastatin on the expression of CX3CR1 in patients with coronary artery disease (Kureishi et al., 2000, Gotto, 2009, Nawrocki et al., 1995). Our results are in agreement with earlier studies revealing atorvastatin suppression for of CX3CR1 expression.

Signaling through the PI3K pathway results in activation of downstream Akt and GSK-3 molecules which are involved in survival and apoptotic cellular processes (Shulby et al., 2004). PI3K/Akt/GSK pathway is a major player involved in many tumor types. Simultaneously, FKN/CX3CR1 axis activation results in activation of PI3K pathway (Mantovani, 1999). Akt is has been found to be amplified in many tumorigenic processes and its presence is related to more aggressive tumors (Mitsiades et al., 2004). GSK-3 is also a downstream target in PI3K pathway and its levels are elevated in PC as it is highly involved in cell proliferation, apoptosis, and migration (Rinnab et al., 2008). Atorvastatin treatment of 22Rv1 cells reduced the level of phosphorylated/active Akt (S473), that is known to be associated with effects on cell proliferation (Gao et al., 2003), survival (Harashima et al., 2012) {Gao, 2003 #55}, invasion (Shukla et al., 2007) and angiogenesis (Jiang and Liu, 2008). Similarly, levels of phosphorylated/inactive GSK-3 α/β (S9/21) were decreased in response to atorvastatin in 22Rv1 cells. This effect on phosphorylation was further enhanced by FNAbs addition. The inhibition of phosphorylation of GSK-3 is linked to inhibition of adhesion as well effects on transcription factors related to cell cycle progression and proliferation (El Touny and Banerjee, 2007). In agreement with our work, effect on cell cycle activation was also noticed to be mediated by FKN through effects on cyclin E and CDK2 CKD 2 and was reversed by FNAbs (Tang et al., 2015). We provide additional information on the inhibitory effect of atorvastatin on the phosphorylation of Akt and GSK-3 α/β in PC cells, which comes in harmony with other studies which investigated the impact of using simvastatin on LNCAP cells (Kochuparambil et al., 2011). Collectively, results show that combined use of atorvastatin and FKN further enhanced the inhibition of PI3K pathway, a major altered pathway during tumorigenesis, ultimately mediating anti-proliferative and anti-apoptotic properties (D'Haese et al., 2010).

The choice of atorvastatin in our study seems appealing as it is considered now as one of the most effective statins because of its significant reduction not only to LDL levels but also to other lipids such as triglycerides (Expert Panel

on Detection and Treatment of High Blood Cholesterol in, 2001). One study has shown that a single daily dose of 10 mg of atorvastatin in 22 subjects can achieve a median concentration 10 μ M, which was within the range of concentrations used in this study (Reddy et al., 2011). A 10 mg dose of atorvastatin is considered the minimum dose used to treat hypercholesterolemia (Medscape, 2019).

5. Conclusions

Atorvastatin induces anti-proliferative effect that is enhanced by blocking the effect of FKN by FNAbs in PC. Moreover, atorvastatin inhibits cell adhesion of PC cells and subsequently could potentially prevent metastasis. Both effects suggest an anticancer and anti-metastatic effect of the combination of atorvastatin and FKN inhibition. Additionally, it decreases the active phosphorylated levels of Akt and GSK-3 α/β . On the other hand, our study found minimal negative impact of this dual inhibition on normal prostatic epithelial cells. Figure 4 is an illustration which summarizes the findings of this study.

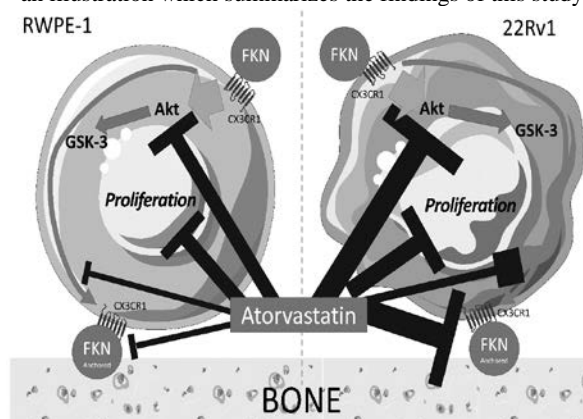


Figure 4. Schematic representation of findings of this study. Thickness of inhibition of arrow relatively expresses extent of inhibition.

Acknowledgements

The research was funded by grant number 20170050 to B.A. from the Deanship of Scientific Research of the Jordan University of Science and Technology.

References

- Al-Husein, B., Goc, A. & Somanath, P. R. 2013. Suppression of interactions between prostate tumor cell-surface integrin and endothelial ICAM-1 by simvastatin inhibits micrometastasis. *J Cell Physiol*, **228**, 2139-48.
- American Cancer Society. (2018). "Cancer Facts & Figures 2018". Atlanta: American Cancer Society. <https://www.cancer.org/content/dam/cancer-org/research/cancer-facts-and-statistics/annual-cancer-facts-and-figures/2018/cancer-facts-and-figures-2018.pdf> (Feb. 2, 2019).
- Bachelerie, F., Ben-Baruch, A., Burkhardt, A., Combadiere, C., Farber, J., Graham, G., Horuk, R., Sparre-Ulrich, A., Locati, M. & Luster, A. 2013. Update on the extended family of chemokine receptors and introducing a new nomenclature for atypical chemokine receptors. *Pharmacol Rev*, **66**, 71P-79.
- Balkwill, F. 2003. Chemokine biology in cancer. *Semin Immunol*, **15**, 49-55.

- Bansal, D., Undela, K., D'cruz, S. & Schifano, F. 2012. Statin use and risk of prostate cancer: a meta-analysis of observational studies. *PLoS one*, **7**, e46691.
- Bazan, J. F., Bacon, K. B., Hardiman, G., Wang, W., Soo, K., Rossi, D., Greaves, D. R., Zlotnik, A. & Schall, T. J. 1997. A new class of membrane-bound chemokine with a CX3C motif. *Nature*, **385**, 640-4.
- Chen, Y. 2012. Cell Adhesion Assay. *Bio-protocol Bio101*: e98.
- Chow, M. T. & Luster, A. D. 2014. Chemokines in cancer. *Cancer Immunol Res*, **2**, 1125-31.
- Ciofu, C. 2012. The statins as anticancer agents. *Maedica (Buchar)*, **7**, 377.
- D'haese, J. G., Demir, I. E., Friess, H. & Ceyhan, G. O. 2010. Fractalkine/CX3CR1: why a single chemokine-receptor duo bears a major and unique therapeutic potential. *Expert Opin Ther Targets*, **14**, 207-19.
- Damás, J. K., Boullier, A., Wæhre, T., Smith, C., Sandberg, W. J., Green, S., Aukrust, P. & Quehenberger, O. 2005. Expression of fractalkine (CX3CL1) and its receptor, CX3CR1, is elevated in coronary artery disease and is reduced during statin therapy. *Arteriosclerosis, thrombosis, and vascular biology*, **25**, 2567-2572.
- El Touny, L. H. & Banerjee, P. P. 2007. Akt-GSK-3 pathway as a target in genistein-induced inhibition of TRAMP prostate cancer progression toward a poorly differentiated phenotype. *Carcinogenesis*, **28**, 1710-1717.
- Expert Panel on Detection, E. & Treatment of High Blood Cholesterol In, A. 2001. Executive Summary of The Third Report of The National Cholesterol Education Program (NCEP) Expert Panel on Detection, Evaluation, And Treatment of High Blood Cholesterol In Adults (Adult Treatment Panel III). *JAMA*, **285**, 2486-97.
- Ferretti, E., Pistoia, V. & Corcione, A. 2014. Role of fractalkine/CX3CL1 and its receptor in the pathogenesis of inflammatory and malignant diseases with emphasis on B cell malignancies. *Mediators of inflammation*, **2014**.
- Fujita, M., Takada, Y. K. & Takada, Y. 2012. Integrins alphavbeta3 and alpha4beta1 act as coreceptors for fractalkine, and the integrin-binding defective mutant of fractalkine is an antagonist of CX3CR1. *J Immunol*, **189**, 5809-19.
- Gao, N., Zhang, Z., Jiang, B. H. & Shi, X. 2003. Role of PI3K/AKT/mTOR signaling in the cell cycle progression of human prostate cancer. *Biochem Biophys Res Commun*, **310**, 1124-32.
- Garton, K. J., Gough, P. J., Blobel, C. P., Murphy, G., Greaves, D. R., Dempsey, P. J. & Raines, E. W. 2001. Tumor necrosis factor-alpha-converting enzyme (ADAM17) mediates the cleavage and shedding of fractalkine (CX3CL1). *J Biol Chem*, **276**, 37993-8001.
- Gbelcova, H., Rimpelova, S., Ruml, T., Fenclova, M., Kosek, V., Hajslova, J., Strnad, H., Kolar, M. & Vitek, L. 2017. Variability in statin-induced changes in gene expression profiles of pancreatic cancer. *Sci Rep*, **7**, 44219.
- Gotto, A. M. 2009. Reducing cardiovascular risk in the metabolic syndrome: What we know and what we still need to know. *Heart Views*, **10**, 17.
- Grip, O., Janciauskiene, S. & Bredberg, A. 2008. Use of atorvastatin as an anti-inflammatory treatment in Crohn's disease. *Br J Pharmacol*, **155**, 1085-92.
- Guo, X., Pan, Y., Xiao, C., Wu, Y., Cai, D. & Gu, J. 2012. Fractalkine stimulates cell growth and increases its expression via NF-kappaB pathway in RA-FLS. *Int J Rheum Dis*, **15**, 322-9.
- Hamilton, R. J., Banez, L. L., Aronson, W. J., Terris, M. K., Platz, E. A., Kane, C. J., Presti, J. C., Amling, C. L. & Freedland, S. J. 2010. Statin medication use and the risk of biochemical recurrence after radical prostatectomy. *Cancer*, **116**, 3389-3398.
- Harashima, N., Inao, T., Imamura, R., Okano, S., Suda, T. & Harada, M. 2012. Roles of the PI3K/Akt pathway and autophagy in TLR3 signaling-induced apoptosis and growth arrest of human prostate cancer cells. *Cancer Immunol Immunother*, **61**, 667-76.
- He, Z., Mangala, L. S., Theriot, C. A., Rohde, L. H., Wu, H. & Zhang, Y. 2012. Cell killing and radiosensitizing effects of atorvastatin in PC3 prostate cancer cells. *J Radiat Res*, **53**, 225-33.
- Imai, T., Hieshima, K., Haskell, C., Baba, M., Nagira, M., Nishimura, M., Kakizaki, M., Takagi, S., Nomiyama, H., Schall, T. J. & Yoshie, O. 1997. Identification and molecular characterization of fractalkine receptor CX3CR1, which mediates both leukocyte migration and adhesion. *Cell*, **91**, 521-30.
- Jiang, B.-H. & Liu, L.-Z. 2008. AKT signaling in regulating angiogenesis. *Current cancer drug targets*, **8**, 19-26.
- Kavalipati, N., Shah, J., Ramakrishnan, A. & Vasawala, H. 2015. Pleiotropic effects of statins. *Indian J Endocrinol Metab*, **19**, 554-62.
- Khosropanah, I., Falahatkar, S., Farhat, B., Heidari Bateni, Z., Enshaei, A., Allahkhah, A. A. & Khosropanah, D. 2011. Assessment of atorvastatin effectiveness on serum PSA level in hypercholesterolemic males. *Acta Med Iran*, **49**, 789-94.
- Kochuparambil, S. T., Al-Husein, B., Goc, A., Soliman, S. & Somanath, P. R. 2011. Anticancer efficacy of simvastatin on prostate cancer cells and tumor xenografts is associated with inhibition of Akt and reduced prostate-specific antigen expression. *J Pharmacol Exp Ther*, **336**, 496-505.
- Kureishi, Y., Luo, Z., Shiojima, I., Bialik, A., Fulton, D., Lefer, D. J., Sessa, W. C. & Walsh, K. 2000. The HMG-CoA reductase inhibitor simvastatin activates the protein kinase Akt and promotes angiogenesis in normocholesterolemic animals. *Nat Med*, **6**, 1004-10.
- Liu, P., Liang, Y., Jiang, L., Wang, H., Wang, S. & Dong, J. 2018. CX3CL1/fractalkine enhances prostate cancer spinal metastasis by activating the Src/FAK pathway. *Int J Oncol*, **53**, 1544-1556.
- Liu, W., Bian, C., Liang, Y., Jiang, L., Qian, C. & Dong, J. 2017. CX3CL1: a potential chemokine widely involved in the process of spinal metastases. *Oncotarget*, **8**, 15213-15219.
- Lodish, H., Berk, A., Zipursky, S. & Et Al. 2000. Cell-Cell Adhesion and Communication. *Molecular Cell Biology*. 4th ed.
- Luster, A. D. 1998. Chemokines—chemotactic cytokines that mediate inflammation. *New England Journal of Medicine*, **338**, 436-445.
- Macor, J. E. 2012. **Annual Reports in Medicinal Chemistry**. Elsevier Science.
- Mantovani, A. 1999. The chemokine system: redundancy for robust outputs. *Immunol Today*, **20**, 254-7.
- Medscape. (2019). "Atorvastatin (Rx)". <https://reference.medscape.com/drug/lipitor-atorvastatin-342446> (July 29th 2019).
- Meucci, O., Fatatis, A., Simen, A. A. & Miller, R. J. 2000. Expression of CX3CR1 chemokine receptors on neurons and their role in neuronal survival. *Proceedings of the National Academy of Sciences*, **97**, 8075-8080.
- Mitsiades, C. S., Mitsiades, N. & Koutsilieris, M. 2004. The Akt pathway: molecular targets for anti-cancer drug development. *Curr Cancer Drug Targets*, **4**, 235-56.
- Moyad, M. A., Merrick, G. S., Butler, W. M., Wallner, K. E., Galbreath, R. W., Kurko, B. & Adamovich, E. 2005. Statins, especially atorvastatin, may favorably influence clinical

- presentation and biochemical progression-free survival after brachytherapy for clinically localized prostate cancer. *Urology*, **66**, 1150-1154.
- Nawrocki, J. W., Weiss, S. R., Davidson, M. H., Sprecher, D. L., Schwartz, S. L., Lupien, P. J., Jones, P. H., Haber, H. E. & Black, D. M. 1995. Reduction of LDL cholesterol by 25% to 60% in patients with primary hypercholesterolemia by atorvastatin, a new HMG-CoA reductase inhibitor. *Arterioscler Thromb Vasc Biol*, **15**, 678-82.
- Nccn. (2017). "NCCN Guidelines®". NCCN. https://www.nccn.org/professionals/physician_gls/default.aspx (November 28th, 2017).
- Nishiyori, A., Minami, M., Ohtani, Y., Takami, S., Yamamoto, J., Kawaguchi, N., Kume, T., Akaike, A. & Satoh, M. 1998. Localization of fractalkine and CX3CR1 mRNAs in rat brain: does fractalkine play a role in signaling from neuron to microglia? *FEBS letters*, **429**, 167-172.
- Reddy, P., Ellington, D., Zhu, Y., Zdrojewski, I., Parent, S. J., Harmatz, J. S., Derendorf, H., Greenblatt, D. J. & Browne, K., Jr. 2011. Serum concentrations and clinical effects of atorvastatin in patients taking grapefruit juice daily. *British journal of clinical pharmacology*, **72**, 434-441.
- Rinnab, L., Schutz, S. V., Diesch, J., Schmid, E., Kufer, R., Hautmann, R. E., Spindler, K. D. & Cronauer, M. V. 2008. Inhibition of glycogen synthase kinase-3 in androgen-responsive prostate cancer cell lines: are GSK inhibitors therapeutically useful? *Neoplasia*, **10**, 624-34.
- Segerer, S., Hughes, E., Hudkins, K. L., Mack, M., Goodpaster, T. & Alpers, C. E. 2002. Expression of the fractalkine receptor (CX3CR1) in human kidney diseases. *Kidney Int*, **62**, 488-95.
- Shukla, S., MacLennan, G. T., Hartman, D. J., Fu, P., Resnick, M. I. & Gupta, S. 2007. Activation of PI3K-Akt signaling pathway promotes prostate cancer cell invasion. *Int J Cancer*, **121**, 1424-32.
- Shulby, S. A., Dolloff, N. G., Stearns, M. E., Meucci, O. & Fatatis, A. 2004. CX3CR1-fractalkine expression regulates cellular mechanisms involved in adhesion, migration, and survival of human prostate cancer cells. *Cancer Res*, **64**, 4693-8.
- Siegel, R. L., Miller, K. D. & Jemal, A. 2019. Cancer statistics, 2019. *CA Cancer J Clin*, **69**, 7-34.
- Sorvina, A., Bader, C. A., Caporale, C., Carter, E. A., Johnson, I. R. D., Parkinson-Lawrence, E. J., Simpson, P. V., Wright, P. J., Stagni, S., Lay, P. A., Massi, M., Brooks, D. A. & Plush, S. E. 2018. Lipid profiles of prostate cancer cells. *Oncotarget*, **9**, 35541-35552.
- Stout, M. C., Narayan, S., Pillet, E. S., Salvino, J. M. & Campbell, P. M. 2018. Inhibition of CX3CR1 reduces cell motility and viability in pancreatic adenocarcinoma epithelial cells. *Biochem Biophys Res Commun*, **495**, 2264-2269.
- Tang, J., Chen, Y., Cui, R., Li, D., Xiao, L., Lin, P., Du, Y., Sun, H., Yu, X. & Zheng, X. 2015. Upregulation of fractalkine contributes to the proliferative response of prostate cancer cells to hypoxia via promoting the G1/S phase transition. *Mol Med Rep*, **12**, 7907-14.
- Wu, Z. 2014. CX3CR1(+) B cells show immune suppressor properties. *J Biol Chem*, **289**, 22630-5.
- Xiao, L. J., Chen, Y. Y., Lin, P., Zou, H. F., Lin, F., Zhao, L. N., Li, D., Guo, L., Tang, J. B., Zheng, X. L. & Yu, X. G. 2012. Hypoxia increases CX3CR1 expression via HIF-1 and NFkappaB in androgen-independent prostate cancer cells. *Int J Oncol*, **41**, 1827-36.
- Yu, O., Eberg, M., Benayoun, S., Aprikian, A., Batist, G., Suissa, S. & Azoulay, L. 2013. Use of statins and the risk of death in patients with prostate cancer. *Journal of Clinical Oncology*, **32**, 5-11.
- Zhuang, L., Kim, J., Adam, R. M., Solomon, K. R. & Freeman, M. R. 2005. Cholesterol targeting alters lipid raft composition and cell survival in prostate cancer cells and xenografts. *J Clin Invest*, **115**, 959-68.

Biochemical Composition, Antioxidant Power and Anti-inflammatory of Dehulled *Sesamum indicum* Seeds and Its Coat Fraction

Laila Elhanafi^{1, 2*}, Zineb Benkhadda Benkhadda³, Chainae Rais⁴, Mariame Houhou^{5, 6}, Siham Lebtar^{7, 8}, Adil Channo⁹ and Hassane Greche^{2, 10}

¹ Laboratory of Functional Ecology and Environment, Faculty of Science and Technology of Fez; ² Laboratory of Engineering, Electrochemistry, Modeling and Environment, Faculty of Sciences DharMahraz; ³ Laboratory of Molecular Bases in Human Pathology and Therapeutic Tools, Faculty of Medicine and Pharmacy; ⁴ Laboratory of Botany, National Agency of Medicinal and Aromatic Plants, Taouanate; ⁵ Laboratory of Natural Resources and Environment, Polydisciplinary Faculty of Taza; ⁶ Laboratory of Bioactive Molecules, Faculty of Sciences and Technology of Fez; ⁷ Laboratory of Biotechnology, Environment and Quality, Faculty of Sciences, University Ibn Tofail, Kenitra; ⁸ Laboratory of Neuroendocrinology and Nutritional and Climatic Environment, Faculty of Sciences DharMahraz, University of Sidi Mohamed Ben Abdellah, Morocco; ⁹ Botany Laboratory, Leiden University, Leiden, Holland, ¹⁰ Applied Organic chemistry Laboratory, Faculty of Science and Technology of Fez, University of Sidi Mohamed ben Abdellah, Fes, Morocco

Received July 18, 2019; Revised August 30, 2019; Accepted September 12, 2019

Abstract

Sesamum indicum is one of the most important ancient oil crops in the world. In fact, this plant, in particular its seeds, is used for food, medicinal and industrial purposes. This article provides an evaluation of the biochemical composition, antioxidant and anti-inflammatory activities of dehulled sesame seeds *Sesamum indicum* and its coat fraction. Results analysis of our investigation showed that the level of total fatty oil, total protein and total sugars were present with 47.27%, 18.84% and 2.18% respectively. However; these compounds were significantly decreased in the coat fraction. On the contrary, the mineral content can be five times higher in the coat fraction, especially for calcium with a value of 831.11mg/100g, compared to dehulled seeds. Quantity of total phenolic and flavonoids were highest in the hydro-methanolic extract of seeds coat with 3.05±0.08mg GAE/g and 0.99±0.02 mg QE/g respectively. The same extract exhibited anti-inflammatory activity and antioxidant power, demonstrated by significantly decreasing in inflammation induced by carrageen in rats (85.56%), significant antioxidant activity (DPPH) (IC50: 2.12 mg/ml) and highest total antioxidant activity (95.5µg/ml). This study suggests that seeds coat of *sesamum indicum* contain interesting phytochemical potential and significant biological activities.

Keywords: *Sesamum indicum*; biochemical composition; mineral composition; phytochemical analysis; antioxidant activity; anti-inflammatory activity.

1. Introduction

Sesame (*Sesamum* genus) belongs to the family of Pedaliaceae that holds around 36 species (Bedigian *et al.*, 1986). Commonly called as “Simsim” in the Arabic world, it represents one of the most economically important and ancient crops. In terms of traditional and popular uses, the seeds are largely used in the cuisine preparation. Nutritionally, they are rich in fatty oil (44 - 58%), protein (18 - 25%), and carbohydrates (13.5%) (Bedigian *et al.*, 1986). The seed contains a high level of unsaturated fatty acids (Were *et al.*, 2006). Its protein fraction is rich in arginine, leucine and methionine amino acids (Namiki, 1995). Recently, studies have shed light on the interesting biological activities of sesame, especially the analgesic effect (Wu *et al.*, 2006), the antioxidant power (Cooney *et al.*, 2001) and the ability to reduce the plasma cholesterol (Moazzami *et al.*, 2006).

It is known that oxygen is the source of life of aerobic organisms; however, it can also represent a source of degradation for organisms (stress oxidative). In fact, it is the ultimate electron acceptor in the electron flow system. Therefore, most biological issues appear during the transfer of unpaired single electrons due to endogenous and exogenous bio processes, which lead to the development of free radicals (Davies, 2004), such as hydrogen peroxide H₂O₂, alkyl peroxides ROOH, superoxide O₂, hydroxyl radicals OH and peroxy ROO (Gülçin, 2012). ROS (Reactive Oxygen Species) residues are the result of several biological and biochemical impairments that affect nucleic acids, lipids, proteins and carbohydrates (Halliwell, 1990; Elmastaş *et al.*, 2006). An antioxidant is defined as a substance that has the ability to significantly delay or inhibit the oxidation process, in low concentrations compared to the oxidizable substrate (Halliwell, 1990). The source of antioxidants could be endogenous (ex: superoxide dismutases), or exogenous (ex:

* Corresponding author e-mail: laila-elhanafi@hotmail.fr.

flavonoids) (Arora *et al.*, 2002). Recently, a growing body of studies has focused on plant origin antioxidants as a safe substance (Namiki *et al.*, 1995). Phenolic compounds represent the major group of natural substances that act as primary antioxidants (Fawole, 2009). On the other hand, inflammation is one of the common manifestations of many diseases (Amabeoku, 2012). It is a biological response of exogenous and/or endogenous aggression such as infections caused by micro-organisms and damaged cells (Ferrero-Miliani *et al.*, 2007). The organism reacts by eliminating possible pathogens in order to revert the damaged tissue to its normal state (Lawrence *et al.*, 2007; Nathan, 2002). However, when inadequately controlled, inflammation can cause severe tissue damages (Alessandri *et al.*, 2013; Coussens *et al.*, 2002). Thus, the anti-inflammatory effect of steroidal and non-steroidal drugs has been widely studied (Barnes *et al.*, 1998; Landolfi *et al.*, 1994).

Sesame seeds are largely processed in many ways; "Tahini" is one of the food products obtained after industrial transformation of sesame seeds. Thus, dehulling is primarily used to obtain clear and white sesame seeds which are a main ingredient in the "Tahini" preparation. The coat fraction is undesirable (industrial residues) (Elleuch *et al.*, 2007). The aim of the current study is to demonstrate that the sesame by-products obtained by means of dehulling may have bio-medicinal properties. For this purpose, this research will shed light on the phytochemical composition, antioxidant effect and anti-inflammatory activity of the dehulled and seed coat of sesame.

2. Materials and Methods

2.1. Preparation of plant material

A Moroccan sesame sample was collected from the agricultural province of Taounat situated in the north of Morocco at 34° 33' North, 4° 39' West. To get fraction coat, raw seeds were soaked in water at room temperature to facilitate the peeling off the coat, the seeds were then dehulled manually. Seeds coat fraction (SC), which is very light in weight and brown in color, and dehulled seeds (DS) were separated and stored at 4 °C.

2.2. Biochemical composition

2.2.1. Total Oil content

Total oil content of SC and DS was extracted using the Soxhlet system (Abaza *et al.*, 2002). In fact, 2g of dried samples was extracted using hexane solvent in a Soxhlet extractor. The oil was then recovered by evaporating the solvent using a rotary vacuum evaporator. Total oil content was calculated according to the following formula (1):

(1) Total oil content (%) = (Weight of extract) / (Weight of sample) x 100

2.2.2. Total protein content

For determination of total nitrogen concentration, the Kjeldahl method was used as described by McKenzie and Wallace (McKenzie *et al.*, 1954). Then, the total nitrogen content was multiplied by 6.25 to determine the protein content of sesame seeds (Khalid *et al.*, 2003). Briefly, a sample of 1g was digested with 8 ml of concentrated H₂SO₄ into the Kjeldahl flask, in the presence of a catalyst

(potassium sulfate, copper sulfate) until the color of the mixture changed to greenish. Then, to distill the sample, 15 ml of NaOH (30%) was added using a semi-automatic distillation system. 4% boric solution was used to collect the produced nitrogen NH₃. The titration was conducted with H₂SO₄ in the presence of mixed indicator solution (bromocresol green and methyl red). The following equation (2) was used to estimate the total Nitrogen concentration:

(2) Total protein content (%) = 6.25 × [V (H₂SO₄) × N (H₂SO₄) × 0.014 × SW]

Where: V (H₂SO₄): volume of H₂SO₄ used for titration, N (H₂SO₄): the normality of H₂SO₄ used for titration, SW: sample dry weight. 0.014: mili equivalent of nitrogen.

2.2.3. Total soluble sugars

100mg of ground seeds of SC and DS was extracted with 4 ml of ethanol (80%); the mixture was then placed in a water bath at 80°C for 30 min. After centrifugation (10 min at 4500 rpm), the supernatant was collected and the sugar content was analyzed with anthrone reagent (0.2% (w/v) anthrone in sulfuric acid). The absorbance was read at 625 nm by using a spectrophotometer and then converted into its glucose equivalent (mg/g) (Dubois *et al.*, 1956).

2.2.4. Mineral content

The mineral contents, including potassium, phosphorus, calcium, sodium, magnesium, were analyzed by inductive coupled plasma mass spectrometry (ICP-MS) (Zhao *et al.*, 1994). Briefly, 0.1 g of dried seeds of SC and DS was digested using concentrated HCl for 5 hours. After being cooled, the sample was then diluted with de-ionized water. All samples were analyzed using ICP-MS.

2.2.5. Total Phenolic Content

For extracts preparations, methanol: water (70:30 v/v) was added to ground and dried samples of SC and DS, with constant shaking for 8 hours. The extracts were then filtered using Whatman filter paper and concentrated under reduced pressure. Total phenolic content of each hydro-methanolic extract was determined according to the method of Folin and Ciocalteu (1927), with minor changes. Briefly, the appropriate dilution of each extract was mixed with 1ml of the diluted Folin-Ciocalteu reagent. Then, 2 ml of 5% sodium carbonate solution was added. After incubation for 2 hours at room temperature, the absorbance was measured at 750 nm. Results are expressed as Gallic Acid Equivalents (GAE).

2.2.6. Total Flavonoids Content

To evaluate the total flavonoids content, 0.1ml of hydro-methanolic extracts of SC and DS were mixed with aluminium chloride methanolic solution (10%) and 0.1ml of sodium acetate. After incubation, the absorbance was measured at 415nm. Results are expressed as Quercetine equivalents (Ordonéz *et al.*, 2006).

2.3. Evaluation of the Antioxidant Activity

2.3.1. DPPH scavenging activity

The effect of extracts on the 1,1-diphenyl-2-picrylhydrazyl (DPPH) radical scavenging was estimated according to the method of Molyneux (Molyneux *et al.*, 2004) with minor modifications. Different concentrations of hydro-methanolic extracts were added to the DPPH

solution (0.5 mM), and then the mixture was incubated at room temperature for 30 min. The absorbance of the solution was measured at 517 nm. Ascorbic acid was used as a positive control. The proportion of the DPPH radical scavenging is calculated using the following equation (3):

$$(3) \% \text{ inhibition of DPPH radical} = [(Ac - Ae)/Ac] * 100$$

With Ac: Absorbance of the control and Ae: Absorbance of the extract.

The inhibition % of DPPH radical was then used to calculate IC50, which is the anti-radical concentration required to cause 50% of inhibition.

2.3.2. Total Antioxidant Capacity (TAC)

Total antioxidant capacity was carried out using the phosphomolybdenum method according to Prieto *et al.* (1999). The tubes, containing a mixture of hydro-methanolic extract solutions of SC or DS, and reaction solution (0.6 M sulfuric acid, 28mM sodium, and 4 mM of ammonium molybdate), were incubated at 95°C for 90 min. After the cooling process, the solution absorbance was measured at 695 nm. The antioxidant activity was expressed as ascorbic acid equivalents.

2.4. Evaluation of the anti-inflammatory activity

The anti-inflammatory activity of SC and DS was evaluated by the carrageenan induced rat paw oedema assay previously reported by Winter *et al.* (1962). Rats were divided into five groups, each containing five adult animals. Group I served as a negative control group receiving normal saline, groups II–IV were given topical application of cream formulated in our laboratory by mixing the neutral cream with each extract at doses of 10% and 15%. Diclofenac gel was used for group V, as a positive control group. Oedema was induced by subplantar injection of 0.1 ml carrageenan (1%, w/v) into the right hind paw of each rat. The paw size was measured just before the carrageenan injection, and then immediately at 3, 4, 5, and 6h after the injection of carrageenan. Percentage inhibition of oedema thickness in treated animals compared to the control group was calculated according to the following formula (4):

$$(4) \% \text{ inhibition of oedema} = [(Sc - St) / Sc] * 100$$

Sc: the Mean increase in paw size of control group; St: the mean increase in paw size of the treated groups.

2.5. Statistical analysis

Statistical analysis was performed using SYSTAT 12. Data were subjected to one-way analysis of variance (ANOVA) in order to determine significant differences among the treatments. The results were considered significant at $P < 0.05$.

3. Results

3.1. Proximate composition

The proximate chemical composition of SC and DS is illustrated in Table 1, total Oil, total protein and total soluble sugars were found to be higher in the whole fraction with 47.27%, 18.84 % and 2.18% respectively than

the coat fraction. Furthermore, we observed variations of mineral distribution between dehulled seeds and its coat fraction (Table 1). In fact, phosphorus was concentrated in the DS with 14.09 ± 1.28 mg/100g. Unlike calcium, which is almost 5 times higher in the coat fraction (831.11 ± 1.5 mg/100g) compared to dehulled seeds (166.28 ± 1.32 mg/100g). Also, the value of sodium was found to be 43.9% higher in SC than DS. As for potassium and

	Dehulled seeds	Seeds coat
Total oil%	47.27±0.6a	5.34±0.15b
Total Protein%	18.84±0.09a	7.57±0.1b
Total soluble sugars %	2.18±0.08a	0.75±0.03b
Mineral compounds		
Calcium(mg/100g)	166.28±1.5b	831.11±1.32a
Potassium(mg/100g)	414.6±4.56a	340.48±3.2a
Magnesium(mg/100g)	239.4±3.21a	278.58±2.5a
Sodium (mg/100g)	14.09±1.28a	25.12±2.67b
Phosphorus(mg/100g)	576.23±2.1a	76.41±1.81b

magnesium, they have the same quantity both in DS and SC with about 377 ± 4.56 and 258 ± 3.2 mg/100g.

Table 1. Biochemical composition of dehulled seeds and seeds coat of sesame

Levels of all components measured in the DS and SC fractions were found significantly different ($P > 0.05$). Data is presented as Means ± Standard Error (SD).

The effect of dehulling on total phenolic content and total flavonoid content is shown in Table 2, indicating that SC was the richest source of poly-phenols. In fact, the

Extract type	Total phenolic content (mg GAE /g)	Total flavonoids content (mg QE/g)
Dehulled seeds	1.13±0.07*	0.1 ± 0.04**
Seeds coat	3.05 ± 0.08*	0.99 ± 0.02**

value of total phenolic compounds and total flavonoids of SC was 37.4% and 67.54% higher than DS.

Table 2. Total phenolic and flavonoids content of dehulled and seeds coat (on dry weight basis)

Total phenolic (*) and flavonoids (**) content of the DS and SC fractions were found significantly different ($P > 0.05$). GAE: gallic acid equivalents; QE: Quercetin Equivalents. Data is presented as Means ± Standard Error (SD).

3.2. Evaluation of the antioxidant Activity

The extract of SC exceeded DS in regards to DPPH scavenging activity, in all doses used Fig.1. However, both extracts showed a low antioxidant activity when compared with the capacity of ascorbic acid to reduce DPPH. In fact, the inhibition percentage of DS was 23%, 51% and 59% for the concentrations of 5mg/ml, 10mg/ml and 15mg/ml respectively, compared to those of the ascorbic acid: 62%, 88% and 99% respectively within the same concentrations. In SC, the inhibition percentage of DPPH radical was 37%, 72% and 85% respectively within the same concentration. Based on Fig.1, the IC50 found for the extract of SC corresponded to 2.39mg/l, compared to ascorbic acid which has an IC50=2.12 mg/ml.

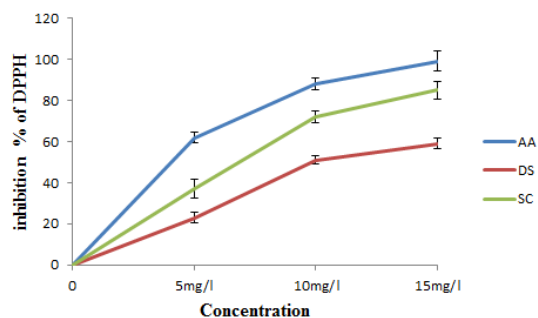


Figure 1. Antioxidant activities of the hydro-methanolic extracts of dehusled and seeds coat as assessed by the DPPH method compared to ascorbic acid. AA: ascorbic acid, DS: dehusled seeds, SC: seeds coat. Data is presented as Means \pm Standard Error (SD).

Concerning Total antioxidant capacity TAC, Fig.2 shows the total antioxidant capacity of SC and DS which increased with concentration of each extract. The value of TAC for SC hydro-methanolic extract showed 95.5 μ g/ml of ascorbic acid equivalent at 100 μ g/ml concentration, this value decreased by 43% for DS ($p < 0.05$).

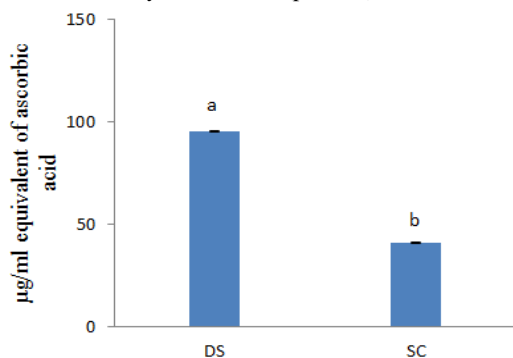


Figure 2. Total antioxidant capacity of the hydro-methanolic extracts of dehusled and seeds coat in ascorbic acid equivalent. DS: dehusled seeds; SC: seeds coat. Data is presented as Means \pm Standard Error (SD).

3.3. Evaluation of the anti-inflammatory activity

As illustrated in Figure3, after 6 hours of carrageenan injection, both doses of 10% and 5% of SC extracts showed maximum inhibition of carrageenan (70% for 5% and 85.56% for 10%) in comparison to Diclofenac at 1% which produced an inhibition of 78.9%. Thus, inhibition of inflammation from DS has shown the lowest effect after 6hours, which reached 46% and 58.17% respectively for 5% and 10% respectively.

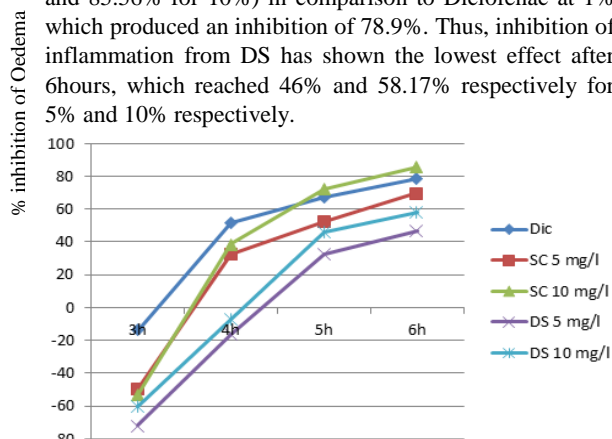


Figure 3. Anti-inflammatory effects of dehusled seeds and seeds coat in the carrageenan induced rat paw oedema test. Dic: Diclofenac 1%, SC: hydro-methanolic extract of seeds coat, DS: hydro-methanolic extract of dehusled seeds.

4. Discussion

In this study, phytochemical composition, antioxidant effect and anti-inflammatory activity of the dehusled and seeds coat of sesame were evaluated.

Concerning our results, the data revealed that the dehusling process increased protein, oil, and soluble sugar content in DS when compared to SC; this difference in concentration is likely due to the storage localization of those natural compounds in the endosperm layers of sesame seeds as has been shown by El-Adawy and Mansour (2000). On the other hand, it is known that magnesium (intracellular cation) and potassium (extracellular cation) play a preventive role in blood pressure and cardiac issues (Swaminathan, 2003 and Weaver, 2013). In fact, it has been reported that a diet containing 20% sesame can slow aging and decrease lipid peroxidation (Yamashita *et al.*, 1990 ; Namiki, 2007). In addition, phosphorus is another important nutrient for maintaining bone formation. Our observation showed that phosphorus was highly concentrated in the DS, contrary to the sodium that was found to be higher in SC than DS. As to potassium and magnesium, they have the same quantity both in DS and SC. These results confirm the findings reported by Wang *et al.* (2008) for *Pisum sativu*. Calcium plays a crucial role not only in physiological reactions (vascular contraction, neural transmission...) but also in preventing osteoporosis (Park *et al.*, 2011). Our study showed that the quantity of calcium was higher in coat fraction than dehusled seeds. Chang *et al.* (2002) reported that oxalate binds to calcium to form calcium oxalate, a type of crystal, which is found to be localized mainly in the seed coat. The nutritionally available calcium was estimated to be less than 25% of the total calcium (Namiki, 2007).

The identification of bioactive compounds and their activities from industrial residues has been the subject of many studies. The peeled parts of many fruits have been found to have a higher concentrate of phenolic compounds than the edible parts. According to our results, the SC extract showed higher phenolic and flavonoids content than the DS extract. Elleuch *et al.* (2007) had shown that the polyphenols are associated with dietary fibers in the sesame coat. The same observation has been registered for coats of numerous fruits like peanut (Yen *et al.*, 1994), pea (Watanabe *et al.*, 1997), wheat (Ohta *et al.*, 1994) and bean (Rodríguez *et al.*, 1994). Phenolic compounds are known for their antioxidant activities and are considered as the most predominant antioxidants (Abaza *et al.*, 2002).

Many studies highlighted the role of plants, whose extracts have a total antioxidant capacity, in prevention of oxidative stress (Abushouk *et al.*, 2017; Uddin *et al.*, 2018). The antioxidant power of the extracts of DS and SC were shown by two complementary spectrometric methods. The free scavenging activity efficiency is indicated by the neutralization of free radicals (DPPH), which are purple-colored (Zhao *et al.*, 1994). The TAC is based on green phosphomolybdenum complex formation. In fact, at acidic pH, Mo (V) is reduced to Mo (VI). Based on our data, the DPPH scavenging activity of SC was found to be higher in DS. This difference can be explained by the ability of coat extract to act as hydrogen atom donors to free radicals. Our results also showed that the

value of TAC for SC hydro-methanolic extract is widely higher when compared with DS. This confirms previous findings of Chang *et al.* (2002), who showed that the seeds coat of soybeans had greater antioxidant activity than whole soybeans. Shahidi *et al.* (2006) found that black sesame coat has significant effects on oxidation of human low density lipoprotein (LDL) cholesterol and also on ferrous ion chelating capacity. Several studies demonstrated the strong and positive relationship between quantity of phenolic compounds and the antioxidant effect (Das *et al.*, 1990). Balasundram *et al.* (2006) showed that phenolic compounds play an important role in antioxidant activity by creation of phenoxyl radicals, which is possible due to giving up hydrogen atoms from their hydroxyl groups to radicals.

It has been clearly shown that significant anti-inflammatory activity was observed in seeds coat extracts. This result can confirm our findings regarding the interesting contents of total phenolic in the hydro-methanolic extract of seeds coat. Geronikaki and Gavalas (2006) had revealed the implication of antioxidant compounds in anti-inflammatory activity. Several previous studies have shown the positive correlation between phenolic compounds quantity and anti-inflammatory activity (Wiseman *et al.* (2001) and Kong *et al.* (2000). Thus, these results suggest that the seed coat of sesame can be valorized as potential resource of antioxidant and anti-inflammatory effects.

5. Conclusion

In this study, coat and dehulled seeds of sesame were evaluated for their basic composition and biological activities. Based on the presented results, the dehulled seeds could be considered as a good source of fixed oil and protein. However, coat is showed rich by phenolic and flavonoids content. Also, it had showed optimum antioxidant efficiency by two complementary test systems. Furthermore, the coat methanolic extract possesses a good anti-inflammatory activity. It is recommended to consider sesame seed coats for therapeutic consideration whereas seeds are rich with nutrients as traditional food.

References

Abaza L, Msallem M, Daoud D, Zarrouk M. 2002. Caractérisation des huiles de sept variétés d'olivier tunisiennes. *OCL.*, **9**: 174-179.

Abushouk AI, Abdo Salem AM, Abdel-Daim MM. 2017. Berberis vulgaris for cardiovascular disorders: A scoping literature review. *Iran J Basic Med Sci.*, **20**: 503-510.

Alessandri AL, Sousa LP, Lucas CD, Rossi AG, Pinho V, Teixeira MM. 2013. Resolution of inflammation: mechanisms and opportunity for drug development. *Pharmacol Ther.*, **139**: 189-212.

Amabeoku, GJ, Kabatende J. 2012. Antinociceptive and anti-inflammatory activities of leaf methanol extract of *Cotyledon orbiculata* L. (Crassulaceae). *Adv Pharmacol Sci.*, **2012**.

Arora A, Sairam RK, Srivastava GC. 2002. Oxidative stress and antioxidative system in plants. *Curr.sci.*, 1227-1238.

Balasundram N, Sundram K, Samman S. 2006. Phenolic compounds in plants and agri-industrial by-products: Antioxidant activity, occurrence, and potential uses. *Food chem.*, **99**: 191-203.

Barnes PJ. 1998. Anti-inflammatory actions of glucocorticoids: molecular mechanisms. *Clin Sci.*, **94**: 557-572.

Bedigian D, Seigler DS, Harlan JR. 1986. Sesamin, sesamol and the origin of sesame. *Biochem. Syst. Ecol.*, **13**: 133-139.

Chang LW, Yen WJ, Huang SC, Duh PD. 2002. Antioxidant activity of sesame coat. *Food chem.*, **78**: 347-354.

Cooney RV, Custer LJ, Okinaka L, Franke AA. 2001. Effects of dietary sesame seeds on plasma tocopherol levels. *Nut cancer.*, **39**: 66-71.

Coussens LM, Werb Z. 2002. Inflammation and cancer. *Nature.*, **420**: 860-867.

Das NP, Pereira TA. 1990. Effects of flavonoids on thermal autoxidation of palm oil: structure-activity relationships. *J Am Oil Chem Soc.*, **67**: 255-258.

Davies MJ. 2004. Reactive species formed on proteins exposed to singlet oxygen. *Photochem & Photobiol Sci.*, **3**: 17-25.

Dubois M, Gilles KA, Hamilton JK, Rebers PA, Smith F. 1956. Colorimetric method for determination of sugars and related substances. *Analytical Chemistry.*, **28**: 350-356.

El-Adawy TA, Mansour EH. 2000. Nutritional and physicochemical evaluations of tahina (sesame butter) prepared from heat-treatment sesame seeds. *Journal Sci Food Agri.*, **80**: 2005-2011.

Elleuch M, Besbes S, Roiseux O, Blecker C, Attia H. 2007. Quality characteristics of sesame seeds and by-products. *Food chem.*, **103**: 641-650.

Elmastaş M, Gülçin I, ÖMER I, Küfrevioğlu Öİ, İbaoglu K, Aboul-Enein HY. 2006. Radical scavenging activity and antioxidant capacity of bay leaf extracts. *JICS.*, **3**: 258-266.

Fawole OA, Ndhala AR, Amoo SO, Finnie JF, Van Staden J. 2009. Antiinflammatory and phytochemical properties of twelve medicinal plants used for treating gastro-intestinal ailments in South Africa. *J. Ethnopharmacol.*, **123**: 237-243.

Ferrero-Miliani L, Nielsen OH, Andersen PS, Girardin SE. 2007. Chronic inflammation: importance of NOD₂ and NALP₃ in interleukin-1beta generation. *Clin. Exp. Immunol.*, **147**: 227-35.

Folin O, Ciocalteu V. 1927. On tyrosine and tryptophane determinations in proteins. *J Biol Chem.*, **73**: 627-650.

Geronikaki AA, Gavalas AM. 2006. Antioxidants and anti-inflammatory diseases: synthetic and natural antioxidants with anti-inflammatory activity. *Comb. Chem. High Throughput Screen.*, **9**: 425-442.

Gülçin I. 2012. Antioxidant activity of food constituents: an overview. *Arch toxicol.*, **86**: 345.

Halliwell B. 1990. How to characterize a biological antioxidant. *Free radic res commun.*, **9**: 1-32.

Khalid EK, Babiker EE, Tinay AE. 2003. Solubility and functional properties of sesame seed proteins as influenced by pH and/or salt concentration. *Food Chem.*, **82**: 361-366.

Kong AN, Yu R, Chen C, Mandlekar S, Primiano T. 2000. Signal transduction events elicited by natural products: role of MAPK and caspase pathways in homeostatic response and induction of apoptosis. *Arch Pharm Res.*, **23**: 1-16.

Landolfi R, Mower RL. 1994. Steiner M. Modification of platelet function and arachidonic acid metabolism by bioflavonoids. Structure Activity relations. *Biochem Pharmacol.*, **33**: 1525-1530.

Lawrence T, Gilroy DW. 2007. Chronic inflammation: a failure of resolution. *Int J Exp Pathol.*, **88**: 85-94.

McKenzie HA, Wallace HS. 1954. The Kjeldahl determination of nitrogen: a critical study of digestion conditions-temperature, catalyst, and oxidizing agent. *Aust J Chem.*, **7**: 55-70.

- Moazzami AA, and Kamal-Eldin A. 2006. Sesame seed is a rich source of dietary lignans. *J Am Oil Chem Soc.*, **83**: 719.
- Molyneux P. 2004. The use of the stable free radical diphenylpicrylhydrazyl (DPPH) for estimating antioxidant activity. *Songklanakarin J Sci Technol.*, **26**: 211–219.
- Nahar L. 2009. Investigation of the analgesic and antioxidant activity from an ethanolic extract of seeds of *Sesamum indicum*. *Pak J Biol Sci.*, **12**: 595-598
- Namiki M. 1995. The chemistry and physiological functions of sesame. *Food Rev Int.*, **11**: 281-329.
- Namiki, M. 2007. Nutraceutical functions of sesame: a review. *Crit Rev Food Sci Nutr.*, **47**: 651-73.
- Nathan C. 2002. Points of control in inflammation. *Nature.*, **420**: 846–852.
- Ohta T, Yamasaki S, Egashira Y, Sanada H. 1994. Anti-oxidative activity of corn bran hemicellulose fragments. *J Agri Food Chem.*, **42**: 653-656.
- Ordonñez AAL, Gomez JD, Vattuone MA, Isla MI. 2006. Antioxidant Activities of *Sechiamedule* (Jacp), Swartz extracts. *Food Chem.*, **97**: 452-458.
- Park HM, Heo J, Park Y. 2011. Calcium from plant sources is beneficial to lowering the risk of osteoporosis in postmenopausal Korean women. *Nutr Res.*, **31**: 27-32.
- Prieto P, Pineda M, Aguilar M. 1999. Spectrophotometric Quantitation of Antioxidant Capacity through the Formation of a Phosphomolybdenum Complex: Specific Application to the Determination of Vitamin E. *Anal Biochem.*, **269**: 337–341.
- Rodríguez DS, Hadley M, Holm ET. 1994. Potato peel waste, stability and antioxidant activity of a freeze-dried extract. *J Food Sci.*, **59**: 1031-1033.
- Shahidi F Lijana-Pathirana CM, Wall DS. 2006. Antioxidant activity of white and black sesame seeds and their hull fractions. *Food Chem.*, **99**: 478-483.
- Shankar RR, Eckert GJ, Saha C, Tu W, Pratt JH. 2005. The change in blood pressure during pubertal growth. *J. Clin. Endocrinol. Metab.*, **90**: 163–167
- Swaminathan R. 2003. Magnesium metabolism and its disorders. *Clin Biochem Rev.*, **24**: 47-66.
- Uddin MS, Hossain MS, Kabir MT, Rahman I, Tewari D, Jamiruddin MR, Al Mamun A. 2018. Phytochemical screening and antioxidant profile of *Syngonium podophyllum* Schott Stems: a fecund phytopharmakon. *J Pharm Nutr Sci.*, **8**: 120-128
- Wang N, Hatcher DW, Gawalko EJ. 2008. Effect of variety and processing on nutrients and certain anti-nutrients in field peas (*Pisum sativum*). *Food Chem.*, **111**: 132-138.
- Watanabe M, Ohshita Y, Tsushida T. 1997. Antioxidant compounds from buckwheat (*Fagopyrum Esculentum*) hulls. *J Agri Food Chem.*, **45**: 1039-1044
- Weaver CM. 2013. Potassium and health. *Adv Nutr.*, **4**: 368S-377S.
- Were BA, Onkware OA, Gudu S, Welander M, Carlsson AS. 2006. Seed oil content and fatty acid composition in East African sesame (*Sesamum indicum* L.) accessions evaluated over 3 years. *Field Crops Res.*, **97**: 254-260.
- Winter C, Risley E, Nuss G. 1962. Carrageenan-induced Edema in hind paw of the rat as an Assay for Anti-inflammatory Drugs. *Proceedings of the Society for Experimental Biology and Medicine.*, **111**: 544– 547.
- Wiseman S, Mulder T, Rietveld A. 2001. Tea flavonoids: bioavailability in vivo and effects on cell signaling pathways in vitro. *Antioxid Redox Signal.*, **3**: 1009-1021.
- Wu WH, Kang YP, Wang H, Jou HJ, Wang TA. 2006. Sesame ingestion affects sex hormones, antioxidant status, and blood lipids in postmenopausal women. *J Nutr.*, **136**: 1270-1275.
- Yamashita K, Kawagoe Y, Nohara M, Namiki M, Osawa T, Kawakashi S. 1990. Effects of sesame in the senescence-accelerated mouse. *Eiyo Shokuryou Gakkaishi.*, **43**: 2440-2446.
- Yen GC, Duh PD. 1994. Scavenging effect of methanolic extracts of peanut hulls on free-radical and active-oxygen species. *J Agri Food Chem.*, **42**: 629-632.
- Zhao FJ, McGrath SP, Crosland AR. 1994. Comparison of three wet digestion methods for the determination of plant sulfur by inductively coupled plasma atomic emission spectrometry (ICP-AES) *Commun. Soil Sci Plant Anal.*, **25**: 407–418.

Anti-inflammatory and Anti-proliferative Activity of Coconut Oil against Adverse Effects of UVB on Skin of Albino Mice

Snur Mohammed Amin Hassan *

Department of Anatomy and Pathology, College of Veterinary Medicine, Sulaimani University, Kurdistan-Iraq, 4601, Sulaimani City, Iraq

Received August 2, 2019; Revised September 4, 2019; Accepted September 16, 2019

Abstract

Excessive exposure of ultraviolet type B (UVB) is the primary cause of skin issues like sunburn, swelling, hyperplasia, skin aging and cancer. Our objective was to assess the effectiveness of topical administration of refined coconut oil (RCO) and virgin coconut oil (VCO) against anti-inflammatory and anti-proliferative UVB adverse effects in mouse skin model by using of tumor necrosis factor- α (TNF)- α and transforming growth factor- β 1 (TGF- β 1). Twenty-four adult, *BALB/c* mice were allocated into 4 groups: group 1 (control negative) not exposed to UVB; group 2 (control positive) exposed to UVB only and left without treatment; group 3 exposed to UVB and treated by RCO topically; groups 4, exposed to UVB and treated topically by VCO. At day 35, the mice were sacrificed. Histomorphometry was achieved for their epidermal thickening with inflammatory reaction measurement, and the expression of TNF- α and TGF- β markers were estimated by immunohistochemistry. VCO reduced epidermal hyperplasia and thickness in comparison to the RCO group including; stratum spinosum thickness for the VCO showed ($26.95 \pm 1.83 \mu\text{m}$) less mean than RCO group ($39.88 \pm 4.24 \mu\text{m}$), stratum granulosum in VCO group ($17.56 \pm 0.69 \mu\text{m}$) in comparison with the RCO ($27.11 \pm 3.04 \mu\text{m}$). Regarding the stratum corneum thickness for the RCO ($38.98 \pm 3.40 \mu\text{m}$) showed high mean than the VCO ($21.49 \pm 2.08 \mu\text{m}$) and the inflammatory score was significantly decreased by (scores 2 and 1) for the RCO and the VCO, respectively as specified by the downregulation of TNF- α and TGF- β markers expression in the skin. The study concluded that anti-inflammatory and anti-proliferative effects of VCO contribute to antioxidant capacity.

Keywords: Albino mice, Anti-inflammatory, Anti-proliferative, TNF- α , TGF- β , Virgin coconut oil, UVB

1. Introduction

Skin, the biggest organ of the body, capacities as the fundamental boundary among the internal and the external milieu. Along these lines, it consistently shields the body from poisonous boosts, e.g., microorganisms, light (UV) illumination, allergens, aggravations and irritants (Lin *et al.*, 2017). Wavelengths in the UVB radiation (290-320 nm) of the sun oriented range are consumed by the skin and in charge of causing an increase in the epidermal, and to a lesser extent the dermal, mitotic activity, which persists from days to weeks, leading to an approximate two-fold thickening of the epidermis including acanthosis and parakeratosis, also thickening of dermis (Surget *et al.*, 2015). UVB also leads to physical inflammatory reactions, oxidative stress (Clydesdale *et al.*, 2001), immune suppression (Ullrich, 2005), DNA mutations, and ultimately non-melanoma skin cancer (Melnikova and Ananthaswamy, 2005).

UV light activates various flagging pathways that modify a translation. This procedure takes after the reaction to growth factors and is known as the UV reaction (Tyrrell, 1996). During UV radiation, the excessive formation of reactive oxygen species (ROS) can interrupt the stability among pro-oxidant production and antioxidant defense (Pillai *et al.*, 2005). ROS overproduction is an inducible factor brought about by the expression of cytokines, prostaglandins, leukotrienes and the pro-

inflammatory molecules that elicit the arrival of inflammatory mediators to the site of disease that is broadly perceived by dermatitis (Lee *et al.*, 2003).

Cytokines such as tumor necrosis factor (TNF)- α plays an important role in photodamage and photoaging (Burke *et al.*, 2001). TNF- α released after UVB exposure induces endothelial cells and keratinocytes to display cell adhesion molecules, thereby recruiting inflammatory cells including keratinocytes, lymphocytes, macrophages and endothelial cells that secrete elastases and collagenases, leading to damage and aging of the skin (Rijken *et al.*, 2006; Moots *et al.*, 2018). TNF- α as pro-inflammatory cytokine also promotes apoptosis, lymphocyte activation, and hyperproliferative skin disorders (Banno *et al.*, 2004).

TGF- β is a family of pluripotent cytokines comprised of three isoforms in mammals such as TGF- β 1,-2, and-3, with TGF- β 1 predominant in most forms of tissue, including the skin (Li *et al.*, 2003). TGF- β 1 plays a critical role in sustaining homeostasis of the body by influencing cell development, differentiation, extracellular matrix accumulation, immune or inflammatory interactions and angiogenesis (Li *et al.*, 2003). UV irradiation induces TGF- β in both the epidermis and dermis of human skin. In the outer compartment of skin, TGF- β is a powerful negative regulator of keratinocyte proliferation (He *et al.*, 2002). Therefore, the induction of TGF- β by UV irradiation contributes to keratinocyte hyperplasia (Quan *et al.*, 2002) and also encourages the development of cancer (Massagué, 2012), TGF β can encourage

* Corresponding author e-mail: snur.amin@univsul.edu.iq, hassan_snur@yahoo.com.

immunosuppression through immediate activation and modification of regulatory T cells (Tregs) (Sakaguchi and Powrie, 2007); also it effectively encourages expression of the fork-box protein P3 (Foxp3) in cluster differentiation (CD4 + T-cells) and converts it into a regulatory phenotype. (Chen *et al.*, 2003). Recent generation specific tiny molecule TGF β pathway inhibitors, such as galunisertib, were shown to be safe, methods that reduce the length of therapy with TGF β inhibitors may be preferred. (Neuzillet *et al.*, 2015).

Skin therapies emphasize combination therapy such as the use of moisturizers, antibiotics, antihistamines, and corticosteroids to treat skin inflammation to repair altered skin barrier function and reduce tingling. The use of steroids for immunosuppression and long-term topical application, however, decreases the amount of collagen causing skin atrophy (Oikarinen *et al.*, 1998). In impact, new therapeutic methodologies are being seriously studied due to these risks. Diverse plant species comprise a few bioactive components that have useful roles for health, such as antioxidant, anti-inflammatory, and antimicrobial effects, thus increasing their use for remedial purposes (Lin *et al.*, 2008). In animal models, several popular plant-derived products were tested for the development of anti-inflammatory therapies (Choi *et al.*, 2009). As a result, natural crop products are increasing as a new option for introducing certain diseases caused by free radicals in individuals, animals, food, and cosmetics (Lim *et al.*, 2007). The research found that vital oils are natural volatile compounds that exhibit powerful odors and are created by aromatic crops as secondary metabolites (Bakkali *et al.*, 2008).

Cocos nucifera fresh juice and kernel extracts, more commonly known as coconut, are usually used for their anti-inflammatory, antipyretic and wound healing characteristics in Southeast Asian countries (Zakaria *et al.*, 2011). Coconut oil is traditionally used for moisturizing and treating skin disorders. The emollient impact of coconut oil has been proved effectively in patients with atopic dermatitis, thus showing that coconut oil is a powerful natural soothing to be used in xerosis therapy (Verallo-Rowell *et al.*, 2008). Tocopherol and fatty acids (FAs) are important components of VCO and add to their antioxidant properties. These elements may cause sunburn, photoaging, and DNA degradation by cell protection (Marina *et al.*, 2009).

In this research, we intended to evaluate the effectiveness of topical administration of refined and extra virgin coconut oil against UVB negative impacts on the mouse's skin, and their effects on inflammation and cell proliferation were assessed using an inflammatory marker (TNF)- α and TGF- β 1 proliferative marker.

2. Materials and Methods

2.1. Animal model and study design

In the animal house of the college of veterinary medicine, twenty-four adult albino mice (*Mus musculus* species, BALB /c strain) were purchased at a weight of 30-35 g. Mice were fed with standard pellet diet (Pico Lab) and provided with water *ad libitum*, were housed in the animal house/College of Veterinary Medicine/Sulaimani University, and were maintained at controlled room temperature about 25°C and photoperiodicity of 12 hours

light/dark system. The animals were used according to the review and institutional guidelines of the Ethics Committee of the College of Veterinary Medicine/Sulaimani University (1235).

After 1 week of acclimatization, mice were allocated into four groups: Control negative group (n=6), mice were not irradiated to UVB irradiation and treated topically with phosphate buffer saline (PBS, 6 drops=300 μ L); Control positive group (n=6), mice were irradiated to UVB irradiation only and left without treatment (nor by PBS or coconut oil); Treatment group with refined coconut oil (n=6), mice were irradiated to UVB irradiation and treated topically with refined coconut oil (RCO) and the last group, which were treated with extra virgin coconut oil (n=6), mice were irradiated to UVB irradiation and treated topically with extra virgin coconut oil (VCO).

2.2. UVB irradiation

Our lamp phototherapy unit consisted of UVB lamps from the (Vilber-Lourmat-France), predominantly emitting UVB light at the range of 280-312 nm. The UVB fluencies used throughout the study were 80mj/Sec. With the exception of the control negative group, mice from other groups were exposed to UVB light for 35 minutes/day (4 days/week for 5 successive weeks) during the experiments. Electric shaver was used to cut the dorsal hairs for making a rectangular area (3*6 cm) prior to the UVB irradiation. Throughout the period of exposure, mice have moved around freely in a specially designed ventilated glass metal-free cabinet (32*25*25 cm).

2.3. Treatment of mice with coconut oils

Various kinds of coconut oils were used in this experiment, including virgin coconut oil (VCO) and refined coconut oils (RCO), both of which were purchased from (CalRoth, Germany). The analysis was carried out on each extracted type of coconut oil using high-performance liquid ultraviolet chromatography (HPLC-UV) separation on a silica column (Lichrosorb Si60 5 μ m particle diameter, 250 mm length x4 mm id) in the Ministry of Agriculture (Baghdad, Iraq), and their chemical composition, including saturated triglyceride, was separated by the Marina et al method. (Marina *et al.*, 2009), whereas polyphenols, vitamins, and phenolic acid have been performed by Puah et al, protocol (Puah *et al.*, 2007).

The mice from both treatment groups were treated with refined and extra virgin coconut oils respectively 4 days/week. Oil treatments were performed topically in two different times 20 min before exposure to UVB (6 drops=300 μ L) and after UVB exposure directly (6 drops=300 μ L). During treatment, the quantity of both types of oil was evaluated by micropipette in order to regulate the amount of oil that was 300 μ L.

2.4. Tissue sampling and histopathological examination

The animals were anesthetized with ketamine and xylazine after 35 days of experimentation and then euthanized by cervical displacement; after that, skin samples were obtained from the dorsal skin, immediately fixed for 24-48 hours in 10 percent neutral buffered formalin and then passed skin samples for series histopathological preparations. Three transverse skin tissue segments (4 μ m thick) were gained using a rotary microtome, hematoxylin, and eosin-stained first section,

IHC stained second and third section followed by microscopic assessment (Leica, Germany) and digital slide photography.

2.5. Histometric assessment

Dorsal skin slide sections were evaluated under a light microscope (Leica, Germany); equipped with an image analysis system (AmScope, AmView). In each case, the epidermal thickness was recorded in 3 layers after 35 days of the study, including stratum spinosum, stratum granulosum, and stratum corneum at 100 magnification (100x) independently, and then the mean was calculated for each layer in the group. When a picture was captured and then divided into 16 squares, inflammatory cells in the dermis were also counted, whereby all inflammatory cells (nuclear polymorphic cells and mononuclear cells) were counted at 400-fold magnification (400x), only the cells that included into the squares while those cells that located outside of it where excluded and mean numbers for each group were attained. Inflammatory cells were scored and categorized as follows: negative or score 0 (0-5 inflammatory cells), mild or score 1 (6-15 inflammatory cells), moderate or score 2 (16-25 inflammatory cells), and severe or score 3 (including 25 inflammatory cells).

2.6. Immunohistochemistry staining

Two skin sections (4 µm thick) were attached to the positively charged slides and allowed to dry in an incubator at 60 °C for 1 hour. With xylene and graded alcohol alternatives, the slices were deparaffinized and rehydrated. Antigen retrieval was accomplished by heating the sections in the pressure cooker that contained citrate buffer for 20 min. Through sinking the slides in 0.3 percent hydrogen peroxidase for 12 minutes, endogenous peroxidase activity was blocked. The sections were then coated with 3% (goat and mouse serum) to block non-specific bindings for about 30 minutes. The slides were then put in a damp chamber and incubated with rabbit anti-TNF-α polyclonal antibody (1:100, Biorybt, USA, orb7100) and rabbit anti-TGF-β1 polyclonal antibody (1:100, Biorybt, USA, orb11468) for 1 hr, followed by three washes in the buffer (2 min each). The sections were then incubated for 20 min with biotinylated anti-rabbit secondary antibodies (Biorybt, USA), washed in a buffer three times, incubated for 25 min in a Horseradish peroxidase-streptavidin (Envision, Biorybt) and washed in a buffer again four times. Tissue staining was visualized with the DAB substrate solution for less than 5 min (Biorybt, USA) and counterstained with hematoxylin. Then by a light microscope (Leica, Germany) examined the slides.

2.7. Assessment of immunohistochemical study

The result of immunohistochemical studies was analyzed quantitatively using the light microscope (Leica, Germany); equipped with an image analysis system (AmScope, AmView). The number of cells expressed TNF-α and TGF-β were calculated a magnification of 400x with in the same length of the epidermal layer for each section. TNF-α and TGF-β1 staining were scored and subsequently calculated in entire representative high power fields for each tissue sample. Three distinct observers (which were blinded to the experiment) subjectively assessed the magnitude and effect of the staining of each

section using the following designations as in Table 1 (Dong *et al.*, 2010; Jammal *et al.*, 2015).

Table 1. Immunoreaction scoring for the TNF-α and TGF-β1.

Quantification and intensity	Grades
No positive cell and no immunostaining	0
1-10% of positive cells and weak (light yellow)	1
11-25% of positive cells and moderate (yellow-brown)	2
26-50% of positive cells and focal strong (brown)	3
> 50% of positive cells and diffuse strong (brown)	4

2.8. Statistical analysis

A one way ANOVA and Duncan's test were used to assess the statistical significance between the groups. Statistical analysis was achieved using SPSS version 25.0 software (SPSS, Chicago, IL, USA). The results were presented as mean ± standard error (SE) and differences significant was reflected at $P < 0.05$; $P < 0.01$ and $P < 0.001$.

3. Results

3.1. Chemical analysis of various coconut oil kinds

The analysis of various types of coconut oils was achieved by normal-phase high-performance liquid chromatography ultraviolet (HPLC-UV). In table 2, generally, the values for RCO were lower than extra VCO. However, fatty acid constituents were considered to be predominant and were about 87.98% in VCO while in the RCO were 78.18%. For example, lauric acid, which made up, the higher percentages among fatty acid (49.90%) in the VCO type in contrast to the RCO type that decreased to 44.89%. In general, less phenolic acids were detected in RCO (3.44%) compared with virgin oil (4.9%) samples because some phenolic compounds were lost or degraded during the refining process; Vanillic was the major phenolic acid in VCO ranged to 2.08% while in the RCO reduced to 1.80 only. Additional constituents that identified were polyphenols and vitamins, in the VCO made up 7.12% in comparison to the RCO type were dropped to 4.49%, and the Catechin was recognized as a significant component in both oil kinds, the unknown elements in the refined oil were 13.89%.

Table 2. Chemical components of various forms of coconut oils

Components		Refined coconut oil %	Extra virgin coconut oil %
Saturated triglyceride (medium-chain)	Lauric acid	44.89	49.90
	Myristic acid	16.99	18.03
	Caprylic acids	6.80	8.10
	Palmitic acids	4.50	5.00
	Stearic acid	1.90	2.65
	Oleic acid	3.10	4.30
Phenolic acids	Protocatechuic	0.10	0.16
	Vanillic	1.80	2.08
	Syringic	0.03	0.45
	P-coumaric	0.45	0.12
	caffeic		
	Ferulic	1.06	2.09
Polyphenols and Vitamins	Gallic acid	1.05	2.0
	Catechin	1.60	2.90
	Vitamin E	0.95	1.02
	Vitamin K	0.89	1.20
Unidentified		13.89	

3.2. Histopathological finding

I- Control groups

Upon histologic examination, the skin section in control negative showed normal epidermal proliferation or thickness value that showed by mean error in each layer including standard error, stratum spinosum ($7.86 \pm 1.28 \mu\text{m}$), in stratum granulosum ($1.80 \pm 0.43 \mu\text{m}$), and stratum corneum ($10.94 \pm 1.36 \mu\text{m}$) as revealed in table 3-5 and figures 1-3a, in comparison to the control positive group that showed significant increase in each mentioned layer's thickness. Histological changes such as diffuse epidermal hyperplasia or acanthosis, hypergranulosis, and hyperkeratosis were evident after 5 weeks of UVB irradiation. Acanthosis was noted in stratum spinosum with maximum mean ($104.87 \pm 9.51 \mu\text{m}$) and highly significant value ($P=0.000$) as in table 3 and figure 1b. Also, severe hyperplasia of stratum granulosum or hypergranulosis was noted in which the granular cell layers increased or thickened to six or more layers from the normal one-three layers as in table 4 and figure 2b with a strong substantial value ($71.20 \pm 10.26 \mu\text{m}$, $P=0.00$), additionally severe hyperplasia of stratum corneum (hyperkeratosis) also detected, in which the horny cell layer becomes abnormally thick and it measured ($107.07 \pm 10.82 \mu\text{m}$) with significant value ($P=0.000$) as in table 5 and figure 3b.

II- Treatment groups

Histological analysis of skin sections in both treatment groups caused in a substantial reduction in UVB-mediated epidermal hyperplasia in contrast to the control positive group. In VCO epidermal hyperplasia mildly increased in contrast to the control negative group in each layer including stratum spinosum ($26.95 \pm 1.83 \mu\text{m}$) with about 12.93 folds less than RCO group ($39.88 \pm 4.24 \mu\text{m}$) with a substantial value ($P=0.00$) as in table 3 and figure 1c and d, that mean rose moderately, stratum granulosum in VCO group slightly increased their mean ($16.52 \pm 0.79 \mu\text{m}$) in comparison with the RCO ($27.16 \pm 3.03 \mu\text{m}$) that moderately thickened about 10.64 folds with significant value ($P=0.00$) as in table 4 and figure 2c and d. Regarding the stratum corneum also the RCO moderately thickened ($38.98 \pm 3.40 \mu\text{m}$) about 17.49 folds with significant value of ($P=0.02$) in contrast to the VCO that mildly increased in their thickness ($21.49 \pm 2.08 \mu\text{m}$) as in table 5 and figure 3c and d.

Table 3. Measurement (μm) of epidermal thickening (stratum spinosum) in different groups.

	Control negative (n=6)	Control positive (n=6)	Refined coconut oil (n=6)	Virgin coconut oil (n=6)
	7.03	81.64	30.25	28.00
Mean \pm SE	5.60	134.05	40.45	25.34
	6.26	112.0	38.01	30.40
	14.2	74.10	58.63	30.42
	7.10	122.97	41.54	18.64
	7.00	104.51	30.42	28.90
	7.86 ± 1.28^a	$104.87 \pm 9.51^{***b}$	$39.88 \pm 4.24^{**c}$	$26.95 \pm 1.83^{**d}$

Mean values with various small alphabetical superscripts differ from one another in the last row by ** $P < 0.01$, *** $P < 0.001$ vs. Control.

Table 4. Measurement (μm) of epidermal thickening (stratum granulosum) in diverse groups.

	Control negative (n=6)	Control positive (n=6)	Refined coconut oil (n=6)	Virgin coconut oil (n=6)
	2.00	65.03	39.28	15.21
Mean \pm SE	1.23	104.60	20.53	16.33
	1.80	47.05	23.8	15.98
	1.00	60.00	33.34	14.4
	3.8	50.12	22.10	20.00
	1.00	100.40	23.93	17.22
	1.80 ± 0.43^a	$71.20 \pm 10.26^{***b}$	$27.16 \pm 3.03^{**c}$	$16.52 \pm 0.79^{**d}$

Mean values with various small alphabetical superscripts differ from one another in the last row by ** $P < 0.01$, *** $P < 0.001$ vs. Control.

Table 5. Measurement (μm) of epidermal thickening (stratum corneum) in different groups.

	Control negative (n=6)	Control positive (n=6)	Refined coconut oil (n=6)	Virgin coconut oil (n=6)
	9.43	90.67	33.34	18.64
Mean \pm SE	7.25	100.96	32.34	30.69
	10.98	79.62	30.98	17.22
	8.34	91.60	50.93	23.93
	16.00	145.84	39.28	20.53
	13.67	133.75	47.05	17.98
	10.94 ± 1.36^a	$107.07 \pm 10.82^{***b}$	$38.98 \pm 3.40^{**c}$	$21.49 \pm 2.08^{**d}$

Mean values with various small alphabetical superscripts differ from one another in the last row by ** $P < 0.05$, *** $P < 0.001$ vs. Control.

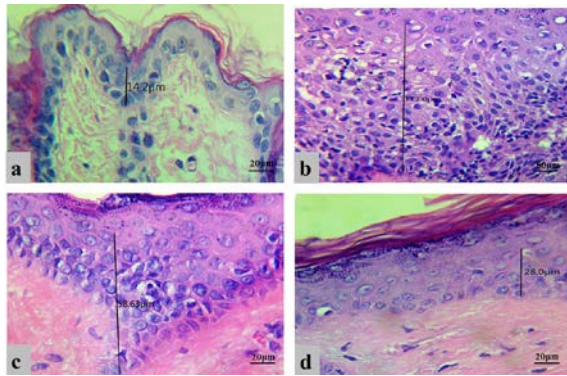


Figure 1. Histopathological skin sections of stratum spinosum thickness in mice. a: Normal thickening in control negative group, b: Marked acanthosis in control positive group, c: Focal-moderate thickening in RCO group, d: Focal-mild thickening in VCO group, (H and E stain).

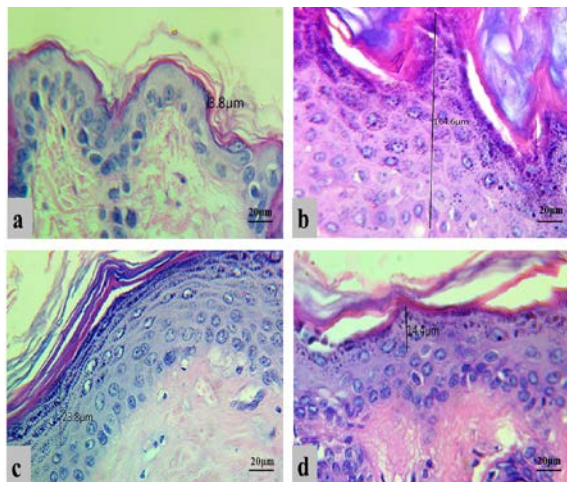


Figure 2. Histopathological skin sections of stratum granulosum thickness in mice. a: Normal thickening in control negative group, b: Severe hypergranulosis in control positive group, c: Moderate thickening in RCO group, d: Mild thickening in VCO group, (H and E stain).

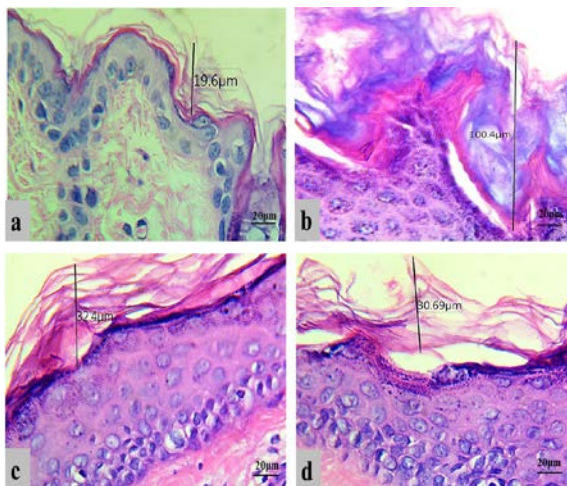


Figure 3. Histopathological skin sections of stratum corneum thickening in mice. a: Normal thickening in control negative group, b: Marked hyperkeratosis in control positive group, c: Moderate thickening in RCO group, d: Mild thickening in VCO group, (H and E stain).

3.3. Assessment of the inflammatory reaction

The statistical analysis of inflammatory polymorphonuclear and mononuclear was provided in

Table 6. The UVB induced raising of inflammatory reactions (polymorphonuclear and mononuclear inflammatory cells) in control positive with highly significant value and the highest score was score 3 for all kinds of inflammatory cells with exception of neutrophil that showed significant only in contrast to the control negative group that showed score 0. In treatment group the infiltration of inflammatory cells was significantly decreased in the mean numbers and scores with scores 2 and 1 for the RCO and the VCO, respectively, in comparison to the control positive group, the differences were significant for all types of inflammatory cells, also among treatment groups, the inflammatory cells decreased significantly in the VCO as well as compared with the RCO with exception for the mast cells that showed no significant. The degree of inflammatory cells infiltration was showed in figure 4.

Table 6. The mean ± SE of the various groups of inflammatory cells.

Variables	Control negative	Control positive	Refined coconut oil	Virgin coconut oil
Neutrophil	1.00±0.60	2.83±0.63*	1.33±0.42	0.66±0.21*
Lymphocytes	1.33±0.55	7.33±1.08**	3.16±0.60*	1.00±0.25
Plasma cells	1.33±0.55	6.00±1.06**	2.66±0.66*	0.83±0.16*
Macrophages	1.50±0.50	8.66±1.70**	4.66±0.49**	4.16±0.47**
Mast cells	1.00±0.63	5.16±0.47**	0.83±0.30	1.16±0.30

Mean values with various small alphabetical superscripts differ from one another in the last row by *P<0.05, **P<0.01 vs. Control.

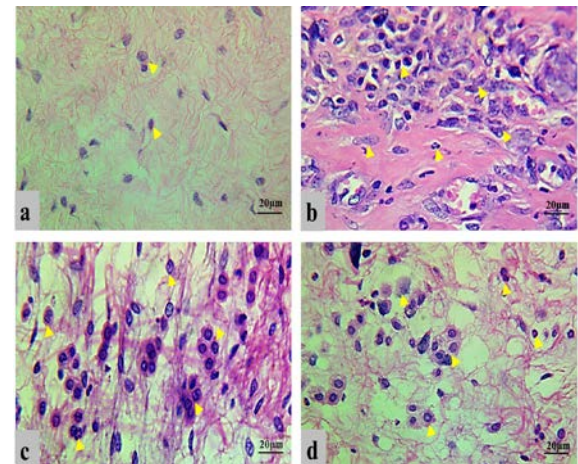


Figure 4. Histopathological skin sections of infiltration of inflammatory cells in mice. a: Normal infiltration in control negative group, b: Marked inflammatory reaction in control positive group, c: Moderate inflammatory reaction in RCO group, d: Mild infiltration in VCO group, (H and E stain).

3.4. TGF-β1 expression detection by IHC

Immunohistochemical analysis of the TGF-β1 marker shown in figure 5 that indicated the increasing of epidermal layer or proliferation of keratinocytes of epidermis, most common expression pattern found was cytoplasmic staining in the keratinocytes of the stratum spinosum of the epidermis of the skin, with a less TGF-β1 expression in the keratinocytes particularly in the stratum granulosum layer. Negative expression (Score 0) was seeming in mice of the control negative group, TGF-β1 expression was increased in the control positive group and showed strong-focal expression (Score 3) in mostly all keratinocytes of epidermis, when compared with the RCO

group, the TGF- β 1 expressed in less than 25% of the epidermal keratinocytes which were stained moderate (Score 2). While in the VCO group the expression of TGF- β 1 decreased if compared to the control positive and even to the RCO group that showed weak expression (Score 1).

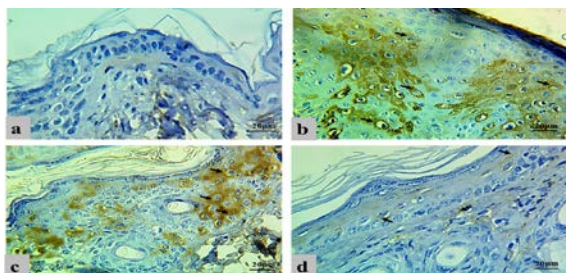


Figure 5. TGF- β 1 expression in epidermal keratinocytes of skin section of different mice groups: a: Negative expression (Score 0) in control negative group, b: Strong-focal expression (Score 3) in control positive group, c: Moderate expression (Score 2) in RCO group, and d: Weak expression (Score 1) in VCO group, (Positive cells indicated by black arrows).

3.5. Immunohistochemical analysis of TNF- α

TNF- α expression showed in all groups with the exception of control negative, and its expression related to the increasing of inflammatory reaction in the dermis, immunohistochemical staining of the keratinocytes in mostly the stratum spinosum and less commonly in stratum granulosum of skin tissue sections that revealed variable scores of TNF- α expression and the pattern of expression was cytoplasmic. Immunohistochemical analysis of the TNF- α marker is shown in figure 6. Negative immunostaining was found in the control negative group (Score 0). In mice of control positive strong-focal expression (Score 3) was apparent, moderate expression of TNF- α (Score 2) was seen in mice of RCO group, whereas weak expression (Score 1) was seen in mice of VCO group in comparison to the control positive and RCO groups in which the TNF- α expression was decreased markedly.

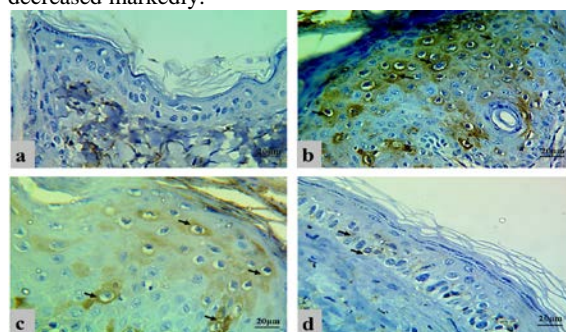


Figure 6. TNF- α expression in epidermal keratinocytes of skin section of different mice groups: a: Negative expression (Score 0) in control negative group, b: Strong-focal expression (Score 3) in control positive group, c: Moderate expression (Score 2) in RCO group, and d: Weak expression (Score 1) in VCO group, (Positive cells are indicated by black arrows).

4. Discussion

Plant oils have been discovered to have numerous helpful physiological features; therefore, they have long been used on the skin for cosmetic and medical reasons. For example, plant oil application can have an occlusive effect as a protective barrier on the skin, allowing the skin

to retain moisture. Topical products also have the benefit of greater bioavailability in the skin and have a localized effect rather than systemic impacts (Patzelt *et al.*, 2012).

In this research, we examined the protective effect of RCO and VCO against UV exposure by following known markers of UV detriment (TNF- α and TGF- β). Our data demonstrated that topical coconut oils treatment on mouse skin significantly reduce epidermal hyperplasia that caused by UVB exposure particularly the group of mice that treated by VCO showed mild thickening of the stratum spinosum, granulosum, and corneum because VCO contain sufficient amounts of medium-chain fatty acids, polyphenols, tocopherols and free radical scavengers which not only improve the antioxidant status, but also reduce free radical-induced protein oxidative damage (Marina *et al.*, 2009; Arunima and Rajamohan, 2013), in contrast to the control positive group that showed marked hyperplasia of skin epidermis and in accordance with study who mentioned that epidermal thickening is regarded as the classical signs of UV exposure mediated damages to the skin (Reagan-Shaw *et al.*, 2006). Our information was also consistent with the earlier research, which documented that UV exposure causes oxidative stress in the skin that can be involved in a wide spectrum of circumstances, including hyperkeratosis and epidermal hyperplasia, which suggested influences on the mitotic cycle and on the macromolecular synthesis.

Triglycerides do not usually penetrate deeper into stratum corneum in plant oil; glycerol leads to the hydration of stratum corneum. Free fatty acids (FFAs), specifically monounsaturated FFAs such as oleic acid discovered in VCO rather than RCO, can interrupt the skin barrier and enhance the permeability of other compounds in coconut oils (Mack Correa *et al.*, 2014). This is the theory why our research showed mild hyperkeratosis to the group of mice who dealt with VCO. Other compounds found in different levels of each vegetable oil are phenolic compounds and tocopherols; they are the basic antioxidants found in virgin coconut oil. These compounds are very essential for the oxidative stability of purified fatty acid (PUFAs) in oil parts. For example, they have an effect on cancer prevention agents and can modulate physiological mechanisms such as homeostasis of the skin barrier, cell proliferation inhibition and inflammation (Servili *et al.*, 2009; Mack Correa *et al.*, 2014). This is the theory why the group topically treated with VCO diminished significantly epidermal hyperplasia instead of control positive group.

In our finding the group treated with RCO showed moderately epidermal thickening in contrast to the group treated with VCO that showed mild changes. The hypothesis why VCO had a potent effect than RCO is that the refined coconut oil is extracted from chemically lightened and deodorized coconut meat; therefore some of the components were decreased or altered by processing or by heating. While virgin coconut oil is obtained without the use of high temperatures or chemicals from the fruit of new, mature coconuts. It is regarded as unrefined and can provide health advantages because it contains elevated quantities of saturated triglycerides, phenolic acids, polyphenols and vitamins (Villarino *et al.*, 2007). Also, Marina *et al.* study revealed that VCO contained higher total phenolic content compared to refined coconut oil and, therefore, had more effective than RCO. It was suggested

that the RCO process being applied through the dry method had considerably destroyed some of the phenolic compounds in the coconut oil (Marina *et al.*, 2009).

The UV-induced proliferation and epidermal hyperplasia depended on gene expression (Yamaguchi and Hearing, 2009). Our information also proved that the topical use of coconut oil also significantly inhibited UVB-mediated cell proliferation in addition to protein expression such as TGF- β 1; for example, the RCO reduced TGF- β 1 expression by score 2, while the VCO decreased TGF- β 1 expression in score 1 in comparison to the control group that exhibited protein expression in high score (Score 3). This is an interesting observation because TGF- β 1 expression has been revealed to be related with cellular proliferation and epidermal thickening that is regarded as a marker of proliferation after UVB irradiation for chronic duration in which in agreement with study of Ichihashi *et al.*, who recognized that UVB generate ROS, and ROS have been shown to activate the latent form of TGF- β 1 (Ichihashi *et al.*, 2003). Also, in agreement with former data, elevated TGF- β 1 expression has been found in keratinocytes of the basal epidermal layer, and TGF- β 1 overexpression associated with the acanthotic and hyperplastic epidermis suggesting that this factor is involved in a negative feedback growth regulatory loop (Li *et al.*, 1999; Liu *et al.*, 2001; Lu *et al.*, 2004). Our finding is in accordance with studies which verified that coconut oil is rich in medium-chain fatty acids such as lauric acid, capric acid, and myristic acid and have been documented to some extent, that such MCFA 's have anti-proliferative and apoptosis-inducing effects (Fauser *et al.*, 2011). These findings suggest that VCO can provide protection against UVB damage, and these protective impacts can be mediated through its antioxidant characteristics, which act as an anti-proliferative agent and reduce the expression of TGF- β 1.

Due to UVB exposure, intracellular reactive oxygen species (ROS) play a crucial role in inflammation, aging, and cancer (Gause and Chauhan, 2016). Likewise, previous reports demonstrate that herbal oils have the capacity to defend against UVB irradiation. In this study, we have found that coconut oil more specifically the VCO markedly reduce the UVB exposure-mediated inflammatory reaction by score 1 in comparison to the control positive group and the RCO also that have score 3 and 2 respectively. In the present investigation, VCO demonstrated insurance against intracellular ROS delivered by UVB illumination irradiation. Our finding is in agreement with the previous report which described that the expression of the inflammatory profile was lower in the coconut oil-treated group after exposure to UVB radiation (Kim *et al.*, 2017). Topical coconut oil defends the cutaneous from UV irradiation (Korac and Khambholja).

For instance, leukocytes (PMNs, macrophages, and lymphocytes), mast cells, and dendritic cells are activated after an inflammatory response. Secreted cytokines such as IL-1 α , TNF- α and-6 stimulate chemokines of chemotaxis that attract the immune cells to the injury and infection site and improve the inflammatory response (Reinke and Sorg, 2012). In the present study, the mice in control positive group showed strong expression of TNF- α (Score 3) with severe dermatitis by means of (29.98) because TNF- α is

pro-inflammatory cytokine and is significant initiator cytokine of inflammatory responses (Neurath *et al.*, 1997).

Our study is in accordance to the former study which mentioned that epidermal keratinocytes, react to proinflammatory cytokines like TNF- α by involving in the expression of many inflammatory mediators during the chronic inflammatory skin disorders induced by UVB irradiation. The chemokines and growth factors of these keratinocytes are the primary force behind the accumulation and proliferation of inflammatory cells in the skin, thus preserving chronic inflammation of the skin (Pastore *et al.*, 2005). This study confirmed that VCO was potent in reducing the TNF- α expression (Score 1) and inflammatory reaction (mild inflammation) in dermis by mean of 7.81 and the inflammation was decreased by 22.17 folds in contrast to the control positive group and RCO group that showed moderate expression of TNF- α (Score 2) and moderate dermatitis by means of 12.64, when compared to the control positive group the inflammatory reaction dropped by 17.34 folds. Our results agree with the study of Varma *et al.*, 2019, who proved that topical use of VCO inhibits anti-inflammatory activity by inhibiting different concentrations of cytokine including TNF- α , IFN γ , IL-6, IL-5 and IL-8 and recovers skin hyperplasia and inflammation (Varma *et al.*, 2019). Other studies documented the anti-inflammatory effects of VCO in reducing atopic dermatitis and enhancing moisturizing to the skin (Evangelista *et al.*, 2014). The outcome suggests photoprotective and anti-inflammatory impacts of VCO against UVB irradiation, making it a significant ingredient in formulations and warranting further clinical studies owing to elevated levels of phenolic and antioxidant elements.

5. Conclusion

From the two types of coconut oil obtainable, VCO appears to carry the highest potential and is more beneficial for skin health by reducing epidermal thickening and inflammatory reaction because its composition varies and contains a higher amount of saturated free fatty acid, polyphenols, and vitamin E compared with RCO. The research indicated that VCO had anti-inflammatory and anti-proliferative impacts through its antioxidant characteristics.

Funding: This research received no external funding.

Conflicts of Interest: No conflict of interest is declared by the writers.

Reference

- Arunima S and Rajamohan T. 2013. Effect of virgin coconut oil enriched diet on the antioxidant status and paraoxonase 1 activity in ameliorating the oxidative stress in rats—a comparative study. *Food & function*, **4(9)**: 1402-1409.
- Bakkali F, Averbeck S, Averbeck D and Idaomar M. 2008. Biological effects of essential oils—a review. *Food and chemical toxicology*, **46(2)**: 446-475.
- Banno T, Gazel A and Blumenberg M. 2004. Effects of tumor necrosis factor- α (tnf α) in epidermal keratinocytes revealed using global transcriptional profiling. *Journal of Biological Chemistry*, **279(31)**: 32633-32642.

- Burke JR, Davern LB, Stanley PL, Gregor KR, Banville J, Remillard R, Russell JW, Brassil PJ, Witmer MR and Johnson G. 2001. Bms-229724 is a tight-binding inhibitor of cytosolic phospholipase α_2 that acts at the lipid/water interface and possesses anti-inflammatory activity in skin inflammation models. *Journal of Pharmacology and Experimental Therapeutics*, **298**(1): 376-385.
- Chen W, Jin W, Hardegen N, Lei KJ, Li L, Marinos N, McGrady G and Wahl SM. 2003. Conversion of peripheral cd4⁺ cd25⁻ naive t cells to cd4⁺ cd25⁺ regulatory t cells by tgfb- β induction of transcription factor foxp3. *Journal of Experimental Medicine*, **198**(12): 1875-1886.
- Choi G, Yoon T, Cheon MS, Choo BK and Kim HK. 2009. Anti-inflammatory activity of chrysanthemum indicum extract in acute and chronic cutaneous inflammation. *Journal of Ethnopharmacology*, **123**(1): 149-154.
- Clydesdale GJ, Dandie GW and Muller HK. 2001. Ultraviolet light induced injury: Immunological and inflammatory effects. *Immunology and cell biology*, **79**(6): 547-568.
- Dong XR, Wang JN, Liu L, Chen X, Chen MS, Chen J, Ren JH, Li Q and Han J. 2010. Modulation of radiation-induced tumour necrosis factor- α and transforming growth factor β 1 expression in the lung tissue by shengqi fuzheng injection. *Molecular medicine reports*, **3**(4): 621-627.
- Evangelista MTP, Abad-Casintahan F and Lopez-Villafuerte L. 2014. The effect of topical virgin coconut oil on scorad index, transepidermal water loss, and skin capacitance in mild to moderate pediatric atopic dermatitis: A randomized, double-blind, clinical trial. *International journal of dermatology*, **53**(1): 100-108.
- Fausser JK, Prisciandaro LD, Cummins AG and Howarth GS. 2011. Fatty acids as potential adjunctive colorectal chemotherapeutic agents. *Cancer biology & therapy*, **11**(8): 724-731.
- Gause S and Chauhan A. 2016. Uv-blocking potential of oils and juices. *International journal of cosmetic science*, **38**(4): 354-363.
- He W, Li AG, Wang D, Han S, Zheng B, Goumans MJ, ten Dijke P and Wang XJ. 2002. Overexpression of smad7 results in severe pathological alterations in multiple epithelial tissues. *The EMBO journal*, **21**(11): 2580-2590.
- Ichihashi M, Ueda M, Budiyo A, Bito T, Oka M, Fukunaga M, Tsuru K and Horikawa T. 2003. Uv-induced skin damage. *Toxicology*, **189**(1-2): 21-39.
- Jammal MP, Araújo da Silva A, Martins Filho A, de Castro Côbo E, Adad SJ, Murta EFC and Nomelini RS. 2015. Immunohistochemical staining of tumor necrosis factor- α and interleukin-10 in benign and malignant ovarian neoplasms. *Oncology letters*, **9**(2): 979-983.
- Kim S, Jang JE, Kim J, Lee YI, Lee D W, Song SY and Lee JH. 2017. Enhanced barrier functions and anti-inflammatory effect of cultured coconut extract on human skin. *Food and chemical toxicology*, **106**: 367-375.
- Korac R and Khambholja K. 2011. Potential of herbs in skin protection from ultraviolet radiation. *Pharmacogn rev*, **5**: 164-173.
- Lee JL, Mukhtar H, Bickers DR, Kopelovich L and Athar M. 2003. Cyclooxygenases in the skin: Pharmacological and toxicological implications. *Toxicology and applied pharmacology*, **192**(3): 294-306.
- Li AG, Koster MI and Wang XJ. 2003. Roles of tgfb signaling in epidermal/appendage development. *Cytokine & growth factor reviews*, **14**(2): 99-111.
- Li J, Foitzik K, Calautti E, Baden H, Doetschman T and Dotto GP. 1999. Tgf- β 3, but not tgfb- β 1, protects keratinocytes against 12-o-tetradecanoylphorbol-13-acetate-induced cell death in vitro and in vivo. *Journal of Biological Chemistry*, **274**(7): 4213-4219.
- Lim Y, Lim T and Tee J. 2007. Antioxidant properties of several tropical fruits: A comparative study. *Food chemistry*, **103**(3): 1003-1008.
- Lin CT, Chen CJ, Lin TY, Tung JC and Wang SY. 2008. Anti-inflammatory activity of fruit essential oil from cinnamomum insularimontanum hayata. *Bioresource Technology*, **99**(18): 8783-8787.
- Lin TK, Zhong L and Santiago J. 2017. Anti-inflammatory and skin barrier repair effects of topical application of some plant oils. *International journal of molecular sciences*, **19**(1): 70.
- Liu X, Alexander V, Vijayachandra K, Bhogte E, Diamond I and Glick A. 2001. Conditional epidermal expression of tgfb1 blocks neonatal lethality but causes a reversible hyperplasia and alopecia. *Proceedings of the National Academy of Sciences*. **98**(16): 9139-9144.
- Lu SL, Reh D, Li AG, Woods J, Corless CL, Kulesz-Martin M and Wang XJ. 2004. Overexpression of transforming growth factor β 1 in head and neck epithelia results in inflammation, angiogenesis, and epithelial hyperproliferation. *Cancer research*, **64**(13): 4405-4410.
- Mack Correa MC, Mao G, Saad P, Flach CR, Mendelsohn R and Walters RM. 2014. Molecular interactions of plant oil components with stratum corneum lipids correlate with clinical measures of skin barrier function. *Experimental dermatology*, **23**(1): 39-44.
- Marina A, Che Man Y, Nazimah S and Amin I. 2009. Chemical properties of virgin coconut oil. *Journal of the American Oil Chemists' Society*, **86**(4): 301-307.
- Marina A, Che Man Y, Nazimah S and Amin I. 2009. Monitoring the adulteration of virgin coconut oil by selected vegetable oils using differential scanning calorimetry. *Journal of Food Lipids*, **16**(1): 50-61.
- Massagué J. 2012. Tgfb signalling in context. *Nature reviews Molecular cell biology*, **13**(10): 616.
- Melnikova VO and Ananthaswamy HN. 2005. Cellular and molecular events leading to the development of skin cancer. *Mutation Research/Fundamental and Molecular Mechanisms of Mutagenesis*, **571**(1-2): 91-106.
- Moots RJ, Curiale C, Petersel D, Rolland C, Jones H and Mysler E. 2018. Efficacy and safety outcomes for originator tnfi inhibitors and biosimilars in rheumatoid arthritis and psoriasis trials: A systematic literature review. *BioDrugs*, **32**(3): 193-199.
- Neurath MF, Fuss I, Pasparakis M, Alexopoulou L, Haralambous S, Meyer zum Büschenfelde KH, Strober W and Kollias G. 1997. Predominant pathogenic role of tumor necrosis factor in experimental colitis in mice. *European journal of immunology*, **27**(7): 1743-1750.
- Neuzillet C, Tijeras-Raballand A, Cohen R, Cros J, Faivre S, Raymond E and de Gramont A. 2015. Targeting the tgfb pathway for cancer therapy. *Pharmacology & therapeutics*, **147**: 22-31.
- Oikarinen A, Haapasaari K, Sutinen M and Tasanen K. 1998. The molecular basis of glucocorticoid-induced skin atrophy: Topical glucocorticoid apparently decreases both collagen synthesis and the corresponding collagen mrna level in human skin in vivo. *The British journal of dermatology*, **139**(6): 1106-1110.
- Pastore S, Mascia F, Mariotti F, Dattilo C, Mariani V and Girolomoni G. 2005. Erk1/2 regulates epidermal chemokine expression and skin inflammation. *The Journal of Immunology*, **174**(8): 5047-5056.

- Patzelt A, Lademann J, Richter H, Darvin M, Schanzer S, Thiede G, Sterry W, Vergou T and Hauser M. 2012. In vivo investigations on the penetration of various oils and their influence on the skin barrier. *Skin Research and Technology*, **18(3)**: 364-369.
- Pillai S, Oresajo C and Hayward J. 2005. Ultraviolet radiation and skin aging: Roles of reactive oxygen species, inflammation and protease activation, and strategies for prevention of inflammation-induced matrix degradation—a review. *International journal of cosmetic science*, **27(1)**: 17-34.
- Puah C, Choo Y, Ma A and Chuah C. 2007. The effect of physical refining on palm vitamin e (tocopherol, tocotrienol and tocotrienol). *American Journal of Applied Sciences*, **4(6)**: 374-377.
- Quan T, He T, Kang S, Voorhees JJ and Fisher GJ. 2002. Ultraviolet irradiation alters transforming growth factor β /smad pathway in human skin in vivo. *Journal of Investigative Dermatology*, **119(2)**: 499-506.
- Reagan-Shaw S, Breur J and Ahmad N. 2006. Enhancement of uvb radiation-mediated apoptosis by sanguinarine in haca human immortalized keratinocytes. *Molecular cancer therapeutics*, **5(2)**: 418-429.
- Reinke J and Sorg H. 2012. Wound repair and regeneration. *European surgical research*, **49(1)**: 35-43.
- Rijken F, Kiekens RC, van den Worm E, Lee PL, van Weelden H and Bruijnzeel PL. 2006. Pathophysiology of photoaging of human skin: Focus on neutrophils. *Photochemical & Photobiological Sciences*, **5(2)**: 184-189.
- Sakaguchi S and Powrie F. 2007. Emerging challenges in regulatory t cell function and biology. *Science*, **317(5838)**: 627-629.
- Servili M, Esposto S, Fabiani R, Urbani S, Taticchi A, Mariucci F, Selvaggini R and Montedoro G. 2009. Phenolic compounds in olive oil: Antioxidant, health and organoleptic activities according to their chemical structure. *Inflammopharmacology*, **17(2)**: 76-84.
- Surget, G., Stiger-Pouvreau, V., Le Lann, K., Kervarec, N., Coureau, C., Coiffard, L. J., Gaillard F, Cahier K, Guérard F and Poupart N. 2015. Structural elucidation, in vitro antioxidant and photoprotective capacities of a purified polyphenolic-enriched fraction from a saltmarsh plant. *Journal of Photochemistry and Photobiology B: Biology*, **143**:52-60.
- Tyrrell RM. 1996. Activation of mammalian gene expression by the uv component of sunlight—from models to reality. *Bioessays*, **18(2)**: 139-148.
- Ullrich SE. 2005. Mechanisms underlying uv-induced immune suppression. *Mutation Research/Fundamental and Molecular Mechanisms of Mutagenesis*, **571(1-2)**: 185-205.
- Varma, S. R., Sivaprakasam, T. O., Arumugam, I., Dilip, N., Raghuraman, M., Pavan, K., Rafiq M and Paramesh R. 2019. In vitro anti-inflammatory and skin protective properties of virgin coconut oil. *Journal of traditional and complementary medicine*, **9(1)**: 5-14.
- Verallo-Rowell VM, Dillague KM and Syah-Tjundawan BS. 2008. Novel antibacterial and emollient effects of coconut and virgin olive oils in adult atopic dermatitis. *Dermatitis*, **19(6)**: 308-315.
- Villarino BJ, Dy LM and Lizada MCC. 2007. Descriptive sensory evaluation of virgin coconut oil and refined, bleached and deodorized coconut oil. *LWT-Food Science and Technology*, **40(2)**: 193-199.
- Yamaguchi Y and Hearing VJ. 2009. Physiological factors that regulate skin pigmentation. *Biofactors*, **35(2)**: 193-199.
- Zakaria Z, Somchit M, Jais AM, Teh LK, Salleh MZ and Long, K. 2011. In vivo antinociceptive and anti-inflammatory activities of dried and fermented processed virgin coconut oil. *Medical Principles and Practice*, **20(3)**: 231-236.

Influence of water quality parameters on larval stages of *Pseudoleptonema quinquefasciatum* Martynov 1935 (Trichoptera: Hydropsychidae) in streams of western Thailand

Penkhae Thamsenanupap¹ and Taeng On Prommi^{2*}

¹Faculty of Environment and Resource Studies, Mahasarakham University, Maha Sarakham, 44150; ²Faculty of Liberal Arts and Science, Kasetsart University, Kamphaeng Saen Campus, Nakhon Pathom, 73140, THAILAND

Received July 27, 2019; Revised September 5, 2019; Accepted September 16, 2019

Abstract

Aspects of the life cycle of *Pseudoleptonema quinquefasciatum* Martynov 1935 (Trichoptera: Hydropsychidae) were investigated including the possible influence of water quality parameters on larval stages. Larvae were sampled by hand picking at five sites in three streams in western Thailand in December 2014 and April 2015. In total, 2,139 larvae were collected and, by measurement of head capsules, the number of larval instars present was confirmed to be five. Analyses were conducted to determine if the number of larval instars present at any time was influenced by physicochemical water quality parameters. The number of first instar larvae was found to be positively correlated with electrical conductivity, whereas number of second instar larvae was correlated with quantity of dissolved solids and water turbidity, orthophosphate, pH, air and water temperature. A positive correlation was found also between third to fifth instar larvae and levels of dissolved oxygen, ammonia-nitrogen, nitrate-nitrogen, and alkalinity. The results suggest that electrical conductivity, total dissolved solids, water turbidity, orthophosphate, pH, air and water temperature, dissolved oxygen, ammonia-nitrogen, nitrate-nitrogen, and alkalinity may be major factors in determining the Trichoptera assemblages present in the streams of western Thailand.

Keywords: Life cycle, *Pseudoleptonema quinquefasciatum*, water variables, larval diet

1. Introduction

Aquatic insects are significant elements in lentic and lotic trophic webs, participating in energy flow and nutrient cycling (Whiles and Wallace, 1997). They are also important food resources for fish (Wallace and Webster, 1996) and some insectivorous birds (Ward *et al.*, 1995). The distribution and abundance of insects in freshwater systems is the result of complex interactions between their ecological roles and the physico-chemical conditions that characterize the habitat, and food availability (Merritt and Cummins, 1996). Thus, the community structure depends on a number of factors, such as water quality, type of substrate, particle size of sediment, water flow, sediment organic matter availability, oxygen concentration as well as environmental conditions surrounding the watercourse (Ward *et al.*, 1995; Buss *et al.*, 2004). Because they reflect environmental changes, aquatic insects are often used as indicators of the effects of human activity on water systems, providing information on habitat and water quality (Woodcock and Hury, 2007). Amongst the aquatic insects, order Trichoptera (or caddisflies) are the most widely distributed; their larvae are common in running water (8-13% of total abundance) (Roback, 1962; Ward, 1992) and they are one of the relatively well-studied orders of aquatic insects in South East Asia (Malicky,

2010; Morse, 2017). The larvae of many species coexist in running waters and are known to have specific habitat and environmental requirements (de Moor, 2007).

Pseudoleptonema Mosely 1933 is a small genus of eight species in the subfamily Macronematinae, family Hydropsychidae. All eight species are described from adults, and larvae have been described for one of the Thai species, *P. quinquefasciatum* (Prommi *et al.*, 2006). The life cycles of a number of Hydropsychidae species have been described (Edington and Hildrew, 2005), but the life cycle of *P. quinquefasciatum* in Thailand is not well known. Data are available on adult emergence periods, which may vary across Thailand and Laos (Hoang *et al.*, 2011). This paper explores aspects of the life cycle of this species, and is the first study on a caddisfly life cycle in streams in the Mae Klong watershed of western Thailand, investigating the relationship between environmental factors and its life history. Also, the study of feeding habits and trophic guilds in aquatic insects is important to understand their functional role and relevance in the conservation of the Asian Tropical streams.

2. Materials and methods

2.1. Study Area

This study was conducted in streams of the Mae Klong Watershed in western Thailand (Fig. 1), the most

* Corresponding author e-mail: faastop@ku.ac.th.

important watershed in western Thailand. Upstream in the watershed area are two main rivers: the Khwae Noi and the Khwae Yai. These rivers run into the Khao Laem and Srinagarind Dams located in the upper region of the Mae Klong Watershed. Downstream in the Kanchanaburi Province, the rivers flow through Ratchaburi Province and enter the Gulf of Thailand in the Samut Songkhram Province. Five sampling sites in three streams were chosen for this study. The streams were in the upstream section of Khwae Noi River before it flows into the Khao Laem Dam. These three streams are the Huai Pakkok, PK1 and PK2; the Huai Kayeng, KY1 and KY2; and the Huai Lijia, LJ (Fig. 1). Details of latitude and longitude of the stations and stream characteristics are shown in Table 1. The streams pass through areas of forest and cultivation, and three of the collecting sites are bordered by villages.

Table 1. Location of the stations and stream characteristics.

Site	Latitude/ Longitude	Description of stream
PK1	13°32.135' N, 099°17.842' E	Cobble predominant, forest and cultivation on both sides
PK2	13°32.077' N, 099°15.495' E	Bedrock and cobble predominant, pool in the middle, gravel and sand. Village and cultivation on both sides
KY1	13°27.658' N, 099°15.348' E	Man-made concrete upstream, gravel, woody debris and other stable substrates. Forest and highland, village both sides
KY2	13°30.241' N, 099°15.883' E	Cobble predominant, pool in the middle, gravel and sand. Village and cultivation on both sides

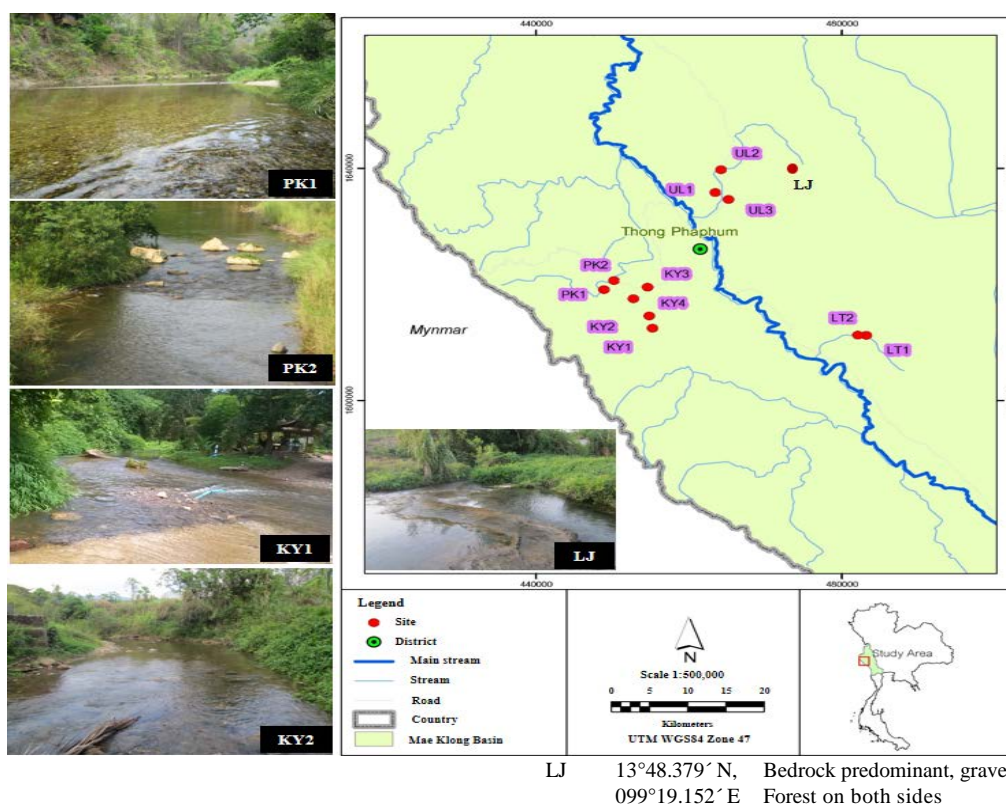


Figure 1. Map of Thailand showing locations of the five sampling sites, PK1, PK2, KY1, KY2 and LJ, and photographs of the streams at the sites.

2.2. Environmental Variables

The physicochemical water quality variables were measured simultaneously with collection of samples. Three replicates of selected physicochemical parameters were recorded directly at the sampling sites: pH (using a portable pH meter); water temperature (WT, °C) and dissolved oxygen (DO, mg/L) (using an oxygen meter — EcoScan DO 110); total dissolved solid (TDS, mg/L) and electrical conductivity (EC, $\mu\text{S}/\text{cm}$) (using an EC meter — CyberScan CON 11). Water samples from each site and sampling period were collected in polyethylene bottles (500 mL) and held at 4°C for study in the laboratory. Ammonia-nitrogen ($\text{NH}_3\text{-N}$, mg/L) was measured by the Nessler method, using a spectrophotometer (DR/2010 model 49300-00; Hach, USA); nitrate-nitrogen ($\text{NO}_3\text{-N}$, mg/L) by the cadmium reduction method, using a

spectrophotometer (DR/2010 model 49300-00; Hach, USA); orthophosphate; (PO_4^{3-} , mg/L) by the ascorbic acid method, using a spectrophotometer (DR/2010 model 49300-00; Hach, USA); and turbidity (TUB, NTU) using a spectrophotometer (DR/2010 model 49300-00; Hach, USA). Alkalinity (ALK, mg/L) was measured by the bromocresol green-methyl red indicator titration in accordance with the standard method procedures (APHA *et al.*, 1992).

2.3. Sampling Procedure

The larvae and pupae of *Pseudoleptonema quinquefasciatum* (Fig. 2A, B) were collected at five sampling sites in the streams of western Thailand (Figure 1). At each sampling site, a stretch of approximately 50 m was chosen for collection of samples. The samples were collected in December 2014 and April 2015, by hand

picking from the surface of boulders that were lifted from water around steps and rapids (Fig. 2C). The sampling time at each site was 2h. Collected *P. quinquefasciatum* larvae and pupae were preserved in 80% ethanol. Larval

characteristics were described and illustrated by Prommi *et al.* (2006). Larvae of *P. quinquefasciatum* construct an open-ended chamber retreat of fine sand, silk and plant debris, and fastened to a rock and capture nets (Fig. 2C).



Figure 2. *Pseudoleptonema quinquefasciatum* larvae (A), head, dorsal view (B) and larval case (red arrows) constructed from sand and detritus attached on stony substrate (C).

2.4. Life Cycle Analysis

A total of 2,139 individual of larvae samples were sampled in this study. In the laboratory, all larvae were sorted to instar using head width, following the method described by MacKay (1978). Head capsule widths were measured using an ocular micrometer. The number of larval instars was determined by analyzing the size frequency distributions of head capsule widths, following which the width ranges for instars were determined for each site. Size frequency distribution diagrams were constructed for each site based on the relative percent of the total number of individuals at each instar collected each month. Once larvae were assigned to instars, the variability in size at each instar was assessed for each site. Voucher specimens were deposited in the Faculty of Liberal Arts and Science, Kasetsart University, Kamphaeng Saen Campus, Nakhon Pathom Province, Thailand.

2.5. Gut Content Analysis

For a qualitative determination of the food items of *P. quinquefasciatum*, 10 larvae from each sampling site and sampling occasion were dissected under a stereomicroscope (Olympus SZ51). The whole digestive tracts were removed to a glass slide with water, shredded, and examined under a compound microscope (Olympus CX31). Contents were separated into plant tissue, algae, plankton, arthropod fragments, and amorphous tissue.

2.6. Data Analysis

The relationship between all larval stages and recorded environmental variables was determined for all sampling

dates together. A Principle Component Analysis (PCA) was performed using the PC-ORD 5.1 software.

3. Results

3.1. Environmental Variables

The means and standard deviations of measured physicochemical water quality parameters at the sampling sites taken during the two sampling periods were summarized in Table 2. The water temperature, dissolved oxygen, turbidity, ammonia-nitrogen, orthophosphate and nitrate-nitrogen did not vary significantly over the sampling period ($P > 0.05$), whereas total dissolved solids, electrical conductivity, pH and alkalinity varied significantly during the period ($P < 0.05$). The temperature varied from 26.38 (KY2) to 29.96 °C (PK2). The lowest mean value for dissolved oxygen (3.58 mg/L) was taken in Huai Lijia (LJ), and the highest values in Huai Kayeng (KY2) (5.76 mg/L). All sampling sites were slightly alkaline with pH showing little variation of (8.05 (LJ) – 8.51 (KY1)); the highest mean value for alkalinity was recorded for KY2 (8.43 mg/L) and lowest was registered for PK1 (12.80 mg/L). The highest mean value of total dissolved solids and electrical conductivity (129.52 mg/L, 258.28 μ S/cm) were observed at KY2 and the lowest at PK1 (40.25 mg/L, 74.08 μ S/cm). The mean turbidity was highest in LJ (18.66 NTU) and lowest at PK1 (6.00 NTU). The mean dissolved nutrients, ammonia-nitrogen, orthophosphate, nitrate-nitrogen concentrations varied from 0.19 (PK2) to 0.36 mg/L (PK1), 0.40 (PK1) to 0.64 mg/L (LJ), and 0.95 (PK2) to 1.70 mg/L (PK1), respectively.

Table 2. Physico-chemical variables recorded at all the sampling sites (Mean \pm SD).

Parameters/sites	PK1	PK2	KY1	KY2	LJ
WT ($^{\circ}$ C)	27.33 \pm 1.97 ^a	29.96 \pm 3.91 ^a	28.48 \pm 5.43 ^a	26.38 \pm 1.34 ^a	27.58 \pm 1.71 ^a
DO (mg/L)	4.59 \pm 2.89 ^a	4.59 \pm 4.89 ^a	5.10 \pm 2.78 ^a	5.76 \pm 1.80 ^a	3.58 \pm 4.12 ^a
TDS (mg/L)	40.25 \pm 997 ^a	63.48 \pm 21.37 ^a	127.3 \pm 53.31 ^b	129.52 \pm 70.92 ^b	114.34 \pm 25.92 ^{ab}
ES (μ S/cm)	74.08 \pm 28.63 ^a	132.17 \pm 35.58 ^{ab}	272.22 \pm 82.18 ^b	258.28 \pm 142.43 ^b	228.16 \pm 51.14 ^b
pH	8.46 \pm 0.09 ^a	8.36 \pm 0.19 ^{ab}	8.51 \pm 0.12 ^{ab}	8.43 \pm 0.00 ^{ab}	8.05 \pm 0.07 ^b
ALK (mg/L)	12.80 \pm 0.28 ^a	16.00 \pm 0.56 ^a	33.3 \pm 10.32 ^{ab}	37.50 \pm 12.02 ^b	29.50 \pm 7.21 ^a
TUB (NTU)	6.00 \pm 4.24 ^a	10.00 \pm 0.46 ^a	16.00 \pm 11.31 ^a	7.50 \pm 5.33 ^a	18.66 \pm 7.54 ^a
NH ₃ -N (mg/L)	0.36 \pm 0.07 ^a	0.19 \pm 0.09 ^a	0.22 \pm 0.03 ^a	0.23 \pm 0.01 ^a	0.20 \pm 0.24 ^a
PO ₄ ³⁻ (mg/L)	0.40 \pm 0.11 ^a	0.59 \pm 0.09 ^a	0.47 \pm 0.12 ^a	0.48 \pm 0.01 ^a	0.64 \pm 0.53 ^a
NO ₃ -N (mg/L)	1.70 \pm 0.07 ^a	0.95 \pm 0.21 ^a	0.96 \pm 0.04 ^a	1.58 \pm 0.63 ^a	1.15 \pm 0.67 ^a

Remark: a, b = the relationship of environmental factors is similar in the sampling sites, ab = the relationship of environmental factors is different in the sampling sites.

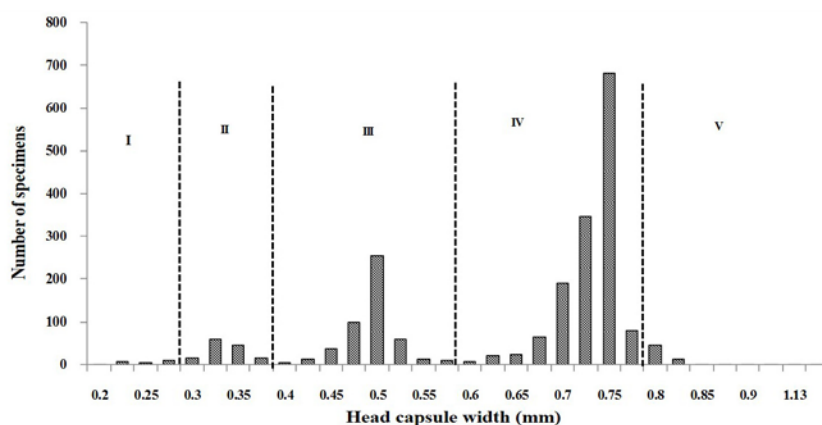
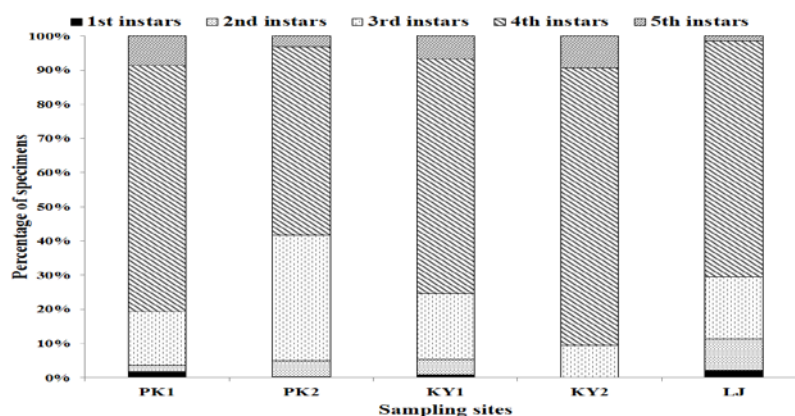
3.2. Larvae Instars of *Pseudoleptonema quinquefasciatum*

Five instars were observed in *Pseudoleptonema quinquefasciatum* using 2,139 specimens. Head widths of first instars ranged from 0.20 to 0.29 mm (n = 22); of second instars from 0.30 to 0.39 mm (n = 143); of third

instars from 0.40 to 0.59 mm (n = 491); of fourth instars from 0.60 to 0.79 mm (n = 1,404); and of fifth instars from 0.80-1.15 mm (n = 73) (Fig. 3-4, Table 3). Accordingly, larvae determined as first to fifth instar were collected from four of the sampling sites; but no first and second instar larvae were found at site KY2 (Table 3).

Table 3. Median and range of head capsule widths (mm) for larval instars of *Pseudoleptonema quinquefasciatum*.

Instar	Number of measurements					Total	Median head width (mm)	Range of head width (mm)
	PK1	PK2	KY1	KY2	LJ			
I	1	1	4	-	22	28	0.245	0.20-0.29
II	1	26	20	-	96	143	0.345	0.30-0.39
III	9	197	89	3	193	491	0.495	0.40-0.59
IV	41	296	316	26	725	1404	0.695	0.60-0.79
V	5	17	31	3	17	73	0.975	0.80-1.15

**Figure 3.** The frequency distribution of larval instars of *Pseudoleptonema quinquefasciatum* Martynov 1935 at all sampling sites, based on head capsule width (n = 2,139) in December 2014 and April 2015.**Figure 4.** Proportion of larval instars of *Pseudoleptonema quinquefasciatum* Martynov 1935 at all sampling sites, assigned on basis of the distribution of head capsule width at each sampling site.

3.3. Gut Content Of *Pseudoleptonema Quinefasciatum* Larvae At Five Sampling Sites

Larval gut contents were assessed qualitatively. Gut contents of 50 larvae were plant tissue, algae, plankton, arthropod fragments, and amorphous detritus. The first three instars appeared to select plankton, algae and plant tissue, whereas guts of larvae of the final two instars contained amorphous detritus and arthropod fragments. Thus, the gut content analysis indicated that larvae are omnivorous filterers (Fig., Table 4).

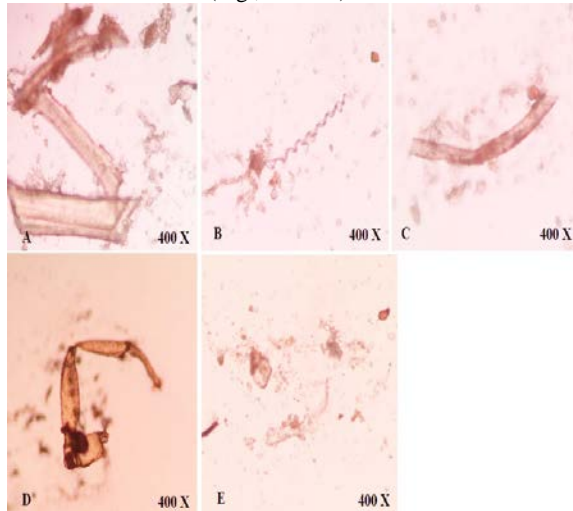


Figure 5. Gut contents from *Pseudoleptonema quinefasciatum* Martynov 1935 larvae. A = plant tissue, B = algae, C = plankton, D = arthropod fragment, E = amorphous detritus.

Table 4. Frequency of food items found in gut contents of each larval instar *Pseudoleptonema quinefasciatum*. + = low, ++ = medium, +++ = high

Larval instar/type of food	1	2	3	4	5
Plant tissue	+	+	++	++	++
Algae	++	++	++	+++	+++
Plankton	+++	+++	+++	+++	+++
Amorphous detritus	+	+	+	++	++
Animal tissue	+	+	+	++	++

3.4. Larval instars of *Pseudoleptonema quinefasciatum* and environmental variables

According to the PCA ordination (Fig. 6), the upper portion of the ordination indicates that the factors with greatest influence on larvae were dissolved oxygen (DO), ammonia-nitrogen (NH₃-N), nitrate-nitrogen (NO₃-N) and alkalinity (AKL) in the 3rd to 5th instar larva at site KY2. The electrical conductivity (EC) appeared to be correlated positively with presence of the 1st instar larva in PK1. In contrast, as shown by the lower portion of the ordination, at sites KY1, PK2 and LJ, number of 2nd instar larvae appear to be correlated with turbidity (TUB), total dissolved solids (TDS), orthophosphate (PO₄³⁻), pH, air temperature (AT) and water temperature (WT).

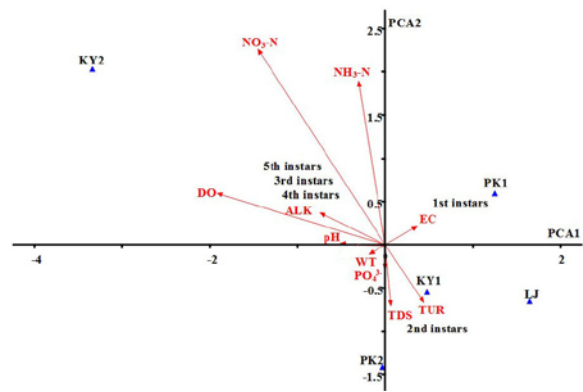


Figure 6. PCA ordination plot based on larval instars of *Pseudoleptonema quinefasciatum* Martynov 1935 and physico-chemical variables and sampling date.

4. Discussion

4.1. Environmental Variables

In freshwater ecosystems, variables such as water temperature and water temperature fluctuations or dissolved oxygen can influence life histories through increased growth rates and number of generations produced annually (Sweeney, 1984). Principle Component Analysis (PCA) showed that dissolved oxygen, ammonia-nitrogen, nitrate-nitrogen and alkalinity had an influence on the 3rd to 5th instar larvae in KY2. The electrical conductivity was correlated positively with number of 1st instar larva in PK1, whereas the turbidity, total dissolved solids, orthophosphate, pH, and water temperature influenced presence 2nd instar larva in the KY1, PK2 and LJ.

Water temperature varied from 26.38 (KY2) to 29.96 C° (PK2). Water temperatures were relatively lower during the wet season than during the dry season. The minimum (25.0°C) and maximum temperatures (35.5°C) were within the range usually observed for tropical waters. At the upstream site, the riparian areas were covered by vegetation that shaded the water and may have kept water temperatures slightly lower — Hauer and Hill (1996) reported that shading from riparian trees beside a smaller watershed stream helped to maintain a lower water temperature.

The lowest mean value of dissolved oxygen (3.58 mg/L) was found in the Huai Lijia (LJ), and the highest values were observed in Huai Kayeng (KY2) (5.76 mg/L). Sources of dissolved oxygen in aquatic environments include the atmosphere and photosynthesis, the concentration being dependent on solubility (which decreases with increasing water temperature). Dissolved oxygen is also reduced by respiration of submerged plants, animals and aerobic bacteria, including their metabolic activity in decomposing dead organic matter (Gupta and Gupta, 2006). Boulton and Brock (1999) pointed out that strong water currents result in turbulent flow which tends to increase or replenish dissolved oxygen.

The pH of the water at all sampling sites was slightly alkaline and showed very little variation (pH 8.05 (LJ) – 8.51 (KY1)). The accumulation of free carbon dioxide due

to reduced photosynthesis by phytoplankton and rooted macrophytes can result in lower pH values in the water while intense photosynthesis reduces free carbon dioxide content and results in higher pH values (Egborge, 1994; Gupta and Gupta, 2006). The pH showed a decrease in the rainy season. This may be attributed to the increased organic matter washed into the stream by surface runoff during the wet season. This would tend to reduce dissolved oxygen through organic decomposition, thus lowering pH.

The highest mean value of total dissolved solids and electrical conductivity (129.52 mg/L, 258.28 μ S/cm) was observed at KY2 and lowest was at PK1 (40.25 mg/L, 74.08 μ S/cm). The general trend in this study was that electrical conductivity tended to increase in the dry season compared with the wet season. Increases in electrical conductivity could result from low precipitation, higher atmospheric temperature resulting in higher evapotranspiration rates, higher total ion concentration, and saline intrusions from underground sources. It could also be due to a high rate of decomposition and mineralization by microbes and by nutrient replenishment from bottom sediments (Egborge, 1994). Increased electrical conductivity and total dissolved solids could also be due to contamination of water from agricultural activities and industrial effluent, degrading water quality (Lenat and Crawford, 1994).

The mean turbidity was highest at LJ (18.66 NTU); the lowest was recorded at PK1 (6.00 NTU). The higher turbidity was recorded during the wet season and may have been due to heavy rainfall, the increase in suspended solids impeding light and thereby increasing turbidity. The adverse effects of turbidity on freshwater include decreased penetration of light which then reduces primary and secondary production, increased adsorption of nutrient molecules to suspended materials, making the nutrients unavailable for plankton production, and decreased oxygen concentration. The particulate matter can clog the filter-feeding apparatus and digestive organs of planktonic organisms, which in turn may adversely affect the development of larvae (Gupta and Gupta, 2006).

The highest mean of alkalinity was recorded in KY2 (8.43 mg/L) and lowest was registered in PK1 (12.80 mg/L). Water bodies in the tropics usually show wide fluctuations in total alkalinity, the values depending on the location, season, plankton populations and nature of bottom depositions. Highly productive waters tend to have alkalinity values above 100 mg/L and for freshwater aquaculture the values optimally should be between 40-200 mg/L. Alkalinity values above 300 mg/L have been reported to affect the spawning and hatching of freshwater fish adversely (Gupta and Gupta, 2006).

The mean dissolved nutrients, ammonia-nitrogen, orthophosphate, nitrate-nitrogen concentrations varied from 0.19 (PK2) to 0.36 mg/L (PK1), 0.40 (PK1) to 0.64 mg/L (LJ), and 0.95 (PK2) to 1.70 mg/L (PK1), respectively. Nitrates are the most oxidized forms of nitrogen and the end product of aerobic decomposition of organic nitrogenous matter. Natural waters in their unpolluted state contain only minute quantities of nitrates. The highest nitrate values occurring during the monsoon/post monsoon season may be primarily due to organic materials entering from the catchment area during periods of high rainfall (Das *et al.*, 1997). The increasing levels of nitrates are likely to be due to freshwater inflow,

litter fall decomposition and terrestrial run-off during the monsoon/post monsoon season (Karuppasamy and Perumal, 2000). Another possible source of nitrate recruitment is through oxidation of ammonia from nitrogen to nitrites (Rajasegar, 2003). The low values during the summer/pre-monsoon period may have been due to utilization of nitrates by phytoplankton activity. In addition, nitrates may be obtained from natural and human activities, both from household wastes and from fertilizers used in agriculture, consistent with observations by Omernik (1977) who indicated that the levels of nutrients in streams were positively correlated with the percentage of land in agriculture. Furthermore, although orthophosphate is usually a minor compound in nature (Jarvie *et al.*, 2002), its higher values in stream water at our sampling sites was probably from agricultural fertilizers which are leached into water when it rains.

4.2. Life Cycle of *P. quinquefasciatum*

The adults of *P. quinquefasciatum* occur all year round (Prommi, 2007; 2015). In our study, pre-pupae and pupae of *P. quinquefasciatum* were recorded throughout the study period. Hydropsychidae undergo five larval instars (Edington and Hildrew, 1995; Waringer and Graf, 1997). In our samples, five larval instars of *P. quinquefasciatum* were recognized at all sampling sites except for the KY2, where no first and second instar larvae were recorded (Table 2). This is due to different collecting efforts but the discrepancy between the lists partly results from the often important adult flight activity.

Trichoptera play an important role in community biomass and secondary production in the stream in Mae Klong watershed. As with many tropical aquatic invertebrates, *P. quinquefasciatum* seems to have a multivoltine life cycle, the year-round favorable environmental conditions resulting in continuous growth and development (Humantincio and Nessimian, 2000). Our study, the first such report for Thailand, showed that larval *P. quinquefasciatum* in the streams from the Mae Klong watershed are mainly omnivorous filterers (Maneechan *et al.*, 2018), moving through several trophic guilds as development from instar to instar takes place. Analyses of gut contents of larvae indicated that the first three instars appear to select plankton, algae and plant tissue, whereas the later instars had consumed amorphous detritus and arthropod fragments.

5. Conclusion

The development of *P. quinquefasciatum* was asynchronous, with many overlapping cohorts coexisting in the rivers. It appears that physico-chemical factors such as electrical conductivity, total dissolved solids, water turbidity, orthophosphate, pH, air and water temperature, dissolved oxygen, ammonia-nitrogen, nitrate-nitrogen, and alkalinity are significant in influencing the life stages and thus the biomass of this hydropsychid caddisfly species in streams of western Thailand. Hydropsychidae are richly diverse in Thai streams and other species can be expected to be affected in the same way.

Acknowledgement

This research work was supported by the Faculty of Liberal Arts and Science, Kamphaeng Saen Campus, Kasetsart University in 2016.

References

- APHA AWWA WPCF. 1992. **Standard method for the examination of water and wastewater**. 18th edition. American Public Health Association. Washington DC.
- Boulton AJ and Brock MA. 1999. **Australian freshwater ecology: Processes and management**. Glen Osmond, Australia: Gleneagles Publishing.
- Buss DF, Baptista DF, Nessimain JL and Egler M. 2004. Substrate specificity, environmental degradation and disturbance structuring macroinvertebrate assemblages in Neotropical Streams. *Hydrobiologia*, **518(1-3)**: 179–188.
- Das J, Das SN and Sahoo RK. 1997. Semidiurnal variation of some physicochemical parameters in the Mahanadi estuary, east coast of India. *Indian J Mar Sci*, **26**: 323–326.
- de Moor FC. 2007. Regional biogeographical differences in Trichoptera diversity in South Africa: Observed patterns and processes. In: Bueno-Soria J, Barba-Alvares R and Armitage B (Eds), **Proceedings of the 12nd International Symposium on Trichoptera**, pp. 211–218.
- Edington JM and Hildrew AG. 1995. A revised key to the caseless caddis larvae of the British Isles, with notes on their ecology. *Freshwater Biological Association Scientific Publication*, **53**: 1–134.
- Egborge ABM. 1994. **Water pollution in Nigeria: Biodiversity and chemistry of Warri River**, Volume 1. Ben Miller Books Nigeria Limited. 331 pp.
- Gupta SK and Gupta RC. 2006. **General and applied ichthyology (fish and fisheries)**. S. Chand and Company Ltd., Ram Nagar, New Delhi. 1130 pp.
- Hauer FR and Hill WR. 1996. Temperature, light, and oxygen. In: Hauer FR and Lamberti GA (Eds.), **Methods in stream ecology**. Academic Press, New York, pp. 93–106.
- Hoang DH Tanida K and Bae YJ. 2005. Records of the Vietnamese Macronematinae (Hydropsychidae, Trichoptera) with description of a new species. In: Tanida K and Rossiter A (Eds.), **Proceedings of the 11th International Symposium on Trichoptera (Osaka)**, Tokai University Press, Kanagawa, Japan. pp. 161–174.
- Humantinc AA and Nessimian JL. 2000. Variation and life strategies of the Trichoptera (Insecta) larvae community in a first order tributary of the Paquequer River, southeastern Brazil. *Rev Bras Biol*, **60(1)**: 73–82.
- Jarvie HP Withers PJA and Neal C. 2002. Review of robust measurement of phosphorus in river water: sampling, storage, fractionation and sensitivity. *Hydrol Earth Syst Sci*, **6(1)**: 113–132.
- Karuppasamy PK and Perumal P. 2000. Biodiversity of zooplankton at Pichavaram mangroves, South India. *Adv Biosci Biotechnol*, **19**: 23–32.
- Lenat DR and Crawford JK. 1994. Effects of land use on water quality and aquatic biota of three North Carolina piedmont streams. *Hydrobiologia*, **294**: 185–199.
- MacKay JR. 1978. Larval identification and instar association in some species of *Hydropsyche* and *Cheumatopsyche* (Trichoptera: Hydropsychidae). *Ann Entomol Soc Am*, **71**: 499–509.
- Maneechan W Kruttha P and Prommi T. 2018. The larva and pupa of *Potamyia flavata* (Banks 1934) (Trichoptera: Hydropsychidae): Description, life cycle, and notes on its biology. *Zootaxa* **4394(3)**: 395–406
- Malicky H. 2010. **Atlas of Southeast Asian Trichoptera**. Biology Department, Faculty of Science, Chiang Mai University. Thailand.
- Merritt RW and Cummins KW. 1996. **An introduction to the aquatic insects of North America**. 3rd ed. Kendall/Hunt Publishing Company.
- Morse JC. 2017. Trichoptera World Checklist. Available from: <http://entweb.sites.clemson.edu/database/trichopt/> (accessed 29 December 2017).
- Omernik JM. 1977. **Nonpoint sources-stream nutrient level relationship: A nationwide study**. PA-600/3-77-105. U.S. Environmental Protection Agency, Corvallis, Oregon.
- Prommi T Permkam S and Malicky H. 2006. The immature stages of *Pseudoleptonema quinquefasciatum* Mart. and *P. supalak* Malicky & Chantaramongkol (Trichoptera: Hydropsychidae). *Braueria*, **33**: 26–30.
- Prommi T. 2007. **Taxonomy of Hydropsychidae (Trichoptera) in mountain streams of Southern Thailand**. Ph.D. Dissertation, Prince of Songkla University, Songkla, Thailand.
- Prommi T. 2015. Trichoptera fauna as stream monitoring of the Mae Klong watershed, Western Thailand. *Adv Environ Biol*, **9(26)**: 1–6.
- Rajasegar M. 2003. Physico-chemical characteristics of the Vellar estuary in relation to shrimp farming. *J Environ Biol*, **24**: 95–101.
- Roback SS. 1962. Environmental requirements of Trichoptera”, In: Tarzwell CM (Ed.), **Third seminar in biological problems in water pollution**, pp. 118-126. No. 999-WP-25, U.S. Public Health Service, Cincinnati, Ohio.
- Sweeney BW. 1984. Factors influencing life history patterns of aquatic insects. In: Resh VH and Rosenberg DM (Eds.), **The ecology of aquatic insects**. Praeger Publishers, New York. pp. 56–100.
- Wallace JB and Webster JR. 1996. The role of macroinvertebrates in stream ecosystem function. *Annu Rev Entomol*, **41**: 115–139.
- Ward D Holmes N and Jose P. 1995. **The new rivers and wildlife handbook**. Bedfordshire: RSPB, NRA. The Wildlife Trusts.
- Ward JV. 1992. **Aquatic insect ecology**. New York: John Wiley & Sons, 438 p.
- Waringer J and Graf W. 1997. **Atlas der österreichischen Köcherfliegenlarven unter Einschluss der angrenzenden Gebiete, Wien**: Facultas Universitätsverlag, 286 p.
- Whiles MR and Wallace JB. 1997. Leaf litter decomposition and macroinvertebrate communities in headwater streams draining pine and hardwood catchments. *Hydrobiologia*, **353(1-3)**: 107–119.
- Woodcock TS and Huryn A. 2007. The response of macroinvertebrate production to a pollution gradient in a headwater stream. *Freshwater Biol*, **52(1)**: 77–196.

Antiviral, Antifungal, and Antibacterial Potential Activities of *Ephedra Sinica* in Vitro

Mohamed M. Deabes¹, Abdou K. Allayeh^{2*}, Mohamed M Seif¹, Abdel-Hamied M. Rasme³ and Khayria M. Naguib¹

¹ Food Toxicology and Contamination Department, ² Virology lab 176, Water Pollution Research Department, National Research Centre, El Buhouth St, Dokki, 12622-Cairo, ³ Botany and Microbiology Department, Faculty of Science, Suez University, Suez, Egypt.

Received July 24, 2019; Revised September 8, 2019; Accepted September 16, 2019

Abstract

This study was conducted to assess the antiviral, antifungal and antibacterial potential of extracts from *Ephedra sinica*. Plant extract activity was screened for four bacterial, three fungal and one viral pathogen including: *Klebsiella pneumoniae*, *Enterobacter cloacae*, *Serratia marcescens*, *Escherichia coli*, *Aspergillus flavus*, *Aspergillus ochraceus*, *Aspergillus niger* and Cocksackie B₃ virus. The findings disclosed promising inhibitory impacts against all pathogens. Ethanol-water extract showed that the greatest inhibition zones (mm) against bacterial and fungal species ranged from 20.7 to 25.0 and 29.0 to 35.0 at a concentration of 150 µl/ml respectively, similar to methanol-water extract inhibition zones against the same pathogens. Interesting outcomes against Cocksackie B₃ virus was observed. For ethanol-water extract (51.6%), followed by ethanol extract (46.6%) and methanol extract (41%) during zero-time infection, the greatest viral inhibition activity was documented. During virucidal process, a limited action of inhibition was observed for ethanol extract (39.4%), methanol extract (36.8%), and ethanol-water extract (31%). No viral inhibition action was notarized in both pre- and post- infection processes. The findings of this study indicated that *Ephedra sinica* is an excellent source of bioactive substances against a wide range of various microbial pathogens.

Keywords: *Ephedra sinica*, Antiviral, Antibacterial, Antifungal

1. Introduction

The quest for new substances with high efficacy, low toxicity, and minor side effects must proceed against microbial diseases due to the global need for these substances to solve drug resistance issues. Growing interest in natural products derived antimicrobial agents still remains the best resource for future advancement as powerful and safe agents for modern medication (Nagai *et al.*, 2011; Allayeh *et al.*, 2015 and 2018). Particularly the medicinal plants; *Ephedra sinica* is regarded one of the most important plants in traditional medicine. *Ephedra sinica* has been used in several disease treatments for over 5000 years (Naidu, 2000; Soni *et al.*, 2004). The dried plant has traditionally been used as a tea to treat asthma, cough, fever, urinary incontinence, lack of sweating, and edema reduction. Furthermore, the *Ephedra* plant includes bronchial dilator, ephedrine, and high quantities of proanthocyanidins with prominent biological activities such as alkaloids, such as bronchodilation and vasorelaxation. Proanthocyanidins were used as antimicrobial, antioxidant, anti-inflammatory, immunosuppressive, antiviral, anti-invasive, antiangiogenic, antitumor, and cytotoxic activity, especially against cancer cell lines such as SGC-7901, HepG2, and HeLa. *Ephedra sinica* has recently been used in the United States market as a supplement for weight loss

and energy gain (Hyuga *et al.*, 2004 and 2007; Zhang *et al.*, 2018). Several reports have documented the antimicrobial activities of *Ephedra* genus against various microorganisms species, including Bacterial species such as; *Staphylococcus aureus*, *Bacillus anthracis*, *B. diphtheriae*, *B. dysenteriae*, *B. typhosus*, *Pseudomonas aeruginosa*, *Lactobacillus acidophilus*, and *Lactobacillus casei*; Fungal species such as *Aspergillus parasiticus*, *Saccharomyces cerevisiae*, *Candida albicans*, *Candida utilis*; viral species such as avian influenza virus (Bagheri-Govkosh *et al.*, 2009; Soltan and Zaki, 2009; Lee *et al.*, 2009; Fazeli-Nasab and Mousavi, 2019). This work will explore the prospective antibacterial, antifungal and antiviral activities of various *Ephedra sinica* crud extracts against eight species of various pathogens, including *Klebsiella pneumoniae*, *Enterobacter cloacae*, *Serratia marcescens*, *Escherichia coli*, *Aspergillus flavus*, *Aspergillus ochraceus*, *Aspergillus niger*, and Cocksackie B₃ virus. We used this virus as model to study the prospective antiviral activity due to its association with several human diseases such as deadly viral myocarditis, hepatitis, meningitis, gastroenteritis, hand foot mouth disease and fibrosis cardiomyopathy that could advance toward heart failure with no effective medication so far.

* Corresponding author e-mail: drallayeh@yahoo.com.

2. Materials and Methods

2.1. Plant Extraction Preparation

Ten grams of *Ephedra sinica* (stem part) powder were extracted by 100 ml of each (ethanol (ET), ethanol: water (ET: H₂O), methanol (MeoH) and methanol: water (MeoH: H₂O)) at room temperature for 24 hours in a shaker. Finally, the extract was concentrated under vacuum with a rotary evaporator and sterilized by using a 0.22 µm syringe filter.

2.2. Antimicrobial Activity Preparation

The experimental bacteria isolates including, *Klebsiella pneumoniae*, *Enterobacter cloacae*, *Serratia marcescens*, and *Escherichia coli* were kindly provided by the Department of Botany and Microbiology, College of Science, Suez University, Egypt. The microbial strains were maintained on nutrient agar slant at 4°C until antimicrobial testing was conducted. According to Sethiet *et al.*, (2013), the antibacterial activity was determined by agar well diffusion assay as the following; Nutrient agar medium was poured at 45°C in pre-seeded sterilized plates with 500 µl of 18 h culture of each bacterial species. Poured plates seeded with test organisms were rotated to allow homogenous spread of the inoculum and left for 30 min at room temperature to solidify. Using a cork-borer, wells of 5 mm in diameter were made in the medium of these plates and injected by *Ephedra* extracts (50, 100 and 150 µl) for each concentration in these wells under aseptic conditions. The Petri-dishes were held in a refrigerator for two hours to allow antimicrobial agent to spread homogeneously before the organism was allowed to grow (Selim *et al.*, 2011). The plates were incubated at 37°C overnight. A positive test showed the appearance of inhibition zone and the diameters of the inhibition zone around the well were measured.

2.3. Antifungal Activity Preparation

Ephedra extracts' antifungal activity was tested against *Aspergillus flavus*, *Aspergillus ochraceus*, *Aspergillus niger* using the agar well diffusion method. Briefly, fungi spore suspensions were prepared and adjusted approximately to 10⁶ spore/ml. Potato dextrose agar (PDA) (Sigma-Aldrich, USA) plates were inoculated with 1 ml of designated fungal spore suspension. Wells of 5 mm diameter were produced on the PDA surface and filled with *Ephedra* extracts at concentration 50, 100 and 150 µl and incubated at 28°C for 72 hours. Fungal growth control was prepared using PDA medium inoculated with spore suspension without any extracts. After incubation, the plates were tested for the inhibitory zones (mm) of the mycelial growth around the wells (Kavanagh, 1972). All experiments were performed in triplicates.

The PDA medium was prepared with distinct plant extract concentrations of 50, 100 and 150 µl by adding extract to the melted medium, followed by the addition of Tween 80 to disperse the extract into the medium. Thirty milliliters of the medium were poured into glass Petri-dishes (9 x 1.5 cm). Each Petri-dish was inoculated at the center with a mycelial disc (6 mm diameter) of the fungal culture. Positive control plates were inoculated following the same procedure. Plates were incubated at 28°C for seven days and the colony diameter was observed daily.

2.4. Antiviral Activity Preparation

Confluent monolayer vero cell (Holding Company for Biological Products and Vaccines, Egypt) was used for the propagation of Coxsackie B₃ virus which was kindly provided by Dr. Mohamed Shaheen, (Shubhada Bopegamage's Lab, Slovak Medical University, Slovakia). This cell line cultured in Dulbecco's modification of eagle's medium DMEM, 13.48 g of DMEM powder was dissolved in one liter of de-ionized H₂O. This culture medium was supplemented with 0.1% L-glutamine, heat-inactivated fetal bovine serum (FBS) from Gibco-BRL in 10% or 2% to prepare growth or maintenance medium, respectively. The following antimicrobials were added: Penicillin/Streptomycin at the final concentration of 50 µg/ml, and Fungal-zone at the final concentration of 2.5 µg/ml obtained from the Gentech Company in Egypt. Using a 0.22 µm syringe filter, fully medium was filtered and sterilized. Virus titer was determined as the next by using Endpoint (limiting) dilution method. At room temperature, a tube of viral stock suspension was thawed. Once thawed, 100 µl of the stock viral solution was serially diluted into a medium sequence of tenfold dilution. Confluent cells (10⁴ cells/ well) prepared in 24-well plates were inoculated with 100 µl of each dilution in triplicate. The plates were then incubated at 37°C (5% CO₂) and observed daily for the development of characteristic CPE. The lowest dilution of viral stock suspension that could still cause 50% of a CPE was taken as the maximum dilution that would result in infection. This was called the TCID₅₀ because it was the minimum concentration of viral particles needed to detect viral CPE and provide a rough indication of the overall concentration of virus present within the stock suspension. The endpoint dilution, expressed as TCID₅₀/ml, was calculated by using Reed-Muench formula (Reed and Muench, 1938; Flint *et al.*, 2003).

2.4.1. Cytotoxicity and Cell Viability

Adding various dilutions of tested extracts to the media can trigger cell modifications. Thus, to ensure that all morphological changes are reported, the maximum concentration of tested extracts at which the cells will display no morphological changes will be determined. Cell suspensions were seeded in 24-well plates and left at 37°C for 24 hours in 5% CO₂ incubator. Upon completion of the confluence, distinct dilutions of the tested extracts were added. The plates then incubated at 37°C in 5% CO₂ atmosphere for two days and cell morphology changes were observed daily. Using the CPE scoring scheme, evidence of morphological change (such as loss of monolayer, granulation, and vacuolization in cytoplasm) was reported (Vijayan *et al.*, 2004). All assays were conducted with approximately 3x10⁴ cells per well in triplicates in 24-well plates.

2.4.2. Cytopathic Inhibition Assay

Vero confluent 24-well plates have been infected at 37°C for 90 min with 100 µl of stock Coxsackie B₃ virus. Then, 100 µl of the extracts were added. For each dilution, three wells were used and 100 µl of the maintenance medium were added per well. Ultimately, plates were incubated for three days until full CPE was observed. The inhibition of CPE was determined by the antiviral activity relative to control and expressed by the formula of Reed

and Munech, (1938). The mechanism of antiviral activity against Coxsackie B₃ virus was investigated in triplicates using cytopathic inhibition assay with some modifications during each process as the next;

2.4.2.1. Pre-Viral Infection Process

Vero cells were cultivated in 24-well plates and inoculated in 5% CO₂ incubator with 100 µl of tested extracts for 90 min at 37°C. The medium was aspired and 100 µl of Coxsackie virus was inoculated for 90 min at 37°C in 5% CO₂ incubator. The maintenance medium was added and further incubation time for 3 days at 37°C in 5% CO₂ incubator. Antiviral activity was determined by the inhibition of CPE related to the control according to Hai-Rog Xiang *et al.*, (2012) and expressed by the formula of Reed and Munech, (1938).

2.4.2.2. Zero-Time Viral Infection Process

One hundred micro-liter of Coxsackie B₃ virus was inoculated into the confluent monolayer of vero cells accompanied by the same volume of tested extracts at 37°C in 5% CO₂ incubator for 3 days until CPE was observed. Antiviral activity was determined by the inhibition of CPE liked to control and expressed by the formula of Reed and Munech as outlined in the prior section.

2.4.2.3. Post-Viral Infection Process

This test was performed with the following variations as mentioned in the prior sections: Confluent of Vero cell line was cultivated in 24-well plates and handled for 90 min with 100 µl of Coxsackie B₃ virus in 5% CO₂ incubator at 37°C. With 100 µl of tested extracts, cells were washed and overlaid. Until CPE was observed, the plates were incubated for 3 days.

2.4.2.4. Virucidal infection process

The direct effect of extracts on Coxsackie B₃ virus was recognized by blending equal volumes of virus suspension with each extract and incubated at 37°C in 5% CO₂ atmosphere for 90 min prior cell infection. The mixture has been introduced to the cells. The same processes in the previous sections have been performed.

2.5. GC/MS Analysis

The assessment was conducted using a GC (Agilent Technologies 7890A) interfaced with a mass-selective detector (MSD, Agilent 7000) equipped with a polar Agilent HP-5ms (5%-phenyl methyl poly-siloxane) capillary column (30 m × 0.25 mm i. d. and 0.25 µm film thickness). The carrier gas was helium with the linear velocity of 1ml/min. The temperature of the injector and detector was 200° C and 250° C, respectively. The volume injected size is 1µl. The operating parameters for MS were as follows: ionization potential 70 eV, interface temperature 250° C, and acquisition mass range 50–800. Component identification was based on a comparison of their mass spectrum and retention time with those of the authentic compounds and by computer matching with NIST and WILEY libraries as well as comparison of the fragmentation pattern of the mass spectral information with those reported in the literature (Sanatana *et al.*, 2013).

2.6. HPLC Conditions

The polyphenols determination from the four *Ephedra* extracts was performed using an Agilent 1260 series.

Column C18 (4.6 mm x 250 mm i.d., 5 µm) was used to separate. The mobile phase consisted of water (A) and 0.02% tri-floro-acetic acid in acetonitrile (B) at a flow rate 1 ml/min. The mobile phase was programmed consecutively in a linear gradient as follows: 0 min (80% A); 0–5 min (80% A); 5–8 min (40% A); 8–12 min (50% A); 12–14 min (80% A) and 14–16 min (80% A). The multi-wavelength detector was monitored at 280 nm. The injection volume was 10 µl for each of the sample solutions. The column temperature was maintained at 35 °C (Amakura *et al.*, 2013).

2.7. Statistical analysis

All experiments were performed in triplicate and the data expressed as means of ± standard deviation (SD) using Microsoft Excel software V2007.

3. Results and Discussion

The genus of *Ephedra* is widespread globally and its composition depends mainly on its species, harvest dates, fractionation processes, and geographical area. In this manner, their pharmacological effect could be quite-species specific. Most of the previous *Edephra* reports have been performed on *Ephedra sinica*, the pharmacological characteristics of which seem to come basically from significant alkaloids, ephedrine, and pseudoephedrine (Walaa *et al.*, 2019). This study is one of very restricted work to our understanding that the antimicrobial actions of *Ephedra sinica* explored. Based on the results of the current study, all *Ephedra sinica* extracts have been shown to inhibit wide range of pathogens as the next in the following sections.

3.1. Antibacterial Activity

To explore *Ephedra sinica*'s crud extracts for antibacterial activity; all crud extracts showed prominent inhibition zones against all bacterial species. Indeed, the largest inhibition zones (mm); 25.0, 22.3, 20.7, and 21.0 have been reported for ethanol: H₂O fraction at 150 µg/ml concentration against *Serratia marcescens*, *Escherichia coli*, *Enterobacter cloacae*, and *Klebsiella pneumoniae*, respectively. Although at the same concentration, methanol: H₂O fraction also displayed elevated inhibition zones; 24.3, 21.0, 19.6, and 20.0 against the same bacterial species. In comparison to prior extracts, inhibition zones of absolute ethanol extract (18.3, 17.0, 15.7 and 14.6) accompanied by absolute methanol extract (21.6, 20.0, 18.0 and 18.6) showed a moderate inhibition of the same species (Table 1). In this respect, Plant *Ephedra sinica* could be regarded as an excellent growth inhibitor against bacterial species. On the other hand, ethanol: aqueous extract has been discovered to be more effective against bacterial species compared to methanol: aqueous extract that also works against the same bacterial species. This outcome is in complete agreement with the previous report about ethanol and aqueous extractions of *Ephedra gerardiana* against *B. atrophaeus*, *Escherichia coli*, *Staphylococcus aureus* and *K. pneumonia* (Khan *et al.*, 2017). Unlike *Ephedra gerardiana*'s ethanol extract against *E. coli*, *S. aureus*, and *P. aeruginosa* also exhibited prominent inhibition zones (Kumar and Sigh, 2011).

Table 1: Inhibition zones (mm) formed by E.S extracts against Bacterial spp.

Extract	Concentration (µl)	Inhibition zone (mm)			
		<i>Serratia marcescens</i>	<i>Escherichia coli</i>	<i>Enterobacter cloacae</i>	<i>Klebsiella pneumoniae</i>
MeOH	50	10.7±1.7	8.6±1.5	8.5±1.1	11.0±2.0
MeOH:H ₂ O		12.3±2.1	10.6±1.2	10.6±2.08	13.0±1.9
ET		8.0±1.8	7.3±2.1	7.0±1.5	8.0±1.0
ET:H ₂ O		13.0±1.8	12.3±2.3	10.0±1.5	11.5±1.5
MeOH	100	16.0±1.5	13.0±1.52	10.0±1.1	12.0±1.0
MeOH:H ₂ O		19.0±2.6	16.0±1.0	14.7±1.52	14.6±2.5
ET		13.0±2.1	10.6±1.6	8.7±1.5	10.7±1.3
ET:H ₂ O		19.6±2.1	16.7±1.6	15.7±2.08	15.0±2.0
MeOH	150	21.6±1.5	20.0±1.7	18.0±1.2	18.6±1.7
MeOH:H ₂ O		24.3±1.15	21.0±2.0	19.6±1.8	20.0±1.5
ET		18.3±2.0	17.0±2.0	15.7±2.3	14.6±1.5
ET:H ₂ O		25.0±2.0	22.3±2.5	20.7±2.1	21.0±2.0

3.2. Antifungal Activity

All crude extracts have been assessed for antifungal activity against *Aspergillus flavus*, *Aspergillus ochraceus* and *Aspergillus niger* based on powerful prospective antibacterial activities. Hence, significant antifungal activity or elevated inhibition zones were documented in this study. Inhibition zones of 29.0, 35.3, and 32.1 (mm) for Ethanol: H₂O fraction (150 µg/ml) were disclosed against *Aspergillus flavus*, *Aspergillus ochraceus*, and *Aspergillus niger*, followed by inhibition zones (26.5, 32.5 and 28.5) of methanol: H₂O fraction, respectively, whereas inhibition zones of absolute methanol (22.6, 29.5 and 25.0) followed by absolute ethanol inhibition zones (18.5, 23.0 and 15.0) showed average inhibition activity against the same fungal species compared to prior extracts at different concentrations (Table 2). Since the growth of the *Aspergillus* species at different levels of 50,100 and 150 µg / ml was considerably inhibited, the current work suggests that *Ephedra sinica* could be used as a therapy against *Aspergillus* species. Our findings are comparable to the previous report on the essential oils of *Ephedra* major which exhibited significant inhibition of fungal growth and Aflatoxin production according to Razzaghi-Abyaneh *et al.*, (2009). For essential oils of *Ephedra* major at the concentration of 1000 µg/ml, powerful inhibition of *Aspergillus parasiticus* and aflatoxin production was reported in other studies (Bagheri-Govkosh *et al.*, 2009; Abou El-Soud *et al.*, 2015; Deabes *et al.*, 2018). On the other hand, few studies showed that there was no obvious inhibition impact of the *Ephedra breana* fractions against *Aspergillus flavus* at 1000 µg / ml levels (Feresin *et al.*, 2001). Another study showed that *Ephedra procera* methanol extract could not influence *Aspergillus flavus* growth at concentrations of 1000 µg/ml (Fazly-Bazzaz and Haririzadeh, 2003). This may refer to the variations in the *Ephedra* plant's compositions or species.

Table 2: Inhibition zones (mm) formed by E.S extracts against Fungi spp.

Extract	Concentration (µl)	Inhibition zone (mm)		
		<i>A. flavus</i>	<i>A. ochraceus</i>	<i>A. niger</i>
MeOH	50	9.0±1.8	15.0±2.1	11.5±1.5
MeOH:H ₂ O		14.7±2.2	18.5±1.1	16.0±1.07
ET		6.5±1.5	9.3±1.5	7.0±1.0
ET:H ₂ O		14.5±1.8	19.0±1.5	16.5±1.5
MeOH	100	16.5±1.5	23.7±1.0	18.1±1.3
MeOH:H ₂ O		21.0±2.0	27.0±1.5	24.5±1.5
ET		9.5±1.0	15.0±1.7	11.5±1.0
ET:H ₂ O		23.5±2.1	28.6±1.4	27.1±1.5
MeOH	150	22.6±1.0	29.5±1.1	25.0±1.5
MeOH:H ₂ O		26.5±1.5	32.5±1.0	28.5±1.0
ET		18.5±1.0	23.0±1.9	15.0±2.0
ET:H ₂ O		29.0±1.0	35.3±2.0	32.1±1.5

3.3. Antiviral Activity

No cytotoxic effect was observed for all the extracts using Vero cell lines. Contrary to the outcomes of antibacterial- or antifungal- experiments in the present study, interesting phenomena was reported during antiviral experimentation; during pre-infection or post-infection mechanisms, neither crude extract nor any fraction showed significant antiviral activity against Coxsackie B₃ virus. But during zero-time infection and virucidal processes for particular extracts, an inhibition activity was reported as shown in (Table 3). The greatest inhibition activity was documented for ethanol: H₂O (51.6%) followed by absolute ethanol (46.6%), absolute methanol (41%), respectively during the zero-time process. For absolute ethanol, absolute methanol, and ethanol: H₂O fractions, 39.4%, 36.8%, and 31% of inhibition activity were reported during the process of virucidal infection, respectively.

Table 3: Antiviral activity of E.S extracts against Coxsackie B₃ virus.

Extract	% of CPE Inhibition of Coxsackie B ₃ virus			
	Pre-infection	Post-infection	Virucidal infection	Zero-time infection
Methanol extract	15.2%	11%	36.8%	41%
Methanol : H ₂ O	5%	2%	31%	33.5%
Ethanol extract	13.8%	16.4%	39.4%	46.6%
Ethanol : H ₂ O	5.5%	9.3%	31%	51.6%

The crud extracts of *Ephedra sinica* have moderate antiviral activity against Coxsackie B₃ virus *in vitro* compared to the outcomes of both antibacterial and antifungal tests in the current work. Contrary to the previous study conducted on plant *Ephedra aphylla* collected from Egypt, mild proportion of antiviral activity (40.7%) against Herpes virus type I was also documented (Khaled *et al.*, 2018). According to Mantani *et al.*, (1999), the inhibition may due to the inhibitory effect of the *Ephedra* on the acidification of intracellular elements such as lysosomes that have capability to inhibit the growth of influenza virus. In another study, (Sumiko *et al.*, 2016) confirmed that the ephedrine alkaloids-free *Ephedra* Herb extract has significant antiviral activity against influenza virus and suggested obtaining a license approval for the therapeutic use of ephedrine alkaloids-free *Ephedra*.

3.4. GC/MS And HPLC Analysis

According to GC/MS analyses, the retention indices (RI) and the composition % of twelve components were identified in *Ephedra sinica* out of which {Lupeol & 2-Nonaprenyl-6-methoxyphenol & Glycodeoxycholic acid & Ledene} and {5, 7-dimethoxyflavone & 4-(Ethylamino)-6-(methylsulfanyl)-1, 3, 5-triazin-2-ol} were the principle principal? Components found in ethanol-water and absolute ethanol extracts, respectively. The profile of GC/MS for methanol-water and absolute methanol extracts was completely different from the previous extracts. Here, twenty-one and eleven components were documented for methanol-water and absolute methanol extracts, respectively (Table 4). On the other hand, higher polyphenol (Gallic acid, Coffeic acid, Syringic acid) content was observed in aqueous-organic solvents extracts in contrast to their absolute solvents by using HPLC (Table 5). Extract of Ethanol-water had the largest polyphenol content followed by extract of methanol-water, while there were no several peaks in both absolute extracts of ethanol and methanol (Figures 1-5). These are comparable to the results of the previous report conducted on black tea and which showed that 50 % of aqueous organic solvents have extracted more polyphenolic compounds than absolute organic solvents (Michael *et al.*, 2016). This phenomenon may be because water swells the plant material and increases extractability by allowing the solvent to penetrate more easily into the solid matrix (Horax *et al.*, 2010). To our knowledge, the phenolic compounds may interact with the membrane proteins, which changes membrane permeability, and causes cell death or penetrates the pathogen itself and coagulates its content according to Tian *et al.*, (2009). These mechanisms support our outcomes and explain why the aqueous-ethanol extracts have significant antibacterial, antifungal and antiviral activities in this work more than

absolute solvent, which may be due to a high content of polyphenol.

Table 4: GC/ MS Profile for each E.S extract according to Retention time and constituents concentration (%)

A- Absolute Ethanol Extract (ET)

No.	Name of compounds	Molecular Formula	Retention time	Ratio (%)
1	Thiourea,N-(4-butoxyphenyl)-N'-[4-(dimethylamino)phenyl]	C ₁₉ H ₂₅ N ₃ OS	6.008	1.05
2	1'-Hydroxymidazolam	C ₁₈ H ₁₃ ClFN ₃ O	14.421	1.31
3	Tetrahydro-L-biopterin	C ₉ H ₁₅ N ₅ O ₃	14.567	1.3
4	4',6-Dimethoxyisoflavone-7-O-β-D-glucopyranoside		14.673	1.67
5	Cholesta-5,7-dien-3-ol, (3β)-	C ₂₇ H ₄₄ O	15.146	6.2
6	Noscapine	C ₂₂ H ₂₃ NO ₇	15.594	1.23
7	Methyl farnesoate	C ₁₆ H ₂₆ O ₂	19.147	3.01
8	Squalene	C ₃₀ H ₅₀	19.786	1.0
9	5,7-dimethoxyflavone	C ₁₇ H ₁₄ O ₄	20.565	25.89725
10	Trp-Cys-Arg, Tryptohan , cystein, arginine		21.437	3.5
11	4-(ethylamino)-6-(methylsulfanyl)-1,3,5-triazin-2-ol	C ₆ H ₁₀ N ₄ OS	22.194	24.51656
12	3-Methoxy-6,7,8,9-tetrahydrobenzo[b,d]furan-2-ol	C ₁₃ H ₁₄ O ₃	22.842	8.716873

B- Ethanol-Water Extract (ET: H2O)

No.	Name of compounds	Molecular Formula	Retention time	Ratio (%)
1	Salicylic acid	C ₇ H ₆ O ₃	3.445	9.04
2	Pyrocatechol	C ₆ H ₄ -1,2-(OH) ₂ C ₆ H ₆ O ₂	3.539	5.13
3	Hydroquinone	C ₆ H ₆ O ₂ C ₆ H ₄ -1,4-(OH) ₂	6.308	6.72
4	4-Pyridinecarboxaldehyde	C ₆ H ₅ NO	3.755	4.37
5	7,3',4',5'-Tetramethoxyflavanone	C ₁₈ H ₁₆ O ₈	6.081	1.36
6	Quercetin 3',4',7-trimethyl ether	C ₁₈ H ₁₆ O ₇	13.199	1.47
7	Propyl gallate	C ₁₀ H ₁₂ O ₅	14.462	2.63
8	2-Nonaprenyl-6-methoxyphenol	C ₁₇ H ₂₄ O ₂	16.522	14.13
9	Glycodeoxycholic acid	C ₂₆ H ₄₃ NO ₅	1.428	11.43
10	Ledene	C ₁₅ H ₂₄	21.327	11.12
11	Lupeol	C ₃₀ H ₅₀ O	21.954	19.75
12	Betulin	C ₃₀ H ₅₀ O ₂	23.091	3.62

C- Absolute Methanol Extract (MeoH)

No.	Name of compounds	Molecular Formula	Retention time	Ratio (%)
1	Pyrocatechol	C ₆ H ₄ -1,2-(OH) ₂ C ₆ H ₆ O ₂	4.02	14.47
2	DL-Homocysteine, S-ethyl-	C ₆ H ₁₃ NO ₂ S	4.207	7.59
3	1-Aminothiurea	CH ₅ N ₃ S	4.529	1.899823
4	Benzoyl isothiocyanate	C ₈ H ₇ NS	4.696	2.226332
5	Salsoline (Alkaloid)	C ₁₁ H ₁₅ NO ₂	5.804	1.058791
6	7,8-Dihydroneopterin	C ₉ H ₁₃ N ₅ O ₄	13.936	1.201704
7	2-Acetyl-5-(tetrahydroxybutyl)imidazole	C ₉ H ₁₄ N ₂ O ₅	14.103	2.353973
8	4',6-Dimethoxyisoflavone-7-O-β-D glucopyranoside		14.861	1.643087
9	Olomoucine	C ₁₅ H ₁₈ N ₆ O	16.136	1.17494
10	2,6-dimethyl-N-(2-methyl-α-phenylbenzyl)aniline	C ₁₀ H ₁₅ N	20.349	44.02967
11	Betulin	C ₃₀ H ₅₀ O ₂	22.529	1.086693

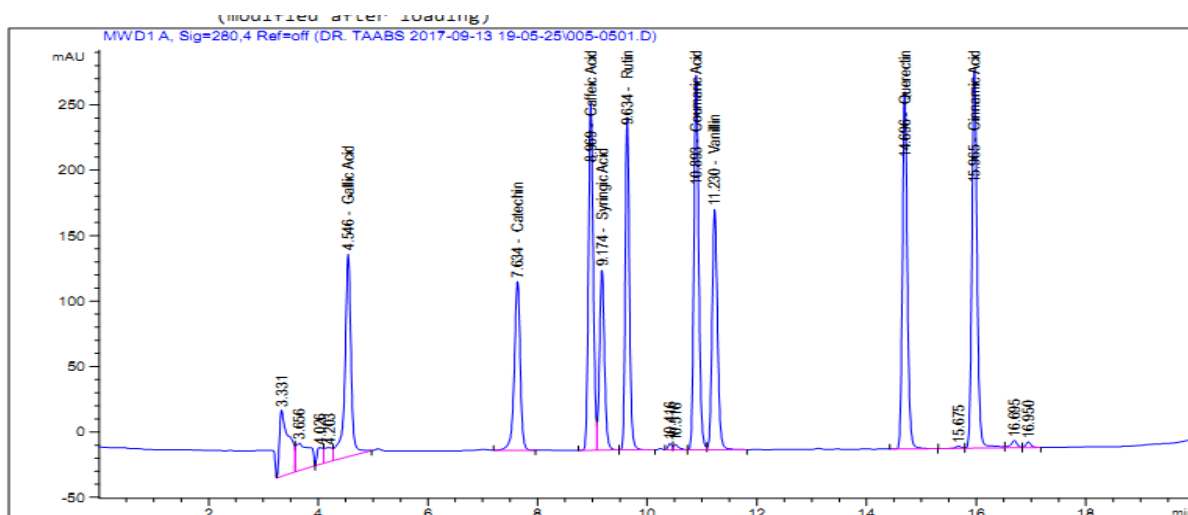
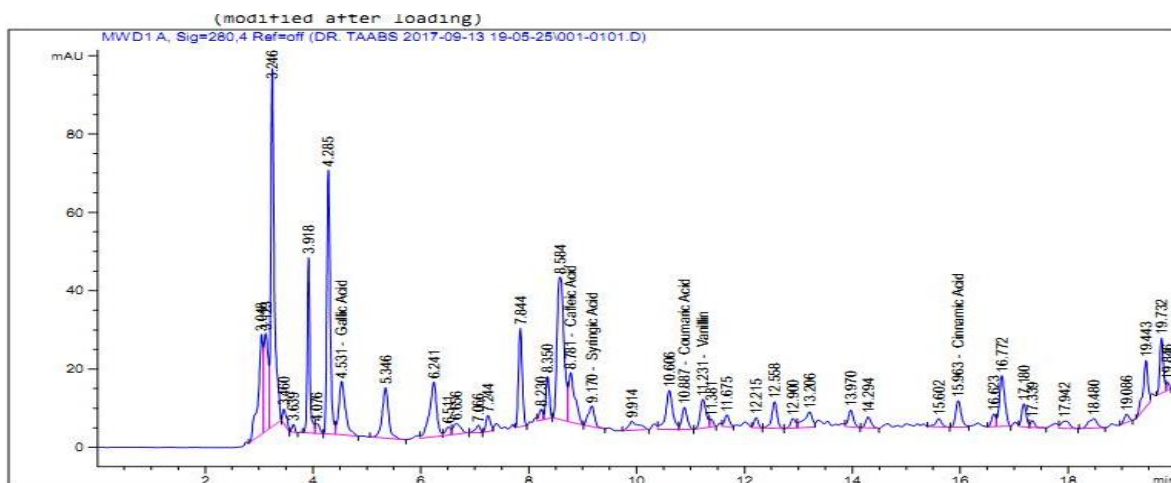
D- Methanol-Water Extract (MeoH: H2O)

No.	Name of compounds	Molecular Formula	Retention time	Ratio (%)
1	Epinephrine	C ₉ H ₁₃ NO ₃	3.906	3.164819
2	Vitexin	C ₂₁ H ₂₀ O ₁₀	3.979	3.9
3	Nopol (terpene)	C ₁₁ H ₁₈ O	4.256	9.81479
4	Benzo[h]quinoline, 2,4-dimethyl-	C ₁₅ H ₁₃ N	5.393	6.24
5	7,3',4',5'-Tetramethoxyflavanone	C ₁₉ H ₂₀ O ₆	6.326	4.602642
6	8-Carboxy-3-methylflavone	C ₁₇ H ₇ D5O ₄	6.99	5.2
7	4-Hydroxychalcone	C ₁₅ H ₁₂ O ₂	7.739	6.72
8	3-(2-Benzothiazolyl)-6-methoxycoumarin	C ₁₇ H ₁₁ NO ₃ S	8.012	3.177727
9	Norepinephrine	C ₈ H ₁₁ NO ₃	8.53	2.45
10	Vanillic acid	C ₈ H ₈ O ₄	9.059	3.82
11	Phloroglucinol	C ₆ H ₆ O ₃	10.119	3.140511
12	Quercetagenin-7-O-glucoside	C ₂₁ H ₂₀ O ₁₃	11.968	3.607574
13	Cholic acid	C ₂₄ H ₄₀ O ₅	12.877	1.80761
14	Tetrahydro-L-biopterin	C ₉ H ₁₅ N ₅ O ₃	13.797	2.809424
15	5,7,3',4',5'-Pentahydroxyflavone	C ₁₅ H ₁₄	14.429	3.711465

16	Gardenin	C ₂₁ H ₂₂ O ₉	14.889	2.320525
17	7-Diethylamino-3-(3,4-dimethoxyphenyl) coumarin	C ₂₁ H ₂₃ NO ₄	15.37	2.170816
18	Quinine	C ₂₀ H ₂₄ N ₂ O ₂	15.566	2.696559
19	5β,7βH,10α-Eudesm-11-en-1α-ol	C ₁₅ H ₂₆ O	15.59	3.245133
20	Baicalein trimethyl ether		15.806	4.48629
21	3,4-Dihydrocoumarin	C ₉ H ₈ O ₂	20.393	1.769145

Table 5: HPLC Separation for Polyphenol content in E.S extracts.

Poly phenol	Concentration (µg/ml)			
	Methanol Extract	Methanol-Water Extract	Ethanol Extract	Ethanol-Water Extract
Gallic Acid	5.66	17.70	1.41	49.54
Catechin	0.0	0.0	0.0	3.27
Coffeic Acid	4.02	8.20	0.0	8.33
Syringic Acid	0.0	2.61	0.0	2.78
Coumaric Acid	0.90	1.41	0.0	1.45
Vanillin	1.9	1.77	0.0	1.79
Cinnamic Acid	0.52	0.45	0.19	1.11

**Figure 1:** HPLC Profile for Polyphenol Standards**Figure 2:** HPLC Profile for E.S extract by absolute Methanol Solvent

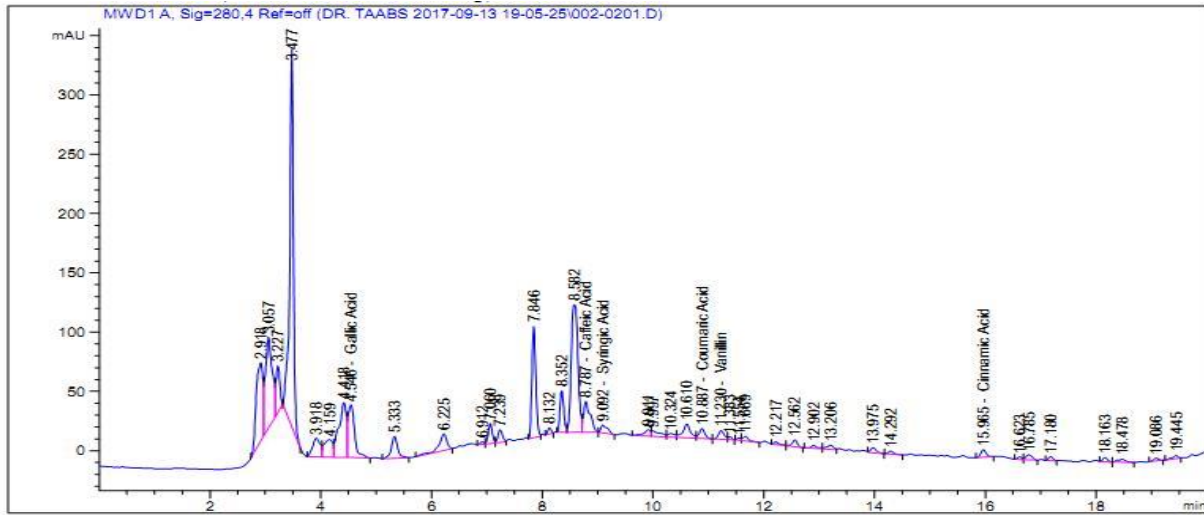


Figure 3: HPLC Profile of E.S extract by Methanol: water extract

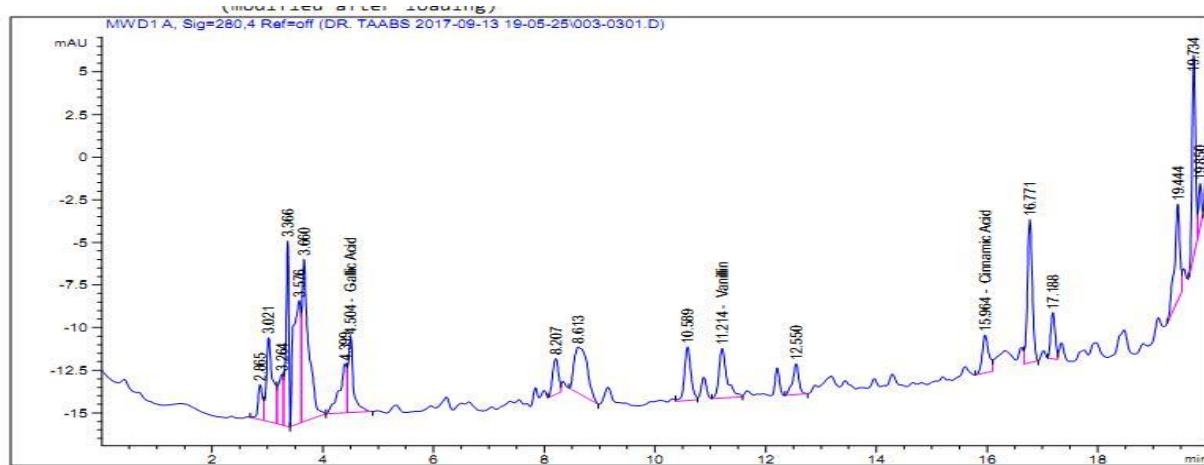


Figure 4: HPLC Profile of E.S extract by absolute Ethanol solvent

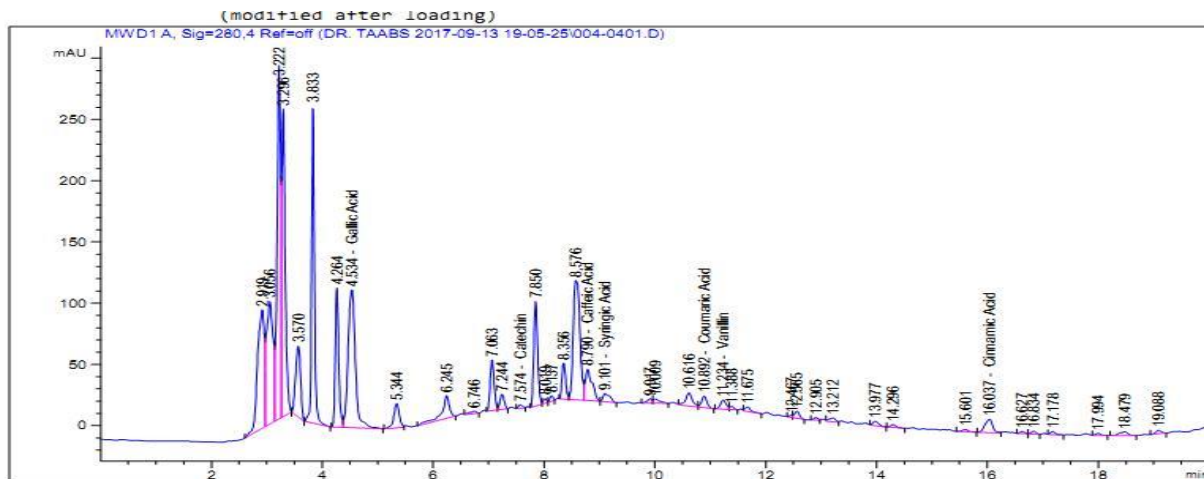


Figure 5: HPLC Profile of E.S by Ethanol: water extract

4. Conclusion

This study explored the aqueous-organic solvents and absolute solvent extracts from *Ephedra sinica* as well as antibacterial, antifungal and antiviral activities of these extracts. Our findings have revealed a significant inhibitory impact on all pathogen species. Ethanol-water extract showed that the greatest inhibition zones (mm) against bacterial and fungal species ranged from 20.7 to

25.0 and 29.0 to 35.0 at a concentration of 150µl/ml, respectively. For antiviral activity, 51.6% was the greatest inhibition documented for ethanol-water extract against coxsackie B₃ virus during zero-time process. We, therefore, suggest that aqueous-ethanol solvent can be used as a useful source for natural polyphenol and alkaloids with anti-wide range of pathogen species. Furthermore, mutagenic and carcinogenic investigations are necessary for safe human use.

5. Conflict of interest

The authors have declared that no competing interests exist.

References

- Abou El-Soud NH, Deabes MM, El-Kassem LA and Khalil M. 2015. Chemical composition and antifungal activity of *ocimum basilicum* L. essential oil. *Open Access Maced J Med Sci*, **3**: 374-379.
- Allayeh Ak, Dardeer EE, and Kotb NS. 2015. Effects of cell-free supernatants of yogurts metabolites on coxsackie B₃ virus *in vitro* and *in vivo*. *Middle East J Appl Sci*, **5**: 353-358.
- Allayeh Ak, El-Baz RM, Osman MO and Saeed NM. 2018. Evaluation of an inhibitory effect of edible mushroom extracts against rotavirus infection. *Egypt Pharmaceut J*, **17**: 77-84.
- Amakura Y, Yamakami S, Yoshida T, Wakana D, Hyuga M, Hyuga S, Hanawa T and Goda Y. 2013. Characterization of phenolic constituents from *Ephedra* herb extract. *Molecules*, **18**: 5326-5334.
- Bagheri-Gavkosh S, Bigdeli M, Shams-Ghahfarokhi M and Razzaghi-Abyaneh M. 2009. Inhibitory effects of *Ephedra* major host on *Aspergillus parasiticus* growth and aflatoxin production. *Mycopathologia*, **168**: 249-255.
- Deabes MM, Khalil WG, Attallah AG, El-Desouky TA and Naguib KM. 2018. Impact of silver nanoparticles on gene expression in *Aspergillus Flavus* producer aflatoxin B₁. *Open Access Maced J Med Sci*, **6**: 600-605.
- Fazeli-Nasab B and Mousavi SR. 2019. Antibacterial activities of *Ephedra sinica* herb extract on standard and clinical strains of *Pseudomonas aeruginosa*. *J Med Bacteriol*, **8**: 40-48.
- Fazly-Bazzaz BS and Haririzadeh G. 2003. Screening of Iranian plants for antimicrobial activity. *Pharm Biol*, **41**: 573-583.
- Feresin GE, Tapia A, Lopez SN and Zacchino SA. 2001. Antimicrobial activity of plants used in traditional medicine of Sun Juan Province, Argentina. *J Ethnopharmacol*, **78**: 103-107.
- Flint SJ, Enquist LW, Racaniello VR and Skallka AM. 2003. **Virus cultivation, detection and genetics: Principles of virology**, Third ed, ASM Press, Washington DC.
- Hai-Rong X, Shen Y, Lu L, Wei H, Luo F, Hong X and Yang Z. 2012. The inhibitory effect of *Rheum palmatum* against coxsackie B₃ *in vitro* and *in vivo*. *American J of Chinese medic*, **40**: 801-812.
- Horax D, Hettiarachchy N and Chen P. 2010. Extraction, quantification, and antioxidant activities of phenolics from pericarp and seeds of bitter melons (*Momordica charantia*) harvested at three maturity stages (immature, mature, and ripe). *J Agric Food Chem*, **58**: 4428-4433.
- Hyuga S, Hyuga M, Yamagata S, Yamagata T and Hanawa T. 2004. Maoto, a Kampo medicine, inhibits migration of highly metastatic osteosarcoma cells. *J Trad Med*, **21**: 174-181.
- Hyuga S, Hyuga M, Nakanishi H, Ito H, Watanabe K, Oikawa T and Hanawa T. 2007. Maoto, Kampo medicine, suppresses the metastatic potential of highly metastatic osteosarcoma cells. *J Trad Med*, **24**: 51-58.
- Khaled AS, Waill AE, Ahmed MT, Ahmed AE, Tahany MA, Ahmed IE and Eman FA. 2018. Antiviral and antioxidant potential of fungal endophytes of Egyptian medicinal plants. *Fermentation*, **4**: 49
- Kavanagh F. 1972. **Analytical microbiology**, First ed. Academic Press, New York.
- Khan A, Gul J, Afsar K, Farzana GJ, Ali B and Muhammad D. 2017. *In vitro* antioxidant and antimicrobial activities of *Ephedra gerardiana* (Root and Stem) crude extract and fractions. *Evid Based Complement Alternat Med*, **6** Pages. Doi: 10.1155/2017/4040254
- Kumar GP and Singh SB. 2011. Antibacterial and antioxidant activities of ethanol extracts from trans *Himalayan* medicinal plants. *J Appl Sci*, **2**: 53-57.
- Lee CH and Lee HS. 2009. Growth inhibiting activity of quinaldic acid isolated from *Ephedra pachyclada* against intestinal bacteria. *Korean Soc Appl Biol*, **52**: 331-335.
- Mantani N, Andoh T, Kawamata H, Terasawa K and Ochiai H. 1999. Inhibitory effect of *Ephedrae* herba, an oriental traditional medicine, on the growth of influenza A/PR/8 virus in MDCK cells. *Antivir Res*, **44**: 193-200.
- Michael B, Thanise N, Batsirai C and Maud M. 2016. Effect of solvent type on total phenolic content and free radical scavenging activity of black tea and herbal infusions. *Food Anal Methods*, **9**: 1060-1067.
- Nagai TS, Makino IS, Hiroyuki I and Haruki Y. 2011. Effects of oral administration of yogurt fermented with *Lactobacillus delbrueckii* ssp. *bulgaricus* OLL1073R-1 and its exopolysaccharides against influenza virus infection in mice. *Int Immunopharmacol*, **11**: 2246-2250.
- Naidu AS. 2000. Phytoantimicrobial (PAM) agents as multifunctional food additives. In: Bidlack WR, Omaye ST, Meskin MS and Topham D (Eds.), **Phytochemicals as bioactive agents**. Technomic Publishing. Lancaster, United Kingdom, pp. 106-110.
- Razzaghi-Abyaneh M, Shams-Ghahfarokhi M, Rezaee MB, Jaimand K, Alinezhad S and Saberi R. 2009. Chemical composition, antiaflatoxigenic activity of *Carum carvil*, *Thymus vulgaris* and Citrus aurantifolia essential oils. *Food Control*, **20**: 1018-1024.
- Reed LJ and Muench HA. 1938. A simple method of estimating fifty percent end points. *Am J Epidemiol*, **27**: 493-497.
- Santana P, Miranda M, Payrol J, Silva M, Hernández V and Peralta E. 2013. Gas chromatography-mass spectrometry study from the Leaves fractions obtained of vernonanthura patens (Kunth). *Int J Org Chem*, **2**: 105-109.
- Selim KA, El-Beih AA, Abd El-Rahman TM and El-Diwanly AI. 2011. Biodiversity and antimicrobial activity of endophytes associated with Egyptian medicinal plants. *Mycosphere*, **2**: 669-678.
- Sethi S, Dutta A, Gupta BL and Gupta S. 2013. Antimicrobial activity of spices against isolated food borne pathogens. *Int J Pharm Pharm Sci*, **5**: 260-262.
- Soltan MM and Zaki AK. 2009. Antiviral screening of forty-two Egyptian medicinal plants. *J Ethnopharmacol*, **126**: 102-107.
- Soni MG, Carabin IJ, Griffiths JC and Burdock GA. 2004. Safety of *Ephedra*: lessons learned. *Toxicol Lett*, **150**: 97-110.
- Sumiko H, Masashi H, Naohiro O, Takuro M, Hiroyuki K, Tadatoshi Y, Morio Y, Yoshiaki A, Takashi H, Hiroshi O, Yukihiro G and Toshihiko H. 2016. Ephedrine alkaloids-free Ephedra Herb extract: a safer alternative to *Ephedra* with comparable analgesic, anticancer, and anti-influenza activities. *J Nat Med*, **70**: 571-583.
- Tian F, Li B, Ji BP, Zhang GZ and Luo YC. 2009. Identification and structure-activity relationship of gallotannins separated from *Galla chinensis*. *LTW-Food Sci. Technol*. **42**: 1289-1295
- Vijayan P, Raghu C, Ashok G, Dhanaraj A and Suresh B. 2004. Antiviral activity of medical plants of Nilgiris. *Indian J Med Res*, **120**: 24-29.
- Walaa A, Marwa A, Rizwan A, Niyaz A, Atta A and Naqvi A. 2019. Clinical uses and toxicity of *Ephedra sinica*. *Pharmacogn J*, **1**: 447-452.
- Zhang B, Wang Z, Xin P, Wang Q, BU H and Kung H. 2018. Phytochemistry and pharmacology of genus *Ephedra*. *Chin J Nat Med*, **16**: 811-828.

Protective effect of Ginger against Sodium Metabisulfite induced Oxidative Stress in Rat

Shahnaz Shekarforoush^{*}, Akbar Afkhami Fathabad and Abbas Taheri

¹Department of Physiology, Arsanjan Branch, Islamic Azad University, Fars, Iran

Received August 19, 2019; Revised September 15, 2019; Accepted September 16, 2019

Abstract

Although sulfiting agents including sodium metabisulfite (SMB) are commonly used as preservative in foods, medicines and beverages, they have also been considered as important risk factors for the initiation and progression of diseases due to oxidative damage. The purpose of this report was to investigate the effect of ginger extract on serum oxidative stress indices and biochemical markers of liver and kidney function in SMB-treated rats. Twenty-four male Wistar rats (200-250 g) were divided into four groups: distilled water, ginger (500 mg/kg/day), sodium metabisulfite (260 mg/kg/day), and sodium metabisulfite + ginger. After 28 days of treatment, serum glutamate oxaloacetate transaminases (SGOT), serum glutamate pyruvate transaminases (SGPT), alkaline phosphatase (ALP), total and direct bilirubin, creatinine, BUN, and total protein and antioxidant enzyme activities including glutathione peroxidase (GPx), glutathion reductase (GR), catalase (CAT) activities, and the levels of glutathione were tested. Differences in parameters among the four groups were assessed by one-way analysis of variance followed by Tukey's test. SMB ingestion resulted in a significant rise in serum liver enzymes (SGOT, SGPT, ALP). Serum antioxidant enzymes (GPx, GR, CAT), and the levels of glutathione were significantly decreased. However, ginger extract supplementation to the SMB treated rats partly reversed these effects to normal levels. Based on these results, sulfite induced oxidative stress was attenuated by ginger extract treatment, thus ginger can be used as a regular protective nutrient.

Keywords: Ginger, liver enzymes, Sodium metabisulfite, Oxidative stress.

1. Introduction

Sulfiting agents including sulfur dioxide and various sulfite salts are widely used as preservatives in pharmaceuticals and food industry. Despite their common uses, sulfites are toxic molecules and can react with a variety of cellular components including proteins, lipids, DNA, etc (Meng et al., 2004, Yi et al., 2005). Adverse effects of sulfite compounds in multiple organs of mammals including the pulmonary system (Vally and Misso, 2012) and the reproductive system (Rezaee et al. 2016, Shekarforoush et al., 2015) have been reported. An immediate increase in reactive oxygen species (ROS) production accompanied by a depletion of intracellular ATP followed by exposure of kidney cells and PC12 cells to sulfites was observed (Vincent et al., 2004, Zhang et al., 2004). Induction of lipid peroxidation was reported in the kidney and liver of rats treated orally with sodium metabisulfite (SMB) at a dose of 520 mg/kg/day (Elmas et al., 2005). Sulfites have been documented to alter the oxidant and antioxidant balance in rat erythrocyte (Ozturk et al., 2010) and serum (Shekarforoush et al., 2018).

Herbal medicines have received considerable attention over the last decades due to their diverse antioxidant activities. Ginger (*Zingiber officinale* Roscoe) is an herbal medicinal product with anti-tumorigenic, anti-inflammatory, and antioxidative activity (Ali et al., 2008).

All ginger's major active ingredients, such as zingerone, gingerdiol, zingibrene, gingerols, and shogaols have antioxidant activities (Sakr and Badawy, 2011). In the alternative and folk medicine in the world, ginger has been used since antiquity to treat diseases like cold, headaches, nausea, gastrointestinal disturbances, rheumatic complaints, parasitic infections, and muscular discomfort. Experimental studies have shown that ginger protects the liver against the toxic effects of alcohol, country liquor, acetaminophen, and heavy metals (Haniadka et al., 2013).

Our previous study has determined the protective effect of ginger against SMB-induced testicular oxidative stress (Afkhami Fathabad et al., 2017).

The daily intake of sulfites through foods and beverages may exceed the acceptable daily intake value (0.7 mg/kg body weight) (Lien et al., 2016). Because consequences of dietary exposure to sulfites are not fully characterized, it is necessary to evaluate how the health risk associated with that can be reduced. There are no published reports in the literature about the protective effect of ginger extract against oxidative stress induced by SMB in the blood of rats. On the basis of these considerations, this study was designed to evaluate whether changes in serum biochemical and oxidative stress markers induced by SMB ingestion could be treated with ginger.

^{*} Corresponding author e-mail: sh.shekar@yahoo.com.

2. Materials and Methods

2.1. Drug and Ginger Extract Preparation

Sodium metabisulfite was obtained from Sigma (EC No: 231-673-0, CAS. No: 7681-57-4) and dissolved in distilled water (260 mg/ml). Dried ginger rhizomes were purchased from Arsanjan grocery and powdered by grinder. 200 g of the powder was soaked in 1 litre of 50% ethanol for 72 hours and extracted by percolation several times until complete exhaustion. The solvent was concentrated using rotavapor device connected to a vacuum pump. 20 g of the concentrate was obtained. Previous studies using HPLC identified the major constituents of ginger including: [6]-gingerol, [8]-gingerol, [10]-gingerol, [6]-shogaol, [8]-shogaol, [10]-shogaol and [6]-paradol, and [1]-dehydrogingerdione (Shao et al., 2010).

2.2. Animals

Twenty-four male Wistar rats weighing 200–250 g were maintained at 12 h light–dark cycles and a constant temperature of 23±1 °C at all times. The rats were fed with a standard rodent pellet diet and drinking water ad libitum. All experimental protocols conducted on rats were performed in accordance with the standards established by the Animal Ethics Committee at the Islamic Azad University. Rats were divided into four groups of 6 animals each: Group 1 (control): rats received distilled water (1 ml/kg); Group 2 (S260): rats treated with SMB (260 mg/kg); Group 3 (Z500): rats treated with ginger (500 mg/kg); Group 4 (SZ), rats treated with SMB + ginger at the same previous dose. The doses of SMB and ginger were prescribed according to the previous studies (Morakinyo et al. 2010, Rezaee et al. 2016). Ginger and SMB were given by gavage via oral cannula and lasted for a period of 28 days.

2.3. Biochemical Evaluation

At the end of the experimental period, rats were anesthetized using diethyl ether and the blood samples were collected by cardiac puncture. The samples were allowed to coagulate for 30 min at room temperature and centrifuged at 3000 rpm for 10 min. The supernatant serum was quickly removed and kept at –20 °C for further analysis.

Serum glutamate oxaloacetate transaminase (SGOT), serum glutamate pyruvate transaminase (SGPT), alkaline phosphatase (ALP), total and direct bilirubin, creatinine, BUN, and total protein values were checked using the standard diagnostic test kits (Pars Azma Co., Iran).

2.4. Serum Antioxidant Enzyme Activities

(GSH) contents with 5-5'-dithiobis, 2-nitrobenzoic acid (DTNB) was measured and followed by a standard

Table 1. Effect of ginger and sodium metabisulfite treatment for 28 days on serum biochemical parameters.

Group	SGOT (IU/L)	SGPT (IU/L)	ALP (IU/L)	TP (g/dl)	BUN (mg/dl)	Cr (mg/dl)	T. Bili (mg/dl)	D. Bili (mg/dl)
Cont	182.5±18.7	111.5±9.5	456±30.9	6.7±0.2	23.6±0.4	0.86±0.02	0.07±0.007	0.02±0.01
Z500	180.5±9.7	107±4.3	364.6±43.6	6.6±0.1	22.5±2.1	0.9±0.03	0.1±0.001	0.04±0.1
S260	266.6±2.6**	148.3±3.8**	683.8±78.1*	5.7±0.2*	26.1±1.2	1.17±0.2	0.1±0.001	0.03±0.01
SZ	202.1±13.7###	117.6±8.8#	509.6±63.7	6.2±0.1	19.3±1.2#	0.82±0.01	0.06±0.008#	0.008±0.01

Each value indicates the mean ± SEM. Z500, administration of 500 mg/kg/day ginger; S260, administration of 260 mg/kg/day sodium metabisulfite; SZ, coadministration of sodium metabisulfite and ginger at the same dose. *P < 0.05, **P < 0.01 vs. control group; #P < 0.05, ###P < 0.01 vs. S260.

Ellman's method (Ellman, 1959). The absorbance of the reaction products was observed after 5 min at 412 nm. The glutathione peroxidase (GPx) activity of serum samples was measured by continuous monitoring of the regeneration of GSH from oxidized glutathione (G-S-S-G) upon the action of glutathione reductase (GR) and NADPH according to the method of Fecondo and Augusteyn (Fecondo and Augusteyn, 1983). The activity of GR was measured spectrophotometrically with a Radox laboratory kit at 340 nm and 37°C using the method described by Carlberg and Mannervik (Carlberg and Mannervik, 1985). Catalase (CAT) was assayed spectrophotometrically by monitoring the decomposition of H₂O₂ using the procedure of Aebi (Aebi, 1984). The activity of SOD was assayed according to Winterbourn et al. (1975) and is based on the ability of superoxide dismutase to inhibit the reduction of nitro-blue tetrazolium by superoxide (Winterbourn et al., 1975).

2.5. Measurement of Lipid Peroxidation

The level of serum malondialdehyde (MDA), a product of lipid peroxidation, was determined using thiobarbituric acid (TBA) method. MDA reacts with TBA and produces a pink colored complex which has the maximum absorbance at 532 nm. The results were expressed as nmol/ml (Mihara and Uchiyama, 1978).

2.6. Statistical Analysis

All data are presented as mean ± standard error of mean (SEM) and analyzed using SPSS (Version 18; SPSS Inc., Chicago, USA). Data was analyzed using one-way ANOVA and a post hoc Tukey test. Statistical significance was accepted when P < 0.05.

3. Results

3.1. Evaluation of Liver and Kidney Function Markers

The effects of SMB and ginger on serum biomarkers of liver and kidney function including SGOT, SGPT, ALP, TP, and bilirubin (as liver function test) and BUN and creatinine (as kidney function test) were examined at the end of treatment period (Table 1). Sulfite treatment for 28 days caused a significant increase in SGOT (P = 0.001), SGPT (P = 0.008), ALP (P = 0.049), and a significant decrease in total protein (P = 0.02). BUN and creatinine levels were increased non-significantly in the SMB treated group. The levels of examined serum biomarkers in the rats fed ginger with SMB did not show any significant difference compared to control group. All measured values in the control and ginger treated groups were almost the same.

3.2. Evaluation of Serum Antioxidant Enzyme Activities

As observed in Table 2, administration of SMB to rats resulted in significant decrease in serum concentrations of GSH ($P = 0.001$) and activities of GPx, GR ($P < 0.001$), and catalase ($P = 0.03$) when compared with the control group. Co-administration of SMB with ginger extract

resulted in significant increase in the GPx and GR activities when compared to the SMB treated rats. No statistically significant difference was observed in GSH level and catalase activity in rats treated with SMB + ginger and control group. No difference was observed between control and ginger treated rats.

Table 2. Effect of ginger and sodium metabisulfite treatment for 28 days on the serum antioxidant enzyme activities.

Groups	SOD (u/ml)	GPx (u/ml)	GR (u/ml)	CAT (u/ml)	GSH ($\mu\text{mol/ml}$)
Control	6.4 \pm 0.74	17.1 \pm 1	3.4 \pm 0.2	19.1 \pm 1.9	0.76 \pm 0.08
Z500	6.1 \pm 1.7	24.3 \pm 1.17	6.7 \pm 0.08	13.1 \pm 1.5	0.63 \pm 0.04
S260	5.2 \pm 1	1.17 \pm 0.26***	1.46 \pm 0.04***	8.1 \pm 3.1*	0.36 \pm 0.06**
SZ	6.5 \pm 1.1	7.93 \pm 0.45****	2.6 \pm 0.04***	9.8 \pm 3.1	0.59 \pm 0.03

Each value indicates the mean \pm SEM. Z500, administration of 500 mg/kg/day ginger; S260, administration of 260 mg/kg/day sodium metabisulfite; SZ, coadministration of sodium metabisulfite and ginger. SOD, superoxide dismutase; GPx, glutathione peroxidase; GR, glutathione reductase; CAT, catalase; GSH, reduced glutathione. * $P < 0.05$, ** $P < 0.01$, *** $P < 0.001$, **** $P < 0.001$ vs. control group; # $P < 0.01$, ## $P < 0.001$ vs. S260.

3.3. Evaluation of Serum Lipid Peroxidation

Serum MDA levels (means \pm SEM) detected in SMB treated rats (33.03 \pm 1 nmol/L) were significantly higher than those detected in rats treated with ginger (23.7 \pm 2.1 nmol/L) and control (18.9 \pm 2.1 nmol/L). Though not significant, MDA levels were observed to decrease in rats treated with SMB + ginger (27.7 \pm 0.5 nmol/L) (Fig. 1).

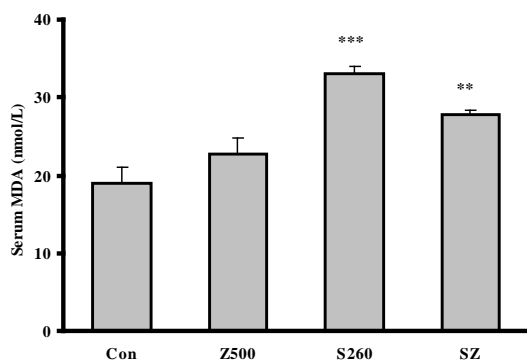


Figure 1. Effect of sodium metabisulfite on serum malondialdehyde (MDA) in rats after 28 days treatment. Values are expressed as mean \pm SE for six rats in each group. Con, control group; Z500, rats treated with ginger (500 mg/kg); S260, rats treated with sodium metabisulfite (260mg/kg); SZ, rats treated with sulfite and ginger. Asterisk, significantly different from the control group. ** $P < 0.01$, *** $P < 0.001$.

4. Discussion

In the present study, the serum biomarkers of oxidative stress and renal and hepatic injuries subsequent to exposing rats to SMB at 260 mg/kg dose were evaluated. The results show that SMB ingestion increased serum levels of MDA, accompanied by significant reduction of GPx, GR, CAT activities and GSH concentration. The present data also confirmed that administration of SMB for 28 days caused liver injury as evidenced by elevation of SGOT, SGPT, ALP, and reduction of total protein. The modification in the values of the investigated parameters confirms the hepatoprotective effect and antioxidant activity of ginger.

The main mechanism by which sulfite mediates its toxic effects is through oxidative stress due to an increased production of sulfur- and oxygen-centered free radicals. ROS overproduction and ATP depletion have been shown

in neurons and human fetal liver cells due to sulfite toxicity (Zhang et al. 2004). Lipid peroxidation was induced in the kidney and liver of rats treated orally with SMB (Elmas et al. 2005). The observed increase in serum MDA levels, as a byproduct of lipid peroxidation, confirms previous observations of sulfite-induced lipid oxidation as a well-established mechanism of cellular injury (Shekarforoush et al. 2018). Sulfite-induced hepatotoxicity is associated with the rapid disappearance of oxidized glutathione (GSSG), followed by the slow depletion of reduced glutathione that potentially diminishes antioxidant defense (Niknahad and O'Brien 2008). Decreased serum antioxidant enzymes activity and GSH content as a result of oxidative stress can reduce the protection against free radicals and lipid peroxidation. The results of an experimental study showed that ingested sulfite by inducing hepatocyte necrosis may cause liver dysfunction (Bai et al. 2013). Hepatotoxicity linked to oxidant stress is reflected by an increase in the levels of hepatic enzymes (Contreras-Zentella and Hernandez-Munoz 2016). Significant increase in the SGOT, SGPT and ALP activities in the SMB treated group could be taken as an index of liver damage. The findings of this study indicated that ginger prevented hepatic enzyme changes in rats. Ginger significantly decreased the serum levels of transaminases towards the respective normal values and increased the activities of GPx and GR compared to SMB ingestion alone. These alterations indicate that the ginger is somewhat able to stabilize plasma membranes and repair hepatic tissue damage caused by SMB. These results are consistent with previous reports indicating that ginger exerts antioxidative effect by decreasing lipid peroxidation and maintaining normal levels of antioxidant enzymes (Ahmed et al. 2000, Mashhadi et al. 2013). Increased serum GSH level was reported in ginger fed rats (Ahmed et al. 2000). Hepatoprotective effect of ginger extract has been demonstrated in earlier studies (Atta et al. 2010, Yemitan and Izebu 2006). The protective effect of ginger may be due to prevention of the decline of hepatic antioxidant status or its direct radical scavenging capacity (Ajith et al. 2007). Recent studies revealed that ginger active components 6-shogaol (Peng et al. 2015) and 6-dehydrogingerdione (Yao et al. 2014) are potent activators of the transcription factor Nrf2 to boost the cellular antioxidant enzymes and GSH.

The previous reported data indicated that SMB, when given at a dose of 520 mg/kg/day, results in increased lipid peroxidation in the kidney (Elmas et al. 2005). Contrary to the finding of abnormal elevation of liver function tests, the sulfite at a dose of 260 mg/kg/day did not significantly increase the serum level of BUN and creatinine. The finding suggests that hepatocytes may be more sensitive to sulfites. On the other hand, because of renal reserve, the serum creatinine level may not rise until 50% of kidney function has been lost (Ronco 2013).

Although this study provides important findings about protective effect of ginger against SMB, the lack of histology was a limitation of our study. Future studies should include histology to confirm the effects of SMB and ginger. In addition, we recommend evaluating the effect of the active gradients, such as 6-shogaol and 6-dehydrogingerdione, as an important line of study.

5. Conclusion

The present results show that sodium metabisulfite (260 mg/kg) induces oxidative stress through decreased serum antioxidant enzyme activities and GSH and increased MDA level.

The observed oxidative effect of sulfite correlates with elevated liver enzymes suggesting that increased ingestion of sulfite may cause damage to the hepatocytes. Increased GPx and GR activity and decreased serum transaminases by co-administration of ginger with sulfites suggest that ginger may partially reduce the observed oxidative damage in the rats after exposure to sulfite.

6. Conflict of Interests

The authors declare that there is no conflict of interests in relation to this work.

Acknowledgment

The present paper was extracted from Msc thesis written by Mr Afkhami Fathabad, financially supported by Arsanjan Branch, Islamic Azad University. We gratefully acknowledge the valuable help of Mr. Kuhpeyma for laboratory works in this research.

References

Aebi H. 1984. Catalase in vitro. *Methods Enzymol*, **105**:121-126.

Afkhami Fathabad A, Shekarforoush S, Hoseini M and Ebrahimi Z. 2017. Attenuation of Sulfite-Induced Testicular Injury in Rats by Zingiber officinale Roscoe. *J Diet Suppl*, **15**(4):398-409.

Ahmed RS, Seth V and Banerjee BD. 2000. Influence of dietary ginger (Zingiber officinales Rosc) on antioxidant defense system in rat: comparison with ascorbic acid. *Indian J Exp Biol*, **38**:604-606.

Ajith TA, Hema U and Aswathy MS. 2007. Zingiber officinale Roscoe prevents acetaminophen-induced acute hepatotoxicity by enhancing hepatic antioxidant status. *Food Chem Toxicol*, **45**:2267-2272.

Ali BH, Blunden G, Tanira MO and Nemmar A. 2008. Some phytochemical, pharmacological and toxicological properties of ginger (Zingiber officinale Roscoe): a review of recent research. *Food Chem Toxicol*, **46**:409-420.

Atta AH, Elkoly TA, Mouneir SM, Kamel G, Alwabel NA and Zaher S. 2010. Hepatoprotective Effect of Methanol Extracts of Zingiber officinale and Cichorium intybus. *Indian J Pharm Sci*, **72**:564-570.

Bai J, Lei P, Zhang J, Zhao C and Liang R. 2013. Sulfite exposure-induced hepatocyte death is not associated with alterations in p53 protein expression. *Toxicology*, **312**:142-148.

Carlberg I and Mannervik B. 1985. Glutathione reductase. *Methods Enzymol*, **113**:484-490.

Contreras-Zentella ML and Hernandez-Munoz R. 2016. Is Liver Enzyme Release Really Associated with Cell Necrosis Induced by Oxidant Stress? *Oxid Med Cell Longev*, **2016**:3529149.

Ellman GL. 1959. Tissue sulfhydryl groups. *Arch Biochem Biophys*, **82**:70-77.

Elmas O, Aslan M, Caglar S, Derin N, Agar A, Aliciguzel Y and Yargicoglu P. 2005. The prooxidant effect of sodium metabisulfite in rat liver and kidney. *Regul Toxicol Pharmacol*, **42**:77-82.

Fecondo JV and Augusteyn RC. 1983. Superoxide dismutase, catalase and glutathione peroxidase in the human cataractous lens. *Exp Eye Res*, **36**:15-23.

Haniadka R, Saxena A, Shivashankara A, Fayad R, Palatty P, Nazreth N, Francis A, Arora R and Baliga M. 2013. Ginger protects the liver against the toxic effects of xenobiotic compounds: preclinical observations. *J Nutr Food Sci*, **3**:1000226.

Lien KW, Hsieh DPH, Huang HY, Wu CH, Ni SP and Ling MP. 2016. Food safety risk assessment for estimating dietary intake of sulfites in the Taiwanese population. *Toxicol Rep*, **3**:544-551.

Mashhadi NS, Ghiasvand R, Askari G, Hariri M, Darvishi L and Mofid MR. 2013. Anti-oxidative and anti-inflammatory effects of ginger in health and physical activity: review of current evidence. *Int J Prev Med*, **4**:S36-42.

Meng Z, Qin G, Zhang B and Bai J. 2004. DNA damaging effects of sulfur dioxide derivatives in cells from various organs of mice. *Mutagenesis*, **19**:465-468.

Mihara M and Uchiyama M. 1978. Determination of malonaldehyde precursor in tissues by thiobarbituric acid test. *Anal Biochem*, **86**:271-278.

Morakinyo A, Achema P and Adegoke O. 2010. Effect of Zingiber officinale (Ginger) on sodium arsenite-induced reproductive toxicity in male rats. *Afr J Biomed Res*, **13**:39-45.

Niknahad H and O'Brien PJ. 2008. Mechanism of sulfite cytotoxicity in isolated rat hepatocytes. *Chem Biol Interact*, **174**:147-154.

Ozturk OH, Oktar S, Aydin M and Kucukatay V. 2010. Effect of sulfite on antioxidant enzymes and lipid peroxidation in normal and sulfite oxidase-deficient rat erythrocytes. *J Physiol Biochem*, **66**:205-212.

Peng S, Yao J, Liu Y, Duan D, Zhang X and Fang J. 2015. Activation of Nrf2 target enzymes conferring protection against oxidative stress in PC12 cells by ginger principal constituent 6-shogaol. *Food Funct*, **6**:2813-2823.

Rezaee N, Nematollahi Z, Shekarforoush S and Hoseini E. 2016. Effect of Sodium Metabisulfite on Rat Ovary and Lipid Peroxidation. *Iranian Journal of Toxicology*, **10**:23-28.

Ronco C. 2013. Kidney attack: overdiagnosis of acute kidney injury or comprehensive definition of acute kidney syndromes? *Blood Purif*, **36**:65-68.

Sakr SA and Badawy GM. 2011. Effect of ginger (Zingiber officinale R.) on metiram-inhibited spermatogenesis and induced apoptosis in albino mice. *J Applied Pharmaceutical Science*, **01**:131-136.

- Shao X, Lv L, Parks T, Wu H, Ho CT and Sang S. 2010. Quantitative analysis of ginger components in commercial products using liquid chromatography with electrochemical array detection. *J Agric Food Chem*, **58**:12608-12614.
- Shekarforoush S, Ebrahimi P, Afkhami Fathabad A and Farzanfar E. 2018. Effect of Sodium Metabisulfite on Oxidative Stress and Lipid Peroxidation Biomarkers. *Curr Nutr Food Sci*, **14**.
- Shekarforoush S, Ebrahimi Z and Hoseini M. 2015. Sodium metabisulfite-induced changes on testes, spermatogenesis and epididymal morphometric values in adult rats. *Int J Reprod Biomed*, **13**:765-770.
- Vally H and Misso NL. 2012. Adverse reactions to the sulphite additives. *Gastroenterol Hepatol Bed Bench*, **5**:16-23.
- Vincent AS, Lim BG, Tan J, Whiteman M, Cheung NS, Halliwell B and Wong KP. 2004. Sulfite-mediated oxidative stress in kidney cells. *Kidney Int*, **65**:393-402.
- Winterbourn CC, Hawkins RE, Brian M and Carrell RW. 1975. The estimation of red cell superoxide dismutase activity. *J Lab Clin Med*, **85**:337-341.
- Yao J, Ge C, Duan D, Zhang B, Cui X, Peng S, Liu Y and Fang J. 2014. Activation of the phase II enzymes for neuroprotection by ginger active constituent 6-dehydrogingerdione in PC12 cells. *J Agric Food Chem*, **62**:5507-5518.
- Yemitan OK, Izegebu MC. 2006. Protective effects of *Zingiber officinale* (Zingiberaceae) against carbon tetrachloride and acetaminophen-induced hepatotoxicity in rats. *Phytother Res*, **20**:997-1002.
- Yi H, Liu J and Zheng K. 2005. Effect of sulfur dioxide hydrates on cell cycle, sister chromatid exchange, and micronuclei in barley. *Ecotoxicol Environ Saf*, **62**:421-426.
- Zhang X, Vincent AS, Halliwell B and Wong KP. 2004. A mechanism of sulfite neurotoxicity: direct inhibition of glutamate dehydrogenase. *J Biol Chem*, **279**:43035-43045.

Molecular Surveillance of Enteroviruses in Al-Zarqa River, Jordan

Ismail Saadoun^{1,*}, Qotaiba Ababneh², Ziad Jaradat² and Mamdoh M. Meqdam³

¹ Department of Applied Biology, College of Sciences, University of Sharjah, P.O. Box 27272, Sharjah-United Arab Emirates; ²Department of Biotechnology and Genetic Engineering, Faculty of Science and Arts; ³Department of Medical Laboratory Sciences, Faculty of Applied Medical Sciences, Jordan University of Science and Technology, Jordan

Received June 18, 2019; Revised September 7, 2019; Accepted September 16, 2019

Abstract

This study is concerned with Al-Zarqa River, one of the major water resources in Jordan. It investigated its surface water quality with respect to the occurrence and serotypes of enteroviruses in different water samples collected from the river over a period of 11 months. Viruses were concentrated from river water, raw sewage and effluent samples with a calculated % recovery yield ranged between 2% and 8%. The concentrations of enteroviruses ranged between 3.3 and 6.3X10³ pdu/ml, with a mean of 2.5X10³ pdu/ml in raw sewage. Thirty-three samples were examined for the presence of enteroviruses by means of RT-PCR and southern blotting hybridization. Enteroviruses were detected in 14 (42%) of the samples. Sequence analysis of RT-PCR products followed by phylogenetic analysis revealed the frequent detection of coxsackievirus B4 and poliovirus serotype type 1, while the remainder comprised coxsackievirus B3, echovirus 9 and echovirus 11. Enteroviruses sequences isolated from samples collected from different sites along the river were similar, but differences were observed in samples collected from the same sites at different times. Circulation of enterovirus in sewage and water, serotyping and phylogenetic analysis enabled us to trace back the source of enterovirus contamination.

Keywords: Enterovirus; phylogeny; serotype; Zarqa River; wastewater

1. Introduction

It is estimated that, more than 100 different types of potentially pathogenic microorganisms that may cause an immense range of diseases and clinical symptoms can be present in polluted water (Iwai *et al.*, 2006). Transmission of pathogens via the environment can clearly result in infections and diseases to both humans and animals, resulting in the circulation of pathogens in the environment (Westrell, 2004). Heavy rains can cause run-offs from agriculture land and will reintroduce pathogens from sludge and manure into rivers, which can contribute substantial loads of pathogens (Hansen and Ongerth, 1991; Kistemann *et al.*, 2002; Ferguson *et al.*, 2003).

Al-Zarqa River is the only inland river in Jordan, and is the second main tributary to River Jordan after Yarmouk River. The pathogens of main concern in the Al-Zarqa River basin include bacteria, protozoa and viruses with the latter being of main concern as they generally pose a greater challenge than bacteria and protozoa in food and wastewater treatment (Sibanda and Okoh, 2012). The risk of viral infections can be 10 to 1,000 times higher than that for bacteria at a similar level of exposure (Rose and Gerba, 1991). In addition, viruses can survive in water longer than bacteria, and can tolerate greater variations in temperature and pH [6, 8] (Maunula *et al.*, 2005; Sibanda and Okoh, 2012). Therefore, the presence of waterborne viruses as enteric viruses in sewage and surface waters is considered

a good indicator of the infectious status of a population, public health in general, (Sibanda and Okoh, 2012), and water safety and quality (Pina *et al.*, 1998). Furthermore, viruses are more resistant to commonly employed water and wastewater disinfection solutions. Thus, viruses can easily be harbored in "microbiologically immaculate" water (Payment *et al.*, 1994; Leeds, 2002).

In Jordan, many cases of enteric viral diseases, such as gastroenteritis, hepatitis A and aseptic meningitis have been reported (Toukan *et al.*, 1988; Meqdam *et al.*, 1997a, 1997b; Battikhi, 2002; Meqdam *et al.*, 2002; Battikhi and Battikhi, 2004; Nimri *et al.*, 2004; Khuri-Bulos and Al Khatib, 2006). These studies indicated that there is a direct or indirect possibility of viral occurrence in and/or viral infection through water environment. Three independent studies were carried out to investigate the enteroviruses prevalence in Jordan (Reichler *et al.*, 1997a, 1997b; Meqdam *et al.*, 2002). However, all these studies were based on detecting enteroviruses from clinical samples collected from children and adults. Another study performed by Malkawi and Shaban (2007) aimed to detect enteroviruses in different domestic water resources such as home water tanks and wells.

The very limited data on viral occurrence in water in Jordan makes it difficult to determine the health risks associated with these viruses. Moreover, to prevent diseases induced by waterborne viruses, a survey of viral occurrence in the water environment is badly needed. Therefore, in this study, Al-Zarqa River, one of the major

* Corresponding author e-mail: isaadoun@sharjah.ac.ae.

water resources in Jordan, was chosen in order to investigate its surface water quality with respect to the presence of waterborne human pathogenic viruses, especially the enteroviruses. The study is considered as the first to investigate the types of enteroviruses in water environmental samples collected from Al-Zarqa River, with a special focus on the serotypes and phylogeny of enteroviruses.

2. Materials and Methods

2.1. Site Location and Background.

Aquifers and basins represent Jordan's primary sources of water. Amman-Zarqa Basin is the second largest basin after The Yarmouk Basin with an area of about 3,900 km². The basin is located in the most densely populated area in Jordan, accounting for 65% of Jordan's population and 90% of the industries in the country (Arab Environment Monitor (AEM) 2006). In addition, the basin provides irrigation for 8,400 hectares of land around. With the high population growth and high demand on water; the basin is subject to increased exploitation of its natural base-flow to an irreversible state (AEM 2006). Moreover, the annual effluent of treated domestic and wastewater treatment plants (total of 60 million cubic meters) has been contributing to nearly all of its summer flow (Optimization for Sustainable Water Resources Management (OPTIMA) 2006).

As-Samra Wastewater Treatment Plant (ASWWTP) (Fig. 1) is heavily overloaded with domestic wastewater effluent from the Amman-Zarqa basin containing high organic loads, plus industrial wastewater containing chemical and organic pollutants. Furthermore, ASWWTP receives domestic wastewater from about 2 million inhabitants in Jordan. Due to this high load, ASWWTP performance has been deteriorating over the years, resulting in lowering the effluent quality and deteriorating the groundwater quality in Zarqa basin to a level that is unsuitable for irrigation (AEM 2006), thus undermining the quality of life of residential communities in the Amman-Zarqa basin (Westrell 2004; De Luca *et al.*, 2013).

2.2. Collection of Raw, Treated Sewage, Surface Water and Pond Water Samples.

A total of 33 samples of raw sewage, treated sewage, surface and pond water were collected over a period of one year (Table 1). All the 33 water and effluent samples were collected from places along the Zarqa River at different distances from the ASWWTP effluent to study the types and quantities of enteroviruses. Figure 1 presents a summary of the samples and the map shows physically the places along the river where the samples were collected. Samples were kept cool and processed as soon as possible or stored at -70 °C until processed.

Table 1. The location, type, number and the volume of the samples collected along Al-Zarqa River.

Site	Description of the site	Type of sample	No. of samples
A	ASWWTP inlet	Composite Raw sewage	3
B	ASWWTP outlet	Composite Treated water	3
C	2 km downstream the ASWWTP, near Al-Hashemia city	Surface river water	7
D	11 km downstream the ASWWTP, Al-Sukhna town	Surface river water	7
E	Al-Sukhna town bridge	Untreated water	3
F	40 km downstream the ASWWTP, Jerash bridge	Pond water	3
G	40 km downstream the ASWWTP, Jerash bridge	Surface river water	7
Total			33

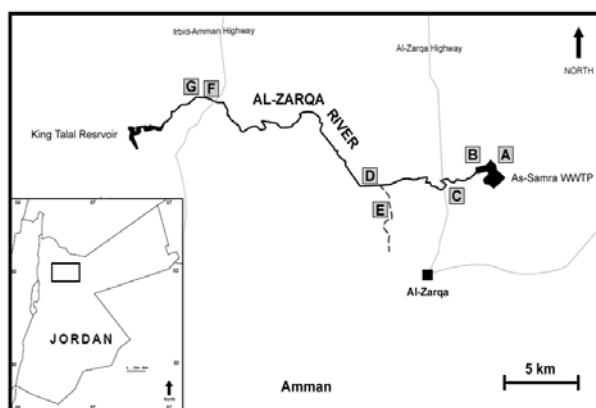


Figure 1. Locations of sampling sites along Al-Zarqa River. A: ASWWTP inlet; B: ASWWTP outlet; C: 2 km downstream the ASWWTP, Al-Hashemia city; D: 10 km downstream the ASWWTP, Al-Sukhna town; E: Al-Sukhna town bridge; F: 40 km downstream the ASWWTP, Jerash bridge, Jordan Modern Private Nursery; G: 40 km downstream the ASWWTP, Jerash bridge, Jordan Modern Private Nursery.

2.3. Concentration of Samples.

Surface water samples were concentrated by the adsorption-elution method (Haramoto *et al.* 2005) with modifications. Seven to eight liters of surface water samples were first allowed to reach the room temperature; the pH was then adjusted to 3.5 with 0.1 N NaOH (Frutarom, UK). The adjusted samples were pumped through a glass filter (Millipore, Ireland) and 0.45 µm mixed cellulose ester (Millipore, Ireland). Filter-adsorbed viruses were eluted with sterile 200 ml of 0.1% skimmed milk (Oxoid, UK) in 0.05 M Glycine buffer (pH 9.5) (Biorad, Italy) and kept in sterile bottles. Further concentration was done by organic flocculation after lowering the pH of the eluent to 4.5, followed by centrifugation at 4500 rpm for 30 min at 12°C. The resulting pellet was resuspended in a 10 ml sterile Phosphate buffered saline (PBS) (pH 7.2) (Lonza, Belgium) and stored at -70°C until subjected to RNA extraction.

Composite raw and treated sewage samples were concentrated by a two-phase separation method described by van den Berg *et al.* (2005). The average concentrate

volume was 2 ml and it was stored at -70°C until subjected to RNA extraction.

2.4. Calculation of Virus Recovery.

The recovery percentage of the applied concentration methods used in this study was calculated by spiking the collected water and sewage samples with the bacteriophage PRD1, provided kindly by The National Institute of Public Health and the Environment (RIVM), The Netherlands. The bacteriophage PRD1 was used to evaluate the efficiency of virus recovery. First, surface water, treated water and raw sewage were spiked with 10⁶ pfu of PRD1, and then the concentration procedures were performed as described earlier. Both, the un-concentrated samples and resulting concentrates were tested for the presence of PRD1 using the double-agar-layer method as described in ISO 10705-1 (ISO, 1995). The percentage of recovery was calculated using the following formula:

$$\% \text{ Recovery} = \frac{\text{No. of PFU} \times \text{volume of concentrate}}{\text{No. of PFU} \times \text{volume of spiked sample}}$$

2.5. RNA extraction, RT-PCR amplification and gel electrophoresis.

Viral RNA was extracted from retentates using the silica beads in the presence of guanidinium isothiocyanate (Fluka, Switzerland) following the method developed by Boom et al. (1990). Primers and probes used were purchased from Alpha DNA (Canada), Midland (Canada) and Invitrogen (Germany). These primers were E1: 5'-CCTCCGGCCCCCTGAATG-3' and E2: 5'-ACCGGATGGCCAATCCAA-3' (Sheih et al., 2003). A 18 µl anti-sense mix composed of 15 µl of extracted RNA plus 50 pmole of the reverse primer E2 and 16 U from the RNase inhibitor RNasin (Promega, USA) was heated at 95°C for 5 min, then chilled on ice for at least 5 min. To make the cDNA, a 12 µl reverse transcription mix containing 1X PCR buffer (10 mM Tris-HCl [pH 8.3]), 3 mM MgCl₂, 1 mM dNTP's and 5 U AMV-RT (All from Promega, USA) was combined with the heated anti-sense mix and incubated at 42°C for 1 h followed by 5 min incubation at 99°C then on ice for at least 5 min. PCR was performed according to van den Berg et al., (2005) by adding 15 µl of cDNA, the forward primer E1, 1X PCR buffer (10 mM Tris-HCl [pH 8.3]), 1.5 mM MgCl₂, 0.2 mM dNTP's and 5 U of Taq Polymerase (All from Promega, USA). PCR cycling was as follows: initial denaturation for 3 min at 94°C, 45 cycle of 1 min at 94°C, 1 min at 37°C and 1 min at 72°C followed by a final extension step for 10 min at 72°C (Applied Biosystems, USA). PCR products were separated onto 2% agarose (Biobasic, Canada) in the presence of 1 µg/ml ethidium bromide (Promega, USA).

2.6. Extraction of PCR products from gels.

After electrophoresis and separation of all PCR products on 2% agarose (Biobasic, Canada), gels were visualized under UV illumination. Purification of PCR products from the gel material was done either using the Qiaquick gel extraction kit (Qiagen, Germany) or the DNA isolation kit (AppliChem, Germany) following the manufacturer's instructions.

2.7. Southern-Blotting Hybridization.

Agarose gels containing the RT-PCR products were first soaked for 1 h in 2 times the gel volume with denaturing solution, neutralized with the same volume of 1X neutralizing solution, and finally soaked in 20X Saline, Sodium Phosphate, EDTA (SSPE) buffer (Lonza, Belgium) for 3 h as described by (Lodder and Husman, 2005). Transfer was made in 20X SSPE to a positively charged nylon membrane (Millipore, Ireland) by using a home-made capillary transfer apparatus. Next day, the membrane was washed with 5X SSC (Lonza, Belgium) two times 5 min each. After that, the transferred DNA was cross-linked by heating the membrane in the microwave (Sharp, Japan) for 8 min. Subsequently, the membrane was pre-hybridized at 55°C with 20 ml of 2XSSPE-0.1%SDS (Promega, USA) for at least 1 h and then hybridized overnight at 55°C with a fresh 20 ml of 2XSSPE-0.1%SDS containing 40 pmole of the biotinylated EV probe (5'-ACTACTTTGGGTGTCCGTGTTTC-3') (Sheih et al., 2003), which is specific for the 5' untranslated region. Detection was made using biotin chromogenic detection kit (Fermentas, EU) following the manufacturer's instructions.

2.8. Calculation of the Enteroviruses RNA Concentration.

The number of virus particles present in all samples was estimated semi-quantitatively by RT-PCR and southern blotting on ten-fold serially diluted RNA (end point dilution) as previously described by (Rutjes et al., 2005). The estimation of the virus RNA concentration (PCR detectable unit per liter [pdu/l]) in the water was based on the most diluted sample, which gave a positive signal after hybridization of the RT-PCR products. Five ml from each sample concentrate (except for the raw sewage samples, where only 1 ml) was used to extract RNA; the final extracted volume was 15 µl. The extracted RNA 10-fold diluted up to 10⁻⁴. All the undiluted and the diluted RNA were subjected to RT-PCR then Southern blotting as described earlier.

2.9. Cloning.

Southern hybridization positive products were cut from the gel with a clean scalpel and purified using the NucleoSpin Extract II kit (Macherey-Nagel, USA). The purified products were then inserted into the pJET1.2/blunt cloning vector provided in the CloneJET PCR cloning kit (Fermentas, EU) according to the manufacturer's instructions. The resulting vectors were transformed into *Escherichia coli* GW2163 (Fermentas, EU) using the TransformAid bacterial transformation kit (Fermentas, EU). Transformed bacteria were selected on 37°C pre-warmed LB agar plates containing 50 µg/ml ampicillin and incubated overnight at 37°C. Next day, 10 colonies from each plate were inoculated into LB broth containing 50 µg/ml ampicillin and incubated for 12-16 hours at 37°C with shaking at 120 rpm. After that, plasmids were extracted from the overnight culture using the GeneJET Plasmid Miniprep Kit (Fermentas, EU). PCR using the primer pair pJET1.2 forward sequencing primer (5'-CGACTACTATAGGGAGAGCGGC-3') and pJET1.2 reverse sequencing primer (5'-AAGAACATCGATTTTCCATGGCAG-3') were used to

ascertain that the isolated plasmids contain the correct insert.

2.10. DNA Sequencing.

Sequencing of all cloned fragments was done using ABI 310 DNA sequencer (Applied Biosystems, USA) available at Princes Haya Biotechnology Center/Jordan University of Science and Technology, Irbid-Jordan, and the pJET1.2 forward sequencing primer (5' CGACTCACTATAGGGAGAGCGGC 3'), and the pJET1.2 backward sequencing primer (5'-AAGAACATCGATTTTCCATGGCAG-3').

Sequencing results were analyzed using the ChromasPro software 1.34. The nucleotide sequences were analyzed by BLASTed against the GeneBank using "blastn" provided by the National Center for Biotechnology Information (NCBI).

2.11. Phylogenetic Analysis.

The 196 base pairs of the 5'NTR enterovirus sequence from 14 isolates obtained in this study were compared to each other and to 56 reference enterovirus strains from GenBank. All sequences were prepared by EditSeq software (DNASTar version 7.0, Inc., Madison, WI, USA) and aligned using the Clustal W method of the MegaAlign software (DNASTar version 7.0, Inc., Madison, WI, USA). The phylogenetic tree was constructed by the neighbor-joining method and the reliabilities were evaluated with 1000 bootstrap replications.

3. Results

3.1. Qualitative detection of enterovirus in the concentrated samples.

Table 2 summarizes the detection of enterovirus and recovery yield of the bacteriophages. For all sites, the recovery yields of spiked bacteriophage PRD1 represent the mean of at least three different samples. The recovery yields means for the surface water samples were between 5 to 6%. The highest recovery yields were obtained from treated sewage.

Table 2. Detection of enterovirus by RT-PCR and southern hybridization assays in the concentrated surface water and raw sewage samples, and recovery yields of bacteriophage PRD1 from the various samples collected.

Sample	No. of Samples	% Recovery mean \pm S.D. ^a	No. (%) of samples positive
Site A	3	2 \pm 0.94	3 (100)
Site B	3	8 \pm 1.2	1 (33)
Site C	7	6 \pm 0.5	2 (29)
Site D	7	5 \pm 2.3	3 (42)
Site E	3	6 \pm 1.4	1 (33)
Site F	3	8 \pm 1.3	0 (0)
Site G	7	5 \pm 1.6	4 (57)
Total	33		14 (42)

^aThe mean and standard deviation (SD) obtained from at least 3 different samples

A sample was considered positive for enteroviral RNA if the 196-bp RT-PCR product gave a positive signal after southern blotting hybridization against a specific probe (EV: 5'-ACTACTTTGGGTGTCCGTGTTTC-3'). Of the

33 samples collected, 14 (42%) were found positive for enterovirus RNA (Table 2). The number of surface river water samples tested positive for enteroviral RNA were 1 (33%) at site B, 2 (29%) at site C, 3 (42%) at site D, and 4 (57%) at site G. Figure 2 shows an example of enterovirus positive results by RT-PCR and southern blotting hybridization. Enterovirus RNA was detected in only 1 out of 3 (33%) treated sewage samples collected from site E. All raw sewage samples (100%) were contained enteroviral RNA (Table 2).

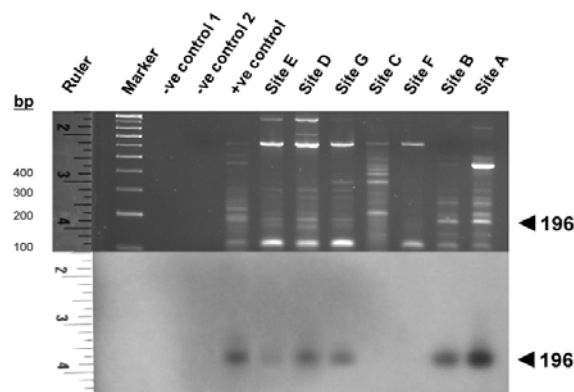


Figure 2. Enterovirus specific RT-PCR products (A) and southern blotting hybridization (B). Ruler: 30 cm long fluorescent ruler; Marker: 100-bp ladder; -ve control 1: negative control for RNA extraction; -ve control 2: negative control for RT-PCR; +ve control: stool sample positive for enterovirus.

3.2. Semi-quantitative estimation of enteroviruses concentration.

The RNA virus concentration of the positive samples ranged from 5 to 10^4 pdu/ml. The highest concentration of enterovirus RNA was in the raw sewage samples with a mean of 2.5×10^3 pdu/ml, whereas the lowest concentration (8.3 pdu/ml) was obtained from the surface river water sample collected from site C (Table 3). Samples collected in March were positively confirmed for enteroviral RNA by RT-PCR and southern blotting hybridization for all sites except for sites C and F (Fig. 2).

Table 3. Enterovirus concentration in all samples collected.

Date of sampling	Concentration (pdu/ml) ^a						
	Site A	Site B	Site C	Site D	Site E	Site F	Site G
28 - Feb	1 X 10^3	0	0	10 *	ND	ND	0
19 - Mar	3.3 X 10^3	6.3 *	8.3 *	10 *	25	ND	10 *
04 - June	ND	ND	0	0	ND	ND	0
23 - Aug	ND	ND	0	0	ND	ND	0
19 - Oct	3.3 X 10^3	0	0	0	0	0	26.6
15 - Nov	ND	ND	0	0	ND	0	11.1
06 - Dec	ND	ND	11.1	25	0	0	66.6

^a pdu/l: PCR detectable units per ml, after detection by RT-PCR and southern hybridization.

* Mean recovery yield was used to calculate concentration.

ND: Not Determined

3.3. Cloning and DNA sequencing

Blast results indicated that one out of the 14 samples contained mixtures of 3 different types of enterovirus

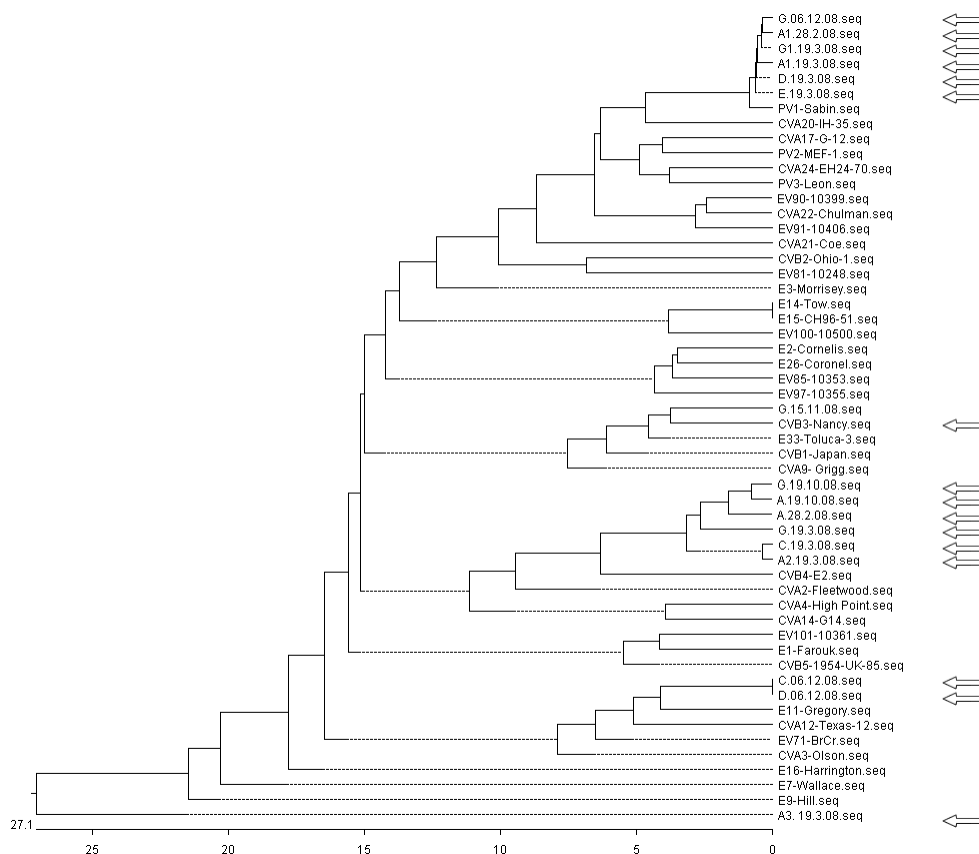


Figure 5. Phylogenetic analysis of enterovirus sequences obtained from different samples. The scale represents the number of nucleotide substitution between the sequences. The arrows locate the enteroviral sequences identified in this study.

4. Discussion

This study is focused primarily on enteroviruses in water environmental samples collected from Al-Zarqa River, Jordan as literature review showed the absence of any qualitative and/or quantitative information about those viruses in the country.

4.1. Concentration of water samples.

It is worth mentioning that the recovery yields of enteroviruses were higher for the less turbid samples (e.g. treated water), compared with more turbid ones (e.g. raw sewage). Similarly, the closer the site of collection to ASWWTP, the better the recovery yield obtained. This observation is consistent with other studies. Katayama *et al.* (2008) obtained recovery yields of 28% and 65% for sewage and treated water, respectively. The possible explanation for the low recovery yields of enteroviruses as well as the bacteriophage PRD1 associated with turbid samples may be the adsorption of the virus into the particles present in the mixture.

4.2. Qualitative and semi-quantitative estimation of enteroviruses.

The annealing temperature of the primers used in enteroviruses PCR protocol was 37°C, which is considered to be low. With this low annealing temperature, there is a high probability of non-specific binding of the primers, which in turn will give a false positive result that necessitates the addition of a confirmatory step. Therefore, southern blotting hybridization against an enteroviral

specific probe was used. A sample was only considered positive for enteroviral RNA by southern blotting if the 196-bp RT-PCR product gave a positive signal.

Of the 33 samples collected, 14 (42%) tested positive for enterovirus RNA. This frequency is similar to that of other studies (Chapron *et al.*, 2002; Lee and Kim, 2002). With the exception of pond water samples (Site F), the presence of enterovirus RNA was detected in all sites. All the collected raw sewage samples also contained enteroviral RNA, which is consistent with other studies (Green and Lewis, 1999; Lodder and de Roda Husman, 2005; Katayama *et al.*, 2008) that showed the raw sewage usually contains high viral loads. The mean concentration of enteroviral RNA in raw sewage samples was 2.5×10^3 pdu/ml. The number of enterovirus pdu present in all samples was estimated semi-quantitatively by RT-PCR and southern blotting hybridization on tenfold serially diluted RNA. Because it detects the enteroviral RNA molecules, the concentration of enteroviral RNA expressed as PCR-detectable unit (pdu) does not usually reflect the concentration of infectious enteroviruses particles, in contrast to the plaque forming unit. Therefore, enterovirus concentrations may be even lower than the obtained result. However, this unit might be beneficial when a comparison between samples is required, especially between raw sewage and treated water samples. Because we were unable to obtain the Buffalo Green Monkey Kidney cell line that usually used to grow enteroviruses, semi-quantitative estimation using the pdu method was the only way to compare samples with respect to enterovirus concentration. Comparisons of enterovirus concentration

obtained from our samples with those of other studies cannot be made, since all studies use the plaque forming unit to express the concentration of enteroviruses.

Only one treated water sample collected from the ASWWTP effluent gave a positive result for enteroviruses RNA. By comparing between the samples collected from the inlet and outlet of ASWWTP, $2.7 \log^{10}$ -unit of enterovirus removal was observed when samples collected on March 19th. This implies that the treated sewage water contains 5 enterovirus pdu discharged into Al-Zarqa River surface water.

Out of the 21 samples of river surface water collected, fifty seven percent tested positive for enteroviral RNA (Table 4). The highest number of samples tested positive for enteroviruses were in site G (4 samples), followed by site D (3) then site C (2). It was noted that as we went downstream ASWWTP, the number of enterovirus-positive samples increased. This can be explained by the fact that, both human (e.g. farming and industrialization) and environmental factors affecting the quality of the river are gradually amplified as the river reaches its final destination in King Talal Dam.

Only one sample collected from site E contained enterovirus RNA. Therefore, untreated water coming from Al-Zarqa city has adverse effects on the water quality of Al-Zarqa River. All samples collected from the private pond were enterovirus RNA free. The pond is fed from groundwater; therefore, filtration of viruses might have occurred during water passage through the soil (Saadoun *et al.*, 2008) resulting in viruses free filtered water.

None of the samples collected in July and August contained enterovirus RNA. In Jordan, the temperature is higher during this period than the rest of the months during which the samples were collected. This observation contradicts other reports showing a peak of enterovirus circulation in the summer and early autumn (Muir *et al.* 1998; Katayama *et al.*, 2002; CDC, 2006; Jiang *et al.*, 2007). However, this may be explained by knowing that the high number of enteroviruses infections comes from using water resources for recreation, which is not the case for Al-Zarqa River that not used for recreation. Furthermore, enteroviruses survive longer at lower temperatures in natural environments, such as river and groundwater (Fong and Lipp, 2005). Although enteroviruses were detected in clinical samples (Meqdam *et al.*, 1997a, 1997b) and house hold water samples (Malkawi and Shaban, 2007), there were no studies in Jordan testing the presence of enteroviruses in river water or water basin to conduct a comparison.

4.3. Typing of enteroviruses detected by sequence analysis.

As cloning was used to test the co-presence of multiple enterovirus serotypes in single samples, we demonstrated the simultaneous presence of 3 different serotypes of enteroviruses in one sample and 2 serotypes of enteroviruses in two different samples. Cloning of virus-positive PCR product has been used extensively to test for the co-presence of multiple virus types in different water environmental samples (Lee and Kim, 2002), especially raw sewage samples, where it is suspected to harbor several serotypes (van den Berg *et al.*, 2005).

Sixteen sequences were obtained from cloning the 14 enterovirus positive RT-PCR products. To identify the

serotype of enterovirus present in each sample, the enterovirus sequences were BLASTed against the GeneBank databases using "blastn" provided by the National Center for Biotechnology Information (NCBI). The BLAST reports obtained demonstrated the presence of both poliovirus type 1 and coxsackievirus B4 in 6 samples for each, Echovirus 11 in two samples, and coxsackievirus B4 and Echovirus 9 in one sample for each.

4.4. Phylogenetic analysis.

Two echovirus 11 isolates were identified in two different surface river water samples collected from sites C and D in December 6th. Alignment and phylogenetic analysis of the two isolates showed that they were identical and related to echovirus 9 Hill strain. The occurrence of these two identical isolates indicates that they came from the same origin. ASWWTP outlet may be the source of echovirus 11 identified in sites C and D. However, this relationship cannot be ascertained, because sewage and treated water samples were not collected from the inlet and outlet of ASWWTP on the same day. The absence of this serotype in site G is due to either dilution of this serotype along the river and/or its inactivation.

The six coxsackievirus B4 isolates obtained were closely related and clustered together with the CVB4-E2 reference strain. By comparing them against each other, the three isolates collected in March 19th were closely related to each other more than to other isolates collected on different dates. This indicates that they may have originated from the same source, ASWWTP inlet. Supporting this presumption is the high similarity of coxsackievirus B4 sequences isolated from the inlet of ASWWTP, 2 and 40 km downstream ASWWTP at sites C and G, respectively. This trend is also strongly supported by 4 poliovirus 1 isolates identified in the same collection day and from overlapping sites (A and G).

5. Conclusion.

This study demonstrated the circulation of enterovirus in large volumes of sewage and water environmental samples collected from and around Al-Zarqa River. Enterovirus serotyping and phylogenetic analysis enabled us to trace back the source of viral contamination in some samples.

Acknowledgments.

The Deanship of Scientific Research at Jordan University of Science and Technology, Irbid-Jordan (Grant No. 58/2008) thankfully funded this study. Authors would like to express their deep thanks to National Institute of Public Health and the Environment (RIVM), the Netherlands, for their technical training and advice, to engineer Sufyan Bataineh from Water Authority of Jordan for his help in collecting samples from ASWWTP, and to Dr. Mustafa Ababneh/JUST-Jordan for providing the DNASTar software. Appreciation is extended to University of Sharjah/Sharjah-UAE for the administrative support.

References

Arab Environment Monitor. (2006). "Tales of water in Zarqa River".

- <http://www.arabenvironment.net/archive/2006/3/29672.html> (July 4, 2007).
- Battikhi MN. 2002. Epidemiological study on Jordanian patients suffering from diarrhea. *New Microbiol*, **25**: 405-412.
- Battikhi MN and Battikhi EG. 2004. The seroepidemiology of Hepatitis A virus in Amman, Jordan. *New Microbiology*, **27**: 215-220.
- Boom R, Sol CJ, Salimans MM, Jansen CL, Wertheim van Dillen PM and der van Noordaa JSO. 1990. Rapid and simple method for purification of nucleic acids. *J Clin Microbiol*, **28**: 495-503.
- Center of Disease Control and Prevention (CDC). Enterovirus Surveillance — United States, 1970–2005. 2006; *MMWR*, **55**: SS-8.
- Chapron CD, Ballester NA, Fontaine JH, Frades CN and Margolin AB. 2000. Detection of astroviruses, enteroviruses, and adenovirus types 40 and 41 in surface waters collected and evaluated by the information collection rule and an integrated cell culture-nested PCR procedure. *Appl Environ Microbiol*, **66**: 2520-2525.
- De Luca G, Sacchetti R, Leoni E and Zanetti F. 2013. Removal of indicator bacteriophages from municipal wastewater by a full-scale membrane bioreactor and a conventional activated sludge process: Implications to water reuse. *Biores Technol*, **129**: 5265-31.
- Ferguson C, Roda Husman AM, Altavilla N, Deere D and Ashbolt N. 2003. Fate and Transport of Surface Water Pathogens in Watersheds. *Critic Rev Environ Sc Technol*, **33**: 299-361.
- Fong TT and Lipp EK. 2005. Enteric viruses of humans and animals in aquatic environments: health risks, detection, and potential water quality assessment tools. *Microbiol Mol Biol Rev*, **69**: 357-371.
- Green DH and Lewis GD. 1999. Comparative detection of enteric viruses in wastewaters, sediments and oysters by Reverse transcription-PCR and cell culture. *Water Res*, **33**: 1195-1200.
- Hansen JS and Ongerth JE. 1991. Effects of time and watershed characteristics on the concentration of Cryptosporidium oocysts in river water. *Appl Environ Microbiol*, **57**: 2790-2795.
- Haramoto E, Katayama H, Oguma K and Ohgaki S. 2005. Application of Cation-Coated Filter Method to Detection of Noroviruses, Enteroviruses, Adenoviruses, and Torque Teno Viruses in the Tamagawa River in Japan. *Appl Environ Microbiol*, **71**: 2403-2411.
- ISO (International Organization for Standardization). 1995. Water Quality: detection and enumeration of bacteriophages-part I: Enumeration of F-specific RNA-bacteriophages, ISO 10705-1, Geneva, Switzerland.
- Iwai M, Yoshida H, Matsuura K, Fujimoto T, Shimizu H, Takizawa T and Nagai Y. 2006. Molecular Epidemiology of Echoviruses 11 and 13, Based on an Environmental Surveillance Conducted in Toyama Prefecture, 2002-2003. *Appl Environ Microbiol*, **72**: 6381-6387.
- Jiang SC, Chu W and He JW. 2007. Seasonal Detection of Human Viruses and Coliphage in Newport Bay, California. *Appl Environ Microbiol*, **80**: 6468-6474.
- Khuri-Bulos N and Al Khatib M. 2006. Importance of rotavirus as a cause of gastroenteritis in Jordan: a hospital based study. *Scand J Infect Dis*, **38**: 639-44.
- Kistemann T, Claßen T, Koch C, Dangendorf F, Fishcheder R, Gebel J, Vacata V and Exner M. 2002. Microbial Load of Drinking Water Reservoir Tributaries during Extreme Rainfall and Runoff. *Appl Environ Microbiol*, **68**: 2188-2197.
- Katayama H, Shimasaki A and Ohgaki S. 2002. Development of a virus concentration method and its application to detection of enterovirus and Norwalk virus from coastal seawater. *Appl Environ Microbiol*, **68**: 1033-1039.
- Katayama H., Haramoto E, Oguma K, Yamashita H, Tajima A, Nakajima H and Ohgaki S. 2008. One-year monthly quantitative survey of noroviruses, enteroviruses, and adenoviruses in wastewater collected from six plants in Japan. *Water Res*, **42**: 1441-1448.
- Lees D. 2002. Viruses and bivalve shellfish International. *J Food Microbiol*, **59**, 81-116.
- Lee SH and Kim SJ. 2002. Detection of infectious enteroviruses and adenoviruses in tap water in urban areas in Korea. *Water Res*, **36**: 248-256.
- Lodder WJ and de Roda Husman AM. 2005. Presence of Noroviruses and Other Enteric Viruses in Sewage and Surface Waters in The Netherlands. *Appl Environ Microbiol*, **81**: 1453-1461
- Malkawi M and Shaban A. 2007. Rapid Detection of Human Enteric Pathogens (Viruses and Bacteria) in Water Resources from Jordan Using Polymerase Chain Reaction (PCR). *J Appl Scient Res*, **3**: 1084-1093.
- Maunula L, Miettinen IT and von Bonsdorff CH. 2005. Norovirus outbreaks from drinking water. *Emerg Infect Dis*, **11**: 1716-21.
- Meqdam MM, Youssef MT, Nimri LF, Shurman AA, Rawashdeh MO and Al-Khdour MS. 1997a. Viral gastroenteritis among young children in northern Jordan. *J Trop Pedc*, **43**: 349-352.
- Meqdam MM, Youssef MT, Rawashdeh MO and Al-Khdour MS. 1997b. Non-seasonal viral and bacterial episode of diarrhea in the Jordan Valley, West of Jordan. *FEMS Immunol Med Microbiol*, **18**:133-138.
- Meqdam MM, Khalousi MM and Al-Shurman A. 2002. Enteroviral meningitis in Northern Jordan: prevalence and association with clinical findings. *J Med Virol*, **66**: 224-128.
- Muir P, Kämmerer U, Korn K., Mulders MN, Poyry T, Weissbrich B, Kandolf R, Cleator GM and van Loon AM. 1998. Molecular typing of Enteroviruses: Current status and future requirements. *Clinic Microbiol Rev*, **11**: 202-227.
- Nimri LF, Elnasser Z and Batchoun R. 2004 Polymicrobial infections in children with diarrhoea in a rural area of Jordan. *FEMS Immunol Med Microbiol*, **42**: 255-259.
- OPTIMA: Optimization for Sustainable Water Resources Management (2006) Case Study: Zarqa River, Jordan. <http://www.ess.co.at/OPTIMA/CASES/JO/zarqa.html> (Accessed 4 July 2007).
- Payment P, Franco E, Fout GS. 1994. Incidence of Norwalk virus infections during a prospective epidemiological study of drinking water-related gastrointestinal illness. *Canad J Microbiol*, **40**: 805-809.
- Pina S, Puig M, Lucena F, Jofre J and Girones R. 1998. Viral Pollution in the Environment and in Shellfish: Human Adenovirus Detection by PCR as an Index of Human Viruses. *Appl Environ Microbiol*, **64**: 3376-3382
- Reichler MR, Kharabsheh S, Rhodes P, Otoum H, Bloch S, Majid MA, Pallansch MA, Patriarca PA, Cochi SL. 1997a. Increased immunogenicity of oral poliovirus vaccine administered in mass vaccination campaigns compared with the routine vaccination program in Jordan. *J Infect Dis*, **175**: (S1), S198-204.
- Reichler MR, Abbas A, Kharabsheh S, Mahafzah A, Alexander JP Jr and Rhodes P. 1997b. Outbreak of paralytic poliomyelitis in a highly immunized population in Jordan. *J Infect Dis*, **175**: (S1), S62-70.
- Rose JB and Gerba CP. 1991 Assessing potential health risks from viruses and parasites in reclaimed water in Arizona and Florida, USA. *Water Sci Technol*, **23(10-12)**: 2091-2098.

- Rutjes SA, Italiaander R, van den Berg HH, Lodder WJ, de Roda Husman AM. 2005. Isolation and detection of enterovirus RNA from large-volume water samples by using the NucliSens miniMAG system and real-time nucleic acid sequence-based amplification. *Appl Environ Microbiol*, **71**: 3734-3740.
- Saadoun I, Schijven J, Shawaqfah M, Al-Ghazawi Z, AL-Rashdan J, Blandford W, Boving T, Ababneh Q and van den Berg H. 2008. Removal of Fecal Indicator Coliforms and Bacteriophages by Riverbank Filtration (RBF) in Jordan, in Al-Mattarneh H, Mohd Sidek, L, Yusoff, M.Z. (Eds), *Innovations in Water Resources and Environmental Engineering. Proceedings of the International Conference on Construction and Building Technology (ICCBT)*. Kuala Lumpur, Malaysia, pp 191-198.
- Sibanda T and Okoh AI. 2012. Assessment of the Incidence of Enteric Adenovirus Species and Serotypes in Surface Waters in the Eastern Cape Province of South Africa: Tyume River as a Case Study. *The Sci World J* 9: doi: [10.1100/2012/949216](https://doi.org/10.1100/2012/949216)
- Shieh YC, Baric RS, Woods JW and Calci KR. 2003. Molecular surveillance of enterovirus and norwalk-like virus in oysters relocated to a municipal-sewage impacted gulf estuary. *Appl Environ Microbiol*, **70**: 7130-7136.
- Toukan AU, Sharaiha ZK, Abu-el-Rob OA, Hmoud MK, Dahbour SS, Abu-Hassan H, Yacoub SM and Margolis HS. 1988. The seroepidemiology of hepatitis A virus infection in Jordan. *Trop Gastroenterol*, **9**: 76-79.
- van den Berg H, Lodder W, Van der Poel W, Vennema H and Husman AM. 2005. Genetic diversity of noroviruses in raw and treated sewage water. *Res Microbiol*, **156**: 532-540.
- Westrell T. 2004. Microbial risk assessment and its implications for risk management in urban water systems. Thesis. Linköping University, Linköping, Sweden.

Phytochemical Analysis, *In Vitro* Antioxidant Activity and Germination Capability of Selected Grains and Seeds

Radka Vrancheva¹, Aneta Popova^{2*}, Dasha Mihaylova³ and Albert Krastanov³

¹Department of Analytical Chemistry and Physicochemistry, ²Department of Catering and Tourism, ³Department of Biotechnology, University of Food Technologies, 26, Maritsa Blvd., 4002, Plovdiv, Bulgaria

Received August 19, 2019; Revised September 17, 2019; Accepted September 27, 2019

Abstract

The present research work was carried out to evaluate the antioxidant potential of several grains and seeds, such as chia, common oat, proso millet, amaranth, quinoa, buckwheat, flax seed, and einkorn. The antioxidant and radical scavenging activity was determined by using different *in vitro* assays. The phytochemical screening revealed that the studied grains contain flavonoids (from 27.80±0.72 to 159.39±2.17 µM QE/g DW), and phenolic materials (from 0.29±0.00 to 2.45±0.02 mg GAE/g DW), their content being in direct connection with the antioxidant activity. Sprouting capability was then characterized by use of conventional and hydroponic methods. The results obtained in the present investigation suggest that grains could be a potential daily source of bioactive substances.

Keywords: sprouting, phenolic profile, antioxidants, flavonoids, functional ingredients

1. Introduction

Food is the main energy source for the human body, and it needs nutritious food to be healthy. Grains are cultivated worldwide and comprise a big percentage of the world's daily meals. Food can be seen as a natural source of beneficial substances. Scientists have identified thousands of different phytochemicals (phenolic acids, flavonoids, etc.), which can aid in the treatment of different ailments. Various studies have shown that plants rich in phytochemicals may supplement the body's needs for free radical combat (Lobo *et al.*, 2010) and attracting more and more attention (Georgieva-Krasteva *et al.*, 2017; Popova and Mihaylova, 2017).

Grains should account for a sizable portion of the daily intake. There are different dietary recommendations for daily grain intake. One of them is serving 16 grams of whole grains. The grain consists of three main parts: bran, endosperm and germ. Most bioactive substances are in the bran (about 52 % by weight) and the germ (at least 24 % by weight) fractions. Non-refined grains have a lower glycemic index and are much more beneficial to the body providing it with sustained energy because they are released into the bloodstream more slowly (Zimmerman and Snow, 2012).

Phenolic compounds presented in cereals have gained much attention as health-promoting phytochemicals due to their strong antioxidant properties (Dapcevic-Hadnadev *et al.*, 2018). They are secondary metabolites with different biosynthetic pathways, which are also associated with their ability to scavenge free radicals and chelate transition metal ions (Huyut *et al.*, 2017). Some crops are a unique source of several compounds not present in other cereals

and pseudocereals. Proso millet (*Panicum miliaceum* L.), mainly used as bird feed, has just recently gained attention for its substantial functional properties and beneficial constituents. This crop is reported to have superior nutritional properties such as high dietary fiber content, low glycemic index and rich micronutrient content (Chandel *et al.*, 2014) and possess good antioxidant properties (Choi *et al.*, 2007). Common oat (*Avena sativa* L.), a cereal of *Poaceae* family, is known for its rich polyphenol content, antioxidant and anti-inflammatory activities (Chu *et al.*, 2013). Buckwheat (*Fagopyrum esculentum* Moench.), is primarily produced in Russia, and is known for its flavonoid content (Morishita *et al.*, 2007). Einkorn (*Triticum monococcum* L.), nature's first and oldest wheat, can significantly contribute to an antioxidant intake with beneficial health effects (Lachman *et al.*, 2012). Amaranth (*Amaranthus hypochondriacus* L.), highly valued for its amino acid composition also has considerable antioxidant activity (Tang and Tsao, 2017). Quinoa (*Chenopodium quinoa* Willd.) rich in phenolic acids, flavonoids, and tannins, is known to possess diverse physiological properties, including antimicrobial, antioxidant, anti-inflammatory, antitumor, and anti-carcinogenic effects (Benavente-Garcia and Castillo, 2008). Chia (*Salvia hispanica* L.) has high levels of phenolic compounds, flavonoids and antioxidant activity (Scapin *et al.*, 2016). Flax seed (*Linum usitatissimum* L.) is rich in phenolic compounds, which are responsible for its antioxidant activities (Rubilar *et al.*, 2010).

Germination is usually defined as the period when an organism grows from a seed. Germination process requires moisture, oxygen, temperature control and light/darkness. Sprouts are different vegetable/plant seeds or beans in a period of growth.

* Corresponding author e-mail: popova_aneta@yahoo.com.

Modern society is subjected to loads of stress, air pollution, climate change, modified products and artificial ingredients. It is reasonable for households to try to find ways to consume food that they trust. Germination is an easy and accessible way to add functional ingredients with beneficial effects to the daily diet. Healthy eating and back-to-nature food choices are trending. The reason why so many people use sprouts for food is that they contain a much higher percentage of vitamins and nutrients than the non-sprouted or mature forms of the abovementioned choices. They are low in calories, easily digestible and a valuable and important source of energy. Regular consumption of sprouts has an overall beneficial effect on health. Germinated seeds speed up metabolism and help reduce the amount of toxins in the body (Benincasa *et al.*, 2019).

Previous work (Morishita *et al.*, 2007; Chandel *et al.*, 2014; Scapin *et al.*, 2016) has only focused on characterizing the phytochemical profile of one or two species at a time as only few researchers have addressed the question of comparing several grains in terms of their beneficial properties. In the available literature, there was no information on the germination process of the studied seeds and grains. The objective of this paper was to investigate the phytochemical constituents profile and antioxidant activity of selective grains and seeds – einkorn, amaranth, common oat, buckwheat, proso millet, flax seed, quinoa and chia. First, the content of phenolic compounds and antioxidant capacities were evaluated in the extracts. Secondly, in order to characterize the samples antioxidant capacities, flavonoid content and phenolic acids have been determined. Finally, the sprouting capability of the studied grains and seeds was characterized with the use of two methods: conventional and hydroponic.

2. Materials and Methods

2.1. Materials and Extracts Preparation

Commercially available samples of eight species (chia, common oat, proso millet, amaranth, quinoa, buckwheat, flax seed, and einkorn) were obtained from local market in Plovdiv (Bulgaria) in spring 2018. The samples were milled into flour to obtain a homogenous particle size. Sample weighing 10g was extracted by stirring with 50 mL of methanol at 25°C at 150 rpm agitation for 24h and filtered through Whatman No. 4 paper. The procedure was repeated twice and the second extraction was carried out with 30 mL solvent. The extracts were pooled together and stored in refrigerator before analyzing.

2.2. Determination of Total Polyphenolic Content (TPC)

The TPC was analyzed following the method of Kujala *et al.* (2000) with some modifications. The TPC was expressed as mg gallic acid equivalents (GAE) per g dry weight of grains (DW).

2.3. Total Flavonoid Content (TFC)

The total flavonoid content was evaluated according to the method described by Kivrac *et al.* (2009). The absorbance was measured at 415 nm. Quercetin was used as a standard and the results were expressed as μM QE/g DW.

2.4. Determination of Antioxidant Activity

2.4.1. DPPH Radical Scavenging Assay

The ability of the extracts to donate an electron and scavenge 2,2-diphenyl-1-picrylhydrazyl (DPPH) radical was determined by the slightly modified method of Brand-Williams *et al.* (1995) as described by Mihaylova *et al.* (2015).

2.4.2. ABTS^{•+} Radical Scavenging Assay

The radical scavenging activity of the extracts against 2,2'-azino-bis(3-ethylbenzothiazoline-6-sulfonic acid) (ABTS^{•+}) was estimated according to Re *et al.* (1999). The results were expressed as TEAC value (μM TE/g DW).

2.4.3. Ferric-Reducing Antioxidant Power (FRAP) Assay:

The FRAP assay was carried out according to the procedure of Benzie and Strain (1999) with slight modification. Results were expressed as μM TE/g DW.

2.4.4. Cupric ion Reducing Antioxidant Capacity (CUPRAC) Assay

The CUPRAC assay was carried out according to the procedure of Apak *et al.* (2004). Trolox was used as a standard and the results were expressed as μM TE/g DW.

2.5. Identification and Quantification of Phenolic Acids

Qualitative and quantitative determination of phenolic acids was performed by using Elite LaChrome (Hitachi) HPLC system equipped with DAD and ELITE LaChrome (Hitachi) software. Separation of the phenolic acids was performed by Supelco Discovery HS C18 column (5 μm , 25 cm \times 4.6 mm), operated at 30°C under gradient conditions with mobile phase consisting of 2 % (v/v) acetic acid (solvent A) and acetonitrile (solvent B) as reported by Terzieva *et al.* (2017).

2.6. Germination

Seed samples were randomly selected from packed bags. Sixteen identical plastic containers were used as germination chambers. Eight chambers were filled with cotton wool soaked in deionized water and the remaining eight containers were filled with plant gel. Seed samples were spread in the containers. Germination was followed by daily counts, and final germination was determined after 5 days. A seed was considered germinated when the radicle protruded through the seed coat of at least 4 mm. Germination process was carried out at 25°C and germination chambers were stored in the dark.

2.7. Statistical Analysis

Data were analyzed using MS Excel software. All assays were performed in at least three repetitions. Results were presented as mean \pm SD (standard deviation). Fisher's least significant difference test at a level of $p < 0.05$ was used to determine the significance of differences between mean values.

3. Results and Discussion

The health benefits of whole grains consumption are often attributed to their unique phytochemical composition. Whole grain phytoconstituents are known for their antioxidant activity, and the ability to scavenge free radicals that may oxidize biologically relevant molecules (Liu, 2007). Based on this, grains could be considered as

contributors to the health benefits of people such as reducing the risk of heart disease, diabetes type 2, cancer, etc.

Phenolics are compounds consisting of one or more aromatic rings with one or more hydroxyl groups, generally categorized as phenolic acids, flavonoids, stilbenes, coumarins and tannins (Liu, 2004). Phenolics are the products of secondary metabolism in plants, providing essential functions in the reproduction and growth of the plant, acting as defense mechanisms against pathogens and parasites, also contributing to the color of plant. In addition to their role in plants, phenolic compounds in our diet provide health benefits associated with reduced risk of chronic diseases. Flavonoids on the other hand, include anthocyanins, flavonols, flavones, flavanones and flavonols. Flavonoids are located in the pericarp of all

Table 1: Total phenolic content (mg GAE/g DW), total flavonoid content (μM QE/g DW) and *in vitro* antioxidant activity of grains methanol extracts (μM TE/g DW).

Sample	TPC	TFC	DPPH	ABTS	FRAP	CUPRAC
chia	2.45 ± 0.02c	152.57±1.84a	5.63±0.04c	76.42±0.69cd	24.12±0.27a	15.83±21.80cd
common oat	1.82 ± 0.02c	159.39±2.17a	1.23±0.01c	44.13±0.17cd	12.13±0.05b	20.61±23.54e
proso millet	0.68 ± 0.01c	36.67±5.05a	1.61±0.01c	<	1.56±0.03b	9.93±8.75e
einkorn	0.61±0.01a	29.16±2.21a	3.64±0.01c	64.02±0.75d	2.15±0.03e	10.38±2.67e
amaranth	0.29±0.00a	27.80±0.72a	0.57±0.01c	<	1.46±0.03e	6.76±7.84bcd
quinoa	0.69±0.64b	364.74±2.82a	3.34±0.06c	52.30±1.83d	6.32±0.08d	10.84±9.04bcd
buckwheat	0.76±0.00a	76.44±1.90a	3.64±0.04c	60.49±1.53d	6.14±0.11a	5.21±2.96e
flax seed	0.61±0.02c	83.60±4.24a	2.76±0.03c	60.19±1.61d	10.72±0.17 a	8.55±13.11cd

< below limit of detection; Means followed by different letters within a column are significantly different at $P < 0.05$ according to Fisher's LSD test.

In comparison, Akin-Idowu *et al.* (2017) established TPC in various amaranth species from 0.27 ± 0.011 to 0.31 ± 0.015 mg GAE/g grains corresponding to the currently reported results. These authors evaluated amaranth as a potent source of antioxidants since the reducing capacity of a compound is usually an indicator of its potential antioxidant activity. Marineli *et al.* (2014) reported total phenolic content of 0.94 ± 0.06 mg GAE/g of chia seeds (Chile). The variations of the results in different research papers could be due to the concentration of phenolic compounds in whole-grain cereals influenced by grain types, varieties and the part of the grain sampled (Adom and Liu, 2002; Adom *et al.*, 2003; Adom *et al.*, 2005).

The investigation of antioxidant properties of natural sources is a very active field of research. Phenolic compounds have antioxidant properties and protect against degenerative diseases like heart diseases and cancer in which reactive oxygen species i.e., superoxide anion, hydroxyl radicals and peroxy radicals are involved (Rhodes and Price, 1997). Based on this and the already established presence of phenolic compounds, the antioxidant activity of eight grains was assessed by four common assays in the current study (Table 1) because it is very difficult to select a single most suitable antioxidant assay method due to the diverse mechanisms of antioxidant action that no assay can capture in their entirety. The results varied significantly from 0.57 ± 0.01 to 76.42 ± 0.69 μM TE/g DW. According to the DPPH assay, the highest results were evaluated for chia (5.63 ± 0.04 μM TE/g DW), followed by buckwheat (3.64 ± 0.04 μM TE/g DW) and einkorn (3.64 ± 0.01 μM TE/g DW). In

cereals. Cereals have only small quantities of flavonoids (McMurrough and Baert, 1994). They are reported to have antioxidant, anticancer, anti-allergic, anti-inflammatory, anticarcinogenic and gastro protective properties (Cook and Sammans, 1996; Liu, 2004; Yao *et al.*, 2004).

The results regarding the total phenol content and total flavonoid content of the methanol extracts of the selected grains are presented on Table 1. The TPC ranged from 0.29 ± 0.00 to 2.45 ± 0.02 mg GAE/g DW and the TFC was established to be from 27.80 ± 0.72 to 159.39 ± 2.17 μM QE/g DW. The total phenolic content was highest in chia (2.45 ± 0.02 mg GAE/g DW), followed by common oat (1.82 ± 0.02 mg GAE/g DW) and then buckwheat (0.76 ± 0.00 mg GAE/g DW). The lowest results according to both assays were evaluated for amaranth.

comparison, Inglett *et al.* (2010) reported 4.15 ± 0.04 μM TE/g for buckwheat 100 % ethanol extract obtained by using a water bath at 50 °C.

ABTS scavenging activity ranged from 44.13 ± 0.17 to 76.42 ± 0.69 μM TE/g DW. The highest values were established for chia (76.42 ± 0.69 μM TE/g DW) and einkorn (64.02 ± 0.75 μM TE/g DW). The lowest values were established for common oat - 44.13 ± 0.17 μM TE/g DW and proso millet and amaranth, where the antioxidant activity toward ABTS^{•+} was even not established. According to Akin-Idowu *et al.* (2017) the ABTS activity of five amaranth species varied from 169.6 ± 3.77 to 201.5 ± 4.04 mM TE/100g and Paško *et al.* (2009) reported 19.63 ± 1.38 mM TE/kg DW for amaranth grain. Despite this, amaranth is a valuable pseudo-cereal, due to its nutritional quality and nutraceutical properties, which contribute to improved human health (Gorinstein *et al.*, 2007; Pasko *et al.*, 2009).

The results with respect to the FRAP assay varied from 1.46 ± 0.03 to 24.12 ± 0.27 μM TE/g DW. The lowest results were evaluated in accordance with those already established in the amaranth extract (1.46 ± 0.03 μM TE/g DW). The highest values were detected for chia and common oat - 24.12 ± 0.27 and 12.13 ± 0.05 μM TE/g DW, respectively. This corresponds to the values established in all conducted antioxidant assays.

According to CUPRAC assay, the antioxidant activity of the investigated grains ranged from 5.21 ± 2.96 to 20.61 ± 23.54 μM TE/g DW. The highest values were detected in common oat and chia samples - 20.61 ± 23.54 and 15.83 ± 21.80 μM TE/g DW, resp. The lowest

antioxidant potential was determined for buckwheat ($5.21 \pm 2.96 \mu\text{M TE/g DW}$) and amaranth methanol extracts ($6.76 \pm 7.84 \mu\text{M TE/g DW}$). Kumar and Kaur (2017) have evaluated the antioxidant capacity of 18 selected cereal crops. According to the CUPRAC assay, the values varied from 0.65 to $4.68 \mu\text{M TE/g}$. Most studies concerning the antioxidant capacity of grains mainly target wheat, rice and rye products.

The most common phenolic compounds found in wholegrain cereals are phenolic acids and flavonoids. Phenolic acids are derivatives of benzoic and cinnamic acids and are present in all cereals. Hydroxybenzoic acid derivatives include p-hydroxybenzoic, protocatechins, vanillic, syringic and gallic acids. Hydroxyl cinnamic acid derivatives include p-coumaric, caffeic, ferulic and sinapic

Table 2: Phenolic acids composition of grains methanol extracts ($\mu\text{g/g g DW}$).

sample/ compound	gallic acid	chlorogenic acid	caffeic acid	ferulic acid	p-coumaric acid	sinapic acid	total phenolic acids
Chia	$14.27 \pm 0.01\text{a}$	$136.42 \pm 2.03\text{a}$	$34.63 \pm 0.01\text{b}$	$26.62 \pm 0.00\text{c}$	-	$168.58 \pm 0.01\text{c}$	$380.52 \pm 0.03\text{a}$
common oat	$13.88 \pm 0.00\text{a}$	$20.44 \pm 0.00\text{a}$	$15.10 \pm 0.00\text{b}$	traces	$21.91 \pm 0.01\text{b}$	$12.17 \pm 1.54\text{b}$	$83.5 \pm 0.01\text{c}$
proso millet	$6.88 \pm 0.01\text{a}$	$2.25 \pm 0.05\text{a}$	$5.37 \pm 0.01\text{b}$	-	$53.43 \pm 0.03\text{a}$	$8.29 \pm 0.01\text{c}$	$76.22 \pm 0.01\text{a}$
Einkorn	$19.19 \pm 0.07\text{a}$	$90.73 \pm 0.07\text{c}$	$6.95 \pm 0.03\text{b}$	-	$21.66 \pm 0.01\text{ba}$	$10.29 \pm 1.69\text{b}$	$148.82 \pm 1.23\text{a}$
Amaranth	$13.2 \pm 0.01\text{a}$	$22.79 \pm 0.08\text{a}$	$6.07 \pm 0.01\text{b}$	-	$21.64 \pm 2.07\text{c}$	$8.22 \pm 0.01\text{c}$	$71.92 \pm 5.06\text{a}$
Quinoa	-	$69.65 \pm 0.01\text{a}$	$19.42 \pm 0.06\text{b}$	$495.59 \pm 0.06\text{c}$	$108.27 \pm 0.0\text{a1}$	$41.41 \pm 0.00\text{a}$	$734.34 \pm 0.01\text{b}$
Buckwheat	-	$29.08 \pm 0.03\text{c}$	$19.41 \pm 0.01\text{b}$	-	$50.35 \pm 0.09\text{b}$	-	$98.84 \pm 0.04\text{a}$
flax seed	$13.54 \pm 0.03\text{a}$	$142.53 \pm 0.01\text{c}$	$5.42 \pm 0.05\text{b}$	-	-	-	$161.49 \pm 0.06\text{c}$

“-” – not detected; “traces” – below limit of detection

Means followed by different letters within a column are significantly different at $P < 0.05$ according to Fisher's LSD test.

However, other research studies evaluated ferulic acid as the most abundant hydroxycinnamic acid found in cereal grains (Santiago *et al.*, 2007; Boz, 2015). It is the main polyphenol present in cereals in which it is esterified to the arabinoxylans of the grain cell wall. Wheat bran is a good source of ferulic acid, which is esterified to the hemicelluloses of the cell walls (Dewanto *et al.*, 2002). It has antioxidant properties to combat destructive free radicals, and astringency that deters consumption by insects and animals (Arnason *et al.*, 1992). Ferulic acid can provide health benefits due to its antioxidant properties (Thompson, 1994).

However, in the present study chlorogenic and caffeic acids were distributed in all of the investigated extracts. On the contrary, the presence of cinnamic acid was not established in detectable amounts. In the chia extract, this compound was detected in traces, which corresponds to the results obtained by Coelho and Salas-Mellado (2014).

Germination is an easy and accessible way to add grains/seeds to the daily diet. For germination to occur, seeds/grains are soaked in water until seed splits open. Roots and shoot begin to occur after 24 h. Einkorn sprouts (Figure 1a) become ready in 72 hours. The conventional method led to a faster development compared to the hydroponic one. The hydroponic method resulted in several sprouts of less quality. Einkorn sprouts (cotton wool) had a length of 10-50 mm and hypocotyl thickness of 2 mm. They had yellow-rose color and attractive fragrance. They possess a slightly crisp texture, and for this reason can be purposely included in salads as functional ingredients. Benincasa *et al.* (2014) have also investigated the potential of einkorn sprouts as functional

ingredients. The major phenolic acids in cereals are ferulic acids and p-coumaric acid (Hahn *et al.*, 1983; Holtekjolen *et al.*, 2006). Therefore, it seems reasonable to evaluate the phenolic acids profile of the investigated grains available on the Bulgarian market, which is the object of the present study (Table 2). The methanol extracts consisted of phenolic acids in wide range in total from 71.92 ± 5.06 to $734.34 \pm 0.01 \mu\text{g/g DW}$. The profile itself in some species was quite similar with respect to the investigated phenolic compounds. In particular, although the total phenolic acids content of einkorn and amaranth extracts differs the presented phenolic acids were the same. The highest content of the studied phenolic acids was established in quinoa extract - $734.34 \pm 0.01 \mu\text{g/g DW}$, where the ferulic acid ($495.59 \pm 0.06 \mu\text{g/g DW}$) was predominant.

ingredients. Common oat sprouts (Figure 1b) did not develop very well. The conventional method resulted in a couple not fully developed sprouts and no sprouts in the hydroponic conditions. Amaranth sprouts (Figure 1c) developed for 72 hours in cotton wool. They had a length of 10-30 mm and hypocotyl thickness of 1 mm. They had a yellow-greenish color and possessed a leafy odor. They resembled the quinoa sprouts. The sprouting conditions did not alter the quality of the sprouts. Both conventional and hydroponic methods resulted in the same sprouts. Chia sprouts (Figure 1d) developed for 30 hours in cotton wool with a length of 40-50 mm, and did not develop in plant gel. They were white with green leaves and no particular odor. Flax seed sprouts (Figure 1e) developed for only 30 hours. They were light green of color with visible leaves. Their hypocotyl thickness was 2 mm. The conventional method in cotton wool led to faster development of the sprout. They possessed an attractive, broccoli like aroma and crisp texture. Quinoa sprouts (Figure 1f) did not develop very well in either condition. There were several sprouts in the cotton wool at a length of about 20-30 mm and a hypocotyl thickness of 0.8 mm. Their color was yellowish with an earthy odor and crispy texture. They are slightly like amaranth sprouts. Sprouts can find an application in the development of whole grain pasta with functional properties (Nataraja *et al.*, 2018). Proso millet and buckwheat did not sprout in either condition. Since the samples were obtained from the local store, the inability of proso millet and buckwheat to germinate could be explained by many reasons i.e. storage conditions, integrity of the package, grains with sprouting inability, storage duration, etc.



(a) Einkorn sprouts conventional method (left), hydroponic (right)

(b) Common oat sprouts conventional method

(c) Amaranth sprouts conventional method (left), hydroponic (right)

(d) Chia sprouts conventional method

(e) Flax seed sprouts conventional method (left), hydroponic (right)

(f) Quinoa sprouts conventional method

Figure 1. Germination capability of selected grains and seeds.

4. Conclusion

Grains are accessible sources of phenolic compounds with potential health benefits. The studied extracts appeared to possess antioxidant activity. Among all investigated species chia, common oat and einkorn revealed the most potential with respect to total flavonoid content and antioxidant capacity. The polyphenol extraction technique applied revealed the most abundant phenolic acids to be chlorogenic and caffeic acids, while ferulic acid was detected in highest amounts. The highest total phenolic acid content was evaluated for quinoa ($734.34 \pm 0.01 \mu\text{g/g} \text{ g DW}$). The study demonstrates and corroborates the importance of whole grains as natural food antioxidants. The current findings add to the growing body of literature concerning whole grains and can improve the available knowledge in food data charts. The current results point out to the opportunity of further investigation the *in vitro* digestibility of the documented phytoconstituents as well as creating a nutrient profile of the sprouts.

5. References

Adom K and Liu R. 2002. Antioxidant activity of grains. *J Agric Food Chem.*, **50**: 6182-6187.

Adom K, Sorrells M and Liu R. 2003. Phytochemical profiles and antioxidant activity of wheat varieties. *J Agric Food Chem.*, **51**: 7825-7834.

Adom K, Sorrells M and Liu R. 2005. Phytochemicals and antioxidant activity of milled fractions of different wheat varieties *J Agric Food Chem.*, **53**: 2297-2306.

Akin-Idowu P, Ademoyegun T, Olagunju O, Aduloju O and Adebo G. 2017. Phytochemical content and antioxidant activity of five grain amaranth species. *Am J Food Sci Technol.*, **5**: 249-255.

Apak R, Güçlü K, Özyürek M and Karademir E. 2004. Novel total antioxidant capacity index for dietary polyphenols and vitamins C and E, using their cupric ion reducing capability in the presence of neocuproine: CUPRAC method. *J Agric Food Chem.*, **52**: 7970-7981.

Arnason J, Gale J, Conilh de Beyssac B, Sen S, Miller A and Philogene B. 1992. Role of phenolics in resistance of maize grain to the stored grain insects, *Prostephanus truncatus* (Horn) and *Sitophilus zeamais* Motsch. *J Stored Prod Res.*, **28**: 119-126.

Benavente-García O and Castillo J. 2008. Update on uses and properties of citrus flavonoids: new findings in anticancer, cardiovascular, and anti-inflammatory activity. *J Agric Food Chem.*, **56**: 6185-6205.

Benincasa P, Galieni A, Manetta A, Pace R, Guiducci M, Pisante M and Stagnari F. 2015. Phenolic compounds in grains, sprouts and wheatgrass of hulled and nonhulled wheat species. *J Sci Food Agric.*, **95**: 1795-1803.

Benincasa P, Falcinelli B, Lutts S, Stagnari F and Galieni A. 2019. Sprouted Grains: A Comprehensive Review. *Nutrients*, **11**: 421-450.

Benzie F and Strain J. 1999. Ferric reducing/antioxidant power assay: Direct measure of total antioxidant activity of biological fluids and modified version for simultaneous measurement of total antioxidant power and ascorbic acid concentration. *Methods Enzymol.*, **299**: 15-27.

Boz H. 2015. Phenolic amides (avenanthramides) in oats – a review. *Cz J Food Sci.*, **33**: 1-7.

Brand-Williams W, Cuvelier E and Berset C. 1995. Use of a free radical method to evaluate antioxidant activity. *LWT - Food Sci Technol.*, **28**: 25-30.

Chandel G, Meena K, Dubey M and Kumari M. 2014. Nutritional properties of minor millets: neglected cereals with potentials to combat malnutrition. *Curr Sci.*, **107**: 1109-1111.

Choi Y, Jeong H and Lee J. 2007. Antioxidant activity of methanolic extracts from some grains consumed in Korea. *Food Chem.*, **103**: 130-138.

Chu Y, Wise L, Gulvady A, Chang T, Kendra D and Van Klinken B. 2013. *In vitro* antioxidant capacity and anti-inflammatory activity of seven common oats. *Food Chem.*, **139**: 426-431.

Coelho M and de las Mercedes Salas-Mellado M. 2014. Chemical characterization of chia (*Salvia hispanica* L.) for use in food products. *J Food Nutr Res.*, **2**: 263-269.

Cook N and Sammans S. 1996. Flavonoids - Chemistry, metabolism, cardioprotective effects, and dietary sources. *J Nutr Biochem.*, **7**: 66-76.

Da Silva Marineli R, Moraes A, Lenquiste A, Godoy T, Eberlin N and Marostica M. 2014. Chemical characterization and antioxidant potential of Chilean chia seeds and oil (*Salvia hispanica* L.). *LWT Food Sci Technol.*, **59**: 1304-1310.

Dapčević-Hadnadev T, Hadnadev M and Pojić M. 2018. The healthy components of cereal by-products and their functional properties. In: Ch. M. Galanakis, editor. **Sustainable Recovery and Reutilization of Cereal Processing By-Products**. Series in Food Science, Technology and Nutrition: Woodhead Publishing, UK, pp. 67-103.

Dewanto V, Wu X and Liu R. 2002. Processed Sweet Corn Has Higher Antioxidant Activity. *J Agric Food Chem.*, **50**: 4959-4564.

- Georgieva-Krasteva L, Hristova I, Mihaylova D and Dobрева K. 2017. Spelt (*Triticum aestivum* ssp. spelta) – from field to cosmetics. *Int J Pharmacogn Phytochem Res.*, **9**: 613-617.
- Gorinstein S, Vargas O, Jaramillo N, Salas I, Ayala A and Arancibia A. 2007. The total polyphenols and the antioxidant potentials of some selected cereals and pseudocereals. *European Food Res Technol.*, **225**: 321-328.
- Hahn D, Faubion J and Rooney L. 1983. Sorghum phenolic acids, their high performance liquid chromatography separation and their relation to fungal resistance. *Cereal chem.*, **60**: 255-259.
- Harborne J and Williams C. 2000. Advances in flavonoid research since 1992. *Phytochem.*, **55**: 481-504.
- Holtekjølen K, Kinitz C and Knutsen H. 2006. Flavanol and Bound Phenolic Acid Contents in Different Barley Varieties. *J Agric Food Chem.*, **54**: 2253-2260.
- Huyut Z, Beydemir Ş and Gülçin İ. 2017. Antioxidant and Antiradical Properties of Selected Flavonoids and Phenolic Compounds. *Biochem Res Int.*, **76**: 167-191.
- Inglett E, Rose J, Chen D, Stevenson G and Biswas A. 2010. Phenolic content and antioxidant activity of extracts from whole buckwheat (*Fagopyrum esculentum* Mönch) with or without microwave irradiation. *Food Chem.*, **119**(3): 1216–1219.
- Kivrak I, Duru M, Öztürk M, Mercan N, Harmandar M and Topçu G. 2009. Antioxidant, anticholinesterase and antimicrobial constituents from the essential oil and ethanol extract of *Salvia potentillifolia*. *Food Chem.*, **116**: 470-479.
- Kujala S, Loponen M, Klika D and Pihlaja K. 2000. Phenolics and betacyanins in red beetroot (*Beta vulgaris*) root: Distribution and effect of cold storage on the content of total phenolics and three individual compounds. *J Agric Food Chem.*, **8**: 5338-5442.
- Kumar H and Kaur C. 2017. A Comprehensive evaluation of total phenolics, flavonoids content and in-vitro antioxidant capacity of selected 18 cereal crops. *Int J Pure Appl Biosci.*, **5**: 569-574.
- Lachman J, Orsák M, Pivec V and Jirů K. 2012. Antioxidant activity of grain of einkorn (*Triticum monococcum* L.), emmer (*Triticum dicoccum* Schuebl [Schrack]) and spring wheat (*Triticum aestivum* L.) varieties. *Plant Soil Env.*, **58**: 15-21.
- Liu R. 2004. Potential synergy of phytochemicals in cancer prevention: mechanism of action. *J Nutr.*, **134**: 79-85.
- Liu R. 2007. Whole grain phytochemicals and health. *J Cereal Sci.*, **46**: 207–219.
- Lobo V, Patil A, Phatak A and Chandra N. 2010. Free radicals, antioxidants and functional foods: Impact on human health. *Pharmacogn Rev.*, **4**: 118–126.
- McMurrough I and Baert T. 1994. Identification of proanthocyanidins in beer and their direct measurement with dual electrode electrochemical detector. *J Inst Brew.*, **100**: 409-414.
- Mihaylova D, Lante A and Krastanov A. 2015. Total phenolic content, antioxidant and antimicrobial activity of *Haberlea rhodopensis* extracts obtained by pressurized liquid extraction. *Acta Alim.*, **44**: 326-332.
- Morishita T, Yamaguchi H and Degi K. 2007. The contribution of polyphenols to antioxidative activity in common buckwheat and tartary buckwheat grain. *Plant Prod Sci.*, **10**: 99–104.
- Nataraja B., Jain S., Jain N., Wadhawan N. and Khidiya M. 2018. Process development of pasta from sprouted and whole grains. *Int J Chem Stud.*, **6**: 2502-2507.
- Pasko P, Barton H, Zagrodzki P, Gorinstein S, Folta M and Zachwieja S. 2009. Anthocyanins, total polyphenols and antioxidant activity in amaranth and quinoa seeds and sprouts during their growth. *Food Chem.*, **115**: 994-998.
- Popova A and Mihaylova D. 2018. Non-traditional grains for balanced diet. *J Hyg Eng Des.*, **(23)**: 64-71.
- Re R, Pellegrini N, Proteggente A, Pannala A, Yang M and Rice-Evans C. 1999. Antioxidant activity applying an improved ABTS radical cation decolorization assay. *Free Rad Biol Med.*, **26**: 1231-1237.
- Rhodes M and Price K. 1997. Identification and analysis of plant phenolic antioxidants. *Eur J Cancer Prev.*, **6**: 518-521.
- Rubilar M, Gutiérrez C, Verdugo M, Shene C and Sineiro J. 2010. Flaxseed as a source of functional ingredients. *J Cereal Sci.*, **10**: 373-377.
- Santiago R, Reid L, Arnason J, Zhu X, Martinez N and Malvar R. 2007. Phenolics in maize genotypes differing in susceptibility to Gibberella stalk rot (*Fusarium graminearum* Schwabe). *J Agric Food Chem.*, **55**: 5186–5193.
- Scapin G, Schmidt M, Prestes R and Rosa S. 2016. Phenolics compounds, flavonoids and antioxidant activity of chia seed extracts (*Salvia hispanica*) obtained by different extraction conditions. *Int Food Res.*, **23**: 2341–2346.
- Tang Y and Tsao R. 2017. Phytochemicals in quinoa and amaranth grains and their antioxidant, anti-inflammatory and potential health beneficial effects: a review. *Mol Nutr Food Res.*, **61**: 16.
- Terzieva V, Vrancheva R and Delchev N. 2017. Antioxidant activity of different extracts of dried and frozen fruits of *Schisandra chinensis* (Turcz.) Baill. *Bul Chem Com.*, **49**: 78–82.
- Thompson L. 1994. Antioxidants and hormone-mediated health benefits of whole grains. *Crit Rev Food Sci Nutr.*, **34**: 473-497.
- Yao L, Jiang Y, Shi J, Tomas-Barberán F, Datta N and Singanusong R. 2004. Flavonoids in food and their health benefits. *Plant Foods Hum Nutr.*, **59**: 113-122.
- Zimmerman M and Snow B. 2012. **An Introduction to Nutrition (v. 1.0)**. University of Maryland publishing, USA, 813p.

Cellulose Content in Selected Plant species along the Dead Sea Coast and the Southern Desert of Jordan

Amal M. Harb* and Jamil N. Lahham

Department of Biological Sciences, Faculty of Science, Yarmouk University, Irbid-Jordan

Received August 21, 2019; Revised September 20, 2019; Accepted October 5, 2019

Abstract

Cellulose is the most abundant organic polymer in nature. It has many vital applications in the human life. The main objective of this study was to determine cellulose content in selected plant species along the Dead Sea coast and the southern desert of Jordan. To fulfill this objective, cellulose content was determined in plant samples according to Updergraff method with some modifications. The results showed significantly high cellulose content in: *Peganum harmala*, *Cleome amblyocarpa*, *Citrullus colocynthis*, *Rumex cyprius*, and *Capparis spinosa* (45.64, 36.44, 36.32, 32.64, and 32.8 % of dry weight, respectively). These values are comparable to cellulose content in biofuel crops such as wheat and barley. Moreover, these plant species are highly adaptive to harsh conditions of water deficiency and high temperature. Therefore, these plant species are promising alternatives in the field of cellulose industry.

Keywords: Cellulose; desert plants; extreme conditions; Dead Sea; Jordan

1. Introduction

There are four principal biogeographical regions in Jordan: Mediterranean, Irano-Turanian, Saharo-Arabian and Sudanian (Al-Eisawi 1996). Because of the diverse bioclimatic regions and subregions, Jordan has rich and highly diverse flora. In addition, different plant adaptations resulted in the characteristic vegetation of the different bioclimatic regions.

The Sudanian biogeographic region includes Jordan Valley to the north, the Dead Sea area, the whole area of Wadi Araba to Aqaba and the granite mountains to the south, including part of Wadi Rum. It has extremely low precipitation of 50 to 100 mm. The soil of this region is saline, sandy and granite. This region also has sand dunes. In this region, *Acacia* woodlands are characteristic of much of the Dead Sea Depression and Wadi Araba. Also, *Calotropis procera* is found in this region (Al-Eisawi 1996).

The Dead Sea is in the Jordan rift valley at the lowest point on Earth (407 m below sea level). It has extremely high salt content (8 times that in the world's oceans). Its name reflects the fact that a very few biological species can survive the extreme environment in this region. The Dead Sea area has two types of vegetations: the dry tropical and the halophytic (Taifour and El-Oqlah 2016). These vegetations types are found in the Saharo-Sindian regional zone. Examples of plant species of the dry tropical vegetation are: *Balanites aegyptiaca*, *Maerua crassifolia*, *Salvadora persica*, *Moringa peregrina*, and *Calotropis procera*. Examples of plant species of the halophytic vegetation are: *Tamarix tetragyna*, *T.*

macrocarpa, *Anabasis setifera*, *Atriplex halimus*, *A. turcomanica*, and *Suaeda fruticosa*.

Drought problems have been exacerbating in the Mediterranean region including Jordan. More than 90% of Jordan area is desert. Hence, the exploitation of natural resources in the desert and saline environments for the benefit of the human communities is of high priority. Plant biomass is made of cellulose, hemicelluloses, lignin, extractives, lipids, proteins, simple sugars, starches, water, hydrocarbon components (HC), ash, and other compounds (Balat et al. 2009). The percentage of the different components of biomass varies among plant species (Bhat et al. 2015). Cellulose is the major component of plant cell wall. It is a polysaccharide made of β -glucose monomer (Mcfarlane et al. 2014). Historically, cellulose was used by humans for clothing, shelter, in medicine and food (Harris et al. 2010). Its ease of extraction resulted in its preference as a biofuel source in the biofuel industry (Abideen et al. 2014). Indeed, 46% of the renewable energy consumption in 2005 was from biomass (Demirbas and Demirbas 2010).

Many previous studies showed the significant negative effect of water deficit and salinity stresses on cellulose synthesis and consequently plant's biomass (Wang et al. 2016; Kesten et al. 2017). Therefore, the main objective of the present study is to test the natural variation in cellulose content in selected plant species along the Dead Sea area coast, and the southern desert of Jordan. Plant species with high cellulose content could be potential target for future applications of cellulose in the different sectors of industry. Indeed, the utilization of these stress adapted plants in the cellulose industry would be an efficient and cost-effective alternative for the growth of highly demanding plant species.

* Corresponding author e-mail: aharb@yu.edu.jo

2. Materials and Methods

2.1. Field Trip and Plant Collection

A field trip to the Dead Sea region and the southern desert of Jordan was conducted between 21 and 23 March 2019. Plant samples of the selected plant species were collected and identified following the Flora Palaestina (Zohary 1966) and were kept in paper bags (Table 1).

Table. 1 Sites of collection of the selected plant species along the Dead Sea coast and the southern desert of Jordan.

Plant species	Site of collection	GPS Coordinates
<i>Prosopis farcta</i> (Banks & Sol.) J.F.Macbr.	Dead Sea	31°33'30.9"N 35°28'30.9"E
<i>Capparis spinosa</i> L.	Dead Sea	31°29'04.2"N 35°34'22.2"E
<i>Aizoon hispanicum</i> L.	Dead Sea	31°29'16.4"N 35°34'13.0"E
<i>Rumex cypricus</i> Murb.	Dead Sea	31°36'06.4"N 35°33'44.7"E
<i>Anabasis setifera</i> Moq.	Dead Sea	31°35'59.3"N 35°33'42.6"E
<i>Citrullus colocynthis</i> (L.) Schrad.	Araba Valley	29°49'21.9"N 35°06'58.4"E
<i>Zygophyllum coccineum</i> L.	Araba Valley	29°49'21.9"N 35°06'58.4"E
<i>Tetraena simplex</i> L.	Araba Valley	29°49'21.9"N 35°06'58.4"E
<i>Blepharis ciliaris</i> (L.) B.L.Burt	Araba Valley	29°49'21.9"N 35°06'58.4"E
<i>Panicum turgidum</i> Forssk.	Araba Valley	30°37'48.8"N 35°16'41.9"E
<i>Cleome amblyocarpa</i> Barratte & Murb.	Araba Valley	29°39'51.3"N 35°02'01.6"E
<i>Peganum harmala</i> L.	Wadi Rum	29°38'14.9"N 35°11'53.2"E
<i>Pulicaria undulata</i> (Forssk.) C.A.Mey.	Wadi Rum	29°34'21.23"N 35°25'7.04"E
<i>Haloxylon persicum</i> Bunge	Aqaba Customs Directorate	29°30'44.9"N 35°00'02.4"E
<i>Zilla spinosa</i> (L.) Prantl	Wadi Alyutum	29°35'46.7"N 35°09'52.8"E
<i>Erodium crassifolium</i> L'Hér. ex Aiton	Aqaba Customs Directorate	29°30'44.9"N 35°00'02.4"E
<i>Atriplex holocarpa</i> F.Muell.	Aqaba Customs Directorate	29°30'44.9"N 35°00'02.4"E

For each plant species, at least samples from three different plants were collected. The developmental stage for each plant species was recorded, and other relevant data about each plant species were retrieved from the Plant list (2013) and the Flora of Israel online by Prof. Avinoam Danin (<https://flora.org.il/en/plants/>) (Table 2).

2.2. Preparation of Plant Samples

Representative plant samples from at least 3 different plants of each plant species were wrapped in Aluminum foil and kept in the oven at 60 °C for 2 weeks for the complete dryness of the samples.

2.3. Cellulose Analysis

Cellulose content was analyzed according to Upergraff (1969) with some modifications. A dry weight of 0.05 g of each plant sample was mixed with 1 ml of acetic: nitric reagent using a vortex mixer. The mixture was then placed in a water bath at 100 °C for 3 min. After that, it was cooled and centrifuged at 10,000 rpm for 15 min. Then, the supernatant was discarded, and the residue was washed with water. Then, 1 ml of 67% H₂SO₄ was added to each sample, and samples were kept for 1 h at room temperature. One hundred (100) µl of the digested cellulose was mixed with 1 ml anthrone reagent (SC208057, Santa Cruz Biotechnology, TX, USA). The mixture was then kept in a water bath at 100 °C for 10 min. The reaction tubes were then cooled. For each reaction tube that represents one plant of each species two technical replicates of 200 µl each were transferred to an ELISA plate. Then, the absorbance was read at 630 nm using the MultiScan Go spectrophotometer (Thermo Fisher Scientific, Finland). The blank was anthrone reagent mixed with water. A standard curve was prepared using cellulose powder (α - cellulose C6429, Sigma Aldrich, USA). Cellulose content was presented in mg.g⁻¹ dry weight (DW).

2.4. Statistical analysis

Data of cellulose content were first analyzed by one-way ANOVA. Then, Tukey pairwise comparisons were used to test the differences between the means of cellulose content for each plant species at a significance level of 0.05 (Minitab 17, Minitab Ltd, UK).

Table. 2 Description of selected plant species along the Dead Sea coast and the southern desert of Jordan.

Plant Species	Developmental stage	Family	Life form	Chorotype
<i>Prosopis farcta</i> (Banks & Sol.) J.F.Macbr.	Flowering	Leguminosae	chamaephyte, hemicryptophyte, phanerophyte shrub	Irano-Turanian
<i>Capparis spinosa</i> L.	Flowering	Capparaceae	chamaephyte, hemicryptophyte	Mediterranean
<i>Aizoon hispanicum</i> L.	Fruit formation	Aizoaceae	Annual	Saharo-Arabian
<i>Rumex cyprius</i> Murb.	Fruit formation	Polygonaceae	Annual	Irano-Turanian - Saharo-Arabian
<i>Anabasis setifera</i> Moq.	Vegetative	Amaranthaceae	Chamaephyte	Saharo-Arabian
<i>Citrullus colocynthis</i> (L.) Schrad.	Fruit formation	Cucurbitaceae	Hemicryptophyte	Saharo-Arabian
<i>Zygophyllum coccineum</i> L.	Flowering	Zygophyllaceae	Chamaephyte	Saharo-Arabian
<i>Tetraena simplex</i> L.	Flowering	Zygophyllaceae	Annual	Sudanian
<i>Blepharis ciliaris</i> (L.) B.L.Burt	Vegetative	Acanthaceae	Chamaephyte	Irano-Turanian - Saharo-Arabian
<i>Panicum turgidum</i> Forssk.	Mature seeds	Poaceae	Chamaephyte, geophyte	Saharo-Arabian - Sudanian
<i>Cleome amblyocarpa</i> Barratte & Murb.	Fruit formation	Capparaceae	Annual	Saharo-Arabian - Sudanian
<i>Peganum harmala</i> L.	Vegetative	Zygophyllaceae	Hemicryptophyte	Irano-Turanian - Saharo-Arabian
<i>Pulicaria undulata</i> (L.) C.A.Mey.	Flowering	Compositae(Asteraceae)	Chamaephyte	Saharo-Arabian - Sudanian
<i>Haloxylon persicum</i> Bunge	Vegetative	Amaranthaceae	Phanerophyte shrub	Irano-Turanian
<i>Zilla spinosa</i> (L.) Prantl	Flowering	Cruciferae (Brassicaceae)	Chamaephyte	Saharo-Arabian
<i>Erodium crassifolium</i> L'Hér. ex Aiton	Mature seeds	Geraniaceae	Hemicryptophyte	Saharo-Arabian
<i>Atriplex holocarpa</i> F.Muell.	Fruit formation	Amaranthaceae	Annual	Australian

3. Results and Discussion

The analysis of variance one-way ANOVA showed a highly significant difference in the cellulose content of the different plant species analyzed in this study (P-value 0.000). A high cellulose content was found in *Peganum harmala*, *Cleome amblyocarpa*, *Citrullus colocynthis*, *Capparis spinosa*, and *Rumex cyprius* (22.82, 18.22, 18.16, 16.44 and 16.32 mg.g⁻¹ DW, respectively) (Table 3). The lowest cellulose content was found in *Zilla spinosa* (1.73 mg.g⁻¹ DW). The following plant species have a cellulose content less than 5 mg.g⁻¹ DW: *Aizoon hispanicum*, *Zygophyllum coccineum*, *Blepharis ciliaris*, *Panicum turgidum*, *Haloxylon persicum*, and *Erodium crassifolium* (Table 3). In the present study, plant species were collected from their natural habitat at different developmental stages. Four out of 17 species were in the vegetative stage, 6 were in the flowering stage, 5 were in the fruit formation stage, and 2 have mature seeds. Cellulose content was found to significantly decrease in the advanced developmental stages (Choon and Ding 2017; Best et al. 2018). However, there was no correlation between the developmental stage and the cellulose content of the plant species with high cellulose content in this study. As some of these species were in the flowering and fruit formation stage, but still have high cellulose content such as: *Cleome amblyocarpa*, *Citrullus colocynthis*, *Capparis spinosa*, and *Rumex cyprius*. Yet, some were at advanced developmental stages and showed extremely low cellulose content such as: *Zilla spinosa* (flowering stage) and *Panicum turgidum* (mature seeds). In general, because

in this study cellulose content was analyzed in different plant species, a consistent correlation between the developmental stage and the cellulose content cannot be shown. Nonetheless, the main objective of this study is to reveal plant species with high cellulose content regardless of the developmental stage.

The ploidy level of plant species was found to affect cellulose content in *Arabidopsis* (Corneille et al. 2019). In *Arabidopsis*, the increase in the ploidy level negatively affected cellulose content. Most of the plant species in this study are diploid such as: *Capparis spinosa*, *Aizoon hispanicum*, *Anabasis setifera*, and *Zygophyllum coccineum* (Al-Turki et al. 2000). Nevertheless, this factor is not significant in our study because cellulose content was analyzed in different plant species regardless of their ploidy level.

The wastes of agricultural crops were used to extract cellulose for biofuel production (Abideen et al. 2011; Sharma et al. 2017). The composition of these wastes was revealed for different crops such as: rice, wheat, and barley (Saini et al. 2015). The percentage of cellulose in the straw of rice, wheat and barley is: 28-36, 33-38, 31-45 (%wt on dry mass basis), respectively. In the present study, some plant species were shown to have high cellulose content when compared to these crops. For example, the cellulose content (%wt on dry mass basis) of *Peganum harmala*, *Cleome amblyocarpa*, *Citrullus colocynthis*, *Rumex cyprius*, and *Capparis spinosa* is 45.64, 36.44, 36.32, 32.64, and 32.88, respectively (Table 3). *Tetraena simplex*, *Prosopis farcta*, and *Pulicaria undulata* also have good cellulose content of 27.98, 27.47, and 24.08, respectively. In general, these species show

high cellulose content like that of the major biofuel crops. Moreover, these species are adapted to the extreme conditions of water deficiency and high temperature. Abiotic stresses were shown to significantly reduce cellulose content in different plant species (Wang et al.

2016; Kesten et al. 2017). Therefore, these species could be good candidates for the future applications in the biofuel industry and other cellulose based applications (Sharama et al. 2017).

Table 3. Cellulose content in selected plant species along the Dead Sea coast and the southern desert of Jordan.

Plant species	Cellulose content (mg g ⁻¹) ± SE	Cellulose content (%wt on dry matter basis)	Analyzed plant part	Number of analyzed plants
<i>Prosopis farcta</i>	13.73 ± 2.84 ^{BCD}	27.47	Leaves	3
<i>Capparis spinosa</i>	16.44 ± 1.43 ^{ABC}	32.88	Leaves	3
<i>Aizoon hispanicum</i>	3.30 ± 0.63 ^{EF}	6.60	Aerial parts*	6
<i>Rumex cyprius</i>	16.32 ± 1.49 ^{ABC}	32.64	Aerial parts	3
<i>Anabasis setifera</i>	7.26 ± 2.29 ^{DEF}	14.52	Aerial parts	3
<i>Citrullus colocynthis</i>	18.16 ± 2.94 ^{AB}	36.32	Leaves	4
<i>Zygophyllum coccineum</i>	2.09 ± 0.28 ^F	4.18	Aerial parts	5
<i>Tetraena simplex</i>	12.04 ± 0.71 ^{BCD}	24.08	Aerial parts	5
<i>Blepharis ciliaris</i>	2.36 ± 0.33 ^{EF}	4.72	Leaves	4
<i>Panicum turgidum</i>	2.04 ± 0.17 ^{EF}	4.08	Leaves	4
<i>Cleome amblyocarpa</i>	18.22 ± 0.46 ^{AB}	36.44	Aerial parts	3
<i>Peganum harmala</i>	22.82 ± 3.06 ^A	45.64	Aerial parts	3
<i>Pulicaria undulata</i>	13.99 ± 1.70 ^{BCD}	27.98	Aerial parts	3
<i>Haloxylon persicum</i>	4.16 ± 0.90 ^{EF}	8.32	Aerial parts	3
<i>Zilla spinosa</i>	1.73 ± 0.21 ^F	3.46	Aerial parts	5
<i>Erodium crassifolium</i>	4.08 ± 0.92 ^{EF}	8.16	Aerial parts	4
<i>Atriplex holocarpa</i>	9.29 ± 0.79 ^{CDE}	18.58	Aerial parts	3

Means of cellulose content that do not share a letter are significantly different.

*Aerial parts are leaves and soft stems

One important factor to be considered for the best utilization of plant species in the different applications of human life is the abundance of these species. According to the Jordan's Plant Red List, *Peganum harmala*, *Citrullus colocynthis*, and *Tetraena simplex* that showed significantly high cellulose content are abundant in Jordan (Taifor and El-Oqlah 2014). *Rumex cyprius* is moderately abundant, while *Cleome amblyocarpa*, *Capparis spinosa*, *Prosopis farcta*, and *Pulicaria undulata* are abundant (Taifor and El-Oqlah 2016). In general, these promising plant species are abundant in nature. Nonetheless, plant tissue culture technique could be used for the homogenous *in vitro* propagation of these promising plant species. In conclusion, the present study revealed new and promising sources of cellulose from the desert plant species of Jordan.

Acknowledgements

This work was supported by the Deanship of Graduate Studies and Scientific Research at Yarmouk University, project number 44-2018.

References

Abideen Z, Ansari R, Khan A. 2011. Halophytes: Potential source of ligno-cellulosic biomass for ethanol production. *Biomass and Bioenerg*, **35**: 1818-1822.

Abideen Z, Hameed A, Koyro HW, Gul B, Ansari R and Khan A. 2014. Sustainable biofuel production from non-food sources – An overview. *Emir J Food Agric*, **26**: 1057-1066.

Al-Eisawi D. 1996. **Vegetation of Jordan**. UNESCO, Cairo Office, Regional Office for Science and Technology for the Arab States.

Al-Turki T, Filfilan S and Mehmood S. 2000. Cytological study of flowering plants from Saudi Arabia. *Willdenowia*, **30**: 339-358.

Balat M, Balat M, Kırtay E and Balat H. 2009. Energy conversion and management main routes for the thermo-conversion of biomass into fuels and chemicals. *Energy Convers Manag*, **50**: 3147–3157.

Best M, Schueller MJ and Ferrieri RA. 2018. Plant cell wall dynamics are regulated by intercellular sugar trafficking. *Int J Plant Stu*, **1**: 1-12.

Bhat AH, Dasan YK and Khan I. 2015. Extraction of lignin from biomass for biodiesel production. In: Hakeem K et al. (Eds.), **Agricultural biomass based potential materials**. Springer International Publishing, Switzerland, pp155- 179.

Corneillie S, De Storme N, Van Acker R and et al. 2019. Polyploidy affects plant growth and alters cell wall composition. *Plant Physiol*, **179**: 74 – 87.

Choon S and Ding P. 2017. Developmental changes in cellular structure and cell wall metabolism of torch ginger (*Etilingera elatior* (Jack) R.M. Smith) inflorescence. *Curr Plant Biol*, **9–10**: 3-10.

Danin A. <https://flora.org.il/en/plants/>

Demirbas T and Demirbas A. 2010. Bioenergy, green energy, biomass and biofuels. *Energy Sources, Part A: Recovery, Utilization, and Environmental Effects*, **32**: 1067 – 1075.

Harris D, Bulone V, Ding SY and DeBolt S. 2010. Tools for Cellulose Analysis in Plant Cell Walls. *Plant Physiol*, **153**: 420–426.

Kesten C, Menna A and Sanchez-Rodriguez C. 2017. Regulation of cellulose synthesis in response to stress. *Curr Opin Plant Biol*, **40**: 106 -113.

McFarlane H, Döring A and Persson S. 2014. The cell biology of cellulose synthesis. *Ann Rev Plant Biol*, **65**: 69 – 94.

Saini J, Saini R and Tewari L. 2015. Lignocellulosic agriculture wastes as biomass feedstocks for second-generation bioethanol production: concepts and recent developments. *3 Biotech*, **5**: 337 – 353.

Sharama V, Joshi A, Ramawat KG and Arora J. 2017. Bioethanol production from halophytes of that desert: A “Green Gold”. In: Basu S, Zandi P and Chalaras S (Eds.), **Environment at crossroads: challenges, dynamics and solutions**. Haghshenas Publishing, Iran, pp 219-235.

Taifor H and El-Oqlah A. 2014. **Jordan plant red list**. Royal botanical gardens, Jordan.

Taifour H and El-Oqlah A. 2016. **The plants of Jordan, an annotated checklist**. Kew Publishing Royal Botanic Gardens, Kew, UK.

The Plant List. 2013. Version 1.1. Published on the Internet; <http://www.theplantlist.org/> (accessed 1st January).

Updegraff D. 1969. Semimicro determination of cellulose in biological materials. *Anal Biochem*, **3**: 420 -424.

Wang T, McFarlane H and Persson S. 2016. The impact of abiotic factors on cellulose synthesis. *J Exp Bot*, **67**: 543 -552.

Zohary M. 1966. **Flora Palaestina**. Israel Academy of Sciences and Humanities, Israel.

Inhibitory Effect of Clay/Chitosan Nanocomposite against *Penicillium digitatum* on Citrus and Its Possible Mode of Action

Khamis Youssef^{1,*} and Ayat F. Hashim²

¹Agricultural Research Center, Plant Pathology Research Institute, 9 Gamaa St., 12619 Giza ; ²Food Industry and Nutrition Division, National Research Centre, 33 El Buhouth 12622 Giza, Egypt

Received August 22, 2019; Revised September 28, 2019; Accepted October 5, 2019

Abstract

Citrus postharvest diseases are commonly controlled by applying synthetic fungicides in packinghouses. Several limitations to pesticides have resulted in a considerable interest in developing alternative non-polluting control means. Clay/chitosan nanocomposite (CCNC) was prepared by an anion exchange reaction between chitosan and clay. The structure and morphology of CCNC was characterized by Fourier-transform infrared spectroscopy (FT-IR), X-ray diffraction (XRD), Transmission electron microscopy (TEM), Scanning electron microscopy (SEM) and energy-dispersive X-ray (EDX). FTIR data and XRD patterns indicate that chitosan was intercalated into the clay layers. TEM result also showed that the dark sheets of clay were dispersion in chitosan matrix. The surface morphology of CCNC in SEM micrograph showed a massive layered structure with some large flakes and some inter layer spaces. The EDX spectra of the prepared nanocomposite show key elements like C, O, Mg, Al and Si. The fungicidal activity of CCNC was tested against *Penicillium digitatum* *in vitro* and *in vivo*. A complete inhibition of *P. digitatum* was achieved at 20 µg mL⁻¹ for clay/chitosan (1:0.5), clay/chitosan (1:1) and clay/chitosan (1:2). CCNC was tested *in vivo* for a direct and indirect action (induction of resistance) against green mold of oranges cv. Valencia late. The results showed that considering CCNC direct action a complete inhibition of green mold was observed, whereas a high reduction (70%) of rot was reported for clay/chitosan (1:2) used as a resistance inducer. The mode of action of CCNC on the pathogens was also demonstrated via the genotoxicity (degradation of *P. digitatum*-DNA) and SEM (severe collapse, malformation and irregular branching of hyphae). CCNC is economically interesting because it is easy to prepare and involves inexpensive alternative control means against green mold of citrus fruit.

Keywords: nanocomposite; *Penicillium digitatum*; chitosan; citrus; clay

1. Introduction

Citrus is a widely spread fruit crop in Egypt, and it is considered to be the most important fruit crop. During 2017, the total Egyptian production was 3013758 tonnes, and 166775 tonnes of Egyptian citrus have been exported (Faostat, 2017). In Egypt, climate is suitable to the production of citrus fruit especially oranges, which accounts for over half of the total fruit production; exported amount of the fresh and dried citrus fruit, especially oranges, reached 2.2% of the total worldwide exported amount. The economic losses due to fungal infection in fruits and vegetables during the postharvest chain are variable and not well documented. They usually reach anywhere from 30 to 50% and, on some occasions, decays can lead to total loss of the produce (Bautista-Baños, 2014).

Penicillium digitatum (Pers.:Fr.) Sacc. is the most severe postharvest fungal pathogen of citrus fruit agent of green mold, which may cause 60–80% of decay under ambient conditions (MoscosoRamírez *et al.*, 2013; Youssef *et al.*, 2014). Citrus postharvest diseases are frequently controlled globally by applying synthetic fungicides in packinghouses before fruit storage. However, the use of chemical fungicides is facing many constraints, including the development of pathogen resistance and

the public concern related to health and environmental hazards. Those problems resulted in a significant interest in developing alternative safer control means (Fallanaj *et al.*, 2015; Youssef *et al.*, 2017).

Chitosan, β-(1,4)-2-amino-2-deoxy-D-glucose, is a natural versatile biopolymer derived by partially deacetylation of chitin, mainly as the structural component of the exoskeletons of crustaceans and insects, as well as in some fungal cell walls (Sanford, 2003). This polymer is among those naturally-occurring compounds that have potential in agriculture, especially for controlling plant diseases. Chitosan has been shown to be fungicidal against several fungal plant pathogens (Liu *et al.*, 2001; Rabea and Steurbaut, 2010). One of the most important attributes of chitosan is its fungistatic/fungicidal activity toward postharvest fungi at various concentrations (*Alternaria alternata*, *Colletotrichum gloeosporioides*, *Fusarium oxysporum*, *Rhizopus stolonifer*, *Penicillium spp.*, *Botrytis cinerea*, *Neurospora crassa*) (Bautista-Banos *et al.*, 2006; Reglinski *et al.*, 2010).

Montmorillonite clay belongs to the smectite group, a diverse group of clay minerals with a 2:1-layer silicate structure that can expand and contract upon wetting and drying, composed of layers of two silica tetrahedral sheets surrounding a central alumina octahedral sheet (Abdeen and Salahuddin, 2013). In addition, the substantial harmlessness of montmorillonite make it a promising

* Corresponding author e-mail: youssefeladawy@yahoo.com.

nanofiller to be broadly utilized in food industry (Xu *et al.*, 2018). Polymer-clay nanocomposites are a class of hybrid materials composed of organic polymer matrices and nanoscale organophilic clay fillers. When nanoclay is mixed with a polymer, three types of composites (tactoids, intercalation, and exfoliation) can be obtained (Xu *et al.*, 2006). For the most part, polymer/clay nanocomposites contain a natural organic/inorganic hybrid polymer network comprising platelet-shaped clay particles that have sizes in the order of a few nm thick and several hundred nm length. Due to clay particles high phase ratio and surface area, if suitably dispersed in the polymer matrix at a loading of 1–5 weight percent, instruct sole combinations of physical and chemical properties to make them attractive for films and coatings in a broad collection of industries (Han *et al.*, 2010).

The purpose of the present research was (i) to prepare and characterize clay/chitosan nanocomposite (CCNC), (ii) to evaluate the efficacy of CCNC *in vitro* against *P. digitatum*, (iii) to assess the efficiency of CCNC against green mold under artificial infection on citrus fruit, and (iv) to evaluate their possible toxicity by using scanning electron microscopy (SEM) and DNA-binding assays.

2. Material and methods

Chitosan was purchased from Acros (Morris Plains, NJ, USA) with a degree of deacetylation and average MW of 85% and 100,000 Da, respectively. Natural montmorillonite (Cloisite®Na⁺) was received from Southern Clay Products Inc (TX; USA). Acetic acid 99–100% was provided from Honeywell (Muskegon, MI, USA).

2.1. Preparation of CCNC

CCNC was prepared following the protocol of Han *et al.* (2010). In particular, aqueous solution of chitosan was prepared by dissolving desired weight ratio of chitosan powder in 100 ml of acetic acid solution (1%, v/v) and stirring for about 2 h. A 1 wt% clay suspension was also prepared by dispersing clay powder in distilled water and stirring for 12 h prior to use. The chitosan solution was then slowly added to the clay suspension at 60°C. During the mixing process, the weight ratio of clay to chitosan was (1:0.5, 1:1 and 1:2) in order to control the chitosan loading level in the clay layers. The reaction mixture was stirred for 2 h, separated by centrifugation and washed three times with distilled water. Then the nanocomposites were dried at 100°C for 12 h and well ground to power.

2.2. Characterization of CCNC

2.2.1. Fourier-transform infrared spectroscopy (FT-IR)

CCNC was analyzed by FT-IR spectroscopy as described by Youssef *et al.* (2017) with minor optimization. The CCNC solution was centrifuged at 25,000 ×g for 25 min and washed twice in deionized water to remove the unbound components. The purified samples and potassium bromide (KBr) were grounded to reduce the diameter size of particle to less than 5 mm. A small amount of sample mixed with the KBr powder then ground the mixture for 3–5 minutes. The powder was added to collar and put it together with the die into press to form pellet and subsequently analysed on a Jasco FT-IR 5300 spectrophotometer. The samples were directly placed in the zinc selenide crystal, and the spectrum was recorded in the transmittance mode.

2.2.2. X-ray diffraction (XRD)

Crystalline materials produce distinct x-ray diffraction (XRD) patterns that can be used for the identification of the phases present in a material. Current approaches use the entire background subtracted spectrum. XRD patterns of CCNC have been recorded using Panalytical Empyrean (PANalytical, Netherlands), using CuK α radiation α 1.5406 Å, and scanning rate 0.1° in the 2 θ range from 20° to 70° and step time 1 s (Hashim *et al.*, 2019).

2.2.3. Transmission electron microscopy (TEM)

TEM imaging was performed as described by Youssef *et al.* (2017). In particular, 20 μ l of diluted CCNC were placed on a film coated 200-mesh copper specimen grid for 10 min. The grid was stained with one drop of phosphotungstic acid (3%) and left to dry for 3 min. The coated grid was dried and examined under the TEM microscope (Philips, CM12), and CCNC was observed by operating at 120 kV.

2.2.4. Scanning Electron Microscopy (SEM)

The surface morphology and shape of the optimized CCNC was studied by SEM (quanta FEG 250, Czech Republic). Samples were coated with gold to avoid charging of the surface. Then, the samples were examined under SEM at HV 25.0 kV, equipped with an energy-dispersive X-ray spectrometer (EDX).

2.3. Antifungal Activity of CCNC against *P. digitatum* *in vitro*

Agar plugs (5 mm Θ) from the growing edge of one-week-old cultures of *P. digitatum* were placed in the center of potato dextrose agar (PDA) Petri dishes amended with 250 mg L⁻¹ of ampicillin and 250 mg L⁻¹ of streptomycin to avoid contamination. For each PDA plate, three holes (5 mm Θ) at the corner of each plate were inoculated with 20 μ l of CCNC. Five concentrations (5, 10, 20, 40 and 60 μ g mL⁻¹) were used. PDA plates with sterilized distilled water were included as control. Five Petri dishes were utilized as replicates for each treatment, and the entire experiment was repeated twice. Colony diameter (mm) was measured after four days of incubation at 24 \pm 1 °C. The percentage of reduction in colony diameter (CD) was calculated according to Salem *et al.* (2016) as follows:

$$CD (\text{reduction, \%}) = (dc - dt) / dc \times 100$$

Where: dc = average colony diameter in control plates

dt = average colony diameter of linear growth in treatment plates

2.4. Antifungal activity of CCNC against green mold *in vivo*

2.4.1. Fruit samples and Conidial Suspension:

Mature *Citrus sinensis* (L. Obseck) fruit cv. Valencia late were harvested from a private orchard in Cairo-Alexandria (desert road), selected for uniformity of size and absence of symptoms of any disorders. Fruits were surface sterilized with a 2% sodium hypochlorite for two min, washed with tap water and air-dried at room temperature. The fruits were divided randomly into two lots to perform the two sets of experiments (direct and indirect activity of CCNC against green mold). *P. digitatum* isolate code MF568039 (Hussien *et al.*, 2018) was grown on PDA plates at 24 \pm 1°C in the dark to produce fungal inoculum. The conidial suspension was

prepared according to the standard protocol to obtain a final concentration of 10^4 conidia ml^{-1} (Youssef *et al.*, 2010).

2.4.2. Direct Antifungal Activity of CCNC

Oranges were wounded (5 mm depth \times 3 mm wide) with a sterile nail-head at two equidistant points in the equatorial zone. A 20 μl aliquot of CCNC solution (20 μg ml^{-1}) was applied into each wound. After 2 h, 10 μl of 10^4 conidia ml^{-1} *P. digitatum* suspension was inoculated into the same wound site. Oranges treated with distilled sterile water and inoculated with the same concentration of the pathogen were included as control. Each treatment was replicated three times, and each replicate consisted of four oranges with two wounds each. Treated fruits were placed in plastic boxes covered with bags to maintain high humidity (90-95%) and incubated at 24 ± 1 °C for one week. The incidence of decay (infected wounds, %) and disease severity (lesion diameter, mm) were recorded. The whole experiment was performed twice.

2.4.3. Indirect Antifungal Activity of CCNC

Oranges were wounded once with a sterile nail-head along the equatorial axis. For each treatment, a 20 μl aliquot of a CCNC solution (20 μg ml^{-1}) was applied into each wound. After 24 h of incubation at 24 ± 1 °C under high relative humidity (90-95%), another wound was made approximately 5 mm apart from the previous one. This wound was inoculated with 10 μl of 10^4 conidia ml^{-1} suspension of *P. digitatum* (Fallanaj *et al.*, 2016). Oranges, treated in the first wound with sterile distilled water and then inoculated with the pathogen conidial suspension in the other one, were included as control. Treatments and replicates were the same as described above. Fruit were incubated and the decay incidence and severity were recorded as described for direct antifungal activity. The entire experiment was performed twice.

For both *in vitro* and *in vivo* experiments, individual chitosan, clay, acetic acid and tecto 50% SC at 9 ml/L (Thiabendazole 50%, Syngenta Agro Egypt) were used for comparison.

2.5. The mode of action of CCNC

2.5.1. Scanning electron microscopy (SEM)

Plugs of *P. digitatum* (6 mm Θ) were cut from cultures grown for four days on PDA amended or not with CCNC at 20 μg ml^{-1} and placed in vials containing 3% glutaraldehyde and 2% paraformaldehyde in 0.1 M sodium cacodylate buffer (pH 7.2) at 4 °C. Samples were kept in this solution overnight for fixation and then washed three times with 0.1 M sodium cacodylate buffer (pH 7.2) for 10 min. Then, the samples were washed three times, for duration of ten minutes each, using different ethanol series (30, 50, 70, 90 and 100%). Samples were critical point dried with CO_2 treated with gold and observed in Quanta FEG 250, Czech Republic (Simionato *et al.*, 2017).

2.5.2. Fungal Genomic DNA Binding/Degradation Assay

Total genomic DNA from *P. digitatum* was extracted following the methods of Moslem *et al.* (2010). After extraction, 10 μl of DNA was treated with CCNC (5 and 20 μg ml^{-1}) for a period of 2 h at 37 °C. The products resulting from interactions of the nanocomposite with DNA were separated by 1.5% (w/v) agarose gel containing

0.05 μg ml^{-1} ethidium bromide, to check the quality of the DNA. A charge-coupled device camera imaging system and UVI soft analysis (Gel Documentation and Analysis Systems, Uvitec, Cambridge, UK) were used to capture the image (Abd-El salam *et al.*, 2018).

2.6. Statistical Analysis

Percentage data were arcsine transformed before analyses to normalize variance. Data were processed statistically using Statistica 6.0 software (Stat Soft Inc., Tulsa, Oklahoma, USA). Mean values of treatments were compared using Duncan's multiple range test (DMRT) and judged at $P \leq 0.05$ level.

3. Results and Discussion

3.1. Preparation of CCNC

CCNC was prepared by an ion exchange process between oligomeric chitosan and Na^+ montmorillonite. The nanocomposites were rapidly prepared within 2 h, due to the high affinity between the chitosan and the clay host. Previous studies have confirmed a great diffusion of montmorillonite in chitosan polymer through the intercalation of cationic chains into montmorillonite interlayers, which grants the resulting nanocomposites with improved mechanical and barrier properties (Darder *et al.*, 2003; Xu *et al.*, 2018). The composites were ordinarily joined through adsorption, gelation, or intercalation due to of the electrostatic cooperation among chitosan and clay (Kumar *et al.*, 2019).

3.2. FT-IR measurements

FT-IR proved to be an appropriate technique to study polymer-clay interaction (Fig. 1). Clay spectrum showed the characteristic absorption bands at 3365 cm^{-1} due to $-\text{OH}$ stretching band for absorbed water. The band at 3626 cm^{-1} was due to AOH band stretch for Al-OH. The overlaid absorption peak at 1624 cm^{-1} might be attributed to OH bending mode of absorbed water. The characteristic peaks at 1120 and 983 cm^{-1} were due to SiAO stretching (out of plane) and Si-O stretching (in-plane) vibration for layered silicate, respectively. Peaks at 903 , 791 , and 679 cm^{-1} might be attributed to AlAlOH, AlFeOH, and AlMgOH bending vibrations, respectively. FT-IR spectrum of chitosan showed peaks at 3346 , 2867 , 1661 , 1587 , 1418 , 1132 and 1077 cm^{-1} , which were due to the asymmetric and symmetric stretching of methylene ($-\text{CH}_2$) groups, amide I, amide II, amide III, C-O-C stretching vibration and C-O stretching vibration respectively.

In the formed chitosan clay nanocomposite in 2:1 ratio, NH_3^+ groups of chitosan interacted electrostatically with the negatively charged sites of the clay; as such, the frequency of vibrational bands at 1587 cm^{-1} in the pure chitosan was shifted toward a lower value (1561 cm^{-1}). In the same context, Han *et al.* (2010) showed a shift in frequency of vibrational bands at 1554 cm^{-1} in the starting chitosan toward lower frequency values depending on the chitosan loading level. The intensity of this absorption was highly decreased due to the electrostatic interaction between cationic chitosan and anionic clay (Abd El-Kader *et al.*, 2015). The amide I band at 1661 cm^{-1} of chitosan may overlap with δHOH bending vibration band at 1624 cm^{-1} of the water molecule associated to the starting clay

as expected for the biopolymers with high water retention capability (Abd El-Kader *et al.*, 2015).

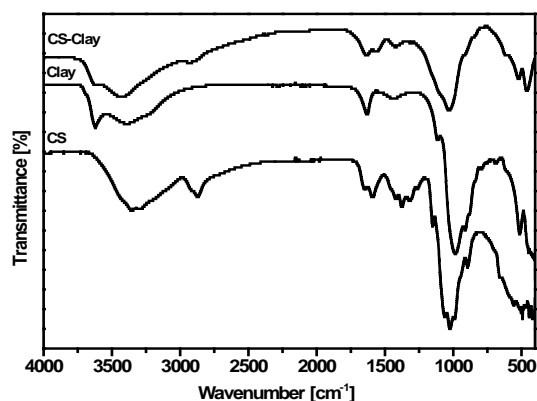


Figure 1. FT-IR spectra of synthesized clay/chitosan nanocomposite.

3.3. XRD analysis

The XRD analysis was used to study the crystallinity and the structural changes of the nanocomposite in the range of $2\text{--}70^\circ$ as shown in (Fig. 2). The XRD pattern of clay presented a distinctive diffraction peak around 7° that corresponds to a d001 spacing (Giannakas *et al.*, 2014). Characteristic peaks of chitosan at around $2\theta = 10^\circ$, 20° and 23° were revealed in harmony with previous publications (Lavorgna *et al.*, 2010; Taghinezhad and Ebadollahi 2017). The peak at 10° shows a hydrated crystallite structure due to the water molecules integration in the crystal lattice. The peak at 18° is recognized to the regular crystal lattice of chitosan (Kittur *et al.*, 2003), whereas the broaden peak around 23° indicates an amorphous structure of chitosan (Rhim *et al.*, 2006; Lavorgna *et al.*, 2010). The XRD ranging up to $2\theta \approx 10$ to 25° shared by both chitosan and clay was quite different than that observed for XRD of both of the two starting materials, indicating the occurred complexation between chitosan and the clay. It is obvious that addition of clay causes a decrease in the crystallinity of chitosan (Giannakas *et al.*, 2014). Both results of XRD and FT-IR supported each other indicating chitosan complexation with clay.

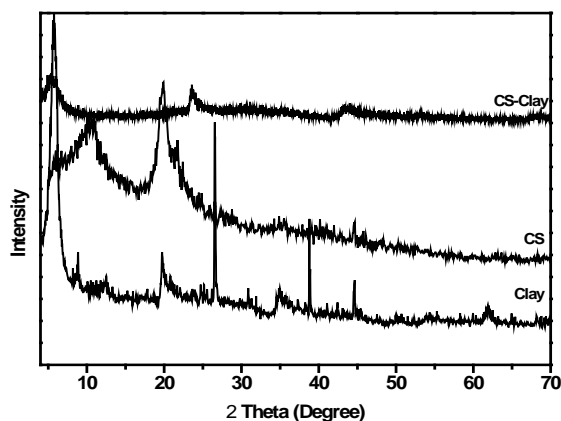


Figure 2. X-ray diffraction pattern of synthesized clay/chitosan nanocomposite.

3.4. Morphological observation by TEM and SEM

The morphology of the prepared CCNC was investigated by TEM and SEM (Fig. 3). There were several single silicate layers, as well as aggregates of silicate layers, dispersed in the polymer matrix. SEM micrograph displayed good and random dispersion of clay within chitosan matrix. From visual analysis of SEM images, a uniform appearance with small irregularities and bumps was noticed. It was also clear that the surface of MMT had an aggregated and foliated appearance due to the presence of the layered structure. The EDX spectra of the prepared CCNC showed key elements like C, O, Mg, Al and Si (Fig. 4). It was observed intercalated, stacked, and partially exfoliated structures of Chitosan/Montmorillonite-K10 nanocomposites Films according to XRD diffraction patterns and TEM observations. Moreover, an interaction between polymer matrix and MMMTK10 was observed from SEM images (Kasirga *et al.*, 2012).

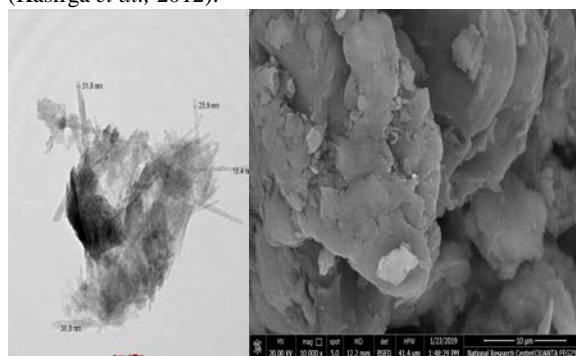


Figure 3. TEM and SEM micrograph of synthesized clay/chitosan nanocomposite.

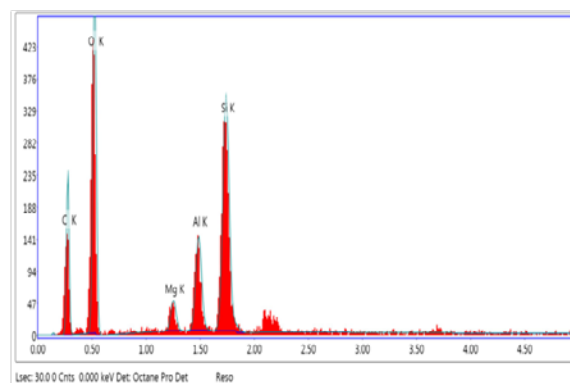


Figure 4. EDX micrograph of synthesized clay/chitosan nanocomposite.

3.5. Antifungal Activity Of CCNC Against *P. digitatum* in Vitro

After 7 days of incubation, a complete inhibition of *P. digitatum* was achieved at $20 \mu\text{g ml}^{-1}$ for clay/chitosan (1:0.5), clay/chitosan (1:1) and clay/chitosan (1:2). At $10 \mu\text{g ml}^{-1}$, the percentage of reduction of colony diameter was 73, 75 and 90% for clay/chitosan (1:0.5), clay/chitosan (1:1) and clay/chitosan (1:2), respectively, whereas a complete inhibition was observed at $60 \mu\text{g ml}^{-1}$ for chitosan and clay as standalone treatments. *P. digitatum* growth was completely inhibited by thiabendazole fungicide at all concentrations used, while acetic acid inhibited the pathogen growth at $20 \mu\text{g ml}^{-1}$ (Fig. 5 and 6). Similarly, chitosan NPs showed the

maximum growth inhibitory effects on *in vitro* mycelial growth of *Trametes versicolor* and *Tyromyces palustris* at 0.1% concentration (Suhartono, 2015). The mode of action by which chitosan affects the growth of fungi may be due to its ability to interfere with the negatively charged residues of macro-molecules exposed on fungal surfaces forming polyelectrolytic complexes, and affecting membrane permeability as well as causing leakage of intracellular electrolytes and proteinaceous constituents (Suhartono, 2015). Chitosan possesses a natural antifungal role by which it increases the permeability of the outer and inner membranes, thus disrupting bacterial cell integrity with the release of cellular metabolites, and finally chelation of trace metals inhibiting enzyme activities (Liu *et al.*, 2004). Chitosan/clay nanocomposites showed also a synergistic effect against *Escherichia coli* and *Staphylococcus aureus* (Han *et al.*, 2010).

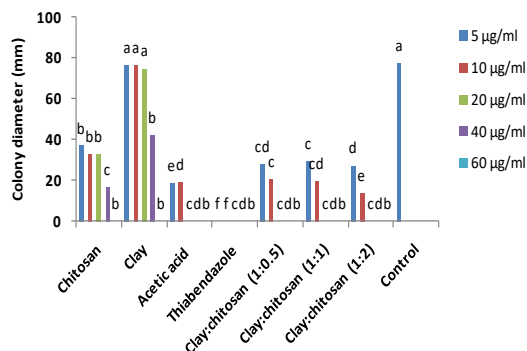


Figure 5. Effect of different concentrations of clay/chitosan nanocomposite on colony diameter (mm) of *P. digitatum* after four days incubation at $24\pm 1^\circ\text{C}$ on PDA. PDA amended with water was utilized as control. Chitosan, clay, acetic acid and thiabendazole were included for comparison. Statistical analysis was performed within each column. Values marked with the same letters are not statistically different according to posthoc test DMRT at $p \leq 0.05$.

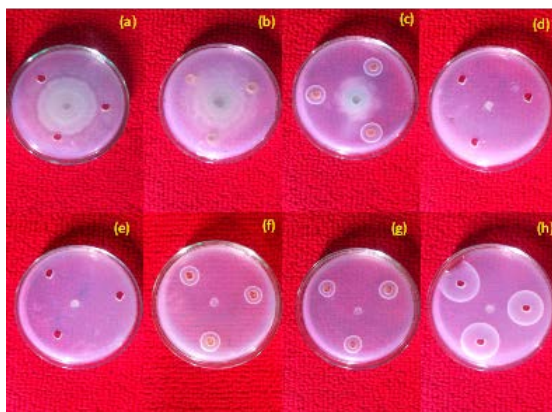


Figure 6. Effect of different concentrations of CCNC on colony diameter of *P. digitatum* after four days incubation at $24\pm 1^\circ\text{C}$ on PDA. A. control; B. clay; C. chitosan; D. acetic acid; E. thiabendazole; F. CCNC 1:0.5; G. CCNC 1:1; H. CCNC 1:2.

3.6. Antifungal Activity Of CCNC Against Green Mold *In Vivo*

In assays evaluating the direct action, decay incidence was 100, 83.3 and 50% for water control, clay and acetic acid, respectively (Fig. 7), while no decay incidence was observed for the remaining treatments. In the case of indirect action (in which compound and pathogen were

added into separate wounds), decay incidence was 100, 66.6, 100, 41.6, 25, 41.6, 33.3 and 33.3 for control, chitosan, clay, acetic acid, thiabendazole, clay:cs,(1:0.5), clay:cs(1:1) and clay:cs (1:2), respectively (Fig. 7). Our results were in agreement with Xu *et al.* (2018) who concluded that chitosan/montmorillonite demonstrated the most significant and extended impact as antifungal agent to decrease the tangerine decay percentage during storage.

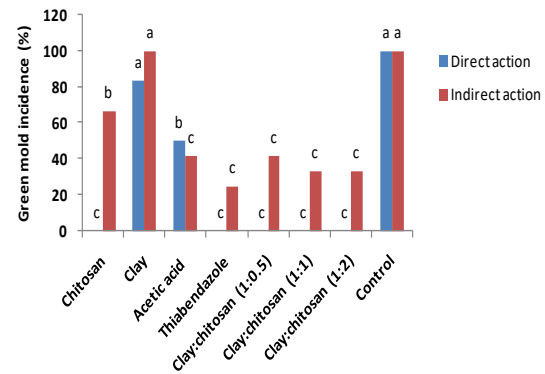


Figure 7. Decay incidence (%) of green mold after seven days of shelf-life at $24\pm 1^\circ\text{C}$ and high RH on "Valencia late" oranges treated with $20\ \mu\text{g/ml}$ of clay/chitosan nanocomposite. Statistical analysis was performed within each column. Values marked with the same letters are not statistically different according to posthoc test DMRT at $p \leq 0.05$. Direct action: the pathogen and clay/chitosan nanocomposite were applied into the same wound; indirect action: the pathogen and clay/chitosan nanocomposite were applied into separated wounds.

In assays evaluating the direct action, lesion diameter was completely inhibited by chitosan, thiabendazole, clay/chitosan (1:0.5), clay/chitosan (1:1) and clay/chitosan (1:2), whereas no complete inhibition of green mold was observed for clay or acetic acid. In case of indirect action, the reduction was 47, 50, 51 and 70% for chitosan, clay/chitosan (1:0.5), clay/chitosan (1:1) and clay/chitosan (1:2), respectively (Fig. 8).

Chitosan NPs were effective elicitors of host resistance to many plant pathogens infections (Pichyangkura and Chatchawan, 2015). Other GRAS compounds such as salts were used on citrus to control postharvest diseases such as sodium carbonate and bicarbonate. The ability to such salts was comprehensively investigated to induce natural resistance in oranges fruit including enzyme activity, gene expression levels, phytoalexin and sugar contents (Youssef *et al.*, 2014; Youssef *et al.*, 2015).

Novel chitosan/Ag/ZnO (CTS/Ag/ZnO) blend films were prepared and evaluated as antimicrobial agent (Li *et al.*, 2010). Their results revealed that ZnO and Ag nanoparticles had a uniform distribution within chitosan polymer; the produced blend had excellent antimicrobial activities against many bacterial, fungal, and yeast strains with higher antimicrobial activities than chitosan alone. In particular, Ag-chitosan nanocomposites might be proposed as efficient fungicidal agents for entire inhibition of *B. cinerea*, and grey mold prevention on strawberries.

Developing chitosan-layered silicate nanocomposites by inserting chitosan chains into interlayers of silicate can improve its mechanical properties. In recent years, polymer nanocomposites have received considerable interest because of their superior thermal and mechanical properties, as compared with the polymer itself (Kumar *et*

al., 2003). The obtained results herein suggest that clay would improve the protection function of chitosan polymer.

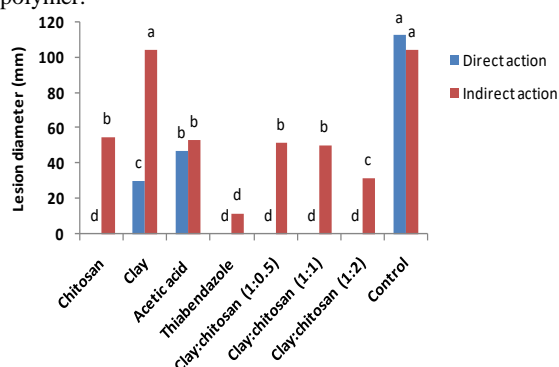


Figure 8. Lesion diameter (mm) of *P. digitatum* after seven days of shelf-life at $24\pm 1^\circ\text{C}$ and high RH on "Valencia late" oranges treated with $20\ \mu\text{g/ml}$ of clay/chitosan nanocomposite. Statistical analysis was performed within each column. Values marked with the same letters are not statistically different according to posthoc test DMRT at $p \leq 0.05$. Direct action: the pathogen and clay/chitosan nanocomposite were applied into the same wound; indirect action: the pathogen and clay/chitosan nanocomposite were applied into separated wounds.

3.7. Scanning Electron Microscopy

On the control samples SEM demonstrated a normal morphology, and linearly shaped and the apical hyphae were tapered with a smooth surface (Fig. 9A). Treatment by CCNC at $20\ \mu\text{g ml}^{-1}$ caused severe collapse, malformation and irregular branching of hyphae in the apical part (Fig. 9B). The microscopic observation of *Rhizoctonia solani* hyphae exposed to chitosan nanocomposite showed severe damage resulting in the separation of layers of hyphal wall and collapse of fungal hyphae (Abd-Elsalam *et al.*, 2018). Nevertheless, much work has to be done regarding the mode of action of chitosan-based nanomaterials against plant pathogens (El Hadrami *et al.*, 2010).

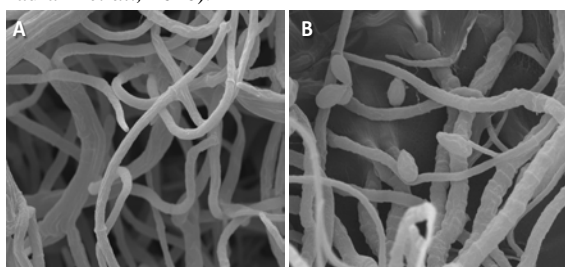


Figure 9. SEM of *P. digitatum* mycelia after 6 days of incubation at $24\pm 1^\circ\text{C}$. A. Normal mycelium and free and linearly shaped hyphae (control); B. severely collapsed mycelium (treated with CCNC1:2). In the magnitude of $3000\times$ (bar $20\ \mu\text{m}$).

3.8. Fungal genomic DNA binding/degradation assay

CCNC was incubated with *P. digitatum* DNA to evaluate DNA binding as a possible molecular basis for their antifungal activities. The genotoxicity exhibited by CCNC was demonstrated by degradation of *P. digitatum* DNA at concentration $20\ \mu\text{g ml}^{-1}$. Control DNA exhibited one major characteristic band of unaffected/intact genomic DNA (Fig. 10). Chitosan-based nanocomposite treatment was effective to prevent amplification of PCR products. Oxidative damage can cause chemical degradation of DNA, which leads to PCR amplification failure when

insufficient copies of DNA are present in the reaction (Abd-Elsalam *et al.*, 2018). Another important mechanism involves penetration of the chitosan oligomer into the cells of microorganisms, which inhibits the growth of cells by preventing the transcription of DNA into mRNA (Hernández-Lauzardo *et al.*, 2011).

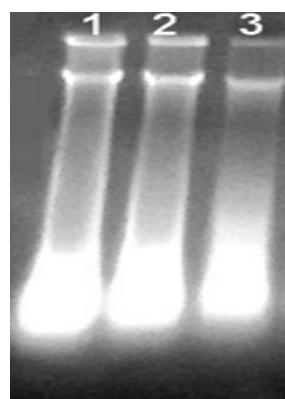


Figure 10. Agarose gel electrophoresis pattern of the fungal genomic DNA treated and untreated with CCNC1:2. Lane 1: DNA for untreated *P. digitatum*, Lane 2: *P. digitatum* treated with $5\ \mu\text{g}$ CCNC, Lane 3: *P. digitatum* treated with $20\ \mu\text{g}$ CCNC.

4. Conclusion

New strategies are needed with the serious goal of controlling green mold of citrus caused by *P. digitatum* with no fungicide residues. Clay/chitosan nanocomposite (CCNC) is economically interesting since it is easy to synthesize and low-cost chemical materials are needed. The chance to integrate at nanometric level clays and chitosan appears as an attractive method to change a portion of the properties of this polysaccharide including its mechanical and thermal behaviour, solubility and antifungal activity. CCNC seems to be an excellent alternative control means against green mold of citrus fruit.

Acknowledgement

We thank Prof. Kamel Ahmed Abd-Elsalam for his scientific advice and helping us to carry out the molecular studies.

References

- Abd El-Kader FH, Shehap AM, Bakr AA and Hussein OT. 2015. Characterization of clay/chitosan nanocomposites and their use for adsorption on Mn(II) from aqueous solution. *Int J Sci Engin Appl*, **4**:174-185
- Abdeen R and Salahuddin N. 2013. Modified chitosan-clay nanocomposite as a drug delivery system intercalation and *in vitro* release of ibuprofen. *J Chem*, **2013**: 1-9
- Abd-Elsalam KA, Vasil'kov AYU, Said-Galiev EE, Rubina MS, Khokhlov AR, Naumkin AV, Shtykova EV and Alghuthaymi MA. 2018. Bimetallic blends and chitosan nanocomposites: novel antifungal agents against cotton seedling damping-off. *Eur J Plant Pathol*, **151**:57-72
- Bautista-Banos S, Hernandez-Lauzardo AN, Velazquez-Del Valle MG, Hernandez-Lopez M, Ait Barka E, Bosquez-Molina E and Wilson CL. 2006. Chitosan as a potential compound to control pre and postharvest diseases on horticultural Commodities. *Crop Prot*, **25**:108-118

- Bautista-Baños S. 2014. Postharvest Decay: Control Strategies. Elsevier Inc, 1-383
- Darder M, Montserrat CA, Ruizhitzky E. 2003. Biopolymer–clay nanocomposites based on chitosan intercalated in montmorillonite. *Chem Mater*, **15**:3774–3780
- El Hadrami A, Adam LR, El Hadrami I and Daayf F. 2010. Chitosan in plant protection. *Marine Drugs* **8**:968–987
- Fallanaj F, Sanzani SM, Youssef K, Zavanella C, Salerno MG, Ippolito A. 2015. A new perspective in controlling postharvest citrus rots: The use of electrolyzed water. *Acta Hort*, **1065**:1599-1606.
- Fallanaj F, Ippolito A, Ligorio A, Garganese F, Zavanella C and Sanzani SM. 2016. Electrolyzed sodium bicarbonate inhibits *Penicillium digitatum* and induces defence responses against green mould in citrus fruit. *Postharvest Biol Technol*, **115**:18–29
- FAOSTAT data: <http://www.fao.org/faostat/en/#data/QC> (Accessed 03 July 2019)
- Giannakas A, Grigoriadi K, Leontiou A, Barkoula N and Ladavos A. 2014. Preparation, characterization, mechanical and barrier properties investigation of chitosan-clay nanocomposites. *Carbohydr Polym*, **108**:103-111
- Han YS, Lee SH, Choi KH and Park I. 2010. Preparation and characterization of chitosan–clay nanocomposites with antimicrobial activity. *J Phys Chem Solids*, **71**: 467
- Hashim AF, Youssef K and Abd-Elsalam KA. 2019. Ecofriendly nanomaterials for controlling gray mold of table grapes and maintaining postharvest quality. *Eur J Plant Pathol*, **154**:377–388
- Hernández-Lauzardo A, Velázquez M and Guerra-Sánchez M. 2011. Current status of action mode and effect of chitosan against phytopathogens fungi. *Afri J Microbiol Res*, **5**:4243–4247
- Hussien A, Ahmed Y, Al-Essawy AH and Youssef K. 2018. Evaluation of different salt-amended electrolysed water to control postharvest moulds of citrus. *Trop Plant Pathol*, **43**:10-20.
- Kasirga Y, Oral A and Caner C. 2012. Preparation and characterization of chitosan/ montmorillonite-K10 nanocomposites films for food packaging applications. *Polym Comp*, **33**:1874-1882
- Kittur FS, Vishu Kumar AB and Tharanathan RN. 2003. Low molecular weight chitosans--preparation by depolymerization with *Aspergillus niger* pectinase, and characterization. *Carbohydr Res*, **338**:1283-1290
- Kumar S, Jog JP and Natarajan U. 2003. Preparation and characterization of poly(methyl methacrylate)–clay nanocomposites via melt intercalation: the effect of organoclay on the structure and thermal properties. *J Appl Polym Sci*, **89**:1186–1194.
- Kumar S, Ye F, Dobretsov S and Dutta J. 2019. Chitosan nanocomposite coatings for food, paints, and water treatment applications. *Appl Sci*, **9**:1-27
- Lavorgna M, Piscitelli F, Mangiacapra P and Buonocore GG. 2010. Study of the combined effect of both clay and glycerol plasticizer on the properties of chitosan films. *Carbohydr Polym*, **82**:291-298
- Li LH, Deng JC, Deng HR, Liu ZL and Li XL. 2010. Preparation, characterization and antimicrobial activities of chitosan/Ag/ZnO blend films. *Chem Eng J*, **160**:378–82
- Liu HY, Du X and Wang LS. 2004. Chitosan kills bacteria through cell membrane damage. *Int J Food Microbiol*, **95**:147-155
- Liu XF, Guan YL, Yang DZ, Li Z and Yao KD. 2001. Antibacterial action of chitosan and carboxymethylated chitosan. *J Appl Polym Sci*, **79**:1324–1335
- Moscoso-Ramírez PA, Montesinos-Herrero C and Palou L. 2013. Characterization of postharvest treatments with sodium methylparaben to control citrus green and blue molds. *Postharvest Biol Technol*, **77**:128-137
- Moslem MA, Abd-Elsalam KA, Bahkali AH and Yassin MA. 2010. First morpho-molecular identification of *Penicillium griseofulvum* and *P. aurantiogriseum* toxicogenic isolates associated with blue mold on apple. *Food-Borne Pathogen Dis*, **7**: 857–861
- Pichyangkura R and Chatchawan S. 2015. Bio stimulant activity of chitosan in horticulture. *SciHortic*, **195**:49-65
- Rabea EI and Steurbaut W. 2010. Chemically modified chitosans as antimicrobial agents against some plant pathogenic bacteria and fungi. *Plant Prot Sci*, **4**:149–158
- Reglinski T, Elmer PAG, Taylor JT, Wood PN and Hoyte SM. 2010. Inhibition of Botrytis cinerea growth and suppression of botrytis bunch rot in grapes using chitosan. *Plant Pathol*, **59**:882–890
- Rhim JW, Hong SI, Park HM and Ng PK. 2006. Preparation and characterization of chitosan-based nanocomposite films with antimicrobial activity. *J Agric Food Chem*, **54**:5814-22
- Salem EA, Youssef K, Sanzani SM. 2016. Evaluation of alternative means to control postharvest Rhizopus rot of peaches. *Sci. Hort*, **198**:86–90.
- Sanford PA. 2003. Commercial sources of chitin and chitosan and their utilization. In: Varum KM, Domard A, Smidsrød O (eds) *Advances in Chitin Science*, vol 6. NTNU, Trondheim, pp 35–42
- Simionato AS, Navarro MOP, de Jesus MLA, Barazetti AR, da Silva CS, Simões GC, Balbi-Peña MI, de Mello JCP, Panagio LA, de Almeida RSC and Andrade G de Oliveira AG. 2017. The Effect of phenazine-1-carboxylic acid on mycelial growth of *Botrytis cinerea* produced by *Pseudomonas aeruginosa* LV strain. *Front Microbiol*, **8**:1102
- Suhartono D. 2015. Preparation of chitosan material and its antifungal activity for bamboo. *Int J Sci Res*, **6**:1586-1590
- Taghinezhad E and Ebadollahi A. 2017. Potential application of chitosan-clay coating on some quality properties of lemon during storage. *Agric Eng Int*, **19**:189-194
- Xu D, Qin H and Ren D. 2018. Prolonged preservation of tangerine fruits using chitosan/montmorillonite composite coating. *Postharvest Biol Technol*, **143**: 50–57
- Xu Y, Ren X and Hanna MA. 2006. Chitosan/Clay Nanocomposite Film Preparation and Characterization. *J Appl Polym Sci*, **99**:1684–1691
- Youssef K, Hashim AF, Margarita R, Alghuthaymi MA and Abd-Elsalam KA. 2017. Antifungal efficacy of chemically-produced copper nanoparticles against *Penicillium digitatum* and *Fusarium solani* on citrus fruit. *The Philip Agric Sci*, **100**:69-78
- Youssef K, Sanzani SM, Ligorio A, Ippolito A and Terry LA. 2014. Sodium carbonate and bicarbonate treatments induce resistance to postharvest green mould on citrus fruit. *Postharvest Biol Technol*, **87**:61–69
- Youssef K, Ahmed Y, Ligorio A, D’Onghia AM, Nigro F, Ippolito A. 2010. First report of *Penicillium ulaiense* as a postharvest pathogen of orange fruit in Egypt. *Plant Pathol*, **59**(6):1174.
- Youssef K, Sanzani SM, Ligorio A, Fallanaj F, Nigro, F, Ippolito A. 2015. Biochemical and transcriptomic changes associated with induced resistance in citrus fruits treated with sodium salts. *Acta Hort*, **1065**:1627–1632

The Role of Turmeric (*Curcuma longa*) Powder in Improving Liver Function to Increase Vitellogenin Synthesis and Deposition in the Oocytes of Catfish (*Pangasianodon hypophthalmus*)

Cut D. Dewi^{1,2}, Wasmen Manalu^{1,*}, Damiana R. Ekastuti¹, and Agus O. Sudrajat³

¹ Department of Anatomy, Physiology, and Pharmacology, Faculty of Veterinary Medicine, IPB University,

²Department of Aquaculture, Faculty of Marine and Fisheries, Universitas Syiah Kuala, Banda Aceh 23111, ³Department of Aquaculture, Faculty of Fishery and Marine Sciences, IPB University, Indonesia

Received June 26, 2019; Revised September 15, 2019; Accepted October 5, 2019

Abstract

This experiment was designed to improve nutrients deposition in the oocytes of catfish by improving the liver functions through supplementation of turmeric powder in the feed and to evaluate the optimum dosage of turmeric powder supplementation in the feed of catfish. The experiment used 40 catfish with the average body weight of 3.75 kg. Forty experimental catfish were divided into 4 treatments, and each treatment used 10 catfish. The treatments were doses of turmeric supplementation in the diet consisting of 0 mg/100 g feed (T0 as a control), 120 mg/100 g feed (T1), 240 mg/100 g feed (T2), and 480 mg/100 g feed (T3). The experimental catfish were fed 2 times a day in the morning and in the afternoon at the level of 3% body weight for 8 weeks. The results of the experiment showed that turmeric powder supplementation at a dose of 480 mg/100 g ration could increase the absolute body weight of the catfish, vitellogenin deposition in the eggs, and gonad development. The results of the present experiment indicate that turmeric powder supplementation of the catfish can be used to improve reproduction performance of catfish and teleost fish.

Keywords: Turmeric powder, Catfish (*Pangasianodon hypophthalmus*), Egg Vitellogenin, Gonad Development

1. Introduction

The production of catfish in Indonesia increases every year, but the production level has not reached the production target. The efforts to increase the production of catfish have been conducted; however, to reach the optimum production, it is required to improve and optimize the physiological functions of body organs of the catfish. Catfish farmers are facing limitations in breeding so that demands for larvae, juvenile, and fries production for catfish farmers have not been achieved optimally. In catfish farming and aquacultures, there are some problems and limitation in the availability of quality larvae, juvenile, and fries by qualities brood stocks. Therefore, to obtain good quality larvae the strategy can be started from improving the quality of eggs (Kjorsvik *et al.*, 1990).

The quality of eggs can be improved by improving the feed quality of the brood stocks. To meet the expectations, one way is to increase reproduction by increasing the brood stocks quality through the feed. The feed is an important component in the process of vitellogenin synthesis. Basically, vitellogenesis is a process of nutrients accumulation in the oocyte so that the availability of egg yolk in the oocyte will determine the qualities of oocytes (Sequeira *et al.*, 2012). The feeding of fish with a quality feed is required for meeting the nutrient requirement during gonad growth and development in the brood

catfish. The nutrients content of ration is an important factor in determining ration quality.

In order to support an optimum reproduction process of the brood catfish, it is required to add materials that contain certain nutrients. One of the materials that can be used is turmeric (*Curcuma longa*). Turmeric (*Curcuma longa*) is a rhizomatous herbaceous perennial plant of the ginger family, Zingiberaceae (Chan *et al.*, 2009). Turmeric powder contains a flavonoid that has phytoestrogen activity acting like estrogen in stimulating the liver to synthesize vitellogenin. Turmeric powder contains curcumin, beta carotene, fat 5.1%, carbohydrate 69.4%, protein 6.3%, vitamin B1, B2, B6, B12, and Vitamin E (Ravindran *et al.*, 2007; Pari *et al.*, 2008; Dono, 2013). Curcumin has a hepatoprotective activity that can prevent and cure the destruction of hepatocytes (Tung *et al.* 2017) and improve the hepatocyte function in synthesizing vitellogenin under the stimulation of estrogen (Saraswati *et al.*, 2013).

Our preliminary studies in catfish strongly confirm that turmeric supplementation improves liver function and increases total egg production (Dewi *et al.*, 2018). The present experiment was designed to investigate the use of curcumin in turmeric powder to improve vitellogenin deposition in the oocyte and gonad development of the experimental catfish.

* Corresponding author e-mail: wasmenmanalu@gmail.com; cutdarabdpunsyiah@gmail.com.

2. Materials and Methods

The experiment was conducted from May to August 2015. The experiment was conducted in the Babakan Experimental Pond, Faculty of Fishery and Marine Science, IPB University. The measurement of vitellogenin contents of the ovulating eggs was conducted in the Laboratory of Biochemistry of Inter-University Center, Bogor Agricultural University. Forty catfish (*Pangasionodon hypophthalmus*), cultured in local freshwater with the average body weight of 3.75 kg, were used as experimental models. The catfish were chosen due to their high fecundity. The experimental catfish were maintained in a 28 x 20 x 6m³ maintenance pond. The optimum supplemental dose of turmeric powder for catfish (2.4 g/kg feed) was calculated according to the method of Laurence and Bacharach (1964) based on the optimum dose of turmeric powder in human. The experimental doses used were no turmeric supplementation, half of the optimum dose, the optimum dose, and twice the optimum dose. Turmeric (with 5.34% curcumin content) was mixed with commercial feed to produce the treatment doses of 0, 120, 240, and 480 mg/100 g feed.

2.1. Catfish Maintenance

The catfish were acclimated to the experimental conditions and the ponds for 1 month before treatment after being selected based on their gonad maturity (stage I). During the maturation process, the experimental catfish were kept in the maintenance pond, which was later partitioned into 4 smaller 7 x 5 x 1.5 m³ experimental net cages. Each net cage contained 10 catfish that were subjected to these conditions for 8 weeks. During the experiment, the catfish were fed commercial feed with a protein content of 38% two times a day (in the morning and in the afternoon). Feed was provided at 3% of the BW, and the nutrient composition of the feed is presented in Table 1.

Table 1. Proximate analyses of experimental rations supplemented with turmeric powder at doses of 0, 120, 240, and 480 mg/100 g commercial ration.

The dose of turmeric (mg/100 g ration)	Protein	Fat	Ash	Water	Carbohydrate	
					Crude Fiber	NFE
0 (T0)	32.99	7.61	9.23	8.06	4.45	37.66
120 (T1)	32.76	7.68	8.95	8.40	5.35	36.86
240 (T2)	31.60	7.09	8.92	8.69	4.63	39.07
480 (T3)	31.81	7.29	9.06	8.37	4.22	39.25

2.2. Samples Collections and Measurements

At the end of 8 weeks of turmeric supplementation, the experimental catfish were sacrificed to observe the gonad. Before being sacrificed, the experimental catfish were weighed for measuring body weight. Each group of experimental catfish was represented by 3 catfish to be sacrificed. The gonad of selected experimental catfish was evaluated by collecting the gonads of 3 selected experimental catfish. The weights of gonads were measured. The eggs vitellogenin concentrations were measured to determine the gonad maturity due to turmeric supplementation.

Vitellogenin concentrations of the eggs were measured in two steps. The first step was the isolation of the vitellogenin from the eggs of experimental catfish by using SDS polyacrylamide gel electrophoresis (SDS-PAGE) (Bio-Rad, Hercules, California, USA) (Walker, 2002). The second step was the quantification of the isolated vitellogenin using the Bradford method (Kruger, 2002).

In the isolation of vitellogenin, 1g of egg sample of the experimental catfish was mixed with 15 µL of sample buffer and the mixture was dissolved in distilled water with the final volume of 1 mL. The mixture was heated at 100°C for 5 minutes. Fifteen microliters (15 µL) of this mixture of sample preparation was used per well, so the weight of egg sample in each well was 15 µg. The electrophoresis was run at 60 mV and 20 mA for 4 hours. After completing the electrophoresis, the gel was processed for silver staining, and then the gel was put into a stop solution for 5 minutes. Then, the gel was washed with ddH₂O for 5 minutes and scanned. The relative mobility (Rf) of the sample was measured, and the molecular weights of the proteins in the sample were calculated using the standard protein marker.

The molecular weight of 240 kDa for avian vitellogenin (Deeley *et al.*, 1975) was used as a criterion for selecting and isolating the vitellogenin. Therefore, in this method, the band with 240 kDa was cut and separated, ground with deionized distilled water (ddH₂O) and then centrifuged at 3360 g for 15 minutes. The supernatant was added with ddH₂O to make a final volume of 200 µL. Then, the supernatant was added to 2 mL of the Bradford solution and then vortexed, and the solution was allowed to sit for 3–15 minutes (stable for 1 hour). Then, 3.3333 µL of the mixture of supernatant and Bradford solution was used to measure the absorbance of the solution using a spectrophotometer at the wave length of 595 nm. The blank solution was made by mixing 200 µL of deionized distilled water with 2 mL of the Bradford solution. The absorbance of the blank solution was also measured. The corrected absorbance of the sample was calculated by reducing the sample absorbance with the blank absorbance.

Then, the standard curve was made by using bovine serum albumen (Sigma) as a standard protein at the ranges of 0, 0.02, 0.04, 0.06, 0.08 and 0.10 mg/mL, which equals the range of concentrations of 0, 20, 40, 60, 80 and 100 ppm. The concentration of sample protein (mg in 200 µL egg) can be calculated from the equation of the standard curve of the BSA. The final concentration of the vitellogenin concentrations of the egg (mg/mL) was calculated by correcting the dilution of the eggs sample in the analysis.

Further, the gonad organs were isolated and then stored in 10% of buffered neutral formalin for histological preparation. Qualitative observations of gonad tissues were determined from the description of histological observations of the gonad by using paraffin and Hematoxylin-Eosin staining (Bancroft and Gamble, 2008).

2.3. Water Quality Parameters

The water quality parameters measured were temperature, pH, and dissolved oxygen. Temperature was measured by using thermometer. The water pH was

measured by using Ph-meter. The dissolve oxygen in the water was measured by DO meter.

2.4. Data Analyses

The collected data were analyzed with Analyses of Variance by using Microsoft Excel 2010 and SPSS version 16.0. When the effect of treatment was significant, the Duncan Test was conducted to test the difference between doses of turmeric supplementation with 95% confidential interval.

3. Results

3.1. Absolute Body Weight

The observation on the absolute body weight gain of experimental catfish fed with commercial ration supplemented with turmeric powder at doses of 0, 120, 240, and 480 mg/100 g ration is presented in Table 2. The statistical analyses showed that the supplementation of catfish with turmeric powder significantly increased absolute body weight gain ($P < 0.05$). The Duncan test also manifested that catfish fed ration supplemented with turmeric powder at a dose of 480 mg/100 g ration showed the highest absolute body weight gain (4.17 kg) that was significantly different from the other doses of turmeric supplementation. Turmeric powder supplementation at doses of 120 and 240 mg/100 g ration did not significantly increase absolute body weight gains compared to control catfish without turmeric powder supplementation ($P > 0.05$).

Table 2. Average absolute body weight gains of experimental catfish fed commercial ration supplemented with turmeric powder at doses 0 mg/100 g ration (T0), 120 mg/100 g ration (T1), 240 mg/100 g ration (T2), and 480 mg/100 g ration (T3) for 8 weeks.

The dose of turmeric powder supplementation (mg/100 g ration)	Absolute body weight gain (kg)
0	3.01±0.86 ^a
120	2.94±0.85 ^a
240	3.14±0.16 ^a
480	4.17±0.43 ^b

Different superscripts in the same column indicate significant differences ($P < 0.05$).

3.2. Vitellogenin Concentration of the Egg

The vitellogenin concentrations of the eggs as an indicator of vitellogenin synthesis and deposition in the oocytes of the experimental catfish fed commercial ration supplemented with turmeric powder at doses 0, 120, 240, and 480 mg/100 g ration are presented in Table 3. The results of statistical analyses showed that turmeric powder supplementation at various doses significantly increased ($P < 0.05$) vitellogenin synthesis and deposition in the oocyte with the final effect on the increased concentrations in the eggs. Further Duncan test showed that the highest vitellogenin deposition in the oocytes was found in the experimental catfish fed ration supplemented with turmeric powder at a dose of 480 mg/100 g ration i.e., 3.99 mg/g egg. The vitellogenin concentration in this experimental catfish fed ration supplemented with turmeric powder at a dose of 480 mg/100 g ration was significantly different ($P < 0.05$) from the experimental catfish fed ration with

turmeric powder at doses of 0, 120, and 240 mg/100 g ration.

Table 3. Mean vitellogenin concentrations in the eggs of experimental catfish fed ration supplemented with turmeric powder at doses of 0 mg/100 g ration (T0), 120 mg/100 g ration (T1), 240 mg/100 g ration (T2), and 480 mg/100 g ration (T3) for 8 weeks.

The dose of turmeric powder supplementation (mg/100 g ration)	Vitellogenin concentration in the eggs (mg/g)
0	0.78±0.15 ^a
120	0.22±0.24 ^a
240	2.06±0.38 ^b
480	3.99±1.29 ^c

Different superscripts in the same column indicate significantly

3.3. Gonad Development

Experimental catfish supplemented with different doses of turmeric powder had significantly different gonad maturities. This result indicates that different doses of turmeric supplementation affect the gonad development of experimental catfish that is the initial stage of effects on reproduction. Gonad development of catfish in this experiment was determined based on the observation of the catfish gonad and the level of gonad maturity in each experimental catfish. The level of gonad maturity of experimental catfish was determined morphologically based on the form, color, size, and the development of gonad contents. Figure 1 and Figure 2 present the photos of the level of gonad maturity of the experimental catfish at the end of the experiment.

From the observation of gonad maturity at the end of the experiment, it was clear that gonad maturity in the experimental catfish supplemented with turmeric at a dose of 480 mg/100 g ration was faster compared to the control catfish (Figures 1 and Figure 2). However, the catfish supplemented with turmeric at doses of 0 mg/100 g ration and 120 mg/100 g ration showed the early gonad maturity at the end of experiment while the experimental catfish supplemented with turmeric at a dose of 480 mg/100 g ration could maintain the gonad maturity until the end of experiment. It could be seen in Figure 2 that there were higher number of eggs in the gonad of experimental catfish.

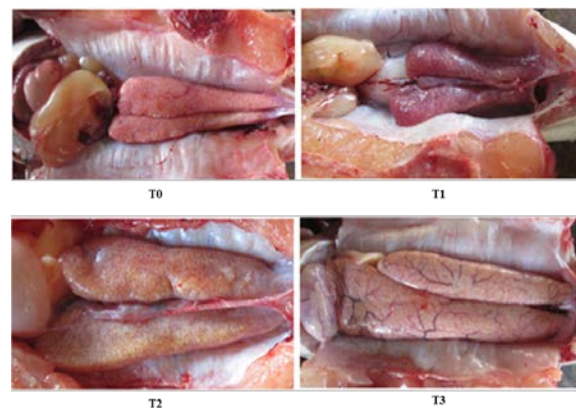


Figure 1. The conditions of ovaries of experimental catfish supplemented with turmeric powder at doses of 0 mg/100 g ration (T0), 120 mg/100 g ration (T1), 240 mg/100 g ration (T2), and 480 mg/100 g ration (T3) for 8 weeks.

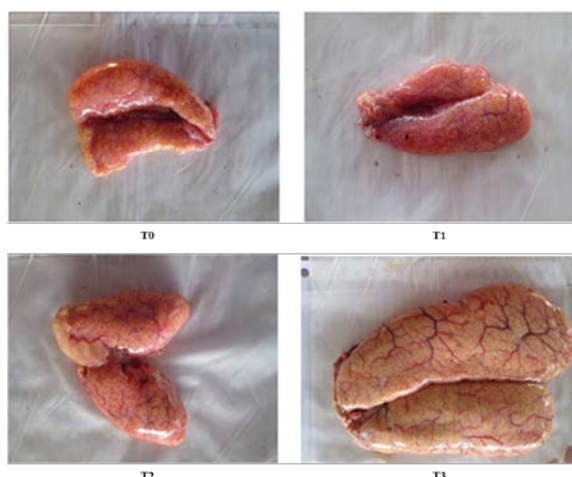


Figure 2. The gonads of experimental catfish supplemented with turmeric powder at doses of 0 mg/100 g ration (T0), 120 mg/100 g ration (T1), 240 mg/100 g ration (T2), and 480 mg/100 g ration (T3) for 8 weeks

3.4. Histology of Gonad

Histologically, catfish supplemented with turmeric powder at a dose of 480 mg/g feed showed a better gonad maturity and ready for ovulation and spawning. There were different stages of oocyte development in one ovary indicating that the experimental catfish have partial or asynchronous spawning. The most significant results from histological observation of gonads were the higher number and size of oocytes in catfish supplemented with turmeric powder at a dose of 480 mg/100 g feed.

3.5. Water Quality

The high quality of the water media was maintained under controlled conditions during the experiment. The water pH ranged from 6.0 to 7.5; the temperature ranged from 27.7 to 30°C; and the dissolved oxygen ranged from 3.5 to 5.42 mg/L. The standard water pH, temperature, and dissolved oxygen ranges were 6.85 to 7.50, 28.0 to 30.0, and 3.0 to 6.0 respectively.

4. Discussion

Supplementation of turmeric powder in the ration improved the growth of experimental catfish during 8 weeks of treatment as was indicated by the increased absolute body weight ($P < 0.05$) (Table 2). At the end of 8 weeks of turmeric powder supplementation, the experimental catfish fed ration supplemented with turmeric powder at a dose of 480 mg/100 g ration had the highest absolute body weight gain compared to the other catfish supplemented with turmeric powder at doses of 0, 120, and 240 mg/100 g ration.

The increases in body weights were related to the increased feed intake as was reported by Rajput et al. (2012) that turmeric powder supplementation in broiler chickens increased appetite that further increased feed intake that eventually met the nutrient requirement of the animals. Supplementation of the ration with *Nigella sativa* or black cumin combined with turmeric at doses of 5-10 g/kg ration for 60 days could increase the daily growth rate of *Lates calcarifer* fingerlings (Abdelwahab and El Bahr, 2012). Mahmoud et al. (2014) concluded that 0.5% turmeric supplementation improved growth performance

of Nile tilapia. The similar result was also observed by Mukherjee et al. (2009) investigating the effect of turmeric powder on growth performance and body color of guppy. In this study, 0.03, 0.06, 0.09, 0.10, and 0.20 percent of turmeric powder were added to the basal diet, and the results revealed that fish fed with diet contained 0.09% turmeric powder had a better growth performance compared to the other groups. Turmeric powder supplementation at a dose of 7.5% ration in African catfish (*Clarias gariepinus*) could also increase body weight gains during 8 weeks of treatment in African catfish (Sodamola et al., 2016). The similar result was also observed in fish supplemented with turmeric powder at a dose of 0.3% ration increased body weight gain of Green terror (*Andinocara rivulatus*) (Mooraki et al., 2019).

Experimental catfish fed ration supplemented with turmeric powder at a dose of 480 mg/100 g ration had the highest vitellogenin concentrations in the eggs i.e., 3.99 mg/mL. This result could be related to the phytoestrogenic effects of flavonoid in the turmeric that could act like estrogen in stimulating the liver to synthesize vitellogenin. The liver is the main site of vitellogenin biosynthesis as a precursor of egg yolk (Turker and Bozcaarmutlu, 2009). Dewi et al. (2018) reported that turmeric powder supplementation at a dose of 480 mg/100 g ration in catfish could increase the plasma vitellogenin concentrations i.e., 5.375 mg/mL. Turmeric powder supplementation dramatically increased the capacity of hepatocytes to synthesize vitellogenin in catfish that eventually increased vitellogenin deposition in the developing oocytes during gonad maturity that was confirmed by the increased fecundity and with the higher diameters. These results in catfish were similar to the results reported by Rawung et al. (2019) that turmeric powder supplementation at a dose of 0.5% ration and thyroxine at a dose of 0.1 mg in african catfish (*Clarias gariepinus*) could increase the vitellogenin concentrations in the eggs i.e., 8.17 mg/mL. Turmeric powder supplementation prior to gonad maturity would stimulate earlier cell growth and receptors that were indicated by the increased synthesis of vitellogenin that eventually increased egg production. The vitellogenin concentration in the eggs found in the present experiment indicated that turmeric powder could increase vitellogenin synthesis and further deposition in the eggs. Turmeric powder supplementation could improve liver capacity and functions to produce the precursor of egg yolk that eventually stimulates the follicle growth during gonad maturity. During the process of vitellogenesis, the number and granules of egg yolk increase so that the volume of oocytes will increase. During the deposition of egg yolk, curcumin as a bioactive component of turmeric is assumed to be deposited in the developing oocytes (Kasiyati et al., 2016a).

The turmeric powder supplementation could increase the diameter of the eggs in the experimental catfish. The increased egg diameter is the results of the increased synthesis, secretion, and deposition of egg yolk precursors in the present experiment. Egg diameter indicates the number of materials and energy deposited in the eggs that will be further used for embryonic growth and development. The egg diameter will increase with the increased gonad development. This increase is related to the increased deposition of nutrients in the oocytes during

gonad maturation that will increase with the increased size of the oocytes. The egg diameter is determined by the amount of vitellogenin deposited in the egg during oocyte growth and development. The increased diameter of the egg is caused by the growth and development of oocytes and the growth and development of the oocytes are related to the deposition of egg yolk. The development of egg during the uptake of vitellogenin will be stopped when the oocyte has reached the maximum size. Dewi et al. (2018) reported that turmeric powder supplementation at doses of 240-480 mg/100 g ration could increase the egg diameter in catfish. Curcumin supplementation in the ration could increase the diameter of F1 follicles in Magelang ducks (Kasiyati et al., 2016b).

The diameters of sample eggs of catfish showed different sizes. In the control catfish, the diameter of the egg was lower compared to those supplemented with turmeric powder at a dose of 480 mg/100 g ration. Lee & Young (2002) stated that the egg size also played a role and determined the survival of the fish developed from this egg. The egg size also correlated with the size of the larvae. Larvae with larger size will survive better during starvation compared to smaller larvae hatched from the egg with the smaller size (Kamler, 1992). The positive relation between the larvae size and egg size was reported in salary Salmon, *Oncorhynchus mykiss*, and turbot (*Scophthalmus maximus*. L) (Kjorsvik et al., 1990). Some researchers showed that eggs with larger sizes produced larvae and fish with better survivals. Kamler (1992) proposed an equation of survival for sea pelagic fish that mortality rate of egg and larvae had a negative correlation with the egg size. If there was no external feed, the larger larvae hatched from a larger egg could survive longer compared to larvae hatched from a smaller egg.

The gonad maturity in fish fed ration supplemented with turmeric powder at doses of 240-480 mg/100 g ration was faster compared to control catfish (Figure 2). The acceleration of gonad maturity is assumed to be related to the role of turmeric powder in improving liver function to synthesize vitellogenin and the vitellogenin will be further transported and deposited in the developing oocytes for the growth and development of follicle hierarchy. The higher the number of developing follicles, the faster the follicle is to be ovulated. Dewi et al. (2018) reported that turmeric powder supplementation at doses of 240-480 mg/100 g ration could produce 100% catfish reached gonad maturity with gonad maturity stage IV (final vitellogenesis) during 8 weeks of treatment. The similar result was also observed in catfish treated with hormone (PMSG+ anti-dopamine, each with doses of 0.25 mL dan 0.1 mg) and turmeric at a dose of 480 mg/100 g in feed could produce 100% gonad maturity in catfish (*Pangasionodon hypophthalmus*) (Arfah et al., 2018).

The differences in histological profiles of gonads in each experimental catfish can be seen in Figure 3. In control catfish, the development of gonad at week 8 is still in the early stage of development; oogonia are very small with a round form and a very large nucleus compared to the cytoplasm, and oogonia are found in group even though some are single. However, the catfish supplemented with turmeric powder at a dose of 480 mg/g feed showed the oocyte that were in the last stage of maturation with a larger size; the number of egg yolk that covered the cytoplasm was higher. Figure 3 shows that the

oocytes of catfish in the same gonad maturity have different and various development stages. The difference in developmental stages of gonad is an indication of the experimental catfish with the partial or asynchronous spawning type. Partial or asynchronous spawning is the development of oocytes when the ovary contains all stadia of oocytes.

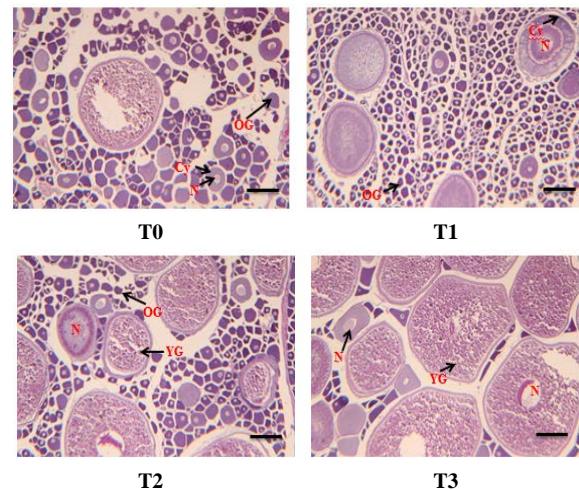


Figure 3. Histology of gonad of experimental catfish supplemented with turmeric powder at doses of 0 mg/100 feed (T0), 120 mg/ 100 g feed (T1), 240 mg/ 100 g feed (T2), and 480 mg/ 100 g feed (T3). Nucleus (N), Cytoplasm (Cy), Yolk Globule (YG), Oogonium (OG). Staining with H&E, Scale line represented 50 μ m. Enlargement 40 x 10 times.

The water quality during catfish maintenance showed the condition that is able to support the maintenance of experimental catfish. The degree of water acidity (pH) during experiment ranged from 6.0-7.5, and this pH range was in the range of optimum pH for catfish as Hossain et al. (2006) stated that the optimum pH to support the life of catfish ranges from 6.85–7.5. The water temperature during the experiment ranged from 27.7-30.0°C, and the temperature was in the normal range. According to Slembrouck et al. (2009), in general, catfish can survive to live in the range of water temperature of 28-30°C. Dissolved oxygen (DO) during experiment ranged from 3.5-5.42 mg/L, and this range was suitable for catfish maintenance to support the optimum catfish growth that ranged 3.0–6.0 mg/L (Rahman et al., 2006).

5. Conclusions

Turmeric powder supplementation can improve absolute body weight gain, vitellogenin synthesis and deposition in the eggs as well as the stage of gonad development of experimental catfish. The improved absolute body weight gain, vitellogenin deposition in the eggs, and gonad development are the initial indicators that curcumin supplementation in the ration has a great prospect to be used in improving reproductive performances of catfish and teleost fish.

Acknowledgments

This study was funded by a PMDSU research grant from the Ministry of Research, Technology and Higher Education of the Republic of Indonesia in 2014.

References

- Abdelwahab AM and El-Bahr SM. 2012. Influence of black cumin seeds (*Nigella sativa*) and turmeric (*Curcuma longa* Linn.) mixture on performance and serum biochemistry of Asian sea bass, *Lates calcarifer*. *World Journal of Fish and Marine Sciences*, **4(5)**: 496-503.
- Arfah H, Sudrajat AO, Supriyadi MA and Zairin M. 2018. Gonad maturation of female striped catfish *Pangasionodon hypophthalmus* (Sauvage, 1878) using a combination of pregnant mare serum gonadotropin+antidopamine, Vitamin E, and curcumin extract mixed feed outside its spawning season. *International Journal of Fisheries and Aquatic Studies*, **6(5)**: 52-57.
- Bancroft JD, and Gamble M. 2008. **Theory and practice of histological techniques**. 6th Ed. Churchill Livingstone, China: Elsevier.
- Chan EWC, Lim YY, Wong SK, Lim KK, Tan SP, Lianto FS, Yong MY. 2009. Effects of different drying methods on the antioxidant properties of leaves and tea of ginger species. *Food Chemistry*, **113(1)**: 166-172.
- Dewi CD, Ekastuti DR, Sudrajat AO, and Manalu W. 2018. Improved vitellogenesis, gonad development and egg diameter in catfish (*Pangasianodon hypophthalmus*) supplemented with turmeric (*Curcuma longa*) powder. *Aquaculture Research*, **49(2)**: 651-658.
- Deeley RG, Mullinix KP, Wetekam W, Kronenberg HM, Meyers M, Eldridge JD, and Goldberger RF. 1975. Vitellogenin synthesis in the avian liver: Vitellogenin is the precursor of the egg yolk phosphoproteins. *The Journal of Biological Chemistry*, **250**: 9060-9066.
- Dono ND. 2013. Turmeric (*Curcuma longa* Linn) supplementation as an alternative to antibiotics in poultry disease. *Wartazoa*, **23(1)**: 41-49.
- Hossain MA, Ali MZ, Rahman MM, and Kader MA. 2006. Evaluation of mixed feeding schedules with varying dietary protein content on the growth performance and reduction of cost of production for sutchi catfish, *Pangasius hypophthalmus* (Sauvage) with Silver Carp, *Hypophthalmichthys molitrix* (Valenciennes). *Journal of Applied Aquaculture*, **18(1)**: 63-7.
- Kamler E. 1992. **Early life history of fish. An energetic approach**. Chapman and Hill, London.
- Kasiyati, Manalu W, Sumiati, and Ekastuti DR. 2016a. Efficacy of curcumin and monochromatic light in improving liver function of sexually mature Magelang ducks. *Journal of the Indonesian Tropical Animal Agriculture*, **41(3)**: 153-160.
- Kasiyati, Sumiati, Ekastuti DR and Manalu W. 2016b. Roles of curcumin and monochromatic light in optimizing liver function to support egg yolk biosynthesis in Magelang ducks. *Int J Poult Sci*, **15(10)**: 414-424.
- Kjorsvik E, Mangor-Jensen A, and Holmfjord I. 1990. Egg quality in fishes. *Advances in Marine Biology*, **26**: 71-113.
- Kruger NJ. 2002. **The Bradford method for protein quantification**. In J. M. Walker (Ed.), *The Protein Protocols Handbook* (pp. 15-21). Totowa, New Jersey: Humana Press.
- Laurence DR, and Bacharach AL. (Eds.) (1964). **Evaluation of Drug Activities: Pharmacometrics (Vol. 900)**. New York: Academic Press.
- Lee WK, and Young SW. 2002. Relationship between ovarian development and serum levels of gonadal steroid hormones, and induction of oocyte maturation and ovulation in the cultured female Korean spotted sea bass *Lateolabrax modulates* (Jeom-nong-one). *Aquaculture*, **207**: 169-183.
- Mahmoud MMA, El Lamie MMM, Dessouki AA, and Yusuf M. 2014. Effect of turmeric (*Curcuma longa*) supplementation on growth performance, feed utilization, and resistance of Nile tilapia (*Oreochromis niloticus*) to *Pseudomonas fluorescens* challenge. *Global Research Journal of Fishery Science and Aquaculture*, **1(12)**: 26-33.
- Mukherjee, A., Mandal, B. and Banerjee, S. 2009. Turmeric as a carotenoid source on pigmentation and growth of fantail guppy (*Poecilia reticulata*). *Proceedings of the zoological Society*, **62(2)**: 119-123.
- Mooraki N, Batman Y, Zoriehzahra S.J, and Kakoolaki Sh. 2019. Evaluating the effect of using turmeric (*Curcuma longa*) on growth performance and hematological parameters of the ornamental fish, Green Terror (*Andinocara rivulatus*). *Journal of Survey in Fisheries Sciences*, **5(2)**: 37-47.
- Pari L, Tewas D, and Eckel J. 2008. Role of curcumin in health and disease. *Physiol Biochem*, **114(2)**: 127-149.
- Rahman MM, Islam MS, Halder GC, and Tanaka. 2006. Cage culture of sutchi catfish, *Pangasius sutchi* (Fowler 1937): effects of stocking density on growth, survival, yield and farm profitability. *Aquaculture Research*, **37**: 33-39.
- Rajput N, Muhammadiyah N, Yan R, Zhong X, Wang T. 2012. Effect of dietary supplementation of curcumin on growth performance, intestinal morphology and nutrients utilization of broiler chicks. *J Poult Sci*, **50**: 44-52.
- Rawung LD, Manalu W, Ekastuti DR, Junior MZ, Rahminiwati M and Sunarma A. 2019. Reproductive performances and egg qualities in african catfish (*Clarias gariepinus*) broodstocks supplemented with curcumin and thyroxine hormone. *Omni Akuatika* (In press).
- Ravindran PN, Babu KN, Sivaraman K. 2007. **Turmeric the genus Curcuma**. London, New York: CRC Press.
- Saraswati TR, Manalu W, Ekastuti DR, and Kusumorini N. 2013. Increased egg production of Japanese quail (*Coturnix japonica*) by improving liver function through turmeric powder supplementation. *Int J Poult Sci*, **12(10)**: 601-614.
- Sequeira AT, Gellida AK, Andre M, Babin PJ. 2012. Vitellogenin expression in white adipose tissue in female teleost fish. *Biology of Reproduction*, **86(2)**: 38.
- Slembrouck J, Baras E, Subagja J, Hung LT, and Legendre M. 2009. Survival, growth and food conversion of cultured larvae of *Pangasianodon hypophthalmus*, depending on feeding level, prey density, and fish density. *Aquaculture*, **294**: 52-59.
- Sodamola M.O, Jimoh WA, Adejola YA, Akinbola DD, Olanrewaju A and Apiakason E. 2016. Effect of turmeric (*Curcuma longa*) root powder (trp) on the growth performance, hematology and serum biochemistry of african catfish (*Clarias gariepinus*). *Academia Journal of Agricultural Research*, **4(9)**: 593-596.
- Tung BT, Hai NT, and Son PK. 2017. Hepatoprotective effect of phytosome curcumin against paracetamol-induced liver toxicity in mice. *Brazilian Journal of Pharmaceutical Sciences*, **53(1)**: 1-13.
- Turker H and Bozcaarmutlu. 2009. Effect of total isoflavones found in soybean on vitellogenin production in common carp. *Kafkas Univ Vet Fak Derg*, **15(4)**: 561-568.
- Walker JM. 2002. **SDS polyacrylamide gel electrophoresis of proteins**. In J. M. Walker (Ed.), *The protein protocols handbook* (pp. 61-67). Totowa, New Jersey: Humana Press.

Effect of Different Applications of Bio-agent *Achromobacter xylosoxidans* against *Meloidogyne incognita* and Gene Expression in Infected Eggplant

Walaa A. Ramadan^{1*} and Gazeia M. Soliman²

¹ Genetics and Cytology Department, Genetic Engineering and Biotechnology Division,² Plant Pathology Department, Nematology Unit, National Research Centre, Dokki, Giza, P.O. 12622, Egypt

Received August 26, 2019; Revised October 10, 2019; Accepted November 2, 2019

Abstract

The present study aimed to evaluate the effect of different applications of the bio-agent *Achromobacter xylosoxidans* (B) against root-knot nematodes, *Meloidogyne incognita* (N) infected eggplant under greenhouse conditions. The different applications are addition of bacteria suspension seven days after / before nematodes, addition of bacteria suspension and nematodes at same time; root dipping in bacteria suspension for 30 and 45 min; foliar spreading by bacteria suspension, in addition two controls; infected plant with nematodes without applying any bacteria, and untreated plant neither with nematodes nor with bacteria. The best application of the bio-agent to maximize bio-control benefits was estimated by studying its effect on eggplant gene expression via protein analysis. The most effective application was when nematodes and *A. xylosoxidans* were added at the same time (N+B at same time). The reduction of nematode parameter; second-stage juveniles in the soil, number of galls and number of egg-masses due to this application had reached 79.80%, 71.09% and 78.26% respectively. These results are in harmony with those of soluble protein electrophoresis of eggplants, which showed that the infected plant gave the lowest number of bands in all total stages of the experiment, while the application (N+B at same time) had the highest number of bands. Four bands at M.W. (55, 53, 47 and 43 kDa.) produced by untreated plant and all application but were absent in infected plant. This indicates the importance of applying the bacterium strain *A. xylosoxidans* which induced the plant to produce these important proteins. The increase or decrease in the number of protein bands refers to the induction or inhibition of the resistance genes, and this change was reflected on plant growth. The effectiveness of the application was clear in increasing the length, fresh and dry weights of shoot and root.

Keywords: Different applications, *Achromobacter xylosoxidans*, eggplant, *Meloidogyne incognita*, bio-agent, gene expression, SDS-PAGE.

1. Introduction

Plant-parasitic nematodes cause serious losses to a variety of agricultural crops worldwide (Ismail *et al.*, 2018). Egyptian agriculture faces a great loss every year incurred from infection by plant diseases, the annual losses up to 23% in eggplant (El-Nagdi *et al.* 2019). The root-knot nematodes, *Meloidogyne incognita* are major plant-parasites, and they are the main problem for many agricultural crops (Hussain *et al.*, 2012; Youssef *et al.*, 2012; Mukhtar *et al.*, 2013, Kassab *et al.*, 2017). In recent years, the main way for their control was the use of chemical nematicides. The risk and harmful effects on humans and environments have focused the attention on the development of biological control agents as an alternative potential eco-friendly strategy for controlling plant diseases. Soil rhizobacteria are repeatedly shown to be promising microorganisms for the biological control of plant-parasitic nematodes (Giannakou *et al.*, 2004). The use of biological agents in particular plant growth-promoting rhizobacteria (PGPR) has been considered as an attractive viable option to the control strategies (Kloepper *et al.*, 1991). B Due to their ability to improve plant

growth, Endophytic bacteria can be considered as PGPR, and their close interactions with plants make them an ideal candidate for enhancing plant growth.

Endophytic bacteria, *Achromobacter xylosoxidans* is a gram-negative bacterium, frequently- isolated from the rhizosphere. *A. xylosoxidans* use in biocontrol is already known to suppress nematode population (Yuen and Schroth, 1986; Vaidya *et al.*, 2001; Tian *et al.*, 2007). *A. xylosoxidans* was included as plant growth -promoting rhizobacteria (PGPR) as it has shown tremendous promise in terms of improvement of NO₃ uptake by roots. *A. xylosoxidans* strain SF2 produces salicylic acids, and another endophytic *A. xylosoxidans* strain 31A was reported to tolerate salinity (Sgroy *et al.*, 2009). Siderophores of *A. xylosoxidans* can act in biocontrol as a determinant of induced systemic resistance in the plant (Vaidya *et al.*, 2001, Forchetti *et al.*, 2007). Also, *A. xylosoxidans* Ax10 has solubilized inorganic phosphate and *A. xylosoxidans* Ax10 has the capability of producing indole acetic acid. In pot experiments, inoculation of *A. xylosoxidans* Ax10 significantly led to an increase of the root length, shoot length, fresh weight, and dry weight of *Brassica juncea* plants compared to the control (Ma *et al.*, 2009). Zhang *et al.* (2016) found that the culture filtrate of

* Corresponding author e-mail: walaanrc70@yahoo.com.

two bacterial strains *A. xylosoxidans* (09X01) and *Bacillus cereus* (09B18) caused high mortality of the second stage juvenile nematodes and reduced *in vitro* egg hatch compared to control.

Using the bacterial suspension simultaneously with nematodes and/or before nematode inoculation was more effective than adding after nematode inoculation. In addition, it recorded a significant increasing in nematode and plant parameters compared to the infected plant with nematodes (Soliman *et al.*, 2017).

Polyacrylamide gel electrophoresis (SDS-PAGE) is commonly employed in biological analysis to determine shifts in protein bands. These bands might be proteins or enzymes. Bio-stress, due to hormonal changes, could cause protein synthesis and enzymatic shifts (Ghasempour *et al.* 1998; Gianello *et al.* 2000; Ghasempour *et al.* 2001; Ghasempour and Kianian 2002; Ghasempour and Maleki 2003). The amount of soluble protein increases in desiccation-hardened plants and undergoes changes in electrophoretic mobility (Faw and Jung, 1972). Cloutier, (1983). detected quantitative changes in the electrophoretic patterns of the soluble proteins of different cultivars grown in different environments. Certain types of stressful environmental conditions can activate stress genes to produce stress proteins that enable organisms to tolerate such stresses. The electrophoretic banding patterns can be used for characterization and identification of eggplant cultivars (Sayed *et al.* 1998). Electrophoretic patterns of soluble proteins and isozymes are powerful tools for the study of genetic variability of cultivars (Barta *et al.*, 2003). Vyomesh *et al.* (2018) detected increasing number of bands in both cultivars upon transition from control to stress environment, and resistant cultivar showed more number of bands as compared to susceptible cultivar

The present study aimed to evaluate the efficacy of different application of *A. xylosoxidans* as bio-agent to maximize its efficiency against *M. incognita* infecting eggplant under greenhouse conditions. Also, this research attempted to study the effect of some different applications on eggplant gene expression via soluble protein analysis.

2. Materials and methods

The bacterial bio-agents *Achromobacter xylosoxidans* 19GES registered under accession number LC214968.1 in the GeneBank (USA) was obtained from previous studies and cultured on Luria broth medium at 30 °C. Luria broth (LB) medium is prepared from Tryptone 10 g, Yeast Extract 5 g, NaCl 5 g, 20 g up to 1000 ml of distilled water according to Davis *et al.* (1980).

2.1. Preparation of Nematode, *M. incognita* culture

The nematode population used in this research, *M. incognita*, was obtained from greenhouse culture of tomato plants which were maintained at Plant Pathology Department. The nematode eggs were extracted from infected roots of tomato in 0.5 % sodium hypochlorite on 25 µm sieve according to the method of Hussey and Barker (1973). The eggs were incubated at 27 °C inside incubator and hatched out the second- stage juveniles (*J*₂) by using Baermann plates.

A. xylosoxidans liquid culture was prepared and activated in (LB) medium. Plastic pots (15 cm diameter) filled with two kilograms of autoclaved soil, 1:1 mixture of

clay and sand, were prepared, and then the eggplant seedlings were transplanted. Pots were arranged in a randomized complete block design under greenhouse conditions at 28°C±2. All plants were watered after nematode inoculation and whenever needed. Six applications of *A. xylosoxidans* were applied in the soil:

The bacterial culture *A. xylosoxidans* was applied as soil drench application (a, b, c), barer root dipping (d and e) and foliar spreading as bio-agent to bio-control of *M. incognita* as follows:

- A. xylosoxidans* (B) inoculated seven days after the nematodes (N) inoculation (B after 7days N).
- Nematodes (N) added after seven days from the *A. xylosoxidans* (B) inoculation (N after 7days B).
- The nematodes (N) and *A. xylosoxidans* (B) inoculated simultaneously (N+B at same time).
- Barer root dipping treatment was given to seedling by immersing their roots in the *A. xylosoxidans* suspension for 30 minutes (Root dipping at 30 min.).
- Barer root dipping treatment was given to seedling by immersing their roots in the *A. xylosoxidans* suspension for 45 minutes (Root dipping at 45 min.).
- Foliar spreading of leaves plant (Foliar spreading with bacteria, *A. xylosoxidans*).
- Plant with nematodes (Infected plant).
- Plant without bacteria and nematodes (Untreated plant).

Applications of rhizobacterial bio-agents were performed by adding 1 ml of *A. xylosoxidans* (around 2×10⁸ cfu / ml) in 2 cm deep around each plant and covered with soil of a seedling at the time of transplant.

Barer root dipping treatment was given to seedling by immersing their roots in the culture of bacteria (2×10⁸ cfu /ml) for two times, 30 min and 45 minutes.

Nematode suspension of *M. incognita* (2000 *J*₂) was added to soil, where seedlings were planted in 2 cm deep around each plant and covered with soil. Plants infected with *M. incognita* and untreated with bacteria served as control. All pots were arranged in a randomized complete block design in a greenhouse at 28 ± 2 °C. Fifty days after nematode inoculation, eggplants were gently uprooted, and the roots were washed and cleaned from the adhering soil particles. The second- stage juveniles (*J*₂) in the soil were extracted by sieving and decanting technique (Barker, 1985) and examined under a light microscope using a Hawksley counting slide. Number of *J*₂ in soil, number of galls and number of egg masses were counted from the whole root system and indexed according to Sharma *et al.* (1994) scale as follows: 1 = no galls or egg-mass, 2 = 1 - 5, 3 = 6 - 10, 4 = 11 - 20, 5 = 21 - 30, 6 = 31 - 50, 7 = 51 - 70, 8 = 71 - 100 and 9 >100 galls or egg-mass / plant. Lengths, fresh and dry weights of both shoot and root systems were recorded.

2.2. SDS-Protein Electrophoresis

Samples of 1 g from leaves exposed to different applications of *A. xylosoxidans* as bio-agent against *M. incognita* infecting eggplant greenhouse conditions in different times were used for protein analyses by Sodium Dodecyl Sulfate –Polyacrylamide Gel Electrophoresis (SDS-PAGE). The protein analysis was performed according to the method of Laemmli (1970). Samples preparations and extraction of water-soluble proteins were performed according to Stegmann (1979). The gel was

photographed and scanned by Gel Doe Bio-Rad System (Gel- Pro analyzer V.3).

2.3. Statistical analysis

All data collected were subjected to analysis of variance (ANOVA) and significant means separated with Duncan Multiple Range Test (DMRT) at $P \leq 0.05$ levels according to Duncan (1955).

3. Results

3.1. Effect of different applications of bio-agent

Achromobacter xylosoxidans against root-knot nematodes *M. incognita* number of J_2 , galls, and egg-masses formation.

Effect of different applications of *A. xylosoxidans* as bio- control agent against *M. incognita* infected eggplant under greenhouse conditions is shown in Table (1). The

results indicated that all application of *A. xylosoxidans* culture had achieved significant reduction ($P < 0.05$) on root-knot nematode parameters as compared to untreated plant. *A. xylosoxidans* (N+B at same time) application was the most effective as reduction reached 79.80%, 71.09% and 78.26% on number of second-stage juveniles in soil, number of galls and number of egg-masses respectively. Application of nematodes after *A. xylosoxidans* (N after 7days B) comes next with some exceptions, recording 75.76%, 68.38% and 75.35% reduction on number of J_2 , number of galls and number of egg-masses, respectively, while the least effective application was in case of barer root dipping, where immersing of seedling root for 30 min. recorded 49.90%, 54.38% reduction in the number of J_2 and number of galls, respectively. Also, the same trend was noticed with respect to galls and egg-masses indexes.

Table 1. Effect of different applications of bio-agent *Achromobacter xylosoxidans* against root-knot nematodes *M. incognita* number of J_2 , galls, and egg-masses formation (after eight weeks applications).[#]

Treatment	No. J_2 200 g in soil	R%. R. %	No. galls / root system	R%. R. %	Root gall index**	No. egg-masses / root system	R%. R. %	Egg-mass index**
B after 7day N	128*c	74.14	51.00b	47.96	7	5.33c	76.83	3
N after 7day B	120d	75.76	31.33de	68.38	6	5.67c	75.35	3
N+B adding the same time	100e	79.80	28.33de	71.09	5	5.00c	78.26	2
Root dipping at 30	248b	49.90	45.00bc	54.08	6	7.00bc	69.57	3
Root dipping at 45 min	124cd	74.95	36.33cd	62.93	6	9.33b	59.43	3
Leaf spraying	123d	75.16	39.67cd	59.52	6	6.67bc	71.00	3
Infected plant	495a	----	98.00a	-----	8	23.00a	-----	5

[#] Values are average of five replicates. * Means followed by the same letter (s) are not significantly different according to Duncan's Multiple Range Test. ** Root galls and egg-masses indexes were determined. R. % = % Reduction.

3.2. Effect of different applications on bio-control efficacy of *A. xylosoxidans* against root-knot nematodes, *M. incognita* on the growth traits of infecting eggplant.

The results shown in Table (2) indicated that the influence of all different applications of *A. xylosoxidans* had increased growth parameters of eggplant significantly ($P < 0.05$). The data revealed that application of *A. xylosoxidans* (N+B at the same time) had achieved the

most effective application in increasing the length, fresh and dry weights of shoot and root length where they reached 58.57 %, 120.30 %, 130.26 %, 93.33 %, compared to other applications and infected plant (plant +nematodes). Generally, application of *A. xylosoxidans* in soil drenching and foliar spraying appeared more effective in increasing growth of eggplants compared to immersing of the seedling roots.

Table (2): Effect of different applications on bio-control efficacy of *Achromobacter xylosoxidans* against root knot nematode *Meloidogyne incognita* on the growth traits of infecting eggplant (after eight weeks of applications).[#]

Treatments	Shoot System				Root System					
	Length (cm)	% Inc.*	fresh weight(g)	% Inc.	Dry weight(g)	% Inc.	Length (cm)	% Inc.	fresh weight(g)	% Inc.
B after 7 days N	24.25*b	38.57	3.13bc	54.95	1.19b	56.58	14.75ab	51.28	2.06bc	19.84-
N after 7days B	26.00 ab	48.57	3.39b	22.28	1.31b	72.37	12.75bc	30.77	2.12bc	-17.51
N+B adding in the same time	27.75a	58.57	4.45a	120.30	1.75a	130.26	18.85a	93.33	2.03c	-21.10
Root dipping at 30 min	18.25c	4.23	3.26b	61.39	1.14bc	50.00	12.75bc	30.77	2.38ab	7.39-
Root dipping at 45 min	20.00c	14.29	2.47c	22.28	1.17bc	53.95	17.75a	82.05	2.23bc	-13.23
Leaf spraying	24.00b	37.14	2.47c	22.28	1.46ab	92.11	16.25ab	66.67	2.33ab	9.39-
Untreated plant	19.00	8.57	3.53		1.50		11.25	15.38	2.18 bc	-15.18
Infected plant	17.50c		2.02c		0.76c		9.75c		2.57a	

[#] Values are average of five replicates. * Means followed by the same letter (s) are not significantly ($P \leq 0.05$) different according to Duncan's Multiple Range Test. % Inc* = Increase over control.

3.3. Effect of *A. xylosoxidans* applications on infected eggplant gene expression by SDS-PAGE:

3.3.1. After one week

Protein profile was performed to detect the biochemical differences due to the different applications of *A. xylosoxidans* as a bio-agent against *M. incognita* which infects eggplant in greenhouse conditions compared with untreated plants and infected plants as shown in Figure (1) and Table (3). The results revealed clear differences in the number and molecular weights of protein bands, 15 bands were found ranging from 17 to 145 kDa. were polymorphic (100% polymorphism). The highest number of protein bands was found in the (root dipping 45 min.)

application (12 bands), followed by (B after 7 days N) application (11 bands) while the lowest number of bands was observed in the infected plant (4 bands). In addition, the application of *A. xylosoxidans* (N+B at same time) displayed eight protein bands. One band with M.W. 145 kDa. appeared in the infected plant but was absent in untreated plant and the rest of applications. On the contrary, two bands at 39 and 24 kDa. were found in untreated plant, leaf spraying and root dipping 45 min. applications, but absent in the infected plant. Also, four bands at M.W. 55, 53, 47 and 43 kDa were produced by untreated plant in normal conditions and all applications but were absent in infected plant.

Table 3: Densitometric analysis represents leaf water soluble-protein electrophoretic patterns for eggplant under normal and different applications after one week.

B.N	M.W.	Untreated plant	Infected plant	B after 7 days N	N after 7 days B	N+B at same time	Root dipping 30 min	Root dipping 45 min	Leaf spraying
1	145	0	1	0	0	0	0	0	0
2	78	0	0	1	0	0	0	0	0
3	67	1	0	1	1	1	1	1	1
4	62	0	0	1	0	0	0	0	0
5	55	1	0	1	1	1	1	1	1
6	53	1	0	1	1	1	1	1	1
7	47	1	0	1	1	1	1	1	1
8	43	1	0	1	1	1	1	1	1
9	39	0	0	0	0	0	0	1	1
10	31	1	0	1	0	0	0	1	0
11	29	1	1	1	0	1	0	1	1
12	26	1	1	1	0	1	1	1	1
13	24	0	0	0	0	0	0	1	1
14	20	1	1	1	0	1	1	1	0
15	17	1	0	0	0	0	0	1	0
Number of Bands		10	4	11	5	8	7	12	9

1 = Presence of band

0 = absence of band

B,N = Band Number

M.W. =Molecular weight

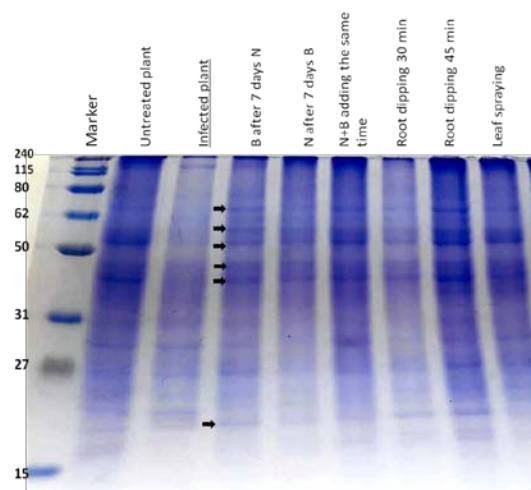


Figure 1. SDS-PAGE of leaf water-soluble protein electrophoretic patterns for eggplant under normal and different applications after one week.

3.3.2. after two weeks of application

Figure (2) and table (4) showed the protein profile of different applications compared with the infected plant (plants + nematode). A total of 12 bands were found in protein pattern ranging from 140 to 19 kDa. Only one band was monomorphic (8.33%) while eleven were polymorphic (91.67% polymorphism). The highest number of protein bands was 11 bands observed in the application of *A. xylosoxidans* (N+B at same time), three of them at M.W. (140, 27 and 21 kDa. respectively) were not detected in untreated plant and the rest of applications, followed by (B after 7 days N) application (six bands). The lowest number of bands (two bands) was observed in the infected plant (plant + nematode). The exposure of plants to stress during root dipping for 45 min. in the bacterial suspension prior to transplantation caused weakness of plants sample, which made it impossible to take sample leaves for protein electrophoresis. We expect that exposure of the plants to this period of time 45 min. is too much, so the bacterial suspension does reverse action to the plants.

Table 4. Densitometric analysis represents leaf water-soluble protein electrophoretic patterns for eggplant under normal and different applications after two-week application.

B.N	M.W	Infected plant	B after 7 days N	N after 7 days B	N+B adding the same time	Root dipping 30 min	Leaf spraying	Untreated plant
1	140	0	0	0	1	0	0	0
2	80	0	1	1	0	0	0	0
3	50	0	1	1	1	1	1	1
4	46	0	1	1	1	1	1	1
5	43	0	1	1	1	0	0	1
6	31	1	1	1	1	1	1	1
7	33	1	0	0	1	0	0	0
8	27	0	0	0	1	0	0	0
9	23	0	0	0	1	0	1	1
10	22	0	1	0	1	0	0	0
11	21	0	0	0	1	0	0	0
12	19	0	0	0	1	0	0	1
Number of Bands		2	6	5	11	3	4	6

1 = Presence of band

0 = absence of band

B,N = Band Number

M.W. =Molecular weight

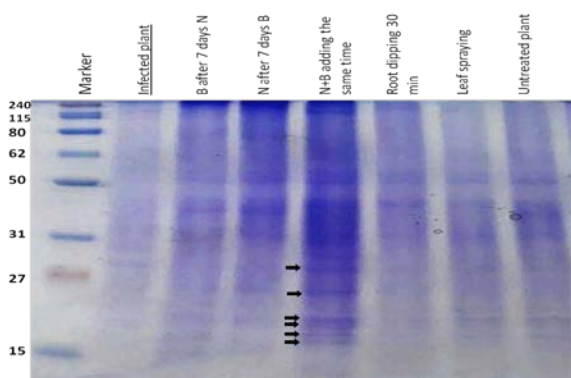


Figure 2. SDS-PAGE of leaf water soluble protein electrophoresis patterns for eggplant under normal and different application after two weeks

3.3.3. End of the experiment (after eight weeks)

Electrophoresis patterns for eggplant under normal and different applications at the end of experiment are shown in Figure (3) and Table (5). The results showed that most of the extracted proteins migrated in the range from 151 to 22 kDa. with total number of 10 bands were polymorphic (100% polymorphism). The highest number of protein polypeptides was found in (N+B at same time) application (7 bands), while the lowest number of bands was observed in the (infected plant) and (root dipping 45 min. application) one band.

Table 5. Densitometric analysis represents leaf water-soluble protein electrophoretic patterns for one eggplant variety under normal and different applications after eight- weeks of experiment.

B.N	M.W	Infected plant	B after 7 days N	N after 7 days B	N+B adding the same time	Root dipping 30 min	Root dipping 45 min	Leaf spraying	Untreated plant
1	151	1	0	0	0	0	0	0	0
2	57	0	1	1	1	1	1	1	1
3	56	0	0	0	1	0	0	0	0
4	44	0	0	1	1	1	1	0	1
5	42	0	0	0	1	1	0	0	0
6	41	0	0	1	0	1	1	0	1
7	29	1	0	0	0	0	0	0	0
8	25	0	0	1	1	1	1	0	1
9	23	0	0	0	0	1	0	0	0
10	22	1	0	1	0	1	1	0	1
Number of Bands		3	1	5	5	7	5	1	5

1 = Presence of band

0 = absence of band

B,N = Band Number

M.W. =Molecular weight

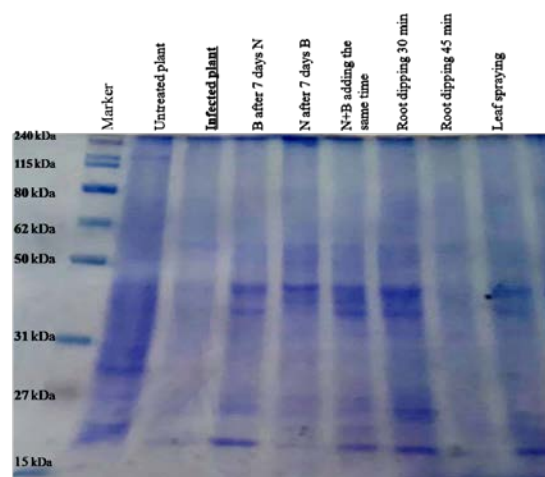


Figure 3. SDS-PAGE of leaf water soluble-protein electrophoresis patterns for one eggplant variety under normal and different application after eight-week of the experiment.

4. Discussion

Plant parasitic nematodes, root-knot nematode (*Meloidogyne incognita*), is one of the most important nematodes associated with low production (Kayani *et al.*, 2017).

Biological control of plant-parasitic nematodes through microorganisms offers an alternative or supplemental management tool to replace chemical methods. Use of biological control agents is considered to be innocuous and economically feasible (Mukhtar *et al.*, 2017). *A. xylosoxidans* can be considered as a potential biocontrol agent to control plant pathogens and improvement of plant growth. These results agreed with those Vaidya *et al.* (2001), Forchetti *et al.* (2007) and Zhang *et al.* (2016). Moreover, Zhang *et al.* (2016) found that the culture filtrate of *A. xylosoxidans* (09X01) strain caused high mortality of the second stage juvenile nematodes and reduced in vitro egg hatch compared to control. The present data are in agreement with Soliman *et al.* (2017) who reported that applying bacterial suspensions simultaneously with nematodes and or before nematode inoculation was more effective in reducing nematode infection than in case of adding after nematode inoculation compared to the infested plant with nematodes and without bacteria.

The application of *A. xylosoxidans* (N+B at the same time) had more effective application in increasing the length, fresh and dry weights of shoot and root length compared to other applications and infested plant (plant +nematodes). The present data agreed with Khan and Tarannum (1999) who reported that root dip treatment was relatively less effective in enhancing the plant growth and yield of tomato compared to soil application. This effect was due to a higher and more uniform distribution of bacterial cells in the root zone during the entire growth period, whereas with root dip treatment, fewer cells may have remained available to the entire root -system. Soliman *et al.* (2017) found the soil where bacterial suspension was applied simultaneously with nematodes and or before nematode inoculation was more effective than adding the bacterial suspension after nematode inoculation. The used applications recorded a significant

increase in the shoot and root lengths and weights when compared to untreated control. The results of soluble protein electrophoresis indicated that the infested plant (plant + nematodes) gave the lowest number of bands in all stages of applications (9 bands). Four bands at M.W. 55, 53, 47 and 43 kDa. Were produced by untreated plant in normal conditions and all application but were absent from infested plant, which indicates the negative effect of nematodes on the infested plant and its inability to produce important proteins for its growth and development in the absence of the bacterium bio-agent. This indicates the importance of applying the bacterium strain *A. xylosoxidans* which helped the plant to produce these important proteins, and the effectiveness of the application was clear in increasing the length, fresh and dry weights of shoot and root length which had high records more than records with infested plant. On the other hand, the application of *A. xylosoxidans* (N+B at same time) showed the highest number of bands in all total stages of experiment (26 bands), three of them at M.W. (140, 27, 21 kDa. respectively) were unique bands and appeared after two weeks but were not detected in untreated plant and the rest of applications. We suggested these bands may be related to gene resistance in plant. The results of electrophoresis coincided with those of greenhouse experiments where bacteria (*A. xylosoxidans*) strain was applied as a bio-agent against nematodes infecting eggplant. The application of *A. xylosoxidans* was generally effective and had achieved reduction of the number of second-stage juveniles in the soil, gall number and number of egg-masses. In addition, this application gave clear increasing in shoot and root lengths and fresh and dry weights compared with the infested plant. The treatment of *A. xylosoxidans* (N+B at the same time) was the most effective application which achieved reduction of 79.80%, 71.09% and 78.26% in the number of second-stage juveniles in the soil, galls number and number of egg-masses, respectively. Moreover, the data revealed that the application of *A. xylosoxidans* (N+B at the same time) achieved clear increasing in length, fresh and dry weights of shoot and root length were recorded 58.57%, 120.30 %, 130.26% and 93.33%, comparedg with the infested (plant + nematodes).

Finally, the increase or decrease in number of protein bands refers to the induction or inhibition of the resistance genes and this change was reflected on plant growth. This result agreed with results obtained by (Faw and Jung, 1972 and Cloutier 1983) who found that the amount of soluble protein increases in desiccation-hardened plants and undergoes changes in electrophoretic mobility detected quantitative changes in the electrophoretic patterns of the soluble proteins of different cultivars grown in different environments; and agreed with those of (Ghasempour and Maleki 2003). The bands obtained might be proteins or enzymes. Bio-stress, due to hormonal changes could cause protein synthesis and enzymatic shifts. The result agreed with those of Vyomesh *et al.* 2018 who detected increasing number of bands in both the cultivars upon transition from control to stress environment and resistant cultivar showed more number of bands as compare to susceptible cultivar

5. Conclusion

In conclusion, the best application of the bacterium strain *A. xylosoxidans* when added with the nematode *Meloidogyne incognita* at the same time, followed by add nematodes (N) after seven days from the *A. xylosoxidans* (B) inoculation, (N after 7days B). This application improved its efficiency as a bio-agent compared to other applications, and could be used as a safe biological alternative to chemical nematicides for suppressing root knot nematode reproduction and improving plant growth parameters. It was found that the best time to study protein bands which produce under nematodes stress and application was after one and two weeks.

Practically, the authors recommend applying the bio-agent *A. xylosoxidans* as soil drench at the time of planting or transfer of plant for protection against *Meloidogyne incognita* infection.

Reference

- Barker TR. 1985. Nematode extraction and bioassays. In: An Advanced Treatise on *Meloidogyne* Vol. II, Barker, T. R., Carter, C. C. and Sasser, J. N. (Eds.). North Carolina University, Graphics, Raleigh, N.C. pp. 19-35.
- Barta J, Curn V and Divis J. 2003. Study of biochemical variability of potato cultivars by soluble proteins, isoenzymes and isoperoxidase electrophoretic patterns. *Plant Soil Environ*, **49**: 230-236.
- Cloutier Y. 1983. Changes in the electrophoretic patterns of the soluble proteins of winter wheat and rye following cold acclimation and desiccation stress. *Plant Physiol*, **71**: 400-403.
- Davis RW, Botstein D and Rotho JR. 1980. Transfection of DNA in Bacterial Genetics: A Manual for Genetic Engineering Advanced Bacterial Genetic. Cold Spring Harbor laboratory cold spring harbor, New York, **67**: 134-137.
- Duncan D B. 1955. Multiple range and multiple F tests. *Biometrics*, **11**: 1-42.
- El-Nagdi MAW, Abd-El-Khair H, Soliman M Gaziea, Ameen HH and El-Sayed M G. 2019. Application of protoplast fusions of *Bacillus licheniformis* and *Pseudomonas aeruginosa* on *Meloidogyne incognita* in tomato and eggplant. *Middle East J of Appl Sci*, **9** (2): 622-629.
- Faw WF and Jung GA. 1972. Electrophoretic protein patterns in relation to low temperature tolerance and growth regulation of alfalfa. *Cryobiol*, **9**: 548-555.
- Forchetti G, Masciarelli O, Alemanno S, Alvarez D and Abdala G., 2007. Endophytic bacteria in sunflower (*Helianthus annuus* L.): isolation, characterization, and production of jasmonates and abscisic acid in culture medium. *Appl Microbiol Biotechnol*, **76**: 1145-1152.
- Ghasempour HR and Kianian J. 2002. Drought stress induction of free proline, total proteins, soluble sugars and its protein profile in drought tolerant grass *Sporobolus elongates*. *J. Sci. Teacher Training Univ*, **1**: 111-118 .
- Ghasempour HR, and Maleki M. 2003. A survey comparing desiccation tolerance in resurrection plant *Notholaena vellea* and studying its protein profile during drought stress against a non resurrection plant *Nephrolepis* sp. *Iranian J. Biol*, **15**: 43-48.
- Ghasempour HR, Anderson EM and Gaff Donald F. 2001. Effects of growth substances on the protoplasmic drought tolerance of leaf cells of the resurrection grass, *Sporobolus stapfianus*. *Aust J Plant Physiol*, **28**: 1115-1120 .
- Ghasempour HR, Anderson EM, Gianello RD and Gaff DF. 1998. Growth inhibitor effects on protoplasmic drought tolerance and protein synthesis in leaf cells of resurrection grass, *S. stapfianus*. *J Plant Growth Regul*, **24**: 179-183.
- Gianello RD, Kuang J, Gaff DF, Ghasempour HR, Blomstedt CK and Hamill JD. 2000. Proteins correlated with desiccation tolerance in a resurrection grass *S. stapfianus*. Chapter 20. Scientific Publishers, Oxford, pp: 161-166.
- Giannakou IO, Karpouzas DG, Prophetou-Athanasiadou D. 2004. A novel non-chemical nematicide for the control of root-knot nematodes. *Appl. Soil Ecol*. **26**:69-79.
- Hussain MA, Mukhtar T, Kayani MZ, Aslam MN and Haque MI. 2012. A survey of okra (*Abelmoschus esculentus*) in the Punjab province of Pakistan for the determination of prevalence, incidence and severity of root-knot disease caused by *Meloidogyne* spp. *Pak J Bot*, **44**(6): 2071-2075.
- Hussey RS, and Barker KR. 1973. A comparison of methods of collecting inocula for *Meloidogyne* spp. including a new technique. *Plant Dis Rep*, **57**: 1025-1028.
- Ismail AE, Soliman M Gaziea, and Badr UM. 2018. Genetic improvement of nematotoxicity of *Serratia liquefaciens* against *Meloidogyne incognita* infected eggplant by gamma irradiation in Egypt. *Pakistan J Parasitol*, **66**(3):28-38.
- Kassab SA, Eissa MF, Badr UM, Ismail AE, Abdel Razik BA and Soliman GM. 2017. The nematicidal effect of a wild type of *Serratia marcescens* and their mutants against *Meloidogyne incognita* juveniles. *Egyptian J Agronematol*, **16**: 95-114.
- Kayani MZ, Mukhtar T and Hussain MA. 2017. Interaction between nematode inoculum density and plant age on growth and yield of cucumber and reproduction of *Meloidogyne incognita*. *Crop Prot*, **92**: 207-212.
- Khan M R and Tarannum Z. 1999. Effects of field application of various micro-organisms on *Meloidogyne incognita* on tomato. *Nematol medit*, **27**:233-238.
- Kloepper JW, Zablowicz RM, Tipping B, Lifshitz R.1991. Plant growth mediated laboratory cold spring harbor, New York., **67**: 134-137.
- Laemmli UK. 1970. Cleavage of structural proteins during the assembly of the head of bacteriophage T4. *Nature*, **227**: 680-685.
- Mukhtar T, Hussain MA and Kayani MZ. 2017. Interaction between nematode inoculum density and plant age on growth and yield of cucumber and reproduction of *Meloidogyne incognita*. *Bragantia*, **75**: 108-112.
- Mukhtar T, Kayani MZ and Hussain MA. 2013. Nematicidal activities of *Cannabis sativa* L. and *Zanthoxylum alatum* Roxb. against *Meloidogyne incognita*. *Ind. Crops Prod*, **42**: 447-453.
- Sayed M, Zain H and MimiL I. 1998. Variability in Eggplant (*Solanum melongena* L.) and its nearest wild species as revealed by Polyacrylamide Gel electrophoresis of seed protein perianth. *J Trop Agric Sci*, **21**(2): 113 - 122.
- Sgroy V, Cassán F, Masciarelli O, Del Papa M F, Lagares A and Luna V. 2009. Isolation and characterization of endophytic plant growth-promoting (PGPB) or stress homeostasis-regulating (PSHB) bacteria associated to the halophyte *Prosopis strombulifera*. *Appl Microbiol Biotechnol*, **85**:371-381.
- Soliman M. Gaziea, Ameen H Hoda and El kelany U S. 2017. Effect of treatment time on biocontrol efficacy of *Bacillus amyloliquefaciens*, *Lysinibacillus sphaericus* and their fusions against root knot nematode *Meloidogyne incognita* infecting tomato plants. *Middle East J Agri Res*, **6** (2): 369-375.
- Stegmann H.1979. Electrophoresis and focusing in slabs using the Pantaphor apparatus for analytical and preparative separations in gel (Polyacrylamide, Agarose, Starch, Sephadex). Messweg 11, D-3300, Braunschweig Institute of Biochemistry, West-Germany, pp: 1-29.

- Tian B, Yang HJ and Zhang K. 2007. Bacteria used in the biological control of plant parasitic nematodes: populations, mechanisms of action, and future prospects. *Microbial Ecol*, **61**:197.
- Vaidya R JI, Shah M, Vyas P R and Chhatpar HS. 2001. Production of chitinase and its optimization: from a novel isolate *Alcaligenes xylooxidans*: Potential in antifungal biocontrol. *World J Microbiol Biotech*, **17**:691-696.
- Vyomesh SP, Pitambara and Shukla YM. 2018 Proteomics study during root knot nematode (*Meloidogyne incognita*) infection in tomato (*Solanum lycopersicum* L.). *J of Pharmacog Phytochem.*, **7** (3): 1740-1747
- Youssef MMA, Mohammed MMM and Korayam AM. 2012. Effect of organic and inorganic fertilizers on *Meloidogyne incognita* infesting sugar beet. *Pak J Nematol*, **30** (2): 143-149.
- Yuen GY and Schroth MN. 1986. Inhibition of *Fusarium oxysporum* f. sp. *dianthi* by Iron competition with an *Alcaligenes* sp. *Phytopathology*, **76**:171-176.
- Zhang J Yonghui Li, Hongxia Y , Bingjian S , Honglian Li. 2016. Biological control of the cereal cyst nematode (*Heterodera filipjevi*) by *Achromobacter xylooxidans* isolate 09X01 and *Bacillus cereus* isolate 09B18. *Biol Control*, **92**: 1–6.

A Preliminary Assessment on the Habitat Use of Carnivores in Al Mujib Biosphere Reserve Using Camera Trapping

Nashat Hamidan¹, Zuhair S. Amr^{2,*} and Mohammad A. Abu Baker³

¹Royal Society for the Conservation of Nature, Amman, Jordan, ²Department of Biology, Jordan University of Science and Technology, Irbid, Jordan, ³Department of Biology, the University of Jordan, Amman, Jordan

Received September 25, 2019; Revised November 3, 2019; Accepted November 13, 2019

Abstract

Carnivore populations in Jordan are on the decline due to continuous habitat loss, fragmentation, and human persecution. Monitoring movement patterns and habitat preferences through noninvasive methods is important to plan effective conservation programs within protected areas. We conducted a camera trap survey of carnivores in Al Mujib Biosphere Reserve, an arid sandstone habitat in southwestern Jordan. Six species were detected: the red fox, caracal, Afghan fox, striped hyena, grey wolf, and the wild cat. Detection of carnivores was higher at night, yet several were active during the day. Captures were also highest within the wilderness zone of the reserve. Most species showed higher preference for wadi systems which provided corridors for movement across their wide ranges and for stalking prey. This is the first study to monitor carnivore distribution and habitat use within protected areas in Jordan using noninvasive survey methods. It provides crucial data through relatively rapid means to assess reserve effectiveness and guide management efforts such as a land use planning within the reserve.

Keywords: camera trapping, carnivores, habitat use, Al Mujib Biosphere Reserve, Jordan, protected area.

1. Introduction

With the current advances in measuring and monitoring mammalian diversity, noninvasive techniques have been developed to reduce disturbance and document the presence of trap-shy and rare species (Kelly *et al.*, 2012; Kays and Slauson, 2008; Long *et al.*, 2008; Saleh *et al.*, 2018). Remote camera trapping is considered an excellent tool for estimating species richness and abundance, habitat use, activity pattern, behavioral ecology and population dynamics (Trolle and Kery, 2005; Lyra-Jorge *et al.*, 2008; Rowcliff and Carbone, 2008; Rowcliffe *et al.*, 2008). It can also provide valuable information for evaluating conservation efforts (Tobler *et al.*, 2008; Balme *et al.*, 2009). The method proved to be useful for studying mammals within protected areas in the Middle East (Cunningham and Wronski, 2009; Abi-Said and Amr, 2012; Ahmed *et al.*, 2016) and provided an exciting transition in wildlife survey methods (Burton *et al.*, 2015).

The carnivores of Jordan were studied extensively over the past three decades using conventional observational and capture methods (Qumsiyeh *et al.*, 1993, Amr *et al.*, 1996; Bunaian *et al.*, 2001; Abu Baker *et al.*, 2004; Qarqaz *et al.*, 2004). Yet, no studies were conducted to monitor the distribution and habitat use of carnivores within protected areas using noninvasive methods. The present study provides crucial preliminary data on the distribution and habitat use of carnivores in Al Mujib Biosphere Reserve in the context of the reserve zoning plan. The study aims to address the relationship between the degree

of protection and the diversity of carnivores in protected areas.

2. Material and Methods

2.1. Site Description

The study site covered an area of approximately 85 km² from the western lower part of Al Mujib Biosphere Reserve. The Reserve is located at the shoreline of the Dead Sea covering an area of 212 km². The highest elevation of the study site starts at 260 m at the eastern site and continues west to reach -420 m below sea level at the western border of the reserve. The reserve is located at the lowest elevation on earth within the Sudanian Penetration biogeographical zone and is characterized by hot summer and warm winter. Three vegetation types dominate the study site including the saline vegetation, the semitropical vegetation, and the water vegetation in the wadis (Al-Eisawi, 2014). The site is dominated by sandstone escarpments characterized by deep slopes and hard terrain especially at the eastern parts, intermixed toward the north-west with large amount of sedimentary hills of Tethys origin locally known as Sab'e Al-Wedyeh (the seven wadis). Nine wadis cross the study area from east to west: Wadi Al-Mujib is one of the oldest wadis at the eastern site of the Rift Valley (Barberi *et al.*, 1979; Abed, 2000). Other wadis include Zarga Maine, Zara, Zgara, Atoun, Abu Irtimih, Um Ghreiba, Hidan, Um Zghaib, and Shgaig.

* Corresponding author e-mail: amrz@just.edu.jo.

The biosphere reserve is governed by a zoning plan that fits with the biosphere designation. Three different zones were identified according to their accessibility and use: Intensive use zone at the outer edge of the reserve, semi-intensive use zone that acts as transitional zone between the semi intensive and the core wilderness zone, and the core wilderness zone where minimum use is practiced except for conservation of wildlife (Figure 2).

2.2. Camera Trapping

Thirty-one Browning Trail Cameras (BTC-6hd) were used during the study period between September 2015 and May 2016. Camera setting mode was set for three photos at each trigger, with five seconds delay between events day and night. Cameras were installed in rock crevices about one meter above ground. Cameras were placed within three designated land use zones in the reserve: 13 in the wilderness, seven semi-intensive use, eight in the intensive use area, and 3 between the wilderness and the semi intensive use zones as shown in Table 1. Animal diversity was calculated using the number of camera trap photos as an estimate for its abundance and the total number of species captured by each camera as an estimate for species richness in the camera site. Species diversity was calculated using Simpson's Diversity Index (SDI). The number of trap nights in each site was used to control for the variation in the effort between the sites.

Table 1. Description of sites and number of cameras used in Al Mujib Biosphere Reserve.

Site	No. of cameras	Description
Wadi Abu Nkhalah	1	Wadi with dense vegetation wide about 4-8 m wide
Al Addadeh	1	Mountain ridge, with steep cliffs facing west, hard terrain intermix with rich vegetation
Al Menqat'ah	2	Mountain ridge overlooking the Mujib wadi system
Marah	4	Open area
Qanani al Hirbah	1	Cliffs with erosion
Qullat Awad	2	Highest peaks on the western side sand stone
Raddas vicinity	4	Open rocky area
Seba'a Wedyeh	1	Sedimentary hills extending from east to west
Um Skhaib	5	Sand stone out crops, deepest wadis with sharp mountain ridges

3. Results

3.1. Species Diversity and Spatial Distribution

The results of camera trapping lasted for 5202 trapping nights, with a total of about 40,000 photos. They were filtered to 2947 informative photos, with only 67 photos for wild carnivores.

A total of six species of wild carnivores were documented in Al Mujib Biosphere Reserve (Figure 1, Table 2), including three canids, two felines and one hyena. During the study period, a total of 67 photos were captured. By far, the red fox, *Vulpes vulpes*, was the most captured species with 49 observations (73.13%), while the wild cat, *Felis silvestris*, was the least species with a single observation (1.5%).

Table 2. Frequency of carnivores photo-trapped in Al Mujib Nature Reserve.

Species	No. of photos	%
<i>Vulpes vulpes</i>	49	73.13
<i>Vulpes cana</i>	5	7.47
<i>Canis lupus</i>	2	2.98
<i>Caracal caracal</i>	6	8.95
<i>Felis silvestris</i>	1	1.50
<i>Hyaena hyaena</i>	4	5.97

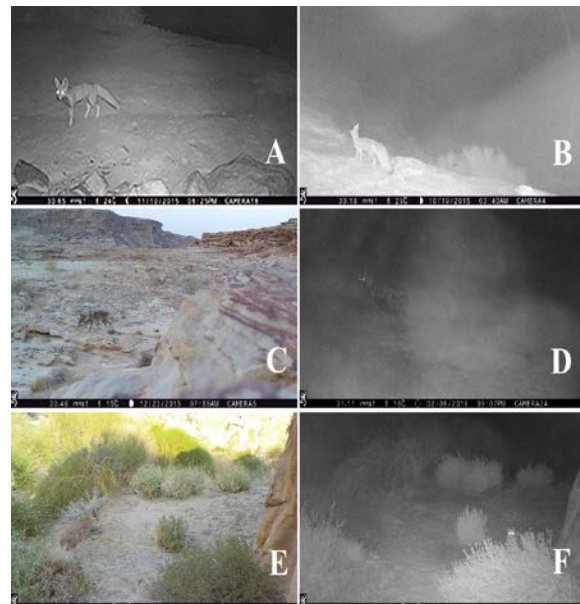


Figure 1. Carnivores captured by camera traps in Al Mujib Biosphere Reserve. **A.** *Vulpes vulpes* in Al Menqat'ah. **B.** *Vulpes cana* in Um Skhaib. **C.** *Canis lupus* in Um Skhaib. **D.** *Hyaena hyaena* in Al Menqat'ah. **E.** *Caracal caracal* in Wadi Abu Nkhalah. **F.** *Felis silvestris* in Wadi Abu Nkhalah.

Detection of carnivores was higher at night, yet several were active during the day. *Vulpes vulpes* was encountered in all types of habitats including open areas and wadi systems. It was found in photo-trapped in 18 locations representing all zones of land use (intensive and semi-intensive, wilderness use). *Vulpes cana* was photographed in four locations around sandstone mountains and cliffs, three and one in the wilderness and intensive zones respectively. The wolf, *Canis lupus*, was found in two locations in the wilderness zone. *Caracal caracal* was located in only one site at the edge of both wilderness and intensive zones. It was photographed along wadi systems that are used by the ibex with relatively rich vegetation cover. *Hyaena hyaena* was spotted in three sites; two within the wilderness zone and one in semi-intensive zone.

Species diversity was highest (SDI 0.24-0.5) in the wilderness zone (Al Mrah, Qanani al Hirbah), and the least in the intensive use zone (SDI 0-0.095). Fourteen cameras recorded only one species; seven in the wilderness, two in the semi intensive, three intensive and two at the edge of both wilderness and semi intensive zones. Six cameras photographed two species; three in the wilderness, two in the semi intensive and one in the intensive zones. Variation in species diversity among the different land use zones is expressed in Figure 2.

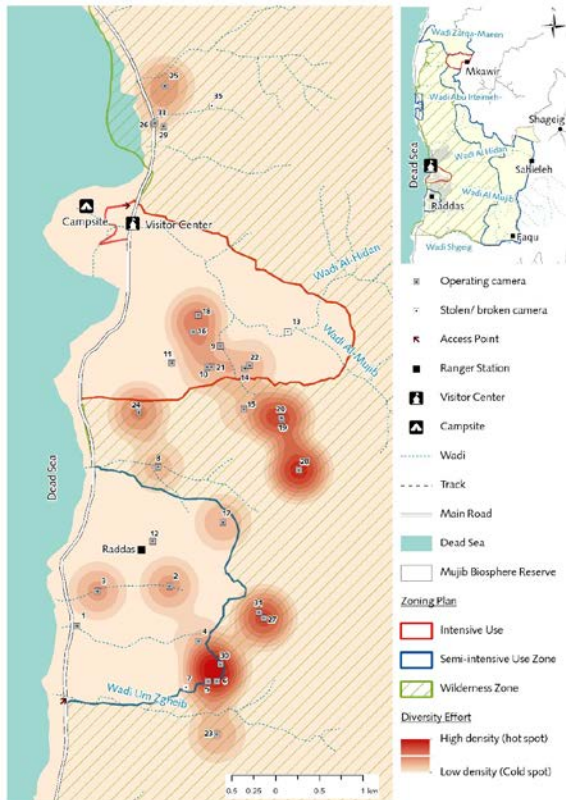


Figure 2. Heat map showing carnivores species diversity in Al Mujib Biosphere Reserve according to zones.

3.2. Seasonal activity patterns

Seasonal activity patterns and diversity of carnivores throughout the study period was highest during the cold winter months (Table 3). Between December and March, 3-5 species were detected, whereas only two were trapped between September and November. The red fox, *V. vulpes*, was recorded throughout the study period. The caracal was observed in the coldest months of the year, with highest number (3) of observations in March.

Table 3. Seasonal activity patterns of carnivores at Al Mujib Biosphere Reserve though out the study period.

Month	<i>C. caracal</i>	<i>C. lupus</i>	<i>F. silvestris</i>	<i>H. hyaena</i>	<i>V. vulpes</i>	<i>V. cana</i>
January	1	0	0	1	5	0
February	1	0	1	1	1	1
March	3	1	0	0	3	0
September	0	0	0	1	3	0
October	0	0	0	0	16	4
November	1	0	0	0	11	0
December	0	1	0	1	10	0

4. Discussion

The present study documents the presence and distribution of carnivores in Al Mujib Biosphere Reserve. Evidently, the red fox, *V. vulpes* was the most common species. This species has a wide spectrum of diet and can survive in all types of habitats in Jordan. Similar results were obtained in the eastern desert and Dana Biosphere reserve (Amr *et al.*, 1996; Bunaian *et al.*, 2001). *Vulpes cana* is associated with sand stone habitat, and was previously reported from around sharp edges and cliffs of different altitudes of Paleozoic sandstone mountains in Al

Mujib Biosphere Reserve, whereas only six individuals were captured during 461 trap nights (Abu Baker *et al.*, 2004). Detection by camera traps suggests that most species showed higher preference for the wadi systems and secluded canyons which provided corridors for movement across their wide ranges and for stalking prey. It seems that the reserve is used by both *C. lupus* and *C. caracal* as feeding grounds, as they ascend from the rocky areas to the west, where they seek large mammals as the Nubian ibex, *Capra nubiana*. The ibex population in Al Mujib Biosphere Reserve is one of the healthiest and most protected in Jordan. Both predators have a wide home range; $34.6 \pm 19.5 \text{ km}^2$ for *C. lupus* (Hefner and Geffen, 1999) and $270\text{-}1116 \text{ km}^2$ for *C. caracal* (van Heezik and Seddon, 1998).

Habitat use and distribution of carnivores can be used to measure management effectiveness within protected areas due to their important role in terrestrial ecosystems and sensitivity to man-made threats such as poaching and habitat loss (Li *et al.*, 2012). Spatial patterns in species diversity drawn from camera trap photos can be used to guide conservation efforts and reserve effectiveness when quantified on spatially explicit maps. The zoning and the degrees of protection have advantages for conserving carnivores by reducing the costs of intensive conservation measures to limited areas, and can provide simple managements procedures in areas of conflicts (Linnell *et al.*, 2005). The current zoning of Al Mujib Biosphere Reserve reflects the effect of conservation on the diversity of carnivores, where the highest diversity was found within the wilderness zones, and the least in the intensive use areas (Fig. 2). In the wilderness zone, no human activities are allowed except for patrolling and research, thus more conservation efforts are implemented, while in the intensive zone, tourism and grazing are allowed. The semi intensive zone is open for eco-tourism only with low patrolling efforts. Conflicts with humans should be minimized in order to protect some of the endangered species of carnivores such as the caracal. This was also observed by Johnson *et al.* (2006) and Carter *et al.* (2012), where they reported that abundance of *Panthera tigris* was related human population and disturbance.

Long-term use of camera-traps proved to be an excellent tool for wildlife monitoring as it can provide quantitative data on spatial patterns of habitat use. This approach can effectively quantify species diversity and habitat use on spatially explicit maps to develop recommendations for managers to improve the degree of protection and land use within protected areas. Noninvasive studies are especially useful in arid environments where animals are rare and disperse over wide ranges. Camera-trapping surveys may be the most effective method in detecting carnivore species (Gecchele *et al.*, 2017). Comparative studies in other protected areas in Jordan should be carried out to relate the effect of conservation and zoning on wildlife.

Acknowledgement

We are grateful to the staff at the Conservation and Monitoring Center and Al Mujib Biosphere Reserve (Royal Society for the Conservation of Nature) for providing access to the site and logistical support, and Mrs. Natalia Boulad for her help in preparing the map.

References

- Abed, AM. 2000. **Geology of Jordan**. Jordanian Geologists Association, Amman, 571 pp.
- Abi-Said M and Amr ZS. 2012. Camera trapping in assessing diversity of mammals in Jabal Moussa Biosphere Reserve, Lebanon. *Vert Zool.*, **62**:145–152.
- Abu Baker M, Al Omari K, Qarqaz M, Khaled Y, Yousef M and Amr Z. 2004. On the current status and distribution of Blanford's Fox, *Vulpes cana* Blanford, 1877, in Jordan (Mammalia: Carnivora: Canidae). *Turk J Zool.*, **28**:1–6.
- Ahmed S, Al Zaabi R, Soorae P, Shah JN, Al Hammadi E, Pusey R and Al Dhaheri S. 2016. Rediscovering the Arabian sand cat (*Felis margarita harrisoni*) after a gap of 10 years using camera traps in the Western Region of Abu Dhabi, United Arab Emirates. *Eur J Wild Res.*, **62**:627–631.
- Al-Eisawi D. 2014. Vegetation Community Analysis in Mujib Biosphere Reserve, Jordan. *Jordan J Nat Hist.*, **1**:35–58.
- Amr ZS, Kalishaw G, Yosef M, Chilcot BJ and Al-Budari A. 1996. Carnivores of Dana Nature Reserve (Carnivora: Canidae, Hyaenidae and Felidae), Jordan. *Zool Middle East*, **13**:5–16.
- Balme G, Hunter LTB and Slotow R. 2009. Evaluation methods for counting cryptic carnivores. *J Wildl Manag.*, **73**:431–443.
- Barberi F, Capaldi G, Gasperini P, Marinelli G, Santacroce R, Scandone R, Treuil M and Jacques V. 1979. Recent basaltic volcanism of Jordan and its implications on the geodynamic evolution of the Afro-Arabian Rift System. *Accademia Nazionale Dei Lincei, Att Del Convegno Lincei*, **47**:667–683.
- Bunaian F, Hatough A, Ababaneh D, Mashqbeh S, Yuosef M and Amr Z. 2001. The Carnivores of the Northeastern Badia, Jordan. *Turk J Zool.*, **25**:19–25.
- Burton AC, Neilson E, Moreira D, Ladle A, Steenweg R, Fisher JT, Bayne E and Boutin S. 2015. Wildlife camera trapping: a review and recommendations for linking surveys to ecological processes. *J Appl Ecol.*, **52**:675–685.
- Carter NH, Shrestha BK, Karki JB, Pradhan NMB and Liu J. 2012. Coexistence between wildlife and humans at fine spatial scales. *Proc Natl Acad Sci.*, **109**:15360–15365.
- Cunningham P and Wronski B. 2009. Blanford's fox confirmed in the At-Tubaiq Protected Area (northern Saudi Arabia) and the Ibex Reserve (Central Saudi Arabia). *Canid News*, **12**:4.
- Gecchele LV, Bremner-Harrison S, Gilbert F, Sultana A, Davison A and Durrant KL. 2017. A pilot study to survey the carnivore community in the hyper-arid environment of South Sinai mountains. *J Arid Environ.*, **141**:16–24.
- Hefner R and Geffen E. 1999. Group size and home range of the Arabian wolf (*Canis lupus*) in southern Israel. *J Mammal.*, **80**:611–619.
- Johnson A, Vongkhamheng C, Hedemark M and Saithongdam T. 2006. Effects of human-carnivore conflict on tiger (*Panthera tigris*) and prey populations in Lao PDR. *Anim Conserv.*, **9**:421–430.
- Kays RW and Slauson KM. 2008. Remote cameras. **In:** Long RA, MacKay P, Zielinski WJ and Ray J C (eds.), **Noninvasive Survey Methods for Carnivores**. Pp. 110–140. Island Press, Washington, D.C.
- Kelly MJ, Betsch J, Wulsch C, Mesa B and Mills LS. 2012. Noninvasive sampling for carnivores. **In:** Boitani L and Powell RA (eds.), **Carnivore Ecology and Evolution**. Pp. 47–69. Island Press, Washington D.C.
- Li S, McShea WJ, Wang D, Lu Z and Gu X. 2012. Gauging the impact of management expertise on the distribution of large mammals across protected areas. *Divers Distrib.*, **18**:1166–1176.
- Linnell JDC, Nilsen EB, Lande US, Herfindal I, Odden J and Skogen K. 2005. Zoning as a means of mitigating conflicts with large carnivores: principles and reality. **In:** Woodroffe R, Thirgood S and Rabinowitz A (eds.), **People and Wildlife: Conflict or Coexistence?** Pp. 162–175. Cambridge University Press, Cambridge.
- Long RA, MacKay P, Zielinski WJ and Ray J. 2008. **Noninvasive survey methods for carnivores**. Island Press, Washington, DC.
- Lyra-Jorge MC, Ciocchi G, Pivello VR and Meirelles ST. 2008. Comparing methods for sampling large- and medium-sized mammals: camera traps and track plots. *Eur J Wild Res.*, **54**:739–744.
- Qarqaz M, Abu Baker M and Amr ZS. 2004. Status and ecology of the Striped Hyaena, *Hyaena hyaena*, in Jordan. *Zool Middle East*, **33**:87–92.
- Qumsiyeh MB, Amr ZS and Shafei D. 1993. The status and conservation of carnivores in Jordan. *Mammalia*, **57**:55–62.
- Rowcliffe JM and Carbone C. 2008. Surveys using camera traps: are we looking to a brighter future? *Anim Conserv.*, **30**:185–186.
- Rowcliffe JM, Field J, Turvey ST and Carbone C. 2008. Estimating animal density using camera traps without the need for individual recognition. *J Appl Ecol.*, **45**:1228–1236.
- Saleh M, Younes M, Basuony A, Abdel-Hamid F, Nagy, A. *et al.* 2018. Distribution and phylogeography of Blanford's Fox, *Vulpes cana* (Carnivora: Canidae), in Africa and the Middle East. *Zool Middle East*, **64**:19–26.
- Tobler MW, Carrillo-Percastegui SE, Pitman RL, Mares R and Powell G. 2008. An evaluation of camera traps for inventorying large- and medium-sized terrestrial rain forest mammals. *Anim Conserv.*, **11**:169–178.
- Trolle M and Kerry M. 2005. Camera-trap study of ocelot and other secretive mammals in the northern Pantanal. *Mammalia*, **69**:405–412.
- van Heezik YM and Seddon PJ. 1998. Range size and habitat use of an adult male caracal in northern Saudi Arabia. *J Arid Environ.*, **40**:109–112.

Evaluation of Nutritional Composition and *In vitro* Antioxidant and Antibacterial Activities of *Codium intricatum* Okamura from Ilocos Norte (Philippines)

Eldrin DLR. Arguelles*

¹Philippine National Collection of Microorganisms, National Institute of Molecular Biology and Biotechnology (BIOTECH), University of the Philippine Los Baños, College, Laguna, Philippines, 4031

Received September 19, 2019; Revised October 31, 2019; Accepted November 13, 2019

Abstract

The nutritional composition of an edible green seaweed *Codium intricatum* Okamura was evaluated, including its potential antioxidant and antibacterial properties. Results showed elemental distribution to be in decreasing order of Na > K > Ca > Mg > Fe > Mn > Pb > Zn > Cu > Cd > Cr. Proximate composition of *C. intricatum* showed high ash and carbohydrate content with estimated value of $37.16 \pm 0.21\%$ and $32.16 \pm 0.29\%$ respectively. Relative antioxidant efficiency of *C. intricatum* exerted radical scavenging activity in a concentration-dependent manner with EC₅₀ value of 40.79 ± 0.015 mg GAE/ml. The tested algal extract exhibited radical scavenging activity that is correlated positively and dose-dependent to its phenolic concentration. Methanol extract of *C. intricatum* showed an extended spectrum of inhibitory activity against Gram-positive drug-resistant bacterium, Methicillin-Resistant *Staphylococcus aureus* (MRSA) with MIC and MBC of 250.00 and 500.00 µg/ml, respectively. It was moderately active against Penicillin-acylase producing *Bacillus cereus* and *Listeria monocytogenes*, each with MIC of 250 µg/ml. Minimum bactericidal concentration of 1000 µg/ml was observed for each of the test organisms. However, no inhibitory effect was observed among the tested Gram-negative bacterial pathogens. This study presented the nutritional profile and functional properties of *C. intricatum*, which make it a good alternative source of compounds possessing diverse bioactivities with prospective usage in the pharmaceutical and food industries.

Keywords: antioxidant activity, biological activity, *Codium intricatum*, Ilocos Norte, polyphenols, proximate analysis, seaweed

1. Introduction

Seaweeds are known in producing several macronutrients (lipids, proteins, carbohydrates, fibers and the like), micronutrients (minerals and vitamins) and other important biologically active compounds (e.g. polyphenols, enzymes, and antibiotics) with potential pharmacological uses (Arguelles *et al.*, 2019a; Ortiz *et al.*, 2006; Muraguri *et al.*, 2016). Analysis of elemental composition and phytochemicals in some seaweed plays a determining role in assessing their nutritional significance. Macroalgae contain high amounts of ash, showing a substantial concentration of macro and micro minerals (Reka *et al.*, 2017). The total elemental composition of seaweed is reported to have an estimated amount of 36% (of its total dried biomass), which is composed mainly of macro-minerals (magnesium, potassium, chloride, sodium, phosphorus, calcium, and sulfur) and micro minerals (copper, iodine, fluoride, zinc, molybdenum, iron, selenium, manganese, nickel, cobalt and boron) (Niranjan & Kim, 2011; Reka *et al.*, 2017). These minerals comprise an addition of up to sixty more trace elements and in much higher amount in comparison to other edible terrestrial plants, thus making these organisms potential dietary food supplements to regulate human nutrition and health

(Kannan, 2014; Reka *et al.*, 2017). In the Philippines, few reports are available on the role of micro and macronutrients in edible seaweeds. The relation between elemental content of seaweeds and their curative ability is not yet properly explained in terms of modern pharmacological concepts. Therefore, it is necessary to quantify the concentration of various trace elements in assessing the impact of several edible seaweeds in the treatment of various diseases to understand their pharmacological action.

Public consumers consider seaweed-derived antioxidants to be non-toxic since it is naturally occurring and have been utilized for several centuries (Fu *et al.*, 2015). Seaweed-derived antioxidants showed a significant part in the prevention of several persistent chronic illnesses like cancer and Parkinson's disease (Fu *et al.*, 2015). Several investigations have shown the antioxidant potential of seaweeds from various parts of the world (Muraguri *et al.* 2016). Some identified antioxidant compounds from marine seaweeds include phlorotannins, carotenoids, fucoxanthin, sulphated polysaccharides, catechins, astaxanthin, and sterols (Tenorio-Rodriguez *et al.*, 2017; Muraguri *et al.*, 2016; Shipeng *et al.*, 2015; Sabeena Farvin & Jacobsen, 2013; Cox *et al.*, 2010). In addition, there are reported studies that describe the antibacterial capability (derived from secondary and primary metabolites) of seaweeds against medically - important pathogenic bacteria such as *Pseudomonas aeruginosa*,

* Corresponding author e-mail: edarguelles@up.edu.ph.

Staphylococcus aureus, *Aeromonas hydrophila*, *Clostridium perfringens*, *Escherichia coli*, *Klebsiella pneumoniae*, and *Enterobacter aerogenes* (Arguelles *et al.*, 2019b; Liu *et al.*, 2017; Ibtissam *et al.*, 2009; Lima-Filho *et al.*, 2002).

Codium intricatum Okamura is a famous edible green seaweed of family Codiaceae commonly called as “pukpuklo” in Ilocos Norte, Philippines. Traditionally, this macroalga is utilized as a vegetable ingredient for food and is noted to have engrossing medicinal attributes such as immunosuppressive, antioxidant, cytotoxic, and anti-metastasis activities (Vasquez & Lirio 2020; Lee *et al.*, 2017; Sanjeeva *et al.*, 2018). However, natural products from edible seaweeds (such as *C. intricatum*) are considered as one of the few studied and underutilized marine resources in the Philippines. The country’s coastline has plentiful edible seaweed resources, but only limited effort has been made to examine the nutritional value, antioxidant, and antibacterial potential of these organisms for food and pharmacological applications. In light of the above information, this investigation was undertaken to evaluate the elemental composition and assess the antioxidant capacity as well as antibacterial activity of *C. intricatum* against selected pathogenic strains of bacteria. Also, quantification of the total phenolic content of the macroalga and correlation studies among the phenolic content of the algal extract and antioxidant capacity were examined.

2. Materials and Methods

2.1. Sample Collection and Extract Preparation

Codium intricatum was collected on 03 December 2018, from Pagudpud (Lat. 18° 35' 21.48" N, Long. 120° 47' 11.04" E), Ilocos Norte, Philippines. The macroalga was characterized and identified based on morphological taxonomic features, according to Algae Base (web site: www.algaebase.org) and Trono (2004). The macroalga was rinsed with sterile tap water to remove contaminating epiphytes and salts and further washed with sterilized distilled water. The alga was dried under shade for 10 days and crushed in a mixer grinder until a coarse powder was obtained. The seaweed powder (1 g) was successively treated with 30 mL methanol in a water bath for 30 minutes with stirring (for 1 hour). The extract was then concentrated via centrifugation at 10,000 rpm at 20 °C for 20 minutes. The liquid extract was collected using a rotary vacuum evaporator and kept under refrigerated conditions at 4 °C until other assays were conducted (Arguelles, 2018).

2.2. Proximate Analysis

The protocol employed for the quantification of percent crude protein, moisture, ash, crude fat, total carbohydrates, and crude fiber were based on AOAC (2011). Proximate composition analysis was performed in triplicates, and biochemical values are presented as means in the results (Arguelles *et al.*, 2018).

2.3. Elemental Composition Analysis

The dried powder of *C. intricatum* was subjected to elemental composition analysis following standard procedures (AOAC, 2011) for the detection of Potassium, Magnesium, Sodium, Manganese, Calcium, Iron, Zinc, Copper, Lead, Chromium and Cadmium using Atomic Absorption Spectrophotometer Perkin Elmer AAAnalyst 400.

2.4. Test Microorganisms

Test microorganisms such as Gram-positive bacteria (Penicillin-Acylase producing *Bacillus cereus* BIOTECH 1635, Methicillin-Resistant *Staphylococcus aureus* BIOTECH 10378, *Listeria monocytogenes* BIOTECH 1958, *Streptococcus mutans* BIOTECH 10231) and Gram-negative bacteria (Penicillin-Acylase producing *Escherichia coli* BIOTECH 1634, *Salmonella typhimurium* BIOTECH 1826, *Aeromonas hydrophila* BIOTECH 10089 and *Pseudomonas aeruginosa* BIOTECH 1824) were used in the study. All test organisms were obtained from the Philippine National Collection of Microorganisms (PNCM), National Institute of Molecular Biology and Biotechnology (BIOTECH), University of the Philippines Los Baños.

2.5. Micro-dilution Antibacterial Assay

The minimum inhibitory concentration (MIC) of the algal extract was determined using two-fold serial dilution technique following the protocol done by Arguelles (2018). Bacterial culture suspension (1×10^5 cells/ml) was prepared for micro-dilution assay against *C. intricatum* extract. The bacterial suspension (100 μ l) was diluted and inoculated to 100 μ l of algal extract distributed in a clear 96-well microtiter plate in different dilutions starting from 1000 to 7.8125 μ g/ml. In this assay, methanol was also used in the experimental set up as negative control. The seeded plate was kept at 35°C for 12 hours, after which the MIC was noted. The MIC is described as the minimum amount of the tested algal extract that inhibited bacterial growth following a 12-h incubation period. The absence or presence of bacterial growth in microtiter plates was evaluated after the incubation period. The MIC of the algal extract at which no visible bacterial growth was detected was noted as the MIC for the extract–bacteria combination under consideration. As for the controls, the MIC of tetracycline against each bacterial species was also determined.

The minimum bactericidal activity (MBC) was noted by inoculating a loop of the sample in microtiter plate wells that exhibited no evident growth from the MIC assay onto a tryptic soy agar (non-selective, rich culture media) plates. The plates were stored at 35°C for 24 hours and were evaluated for visible colony growth or lack of bacterial growth for each dilution subculturing being considered. Lack of growth confirms that the seaweed extract was bactericidal at that particular dilution. Bacterial growth on agar plates shows that the sample was bacteriostatic at that dilution. The lowest concentration of the algal extract exhibiting no visible growth of the bacterial pathogen on agar was noted as the minimum bactericidal activity (MBC) value (Arguelles & Sapin, 2020).

2.6. Determination of Total Polyphenolic Content

The total phenolic compound present in *C. intricatum* extract was calculated by Folin-Ciocalteu method following the protocol done by Nuñez Selles *et al.*, (2002). *C. intricatum* extract was diluted with sterile distilled water. Aliquot of about 0.5 ml of Folin-Ciocalteu’s reagent and 0.5 ml of 10% Na₂CO₃ solution was placed to 0.5 ml of the diluted seaweed extract and were thoroughly mixed in a test tube using a vortex mixer. The mixture was kept for 5 minutes, and 5 mL of sterile water was added to each of the solutions. Spectrophotometric readings were done using a Shimadzu UV-1601 spectrophotometer at 720 nm wavelength with reagent plus water as the blank sample (Arguelles & Sapin, 2020). Construction of the calibration curve was done using gallic acid as the standard, and gallic acid

equivalent (GAE) was utilized to show the total phenol content in *C. intricatum* extract.

2.7. DPPH Radical Scavenging Assay

The test for antioxidant activity of *C. intricatum* was done following the method proposed by Ribeiro *et al.*, (2008) using 2,2-diphenyl-1-picrylhydrazyl (DPPH) with few modifications. Aliquot of 100 µl of *C. intricatum* extract was mixed with 5.0 ml of 0.1 mM DPPH methanolic solution. The solution was thoroughly mixed by a vortex mixer and set aside at 30 °C for 20 minutes. The absorbance readings of the tested sample solutions were done using a Shimadzu UV-1601 spectrophotometer at 517 nm wavelength. The amount of inhibition was evaluated using the mathematical expression used by Ribeiro *et al.*, (2008).

$$\text{Inhibition (\%)} = [(A_{\text{control}} - A_{\text{sample}}) / A_{\text{control}}] \times 100$$

Where: A_{sample} = absorbance reading of the seaweed extract (DPPH solution and test extract) and A_{control} = absorbance reading of the control (DPPH solution only). In this investigation, gallic acid served as a positive control. The antioxidant activity of the seaweed extract was determined and noted as EC_{50} value (the amount of the seaweed extract showing 50% scavenging activity of DPPH radical expressed in µg/ml).

2.8. Statistical analyses

The data obtained from the experimental set-ups were given as means \pm standard deviations (mean \pm SD) of three simultaneous experimental readings. Estimation of the linear correlation coefficient and evaluation of the correlation analysis were done using MS Office Excel 2007.

3. Results And Discussion

3.1. Proximate Composition Analysis

Biochemical composition of *C. intricatum* collected from Pagudpud, Ilocos Norte, showed that the biochemical composition of this seaweed displayed a good nutritional profile (Table 1). In this study, *C. intricatum* exhibited high ash and carbohydrate content with 37.16 \pm 0.21% and 32.16 \pm 0.29% respectively. The total amount of ash observed in the seaweed sample was almost similar to ash content reported for *Codium geopiorum* (37.96 \pm 0.05) but is higher to *Codium fragile* (21.79 \pm 0.52). On the other hand, other species, such as *Codium dworkense* have relatively higher crude ash content (in comparison to *Codium intricatum*) with an estimated value of 69.94 \pm 0.11% (Mwalugha *et al.*, 2015; Turan *et al.*, 2015). High concentration of ash would mean presence of considerable concentration of macro (such as magnesium, phosphorus, potassium, sodium, chloride, calcium, and sulfur) and micro minerals (such as copper, iodine, zinc, molybdenum, iron, selenium, manganese, cobalt, nickel and boron) present in *C. intricatum* biomass (Niranjan & Kim, 2011; Reka *et al.*, 2017). Carbohydrates are regarded as the most significant biochemical component in seaweeds for the reason that it serves as the primary source of energy to execute important metabolic processes in the alga (El-Manawy *et al.*, 2019). The carbohydrate content obtained from *C. intricatum* is significantly higher compared to some of the seaweeds (*Hormophysa cuneiformis* and *Padina boergesenii*) obtained from the Red Sea coast in Egypt but is lower than *C. fragile* obtained from the coastline region of Northern Chile (El-Manawy *et al.*, 2019; Ortiz *et al.*, 2008). On the other hand, Akhtar & Sultana (2002) observed similar

carbohydrate content range for other known seaweeds such as *Caulerpa* sp. (32.9%) and *Sargassum* sp. (32.3%).

Table 1. Proximate composition of *Codium intricatum* Okamura.

Proximate Composition	Percent Composition (%)*
Moisture Content	12.34 \pm 0.12
Ash Content	37.16 \pm 0.21
Crude Protein	5.03 \pm 0.05
Crude Fat	2.17 \pm 0.17
Crude Fiber	11.14 \pm 0.32
Carbohydrate	32.16 \pm 0.29

* All values are reported as mean \pm standard deviation (n = 3)

Proteins are also considered as one of the principal constituent in the proximate analysis of *C. intricatum* showed in the study. In collation with other *Codium* species, the protein content of *C. intricatum* (5.03 \pm 0.05%) is within the reported range (Mwalugha *et al.*, 2015; Ortiz *et al.*, 2008). However, the protein concentration of *C. intricatum* is relatively lower than the reported protein contents of other brown (*Dictyota cervicornis*, *Dictyota bartaynesiana*, *Sargassum cristaefolium*, and *Spatoglossum asperum*) and red (*Acanthophora spicifera*, *Hypnea musciformis*, and *Gracilaria arcuata*) seaweeds (Mwalugha *et al.*, 2015). The total amount of protein in macroalga changes not only among species of certain genera of seaweeds but also between habitats and maturity level (Fathy, 2007). Variations in the biochemical constituents of seaweeds are attributable to environmental factors (salinity, temperature, and dissolved oxygen) and seasonal differences. Generally, seaweeds contain a low concentration of lipids ranging from 0.92 to 5 % of the total algal biomass (Schmid *et al.*, 2014; El-Manawy *et al.*, 2019; Arguelles & Martinez-Goss, 2020). The lipid content obtained for *C. intricatum* is within the reported range, with an estimated value of 2.17 \pm 0.17%. On the other hand, the average amount of dietary fiber in seaweeds varies from 9 to 21% of the total dried algal biomass (Mwalugha *et al.*, 2015). *C. intricatum* showed a total crude fiber content of 11.14 \pm 0.32%, which is within the range of those reported crude fiber content of red, brown, and green seaweeds. Moisture content gives information about the storage/shelve life of food products. The moisture content for commercially dried seaweeds should be maintained between 15 to 35% and must remain stable even below 15% (Blakemore, 1990). The result of the proximate analysis for moisture content of *C. intricatum* (12.34 \pm 0.12%) suggests its stability during storage and marketing. This study presents preliminary data regarding the biochemical composition of *C. intricatum* obtained from the coast of Ilocos Norte, Philippines. Results of the proximate composition of *C. intricatum* suggest that it could be an excellent source of carbohydrates, ash, and crude fiber.

3.2. Elemental Composition Analysis

Seaweeds contain a high concentration of minerals because of the diverse kinds of substances they absorb from the marine habitat where they grow and proliferate (MacArtain *et al.*, 2007). Ash content of edible seaweeds is usually considered as a benchmark of quality for the evaluation of the nutritional and bifunctional properties of the edible alga (Reka *et al.*, 2017). *C. intricatum* possesses a high amount of ash, up to 37.16 \pm 0.21%, in the dried algal biomass. The average concentration of some

important minerals in *Codium intricatum* is presented in Table 2. The elemental distribution in *C. intricatum* was observed to be in decreasing order of Na > K > Ca > Mg > Fe > Mn > Pb > Zn > Cu > Cd > Cr. High concentration of sodium ($174,900 \pm 0.88$ ppm) followed by potassium ($75,680 \pm 4,187$ ppm), calcium ($55,081 \pm 4,289$ ppm) and magnesium ($13,941 \pm 861$ ppm) were observed in the algal biomass. The high level of sodium in *C. intricatum* biomass (Table 2) is similar to the findings reported in seaweeds such as *Fucus vesiculosus*, *Halimeda opuntia*, *Gracillaria corticata*, and *Turbinaria arriquetra* (Balina *et al.*, 2016; Omar *et al.*, 2013). The current consumption of sodium in some of the local foods in the Philippines is far beyond the recommended concentration levels. Thus, consumption of this edible seaweed (with high sodium concentration) can contribute to a greater intake of sodium, thus causing health-associated diseases such as hypertension. This attribute may, nevertheless, be favorable if considering *C. intricatum* as a replacement of salt in several processed meat foods, for the reason that its rich mineral content can help in maintaining the salty taste of food without adding table salt (NaCl) (Circunsisão *et al.*, 2018). Recent studies show the formulation of processed meat products (such as frankfurters and meat patties) fortified with seaweeds (such as *Porphyra umbilicalis*, *Himanthalia elongata* or *Undaria pinnatifida*) targeting the decrease of the use of traditional salt (NaCl) and enhancing its mineral composition and content (López-López *et al.*, 2011; López-López *et al.*, 2009). Potassium is the second most abundant mineral element in *C. intricatum*, which is higher than that obtained by Omar *et al.*, (2013) from seaweeds (*Halimeda opuntia*, *Gracillaria corticata*, and *Turbinaria arriquetra*) at the Southern coast of Jeddah in Saudi Arabia. The abundance of potassium in this edible macroalgae is good in preventing potassium related diseases such as hypokalemia. The third most abundant element in the algal biomass is calcium. *C. intricatum* can be regarded as a suitable mineral source of calcium for the maintenance of the proper functional role of some important processes in the human body (such as glandular secretion, muscle contraction and nerve transmission) as well as resolve vascular vasodilation and contraction (Ooi *et al.*, 2012). High concentration of calcium was also noted by MacArtain *et al.*, (2007) in *Ulva lactuca* (a green seaweed) and proved to have higher concentration as compared to calcium concentration present in other terrestrial foodstuffs (MacArtain *et al.*, 2007). Furthermore, *C. intricatum* can also be considered as a good alternative source of magnesium since high concentration of the element was also observed in the macroalga. Magnesium supports the proper functioning of the immune, muscular, and nervous system. This trace element fortifies bones, control blood pressure and sugar as well as protein synthesis. However, high magnesium intake can cause a lowering of blood pressure, reduced kidney function, diarrhea and cardiac arrest (Jahnen-Dechent & Kettleler, 2012).

Trace microelements are metal constituents that are divided into two main subclasses. The first group includes cobalt, copper, iron, manganese, and zinc, which are important to the human body for the proper functioning of biochemical processes but can be toxic at very high concentrations. On the other hand, the second group includes mercury, cadmium, chromium, and lead, which are metals that do not have a biological function and includes critical metallic chemical contaminants in the marine

ecosystem (Omar *et al.*, 2013). Manganese was noted in the biomass of *C. intricatum* (32.40 ± 1.67 ppm) in significant amount but is lower than that obtained by Balina *et al.*, (2016) from *Fucus vesiculosus* (1680 ppm). Based on the result, this edible seaweed can also be used to supplement manganese in food which is important in controlling blood sugar levels, formation of bone and tissues as well as prevention of diseases (diabetes, osteoporosis, arthritis and epilepsy) (Nielsen, 1999).

Iron deficiency is a frequent problem affecting several people globally. Limitation of iron can result in chronic infections and bleeding, as well as a deficiency in folic acid, vitamin A and vitamin B12. The high concentration of iron observed in *C. intricatum* (290.53 ± 24.74 ppm) suggests that the edible seaweed can serve as an excellent alternative source of dietary iron to address iron deficiency (Ooi *et al.*, 2012). Zinc and copper are important metallic chemical elements that are required at most in minimal concentration by humans for the proper function of some important biochemical processes in the body. Zinc acts as a stimulus for the formation of metallothionein that possesses a strong affinity for copper, which hampers systemic assimilation of copper inside the cells of the intestine (Ooi *et al.*, 2012). *C. intricatum* contains minimal amounts of copper and zinc that can be used as a source of food to address copper-zinc deficiency and disparity. The amount of copper and zinc obtained in this study is lower than that obtained from *F. vesiculosus* with copper and zinc concentration of 12.7 ppm and 89 ppm, respectively (Balina *et al.*, 2016). Chromium, cobalt, and copper are three microelements that support important biological processes in the human body. Chromium is a mineral that helps in the regulation of blood sugar and pressure levels as well as the normal development of body muscle (Nriagu, 1988). On the other hand, cobalt is an important microelement needed for vitamin C and vitamin B12 synthesis. This mineral helps in the normal cardiac functioning of the human body and facilitates iron absorption within the body (Kazantzis, 1981).

Copper is important in the synthesis of phospholipids and hemoglobin as well as helping in the production of melanin pigment for the skin (Uauy *et al.*, 1988). *C. intricatum* contains these microelements in considerable amounts (Table 2) and thus serves as a potential natural source of these important nutrients.

Toxic microelements such as cadmium and lead, if present at minimal concentrations, can be detrimental to human health. These elements are not needed in the proper functioning of the body. Thus, non-inhalation and non-ingestion of these microelements are encouraged for the reason that serious toxic poisoning can result in death (Kisten *et al.*, 2017). Cadmium, although not considered essential, helps in the proper functioning of important internal organs such as kidney and liver. However, it is also considered toxic in high amounts, causing damage to important organs (kidneys, liver, and lungs), diarrhea, cardiovascular problems, anemia, and severe damage to the brain (Bernard & Lauwerys, 1986). On the other hand, lead is noted for its importance in the normal brain, bone, and muscle functions but has also been known to cause seizures, kidney failure, comas, anemia, and heart attacks (Schroeder & Tipton, 1968). *C. intricatum* revealed the presence of these microelements but in amounts that are not toxic and confirms the nutritional potential and benefit of this edible seaweed.

Table 2. Concentrations of macro and micro-elements of *Codium intricatum* Okamura.

Seaweed	Elemental Parameter*										
	Ca (ppm)	Mg (ppm)	Na (ppm)	Mn (ppm)	K (ppm)	Fe (ppm)	Zn (ppm)	Cu (ppm)	Pb (ppm)	Cr (ppm)	Cd (ppm)
<i>Codium intricatum</i>	55,081 ±4,289	13,941 ± 861	174,900 ±0.88	32.40 ±1.67	75,680 ±4,187	290.53 ±24.74	4.65 ±0.25	2.27 ±0.08	6.47 ±0.25	0.84 ±0.03	1.70 ±0.04

* All values are reported as mean ± standard deviation (n = 3)

C. intricatum is potentially a good alternative source of microelements needed for human health and nutrition. Differences in the concentration of trace element content in *C. intricatum* in comparison to other seaweed species are highly influenced by several environmental and cultural factors including: pH, interactions, salinity and interactions among elements, light intensity, amount of trace elements in water, and other metabolic influences like dilution of elemental composition caused by growth and development of seaweed (El-Said & El-Sikaily, 2013; Zbikowski *et al.*, 2006). The result of this study provides baseline information on the nutritional value of *C. intricatum* that can be used in the food industry for human consumption to address nutrient deficiency in the world.

3.3. Total Phenolic Content

Several studies have demonstrated that polyphenols are the primary compounds responsible for the antioxidant activities of diverse kinds of marine macroalgae (Zhang *et al.*, 2007; Shipeng *et al.*, 2015). The total polyphenolic content (TPC) in the algal extract was evaluated using Folin-Ciocalteu method and is given as mg GAE/g of the dried seaweed biomass (Table 3).

Table 3. Phenolic content and DPPH free radical scavenging activity of methanol extract of *Codium intricatum* Okamura.

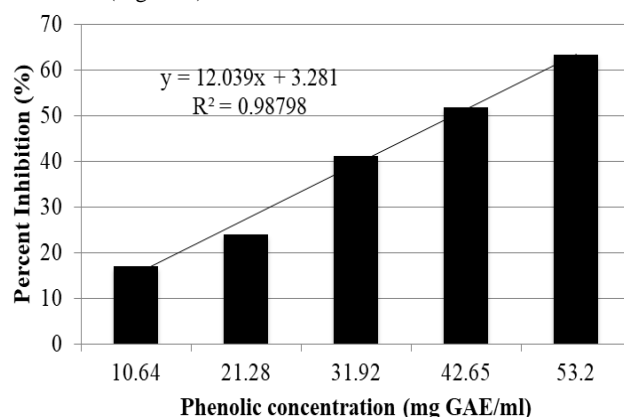
Seaweed	Solvent Extractant	Total Phenolic Content (mg GAE/g)	EC ₅₀ (mg GAE/ml)
<i>Codium intricatum</i>	Methanol	0.934±0.02	40.79 ±0.015

The TPC in the algal biomass is 0.934±0.02 mg GAE/g which is greater than that obtained from the methanol extracts of other seaweeds such as *Gracilaria bursa-pastoris* from Marmara Sea coast of Turkey with 0.35 ± 0.05 mg GAE/g and *Sargassum horneri* from the seacoast of Bijin-do, South Korea with 0.51 ± 0.02 mg GAE/g (Shipeng *et al.*, 2015; Yildiz *et al.*, 2011). However, higher phenolic concentrations were observed by Ismail (2017) from three Egyptian seaweeds (*Sargassum linifolium*, *Corallina officinalis* and *Ulva fasciata*) with maximum value of 10.35 mg GAE/g, 4.89 mg GAE/g, and 11.95 mg GAE/g dry weight respectively. Variations in the total polyphenolic contents among species of seaweeds are caused by several influencing environmental factors like seasonal variation, physiological condition, and geographical origin (Machu *et al.*, 2015).

3.4. Antioxidant Activity

Seaweeds are often exposed to stressful conditions because of exposure to high light and oxygen that results in the emergence of free radicals; thus, seaweeds form a defense mechanism and produce substances such as antioxidants (Cox *et al.*, 2010). In this study, assessment of the antioxidant capacity of the solvent extract of *C. intricatum* was established by assessing the DPPH

radical scavenging activity at different prepared concentrations of seaweed extract, and EC₅₀ value of the seaweed extract was calculated and presented in Table 3. DPPH is a quick method for evaluating the antioxidant activity by measuring the DPPH scavenging capability of the extracts. The seaweed extract was capable of reducing DPPH free radical into diphenyl picryl hydrazine. DPPH scavenging activity of the extract of *C. intricatum* showed that at 53.2 mg GAE/ml concentration, the maximum antioxidant activity was found to be 63.21 ± 0.21%. The results of the analysis exhibited that the DPPH scavenging activity increases when the amount of the seaweed extract is increased (Figure 1).

**Figure 1.** Correlation between total phenolic content and total antioxidant activity (DPPH radical scavenging assay) of *Codium intricatum*.

The results suggested that the algal extracts could inhibit oxidation through free radical scavenging, which can be attributed to phenolic compounds that can act as natural antioxidants. The computed EC₅₀ value of the algal extract is 40.79 ± 0.015 mg GAE/ml. Lower EC₅₀ concentrations are indicative of high antioxidant activity. In collation to the EC₅₀ of other edible seaweed such as *Enteromorpha spirulina* (50.00 ± 0.04 mg GAE/ml), *C. intricatum* had a comparatively greater antioxidant activity (Cox *et al.*, 2010). Polyphenolic compounds are largely distributed in seaweeds, and several factors such as extraction methods and polarity of solvents used for polyphenol extraction must also be considered in order to obtain the target polyphenols in the sample. Generally, polyphenols are usually soluble in polar organic solvents than in aqueous mixtures of ethanol, acetone and methanol (Aili Zakaria *et al.*, 2011; Arguelles *et al.*, 2017).

3.5. Correlation Study Between Antioxidant Activity And Total Polyphenolic Content

Several studies suggested a direct relationship between the antioxidant activity and total phenolic content in several species of seaweeds (Shipeng *et al.*, 2015; Ismail, 2017; Arguelles *et al.*, 2019b). Nevertheless, other studies show the absence of such a relationship (Tenorio-Rodriguez *et al.*, 2017). In this study,

antioxidant activities of the seaweed extract tested follow a dose-dependent manner and increased with the increase in the concentration extract. A strong and direct correlation between DPPH assay and TPC ($R^2=0.988$) indicated that polyphenols present in *C. intricatum* crude extract are involved in antioxidant activity by scavenging DPPH (Figure 1). Several species of seaweeds contain active antioxidant compounds such as flavonoids and polyphenols from which the antioxidant activity of *C. intricatum* extract tested in the study could be attributed to (Farasat, 2013; Fu *et al.* 2015). Phenolic profiling of the crude extract is essential to identify the components of active substances to get a more appropriate correlation among the role of polyphenols and antioxidant activity (Arguelles *et al.*, 2017).

3.6. Antibacterial Activity

Seaweeds are potential renewable resources of bioactive compounds with diverse beneficial effects. In the Philippines, several studies report that bioactive secondary metabolites isolated from various seaweed exhibit potential for being used as antimicrobial molecules (Arguelles *et al.*, 2019b; Jerković *et al.*, 2019; Vasquez & Lirio, 2020; Moubayed *et al.*, 2017). Nevertheless, the possible use for the biomedical application of species belonging to the genus *Codium* has been the least investigated for their biological activities among all members of Chlorophyceae (Jerković *et al.*, 2019; Vasquez & Lirio, 2020). Methanol extract of *C. intricatum* was subjected to antibacterial assay against a wide array of bacterial pathogens. *Codium intricatum* showed an extended spectrum of inhibitory activity against Methicillin-Resistant *Staphylococcus aureus* (MRSA) with MIC and MBC of 250 and 500 µg/ml, respectively (Figure 2). It was moderately active against Penicillin-acylase producing *Bacillus cereus* and *Listeria monocytogenes*, each with MIC of 250 µg/ml. MBC of 1000 µg/ml was observed for each of the test organisms. Moreover, no inhibitory effect was observed in *S. mutans* and among the Gram-negative bacterial pathogens used in the study, which is similar to that observed by Lavanya & Veerappan (2011) as well as Ibtissam *et al.*, (2009) against *Escherichia coli*, *Pseudomonas aeruginosa* and *Klebsiella pneumoniae*. However, other studies such as that of Koz *et al.*, (2009), antibacterial activity of *C. fragile* extract against *E. aerogenes*, *E. coli* and *B. subtilis* was observed. Antibacterial activity of *C. intricatum* extract in opposition to *S. aureus*, and MRSA is similar to that reported from methanol extracts of three *Codium* species (*C. tomentosum*, *C. dichotomum*, and *C. fragile*) where high inhibitory activity were noted (Ibtissam *et al.*, 2009; Koz *et al.*, 2009). However, when *S. aureus* was tested against *C. bursa*, no antibacterial activity was observed (Ibtissam *et al.*, 2009; Jerković *et al.*, 2019). As previously shown in several studies, antibacterial activity of marine seaweeds inhibited the growth of a wide array of bacteria. Also, variations in the inhibitory activity of seaweed extracts against microorganisms are highly dependent on several factors like habitat and place of collection, physiological phenomena (developmental stage of the macroalga), ecological parameters (irradiance and nutrients) as well as seasonality variations (Salvador *et al.*, 2007). The findings of the present investigation are analogous to those observed by Tuney *et al.*, (2006) and Taskin *et al.*, (2001) where Gram-positive bacteria are, to a greater extent, vulnerable to seaweed extracts used in their investigation compared to Gram-negative bacteria. The sensitivity of a specific kind of bacteria to the activity of bioactive substances found in the algal extract is attributed to the difference in structure and composition of the

cell walls (Arguelles & Sapin, 2020). Gram-positive bacteria are marked by dense peptidoglycan in the outer layer of its cell wall, while Gram-negative bacteria have composite, multilayered cell wall structure that makes the entry of bioactive compounds more difficult (Arguelles & Sapin, 2020).

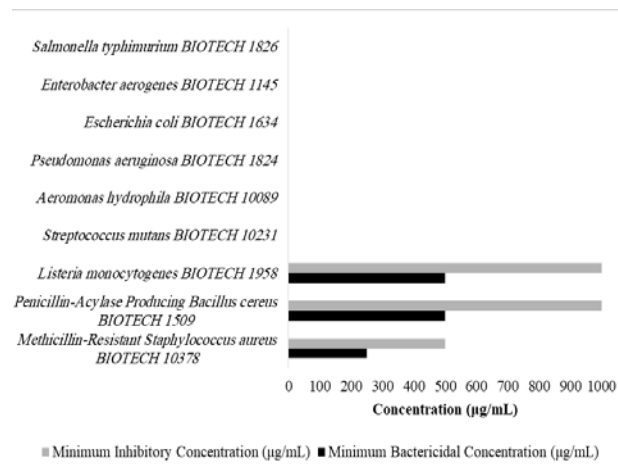


Figure 2. Antibacterial activity of *Codium intricatum* extract.

In the Philippines, no extensive and individual scientific studies are available, showing the potential antibacterial property of *C. intricatum*. This study is the first investigation in the country about the antibacterial property of *C. intricatum* against Methicillin-resistant *Staphylococcus aureus*, Penicillin-acylase producing *Bacillus cereus*, and *Listeria monocytogenes*. In light of the recent findings in this study, *C. intricatum* extract exhibited the existence of bioactive compounds with promising antibacterial property against these important pathogenic bacteria. Further study should be conducted to purify and identify these bioactive substances.

4. Conclusion

Seaweeds are potential renewable resources that have been reported to provide several beneficial effects. The elemental composition and proximate composition of *C. intricatum* suggest that the alga has potential food value that can be used in the food industry. Also, this study concludes that *C. intricatum* represents an alternative natural source of polyphenols and other bioactive compounds for the development and production of novel antibiotics and natural antioxidants. Further studies should be conducted to identify the structure and elucidate the mechanism of action of different biologically active substances present in the algal extract that showed promising antibacterial activity.

Acknowledgements

The author wishes to thank the support of the Food Laboratory and the Philippine National Collection of Microorganisms, National Institute of Molecular Biology and Biotechnology (BIOTECH), University of the Philippines Los Baños during the course of the study. The technical assistance of Mrs. Arsenia B. Sapin in conducting some experiments in the study is acknowledged with gratitude.

References

- Aili Zakaria N, Ibrahim D, Fariza Sulaiman S, and Afifah Supardy N. 2011. Assessment of antioxidant activity, total phenolic content and in-vitro toxicity of Malaysian red seaweed, *Acanthophora spicifera*. *J Chem Pharm Res*, **3**(3): 182-191.
- Akhtar P, and Sultana V. 2002. Biochemical studies of some seaweed species from Karachi coast. *Rec Zool Surv Pakistan* **14**: 1-4.
- AOAC. 2011. Official methods of analysis. 18th (Ed.). Association of Official Analytical Chemists, Gaithersburg, MD.
- Arguelles EDLR, and Martinez-Goss MR. 2020. Lipid accumulation and profiling in microalgae *Chlorolobion* sp. (BIOTECH 4031) and *Chlorella* sp. (BIOTECH 4026) during nitrogen starvation for biodiesel production. *J Appl Phycol*, <https://doi.org/10.1007/s10811-020-02126-z>.
- Arguelles EDLR, and Sapin AB. 2020. Bioactive properties of *Sargassum siliquosum* J. Agardh (Fucales, Ochrophyta) and its potential as source of skin-lightening active ingredient for cosmetic application. *J Appl Pharm Sci*, **10**(7): 51-58
- Arguelles EDLR, Laurena AC, Monsalud RG, and Martinez-Goss MR. 2019a. High lipid and protein-producing epilithic microalga, *Desmodesmus* sp. (U-AU2): A promising alternative feedstock for biodiesel and animal feed production. *Philipp J Crop Sci*, **44**(2): 13-23.
- Arguelles EDLR, Monsalud RG, and Sapin AB. 2019b. Chemical composition and *In vitro* antioxidant and antibacterial activities of *Sargassum vulgare* C. Agardh from Lobo, Batangas, Philippines. *J ISSAAS*, **25**(1): 112-122.
- Arguelles EDLR. 2018. Proximate analysis, antibacterial activity, total phenolic content and antioxidant capacity of a green microalga *Scenedesmus quadricauda* (Turpin) Brébisson. *Asian J Microbiol, Biotechnol Env Sci*, **20**(1): 150-158.
- Arguelles EDLR, Laurena AC, Martinez-Goss MR, and Monsalud RG. (2017). Antibacterial activity, total phenolic content, and antioxidant capacity of a green microalga *Desmodesmus* sp. (U-AU2) From Los Baños, Laguna (Philippines). *J Nat Stud*, **16**(2): 1-13.
- Balina K, Romaglina F, and Blumberga D. 2016. Chemical composition and potential use of *Fucus vesiculosus* from Gulf of Riga. *Energy Procedia*, **95**: 43-49.
- Bernard A, and Lauwerys R. 1986. Effects of cadmium exposure in humans. In: *Cadmium*. Berlin: Springer.
- Blakemore WR. 1990. Post harvest treatment and quality control of Eucheuma seaweeds. In: *Proceedings of the regional workshop on seaweed culture and marketing*. South Pacific aquaculture development project, Food and Agriculture Organization of the United Nations, Suva, Fiji, 48-52.
- Circuncisão AR, Catarino MD, Cardoso SM, Silva AMS. 2018. Minerals from Macroalgae Origin: Health Benefits and Risks for Consumers. *Marine Drugs*, **16**: 400. <https://doi.org/10.3390/md16110400>
- Cox S, Abu-Ghannam N, Gupta S. 2010. An assessment of the antioxidant and antimicrobial activity of six species of edible Irish seaweeds. *Int Food Res Journal*, **17**: 205-220.
- El-Manawy IM, Nassar MZ, Fahmy NY, Rashedy SH. 2019. Evaluation of proximate composition, antioxidant and antimicrobial activities of some seaweeds from the Red Sea coast, Egypt. *Egyptian J Aquat Biol Fisheries*, **23**(1): 317-329.
- El-Said FG, El-Sikaily A. 2013. Chemical composition of some seaweed from Mediterranean Sea coast, Egypt. *Environ Monit Assess*, **185**: 6089-6099.
- Farasat M, Khavari-Nejad RA, Nabavi SMB, and Namjooyan F. 2013. Antioxidant Properties of two Edible Green Seaweeds From Northern Coasts of the Persian Gulf. *Jundishapur J Nat Pharm Prod*, **8**(1): 47-52.
- Fu CWF, Ho CW, Yong WTL, Abas F, and Tan CP. 2015. Effects of phenolic antioxidants extraction from four selected seaweeds obtained from Sabah. *Int Food Res J*, **23**(6): 2363-2369.
- Guiry M D, in Guiry M D, and Guiry G M. (2017). AlgaeBase. World-wide electronic publication, National University of Ireland, Galway. <http://www.algaebase.org>; searched on 18 December 2018.
- Ibtissam C, Hassane R, Martinez-Lopez J, Dominguez Seglar J F, Gomez Vidal J A, Bouziane H, and Kadiri M. 2009. Screening of antibacterial activity in marine green and brown macroalgae from the coast of Morocco. *Afr J Biotechnol*, **8**(7): 1258-1262.
- Ismail GA. 2017. Biochemical composition of some Egyptian seaweeds with potent nutritive and antioxidant properties. *Food Sci Tech*, **37**(2): 294-302.
- Jahren-Dechent W, Ketteler M. (2012). Magnesium basics. *Clin Kidney J*, **5**(Suppl 1): i3-i14.
- Jerković I, Kranjac M, Marijanović Z, Šarkanj B, Cikoš A-M, Aladić K, Pedišić S, and Jokić S. 2019. Chemical diversity of *Codium bursa* (Oliv) C. Agardh headspace compounds, volatiles, fatty acids and insight into its antifungal activity. *Molecules*, **24**: 842-858.
- Kisten K, Moodley R, and Jonnalagadda SB. 2017. Elemental analysis and nutritional value of seaweed from KwaZulu-Natal, South Africa. *Analytical Letters*, **50**(3): 580-590.
- Kannan S. 2014. FT-IR and EDS analysis of the seaweeds *Sargassum wightii* (brown algae) and *Gracilaria corticata* (red algae). *Int J Curr Microbiol Appl Sci*, **3**(4): 341-351.
- Kazantzis G. 1981. Role of cobalt, iron, lead, manganese, mercury, platinum, selenium, and titanium in carcinogenesis. *Environ Health Perspect*, **40**:143.
- Koz FFY, Yavasoglu NUK, Demirel Z, Sukatar A, and Ozdemir G. 2009. Antioxidant and antimicrobial activities of *Codium fragile* (Suringar) Hariot (Chlorophyta) essential oil and extracts. *Asian J Chem*, **21**(2): 1197-1209.
- Lavanya R, and Veerappan N. 2011. Antibacterial potential of six seaweeds collected from gulf of Mannar of southeast coast of India. *Adv Biol Sci*, **5**(1): 38-44.
- Lee SA, Moon SM, Choi YH, Han SH, Park BR, Choi MS, Kim JS, Kim YH, Kim DK, and Kim C S. 2017. Aqueous extract of *Codium fragile* suppressed inflammatory responses in lipopolysaccharide-stimulated RAW264.7 cells and carrageenan-induced rats. *Biomed Pharmacother*, **93**:1055-1064.
- Lima-Filho JVM, Carvalho AFFU, and Freitas SM. 2002. Antibacterial activity of extracts of six macroalgae from the Northeastern Brazilian Coast. *Brazilian J Microbiol*, **33**: 311-313.
- Liu M, Liu Y, Cao MJ, Liu GM, Chen Q, Sun L, and Chen H. 2017. Antibacterial activity and mechanisms of depolymerized fucoidans isolated from *Laminaria japonica*. *Carbohydr Polym*, **172**: 294-305.
- López-López I, Cofrades S, and Jiménez-Colmenero F. 2009. Low-fat frankfurters enriched with n-3 PUFA and edible seaweed: Effects of olive oil and chilled storage on physicochemical, sensory and microbial characteristics. *Meat Sci*, **83**(1):148-154.
- López-López I, Cofrades S, Cañeque V, Díaz M T, López O, and Jiménez-Colmenero F. 2011. Effect of cooking on the chemical composition of low-salt, low-fat Wakame/ olive oil added beef patties with special reference to fatty acid content. *Meat Sci*, **89** (1): 27-34.
- MacArtain P, Gill CIR, Brooks M, Campbell R, and Rowland R. 2007. Nutritional value of edible seaweeds. *Nutr Rev*, **65**: 535-543.
- Machu L, Misurcova L, Ambrozova JV, Orsavova J, Mlcek J, Sochor J, and Jurikova T. 2015. Phenolic content and antioxidant capacity in alga food product. *Molecules*, **52**: 873-885.

- Moubayed NMS, Al Hourri HJ, Al Khulaifi MM, and Al Farraj, DA. 2017. Antimicrobial, antioxidant properties and chemical composition of seaweeds collected from Saudi Arabia (Red Sea and Arabian Gulf). *Saudi J Biol Sci*, **24**: 162–169. [\[CrossRef\]](#)
- Muraguri EN, Wakibia JG, Kinyuru JN. 2016. Chemical composition and functional properties of selected seaweeds from the Kenya coast. *J Food Res* 5(6): 114-123.
- Mwalugha MH, Wakibia JG, Kenji GM, and Mwasaru MA. 2015. Chemical composition of common seaweeds from the Kenya Coast. *J Food Res*, **4**(6): 28-38.
- Nielsen F H. (1999). Ultra-trace minerals. *Modern Nutrition in Health and Disease*, **9**: 283-303.
- Niranjan RM, and Kim SK. 2011. Nutritional and digestive health benefits of seaweed. *Adv Food Nutr Res*, **64**: 1043-4526.
- Nriagu J O. 1988. Production and uses of chromium. In: *Chromium in the Natural and Human Environments*. New York: Wiley.
- Núñez Selles A, Castro HTV, Aguero JA, Gonzalez JG, Naddeo F, De Simone F, and Pastrelli L. 2002. Isolation and quantitative analysis of phenolic antioxidants, free sugars and polyols from mango (*Mangifera indica* L.) stem bark aqueous decoction used in Cuba as a nutritional supplement. *J Agric Food Chem*, **50**: 762-766.
- Omar HH, Abdullatif BM, El-Kazan MM, and El-Gendy AM. 2013. Read sea water and Biochemical composition of seaweeds at southern coast of Jeddah, Saudi Arabia. *Life Sci J* **10**(4): 1073-1080.
- Ooi D-J, Iqbal S, and Ismail M. 2012. Proximate composition, nutritional attributes and mineral composition of *Peperomia pellucida* L. (Ketumpangan Air) grown in Malaysia. *Molecules*, **17**: 11139-11145.
- Ortiz J, Romero N, Robert P, Araya J, Lopez-Hernández J, Bozzo C, and Rios A. 2006. Dietary fiber, amino acid, fatty acid and tocopherol contents of the edible seaweeds *Ulva lactuca* and *Durvillaea antarctica*. *Food Chemistry*, **99**(1): 98-104.
- Ortiz J, Uquiche E, Robert P, Romero N, Quitral V, and Llantén C. 2008. Functional and nutritional value of the Chilean seaweeds *Codium fragile*, *Gracilaria chilensis* and *Macrocystis pyrifera*. *Eur J Lip Sci Tech*, **111**(4): 320-327.
- Reka P, Thahira Banu A, and Seethalakshmi M. 2017. Elemental composition of selected edible seaweeds using SEM- energy dispersive spectroscopic analysis. *Int Food Res J* **24**(2): 600-606.
- Ribeiro SMR, Barbosa LCA, Queiroz JH, Knodler M, and Schieber, A. 2008. Phenolic compounds and antioxidant capacity of Brazilian mango (*Mangifera indica* L.) varieties. *Food Chemistry*, **110** (3): 620-626.
- Salvador N, Garreta A G, Lavelli L, and Ribera M A. 2007. Antimicrobial activity of Iberian macroalgae. *Scientia Marina*, **71**(1): 101-113.
- Sanjeeva K K A, Lee W W, and Jeon Y-J. 2018. Nutrients and bioactive potentials of edible green and red seaweed in Korea. *Fish Aquat Sci*, **21**:19.
- Schmid M, Guihéneuf F, and Stengel D. 2014. Fatty acid contents and profiles of 16 macroalgae collected from the Irish Coast at two seasons. *J Appl Phycology*, **26**: 451–463.
- Schroeder H A, and Tipton I H. 1968. The human body burden of lead. *Arch Environ Health*, **17**(6): 965-978.
- Shipeng Y, Woo H-C, Choi, J-H, Park Y-B, and Chun B-S. 2015. Measurement of antioxidant activities and phenolic and flavonoid contents of the brown seaweed *Sargassum horneri*: comparison of supercritical CO₂ and various solvent extractions. *Fish and Aquatic Sci*, **18**(2): 123-130.
- Taskin E, Ozturk M, and Kurt O. 2001. Antibacterial activities of some marine algae from the Aegean Sea (Turkey). *Afr J Biotechnol*, **6**: 2746-2751.
- Tenorio-Rodriguez P A, Murillo-Álvarez J I, Campa-Cordova Á I, Angulo C. (2017). Antioxidant screening and phenolic content of ethanol extracts of selected Baja California Peninsula macroalgae. *J Food Sci Tech*, **54**(2): 422–429.
- Trono G C. 2004. *Field Guide and Atlas of the Seaweed Resources of the Philippines, Vol. 2*. Quezon City: Bureau of Agricultural Research and Marine Environment and Resources Foundation.
- Tuney I, Cadirci B H, Unal D, and Sukatar A. 2006. Antimicrobial activities of the extracts of marine algae from the coast of Ural (Izmir, Turkey) Brittany France. *Turk J Biol*, **30**:171-175.
- Turan F, Ozgun S, Sayin S, and Ozyilmaz G. 2015. Biochemical composition of some red and green seaweeds from Iskenderun Bay, the northeastern Mediterranean coast of Turkey. *J Black Sea/Mediterranean Environ*, **21**(3): 239-249.
- Uauy R, Olivares M, and Gonzalez M. 1998. Essentiality of copper in humans. *American J Clin Nutr*, **67**(5): 952S-959S.
- Vasquez RD, and Lirio S. (2020). Content analysis, cytotoxic, and anti-metastasis potential of bioactive polysaccharides from green alga *Codium intricatum* Okamura. *Curr Bioact Compd*, **16**(3):320-328. <https://doi.org/10.2174/1573407214666181019124339>
- Yildiz G, Vatan Ö, Çelikler S, and Dere Ş. 2011. Determination of the phenolic compounds and antioxidative capacity in red algae *Gracilaria bursa-pastoris*. *Int J Food Propert*, **14**: 496-502.
- Zhang WW, Duan XJ, Huang HL, Zhang Y, and Wang BG. 2007. Evaluation of 28 marine algae from the Qingdao coast for antioxidative capacity and determination of antioxidant efficiency and total phenolic content of fractions and sub-fractions derived from *Symphyclocladia latiuscula* (Rhodomelaceae). *J Appl Phycol*, **19**: 97–108.
- Zbikowski R, Szefer P, and Latała A. 2006. Distribution and relationships between selected chemical elements in green alga *Enteromorpha* sp. from the southern Baltic. *Environ Poll*, **143**: 435–448.

Associations of GCKR, TCF7L2, SLC30A8 and IGFB Polymorphisms with Type 2 Diabetes Mellitus in Egyptian Populations

Eman A. Awadallah^{1,*}, Nehal S. Hasan¹, Mona A.M. Awad¹, Solaf A. Kamel¹, Rasha N. Yousef¹, Nevine I. Musa² and Eman M. Hassan¹

¹ Department of Clinical and Chemical Pathology, National Research Centre (NRC), Giza, 12622; ² Department of Internal Medicine, Ain Shams University, Cairo, Egypt

Received: September 23, 2019; Revised: November 3, 2019; Accepted: November 22, 2019

Abstract

Novel genes have been identified by Genome-wide association studies (GWAS) to be associated with type 2 diabetes mellitus (T2DM) which have been replicated in different ethnic populations and yielded inconsistent results. We aimed to study the possible association between glucokinase regulator gene (GCKR), transcription factor 7 like 2 (TCF7L2), Solute Carrier Family 30 Member 8 (SLC30A8) and insulin like growth factor binding (IGFB) genes polymorphisms (rs 780094, rs 7903146, 12255372, rs 11558471 and rs 2854843) and T2DM in Egyptian people. This case control study was conducted on 228 subjects divided into two groups; the control group which contains 96 healthy individuals and 132 patients with T2DM. Single nucleotide polymorphisms (SNPs) (rs 780094, rs 7903146, 12255372, rs11558471 and rs 2854843) were detected by real-time polymerase chain reaction (Rt-PCR). For GCKR gene (rs 780094) the variant T allele was associated with T2DM ($p=0.001$) and the frequency of (TT and CT) genotypes vs. CC genotype was significantly higher in T2DM patients than control ($p = 0.001$). These genotypes showed higher risk for T2DM (OR = 8.4, 95% CI= 3.2 -22.0 and OR= 5.4, 95% CI= 2.9- 10.0 respectively, $p= 0.001$). IGFB gene (rs 2854843) showed that the risk of T2DM is increased with TT and CT genotypes (OR= 13.3, 95% CI=6.26 - 28.4, OR= 3.0, 95% CI= 1.5 – 6.0, respectively, $p= 0.001$). With regard to SLC30A8 gene (rs 11558471) the only genotype that showed significant association with type 2 diabetes is AG genotype ($p=0.01$). Also, we identified strong association between T2DM and TCAGT, TTGTT haplotypes ($p= 0.001$ and 0.01 respectively). Conclusion: Our study revealed a significant association between T2DM and TCAGT, TTGTT, TTATT and TCATT haplotypes.

Keywords: type 2 diabetes mellitus, single nucleotide polymorphisms, haplotype, Polymerase Chain Reaction.

1. Introduction

Diabetes mellitus (DM) is a chronic life-threatening disease, and it is the second leading cause of death over the world among adults between age of 35 and 64 years; 1 of every 10 deaths is caused by DM (El-Lebedy *et al.*, 2014). DM is one of metabolic diseases caused by impaired insulin action, insulin secretion or defect in both mechanisms. The underlining cause of type 2 diabetes mellitus (T2DM) can be attributed to combination of increased production of insulin hormone as a compensatory response to resistance to its action and inadequate secretory response (Sturgeon *et al.*, 2016); meanwhile, expansion of low physical activity life style and obesity increased prevalence of diabetes (Hasan *et al.*, 2017). On the other hand, genetic factors have an important role in the development of the underlining pathology of diabetes (Murea *et al.*, 2012). The rising prevalence of diabetes highlights the urgent need for aggressive strategies aimed at the prevention and control of diabetes (Liu *et al.*, 2015; Guo *et al.*, 2012).

Establishment of single-nucleotide polymorphism (SNP) databases, development and improvement of cost-effective high-throughput genotyping technology, and multi-center consortium large-scale genome-wide association studies (GWAS) are effective methods to investigate genetic susceptibility to T2DM (Xiao *et al.*, 2016). Glucokinase (GCK), expressed in beta cells of pancreas and in the liver, is the key enzyme that encodes rate-limiting step of glycolysis, glucose stimulated insulin secretion and regulating glucose balance (Wang *et al.*, 2018). The activity of GCK is controlled by the glucokinase regulatory protein (GCRP), which binds to GCK. Its inhibitory effect is antagonized by fructose 1-phosphate and enhanced by fructose 6-phosphate. The glucokinase regulator gene (GCKR) encodes GCRP. GCKR (rs780094) is the most commonly reported SNP that has been shown by GWAS studies to be associated with insulin levels, triglycerides (TG), fasting glucose (Wang *et al.*, 2018), and susceptibility to T2DM (Zhou *et al.*, 2018; Ma *et al.*, 2016). The transcription factor 7 like 2 (TCF7L2) gene is considered as an important gene of susceptibility for diabetes in European populations.

* Corresponding author e-mail: emanawad_28@yahoo.com.

Lyssenko *et al.* 2007 found that SNPs in TCF7L2 gene (rs12255372 and rs7903146) have strong association with the risk of diabetes. These gene risk alleles are associated with β -cells dysfunction of pancreases in all subjects (Grant *et al.*, 2006).

A number of susceptibility variants for T2DM have been identified by GWAS. The common alleles of SNPs, rs13266634(C/T, Arg276Trp), and rs11558471 (A/G) in the Solute Carrier Family 30 Member 8 (SLC30A8) gene are found to confer the risk susceptibility in T2DM (Abu Seman *et al.*, 2015). The genes including SLC30A8 identified by GWAS, however, can only explain approximately 10% of the overall heritable risk of T2DM, which challenges our expectations to translate genetic information into clinical practice (Imamura *et al.*, 2011). Insulin-like growth factor 2 mRNA (messenger-ribonucleic acid) binding protein 2 (IGF2BP2) belongs to a family of IGF2 mRNA-binding proteins that is implicated in Insulin growth factor 2 (IGF2) translational regulation, mRNA localization and turnover (Bell *et al.*, 2013; Dai *et al.*, 2011). IGF-2 plays a role in glucose homeostasis through inhibiting the gluconeogenesis by the liver as well as increasing the uptake of glucose by peripheral tissues (Zachariah *et al.*, 2007). Several IGF2BP2 gene variants were identified and investigated for association with T2DM (Gu *et al.*, 2012). This study identified 4 novel susceptibility genes associated with T2DM including GCKR, TCF7L2, SLC30A8 and IGFB. We aim to assess the association between GCKR polymorphisms (rs 780094), TCF7L2 polymorphisms (rs 7903146 and 12255372), SLC30A8 polymorphisms (rs 11558471), and IGFB polymorphisms (rs 2854843) and T2DM in Egyptian people.

2. Materials and Methods

2.1. Studied Population

This study is a case-control study that included 228 subjects. They are divided into 96 apparently healthy control subjects who were age and sex matched and 132 patients with T2DM. The cases were recruited from out patients' clinic of the National Research Centre, National Egyptian Institute of Diabetes, and Coronary Care Unit (CCU) of Ain Shams Hospital, Cairo Egypt.

According to American Diabetes Association (ADA) [American Diabetes Association (2018)]; DM is diagnosed when fasting blood glucose (FBG) level ≥ 126 mg/dl and/or 2 hours post prandial (2HPP) ≥ 200 mg/dl and/or random blood glucose (RBG) ≥ 200 mg/dl and/or glycated hemoglobin (HbA1c) ≥ 6.5 %.

All participants answered a questionnaire used for collecting socioeconomic data, as well as family history of diabetes and other diseases. Anthropometric measurements

were performed: weight (kg), height (cm), body mass index (BMI) (kg/m^2), waist circumference (cm) (Ong *et al.*, 2017).

Hepatic, renal, autoimmune, endocrinal diseases, metabolic disorders and autoimmune diseases were exclusion criteria for diabetic patients.

Ethics Committee's approval and participants' consents were obtained.

2.2. Laboratory Investigations

2.2.1. Biochemical markers

Venous blood samples after a 10-hours fasting were collected from each subject in a sterile EDTA and plain vacutainer tubes. 2 EDTA tubes blood samples were collected one of them stored at -20 C° till DNA (double stranded nucleic acid) extraction for genotyping and the other used for measuring HbA1c. Blood on the plain tubes was allowed to clot for 30 minutes, and then centrifuged at 3000g for 10 minutes at -4 C°. Sera were stored at -20 C° till time of analysis. Measurement of serum levels of FBG, lipid profile [total cholesterol (CHO), high density lipoprotein (HDL) cholesterol (HDL-C), TG] and HbA1c were performed on automated clinical chemistry analyzer (OLYMPUS AU400). Low density lipoprotein cholesterol (LDL-C) level was calculated using Friedewald formula (Friedewald *et al.*, 1972).

2.2.2. Genotyping of GCKR, TCF7L2, SLC30A8, and IGFB SNPs

DNA was extracted using QIA amp DNA Blood Mini Kits-50-Catalog no. 51104 (Qiagen, Hilden, Germany) according to manufacture instruction. DNA integrity was determined by 1% agarose gel electrophoresis, stained with ethidium bromide, and visualized through GEL documentation (E-Gel® Imager System with UV Light Base, Thermo scientific). DNA concentration was determined by Nano Drop 2000 Spectrophotometer (Thermo scientific). GCKR rs780094, TCF7L2 rs7903146, TCF7L2 rs12255372, SLC30A8, rs11558471, and IGFB rs2854843 polymorphisms (Applied Biosystems, Foster City, CA, USA) were detected by Rt-PCR using the Rotor Gene Q Rt-PCR (QIAGEN, Germany) (Table 1).

Allele discrimination was performed using the TaqMan genotyping protocol (Applied Biosystems, Foster City, CA, USA). PCR reactions were set up in 20 μ l reaction volume including 20–30 ng DNA, 10 μ l TaqMan genotyping PCR Master Mix and 1 μ l TaqMan SNP genotyping assay. The PCR assay was carried out according to manufacturer's instructions including one step of 10 min at 95 °C followed by 40 cycles of DNA denaturation at 95 °C for 15 s and annealing/extension at 60 °C for 1 min. Final products were analyzed by Rotor Gene software.

Table 1: Genotyping SNPs

Mapped gene	dbSNP	Sequence [VIC/FAM]
GCKR	rs780094	CTCAACAAATGTATTGATCAGCAAA[C/T]ATGTGTCAGTCATGGTCTAAAAA
TCF7L2	rs7903146	TAGAGAGCTAAGCACTTTTATAGATA[C/T]TATATAATTTAATTGCCGTATGAGG
TCF7L2	rs12255372	TGCCAGGAATATCCAGGCAAGAAT[G/T]ACCATATTCTGATAATTACTCAGGC
SLC30A8	rs11558471	CAGATAATTTAGATATTTACCTGCA[A/G]GAAGGAATAAAGCAGATGCAACCAA
IGFB	rs2854843	AGGAAAGTTATTCAAAATCTAGAAA[C/T]GTCTTCTGCTAAATTCTTAATTAAG.

2.3. Statistical Analysis

The data were analyzed using Microsoft Excel 2010 and statistical package for social science (SPSS version 24.0) for windows (SPSS IBM., Chicago, IL). Continuous normally distributed variables were represented as mean \pm SD. with 95% confidence interval, and using the frequencies and percentage for categorical variables, a p value ≤ 0.05 was considered statistically significant. To compare the means of normally distributed variables between groups, the Student's t test was performed. χ^2 test or Fisher's exact test was used to determine the distribution of categorical variables between groups. Spearman's rank correlation coefficient (r) was done to show the correlation between different parameters in this study. Effect modifications were evaluated by stratification, and statistical interaction was assessed by including main effect variables and their product terms in the logistic regression model.

2.3.1. Haplotype Analysis

The data was analyzed using HAPLOTYPE ANALYSIS softwear v1.05 which is a software written in Visual Basic for Applications (VBA) within Excel. This is new software for analysis of data from organelle based on the frequency of haplotypes. Population genetic structure from the population samples (inter-population analysis) was computed, utilizing: Nei's minimum genetic distance and genetic differentiation among the populations and contribution of each of them to the total diversity (Finkeldey and Murillo 1999).

3. Results

3.1. Characteristics of the Studied Population

This study is a case-control comparative study consisting of 132 patients with T2DM and control group ($n = 96$). The 2 studied groups showed statistical significant differences as regards height, weight, waist, BMI, FBG, 2HPP, HbA1c, CHO, TG, and LDL among the T2DM group when compared to control group (p of all parameters = 0.001 except height and BMI were $p = 0.04$ and 0.004 , respectively) (Table 2).

Table 2. Demographic and biochemical variables of the studied populations:

	Control N= 96 Mean \pm SD	Diabetic N= 132 Mean \pm SD	P. value
Weight (kg)	77.6 \pm 14.2	82.4 \pm 10.9	0.006*
Height (cm)	164.4 \pm 12.4	161.4 \pm 8.4	0.04*
BMI (kg/m ²)	29.2 \pm 7.6	31.7 \pm 4.1	0.004*
Waist (cm)	88.5 \pm 14.3	106.9 \pm 12.7	0.001**
FBS (mg/dl)	93.0 \pm 23.1	195.3 \pm 75.9	0.001**
2H PP (mg/dl)	99.8 \pm 27.3	222.3 \pm 73.5	0.001**
HbA1c (%)	5.2 \pm 0.7	8.6 \pm 2.0	0.001**
CHO (mg/dl)	162.4 \pm 34.5	211.4 \pm 50.6	0.001**
TG (mg/dl)	102.4 \pm 34.3	199.2 \pm 87.0	0.001**
HDL (mg/dl)	48.4 \pm 10.2	47.5 \pm 16.0	0.625
LDL (mg/dl)	92.3 \pm 36.2	123.8 \pm 45.8	0.001**

†Weight, Height, BMI, Waist, FBS, 2H PP, HbA1c, CHO, TG, HDL and LDL are represented as mean \pm SD; the data were analyzed by t test.

*P-value ≤ 0.05 is significant, **P-value ≤ 0.001 is highly significant.

3.2. Association Studies for Different SNPs

For the GCKR rs 780094 the T allele showed higher frequency in T2DM patients than in controls (OR =3.99, 95% CI= 2.565-6.215, $p = 0.001$). The frequency of (CT and TT) genotypes vs. CC genotype was significantly higher in T2DM patients (50% in patients vs., 22.9% in controls and 21.2% in patients vs. 6.3% in controls, respectively) ($p = 0.001$); these genotypes showed higher risk for T2DM (OR= 5.4, 95% CI =2.9 - 10.0 and OR= 8.4, 95% CI = 3.2 - 22.0 respectively) ($p =0.001$). Meanwhile, the frequency of (CT + TT) genotypes vs. the CC genotype was significantly higher in T2DM patients than in controls (71.2% in patients vs. 29.2% in controls), with higher risk for T2DM (OR=6, 95% CI=3.4- 10.7) ($p=0.001$).

Considering the IGF1 rs 2854843, the T allele frequency was significantly associated with increased risk of T2DM (OR= 5.8, 95% CI=3.850-8.712, $p=0.001$). The frequency of TT genotypes vs. CC genotype was significantly higher in T2DM patients when compared to control (57.6% in patients vs. 14.6% in controls) ($p = 0.001$); it showed increased risk of T2DM (OR= 13.3, 95% CI=6.26 - 28.4). Also, the frequency of (CT + TT) genotypes vs. the CC genotype was significantly higher in T2DM patients than in controls (83.3% in patients vs. 33.8% in control) (OR= 6.4, 95% CI= 3.5 - 11.8, $p = 0.001$).

As regards the SLC30A8 rs 11558471, the only genotype that showed significant difference between diabetic patients and control group is AG genotype (37.9% in patients vs. 18.8% in control) ($p=0.01$).

However, the other two SNPs (TCF7L2 rs 7903146 and rs 12255372) were not found to be associated with T2DM. The genetic models are summarized in table 3.

3.3. Associations of Haplotypes with T2DM

The haplotype block was constructed for the five SNPs (rs780094, rs 7903146 and 12255372, rs 11558471 and rs 2854843). All five SNPs fell into one block. CCAGC haplotype was the most frequent and associated with control group than in cases ($p =0.001$) followed by CTATT haplotype ($p =0.03$), while TCAGT was the most frequent haplotype in T2DM patients followed by TTGTT, TTATT and TCATT and they were strongly associated with the disease ($P = 0.001$, 0.01, 0.04 and 0.05 respectively), meanwhile taking CCAGC haplotype as reference (OR = 28.6, 7.9, 10.7 and 8.9 respectively) (Table 4). Another finding in this study is that subjects having TCGGT and TTGGT haplotypes are not protective against diabetes ($p=0.001$ and 0.02 respectively) as they were found in cases only, while, CCATC and CTGTC could be considered protective haplotypes as they were found only in control group ($p = 0.001$ for both) (Table 4) (Figure 1).

Table 3: Association study of different SNPs variants with T2DM under different genetic models

SNPs	Genotype	Groups		P. value	OR	95% CI	P. value	
		Control	Diabetic					
GCKR	CC	68(70.8%)	38(28.8%)	0.001**	1(reference)			
	CT	22(22.9%)	66(50.0%)	0.001**	5.4	2.9 - 10.0	0.001**	
	TT	6(6.3%)	28(21.2%)	0.001**	8.4	3.2 - 22.0	0.001**	
	CT+TT	28(29.2%)	94(71.2%)	0.001**	6.0	3.4- 10.7	0.001**	
	Allele	C	158(0.823)	142(0.538)	0.001**	1(reference)		
		T	34(0.177)	122(0.462)	0.001**	3.993	2.565-6.215	0.001**
SLC30A8	AA	63(65.6%)	68(51.5%)	0.1	1(reference)			
	AG	18(18.8%)	50(37.9%)	0.01*	2.6	1.4 - 4.9	0.01*	
	GG	15(15.6%)	14(10.6%)	0.29	0.9	0.4 - 1.9	0.7	
	AG+GG	33(34.4%)	64(48.5%)	0.1	1.8	1.05 - 3.1	0.03*	
	Allele	A	144(0.750)	186(0.705)	0.5	1(reference)		
		G	48(0.250)	78(0.295)	0.3	1.258	0.826 - 1.915	0.2
IGFB	CC	54(56.3%)	22(16.7%)	0.001**	1(reference)			
	CT	28(29.2%)	34(25.8%)	0.6	3.0	1.5 - 6.0	0.001**	
	TT	14(14.6%)	76(57.6%)	0.001**	13.3	6.26 - 28.4	0.001**	
	CT+TT	42(33.8%)	110(83.3%)	0.001**	6.4	3.5 - 11.8	0.001**	
	Allele	C	136(0.708)	78(0.295)	0.001**	1(reference)		
		T	56(0.292)	186(0.705)	0.001**	5.8	3.850-8.712	0.001**

†OR: Odds Ratio; †CI: Confidence Interval.

††Allele frequency was calculated in 2 N.

*P value ≤ 0.05 significant; **P value ≤ 0.01 highly significant.

Table 4. Association of different SNPs haplotypes and T2DM

Haplotype association	Control		Cases		P. value	OR	95% CI	P. value
	N	%	N	%				
Significant Haplotypes association in control								
CCAGC	68	35.4%	38	14.4%	0.001**	1(reference)		
CTATT	10	5.2%	4	1.5%	0.03*	0.72	0.2 - 2.4	0.6
Significant Haplotypes association in cases								
TCAGT	2	1.0%	32	12.1%	0.001**	28.6	6.5 - 126.12	0.001**
TTGTT	5	2.6%	22	8.3%	0.01*	7.9	2.8 - 22.5	0.001**
TTATT	2	1.0%	12	4.5%	0.04*	10.7	2.3 - 50.5	0.003*
TCATT	2	1.0%	10	3.8%	0.05*	8.9	1.9 - 42.9	0.01*
Specific Haplotypes for control group								
CCATC	12	6.3%	0	0.0%	0.001**			
CTGTC	10	5.2%	0	0.0%	0.001**			
TTATC	2	1.0%	0	0.0%	0.1			
TCGTT	2	1.0%	0	0.0%	0.1			
TCGTC	2	1.0%	0	0.0%	0.1			
CTGGC	2	1.0%	0	0.0%	0.1			
TCATC	2	1.0%	0	0.0%	0.1			
Specific Haplotypes for cases group								
TCGGT	0	0.0%	12	4.5%	0.001**			
TTGGT	0	0.0%	8	3.0%	0.02*			
CTGGT	0	0.0%	4	1.5%	0.09			
TTAGT	0	0.0%	4	1.5%	0.09			
TTAGC	0	0.0%	4	1.5%	0.09			
CCGTT	0	0.0%	2	0.8%	0.23			

*P value ≤ 0.05 is significant; **P value ≤ 0.01 is highly significant.

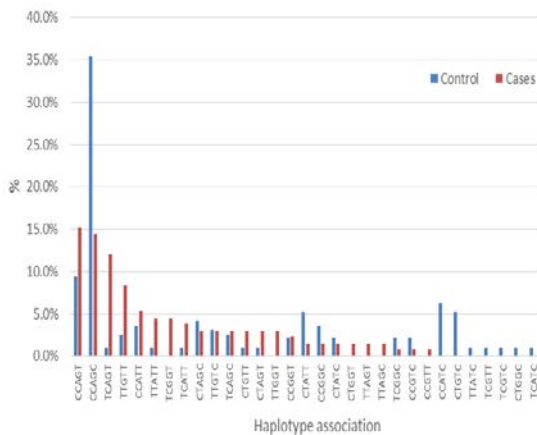


Figure 1. Total haplotype association in control and cases:

4. Discussion

Type 2 diabetes mellitus (T2DM) is a complex disorder resulting from an interaction between environment and genetic factors. Genetic variations can insert major or minor impacts on the disease. For initial prevention of T2DM, it is necessary to recognize genes potentially underlying the disease (Pourahmadi *et al.*, 2015). Our study is the first one of GCKR, TCF7L2, SLC30A8 and IGF2BP2 risk variants, rs 780094, rs 7903146, rs 12255372, rs 11558471 and rs2854843 in Egyptians.

The association between T2DM and GCKR rs780094 has been replicated in many studies of different ethnic populations since the Diabetes Genetics Initiative GWAS (Ling *et al.*, 2011). This association is confirmed again in our study in Egyptian population as TT mutant genotype distributions were significantly different between control and cases ($p=0.001$ OR= 8.4 with 95% CI= 3.2 – 22.0), also, the frequency of T allele was different ($p=0.001$ and OR = 3.993 with 95% CI= 2.565 – 6.215).

The decrease in β -cell mass and function in pancreatic islets are the underlying mechanisms of the progress of T2DM. TCF7L2 influences β -cell functions by affecting β -cell survival in pancreatic islets (Huang *et al.*, 2018).

An Egyptian study conducted by Alnaggar *et al.*, 2018 showed that there was statistically significant association between type 2 diabetic patients and diabetic nephropathy and TCF7L2 gene polymorphism rs 12255372, $P=0.005$, the allelic frequency differed significantly between the studied groups $P=0.005$, denoting that the G allele was the risky allele for developing T2DM and diabetic nephropathy. Another study on TCF7L2 gene polymorphism (rs12255372) was performed by Hassan *et al.*, 2019 in Al Najaf governorate, and it found that minor T allele showed significant association with the risk of T2DM with an OR of 3.52 (95% CI 1.96 – 6.33, $p < 0.0001$).

As regards TCF7L2 gene polymorphism (rs 7903146) Shah *et al.* studied 120 individuals, one half of them were homozygous for CC while, the other half were homozygous for TT. In their study, β -cell responsiveness was slightly impaired in the TT genotype group and differed significantly between genotypes, implying that a genetic variant of TCF7L2 impairs glucose tolerance through effects on insulin secretion and on glucagon (Shah *et al.*, 2016).

A study on three TCF7L2 variants (rs7903146, rs12255372, and rs4506565) was performed in India, and an association was detected between these three SNPs and T2DM (Pourahmadi *et al.*, 2015). Four TCF7L2 gene SNPs (rs11196205, rs7901695, rs12255372, and rs7903146) were investigated within a Japanese sample, this study showed a significant association between these four variants and T2DM, of all SNPs, rs12255372 showed the strongest association (Hayashi *et al.*, 2007). However, studies performed in China (Chang *et al.*, 2007), India (Guo *et al.*, 2007), and the United Arab Emirates (Saadi *et al.*, 2008) found no significant association between this SNP in the TCF7L2 gene and T2DM. Meanwhile, a study in Iran found that genotype distribution of TT mutant of rs7903146 (C/T) and rs12255372 (G/T) were not different between control subjects and T2DM patients ($p \geq 0.05$ for both, OR= 0.564, 95% CI= 0.280-1.135 and OR = 0.473 95% CI= 0.170-1.314 respectively) in the sample recruited from Jahrom city (Pourahmadi *et al.*, 2015), and this is concordant with our results which showed no significant difference in the frequency of the two studied SNPs (rs 7903146 and rs 12255372 in TCF7L2 gene) ($p = 0.2$ and 0.6 with OR= 1.9, 95% CI= 0.8- 4.5 and OR= 0.7 95% CI= 0.31-1.6 respectively).

GWAS identified IGF2BP2 gene to be associated with T2DM, and this association has been repeatedly confirmed among different ethnic populations (Grant *et al.*, 2006). While many studies confirmed the association (Cauchi *et al.*, 2012; Gamboa-Meléndez *et al.*, 2012), other studies reported no association (Kommoju *et al.*, 2013; Duesing *et al.*, 2008). Our results showed a strong association of SNP (rs 2854843) with T2DM as TT and CT+ TT genotypes distribution significantly different between cases and control ($p=0.001$, 0.001, OR= 13.3 with 95% CI= 6.26 – 28.4 and OR= 6.4 with 95% CI= 3.5 – 11.8 respectively). The common alleles of SNPs, rs13266634(C/T, Arg276Trp), and rs 11558471(A/G) in the SLC30A8 gene are found to confer the risk susceptibility in T2DM (Abu Seman *et al.*, 2015). We studied the risk of SLC30A8 polymorphism (rs 11558471), and we found that AG genotype is the only genotype which showed an increased frequency in T2DM patients than control ($p=0.01$ and OR= 2.6 with 95% CI= 1.4 – 4.9).

In our patients, haplotype analysis showed strong association between T2DM and TCAGT, TTGTT, TTATT and TCATT haplotypes ($p=0.001, 0.01, 0.04$ and 0.05 respectively). Taking CCAGC as a reference showed increased risk of developing T2DM (OR= 28.6, 7.9, 107 and 8.9 respectively), while other haplotypes which include CCAGC and CTATT could be protective against T2DM as they were significantly higher in the control group. Meanwhile, haplotype analysis showed us another finding that there were specific haplotypes for control group (CCATC and CTGTC) and others were specific for

cases group (TCGGT and TTGGT). One of the limitations of our study is that we cannot compare our results with other research works because we did not find another haplotype studies on these five SNPs at the same time.

5. Conclusion

In conclusion, our study identified a significant association of GCKR rs 780094 and IGF2 rs 2854843 variants with T2DM in Egyptians. Also, we identified strong association between T2DM and TCAGT, TTGTT, TTATT and TCATT haplotypes. However, CCATC and CTGTC haplotypes were higher in control group than in diabetic patients. Further studies are to be addressed to assess other variants that could modify the risk of T2DM in our population.

Acknowledgment

All authors have appreciated the role of National Research Centre in funding this work.

References

- Abu Seman N, Mohamud WNW, Östenson CG, Brisma KR, and Gu H F. 2015. Increased DNA methylation of the SLC30A8 gene promoter is associated with type 2 diabetes in a Malay population *Clin epigenetic*, **7(1)**: 30.
- Alnaggar AR, Abd El-salam RF, Rady NH, Ishak MF and Ammar SH. 2018. Study of the association of transcription factor 7 like 2 gene polymorphism with type 2 diabetes mellitus and diabetic nephropathy in the Egyptian population. *Endocrine Abstracts*, **56** P335 DOI: [10.1530/endoabs.56.P335](https://doi.org/10.1530/endoabs.56.P335)
- American Diabetes Association 2018. *Diabetes Care* **41** (Suppl.1)p. S13–27.
- Bell JL, Wächter K, Mühleck B, et al. 2013. Insulin-like growth factor 2 mRNA-binding proteins (IGF2BPs): post-transcriptional drivers of cancer progression. *Cell Mol Life Sci*, **70** (15):2657-2675.
- Cauchi S, Ezzidi I, El Achhab Y, Mtiraoui N, Chaieb L, Salah D, Nejari C, Labrune Y, Yengo L, Beury D, Vaxillaire M, Mahjoub T, Chikri M, Froguel P. 2012. European genetic variants associated with type 2 diabetes in North African Arabs. *Diabetes Metab*, **38(4)**:316-323.
- Chang YC, Chang TJ, Jiang YD, Kuo SS, Lee KC, Chiu KC, Chuang L M. 2007. Association study of the genetic polymorphisms of the transcription factor 7-like 2 (TCF7L2) gene and type 2 diabetes in the Chinese population. *Diabetes*, **56**:2631–2637.
- Dai N, Rapley J, Angel M, et al. 2011. mTOR phosphorylates IMP2 to promote IGF2 mRNA translation by internal ribosomal entry. *Genes Dev*, **25(11)**:1159-1172.
- Duesing K, Fatemifar G, Charpentier G, Marre M, Tichet J, Hercberg S, et al. 2008. Evaluation of the association of IGF2BP2 variants with type 2 diabetes in French Caucasians. *Diabetes*, **57(7)**:1992–1996.
- El-Lebedy D, Kafoury M, Abd-El Haleem D, Ibrahim A, Awadallah E and Ashmawy I. 2014. Paraoxonase-1 gene Q192R and L55M polymorphisms and risk of cardiovascular disease in Egyptian patients with type 2 diabetes mellitus. *Journal of Diabetes & Metabolic Disorders*, **13(125)**: 2-7.
- Finkeldey R, Murillo O 1999. Contributions of subpopulations to total gene diversity. *Theoretical and Applied Genetics*, **98**: 664-668.
- Friedewald WT, Levy RI, Fredrickson D S. 1972. *Clin Chem*, **18**: 499 502.
- Gamboa-Meléndez MA, Huerta-Chagoya A, Moreno- Macías H, Vázquez-Cárdenas P, et al. 2012. Contribution of common genetic variation to the risk of type 2 diabetes in the Mexican Mestizo population. *Diabetes*, **61(12)**: 3314-3321.
- Grant SF, Thorleifsson G, Reynisdottir I, Benediktsson R, et al. 2006. Variant of transcription factor 7-like 2 (TCF7L2) gene confers risk of type 2 diabetes. *Nat Genet*, **38**:320–323.
- Gu T, Horová E, Möllsten A, et al. 2012. IGF2BP2 and IGF2 genetic effects in diabetes and diabetic nephropathy. *J Diabetes Complications*, **26** (5):393-398.
- Guo T, Hanson RL, Traurig M, Muller YL, Ma L, Mack J, Kobes S, Knowler WC, Bogardus C, Baier LJ. 2007. TCF7L2 is not a major susceptibility gene for type 2 diabetes in Pima Indians: analysis of 3,501 individuals. *Diabetes*, **56**:3082–3088.
- Guo XH, Yuan L, Lou QQ, Shen L, Sun ZL, Zhao F, et al. 2012. A nationwide survey of diabetes education, self- management and glycemic control in patients with type 2 diabetes in China. *Chin Med J*, **125**:4175–4180.
- Hasan NS, Kamel SA, Hamed M, Awadallah E, Abdel Rahman AH, Musa NI and Hussein GH S. 2017. Peroxisome proliferator-activated receptor- α polymorphism (rs1801282) is associated with obesity in Egyptian patients with coronary artery disease and type 2 diabetes mellitus. *Journal of Genetic Engineering and Biotechnology*, **15**: 409–414.
- Hassan BG, Ridha MM and Mohammed AJ. 2019. The association of TCF7L2 Gene (rs12255372) single nucleotide Polymorphism with Type Two Diabetes Mellitus in Al Najaf Governorate. *Pharm. Sci. and Res.* **10(9)**: 2163-2165.
- Hayashi T, Iwamoto Y, Kaku K, Hirose H, Maeda S. 2007. Replication study for the association of TCF7L2 with susceptibility to type 2 diabetes in a Japanese population. *Diabetologia*, **50**:980–984.
- Huang ZQ, Liao YQ, Huang RZ, Chen JP and Sun HL. 2018. Possible role of TCF7L2 in the pathogenesis of type 2 diabetes mellitus. *Journal of Biotechnology and Biotechnological Equipment*, **32(4)**:830-834.
- Imamura M, Maeda S. 2011. Genetics of type 2 diabetes: the GWAS era and future perspectives. *Endocr J*, **58(9)**:723–739.
- Kommoju UJ, Maruda J, Kadarkarai S, Irgam K, Kotla JP, Velaga L, Reddy B M. 2013. No detectable association of IGF2BP2 and SLC30A8 genes with type 2 diabetes in the population of Hyderabad, India. *Meta Gene*, **1**: 15–23.
- Ling Y, Li X, Gu Q, Chen H, Lu D and Gao X. 2011. Associations of common polymorphisms in GCKR with type 2 diabetes and related traits in a Han Chinese population: a case585 control study. *MC Medical Genetics*, **12(66)**: 1-9.
- Liu L, Lou Q, Guo X, Yuan L, Shen L, Sun Z, et al. 2015. Management status and its predictive factors in patients with type 2 diabetes in China: a nationwide multicenter study: a nationwide multicenter study. *Diabetes Metab Res Rev*, **31**:811–816.
- Lyssenko V, Lupi R, Marchetti P, Del Guerra S, Orho- Melander M, Almgren P, Sjogren M, et al. 2007. Mechanisms by which common variants in the TCF7L2 gene increase risk of type 2 diabetes. *J Clin Invest*, **117**: 2155–2163.
- Ma Q, Wang L, Yao H, Zhu J, Wang S, Zhang X, Wang T, Ma Y, Su Y, Wang Z, Ding L. 2016. Association of GCKR gene polymorphisms and type 2 diabetes among ethnic Uyghurs. *Chin J Med Genet*, **33**: 532-536.
- Murea M, Ma L and Freedman B I. 2012. Genetic and environmental factors associated with type 2 diabetes and diabetic vascular complications. *Review of Diabetic Studies*, **9** (1): 6–22.

- Ong KL, Cheung BMY, Man YB, Lau CP, Lam KSL. 2007. Prevalence, awareness, treatment, and control of hypertension among United States adults 1999-2004. *Hypertension*, **49**: 69–75.
- Pourahmadi M, Erfanian S, Moradzadeh M, and Jahromi A S. 2015. Non-Association between rs7903146 and rs12255372 Polymorphisms in Transcription Factor 7-Like 2 Gene and Type 2 Diabetes Mellitus in Jahrom City, Iran. *Diabetes Metab J*. **39(6)**: 512–517.
- Saadi H, Nagelkerke N, Carruthers S G, Benedict S, Abdulkhalek S, Reed R, Lukic M, Nicholls M G. 2008. Association of TCF7L2 polymorphism with diabetes mellitus, metabolic syndrome, and markers of beta cell function and insulin resistance in a population-based sample of Emirati subjects. *Diabetes Res Clin Pract*, **80**:392–398.
- Shah M, Varghese RT, Miles JM, et al. 2016. TCF7L2 genotype and α -cell function in humans without diabetes. *Diabetes*. **65(2)**:371–380.
- Sturgeon LP, Bragg-Underwood TM, and Blankenship M. 2016. Practice matters: prevention and care of individuals with type 2 diabetes. *International Journal of Faith Community Nursin,g* **2(1)**: 32-39.
- Wang L, Ma Q, Yao H, He2 LJ, Fang BB, Cai W, Zhang B, Wang ZQ, Su YX, Du GL, Wang SX, Zhang ZX, Hou QQ, Cai R, He FP. 2018. Association of GCKR rs780094 polymorphism with circulating lipid levels in type 2 diabetes and hyperuricemia in Uyghur Chinese. *Int J Clin Exp Pathol*, **11(9)**:4684- 4694.
- Xiao S, Zeng X, Fan Y, Su Y, Ma Q, Zhu J, and Yao H. 2016. Gene Polymorphism Association with Type 2 Diabetes and Related Gene-Gene and Gene-Environment Interactions in a Uyghur Population. *Med Sci Monit*, **22**: 474–487.
- Zachariah S, Brackenridge A, Shojaee-Moradie F, Camuncho-Hubner C, Umpleby A M, Russell-Jones D. 2007. The mechanism of non-islet cell hypoglycaemia caused by tumour produced IGF-II. *Clin Endocrinol*, **67(4)**: 637-638.
- Zhou WLY, Zhang L, Shi Y, Wang C, Zhang D, Liu X, Mao Z, Li L. 2018. Gene-gene interactions lead to higher risk for development of type 2 diabetes in a Chinese Han population: a prospective nested case-control study. *Lipids Health Dis*, **17**: 179.

Toxicities of *Parkia biglobosa* Extract and Dimethoate + Cypermethrin Insecticide on Kidney and Liver of Wistar Rats Fed Treated Okra Fruits

Olajumoke O. Fayinminnu^{1,*}, Olufunso O. Adeniyi^{1,2} and Rotimi Olatunde³

¹Department of Crop Protection and Environmental Biology, University of Ibadan, ²Forestry Research Institute of Nigeria; ³Department of Pharmacognosy, College of Medicine, University of Ibadan, Nigeria

Received: October 6, 2019; Revised: November 8, 2019; Accepted: November 22, 2019

Abstract

This study evaluated the sub-acute toxicities of *Parkia biglobosa* aqueous pod husk extract (PAPHE) and Dimethoate + Cypermethrin (D+C) insecticides treated okra fruits (milled) on the kidney and liver of wistar rats. Thirty-two male wistar rats randomly divided into eight experimental groups of four rats each were used for this study. The treatments were animals fed with: Standard Ratio Feed (SRF) + untreated okra (T1), SRF+ 2.5ml D+C okra treated (T2), SRF+5.0 ml D+C okra treated (T3), SRF + 20% PAPHE okra treated (T4), SRF+ 15% PAPHE (T5), SRF+10% PAPHE (T6), SRF+ 5% PAPHE (T7) and SRF only (Control 0%) (T8). Drinking water was given *ad libitum* for 21 days. Animal groups were sacrificed at the end of the experiment and vital organs were removed. Hematology and serum biochemical assays and histopathological identifications were done using standard procedures. Data were analyzed using ANOVA ($p < 0.05$), while histopathology was examined. Results revealed no significant differences ($p > 0.05$) amongst the treatments with the exception of treatment T5. The STR+15% PAPHE okra treated (T5) revealed highest values of platelets ($219 \times 10^3/\mu\text{L}$), Mean Corpuscular Hemoglobin (21.61 g/dL), Globulin (4.57 g/dL), AST (45.67 U/L) and Creatinine (1.13 mg/dL). Treatment T5 was more toxic than the other treatments. Photomicrographs of sections of liver and kidney organs of the wistar rats showed lesions (necrosis) in all the treatments except the control groups fed on SRF and SRF + untreated okra and SRF+ okra treated with 5% PAPHE. As such, the aqueous pod husk extract of *P. biglobosa* (PAPHE) appeared to be safe for consumption at 5% concentration in agricultural sustainability for food quality and safety.

Keywords: *Parkia biglobosa* pod husk extract, Dimethoate+Cypermethrin, Okra, Wistar rats

1. Introduction

Okra (*Abelmoschus esculentus* (L.) Moench) is a fruit vegetable that is widely cultivated and consumed in Nigeria; it is cultivated for its fibrous fruits (or pods) and its leaves. It is a good source of carbohydrate, protein, fats, vitamins and minerals (Akintoye *et al.*, 2011; Ojo *et al.*, 2014). Okra fruit can be cooked in a variety of ways; its leaves may also be cooked, eaten raw in salads or used as cattle feed (Fagwalawa and Yahaya, 2016). Mature fruits and stems of okra plant containing crude fiber are used in the paper industry (Moekchantuk and Kumar, 2004). Extracts from the seeds of the okra are viewed as an alternative source for edible oil. Okra is said to be very useful against genito-urinary disorders, spermatorrhoea and chronic dysentery (Robert *et al.*, 2011). Its mucilage is also suitable for medicinal (curing ulcers and relief from hemorrhoids) and industrial applications (Akinyele and Temikotan, 2007).

Okra is prone to damage by various insects such as: *Podagrica uniforma* and *P. sjostedti*, others include *Anomis flava*, *Earias biplaga*, *Aphis gossypii*, *Aphis craccivora* (Kumar, 2010). Incidence of attacks on okra leaves starts as early as the germination stage by

Podagrica species that create circular and irregular holes on okra leaves and punctures on pods. *Sylepta derogate* rolls okra leaves prior to pupation causing a reduction in the photosynthetic sites of the leaves (Ogbalu *et al.*, 2015).

The exposure of synthetic pesticides (insecticides, fungicides, herbicides) to fruits and vegetable production has been causing adverse health implication and environmental pollution. Pesticides have deleterious effects on non-target species; they affect animal and plant biodiversity, food webs and the ecosystem (Mahmood *et al.*, 2016). This problem led to a more sustainable approach to pest control and natural crop protection (botanicals) (Fayinminnu, 2010) with pesticidal potency. Pesticidal effects of many plants have been discovered and researched, such as Neem (*Azadirachta indica*), *Derris elliptica*, Chilli pepper (*Capsicum annum*), Giant milkweed (*Calotropis procera*), Mint weed (*Hyptis suaveolens*), Tobacco (*Nicotiana tabacum*), Cassava (*Manihot esculenta*), Eggplant (*Solanum melongena*), African locust bean tree (*Parkia biglobosa*) (Salako *et al.*, 2015), Purple weed (*Alternanthera brasiliana*) (Fayinminnu and Shiro, 2014) Drumestick (*Moringa oleifera*) (Fayinminnu *et al.*, 2015). Phytochemicals inherent in *P. biglobosa* have increased their use as a

* Corresponding author e-mail: olorijkb2008@gmail.com.

biopesticide to suppress different insect pests of okra (Fayinminnu *et al.*, 2017).

Biopesticides result in lower pesticide residues in food and environment, thereby preventing pollution problems and health hazards associated with synthetic pesticides; but toxic effects of some of these biopesticides on rats and humans have been reported. Awe and Oyetunji (2013) reported the toxicity of cassava leaf aqueous extracts on rats. Kadiri *et al.* (1999) found out that the traditional neem leaf-based medicines also used as biopesticide had acute toxic effects. Builders *et al.* (2012) administered graded doses of *Parkia biglobosa* stem bark methanolic and aqueous extracts orally to rats and found out that they were non-toxic.

Sherah *et al.* (2014) discovered the presence of substances that are cytotoxic enough to kill shrimp larvae in extracts of the seed-husk and stem-bark of *Parkia biglobosa*. The effectiveness of aqueous extract of *P. biglobosa* as a bio-insecticide in managing insect pests on okra plants had been reported by Fayinminnu *et al.* (2017). Therefore, the use of *P. biglobosa* aqueous extract as an insecticide on okra fruit vegetable necessitated the study of its toxicological effects. Information on the toxicity of residues of aqueous extract of *P. biglobosa* pod husk on rats is scanty. This study, therefore, aimed at assessing the sub-acute toxicity of residues of aqueous extract of *Parkia biglobosa* pod husk (PAPHE) on treated okra milled fruit feed on haematology, serum biochemistry and histology of kidney and liver organs of male wistar rats.

2. Materials and Methods

2.1. Preparation of aqueous extract of *Parkia biglobosa* pod husk

The pods of *Parkia biglobosa* were collected from Tede town in Atisbo Local Government Area, Oyo State (latitude 08°34'N and longitude 003°27'E). They were identified and authenticated at the herbarium of Forestry Research Institute of Nigeria, Jericho, Ibadan, Oyo State, Nigeria with voucher number 110449 (Fayinminnu *et al.*, 2017). The extraction procedure of *Parkia biglobosa* pod husk was carried out at the Toxicology Research Laboratory of the Department of Crop Protection and Environmental Biology, University of Ibadan, Nigeria as reported by Fayinminnu *et al.* (2017). The pods of *P. biglobosa* were dehusked and the husks were air dried at room ambient temperature of 28.71±1.77°C and relative humidity of 77.64 ± 8.07% for two weeks. They were milled into powder using Rico MG '601' Grinder Mixer and sieved through a 2 mm sieve to remove the fibers (Fawole and Abikoye, 2002). Aqueous extract was obtained by soaking 250 grams of milled pod husk in 1250 ml of water (ratio 1:5) for 24 hours according to the method of Oshimagye *et al.* (2014). The extract was concentrated by placing it in water bath at low temperature (45- 50°C) in order to determine its yield.

$$\% \text{ yield} = \frac{\text{weight of extract (grams)}}{\text{weight of plant material (grams)}} \times 100$$

The concentration of the stock solution of the biopesticide (aqueous extract of *P. biglobosa* pod husk (PAPHE)) was 20%; other concentrations were prepared from the stock solution by serial dilution. A 5% concentration was prepared by diluting 125 ml of the stock

solution in 500 ml of water; 10% was prepared by diluting 250 ml of stock solution in 500 ml of water; 15% was prepared by diluting 375 ml of stock solution in 500 ml of water. The prepared extracts were labeled and stored in refrigerator at 20°C for 24 hours prior to use to prevent putrefaction and degradation of phytochemicals present in them (Fayinminnu and Shiro, 2014).

2.1.1. Preparation of synthetic chemical pesticide

The synthetic chemical insecticide 'Scorpion' (Dimethoate 14.5% + Cypermethrin 5.5% (D+C)) was purchased from SARO Agrosociences Limited, Oluyole, Ibadan, Oyo State, Nigeria. Synthetic insecticide treatments were prepared as follows: 2.5 ml of dimethoate + cypermethrin in 500 ml (recommended dose) and 5 ml of dimethoate + cypermethrin in 500 ml of water (Dey *et al.*, 2013).

2.2. Experimental Compounds

Qualitative and quantitative analyses of the following phytochemicals were performed on the milled *Parkia biglobosa* plant parts (leaves, bark, pod husk and seeds) at the Organic Chemistry (Pharmchem) Research Laboratory of the Faculty of Pharmacy, University of Ibadan and Femtop Analytical Laboratory, Idi-Ishin, Ibadan. According to the earlier work and report of Fayinminnu *et al.* (2017), the identified phytochemicals: Phenol, Flavonoid, Tannin, Saponin, Cardiac glycoside, Steroid, Terpenoid, Alkaloid and Antraquinone in *Parkia biglobosa* pod husk formed the basis for its potential biopesticide (insecticide) and baseline for this present study.

2.3. Field Study

This was carried out at the Crop Garden of the Department of Crop Protection and Environmental Biology (CPEB), University of Ibadan, Nigeria as reported earlier by Fayinminnu *et al.* (2017). The field seven treatments were: 2.5 and 5.0 ml D+C, 5, 10, 15, 20% PAPHE and control (0%). The gross area at the crop garden of CPEB was 22.3 m x 10.7 m with individual plot sizes of 0.9 m x 0.9 m and an alley of 2 m. Each of the seven treatments was replicated three times and laid out in a randomized complete block design.

Two seeds of okra (variety NHAe-47-4 purchased from National Horticulture Research Institute ((NIHORT), Idi-Ishin, Ibadan, Oyo State, Nigeria) were sown per stand at a depth of 2cm, spacing of 0.3m x 0.3m between each stand to obtain a plant population of 2651 plants ha⁻¹. Missing stands were supplied at one (1) week after sowing (WAS), while seedlings were later thinned to one (1) seedling per stand two (2) WAS. Watering was done manually on a daily basis. Regular weeding was carried out manually in order to prevent competition, infestation of pests and diseases and also to ensure maximum growth of the crops. The plants were sprayed with the aforementioned seven treatments weekly from two (2) WAS till twelve (12) WAS to control *Podagrica unifirma* and *sjustedti* (Flea beetles) using a 7.5 Litre knap sack sprayer.

At maturity, sprayed okra fruits were harvested at 9 to 12 weeks after sowing every week by plucking from each treated plot. Harvested sprayed okra fruits from each treatment were chopped into smaller pieces and air dried at an average room temperature of 28.71±1.77°C and relative

humidity of $77.64 \pm 8.07\%$, milled separately and stored in the refrigerator at 4°C for 24 hrs prior to use.

2.4. Experimental Animals

Thirty-two male wistar rats (*Ratus norvegicus*) weighing $80 \pm 20\text{gm}$ were obtained from the Central Animal House of the Department of Physiology, College of Medicine, University of Ibadan, Nigeria. Prior to the arrival of the wistar rats, the rat cages (wooden wire) were properly cleaned and disinfected at the Department of Pharmacognosy, College of Medicine, University of Ibadan. Cages were fitted with drinkers that could comfortably drop water when imbibed by rats and the feeders were properly placed to eliminate feed spillage. The animals were kept under and maintained at $27 \pm 2^{\circ}\text{C}$, with 12 hour light, 12 hour dark cycles, relative humidity of 70-80%.

The rats were divided into eight experimental groups (treatments) with four rats and were labeled T1, T2, T3, T4, T5, T6, T7 and T8 in each cage and were acclimatised for seven days before the commencement of the feeding treatments which lasted for 21 days. Locally grower mash feed (Standard Ratio Feed) and water was given to the rats during acclimatisation and treatment periods *ad libitum*. During the experiment, the experimental procedures were approved and conducted following the guidelines of University of Ibadan Ethical Committee which conforms to the Ethical use of Animals (Clarke *et al.*, 1996).

2.5. Sub Chronic Toxicity of the Plant Extract and Synthetic Insecticide

2.5.1. *Parkia biglobosa* and Dimethoate + Cypermethrin

The grouped experimental animals were tagged T1, T2, T3, T4, T5, T6, T7 and T8 of four rats per cage. They were administered: Standard Ration Feed (SRF) + treated okra milled feed of *Parkia biglobosa* pod husk extract (PPHE) at 5, 10, 15 and 20%, SRF+ Dimethoate 14.5% + Cypermethrin (D+C) at 2.5 and 5.0 ml and two controls (control group rats were fed with SRF (standard ration feed only) and untreated okra milled feed +SRF),

T1 – Group of rats fed on SRF (Standard Ration Feed) + untreated okra milled feed

T2 – Group of rats fed on SRF 93g +7g of okra milled feed sprayed with 2.5 ml of dimethoate + cypermethrin in 500 ml of water (recommended dose)

T3- Group of rats fed on SRF 93g +7g of okra milled feed sprayed with 5 ml of dimethoate + cypermethrin in 500 ml of water

T4- Group of rats fed on SRF 93g + 7g of okra milled feed sprayed with 20% extract of *Parkia biglobosa* pod husk extract

T5 – Group of rats fed on SRF 93g + 7g of okra milled feed sprayed with 15% extract of *Parkia biglobosa* pod husk extract

T6 – Group of rats fed on SRF 93g + 7g of okra milled feed sprayed with 10% extract of *Parkia biglobosa* pod husk extract

T7 – Group of rats fed on SRF 93g + 7g of okra milled feed sprayed with 5% extract of *Parkia biglobosa* pod husk extract

T8 – Group of Control rats (0%) (SRF only) 100g + 0g of okra milled feed

All groups were fed with okra treated milled feed + SRF and drinking water *ad libitum* was given for

21 days according to the treatments stated above everyday (from morning till night).

Weights of the animals were taken weekly and at the end of the experiment. Toxicity of the administered feed such as sluggishness, aggressiveness, weight gain / loss, convulsion, paralysis and mortality were observed on the experimental animals as daily routine as earlier reported by Fadina *et al.* (1999); Oshoke *et al.* (2016) and Fayinminnu *et al.* (2017).

2.6. Collection of Blood samples for hematology and Serum Biochemistry

2.6.1. Blood hematology and Serum Biochemistry Analyses

The termination of the experiment was done at 21 days; all the living wistar rats were sacrificed through cervical dislocation. Blood samples (2 ml) were collected by cardiac puncture into EDTAK3 bottles. They were arranged in heparinized capillary tubes and analyzed for hematological parameters according to the method of Schalm *et al.* (1975). The hematological parameters include Packed Cell Volume (PCV), Hemoglobin concentration (Hb), Red Blood Cell (RBC), White Blood Cell (WBC), Platelets (PLT), Lymphocytes (LYM), Neutrophils (Neut), Monocytes (MON), Eosinophils (EOS), Mean Corpuscular Volume (MCV), Mean Corpuscular Hemoglobin (MCH) and Mean Corpuscular Hemoglobin Concentration (MCHC).

Blood samples for serum biochemical analyses were collected into plain bottles and centrifuged at 3000 revolutions per minute for 10minutes. The supernatant was analyzed for Total protein (TP) using Biuret method (Bradford, 1976), Albumin (ALB), Globulin (GLB), Total bilirubin (TB) concentrations were calculated according to Doumas *et al.* (1971). Alkaline Phosphatase (ALP), Alanine aminotransferase (ALT) and Aspartate aminotransferase (AST) were determined using the method of Reitman and Frankel (1957), Glucose level, Creatinine and Urea.

2.7. Histopathological Examination

The experimental animals' abdomens were dissected immediately after blood collection to harvest organs of interest (liver and kidney). The tissues (livers and kidneys) were weighed and were preserved in 10% formalin in universal bottles for histopathological examination. They were then processed and stained with hematoxylin and eosin (H & E) stain for histopathology examination. For preparing the animal tissues for microscopic examination, histological procedures were followed in a stepwise protocol they include: Fixation, Dehydration, Clearing, Infiltration, Embedding, Blocking, Sectioning and Staining. Detailed microscopic examination was carried out on the organs of both control and treated groups.

The hematological and serum biochemistry analyses and histopathological examinations were carried out by qualified pathologists at the Clinical Pathology and Histopathology Laboratories of the Department of Veterinary Pathology, Faculty of Veterinary Medicine, University of Ibadan, Ibadan, Nigeria.

2.8. Statistical Analysis

Data were analyzed using analysis of variance (ANOVA) with Statistical Analysis System (SAS) software at 5% ($p < 0.05$) level of significance. Means were

separated using Duncan Multiple Range Test (DMRT). Results were presented as mean \pm standard error of the mean (SEM).

3. Results and Discussions

3.1. Behavioral Observations

The behavioral observation of the experimental animals during the study showed restlessness after each feeding to the treatments of *Parkia biglobosa* pod husk extract and dimethoate + cypermethrin treated okra. Restlessness, which is a sign of pesticide poisoning, was observed in animals fed okra treated with SRF + 5 ml of dimethoate + cypermethrin. This might be due to the inhibitory action of dimethoate (an organophosphate insecticide) on acetylcholinesterase leading to accumulation of acetylcholine at the nerve synapses (Chedi and Aliyu, 2010).

3.2. Toxic effects of treated okra with *Parkia biglobosa* pod husk extract (PAPHE) and dimethoate+ cypermethrin (D+C) on food intake of wistar rats

Result of treated okra feed intake of the experimental animals from this study varied across the three (3) weeks of feeding as shown in Figure 1. No significant differences ($p > 0.05$) were observed at week one (1), although SRF+ 5 ml D+C (T3) had the highest value (79.7 g), followed by SRF only (T8) with 74.3g, the least value (52.5 g) was obtained from SRF+ 20% PAPHE (T4). Significant differences ($p > 0.05$) in feed intake were not observed amongst the treatments at week two (2). However, SRF+5% PAPHE (T7) had highest value (74.3 g) followed by SRF+2.5 ml D+C (T2; 73.7 g), while treatment T1 (SRF+ untreated okra) had the least value of 42.9 g. The same trend as in week two was observed in week three with no significant differences among the treatments. Treatment SRF+ 5% PAPHE (T7) had the highest value (74.7 g), followed by SRF+ 2.5 ml D+C (T2; 69.4 g), while T1 (SRF+ untreated okra) had the lowest value (50.8 g) though it increased compared to week two (2).

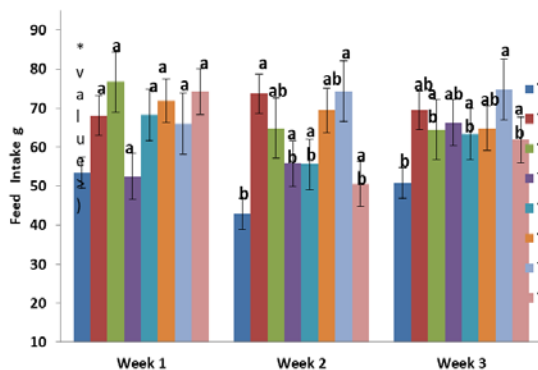


Figure 1: Toxic effects of treated okra with *Parkia biglobosa* pod husk extract (PAPHE) and dimethoate+ cypermethrin (D+C) on feed intake of wistar rats .T1= rats fed untreated okra + standard ration feed, T2 = rats fed okra treated with 2.5 ml of synthetic insecticide in 500 ml of water + standard ration feed, T3 = rats fed okra treated with 5 ml of synthetic insecticide in 500 ml of water + standard ration feed, T4 = rats fed okra treated with 20% PAPHE + standard ration feed, T5 = rats fed okra treated with 15% PAPHE + standard ration feed, T6 = rats fed okra treated with 10% PAPHE + standard ration feed, T7 = rats fed okra treated with 5% PAPHE + standard ration feed, T8 = control (rats fed with standard ration feed).

3.3. Toxic effects of (PAPHE) and dimethoate+ cypermethrin (D+C) on body weight of wistar rats

The toxic effect of varying doses of PAPHE and dimethoate + cypermethrin on mean body weights of wistar rats is presented in Figure 2. There were no significant differences in mean body weights among all the experimental animals at week zero (0) before the commencement of the treatments. Control animals (T8) had the highest mean weight (118.17g) which was not significantly different from treatments T1 (94.43g), T2 (97.83g), T4 (98.67g), T5 (95.5g) and T6 (98.6g) at the first week of treatment (week one). The mean weight of the control animals was significantly higher than that of treatments T3 and T7. Results shown at week two (2) revealed no significant differences in the mean weight of the animals. Treatment T6 had the highest mean weight (121.87g), closely followed by T7 (120.4g), T1 (118.47g), T5 (118.23g), T8 (118.1g), T2 (116.1), T4 (105.7g) and treatment T3 had the lowest (97.2 g) which was not significantly different. The body weight of the animals at week three showed that treatment T1 had the highest mean weight (136.87g) which was not significantly different from T2 (115.13g), T4 (113.23g), T5 (118.73g), T6 (112.73g), T7 (131.63g) and T8 (131.9g). However, this was significantly higher than treatment T3 (104.9g) which had the lowest weight among the treated animals.

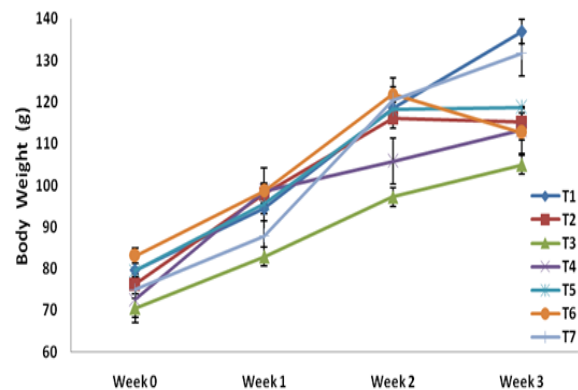


Figure 2: Toxic effects of treated okra with *Parkia biglobosa* pod husk extract (PAPHE) and dimethoate+ cypermethrin (D+C) on body weight of wistar rats .T1= rats fed untreated okra + standard ration feed, T2 = rats fed okra treated with 2.5 ml of synthetic insecticide in 500 ml of water + standard ration feed, T3 = rats fed okra treated with 5 ml of synthetic insecticide in 500 ml of water + standard ration feed, T4 = rats fed okra treated with 20% PAPHE + standard ration feed, T5 = rats fed okra treated with 15% PAPHE + standard ration feed, T6 = rats fed okra treated with 10% PAPHE + standard ration feed, T7 = rats fed okra treated with 5% PAPHE + standard ration feed, T8 = control (rats fed with standard ration feed)

The decrease in mean body weight of treated experimental animals was relatively non-significant in this study. This may be due to the rich diet they were fed with. Standard ration feed (SRF) was compounded according to the nutritional requirements of the rats (NebGuide, 2008) and mixed with milled okra which also contains nutrients required for proper growth (Sorapong, 2012) of the animals. This conformed to the findings of Builders *et al.* (2012) who observed no significant changes in the body weight of rats exposed to extracts of *Parkia biglobosa* stem bark.

3.4. a. Toxic Effects of *Parkia biglobosa* Pod Husk Extract (PAPHE) and dimethoate + cypermethrin treated okra on Hematological parameters of Wistar rats

Results presented in Table 1 showed Hematological parameters: Packed cell volume (PCV), Hemoglobin concentration (Hb), Red blood cell count (RBC), White blood cell count (WBC), Platelet count (PLT) and Lymphocyte (LYM) of the male wistar rats. There were no significant differences ($p>0.05$) in PCV, HB, RBC, WBC and LYM across all the treated animals. Rats fed on okra treated with 15% PAPHE + SRF (treatment T5) had a significantly ($p<0.05$) higher platelet count (PLT) ($129 \times 10^3/\mu\text{L}$) over other treated animals.

Platelets are blood cells that circulate within the blood and bind together when they recognize damaged blood vessels. A higher number of platelets is referred to as Thrombocytosis. Thrombocytosis could be primary (when abnormal cells in the bone marrow cause an increase in

platelets, but the reason is unknown) or secondary (abnormal cells in the bone marrow that may be caused by an ongoing condition or disease such as anaemia, cancer, inflammation or infection) (Williams, 2016). The 15% *Parkia biglobosa* aqueous pod husk extract (PAPHE) concentration increased the platelets of experimental animals; this could have been due to its ability to catalyze the bone marrow's activity of producing more platelets. Increased platelet counts could lead to increased platelet plug formation (Thrombosis). This could eventually lead to Thrombocytosis (restricted blood flow due to platelet formation), a condition that can cause severe ill health and death of animals. A lower platelet count was observed in animals fed okra treated with 20% (a higher) extract concentration. It may be deduced that 15% concentration of *P. biglobosa* aqueous pod husk extract is a threshold limit that causes a higher platelet count.

Table 1a. Toxic Effects of *Parkia biglobosa* Pod Husk Extract (PAPHE) and dimethoate + cypermethrin treated okra on Hematological parameters of Wistar rats

Treatments	PCV (%)	HB (g/dl)	RBC ($\times 10^3/\mu\text{L}$)	WBC ($\times 10^3/\mu\text{L}$)	PLT ($\times 10^3/\mu\text{L}$)	LYM ($\times 10^3/\mu\text{L}$)
T1	38.0 \pm 1.0 ^a	12.63 \pm 0.34 ^a	6.35 \pm 0.13 ^a	8.13 \pm 1.31 ^a	113 \pm 1.76 ^a	6.0 \pm 1.20 ^a
T2	41.67 \pm 1.76 ^a	13.50 \pm 0.59 ^a	6.75 \pm 0.34 ^a	6.13 \pm 0.61 ^a	103 \pm 13.3 ^a	4.08 \pm 0.37 ^a
T3	45.33 \pm 3.18 ^a	14.93 \pm 1.14 ^a	7.50 \pm 0.60 ^a	5.32 \pm 0.86 ^a	115 \pm 7.42 ^a	4.20 \pm 0.53 ^a
T4	42.00 \pm 1.73 ^a	13.70 \pm 0.49 ^a	7.04 \pm 0.35 ^a	3.90 \pm 0.17 ^a	96.0 \pm 6.7 ^a	2.67 \pm 0.21 ^a
T5	47.33 \pm 0.88 ^a	16.50 \pm 0.95 ^a	7.62 \pm 0.26 ^a	7.45 \pm 0.32 ^a	219 \pm 1.21 ^{ab}	5.27 \pm 0.35 ^a
T6	41.33 \pm 3.18 ^a	13.40 \pm 1.06 ^a	6.64 \pm 0.69 ^a	6.13 \pm 1.60 ^a	103 \pm 3.0 ^a	4.61 \pm 1.26 ^a
T7	42.00 \pm 1.53 ^a	13.60 \pm 0.40 ^a	6.96 \pm 0.35 ^a	5.70 \pm 2.19 ^a	126 \pm 29.1 ^a	4.23 \pm 1.62 ^a
T8	45.17 \pm 2.91 ^a	15.10 \pm 0.89 ^a	7.54 \pm 0.55 ^a	5.13 \pm 1.26 ^a	117 \pm 6.66 ^a	3.49 \pm 0.93 ^a
NS	NS	NS	NS	NS	NS	NS

Note: Values with the same superscripts (a) in the column indicate no significant difference from each other. $P>0.05$ means there is no significant difference, $P<0.05$ means there is significant difference at 5% level of probability using Duncan Multiple Range Test, NS= Not Significant. T1= rats fed untreated okra + standard ration feed, T2 = rats fed okra treated with 2.5 ml of synthetic insecticide in 500 ml of water + standard ration feed, T3 = rats fed okra treated with 5 ml of synthetic insecticide in 500 ml of water + standard ration feed, T4 = rats fed okra treated with 20% PAPHE + standard ration feed, T5 = rats fed okra treated with 15% PAPHE + standard ration feed, T6 = rats fed okra treated with 10% PAPHE + standard ration feed, T7 = rats fed okra treated with 5% PAPHE + standard ration feed, T8 = control (rats fed with standard ration feed). PCV= Packed cell volume, Hb= Hemoglobin concentration, RBC=Red blood cell count, WBC= White blood cell count, PLT =Platelet, LYM= Lymphocyte

b. Toxic Effects of *Parkia biglobosa* Pod Husk Extract (PAPHE) and dimethoate + cypermethrin treated okra on Hematological parameters of Wistar rats

The results shown in Table 1b revealed that rats fed on okra treated with 15% PAPHE + SRF (treatment T5) had a significantly higher (21.6 g/dL) Mean Corpuscular Hemoglobin (MCH). The other parameters (NEUT, MON,

EOS, MCV and MCHC) across all other treatments were not significantly different ($p>0.05$).

Mean Corpuscular Hemoglobin (MCH) is the average amount of hemoglobin per red blood cell in a blood sample. Significantly higher MCH observed in experimental animals fed okra treated with 15% PAPHE is indicative of red blood cells with increased hemoglobin content. This might be suggestive of a macrocytic anemic condition (Ashaolu *et al.*, 2011).

Table 1b: Toxic Effects of *Parkia biglobosa* aqueous pod husk extract (PAPHE) and dimethoate + cypermethrin treated okra on Hematological parameters of male wistar rats

Treatments	NEUT ($\times 10^3$)	MON ($\times 10^3$)	EOS ($\times 10^3$)	MCV (fl)	MCH(g/dL)	MCHC (pg)
T1	1.81 \pm 0.31 ^a	0.16 \pm 0.1 ^a	0.17 \pm 0.04 ^a	59.80 \pm 0.33 ^a	19.88 \pm 0.12 ^a	33.25 \pm 0.16 ^a
T2	1.78 \pm 0.26 ^a	0.16 \pm 0.1 ^a	0.12 \pm 0.03 ^a	61.80 \pm 0.48 ^a	20.02 \pm 0.13 ^a	32.4 \pm 0.05 ^a
T3	0.90 \pm 0.26 ^a	0.13 \pm 0.1 ^a	0.17 \pm 0.02 ^a	60.63 \pm 0.69 ^a	19.95 \pm 0.24 ^a	32.91 \pm 0.28 ^a
T4	1.04 \pm 0.1 ^a	0.12 \pm 0.1 ^a	0.08 \pm 0.1 ^a	59.74 \pm 0.75 ^a	19.50 \pm 0.28 ^{ab}	32.63 \pm 0.21 ^a
T5	1.60 \pm 0.17 ^a	0.1 \pm 0.0 ^a	0.17 \pm 0.02 ^a	62.16 \pm 1.18 ^a	21.61 \pm 0.49 ^{abc}	34.81 \pm 1.38 ^a
T6	1.31 \pm 0.31 ^a	0.1 \pm 0.0 ^a	0.12 \pm 0.1 ^a	62.65 \pm 1.98 ^a	20.30 \pm 0.62 ^a	32.41 \pm 0.13 ^a
T7	1.22 \pm 0.48 ^a	0.16 \pm 0.1 ^a	0.12 \pm 0.1 ^a	60.40 \pm 0.93 ^a	19.57 \pm 0.42 ^{ab}	32.40 \pm 0.30 ^a
T8	1.40 \pm 0.26 ^a	0.15 \pm 0.4 ^a	0.1 \pm 0.03 ^a	60.65 \pm 0.56 ^a	20.07 \pm 0.32 ^a	33.09 \pm 0.36 ^a
NS	NS	NS	NS	NS	NS	NS

Note: Values with the same superscripts (a, ab) in the column indicate no significant difference from each other. $P>0.05$ means there is no significant difference, $P<0.05$ means there is significant difference at 5% level of probability using Duncan Multiple Range Test, NS= Not Significant. T1= rats fed untreated okra + standard ration feed, T2 = rats fed okra treated with 2.5 ml of synthetic insecticide in 500 ml of water + standard ration feed, T3 = rats fed okra treated with 5 ml of synthetic insecticide in 500 ml of water + standard ration feed, T4 = rats fed okra treated with 20% PAPHE + standard ration feed, T5 = rats fed okra treated with 15% PAPHE + standard ration feed, T6 = rats fed okra treated with 10% PAPHE + standard ration feed, T7 = rats fed okra treated with 5% PAPHE + standard ration feed, T8 = control (rats

fed with standard ration feed). Neutrophils (NEUT), Monocytes (MON), Eosinophils (EOS), Mean Corpuscular Volume (MCV), Mean Corpuscular Hemoglobin (MCH) and Mean Corpuscular Hemoglobin Concentration (MCHC)

This present study showed that other hematological parameters such as Packed cell volume, Hemoglobin concentration, Red blood cell count, White blood cell count, lymphocytes, neutrophils, monocytes, eosinophils, mean corpuscular volume and mean corpuscular hemoglobin concentration had no significant differences in all treated experimental animals. This is similar to the findings of Builders *et al.* (2012).

3.5. Toxic Effects of *Parkia biglobosa* aqueous pod husk extract (PAPHE) and dimethoate + cypermethrin treated okra on Serum biochemical parameters of wistar rats

The serum biochemical parameters include Total protein (TP), Albumin (ALB), Globulin (GLOB), Albumin – Globulin (AG) ratio and Glucose (GLU) level (Table 2). The Total Protein of rats fed okra treated with 15% extract (PAPHE) + SRF (treatment T5) was significantly higher (8.7 g/dl) than all other treatments as shown on Table 2. The increase in serum Total Protein observed in animals administered treatment T5 (okra treated with 15% PAPHE + SRF) may have been due to increased release of tissue specific enzymes, intracellular proteins (Orhue *et al.*, 2005) or acute phase proteins. Acute phase proteins are proteins whose concentration in the blood may increase as the body fights infection or some other inflammation.

Experimental animals fed on okra treated with 15% extract + SRF (T5) had a significantly higher albumin value (4.1 g/dl) than other animals. The Albumin of rats fed on untreated okra + SRF (T1) (2.4 g/dl), rats fed okra treated with SRF + 5 ml D+C (T3) (2.97 g/dl) and rats fed okra treated with 20% extract + SRF (T4) (3.07 g/dl) were significantly lower than that of rats fed on okra treated with SRF +2.5 ml D+C (T2) (3.40 g/dl) and rats fed okra treated with 10% extract + SRF (T6) (3.40 g/dl). There was no significant difference between rats fed okra treated with 5% extract + standard ration feed (T7) (3.27 g/dl) and the control T8 (3.47 g/dl). Albumin is produced entirely in the liver and is of great importance in regulating the flow of water between the plasma and tissue fluid by its effect on colloid osmotic pressure (Orhue *et al.*, 2005). Damage in liver cells might have led to slightly higher blood albumin value as observed in animals to which treatment T5 was administered (Obaineh and Matthew, 2009).

The globulin of treatment T5 (4.57 g/dl) was significantly higher, while lower values of globulin were observed from treatments T2 (3.27 g/dl) T4 (3.90 g/dl), T6 (3.83 g/dl) and control (3.93 g/dl) with no significant differences. Slightly higher globulin value also observed in animals administered treatment T5 might have been due to enhanced antibody secretion in response to infection or allergy (Orhue *et al.*, 2005).

Table 2. Toxic Effects of *Parkia biglobosa* aqueous pod husk extract (PAPHE) and dimethoate + cypermethrin treated okra on serum biochemical parameters of Wistar rats

Treatments	TP (g/dl)	ALB (g/dl)	GLOB (g/dl)	A.G Ratio	GLUC (mg/L)
T1	6.60±0.06 ^a	2.43±0.19 ^a	4.17±0.15 ^a	0.57±0.07 ^a	122±4.91 ^a
T2	7.17±0.12 ^a	3.40±0.15 ^b	3.77±0.07 ^{ab}	0.87±0.07 ^a	119±3.18 ^a
T3	7.03±0.13 ^a	2.97±0.22 ^a	4.07±0.09 ^a	0.67±0.07 ^a	122±2.91 ^a
T4	6.97±0.32 ^a	3.07±0.29 ^a	3.90±0.06 ^{ab}	0.77±0.09 ^a	130±3.7 ^a
T5	8.67±0.09 ^b	4.10±0.06 ^{abc}	4.57±0.09 ^{abc}	0.87±0.03 ^a	117±1.76 ^a
T6	7.23±0.07 ^a	3.40±0.21 ^b	3.83±0.15 ^{ab}	0.80±0.06 ^a	131±4.04 ^a
T7	7.27±0.15 ^a	3.27±0.07 ^{ab}	4.00±0.10 ^a	0.77±0.03 ^a	121±3.51 ^a
T8	7.40±0.15 ^{ab}	3.47±0.12 ^{ab}	3.93±0.13 ^{ab}	0.83±0.03 ^a	115±1.33 ^a
				NS	NS

Note: P>0.05 means there is no significant difference, P<0.05 means there is significant difference at 5% level of probability using Duncan Multiple Range Test, NS = Not Significant

T1= rats fed untreated okra + standard ration feed, T2 = rats fed okra treated with 2.5 ml of synthetic insecticide in 500 ml of water + standard ration feed, T3 = rats fed okra treated with 5 ml of synthetic insecticide in 500 ml of water + standard ration feed, T4 = rats fed okra treated with 20% PAPHE + standard ration feed, T5 = rats fed okra treated with 15% PAPHE + standard ration feed, T6 = rats fed okra treated with 10% PAPHE + standard ration feed, T7 = rats fed okra treated with 5% PAPHE + standard ration feed, T8 = control (rats fed with standard ration feed) TP= Total protein, ALB =Albumin, GLOB =Globulin, AG= Globulin ratio, GLU = Glucose level

3.6. Toxic Effects of *Parkia biglobosa* aqueous pod husk extract (PAPHE) and dimethoate + cypermethrin on enzyme markers of kidney function of male wistar rats

The results as shown on Table 3 revealed no significant differences (p>0.05) in TB, ALP, ALT and Urea across all treated experimental animals. The creatinine level in treatment T5 was significantly higher (1.13 mg/dL) than other experimental animals. Creatinine is excreted from the body in the urine via the kidneys. As a result, creatinine measurement is used almost exclusively in the assessment of kidney function. Creatinine level was higher in animals administered treatment T5 when compared to other treatments. Elevation of creatinine is indicative of under-excretion, suggesting kidney impairment (Oyebanji *et al.*, 2013).

A significant similar trend was also observed in AST level (45.67 U/L). Aspartate Amino Transferase (AST) a serum liver enzyme had a slightly higher value in animals administered treatment T5 when compared to the control and other treatments. This might be indicative of liver cell damage (Aniagu *et al.*, 2005).

Table 3: Toxic Effects of *Parkia biglobosa* aqueous pod husk extract (PAPHE) and dimethoate + cypermethrin on enzyme markers of kidney and liver functions of male wistar rats

Treatments	TB (mg/dL)	AST (U/I)	ALT (U/I)	ALP (U/I)	UREA (mg/dL)	CREAT (mg/dL)
T1	0.3±0.1 ^a	43.0±1.53 ^a	31.33±0.88 ^a	112±2.52 ^a	15.73±0.44 ^a	0.67±0.03 ^{ab}
T2	0.23±0.09 ^a	39.67±0.88 ^a	27.33±1.45 ^a	111±7.84 ^a	16.33±0.69 ^a	0.73±0.03 ^{ab}
T3	0.23±0.09 ^a	43.33±2.03 ^a	30.67±1.20 ^a	111±4.67 ^a	14.77±0.58 ^a	0.67±0.03 ^{ab}
T4	0.33±0.03 ^a	37.0±0.58 ^a	25.33±0.33 ^a	111±3.93 ^a	15.30±0.44 ^a	0.733±0.03 ^{ab}
T5	0.27±0.03 ^a	45.67±0.88 ^{ab}	33.33±0.33 ^a	118±7.31 ^a	16.73±0.79 ^a	1.13±0.07 ^{abc}
T6	0.17±0.03 ^a	42.67±1.45 ^a	31.0±1.53 ^a	118±1.0 ^a	14.30±1.11 ^a	0.80±0.0 ^{ab}
T7	0.23±0.88 ^a	40.33±0.88 ^a	29.0±2.0 ^a	130±1.20 ^a	16.77±0.32 ^a	0.73±0.03 ^{ab}
T8	0.23±0.88 ^a	37.0±1.16 ^a	26.0±0.58 ^a	121±6.25 ^a	16.40±0.58 ^a	0.67±0.07 ^{ab}
	NS		NS	NS	NS	

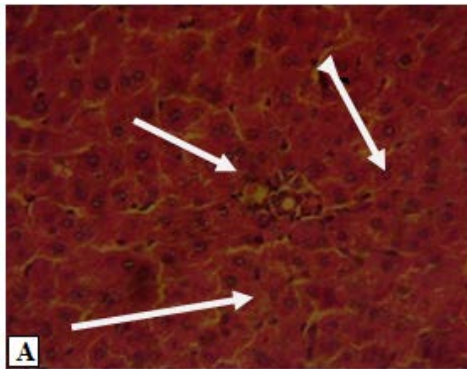
Note: Values with the same superscripts (a, ab) in the column indicate no significant difference from each other. P>0.05 means there is no significant difference, P<0.05 means there is significant difference at 5% level of probability using Duncan Multiple Range Test, NS= Not Significant. T1= rats fed untreated okra + standard ration feed, T2 = rats fed okra treated with 2.5 ml of synthetic insecticide in 500 ml of water + standard ration feed, T3 = rats fed okra treated with 5 ml of synthetic insecticide in 500 ml of water + standard ration feed, T4 = rats fed okra treated with 20% PAPHE + standard ration feed, T5 = rats fed okra treated with 15% PAPHE + standard ration feed, T6 = rats fed okra treated with 10% PAPHE + standard ration feed, T7 = rats fed okra treated with 5% PAPHE + standard ration feed, T8 = control (rats fed with standard ration feed). TP= Total protein, ALB =Albumin, GLOB =Globulin, AG= Globulin ratio, GLU = Glucose level

3.7. Toxic effects of *Parkia biglobosa* Pod Husk Extract and dimethoate + cypermethrin treated okra on Histological organs (liver and kidney) of male wistar rats

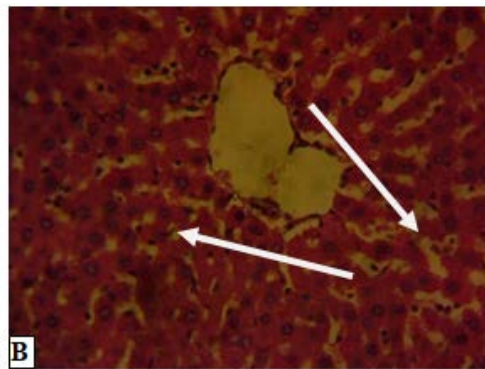
Photomicrographs showing sections of organs of interest (liver and kidney) of the treated rats are presented in plates 1 and 2. Parenchymal cells of the liver (i.e. the hepatocytes) and kidney (i.e. glomerulus and tubular epithelial cells) were normal in treatments T1: rats fed untreated okra + standard ration feed (control), T7: rats fed okra treated with 5% PAPHE + standard ration feed, and T8: control (rats fed with standard ration feed only). Lesions were observed in the livers of the following treatments: T2: rats fed okra treated with 2.5 ml of dimethoate + cypermethrin + standard ration feed, T3: rats fed okra treated with 5 ml of dimethoate + cypermethrin + standard ration feed, T4: rats fed okra treated with 20% PAPHE + standard ration feed, T5: rats fed okra treated with 15% PAPHE + standard ration feed, T6: rats fed okra treated with 10% PAPHE + standard ration feed. Similarly, lesions were also observed in the kidneys of treatments T4 and T6.

Experimental rats fed on T1 showed normal hepatocytes, glomerulus and tubules in their liver and kidney, respectively (control). Moderate centrilobular vacuolar degeneration and atrophy of hepatocytes were observed in liver, while kidney had normal histological structures in T2 treatment. Examination showed diffuse atrophy of hepatic cords and Kupffer cells hyperplasia in the liver of T3 with normal histological structures in the kidney. Observations in T4 showed mild random degeneration of hepatocytes in liver, while the kidney revealed diffuse vacuolar degeneration of medullary tubular epithelial cells (T1-T4 shown in plate 1).

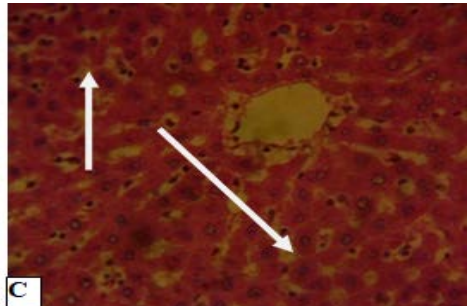
Diffuse degeneration of hepatocytes; Hepatocellular necrosis and infiltrate of inflammatory cells were shown in liver of T5, while kidney showed normal histological structures. Experimental rats fed on T6 treatment showed liver with marked random degeneration and necrosis of hepatocytes, while the kidney had coagulation necrosis of tubular epithelial cells. Normal histological structures were observed in both liver and kidney of T7 as well as in T8 (control) (T5-T8 as shown in plate 2).



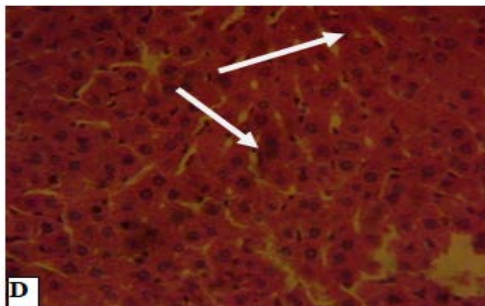
Arrows showing Normal hepatocytes



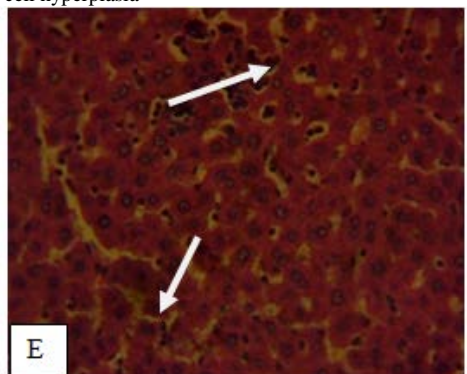
Arrows showing Moderate centrilobular vacuolar degeneration and atrophy of hepatocytes



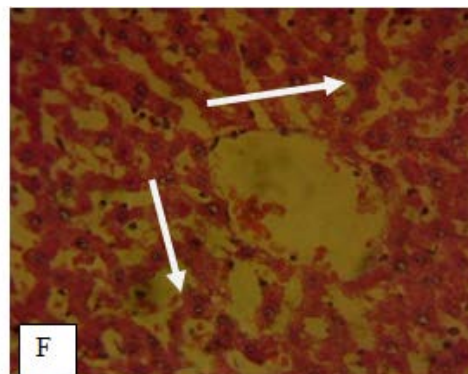
Arrows showing Diffuse atrophy of hepatic Kupffer cell hyperplasia



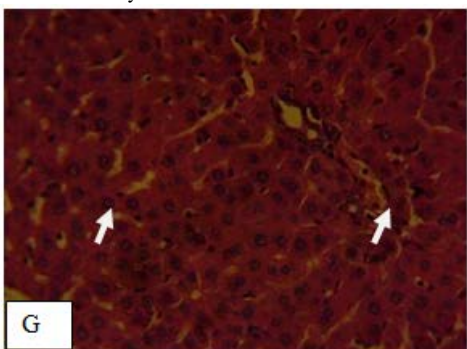
Arrows showing Mild random degeneration of cord and hepatocytes



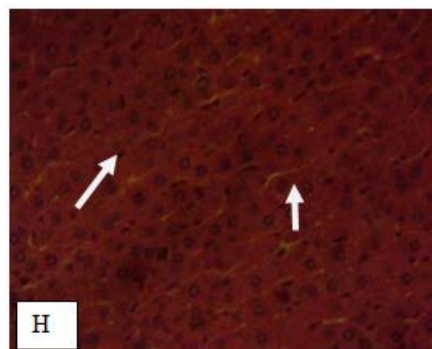
Arrows showing Focus of hepatocellular infiltrate of inflammatory cells



Arrows showing Random degeneration and necrosis of hepatocyte

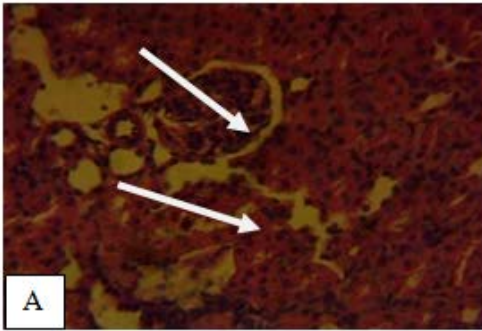


Normal histological structures

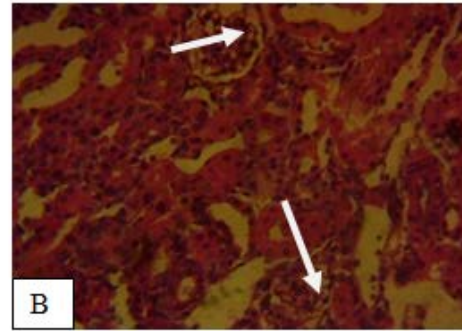


Normal histological structures

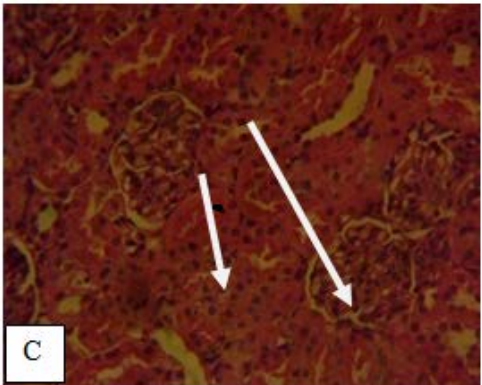
Plate 1: Photomicrograph of section of rat liver fed with okra treated with *Parkia biglobosa* and dimethoate + cypermethrin treatments. **A - T1:** Liver of rat fed with untreated okra + standard ration feed, **B - T2:** Liver of rat fed okra treated with 2.5 ml of dimethoate + cypermethrin + standard ration feed (SRF), **C- T3:** Liver of rat fed okra treated with 5 ml of dimethoate + cypermethrin + SRF, **D - T4:** Liver of rat fed okra treated with 20% extract (PAPHE) + SRF, (H & E Magnification X 400). **E - T5:** Liver of rat fed okra treated with 15% PAPHE + SRF. **F - T6:** Liver of rat fed okra treated with 10% PAPHE + SRF. **G - T7:** Liver of rat fed okra treated with 5% PAPHE + SRF. **H - T8:** Liver of rats fed with SRF only (control). (H & E Magnification X 400)



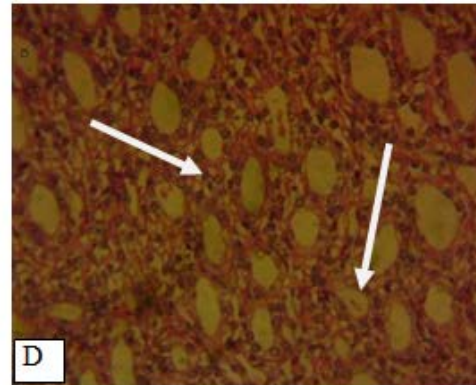
Arrows showing Normal glomerulus and tubules



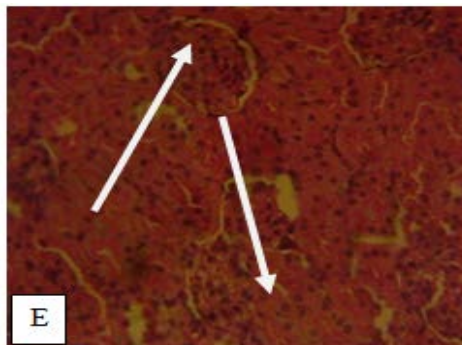
Arrows showing Normal histological structures



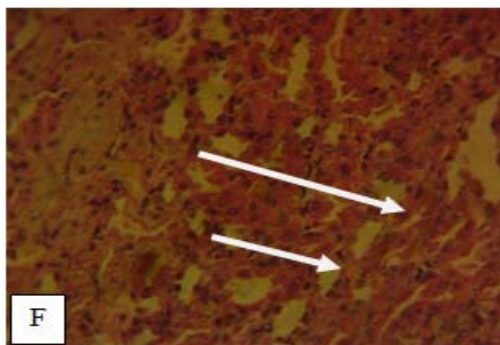
Arrows showing Normal histological structures of medullary



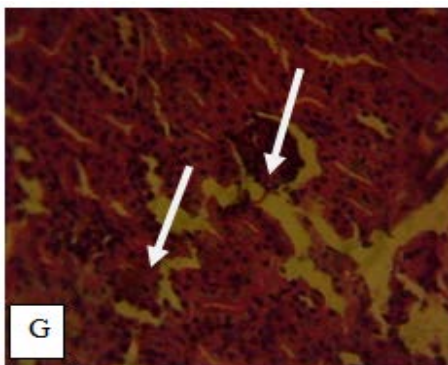
Arrows showing Diffuse vacuolar degeneration tubular epithelial cells



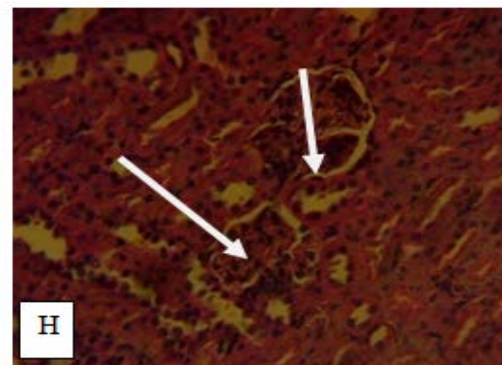
Arrows showing Normal histological structures



Arrows showing Coagulation necrosis of tubular epithelial cells



Arrows showing Normal histological structures



Arrows showing Normal histological structures

Plate 2: Photomicrograph of section of rat kidneys fed with okra treated with *Parkia biglobosa* and dimethoate + cypermethrin treatments
A - T1: Kidney of rat fed with untreated okra + Standard Ration Feed, **B - T2:** Kidney of rat fed okra treated with Standard Ration Feed + 2.5 ml of D+C, **C- T3:** Kidney of rat fed okra treated with Standard Ration Feed + 5 ml of D+C, **D - T4:** Kidney of rat fed okra treated with 20% PAPHE + Standard Ration Feed, **E - T5:** Kidney of rat fed okra treated with 15% PAPHE + Standard Ration Feed, **F - T6:** Kidney of rat fed okra treated with 10% PAPHE + Standard Ration Feed, **G - T7:** Kidney of rat fed okra treated with 5% PAPHE + Standard Ration Feed, **H - T8:** Kidney of rats fed with Standard Ration Feed only (control)
 (H & E Magnification X 400)

Histopathology analyses conducted in this study revealed lesions such as vacuolar degeneration, atrophy, necrosis of hepatocytes and kupffer cells in photomicrographs of liver of the following treatments: rats fed okra treated with SRF+ 2.5 ml of Dimethoate + Cypermethrin (T2), rats fed okra treated with SRF+ 5 ml of Dimethoate + Cypermethrin (T3), rats fed okra treated with 20% PAPHE + SRF (T4), rats fed okra treated with 15% PAPHE + SRF (T5) and rats fed okra treated with 10% PAPHE + SRF (T6). This might be indicative of liver cell damage or hepatotoxicity (Gregorio, 2001) as the liver is the primary site of metabolism and detoxification. The plant extract (*Parkia biglobosa* aqueous pod husk extract) and synthetic insecticide (Dimethoate + Cypermethrin) did not really alter the morphology of the kidney, as lesions were observed in photomicrographs of kidney of animals administered treatments T4 and T6 only. This might be indicative of renal toxicity. Lesions were not observed both in the liver and kidney organs of animals fed with untreated okra + SRF (treatment T1), okra treated with 5% extract + SRF (treatment T7) and standard ration feed (SRF) only (treatment T8/ control).

Vacuolar degeneration is a reversible cell injury (Seely and Brix, 2016); the liver of experimental animals in which vacuolar degeneration was observed could revert back to normal if the treatment is stopped. Atrophy refers to a reduction in cell size; on the other hand, necrosis (also a type of lesion) is an irreversible reaction to injury otherwise called cell death (Syntichaki and Tavernarakis, 2002). If treatments of the experimental animals with the toxicants continue for a longer period or at higher concentrations, death of the cells may occur.

4. Conclusion

The variations observed in the levels of hematology and serum biochemical parameters were results of different concentrations of *Parkia biglobosa* aqueous pod husk extract (PAPHE) and synthetic insecticide (Dimethoate + Cypermethrin) used in the treatments relative to the control. The toxic effects of PAPHE and dimethoate + cypermethrin on the organs of fed okra wistar rats may be due to any or a combination of all the phytochemicals present in the aqueous pod husk extract.

This study revealed that rats exposed to feed containing untreated okra + standard ration feed, standard ration feed only and okra treated with 5% PAPHE + standard ration feed were free from organ damages. As such, the aqueous pod husk extract of *Parkia biglobosa* appears to be safe for consumption at 5% concentration in agricultural sustainability, food quality and safety.

Acknowledgments

This work was carried out in the Research Laboratories of the Department of Crop Protection and Environmental Biology, Department of Pharmacognosy, College of Medicine and Department of Pathology, Faculty of Veterinary Medicine, all in the University of Ibadan. The authors are grateful to Mr. David Omobusuyi, Prof. Ben. Emikpe and Dr. Theophilus for their technical support and encouragement.

References

- Akintoye, HA, Adebayo, AG, and Aina, OO. 2011. Growth and yield response of okra intercropped with live mulches. *Asian J. Agric. Res.* **5**: 146-153.
- Akinyele, BO, and Temikotan, T. 2007. Effect of variation in soil texture on the vegetative and pod characteristics of okra (*Abelmoschus esculentus* (L.) Moench). *Intern. J. Agric. Res.* **2**: 165-169.
- Aniagu, SO, Nwinyi, FC, Akumka, DD, Ajoku, GA, Dzarma, S, Izebe, KS, Ditse, M, Patrick, E., Nwaneri, C, Wambebe, C, and Gamaniel, K. 2005. Toxicity studies in rats fed nature cure bitters. *Afr. J. Biotech.* **4**: 72-78
- Ashaolu, JO, Ukwenya, VO, Okonoboh, AB, Ghazal, OK, Jimoh, AA. 2011. Effect of monosodium glutamate on hematological parameters in wistar rats. *Inter J of Medicine and Medical Sci* **3**(6): 219- 222
- Awe, EO, and Oyetunji, KT. 2013. Biochemical, haematological and histopathological assessment of toxic effects of *Mammoth esculenta* Crantz leaf aqueous extract in rats. *International Journal of Pharma and Bio Sciences* **4**(3): 228 – 235
- Bradford, MM. 1976. A rapid and sensitive method for the quantitation of quantities of protein utilizing the principle of protein-dye binding. *Anal. Biochem.* **72**: 248-254
- Builders, MI, Isichie, CO, and Aguiyi, JC. 2012. Toxicity studies of the extracts of *Parkia biglobosa* stem bark in rats. *British Journal of Pharmaceutical Research* **2**(1): 1-16
- Chedi, BA, and Aliyu, M. 2010. Effect and management of acute dichlorvos poisoning in wistar rats. *Bayero Journal of Pure and Applied Sciences* **3**(2): 1 – 3
- Clarke, JD. 1996. The guide for the care and use of laboratory animals. National Academy of Science Revision Committee
- Doumas, BT, Watson, WA, and Biggs, HG. 1971. Albumin standards and the measurement of serum albumin with bromocresol green. *Clin. Chem. Acta* **31**: 87
- Fagwalawa, LD, and Yahaya, SM. 2016. Effect of organic manure on the growth and yield of okra. *Imperial Journal of Interdisciplinary Research* **2**(3): 130-133.
- Fayinminnu, OO, Adeniyi, OO, Alabi, OY, and Omobusuyi, DO. 2017. Potentials of aqueous extract of pod husk *Parkia biglobosa* (Jacq.) Benth as a biopesticide in okra (*Abelmoschus esculentus* (L.) Moench) Production. *Journal of Agriculture and Ecology Research International.* **12**(1): 1-12
- Fayinminnu, OO, and Shiro, OO. 2014. The pesticidal potential of *Alternanthera brasiliana* (L.) O.Kuntze in solving pest problem in organic agriculture. Proceedings of the 4th ISOFAR Scientific Conference. 'Building Organic Bridges', at the Organic World Congress Istanbul, Turkey. 13-15 October, 2014. Pp 875- 878
- Fayinminnu, OO. (2010). Crude Cassava Water Extract as a natural emergence effects on growth, yield and food components of cowpea (*Vigna unguiculata*(L) Walp.). Ph.D. Thesis: Department of Crop Protection and Environmental Biology, University of Ibadan, Ibadan. 225 pp
- Mahmood, I, Imadi, SR, Shazadi, K, Gul, A, and Hakeem, KR. 2016. Effects of pesticide on environment. Plant, Soil and Microbes Hakeem, KR et al. (eds.), Springer International Publishing Switzerland pp 260.
- Kadiri, S, Arije, A, and Salako, BL. 1999. Traditional herbal preparations and acute renal failure in South West Nigeria. *Tropical Doctor* **29**: 244–246
- Kumar, S, Dagnoko, S, Haougui, A, Ratnadass, A, Pasternak, D, Kouame, C. 2010. Okra (*Abelmoschus* spp.) in West and Central Africa: Potential and progress on its improvement. *African Journal of Agricultural Research* **5**(25), pp. 3590-3598

- Moekchantuk, T, and Kumar, P. 2004. Export okra production in Thailand. Inter-country programme for vegetable IPM in South and SE Asia phase II Food and Agriculture Organization of the United Nations, Bangkok, Thailand
- NebGuide. 2008. Understanding and Using a Feed Analysis Report. University of Nebraska pp 1-4
- Obaineh, OM, and Matthew, AO. 2009. Toxicological effects of chlorpyrifos and methidathion in young chickens. *African Journal of Biochemistry Research* **3** (3): 048-051
- Ogbalu, OK, Manuel, RB, and Gbarakoro, T. 2015. The role of *Sylepta Derogata* [Lepidoptera: Pyralidae] in the abscission and defoliation of okra flowers, seeds and pods In Monocrop gardens pn Port Harcourt, Nigeria. *Journal of Pharmacy and Biological Sciences* **10**(6): 134-138
- Ojo, JA, Olunloyo, AA, and Ibitoye, O. 2014. Evaluation of botanical insecticides against flea beetles *Podagrica sjostedti* and *Podagrica uniforma* of okra. *International Journal of Advanced Research* **2** (4): 236-244
- Orhue, NE, Nwanze, EA, and Okafor, A. 2005. Serum total protein, albumin and globulin levels in Trypanosoma brucei-infected rabbits: Effect of orally administered *Scoparia dulcis*. *African Journal of Biotechnology* **4** (10): 1152-1155
- Oshimagyne, MI, Ayuba, VO, and Annunne, PA. 2014. Toxicity of aqueous extracts of *Parkia biglobosa* pods on *Clarias gariepinus* (Burchell, 1822) juveniles. *Nigerian Journal of Fisheries and Aquaculture* **2**(2): 24-29
- Oyebanji, BO, Saba, AB, Oridupa, OA. 2013. Studies on the anti-inflammatory, analgesic and antipyretic activities of betulinic acid derived from *Tetracera potatoria*. *Afr J Tradit Complement Altern Med*. **11** (1):30-3
- Pankaja, SC. 2013. Phytochemical analysis of *Citrus sinensis* Peel. *International Journal of Pharma and Bio Sciences* **4** (1): 339 – 343
- Robert, L, Ming, L and Irvin, J. 2011. Seed oil and fatty acid content in okra (*Abelmoschus esculentus*) and related species. *Journal of Agricultural and Food Chemistry* **59** (8):4019–4024
- Salako, EA, Anjorin, TS, and Ulelu, AJ. 2015. Ethnobotanical survey of pesticidal plants used in Edo State, Nigeria. *African Journal of Agricultural Science and Technology* (AJAST) **3** (11): 448- 460
- Schalm, OW, Jain, NC, and Carroll, EJ. 1975. Veterinary Hematology. 3rd Lee and Febriger, Philadelphia. *Indian Vet. J.*, **39**: 157-161
- Seely, JC, and Brix, A. 2016. Kidney, Renal Tubule – Vacuolation, Cytoplasmic. National Toxicology Program Nonneoplastic Lesion Atlas pp 1-3
- Sherah, SB, Onche, EU, Mbonu, IJ, Olotu, PN, and Lajide, L. 2014. *Parka Biglobosa* plants parts: phytochemical, antimicrobial, toxicity and antioxidant Characteristics. *Journal of Natural Sciences Research* **4**(2): 130-133
- Sorapong, B. 2012. Okra (*Abelmoschus esculentus* (L.) Moench) as a valuable vegetable of the world. *Ratar. Povrt.* **49**: 105-112
- Syntichaki, P, and Tavernarakis, N. 2002. Death by necrosis. Uncontrollable Catastrophe, or is there order behind the chaos? *European Molecular Biology Organization Reports* **3**(7): 604-609
- Williams, M. 2016. What are Platelets and why are they important? Heart and Vascular Institute. Johns Hopkins Medicine.

Pomegranate Peel Extract Activities as Antioxidant and Antibiofilm against Bacteria Isolated from Caries and Supragingival Plaque

Sabria Benslimane, Ouafa Rebai*, Rachid Djibaoui, and Abed Arabi

Laboratory of Microbiology and Vegetal Biology, Faculty of Natural Sciences and Life, University of Mostaganem, Algeria

Received: October 5, 2019; Revised: November 20, 2019; Accepted: November 22, 2019

Abstract

The present study aimed to extract polyphenols from pomegranate (*Punica granatum* L.) peel extract (PPE) by maceration using three different solvents: acetone 70%, ethanol 70% and methanol 70% (v/v). The antioxidant capacity potential was determined by scavenging activity of free radicals (DPPH) and ferric reducing power (FRAP) assays. The antimicrobial activity of PPE was evaluated against six oral pathogens isolated from dental caries and supragingival plaque (*Streptococcus mutans*, *Enterococcus faecalis*, *Gemella morbillorum*, *Staphylococcus epidermis*, *Enterococcus bugandensis* and *Klebsiella oxytoca*). The highest total phenolic and flavonoid contents were obtained with ethanolic PPE (204.67 ± 15.26 26 mg gallic acid equivalents (GAE)/g dry weight (DW), 67.67 ± 1.53 mg quercetin equivalent (QE)/g DW respectively). The highest proanthocyanidin content was observed with acetonetic extract (220 ± 17.32 mg catechin equivalent (CE)/g DW). The phenolic profile of ethanolic PPE was determined by HPLC analysis; pedunculagin, punigluconin and punicalagin as a predominant ellagitannin have been identified. The highest scavenging activity (87.37 ± 1.36%) was exhibited by ethanolic PPE with the lowest IC50 value (220 ± 14µg/ml) for DPPH, whereas the highest reducing power assay was observed with acetonetic PPE with a value of 1.48 at 700 nm. The antibacterial activity was investigated by microdilution method, all bacteria were sensitive to the extract with MIC (minimum inhibitory concentration) ranging from 0.0125 to 100 mg/ml, the Gram-positive bacteria are the most sensitive. Antibiofilm activity of ethanolic PPE was tested by crystal violet. The maximum biofilm inhibition was observed at the highest concentration of the extract (MIC) with *E. faecalis* (91.95%) and *S. epidermis* (90.7%). Results indicate the potential application of PPE as antioxidant and antibacterial agent against oral pathogens and that it has great potential for prevention and treatment of dental caries.

Keywords: *Punica granatum* peel, polyphenols, antioxidant, oral biofilm, minimum inhibitory concentration (MIC).

1. Introduction

For a long period in history, a large number of aromatic, spicy, medicinal, and other plants have been used for their medicinal or aromatic properties. The plant derived extracts and essential oils are a potential source of natural and safer antibacterial, antioxidant, anticarcinogenic, antifungal, analgesic, insecticidal, anticoccidial and hypoglycemic agents (Hussain *et al.*, 2008 ; Dadashi *et al.*, 2016). During the growth, Plants generate a variety of secondary metabolites for their defense against negative biotic and abiotic environmental factors. Polyphenols, one of the main bioactive secondary metabolites, are natural antioxidant agents which have an important role in human health because of their ability to scavenge free radicals (Saeed *et al.*, 2012) which have been implicated in the development of a number of disorders, including cancer, neurodegeneration and inflammation (Halliwell, 2007; Ferguson, 2010), giving rise to studies of antioxidants for the prevention and treatment of diseases.

Punica granatum Linn is a plant of puniceae family; the tree may grow up to five meters in height. It has

glossy, leathery leaves and bears red flowers at the branch tips (Khalil, 2004). The pomegranate is fruit of this plant, locally known as romane variety safferi. The tree is native in Asian countries; it has been cultivated and naturalized over the whole Mediterranean region since ancient times (Ahangari *et al.*, 2012). Pomegranates have prominent medical history, and possess remarkable medicinal properties (Longtin, 2003) such as anti-inflammation, anti-diabetes, anti diarrhea, treat dental plaque and aphtae and to combat intestinal infections and malarial parasites (Ismail *et al.*, 2012). Recent studies also revealed the efficacy of the pomegranate fruit against cancer, atherosclerosis, infectious and coronary heart diseases (Lansky *et al.*, 2007; Fischer *et al.*, 2011).The pomegranate peels represent 50% of total weight of fruit, they are an important source of bioactive compounds as phenolics, flavonoids, ellagitannins, and proanthocyanidin compounds (Li *et al.*, 2006), minerals, mainly potassium, nitrogen, phosphorus, magnesium, sodium, and calcium (Mirdehghan and Rahemi, 2007), and complex polysaccharides (Jahfar *et al.*, 2003).

The oral cavity harbors diverse and complex microbial community, more than 700 species have been detected in human oral cavity, and they are composed by both

* Corresponding author e-mail: : rebaiouafa@yahoo.fr.

commensal and pathogenic species (Paster *et al.*, 2001; Dewhirst *et al.*, 2010). Some of these adhere to the teeth and initiate formation of a dental biofilm, which is the major cause of dental caries and periodontal disease (Hardie, 1992; Aas *et al.*, 2005; Do *et al.*, 2013). Oral pathologies such as cavities and periodontal disease are among the most prevalent worldwide (Petersen *et al.*, 2005). The poor oral health has a significant impact on quality of life, as well as implications for systemic health; there is a strong association between severe periodontal diseases and diabetes, cardiovascular diseases, rheumatoid arthritis, osteoporosis, stomach ulcers and gastric cancer and the risk of pregnancy complications, such as preterm low-birth weight (Watabe *et al.*, 1998; Petersen *et al.*, 2005; Yeo *et al.*, 2005; Rautemaa *et al.*, 2007).

The aim of this research is to investigate the effects of different solvents on the extraction of polyphenol from pomegranate peels extract. We also investigate and compare antioxidant, antimicrobial and antibiofilm activity of acetone, ethanol and methanol pomegranate peel extract. This study hints for a plausible economic exploitation of an agroindustrial wastes in pharmaceutical and food industries.

2. 2. Materials and Methods

2.1. Preparation of the Samples

The pomegranate fruits were collected from the region of Hassi Mameche (Mostaganem, Algeria), during the months of September and October, and identified by Microbiology and vegetal biology laboratory at Mostaganem University. Fresh pomegranate fruits were peeled manually and collected peels were then rinsed with distilled water. Peels were further cut into small pieces and dried in an incubator at 30 °C for several days (6-7 days). Dried pieces were ground into a fine powder by a blender and stored away from light for further studies. The solvent extraction procedure was carried out according to the method described by Soares *et al.* (2009). The plant extracts were prepared by mixing 5 g of grounded material in 100 mL of different solvents with increasing polarity: acetone 70%, ethanol 70% and methanol 70% (v/v). The mixture was then shaken for 24 hours at ambient temperature prior to filtration. The filtrates were concentrated under reduced pressure with a rotary evaporator (Heidolph Laborota 4000) at 40°C. The resulting crude extracts were stored at 4°C for further analysis.

2.2. Phytochemical Analysis of Plant Extracts

2.2.1. Total Phenolic Content

The total phenolic content of all extracts was measured using the Folin-Ciocalteu method described by the International Organization for Standardization (ISO 14502-1:2005(E)). Aliquots of 1 mL of diluted extracts (2 mg/mL) were mixed with 5 mL Folin-Ciocalteu reagent at 10% (v/v). After 5 minutes, 4 mL of 7.5% sodium carbonate solution was added to the mixture and incubated for 60 minutes at room temperature in the dark. The absorbance was measured at 765 nm against a blank. The total phenolic content was calculated by the regression equation of the calibration curve of gallic acid (ranging from 10 to 50 µg/mL), and the results were expressed as

mg of gallic acid equivalents per gram of dry weight (mg GAE/g of DW).

2.2.2. Total Flavonoid Content

Total flavonoids of the samples were measured by the aluminum chloride spectrophotometric assay according to Kumazawa *et al.* (2004). Briefly, 0.5 mL of trichloridric aluminium (AlCl₃) at 2% (ethanolic solution) was added to 0.5 mL of appropriately diluted extract. After 10 minutes of incubation at room temperature, absorbance was measured at 420 nm. Quercetin was used as a standard for the construction of the calibration curve (ranging from 0.125 to 40µg/mL). The results were expressed in mg equivalent of quercetin per g dry weight (mg QE/g DW).

2.2.3. Proanthocyanidin Content

The proanthocyanidin content was carried out by the modified vanillin assay (Sun *et al.*, 1998b). 2.5 mL of each methanolic solutions of a 1:3 (v/v) sulfuric acid and 1% (w/v) of a vanillin solution were mixed with 1mL of appropriately diluted extract in distilled water (1mg/mL). The tubes were incubated at 30°C for 15 minutes, the absorbance was measured using a spectrophotometer (6715 UV / VIS, Jenway) at a wavelength of 500 nm. The tannin content is estimated in mg equivalent of catechin per gram of dry weight (CE/ g) from the calibration curve (ranging from 50 to 400µg/mL).

2.3. High Performance Liquid Chromatography Analysis

HPLC analyses are performed using a Shimadzu instrument equipped with a high pressure liquid chromatography pump (LC-2030C) with a deuterium UV detector (LC-2030/2040 PDA). Phenolic compounds were separated on Restek IBD ultra C8 reversed-phase column (250mm x4.6mm ,5µm), using water/acetic acid (0.075%) (Solvent A) and methanol/ acetic acid (0.075%) (Solvent B) at pH 3. Flow rate for each sample was 0.8 mL/min, column temperature was 35°C and the detection was monitored at 280 nm. The phenolic compounds were identified by comparing their retention times with those of pure standards.

2.4. Antioxidant Activity

2.4.1. DPPH Scavenging Assay

The antioxidant activity of the PPE was measured in terms of radical scavenging ability, using the DPPH modified method of Sanchez-Moreno *et al.* (1998). 50 µl of each plant extracts at different concentrations from 0.025 to 5 mg/mL was added to 1950 µl of methanolic solution of DPPH (0.025 g/l). The mixture was shaken vigorously and left to stand for 30 minutes in the dark, at room temperature. The absorbance was recorded at 515 nm on spectrophotometer. The control was prepared as above without any extract and methanol was used as blank. The scavenging ability (SA) was calculated as follows:

DPPH scavenging activity (%) = $(A_c - A_s / A_c) \times 100$.
Where, A_c is the absorbance of the control reaction and A_s is the absorbance of the test compound.

The EC50 value is the concentration of the sample necessary to decrease initial concentration of DPPH by 50%; it was calculated from the nonlinear graph of scavenging activity (%) versus concentration of samples. Lower absorbance of the sample indicated the higher free

radical scavenging activity but higher IC 50 value indicates a weaker capacity to scavenge DPPH radicals.

2.4.2. Ferric Reducing Power Assay

The reducing power of the PPE was carried out according to the method of Oyaizu (1986). 2.5 mL of phosphate buffer solution (0.2 M, pH 6.6) and 2.5 mL of 1% potassium ferricyanide solution (K₃[Fe(CN)₆]), were mixed with 1 mL of various concentrations of the extracts (0.1, 0.2, 0.3, 0.4 and 0.5 mg/mL) diluted in distilled water. After incubation for 20 minutes at 50°C, 2.5 mL of 10% trichloroacetic acid (w/v) was added to the mixture. After the centrifugation (Rotofix 32A) at 3000 rpm for 10 minutes, 2.5 mL of the supernatant was mixed with 2.5 mL of distilled water and 0.5 ml of 0.1% ferric chloride solution. The absorbance of the mixture was measured at 700 nm. Ascorbic acid was used as a positive control.

2.5. Antibacterial Activity

2.5.1. Sample Collection and Culturing Conditions

Samples were taken from the patients who exhibited the sign and symptoms of dental caries and periodontal diseases (gingivitis, periodontitis). Sterile cotton swabs were used to collect microbial samples (from caries and supragingival plaque) appropriately under the assistance of dentist. Sample collection was performed at a community health center in Mostaganem Algeria, on a total of 37 patients (male and female, age ranging from 4 to 61 year). Informed consent was obtained from all patients in accord with the protocol approved by the local ethics committee. The samples were taken to the laboratory of microbiology and vegetal biology at Mostaganem. The sticks were taken out and put in nutrient broth and incubated at 37°C for 24 hours. For the isolation of etiological agents involved in causing dental caries and teeth plaques, several media are used to inoculating all samples; Trypticase soy agar (TSA) + 5% blood for the isolation of a facultative anaerobic bacteria, Mac Conckey's medium for the isolation of aerobic Gram-negative bacteria, Chapman agar for isolation of staphylococcus strains. Then the inoculated plates are incubated at 37°C for 24 or 48 hours in aerobic or anaerobic conditions. After the purification of the isolates, a bacterial identification is carried out by the conventional methods of microbiology (morphology of colony, gram stain reaction, and biochemical tests including catalase, oxidase, Voges-Proskauer and methyl red), hemolytic test and the utilization of API 20 strep, API staph and API 20E (Biomérieux, France). Isolated cultures were identified and screened for biofilm formation.

2.5.2. Determination of Minimum Inhibitory Concentration (MIC) and Minimum Bactericidal Concentration (MBC)

MIC of ethanolic, methanolic and acetonc crude extract of pomegranate peels was evaluated by the microdilution method by using 96-well microplates (Gulluce *et al.*, 2007). The stock solution of each extract (200 mg/mL) was prepared in 10% dimethylsulfoxide (DMSO), from this solution twofold serial dilutions were made in a concentration range from 200 mg/mL to 0.0125 mg/mL. 100 µl of stock solution, is added to the wells of the first line of the microplate, then 100 µl of the different dilutions are added successively in the following lines. 90 µl of nutrient broth and 10µl of inoculums (adjusted at 0.5

Mc Farland) were introduced in each well. The microplates were incubated at 37°C for 24 hours. The MIC was determined as the lowest extracts concentration of the permitting no visible growth of microorganism (no turbidity).

The minimum bactericidal concentration (MBC) is the lowest concentration of the extract that inhibited visible growth of the microorganism. The MBC were determined by subculturing 10 µL of the culture from each negative well on Mueller Hinton Agar, and incubated at 37°C for 24 hours. All these analyses were performed in triplicate.

2.6. Determination of Antibiofilm Activity

2.6.1. Biofilm Formation Assay

The ability of the isolates to adhere to the abiotic surface *in vitro* was tested by the adopted tube method (Lim *et al.*, 2008) with some modifications. The bacterial strains were inoculated in TSB at 37°C with stirring overnight, then the density was adjusted to 10⁸CFU/mL at 600 nm. Isolates were inoculated (200µl) in 2 mL trypticase soy broth (TSB) with 5% sucrose and incubated for 2, 4, 6, 24 and 48 hours at 37°C at static condition. The quantitative analysis of biofilm formation was performed using crystal violet staining of the attached cells (Djordjovic *et al.*, 2002). The planktonic-phase cells were gently removed and the glass tubes were washed three times with PBS, allowed to air dry for 20 minutes, then stained for 20 minutes with 0.1 % crystal violet (w/v) and rinsed thoroughly to remove excess stain and dried for 20 minutes. 2 mL of 95% ethanol was added into each tube and incubated for 30 minutes. The optical density of 2 mL distained solution was examined at 595 nm using a spectrophotometer. All tests were performed in triplicate.

2.6.2. Quantitative Assay of Biofilm Inhibition

In this study, the ethanolic PPE was chosen because of its efficacy. The ability of the extract to inhibit biofilm formation of oral pathogen was tested by tube method, by the adopted method from Cramton *et al.*, (1999) with little modifications. Briefly 1mL of inoculated fresh TSB+5% sucrose (adjusted to 10⁸ CFU/mL at 600 nm) was dispensed into each test tube in presence of 1 mL of different concentrations of PPE (ranging from final concentration MIC to 6.25% MIC). The tubes with bacterial suspension and D.W are considered as negative control. All the tubes are incubated at 37°C for 48 hours. After incubation, the biofilm was assayed using the crystal violet staining method (Djordjovic *et al.*, 2002).

The results are expressed as percentage inhibition: [(OD growth control – OD sample) / OD growth control] × 100.

2.7. Statistical Analysis

All analyses were carried out in triplicate; the values were then presented as average values along with their standard derivations. Data were statistically analyzed by One-way analysis of variance (ANOVA) complemented with Tukey's test with SPSS version 25. Results were considered significant if p <0.05.

3. Results

3.1. Determination of Polyphenol, Flavonoid and Proanthocyanidin Contents

Data in table 1 summarizes the contents of total phenolic, flavonoid and proanthocyanidin of the 70% acetic, 70% ethanolic and 70% methanolic extracts of pomegranate peels. The total polyphenol contents of PPE are in the range of 80.67 ± 1.15 to 204.67 ± 15.26 mg gallic acid equivalents (GAE)/g dry weight (DW). The highest TPC was obtained with 70% ethanol. With respect to TPC extraction yield, solvents used in the present study could be classified in the following decreasing order: ethanol 70% (204.67 ± 15.26 mg GAE/g DW), acetone 70% (176.67 ± 3.06 mg GAE/g DW) and methanol 70% (80.67 ± 1.15 mg GAE/g DW). The total flavonoids contents in PPE ranged from 54.67 ± 4.62 to 67.67 ± 1.53 mg quercetin equivalent (QE) /g DW.

The solvent classification with respect to their extraction efficiency was similar for polyphenols and flavonoids. Ethanolic extract showed the highest value of the flavonoids contents, while the lowest value was obtained by methanolic extract.

Based on the results, it is evident that the PPE is rich in proanthocyanidin and ranged from 115 ± 13.23 to 220 ± 17.32 mg CE/g; the highest level of condensed tannins was observed with acetic extract, followed by ethanolic extract.

Table 1. The total phenolic, flavonoid and tannin contents of pomegranate peel extracts

Pomegranate peel extract	Total phenolic mg GAE/g	Total flavonoid mg QE/g	Proanthocyanidin mg CE/g
Acetic PPE	176.67 ± 3.06	60 ± 20	220 ± 17.32
Ethanolic PPE	204.67 ± 15.26	67.67 ± 1.53	145 ± 50
Methanolic PPE	80.67 ± 1.15	54.67 ± 4.62	115 ± 13.23

The data are displayed with mean standard deviation of twice replications.

3.2. HPLC Analysis

In order to identify components from PPE, HPLC analysis was performed on ethanolic PPE (Figure 1), which has shown the highest level of polyphenols. The results revealed the presence of tannins as pedunculagin, punicalagin and punigluconin respectively in ethanolic PPE by comparisons to the retention time and UV spectra of authentic standards. In the present study, the punicalagin was determined as predominant in the extract; it constituted of 36.451% of the total extracted compounds followed by pedunculagin (23.430%) and punigluconin (9.486%).

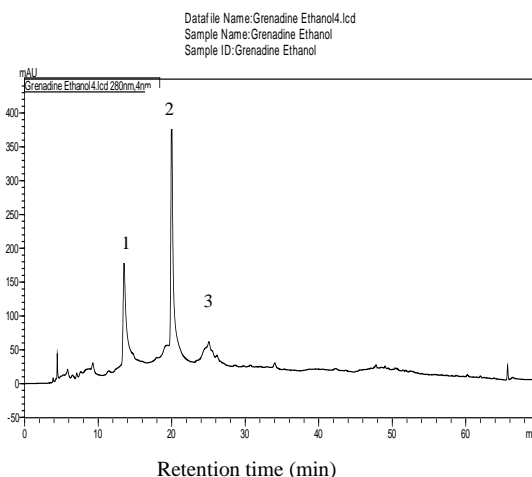


Figure 1. HPLC chromatogram of ethanolic pomegranate peels extract recorded at 280 nm. Peak 1 is pedunculagin; peak 2 is punicalagin; peak 3 is punigluconin.

3.3. DPPH Assay

In the present study, we have evaluated the free radical scavenger activity of ethanol 70%, acetone 70% and methanol 70% PPE; the scavenging activity of DPPH in PPE solution was determined in percentage and compared with a standard ascorbic acid. The decrease in absorbance of DPPH radical is caused by the reaction between antioxidant found in a mixture solution of the PPE and DPPH, which induces the change in color of the mixture from purple to yellow. The hydroalcoholic extracts showed concentration dependant on antiradical activity. Antioxidant activity of phenolic compounds varied greatly according to tested solvent as given in Table 2. The highest scavenging activity ($87.37 \pm 1.36\%$) was exhibited by ethanolic PPE followed by acetic PPE ($57.84 \pm 4.85\%$), their DPPH radical scavenging activity are not significantly different, whereas methanolic PPE had the lowest antioxidant property ($22.23 \pm 0.76\%$) and is significantly different from ethanolic PPE ($p = 0.043$). When compared to a standard ascorbic acid, the DPPH radical scavenging activity of ethanolic PPE was higher at concentrations ranging from $25 \mu\text{g/mL}$ to $50 \mu\text{g/mL}$; however, its antiradical activity is lower than ascorbic acid at concentrations ranging from $100 \mu\text{g/mL}$ to $1000 \mu\text{g/mL}$. The EC 50 values obtained for the investigated plant extracts were in the range from $220 \pm 0.02 \mu\text{g/mL}$ to $700 \pm 37 \mu\text{g/mL}$. The EC50 of ethanolic PPE had the lower value ($220 \pm 0.02 \text{ mg/mL}$) in comparison with the different extracts (Table 3).

In this present study, a positive relationship exists between the total phenolic content, flavonoid content and the antioxidant activity of the PPE. This is because the highest antioxidant capacity was exhibited by 70% ethanolic extract which also showed the highest concentrations of phenolics and flavonoids. Likewise, methanolic PPE extract exhibited the lowest concentrations of phenolics, flavonoids and antioxidant activity.

Table 2. DPPH radical scavenging activities (%) of 70% acetonetic, 70% ethanolic and 70% methanolic PPE. Ascorbic acid was used as positive control

Concentration (µg/mL)	% of inhibition			
	Acetonetic PPE	Ethanolic PPE	Methanolic PPE	Ascorbic acid
25	20.27± 0.88	44.74± 1.05	4.57± 2.16	5.41± 2.19
50	34.81± 0.54	46.79± 0.68	13.09± 0.82	21.04± 3.92
100	44.53± 1.97	50.96± 0.84	17.03± 2.28	63.61± 6.61
500	46.01±1.84	70.54± 0.63	22.01± 0.55	90.24± 1.78
1000	57.84±4.85	87.37± 1.36	22.23± 0.76	97.24± 0.90

The data are displayed with mean ± standard deviation of twice replications.

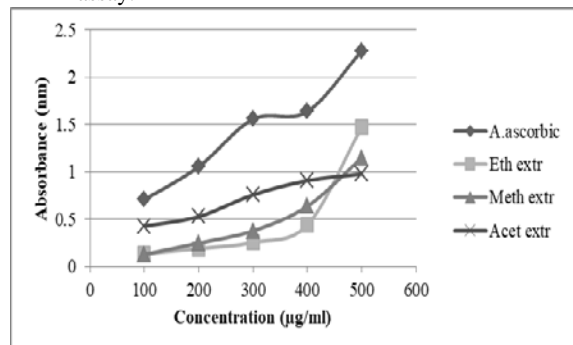
Table 3. EC50 concentrations of DPPH scavenging activity from bioactive compounds.

Bioactive compounds (PPE)	EC50 (µg/mL)
Acetonetic PPE	510± 20
Ethanolic PPE	220± 14
Methanolic PPE	700± 37
Ascorbic acid	200± 26

Values are expressed as mean of three replicates. EC50: the sample concentration required to scavenge 50% free radicals. Ascorbic acid was used as positive control.

3.4. FRAP Assay

The reducing power was used to investigate the ability of the antioxidants found in the extract to donate an electron and reduce Fe^{+3} to Fe^{+2} . In this experiment, depending on the reducing power of the sample, the yellow color of the test solution changes to pale green and blue color. As shown in Figure 2, it was found that the increase in extract concentration increases the reducing power activity. The reducing power of acetonetic, ethanolic and methanolic PPE at different concentrations showed a range of absorbance values from 0.13 to 1.48 at 700 nm; the activity of the three extracts was not significantly different ($p= 0.657$). These values were lower than those obtained with ascorbic acid with absorbance values from 0.71 to 2.28; the reducing power of the reference compound is significantly higher ($p < 0.05$) than that of methanolic and ethanolic PPE. The lowest reducing power was found in the methanolic PPE; this result confirmed that obtained by DPPH assay.

**Figure 2.** Reducing power of PPE. Eth extr = ethanol extract; Meth extr = methanol extract; Acet extr = acetone extract; Ascorbic acid was used as positive control.

3.5. Identification and Selection of Oral Pathogen

In this study, samples were collected from 37 patients, males and females, of different age groups; all samples were cultured on different media, and conventional methods were used for isolation and identification. Strains were identified as *Streptococcus mutans*, *Streptococcus salivarius*, *Streptococcus constellatus*, *Enterococcus faecalis*, *Enterococcus faecium*, *Staphylococcus epidermis*, *Staphylococcus aureus*, *Lactobacillus sp*, *Klebsiella oxytoca*, *Enterobacter bugandensis*. Six strains exhibiting significant biofilm formation were selected for our study, for which four were selected for antibiofilm activity and subjected to molecular identification (data not shown).

Table 4. Gram staining and cell morphology of isolated bacteria.

Strains	Gram staining	Morphology
<i>Streptococcus mutans</i>	+	Cocci
<i>Gemella morbillorum</i>	+	Cocci
<i>Enterococcus faecalis</i>	+	Cocci
<i>Staphylococcus epidermis</i>	+	Cocci
<i>Klebsiella oxytoca</i>	-	Rod
<i>Enterobacter bugandensis</i>	-	Rod

3.6. Antibacterial Effect

Antibacterial activity was evaluated by determining the MIC and MBC of the PPE against oral pathogen by microdilution method, according to Gulluce *et al.* (2008).

The three PPE, screened for antimicrobial activity, showed antibacterial activity against all strains. As evident from the Table 5, the intensity of antibacterial activity of the extracts varied depending on the species of bacteria. Statistical analysis reveals that extracts from pomegranates peels exhibited significantly different antimicrobial potential against tested strains ($p= 0.026$). Gram-negative bacteria are more resistant to the extracts. The highest MIC values were observed with *E. bugandensis* (from 3.15 mg/mL to 100 mg/mL), followed by *K. oxytoca* with action interval of PPE from 12.5 to 25 mg/mL. PP extracts are the most effective against *S. mutans* and *E. faecalis* (MIC values from 0.0125 to 0.025 mg/mL). In comparison between the effects of the ethanolic, methanolic and acetonetic PPE on each strain, there is not statistically significant difference in activity ($p < 0.05$). Action interval of acetonetic, ethanolic and methanolic extract was from 0.0125 mg/mL to 12.5 mg/mL, from 0.025 mg/mL to 100 mg/mL and from 0.0125 mg/mL to 100 mg/mL respectively.

On the other hand, results of minimum bactericidal concentrations (MBC) are listed in Table 5, where the ethanolic and acetonetic PPE have the lowest MBC values and have approximately the same values against oral pathogens. They were in the range from 6.25 mg/mL to >200 mg/mL. CMBs of methanolic PPE were in the range from 25 mg/mL to 200 mg/mL; there are no significantly differences between the MBC values of the three extracts. MBC results show that *S. mutans* and *E. faecalis* were the most sensitive, *E. bugandensis* and *K. oxytoca* were the most resistant microorganisms and have significantly different values of MBC than the other strains, which confirm the results of the MIC. A bacteriostatic activity of the PPE was observed in all the strains.

Table 5. MIC and MBC of acetic, ethanolic and methanolic PPE.

Species	Acetone	Ethanol	Methanol	Acetone	Ethanol	Methanol
	MIC (mg/mL)			MBC (mg/mL)		
<i>S. mutans</i>	0.0125	0.025	0.025	6.25	6.25	100
<i>G.morbillorum</i>	12.5	12.5	25	12.5	12.5	25
<i>E. faecalis</i>	0.0125	0.025	0.0125	6.25	12.5	25
<i>S. epidermis</i>	0.4	0.05	0.05	25	12.5	12.5
<i>K. oxytoca</i>	12.5	12.5	25	>200	>200	200
<i>E.bugandensis</i>	3.15	100	100	100	200	200

MIC: minimum inhibitory concentration; MBC: minimum bactericidal concentration.

3.7. Antibiofilm Activity

In this study, the in vitro antibiofilm effect of the ethanolic PPE was evaluated against four selected oral pathogens by tube method. The effect of PPE on biofilm formation was evaluated by staining with crystal violet as previously reported (Djordjevic *et al.*, 2002). The adherence capabilities of the strains were classified into four categories, no/low ($OD_{595} < 0.2$), moderate ($0.2 < OD_{595} < 0.4$), high ($0.6 < OD_{595} < 1$), and very high ($OD_{595} > 1$) biofilm producers (Russo *et al.*, 2018). All the strains showed positive result on their capability of biofilm formation (Figure 3). *G. morbillorum* and *E. bugandensis* formed the thickest biofilm (very high producer), *E. faecalis*, *S. epidermis*, *K. oxytoca* were classified as high biofilm producers and *S. mutans* as moderate biofilm producer. There are no significant differences in biofilm formation between strains.

Susceptibility of biofilms against plant extract showed that the effect of tested ethanolic PPE inhibited the biofilm formation of all the strains (Figure 4), and the obtained effect was dose dependent. The extract showed good antibiofilm activity >50% against all tested bacteria. Significant differences ($p < 0.05$) were observed between different extract concentrations in biofilm inhibition values. Doses of MIC, 50% MIC and 25% MIC had a greater influence in biofilm eradication than doses of 12.25% MIC and 6.25% MIC. The maximum biofilm inhibition was observed at the highest concentration of the extract (MIC) with *E. faecalis* (91.95%) and *S. epidermis* (90.7%), and the lowest biofilm reduction was observed with *E. bugandensis* (62.66%).

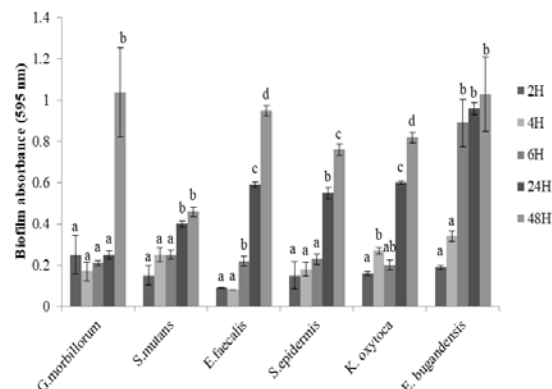


Figure 3. Quantification of biofilm formation by tube method after 2, 4, 6, 24 and 48 hours of incubation. Values represent means \pm standard errors for three replicates. Data with different letters indicate significant difference at $p < 0.05$.

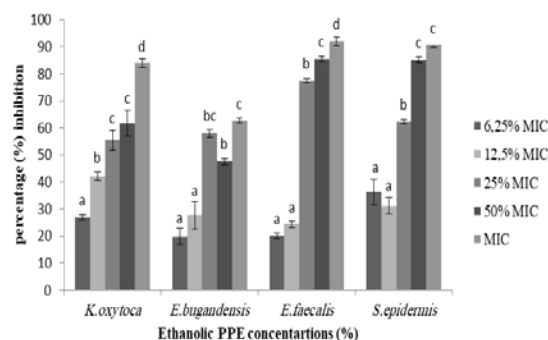


Figure 4. The effect of ethanolic PPE on the formation of bacterial biofilms. Values represent means \pm standard errors for three replicates. Different letters denote significant difference from one another ($p < 0.05$).

4. Discussion

Recently, the use of medicinal plants as antibacterial agent has increased due to opposing effects of antibiotics and the increasing resistant pattern of bacteria which made that antibiotics lose their efficacy (Davies, 1994; Service, 1995; Ahmad *et al.*, 1998). For this, it is necessary to find an alternative of antibiotics for the treatment of infectious diseases. Among these, *Punica granatum*, known for its antioxidant and antimicrobial activities, these properties could be attributed to the production of several secondary metabolites by the plants (Khan *et al.*, 2017). Therefore, in the current study we have evaluated different classes of phenolic compounds. The results indicated that the pomegranate peel extract is rich in polyphenol and proanthocyanidin contents. Our results are in agreement with Elfalleh *et al.* (2012) and Shinde *et al.* (2015) who reported that total phenolic content of pomegranate peels is 85.60 ± 4.87 and 212 ± 20.55 mg GAE/g DW respectively. The ethanolic PPE has the highest polyphenol and flavonoid contents. Ethanol has been known as a good solvent for polyphenol extraction and is safe for human consumption (Dai and Mumper, 2010). Malviya *et al.* (2014) and Wang *et al.* (2011) also reported that content of polyphenols and flavonoids in ethanol extract of pomegranate peels are higher than water, methanol and acetone extracts. There is a different factor that influenced the variation in the recovery of phenolics and flavonoids from natural products, the type of plant, the nature of compounds to extract and the efficiency of extraction solvents to dissolve such compounds (Shabir *et al.*, 2011; Roudsari *et al.*, 2007). Also, the use of mixed solvents (solvent+ DW) results in an enrichment of the extracts in polyphenols, which is due to the increase in the solubility of the phenolic compounds in the extracts (Mohammedi and Atik, 2011; Trabelsi *et al.*, 2010). The results indicated that PPE contained higher level of tannins compounds, which is in compliance with the literature (Machado *et al.*, 2002; Voravuthikunchai *et al.*, 2005; Al zoreky, 2009). Wang *et al.* (2011) found that the proanthocyanidins content of ethanol and acetone extracts were higher than the methanol extract. Also, Vijayalakshmi *et al.* (2017) revealed the presence of highest total tannin content in the ethanolic PPE.

HPLC analysis was performed to obtain more information about the nature of the phenolic compounds present in the ethanolic PPE. The results showed the

presence of three ellagitannins with punicalagin as major components. The pomegranate peel is a rich source of ellagitannins, especially punicalagin, gallic acid, ellagic acid (Gil *et al.*, 2000; Cerdà *et al.*, 2003). Punicalagin, which belongs to the class of hydrolysable tannins, is the most abundant component and is characteristic compounds in pomegranate peel (Seeram *et al.*, 2006; Bakkalbaşı *et al.*, 2009). Our findings are in correlation with other studies, Middha *et al.* (2013) and Kwak *et al.* (2005) revealed the presence of punicalagin as a major ellagitannin in PPE. Other authors (Choi *et al.*, 2011; Çam and Hişil, 2010) found in addition to punicalagin other compounds such as ellagic acid and gallic acid. Furthermore, HPLC analysis of methanolic PPE carried out by Ali *et al.* (2014) revealed the presence of pyrogallol, chlorogenic acid, coumaric acid, ferulic acid, cinnamic acid, benzoic acid, catechin, rutin, acacetin, genistein and kaempferol. These variations in results are probably due to the used solvent, which have an impact on the composition of PPE (El-Falleh *et al.*, 2012). Also several factors (environmental, processing and post harvesting) influenced the composition of the peel (Houston, 2005).

In vitro radical scavenging and antioxidant capacity of the PPE were studied by using DPPH free radical scavenging assay and Ferric reducing power assay. The DPPH test is used to measure the capability of antioxidants in plants extracts to scavenge free radicals from the DPPH solution by donating hydrogen atoms or electrons, which converts free radicals into more stable products (Roudsari, 2007; Sajid *et al.*, 2012).

In the DPPH test, the scavenging activity of the extract varies according to the extraction methodology and the polarity of solvent used for extraction; this could be due to the solubility or insolubility of different antioxidant compounds found in the extract with different chemical characteristics and polarities in particular solvent (Bushra *et al.*, 2009; Boeing *et al.*, 2014). In the present studies, ethanol is a better solvent than acetone and methanol. Results were consistent with the findings of Malviya *et al.* (2014), who reported such higher antioxidant activity was found in 100 % water and 70 % ethanol: 30 % water.

The FRAP assay is a simple method frequently used in the evaluation of antioxidant compounds of fruits, vegetables and some biological samples (Wong *et al.*, 2006). In this method, acetonic extract gave the highest reducing power followed by ethanolic extract. Similar results were reported by Thitipramote *et al.* (2019) where acetonic and ethanolic PPE exhibited the highest bioactive compound and antioxidant activity in ferric reducing power assay. Other authors found the best results of antioxidant activity in methanolic PPE (Li *et al.*, 2006; Pagliarulo *et al.*, 2016). The differences in results may be attributed to the type of pomegranate variety, storage time, harvesting date, climate conditions and method of extraction, as well as solvent concentration (Moure *et al.*, 2001; Robards, 2003; Pinelo *et al.*, 2004).

In the current study, PPE showed antibacterial activity against all tested bacteria. The intensity of antibacterial activity varied depending on the tested bacteria. Gram-positive strains are more sensitive to PPE than Gram-negative bacteria. This variation in sensitivity is ascribed to the differences in cell wall composition. The cell wall of Gram-positive bacteria contains a thick peptidoglycan

layer, while the cell wall of Gram-negative bacteria contains a thin peptidoglycan layer that is surrounded by a thick cytoplasmic membrane and periplastic space, which prevents the penetration of antimicrobial substances (Staszewski *et al.*, 2011; Oliveira *et al.*, 2013). Alvarez-Ordóñez *et al.* (2014) reported that the plant extracts were able to disrupt the molecular structure of the bacteria cell wall and caused leakage of intracellular content, causing increasing in membrane permeability. Several authors have also observed low MIC values for plant extracts for Gram-positive bacteria and high values was reported for Gram-negative bacteria (Burt, 2004; Al-Zoreky, 2009; Hayrapetyan *et al.*, 2012; Tayel *et al.*, 2012). The present research was in line with other studies demonstrating antibacterial effect of *punica granatum* L. peel extracts against *S. aureus*, *Salmonella enterica*, *Shigella sonnei*, *E. coli*, *Bacillus subtilis* and *Enterococcus faecalis* (Machado *et al.*, 2002; Voravuthikunchai *et al.*, 2005; Pagliarulo *et al.*, 2016; Rosas-Burgos *et al.*, 2017). In the work carried by Malviya *et al.* (2014) the antibacterial activity of ethanolic PPE of Ganesh variety was demonstrated on *Staphylococcus aureus*, *Enterobacter aerogenes*, *Salmonella typhi* and *Klebsiella pneumoniae*. In the study by Jaisinghani *et al.* (2018), the inhibitory effect of ethanolic PPE cultivars against both Gram-negative and positive bacteria strains have been reported. The ellagitannins are the major components of pomegranate peel polyphenols, which have been implicated in antimicrobial, anti-inflammatory and anti-cancer activities (Adams *et al.*, 2006; Glazer *et al.*, 2012). Bialonska *et al.* (2009) has reported effect of pomegranate tannin constituents on the growth of various species of human gut bacteria *in vitro*. The tannins increase bacteriolysis, interfere with mechanisms of bacterial adhesion onto the tooth surfaces (Pereira *et al.*, 2006).

The six oral isolates were screened for the biofilm formation by tube method. All the strains showed adherence of the stain in test tube. The antibiofilm activity was tested at concentrations \leq CMI of ethanolic PPE against four selected oral pathogens. Results showed that the tested extract could inhibit the biofilm formation for all tested bacteria in a dose-dependent manner, the inhibitory effect increased with increasing concentration. Vasconcelos *et al.* (2006) demonstrate the potential of PPE to significantly reduce the adherence of three standard streptococci strains (mutans ATCC 25175, sanguis ATCC 10577, and mitis ATCC 9811) of dental plaque and the high efficiency of pomegranate gel in inhibition of bacterial adherence. Menezes *et al.* (2006) observed the effect of the pomegranate hydroalcoholic extract to significantly reduce the bacteria of dental plaque and concluded that this extract could be helpful in the prevention of diseases caused by plaque bacteria. These results are supported by an *in vitro* study of several authors (Kakiuchi *et al.*, 1986, Pereira *et al.*, 2006) who demonstrated that the antimicrobial action of *Punica granatum* Linn on the inhibition of adherence of dental biofilm bacteria is the result of disturbance of glucan synthesis, thus preventing the adhesion of these bacteria to dental surface.

5. Conclusion

This study showed that pomegranate peels are a potential resource for phenolics, flavonoids and proanthocyanidins. The phytochemistry of ethanolic extract was the highest followed by acetonetic extract.

This research revealed the highest antioxidant activities of pomegranate peels which may be attributed to ellagitannins identified by HPLC analysis. All extracts of pomegranate peels have inhibitory effect against both Gram-negative and Gram-positive bacteria. Also, the ethanolic PPE are able to inhibit biofilm formation of *E. faecalis*, *S. epidermis*, *K. oxytoca* and *E. bugandensis*. So, the use of pomegranate peels, which is the by product, could be interesting for its antioxidant and antimicrobial activities against oral pathogen by its incorporation in gum, mouthwash, toothpaste and in the elaboration of products to reduce caries and dental plaque.

Acknowledgment

The authors would like to thank laboratory of Microbiology and Vegetal Biology at University of Mostaganem (Algeria) for their financial support, Ms. Katarina Kvoriaková, Dr. Dahloum Lahouari and Mr. Benchehida Abdelkader for their help with the article.

References

Aas JA, Paster BJ, Stokes LN, Olsen I and Dewhirst FE. 2005. Defining the normal bacterial flora of the oral cavity. *J Clin Microbiol*, **43**: 5721-5732.

Adams LS, Seeram NP, Aggarwal BB, Takada Y, Sand D and Heber D. 2006. Pomegranate juice, total pomegranate ellagitannins, and punicalagin suppress inflammatory cell signaling in colon cancer cells. *J Agric Food Chem*, **54**: 980-985.

Ahangari B and Sargolzaei J. 2012. Extraction of pomegranate seed oil using subcritical propane and supercritical carbon dioxide. *Theor Found Chemen*, **46**:258-265.

Ahmad I, Mehmood Z and Mohammad F. 1998. Screening of some Indian medicinal plants for their antimicrobial properties. *Journal of Ethnopharmacology*, **62**: 183-193.

Ali SL, El-Baz FK, El-Emary GAE, Khan EA and Mohamed AA. 2014. HPLC analysis of poly phenolic compounds and free radical scavenger activity of pomegranate. *International journal of pharmaceutical and clinical research*, **6**: 348-355.

Alvarez-Ordóñez A, Begley M, Clifford T, Deasy T, Considine K, O'Connor P, Ross RP and Hill C. 2014. Investigation of the Antimicrobial Activity of *Bacillus licheniformis* Strains Isolated from Retail Powdered Infant Milk Formulae. *Probiotics and Antimicrobial Proteins*, **6**: 32-40.

Al-Zoreky NS. 2009. Antimicrobial activity of pomegranate (*Punica granatum* L.) fruit peels. *Int. J. Food Microbiol*, **134**: 244-248.

Bakkalbaşı E, Menten O and Artik N. 2009. Food Ellagitannins-Occurrence, Effects of Processing and Storage, *Crit. Rev. Food Sci. nut*, **49**: 283- 298.

Bialonska D, Kasimsetty SG, Schrader KK and Ferreira D. 2009. The effect of pomegranate (*Punica granatum* L.) by products and ellagitannins on the growth of human gut bacteria. *Journal of agricultural and food chemistry*, **57**: 8344-8349.

Boeing JS, Barizão ÉO, E Silva BC, Montanher PF, Cinque Almeida V and Visentainer JV. 2014. Evaluation of solvent effect on the extraction of phenolic compounds and antioxidant capacities from the berries: application of principal component analysis. *Chem Cent J*, **8**:48.

Burt S. 2004. Essential oils: their antibacterial properties and potential applications in foods – a review. *International Journal of Food Microbiology*, **94**: 223-253.

Bushra S, Farooq A and Muhammad A. 2009. Effect of Extraction Solvent/Technique on the Antioxidant Activity of Selected Medicinal Plant Extracts. *Molecules*, **14**: 2167-2180.

Çam M and Hişil Y. 2010. Pressurized water extraction of polyphenols from pomegranate peels. *Food Chem*, **123**: 878-885.

Cerda B, Llorach R, Cerón JJ, Espín JC and Tomàs-Barberà FA. 2003. Evaluation of the bioavailability and metabolism in the rat of punicalagin, an antioxidant polyphenol from pomegranate juice. *Eur J Nutr*, **42**:18-28.

Choi JG, Kang OH, Chae YS, Oh YC, Brice OO, Kim MS, Sohn DH, Kim HS, Park H, Shin DW, Rho JR and Kwon DY. 2011. In Vitro and in Vivo Antibacterial Activity of Punica granatum Peel Ethanol Extract against Salmonella. *Evidence- Based complementary and Alternative Medicine*, **5**: 690518.

Cramton SE, Gerke C, Schnell NF, Nichols WW and Götz F. 1999. The intercellular adhesion (ica) locus is present in *Staphylococcus aureus* and is required for biofilm formation. *Infect Immun*, **67**: 5427-33.

Dadashi M, Hashemi A, Eslami G, Fallah F, Goudarzi H, Erfanimesh S and Taherpour A. 2016. Evaluation of antibacterial effects of Zataria multiflora Boiss extracts against ESBL-producing *Klebsiella pneumoniae* strains. *Avicenna Journal of Phytomedicine*, **6**:336-343.

Dai J and Mumper RJ. 2010. Plant Phenolics: Extraction, Analysis and Their Antioxidant and Anticancer Properties. *Molecules*, **15**: 7313-7352.

Davies J. 1994. Inactivation of antibiotics and the dissemination of resistance genes. *Science*, **264**: 375-382.

Dewhirst FE, Chen T, Izard J, Paster BJ, Tanner AC, Yu WH, Lakshmanan A and Wade WG. 2010. The human oral microbiome. *J Bacteriol*, **192**: 5002-5017.

Djordjevic D, Wiedmann M and Mc Landsborough LA. 2002. Microtiter plate assay for assessment of *Listeria monocytogenes* biofilm formation. *Applied and Environmental Microbiology*, **68**: 2950-2958.

Do T, Devine DA and Marsh PD. 2013. Oral biofilms: molecular analysis, challenges, and future prospects in dental diagnostics. *Clin Cosmet Investig Dent*, **5**: 11-19.

Elfalleh W, Hannachi H, Tlili N, Yahia Y, Nasri N and Ferchichi A. 2012. Total phenolic contents and antioxidant activities of pomegranate peel, seed, leaf and flower. *J Med Plants Res*, **6**: 4724-4730.

Ferguson LR. 2010. Chronic inflammation and mutagenesis. *Mutat. Res. Fund. Mol*, **690**: 3-11.

Fischer UA, Carle R and Kammerer DR. 2011. Identification and Quantification of Phenolic Compounds from Pomegranate (*Punica granatum* L.) Peel, Mesocarp, Aril and Differently Produced Juices by HPLC-DAD– ESI/MSn. *Food Chemistry*, **127**: 807-821.

Gil MI, Tomàs- Barberà FA, Hess-Pierce B, Holcroft DM and Kader AA. 2000. Antioxidant activity of pomegranate juice and its relationship with phenolic composition and processing. *Food Chem*, **68**:4581-4589.

Glazer I, Masaphy S, Marciano P, Bar-Ilan I, Holland D, Kerem Z and Amir R. 2012. Partial identification of antifungal compounds from Punica granatum peel extracts. *J Agric Food Chem*, **60**: 4841-4848.

Gulluce M, Sahin F, Sokmen M, Ozer H, Daferara D, Sokmen A, Polissiou M, Adiguzel A and Ozkan H. 2007. Antimicrobial and antioxidant properties of the essential oils and methanol extract from *Mentha longifolia* L. ssp. longifolia. *Food Chem*, **104**: 1449-1456.

- Halliwell B. 2007. Oxidative stress and cancer: have we moved forward? *Biochem. J.* **401**: 1-11.
- Hardie JM. 1992. Oral microbiology: Current concepts in the microbiology of dental caries and periodontal disease. *Br Dent J.* **172**:271.
- Hayrapetyan H, Hazeleger WC and Beumer RR. 2012. Inhibition of *Listeria monocytogenes* by pomegranate (*Punica granatum*) peel extract in meat pate at different temperatures. *Food Control.* **23**: 66-72.
- Houston MC. 2005. Nutraceutical, vitamins, antioxidants and minerals in the prevention and treatment of hypertension. *Progress in Cardiovascular Diseases.* **47**: 396-449.
- Hussain AI, Anwar F, Hussain ST and Przybylski R. 2008. Chemical composition, antioxidant and antimicrobial activities of basil (*Ocimum basilicum*) essential oils depends on seasonal variations. *Food chemistry.* **108**: 986-995.
- Ismail T, Sestili P and Akhtar S. 2012. Pomegranate peel and fruit extracts. A review of potential anti-inflammatory and anti-infective effects. *Journal of Ethnopharmacology.* **143**: 397-405.
- ISO 14502-1: 2005. Determination of substances characteristic of green and black tea. Part 1: Content of total polyphenols in tea. Colorimetric method using Folin-Ciocalteu reagent.
- Jahfar M, Vijayan KK and Azadi P. 2003. Studies on a polysaccharide from the fruit rind of *Punica granatum*. *Res. J. Chem. Environ.* **7**: 43-50.
- Jaisinghani RN, Makhwana S and Khanojia A. 2018. Study on antibacterial and flavonoid content of ethanolic extract of punica granatum (pomegranate) peel. *Microbiology research.* **9**:7480.
- Kakiuchi N, Hattori M and Nishizawa M. 1986. Studies on dental caries prevention by traditional medicines. Inhibitory effect of various tannins on glucan synthesis by glycosyltransferase from *Streptococcus mutans*. *Chem Pharm Bull.* **34**:720-725.
- Khalil EA. 2004. Antidiabetic effect of an aqueous extract of pomegranate (*Punica granatum* L.) peels in normal and alloxan diabetic rats. *Egy. J. Hosp. Med.* **16**: 92-99.
- Khan NH, Ying ALT, Tian CGZ, Yi OW and Vijayabalan S. 2017. Screening of *Punica granatum* seeds for antibacterial and antioxidant activity with various extracts. *J Gastroenterol Dig Dis.* **1**:1-7.
- Kumazawa S, Hamasaka T and Nakayama T. 2004. Antioxidant activity of propolis of various geographic origins. *Food Chemistry.* **84**: 329-339.
- Kwak HM, Jeong HH, Sohng BH et al. 2005. Quantitative analysis of antioxidants in Korea pomegranate Husk (*Granati pericarpium*) cultivated in different site. *Journal of the Korean Society for Applied Biological Chemistry.* **48**: 431-434.
- Lansky EP and Newman RA. 2007. *Punica granatum* (Pomegranate) and Its Potential for Prevention and Treatment of Inflammation and Cancer. *Journal of Ethnopharmacology.* **109**: 177-206.
- Li Y, Guo C, Yang J, Wei J, Xu J and Cheng S. 2006. Evaluation of antioxidant properties of pomegranate peel extract in comparison. *Food Chemistry.* **96**: 254-260.
- Lim J, Lee KM, Kim SH, Nam SW, Oh YJ, Yun HS, Jo W, Oh S, Kim SH and Park S. 2008. Nanoscale characterization of *Escherichia coli* biofilm formed under laminar flow using atomic force microscopy (AFM) and scanning electron microscopy (SEM). *Bull. Kor. Chem. Soc.* **29**: 2114-2118.
- Longtin R. 2003. The pomegranate: nature's power fruit? *JNCI J Natl Cancer Inst.* **95**: 346-348.
- Machado TDB, Leal ICR, Amaral ACF, Dos Santos KRN, Da Silva MG, and Kuster RM. 2002. Antimicrobial ellagitannin of *Punica granatum* fruits. *Journal of the Brazilian Chemical Society.* **13**: 606-610.
- Malviya S, Jha A and Hettiarachchy N. 2014. Antioxidant and antibacterial potential of pomegranate peel extracts. *Journal of food science and technology.* **51**: 4132-4137.
- Menezes SMS, Cordeiro LN and Viana GSB. 2006. *Punica granatum* (pomegranate) extract is active against dental plaque. *Journal of Herbal Pharmacotherapy.* **6**: 79-92.
- Middha SK, Talambedu U and Pande V. 2013. HPLC evaluation of phenolic profile, nutritive content, and antioxidant capacity of extracts obtained from *Punica granatum* fruit peel. *Advances in Pharmacological Sciences.* **2013**: 1-6.
- Mirdehghan SH and Rahemi M. 2007. Seasonal changes of mineral nutrients and phenolics in pomegranate (*Punica granatum* L.) fruit. *Scientia Horticulturae.* **111**: 120-127.
- Mohammedi Z and Atik F. 2011. Impact of solvent extraction type on total polyphenols content and biological activity from *Tamarix aphylla* (L.) karst. *Inter J Pharma Bio Sci.* **2**: 609-615.
- Moure A, Franco D, Sineiro J, Domínguez H, Núñez MJ and Lema JM. 2001. Antioxidant activity of extracts from *Gevuina avellana* and *Rosa rubiginosa* defatted seeds. *Food Research International.* **34**: 103-109.
- Oliveira DA, Salvador AA, Smânia A, Smânia EF, Maraschin M, Ferreira SR. 2013. Antimicrobial activity and composition profile of grape (*Vitis vinifera*) pomace extracts obtained by supercritical fluids. *J Biotechnol.* **164**: 423-432.
- Oyaizu M. 1986. Studies on products of browning reactions: Antioxidant Activities of Products of browning reaction prepared from glucose amine. *Jpn J Nutr.* **44**: 307-315.
- Pagliarulo C, De Vito V, Picariello G, Colicchio R, Pastore G, Salvatore P and Volpe MG. 2016. Inhibitory effect of pomegranate (*Punica granatum* L.) polyphenol extracts on the bacterial growth and survival of clinical isolates of pathogenic *Staphylococcus aureus* and *Escherichia coli*. *Food Chemistry.* **190**: 824-831.
- Paster BJ, Boches SK, Galvin JL, Ericson RE, Lau CN, Levanos VA, Sahasrabudhe A and Dewhirst FE. 2001. Bacterial diversity in human subgingival plaque. *J Bacteriol.* **183**: 3770-3783.
- Pereira JV, Pereira MSV, Sampaio FC, Sampaio MCC, Alves PM, Araújo CRF and Higinio JS. 2006. In vitro antibacterial and antiadherence effect of *Punica granatum* Linn extract upon dental biofilm microorganisms. *Braz J Pharmacogn.* **16**: 88-93.
- Petersen PE, Bourgeois D, Ogawa H, Estupinan-Day S and Ndiaye C. 2005. The global burden of oral diseases and risks to oral health. *Bulletin of the World Health Organization.* **83**: 661-669.
- Pinelo M, Manzocco L, Nunez MJ and Nicoli MC. 2004. Interaction among phenols in food fortification: negative synergism on antioxidant capacity. *J Agric Food Chem.* **52**: 1177-1180.
- Rautemaa R, Lauhio A, Cullinan MP and Seymour GJ. 2007. Oral infections and systemic disease—an emerging problem in medicine. *Clinical Microbiology and Infection.* **13**: 1041-1047.
- Robards K. 2003. Strategies for the determination of bioactive phenols in plants, fruit and vegetables. *J Chromatogr A.* **1000**: 657-691.
- Rosas-Burgos EC, Burgos-Hernández A, Noguera-Artiaga L, Kacániová M, Hernández-García F, Cárdenas-López JL and Carbonell-Barrachina AA. 2017. Antimicrobial activity of pomegranate peel extracts as affected by cultivar. *J Sci Food Agric.* **97**: 802-810.
- Roudsari MH. 2007. Subcritical water extraction of antioxidant compounds from canola meal, M.Sc. Thesis, University of Saskatchewan, Saskatoon.

- Russo P, Hadjilouka A, Beneduce L, Capozzi V, Paramithiotis S, Drosinos EH and Spano G. 2018. Effect of different conditions on *Listeria monocytogenes* biofilm formation and removal. *Czech J. Food Sci*, **36**: 208-214.
- Saeed N, Khan MR and Shabbir M. 2012. Antioxidant activity, total phenolic and total flavonoid contents of whole plant extracts *Torilis leptophylla* L. *BMC Complement. Altern. Med*, **12**: 221.
- Sajid ZI, Anwar F, Shabir G, Rasul G, Alkharfy KM and Gilani AH. 2012. Antioxidant, antimicrobial properties and phenolics of different solvent extracts from bark, leaves and seeds of *Pongamia pinnata* (L.) pierre. *Molecules*, **17**: 3917-3932.
- Sanchez-Moreno C, Larrauri JA and Saura-Calixto F. 1998. A procedure to measure the antiradical efficiency of polyphenols. *J. Sci. Food Agric*, **76**: 270-276.
- Seeram Np, Zhang Y, Reed JD, Krueger CG and Vaya J. 2006. *Pomegranates: Ancient Roots to Modern Medicine*, CRC press, Taylor and Francis Group, Boca Raton, FL.
- Service RF. 1995. Antibiotics that resist resistance. *Science*, **270**: 724-727.
- Shabir G, Anwar F, Sultana B, Khalid ZM, Afzal M, Khan QM, and Ashrafuzzaman M. 2011. Antioxidant and antimicrobial attributes and phenolics of different solvent extracts from leaves, flowers and bark of gold mohar [*Delonix regia* (Bojer ex Hook.) Raf.]. *Molecules*, **16**: 7302-7319.
- Shinde PA, Reddy VKS and Patange SB. 2015. Quality of Indian mackerel as affected by pomegranate peel and tea leaf extracts during ice storage. *SAARC J. Agr*, **13**: 109-122.
- Soares AA, Marques de Souza CG, Daniel FM, Ferrari GP, Gomes da Costa SM and Peralta RM. 2009. Antioxidant activity and total phenolic content of *Agaricus brasiliensis* (*Agaricus blazei* Murril) in two stages of maturity. *Food Chemistry*, **112**: 775-781.
- Sun B, Ricardo da Silva J and Spranger I. 1998b. Critical factors of the vanillin assay for catechins and proanthocyanidins. *Journal of Agricultural and Food Chemistry*, **46**: 4267-4274.
- Tayel AA, El-Tras WF, Moussa SH and El-Sabbagh SM. 2012. Surface decontamination and quality enhancement in meat steaks using plant extracts as natural biopreservatives. *Foodborne Pathog. Dis*, **9**: 755-761.
- Thitipramote N, Maisakun T, Chomchuen C, Pradmeeteekul P, Nimkamnerd J, Vongnititorn P, Chaiwut P, Thitilertdecha N and Pintathong P. 2019. Bioactive Compounds and Antioxidant Activities from Pomegranate Peel and Seed Extracts. *Food and Applied Bioscience Journal*, **7**: 152-161.
- Trabelsi N, Megdiche W, Ksouri R, Falleh H, Oueslati S, Bourgo S, Hajlaoui H and Abdelly C. 2010. Solvent effects on phenolic contents and biological activities of the halophyte *Limoniastrum monopetalum* leaves. *Food Sci Tech*, **43**: 632-639.
- Vasconcelos LCDS, Sampaio FC, Sampaio MCC, Pereira MDSV, Higino JS, and Peixoto MHP. 2006. Minimum inhibitory concentration of adherence of *Punica granatum* Linn (pomegranate) gel against *S. mutans*, *S. mitis* and *C. albicans*. *Brazilian Dental Journal*, **17**: 223-227.
- Vijayalakshmi K, Sreedevi P and Venkateswari R. 2017. Phytochemical evaluation of *Punica granatum* L. leaf extract. *Int J Curr Pharm Res*, **9**: 14-18.
- Von Staszewski M, Pilosof AM and Jagus RJ. 2011. Antioxidant and antimicrobial performance of different Argentinean green tea varieties as affected by whey proteins. *Food Chem*, **125**: 186-192.
- Voravuthikunchai SP, Sririrak T, Limsuwan S, Supawita T, Iida T, and Honda T. 2005. Inhibitory effects of active compounds from *Punica granatum* pericarp on verocytotoxin production by enterohemorrhagic *Escherichia coli* O157:H7. *Journal of Health Science*, **51**: 590-596.
- Wang Z, Pan Z, Ma H and Atungulu GG. 2011. Extract of phenolics from pomegranate peels. *The Open Food Sci. J*, **5**: 17-25.
- Watabe K, Nishi M, Miyake H and Hirata K. 1998. Lifestyle and gastric cancer: a case-control study. *Oncol Rep*, **5**: 1191-1194.
- Wong CC, Li HB, Cheng KW and Chen F. 2006. A systematic survey of antioxidant activity of 30 Chinese medicinal plants using the ferric reducing antioxidant power assay. *Food Chem*, **97**: 705-711.
- Yeo BK, Lim LP, Paquette DW and Williams RC. 2005. Periodontal disease—the emergence of a risk for systemic conditions: pre-term low birth weight. *Annals of the Academy of Medicine Singapore*, **34**: 111-116.

Jordan Journal of Biological Sciences

An International Peer – Reviewed Research Journal

Published by the Deanship of Scientific Research, The Hashemite University, Zarqa, Jordan



Name: الاسم:
 Specialty: التخصص:
 Address: العنوان:
 P.O. Box: صندوق البريد:
 City & Postal Code: المدينة: الرمز البريدي:
 Country: الدولة:
 Phone: رقم الهاتف:
 Fax No.: رقم الفاكس:
 E-mail: البريد الإلكتروني:
 Method of payment: طريقة الدفع:
 Amount Enclosed: المبلغ المرفق:
 Signature: التوقيع:
 Cheque should be paid to Deanship of Research and Graduate Studies – The Hashemite University.

I would like to subscribe to the Journal

For

- One year
 Two years
 Three years

One Year Subscription Rates

	Inside Jordan	Outside Jordan
Individuals	JD10	\$70
Students	JD5	\$35
Institutions	JD 20	\$90

Correspondence

Subscriptions and sales:

The Hashemite University
 P.O. Box 330127-Zarqa 13115 – Jordan
 Telephone: 00 962 5 3903333
 Fax no. : 0096253903349
 E. mail: jjbs@hu.edu.jo

المجلة الأردنية للعلوم الحياتية
Jordan Journal of Biological Sciences (JJBS)

<http://jjbs.hu.edu.jo>

المجلة الأردنية للعلوم الحياتية: مجلة علمية عالمية محكمة ومفهرسة ومصنفة، تصدر عن الجامعة الهاشمية وبدعم من صندوق دعم البحث العلمي والإبتكار – وزارة التعليم العالي والبحث العلمي.

هيئة التحرير

رئيس التحرير

الأستاذ الدكتورة منار فايز عتوم
الجامعة الهاشمية، الزرقاء، الأردن

الأعضاء:

الاستاذ الدكتور زهير سامي عمرو
جامعة العلوم و التكنولوجيا الأردنية
الاستاذ الدكتور عبدالرحيم أحمد الحنيطي
الجامعة الأردنية

الأستاذ الدكتور جميل نمر اللحام
جامعة اليرموك
الأستاذ الدكتورة حنان عيسى ملكاوي
جامعة اليرموك

الاستاذ الدكتور خالد محمد خليفات
جامعة مؤتة

فريق الدعم:

المحرر اللغوي

الدكتور شادي نعامنة

تنفيذ وإخراج

م. مهند عقده

ترسل البحوث الى العنوان التالي:

رئيس تحرير المجلة الأردنية للعلوم الحياتية
الجامعة الهاشمية

ص.ب , 330127 , الزرقاء, 13115 , الأردن

هاتف: 0096253903333

E-mail: jjbs@hu.edu.jo, Website: www.jjbs.hu.edu.jo



المملكة الأردنية الهاشمية



المجلة الأردنية



للعلوم الحياتية

مجلة علمية عالمية محكمة

تصدر بدعم من صندوق دعم البحث العلمي و الابتكار



<http://jjbs.hu.edu.jo/>